

WL-TR-91-2036

AD-A240 650



PROPERTIES OF AIRCRAFT FUELS AND RELATED MATERIALS

T. B. Biddle, et al.
United Technologies Corporation
Pratt & Whitney
P.O. Box 109600
West Palm Beach, Florida 33410-9600



July 1991

Final Report for Period Ending July 1985 - November 1990

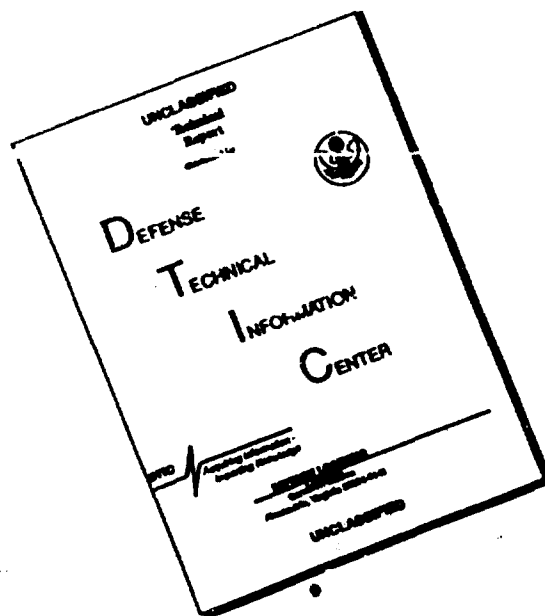
Approved for public release; distribution unlimited

91-11218



AERO PROPULSION AND POWER DIRECTORATE
WRIGHT LABORATORY
AIR FORCE SYSTEMS COMMAND
WRIGHT-PATTERSON A'IR FORCE BASE, OHIO 45433-6563

DISCLAIMER NOTICE




**THIS DOCUMENT IS BEST
QUALITY AVAILABLE. THE COPY
FURNISHED TO DTIC CONTAINED
A SIGNIFICANT NUMBER OF
PAGES WHICH DO NOT
REPRODUCE LEGIBLY.**


NOTICE

When Government drawings, specifications, or other data are used for any purpose other than in connection with a definitely Government-related procurement, the United States Government incurs no responsibility or any obligation whatsoever. The fact that the government may have formulated or in any way supplied the said drawings, specifications, or other data, is not to be regarded by implication, or otherwise in any manner construed, as licensing the holder, or any other person or corporation; or as conveying any rights or permission to manufacture, use, or sell any patented invention that may in any way be related thereto.

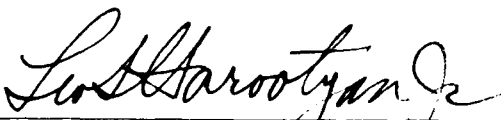
This report is releasable to the National Technical Information Service (NTIS). At NTIS, it will be available to the general public, including foreign nations.

This technical report has been reviewed and is approved for publication.


STEVEN D. ANDERSON
Fuels Branch
Fuels and Lubrication Division


CHARLES L. DELANEY, Chief
Fuels Branch
Fuels and Lubrication Division
Aero Propulsion and Power Directorate

FOR THE COMMANDER


LEO S. HAROOTYAN, JR., Chief
Fuels and Lubrication Division
Aero Propulsion and Power Directorate

If your address has changed, if you wish to be removed from our mailing list, or if the addressee is no longer employed by your organization please notify WL/POSF, WPAFB, OH 45433-6563 to help us maintain a current mailing list.

Copies of this report should not be returned unless return is required by security considerations, contractual obligations, or notice on a specific document.

UNCLASSIFIED

SECURITY CLASSIFICATION OF THIS PAGE

REPORT DOCUMENTATION PAGE

Form Approved
OMB No. 0704-0188

1a. REPORT SECURITY CLASSIFICATION <u>Unclassified</u>			1b. RESTRICTIVE MARKINGS	
2a. SECURITY CLASSIFICATION AUTHORITY			3. DISTRIBUTION/AVAILABILITY OF REPORT Approved for Public Release; Distribution Unlimited	
2b. DECLASSIFICATION/DOWNGRADING SCHEDULE				
4. PERFORMING ORGANIZATION REPORT NUMBER(S) FR-21509			5. MONITORING ORGANIZATION REPORT NUMBER(S) WL-TR-91-2036	
6a. NAME OF PERFORMING ORGANIZATION Pratt & Whitney		6b. OFFICE SYMBOL (If applicable)	7a. NAME OF MONITORING ORGANIZATION Aero Propulsion and Power Directorate (WL/POSF) Wright Laboratory	
6c. ADDRESS (City, State, and ZIP Code) P.O. Box 109600 West Palm Beach, FL 33410-9600			7b. ADDRESS (City, State, and ZIP Code) Wright-Patterson AFB, OH 45433-6563	
8a. NAME OF FUNDING/SPONSORING ORGANIZATION Aero Propulsion and Power Directorate		8b. OFFICE SYMBOL (If applicable) WL/POSF	9. PROCUREMENT INSTRUMENT IDENTIFICATION NUMBER F33615-85-C-2508	
8c. ADDRESS (City, State, and ZIP Code) Wright-Patterson AFB, OH 45433-6563			10. SOURCE OF FUNDING NOS.	
			PROGRAM ELEMENT NO.	PROJECT NO. 3048
			TASK NO. 05	WORK UNIT ACCESSION NO. 51
11. TITLE (Include Security Classification) PROPERTIES OF AIRCRAFT FUELS AND RELATED MATERIALS				
12. PERSONAL AUTHOR(S) Biddle, Tedd B., et al.				
13a. TYPE OF REPORT Final		13b. TIME COVERED FROM 7/8/85 TO 11/30/90	14. DATE OF REPORT (Year, Month, Day) 91 July 29	
15. PAGE COUNT 514				
16. SUPPLEMENTARY NOTATION				
17. COSATI CODES			18. SUBJECT TERMS (Continue on reverse if necessary and identify by block number)	
FIELD	GROUP	SUB. GR.	Aircraft Fuels, Lubricity, Thermal Stability,	
07	01	03	Vapor Pressure, Thermal Conductivity, High Density Fuels,	
21	04	09	Corrosion Inhibitor, Combustion	
19. ABSTRACT (Continue on reverse if necessary and identify by block number)				
<p>The technical effort described herein was conducted over a period from July 1985 through November 1990 and represents a diverse range of subject areas. Topics of study include: general analysis and characterization of conventional and experimental fuel properties which are unique and/or critical to engine performance and durability; special investigations; development and evaluation of new test methods; refinement of existing test methods; additive evaluation and quantification; investigation of fuel and material related field problems; advanced fuel requirements; and fuel system parameters for current and advanced engines.</p>				
20. DISTRIBUTION/AVAILABILITY OF ABSTRACT <input checked="" type="checkbox"/> UNCLASSIFIED/UNLIMITED <input type="checkbox"/> SAME AS RPT <input type="checkbox"/> DTIC USERS			21. ABSTRACT SECURITY CLASSIFICATION Unclassified	
22a. NAME OF RESPONSIBLE INDIVIDUAL Steven D. Anderson			22b. TELEPHONE (Include Area Code) 513-255-3190	22c. OFFICE SYMBOL WL/POSF

DD Form 1473, JUN 86

Previous editions are obsolete.

UNCLASSIFIED

SECURITY CLASSIFICATION OF THIS PAGE

FOREWORD AND ACKNOWLEDGEMENTS

This final report describes the technical effort conducted under Air Force Contract No. F33615-85-C-2508, entitled "Properties of Aircraft Fuels and Related Materials." The technical effort described herein was conducted over a period from July 1985 through November 1990 and represents a diverse range of subject areas. Topics of study and technical activity include: general analysis and characterization of conventional and experimental fuels possessing properties which are unique and/or critical to engine performance and durability; special investigations; development and evaluation of new test methods; refinement of existing laboratory techniques; additive evaluation and quantification; investigation of fuel and material related field problems; advanced fuel requirements; and fuel system parameters for current and advanced engines.

The research conducted under this contract was administered under the direction of Mr. Timothy Dues, WRDC, from July 1985 through January 1987 and by Mr. Steven Anderson, WRDC, from February 1987 through November 1990. Mr. Paul Warner was the P&W Program Manager and Mr. Tedd Biddle the Deputy Program Manager from July 1985 to October 1988. Tedd Biddle assumed the role of P&W Program Manager from November 1988 through November 1990.

The research conducted under this program was the product of many contributors. Among those who provided guidance and practical experience in pursuit of the various areas of study and investigation included Tim Dues, Steven Anderson, Royce Bradley, Herb Lander, Randy Howard, Ronald Butler, Brian Bergsten, Mel Roquemore, William Harrison, Charles Martel, Art Churchill, and Charles Delaney of WRDC. Contributors from the P&W Fuels and Lubricants and Analytical Chemistry Laboratories who worked as Task Managers, Primary Investigators, and performed the laboratory tests, evaluations, and investigations included Paul Warner, William Edwards, Richard Meehan, Susan Guisinger, Marc Rippen, Susan Brown, Michael Gehron, Tedd Biddle, Donald Yost, Michael Polito, William Cellich and James Stoorza. A great deal of support in the areas of system hardware, thermal management, and computer modeling was provided by P&W Project Groups under the supervision of Sam Arline, Engine Controls; Jim Shadowen, Combustor Design; Jim Mohn, Ed Kichura, Paul McClure, and Nat Kosowski, Mechanical Components and Systems. Bennett Croswell of P&W Advanced Engineering Programs was invaluable in his management and performance of a study directed at high temperature fuel requirements and payoffs in the design of advanced fighter engines.

In addition, technical support was provided by Dr. Henk Meuzelaar of University of Utah Biomaterials Profiling Center in the investigation of a JP-10 fuel related field problem; Dr. Louis Hall of Sun Refinery in the development of RJ-7 High Density Fuel; Dr. Arthur Krawetz of Phoenix Chemical Laboratory, Inc. for thermal conductivity data; Dr. Gene Strum of NIPER for hydrocarbon type analysis; Dr. Richard Yost of the University of Gainesville in the development of a method for hydrocarbon type analysis using tandem mass spectroscopy; and Dr. Jane Callanan of the National Bureau of Standards for development of standard measurement techniques and standard reference materials for heat capacity and heat of vaporization of jet fuels. Further, the forum provided by ASTM and the Coordinating Research Council and insight by its members in areas of fuel lubricity and thermal stability was greatly appreciated.

Accession For	
NTIS	GRACI
DTIC	145
Unannounced	
Justification	
By	
Date	
Distribution	
D-1	
A-1	

TABLE OF CONTENTS

<i>Topic Area</i>	<i>Page</i>
DEVELOPMENT OF AN IMPROVED METHOD FOR HIGH-TEMPERATURE VAPOR PRESSURE DETERMINATIONS	1
1.0 INTRODUCTION.....	1
1.1 BACKGROUND.....	1
1.2 OVERVIEW	1
2.0 EXPERIMENTAL.....	2
2.1 DISTILLATION AND VAPOR PRESSURE METHODS	2
2.1.1 ASTM D2887 Simulated Distillation	2
2.1.2 ASTM D86 Distributions	3
2.1.3 Vapor Pressure Determinations	3
3.0 RESULTS AND DISCUSSION.....	3
3.1 DISTILLATIONS AND VAPOR PRESSURE DETERMINATIONS.....	3
3.1.1 ASTM D86 Distillation.....	3
3.1.2 ASTM D2887 Simulated Distillation	4
3.1.3 Vapor Pressure Determinations	4
3.2 DATA ANALYSIS AND CORRELATIONS	11
3.2.1 Percent Recovered Versus Temperature Modeling for ASTM D2887 and ASTM D86 Data	12
3.2.2 Vapor Reflux Modeling	12
3.2.3 Vapor Pressure Versus Percent Recovered Modeling	13
3.2.4 ASTM D86 Versus ASTM D2887 Modeling.....	16
4.0 CONCLUSIONS AND RECOMMENDATIONS	28
APPENDIX A: REFLUX VAPOR PRESSURE TEST	29
DETERMINATION OF FUEL PROPERTIES AND GENERAL ANALYSIS	34
1.0 INTRODUCTION.....	34
2.0 EXPERIMENTAL.....	35
2.1 DETERMINATION OF FUEL PROPERTIES AND GENERAL ANALYSIS.....	35
2.1.1 Hydrocarbon Type by Mass Spectroscopy and FIA	35
2.1.2 Gross and Net Heats of Combustion.....	35
2.1.3 Kinematic Viscosity as a Function of Temperature	35
2.1.4 Simulated Distillation	36
3.0 RESULTS AND DISCUSSION.....	36
3.1 DETERMINATION OF FUEL PROPERTIES AND GENERAL ANALYSIS.....	36
3.1.1 Hydrocarbon Type Analysis by Mass Spectroscopy and FIA.....	36
3.1.2 Gross and Net Heats of Combustion.....	36
3.1.3 Kinematic Viscosity as a Function of Temperature	37
3.1.4 Simulated Distillation	37
4.0 CONCLUSIONS.....	42
DETERMINATION OF THERMAL CONDUCTIVITY OF AIRCRAFT/MISSILE FUELS.....	43
1.0 INTRODUCTION.....	43
2.0 EXPERIMENTAL.....	43
3.0 RESULTS AND DISCUSSION.....	44
4.0 CONCLUSIONS AND RECOMMENDATIONS	59
REFERENCES.....	59

CHARACTERIZATION OF CANDIDATE HIGH DENSITY FUELS	60
1.0 INTRODUCTION AND BACKGROUND	60
2.0 EXPERIMENTAL	61
2.1 HYDROCARBON TYPES BY MASS SPECTROMETRY AND FIA	61
2.2 SIMULATED DISTILLATION	61
2.3 GROSS AND NET HEATS OF COMBUSTION	62
2.4 SPECIFIC HEAT AS A FUNCTION OF TEMPERATURE	62
2.5 KINEMATIC VISCOSITY AS A FUNCTION OF TEMPERATURE	62
2.6 DENSITY AS A FUNCTION OF TEMPERATURE	62
2.7 DIELECTRIC CONSTANT AS A FUNCTION OF TEMPERATURE	63
2.8 TRUE VAPOR PRESSURE AS A FUNCTION OF TEMPERATURE	63
2.9 SURFACE TENSION AS A FUNCTION OF TEMPERATURE	63
2.10 THERMAL CONDUCTIVITY AS A FUNCTION OF TEMPERATURE	63
3.0 RESULTS AND DISCUSSION	64
3.1 FUEL PROPERTIES	64
3.1.1 Hydrocarbon Types by Mass Spectrometry and FIA	64
3.1.2 Simulated Distillation	64
3.1.3 Gross and Net Heats of Combustion	65
3.1.4 Specific Heat as a Function of Temperature	65
3.1.5 Kinematic Viscosity as a Function of Temperature	65
3.1.6 Density as a Function of Temperature	66
3.1.7 Dielectric Constant as a Function of Temperature	66
3.1.8 Vapor Pressure as a Function of Temperature	66
3.1.9 Surface Tension as a Function of Temperature	66
3.1.10 Thermal Conductivity as a Function of Temperature	67
3.2 POTENTIAL FUEL EFFECTS ON ENGINE PERFORMANCE AND LIFE	67
4.0 CONCLUSIONS	68
REFERENCES	86
 CHARACTERIZATION OF EXPERIMENTAL COAL TARS	 87
1.0 INTRODUCTION	87
1.1 HISTORICAL BACKGROUND	87
1.2 THE GREAT PLAINS COAL GASIFICATION PLAN	88
1.3 STUDY OBJECTIVES	90
2.0 EXPERIMENTAL	90
2.1 SAMPLE COLLECTION	90
2.2 SAMPLE CHARACTERIZATION	91
2.2.1 Thermogravimetry	91
2.2.2 Liquid Chromatography	91
2.2.3 Low Voltage Mass Spectrometry	91
2.2.4 Fourier Transform Infrared Spectrometry	91
2.2.5 Elemental Analysis	92
2.2.6 Trace Metals Analysis	94
2.2.7 Simulated Distillation	94
2.2.8 Proton Nuclear Magnetic Resonance Spectrometry	94
2.2.9 Conventional Analyses	94
2.2.10 Data Analysis	94
3.0 RESULTS AND DISCUSSION	95
3.1 NAPHTHA STREAM	95
3.2 TAR OIL STREAM	95

<i>Topic Area</i>	<i>Page</i>
3.3 TAR OIL FRACTIONS: LIGHT AND HEAVY	95
3.4 CRUDE PHENOLS STREAM SAMPLES	98
3.5 WEATHERING AND LONG TERM STABILITY STUDIES OF THE TAR OIL	99
3.5.1 Laboratory Weathering	99
3.5.2 Long-Term Stability	99
4.0 CONCLUSIONS	116
4.1 LIQUID YIELDS	116
4.2 COMPOSITION	116
4.3 STABILITY	116
4.4 SUITABILITY FOR TRANSPORTATION FUELS	116
REFERENCES	117
RJ-7 HIGH DENSITY FUEL DEVELOPMENT	119
1.0 INTRODUCTION	119
2.0 EXPERIMENTAL	119
2.1 COTRIMER FUEL COMPONENT	119
2.2 CYCLOPENTADIENE COTRIMER/INDENE ADDUCT	121
3.0 DISCUSSION	122
4.0 CONCLUSIONS AND RECOMMENDATIONS	123
REFERENCES	125
PURIFICATION OF RJ-5 AND JP-10 FUELS FOR USE AS STANDARDS	126
1.0 INTRODUCTION	126
2.0 EXPERIMENTAL	126
2.1 DISTILLATION OF JP-10 AND RJ-5 FUELS	126
2.2 GAS CHROMATOGRAPHIC ANALYSES OF DISTILLED FUELS	127
3.0 RESULTS AND DISCUSSION	127
ALTERNATE HIGH FLASH POINT CALIBRATION FLUID	132
1.0 INTRODUCTION	132
2.0 DISCUSSION	132
3.0 CONCLUSION AND RECOMMENDATIONS	133
REFERENCES	134
JP-10 FUEL DISCOLORIZATION INVESTIGATION	135
1.0 BACKGROUND	135
1.1 JP-10 PROBLEMS EXPERIENCED BY THE AIR FORCE	135
1.2 JP-10 PRODUCTION PROCESS INFORMATION	136
1.3 LITERATURE DATA ON JP-10 COMPOSITION AND STABILITY	136
2.0 EXPERIMENTAL	136
2.1 SAMPLE DESCRIPTION	136
2.2 DYNAMIC AND STATIC TEST PROCEDURES	138
2.3 LIQUID CHROMATOGRAPHY (LC)	139
2.4 FTIR ANALYSIS	139
2.5 LOW VOLTAGE DIRECT MASS SPECTROMETRY	139
2.6 GAS CHROMATOGRAPHY / MASS SPECTROMETRY (GC/MS)	141
3.0 RESULTS AND DISCUSSION	142
3.1 ANALYSIS OF JP-10 BULK COMPONENTS	142
3.2 ANALYSIS OF JP-10 TRACE COMPONENTS	147
3.2.1 (Alkylsubstituted) Aromatic Hydrocarbons	150

<i>Topic Area</i>	<i>Page</i>
3.2.2 JP-10 Related Oligomers, Homologs and Analogs	152
3.2.3 Long Chain Paraffins	154
3.2.5 Dioctylphthalate (DOP)	157
3.2.6 Unknown Peak Series at m/z 210, 238, 266	158
3.2.7 Miscellaneous Compounds (e.g., silicone oil)	158
3.3 FTIR AND PYROLYSIS MS ANALYSIS OF GUM COMPONENTS	158
3.4 STATIC AND DYNAMIC EXPOSURE TESTS RESULTS	161
4.0 CONCLUSIONS	161
4.1 CHEMICAL COMPOSITIONAL CHANGES	161
4.2 SUSPECTED CAUSE OF FIELD PROBLEM	162
REFERENCES	164
EVALUATION OF PARTICULATE MATTER	165
1.0 INTRODUCTION	165
2.0 EXPERIMENTAL	165
3.0 DISCUSSION	166
4.0 CONCLUSION	168
EVALUATION OF THE SHELL PREMIXED BURNER	169
1.0 INTRODUCTION	169
2.0 EXPERIMENTAL	170
3.0 RESULTS AND DISCUSSION	172
4.0 CONCLUSIONS	179
STANDARDIZATION OF LUBRICITY TEST	180
1.0 INTRODUCTION	180
2.0 EXPERIMENTAL	181
2.1 REFERENCE FLUID INVESTIGATION	181
2.2 TEST CYLINDER SURFACE FINISH INVESTIGATION	182
2.3. FALEX RING INVESTIGATION	183
2.4 INTERLABORATORY EVALUATION OF THE FALEX RING	185
2.5 TEST BALL INVESTIGATION	185
3.0 RESULTS AND DISCUSSION	186
3.1 REFERENCE FLUID SELECTION	186
3.1.1 Ability to Discern Cylinder Quality	187
3.1.2 Reproducibility of Candidate Fluid	188
3.1.3. Repeatability Across Running Surface	188
3.2 TEST CYLINDER SURFACE FINISH INVESTIGATION	189
3.3 FALEX RING INVESTIGATION	193
3.4 INTERLABORATORY EVALUATION OF THE FALEX RING	196
3.5 FALEX RING LUBRICITY VALUES FOR TYPICAL JET FUELS	203
3.6 TEST BALL INVESTIGATION	204
4.0 CONCLUSIONS AND RECOMMENDATIONS	206
APPENDIX A: ISOPAR M PROPERTY DATA SHEET	207
APPENDIX B: BOCLE MODIFICATION FOR USE WITH FALEX RING	208
EVALUATION OF CORROSION INHIBITORS AS LUBRICITY IMPROVERS	209
1.0 INTRODUCTION	209
1.1 BACKGROUND	209
1.2 QUANTIFICATION OF CORROSION INHIBITORS	211

1.3 PROGRAM OBJECTIVES	211
2.0 EXPERIMENTAL.....	212
2.1 CORROSION INHIBITOR EVALUATIONS	212
2.1.1 Ball-On-Cylinder Lubricity Evaluator (BOCLE).....	212
2.1.2 Additives Evaluated.....	213
2.1.3 Test Fuels	213
2.1.4 Additive/Fuel Blends	216
2.1.5 Test Temperatures	216
2.1.6 Summary of Test Matrix	216
2.2 REFINEMENT OF RPHPLC METHOD FOR DETERMINING CI CONTENT IN JET FUELS	216
2.2.1 Equipment and Instrumental Conditions	216
2.2.2 Materials.....	217
3.0 RESULTS AND DISCUSSION.....	217
3.1 CORROSION INHIBITOR EVALUATIONS	218
3.1.1 Lubricity Test Data.....	218
3.1.2 Criteria Used to Assess Performance.....	218
3.1.3 Performance Profile	218
3.1.4 Effect of Fuel Type on Additive Performance.....	219
3.1.5 Effective Concentrations for Lubricity Improvement	222
3.1.6 Performance Ranking	222
3.1.7 Effect of Temperature.....	224
3.2 PROPOSED MIL-I-25017 LUBRICITY REQUIREMENT	225
3.3 REFINEMENT OF RPHPLC METHOD FOR DETERMINING CI CONTENT IN JET FUELS.....	231
3.3.1 Method Development Goals.....	231
3.3.2 Preliminary Method Development-- Theory and Mechanism	231
3.3.3 Method Modification	232
3.3.4 Finalized Test Method	235
3.3.5 Applicability to QPL-25017-15.....	238
3.3.6 Chromatograms	239
4.0 CONCLUSIONS AND RECOMMENDATIONS	239
4.1 CORROSION INHIBITOR EVALUATIONS	240
4.2 PROPOSED MIL-I-25017 LUBRICITY REQUIREMENT.....	240
4.3 REFINEMENT OF RPHPLC METHOD	241
REFERENCES.....	242
APPENDIX A.....	243
APPENDIX B.....	244
APPENDIX C	252
APPENDIX D	257
APPENDIX E.....	323
DETERMINATION OF CORROSION INHIBITOR CONTENT IN AVIATION FUELS.....	355
1.0 INTRODUCTION.....	355
2.0 EXPERIMENTAL.....	357
2.1 MATERIALS	357
2.2 METHOD	357
3.0 RESULTS AND DISCUSSION.....	358
4.0 CONCLUSIONS AND RECOMMENDATIONS	363
REFERENCES.....	364

ASSESSMENT OF THE FIBER OPTIC MODIFIED JET FUEL THERMAL

OXIDATION TESTER	365
1.0 INTRODUCTION AND BACKGROUND	365
2.0 EXPERIMENTAL	366
2.1 EQUIPMENT	366
2.1.1 Jet Fuel Thermal Oxidation Tester (JFTOT)	366
2.1.2 Configuration Of Fiber Optic Modified JFTOT	366
2.2 SOFTWARE	366
2.3 THEORY	367
2.4 TEST APPROACH	367
2.4.1 Test Fuels	367
2.4.2 FOM-JFTOT Test Conditions	367
2.4.3 Summary Of Test Matrix	368
3.0 RESULTS AND DISCUSSION	368
3.1 ESTABLISHMENT OF HARDWARE MAINTENANCE PROCEDURE	368
3.2 SOFTWARE LIMITATIONS AND IMPROVEMENTS	368
3.3 EVALUATION OF NAVY FUELS	369
3.3.1 FOM-JFTOT Data	369
3.3.2 Effect Of Fuel Quality And Temperature On Deposition Rate	370
3.3.3 Repeatability And Reproducibility	370
3.3.4 Activation Energy And Fiber Optic Breakpoint Temperature	370
3.3.5 Arrhenius Plots	371
Trace Interpretation	372
3.4 EVALUATION OF A P&W JP-5	373
4.0 CONCLUSIONS AND RECOMMENDATIONS	374
4.1 STRENGTHS AND POTENTIAL	374
4.2 LIMITATIONS	374
4.3 DEVELOPMENT NEEDS	375
REFERENCES	375

THERMAL OXIDATION CLOSED CELL EXPERIMENTS..... 408

1.0 INTRODUCTION	408
2.0 EXPERIMENTAL	409
2.1 MATERIALS	409
2.2 INSTRUMENTATION	409
2.3 TECHNIQUES	409
2.4 PROCEDURE DEVELOPMENT	410
2.5 DATA ANALYSIS	411
3.0 RESULTS AND DISCUSSION	412
3.1 TOTAL CARBON	412
3.2 TOTAL FILTERABLE CARBON	416
3.3 TOTAL CARBON TO TOTAL FUEL VOLUME RATIO ANALYSIS (TC/TV)	417
3.4 TOTAL WALL CARBON TO TOTAL CARBON RATIO (TWC/TC)	418
4.0 CONCLUSIONS AND RECOMMENDATIONS	427

DESIGN REQUIREMENTS FOR A LABORATORY SCALE THERMAL

OXIDATION STABILITY TEST	428
1.0 INTRODUCTION	428
2.0 STUDY APPROACH	430
2.1 COMPONENTS SUSCEPTIBLE TO THERMAL INSTABILITY	430

2.2 FUEL SYSTEM PARAMETERS	430
2.3 CRITICAL FUEL SYSTEM PARAMETERS	430
2.4 TYPE OF INFORMATION NEEDED BY DESIGNERS AND DEVELOPERS	431
2.5 CAPABILITIES AND LIMITATIONS OF CURRENT TEST DEVICES	431
2.6 COLLATED DESIGN REQUIREMENTS FOR A THERMAL STABILITY TEST	431
2.7 CONCEPTUAL CONFIGURATION FOR A TEST DEVICE	431
3.0 SOURCES USED FOR COMPILING DESIGN REQUIREMENTS	432
3.1 ASTM/CRC ACTIVITIES	432
3.2 UNITED KINGDOM THERMAL STABILITY STEERING GROUP	432
3.3 P&W PROJECT GROUPS	433
3.4 OVERHAUL AND REPAIR DEPOTS	433
3.5 INDUSTRY AND MILITARY SURVEY	433
3.6 LITERATURE SEARCH	433
4.0 STUDY RESULTS	434
4.1 FUEL SYSTEM COMPONENTS AFFECTED BY THERMAL STABILITY	434
4.2 FUEL SYSTEM PARAMETERS	436
4.3 CRITICAL FUEL SYSTEM PARAMETERS	437
4.4 FLIGHT CONDITIONS AFFECTING COMPONENTS	441
4.5 TYPE OF INFORMATION NEEDED BY DESIGNERS AND DEVELOPERS	443
4.6 CAPABILITIES AND LIMITATIONS OF CURRENT TEST DEVICES	447
4.7 THERMAL STABILITY CRITERIA USED IN COMPONENT DESIGN	453
5.0 SUMMARY AND CONCLUSIONS	454
5.1 DESIGN REQUIREMENTS	455
5.2 TRADE-OFFS	457
5.3 FEASIBILITY OF CONSTRUCTING THE CONCEPTUAL TEST DEVICE	457
APPENDIX A	459
HIGH TEMPERATURE FUEL REQUIREMENTS AND PAYOFFS STUDY	464
1.0 INTRODUCTION	464
1.1 OVERVIEW	464
1.2 BACKGROUND	464
1.3 APPROACH	466
2.0 FACTORS INFLUENCING FUEL TEMPERATURE REQUIREMENTS	469
2.1 ADVANCED APPLICATIONS / MISSIONS	469
2.2 AIR FRAME HEAT LOADS	471
2.3 PROPULSION SYSTEM HEAT LOADS	471
3.0 THERMAL MANAGEMENT MODELS	473
3.1 OVERVIEW	473
3.2 ENGINE LUBRICATION SYSTEM	475
3.3 FUEL RECIRCULATION SYSTEM	476
4.0 STUDY RESULTS	478
4.1 FUEL REQUIREMENTS WITH FIXED AIRFRAME HEAT LOADS AND NO RECIRCULATION SYSTEM	478
4.1.1 IHPTET Phase I Advanced Tactical Fighter Mission	480
4.1.2 IHPTET Phase II Air Superiority Fighter (ASF) Mission	481
4.1.3 IHPTET Phase III Air Superiority Fighter (ASF) Mission	483
4.1.4 Other Missions Investigated	484
4.1.5 Summary	486

4.2 PARAMETRICS OF MAXIMUM FUEL TEMPERATURE AND AIRFRAME HEAT LOAD TO ESTABLISH RECIRCULATION SYSTEM REQUIREMENTS	487
4.2.1. Recirculation Requirements	487
4.2.2 Preliminary Sizing of Recirculation System Components	491
4.2.3 Summary	492
5.0 CONCLUSIONS	493
6.0 RECOMMENDATIONS	494

LIST OF FIGURES

Figure

Page

Development of An Improved Method for High-Temperature Vapor Pressure Determinations

1. Chromatographs From ASTM D2887 Analyses	6
2. ASTM D86 Distillation Data for Sample No. DODX 1422-1 (JP-7)	13
3. ASTM D86 Distillation Data for Sample No. 84-POSF-2038 (JP-8)	14
4. ASTM D86 Distillation Data for Sample No. 85-POSF-1758 (Light Pyrolysis Fuel).....	15
5. ASTM D2887 Distillation Data for Sample No. DODX 1422-1 (JP-7).....	16
6. ASTM D2887 Simulated Distillation Data for Sample No. 84-POSF-2038	17
7. ASTM D2887 Simulated Distillation Data for Sample No. 85-POSF-1758 (Light Pyrolysis Fuel)	18
8. Vapor Pressure Data for Sample No. DODX 1422-1 (JP-7)	19
9. Vapor Pressure Data for Sample No. 84-POSF-2038 (JP-8)	20
10. Vapor Pressure Data for Sample No. 85-POSF-1758 (Light Pyrolysis Fuel).....	21
11. Correlation Model for Predicting Vapor Pressure of JP-7 Using ASTM D2887 Data	22
12. Correlation Model for Predicting Vapor Pressure of JP-8 Using ASTM D2287 Data	23
13. Correlation Model for Predicting Vapor Pressure of Light Pyrolysis Fuel Using ASTM D2887 Data	24
14. Correlation Model for Predicting ASTM D86 Results from ASTM D2887 Data for JP-7	25
15. Correlation Model for Predicting ASTM D86 Results from ASTM D2887 Data for JP-8	26
16. Correlation Model for Predicting ASTM D86 from ASTM D2887 Data for Light Pyrolysis Fuel	27
A1. Vapor Pressure Apparatus Reflux Method.....	33

Determination of Fuel Properties and General Analysis

1. Kinematic Viscosity As a Function of Temperature For Candidate High Density JP-8X Fuels.....	41
---	----

Determination of Thermal Conductivity of Aircraft/Missile Fuels

1. Thermal Conductivity Data Fit for Toluene	48
2. Comparison of Measured Toluene Thermal Conductivity to Literature Values	49
3. Thermal Conductivity Data Fit for Dimethyl Phthalate	50
4. Comparison of Measured Dimethyl Phthalate Thermal Conductivity to Literature Values	51
5. Thermal Conductivity Data Fit for JP-10	52
6. Thermal Conductivity Data Fit for JP-8	53
7. Thermal Conductivity Data Fit for JP-4	54
8. Thermal Conductivity Data Fit for JP-7	55
9. Thermal Conductivity Data Fit for RJ6	56
10. Thermal Conductivity Data Fit for JP-TS	57
11. Comparison of Thermal Conductivity and Thermal Coefficients (slope) For All Fuel Types	58

Characterization of Candidate High Density Fuels

1. Specific Gravity As a Function of Temperature For Combustion Test Fuels	79
2. Kinematic Viscosity As a Function of Temperature For Combustion Test Fuels	80
3. Density A a Function of Temperature For Combustion Test Fuels	81
4. Dielectric Constant As a Function of Temperature For Combustion Test Fuels.....	82
5. True Vapor Pressure As a Function of Temperature For Combustion Test Fuels.....	83
6. Surface Tension As a Function of Temperature For Combustion Test Fuels	84
7. Thermal Conductivity As a Function of Temperature For Combustion Test Fuels	85

Characterization of Experimental Coal Tars

1. Simplified flow diagram of Great Plains Gasification Associates process	89
2. Low voltage mass spectrometry system with special inlet for low volatile liquids and/or solids.....	92
3. Schematic of capillary sample introduction system.....	93

4. Low voltage mass spectra of main product streams obtained from ANG coal gasification plant	100
5. Score plot of discriminant functions obtained on set of 24 low voltage mass spectra ANG tar oil ...	101
6. Low voltage mass spectra of the light (<200°C) and heavy (>200°C) fractions of tar oil	102
7. Fourier transform infrared (FTIR) spectra of the light and heavy fractions of tar oil	103
8. High resolution ¹ H-NMR spectra of light and heavy fractions of tar oil	104
9. Low voltage mass spectra of four ANG light tar oil fractions	107
10. Low voltage mass spectra of four heavy tar oil fractions	108
11. Infrared and ¹ H-NMR spectra of crude phenols (stream c) obtained from ANG gasification plant....	110
12. Score plot of two factors obtained on low voltage mass spectra of weathered ANG tar oil	112
13. Factor spectrum of the weathering axis showing the effect of oxygen exposure on ANG tar oil	113
14. Score plot of the first three functions obtained on low voltage mass spectra of stored ANG tar oil ..	114
15. Discriminate spectrum of the time axis showing the effect of storage time on ANG tar oil	115

Purification of RJ-5 and JP-10 Fuels For Use As Standards

1. Gas Chromatogram of Distilled JP-10	130
2. Gas Chromatogram of Distilled JP-10	131

JP-10 Fuel Discoloration Investigation

1. Apparatus for Dynamic JP-10 Tests	138
2a. Low voltage mass spectrometry system	140
2b. Detailed schematic of capillary sample introduction system	140
3. Gas Chromatogram Of Sample V39	143
4. Gas Chromatograms Showing The Four Major Components Of JP-10	144
5a. Low Voltage Mass Spectra Of V39 And Two Control Samples Showing Bulk Compositions	145
5b. Low voltage mass spectra of V39 and two control samples showing trace components	146
6. Gas Chromatogram Sample V39, Showing Four Compound Types Present As Trace Components ..	148
7. GC/MS Of The Three Control Samples A, B, And C Showing Trace Components	150
8. Low Voltage Mass Spectra Of Three Control Samples Of JP-10 Using Curie Point Wires	152
9. Low Voltage Mass Spectra Of Control Sample S4	153
10. Low Voltage MS Polar LC Fraction And Visible Gum Sample From Laboratory Weathering Test ..	155
11. Low Voltage Mass Spectra Of Discolored Field Samples And Extracted Fuel Pump Ring Sample ..	156
12. Fourier Transform Infrared Spectra Of Samples V39 And Control	157
13. Fourier Transform Infrared Spectrum Of V39 With Superimposed Spectrum Of Dioctyl Phthalate ..	158
14. Photograph Of A Clean Armature And The Armature Coated With Gum From Sample S3	159
15. Fourier Transform Infrared Spectra Of Sample S3 And The Gum Precipitate From S3	160

Evaluation of the Shell Premixed Burner

1. Shell Premixed Burner	171
2. Repeatability of Shell Thornton Measurements	175
3. Repeatability of P&W Measurements	176
4. Repeatability of the Naval Research Laboratory Measurements	177
5. Reproducibility Between Laboratories Using the OSD 50-5 Detector	178
6. Reproducibility Between Laboratories Using the OSD 50-E Eye Response Detector	179

Standardization of Lubricity Test

1. Falex Ring and Mandrel Assembly	184
2. Wear Scar Interpretation	196
3. Nominal Falex Ring Lubricity Values for Typical Jet Fuels	204

Evaluation of Corrosion Inhibitors As Lubricity Improvers

1. Typical BOCLE Wear Scars Produced by Jet Fuels	213
---	-----

2. InterAv Ball-On-Cylinder Lubricity Evaluator	214
3. BOCLE Load Correlation	215
4. Varian High Performance Liquid Chromatograph	217
5. Effect of IPC-4410 in Clay Treated JP-4	220
6. Effect of Tolad 249 in Clay Treated JP-4	221
7. Effect of Temperature on PRI-19 in Clay Treated JP-4	224
8. Effect of Temperature on Hitec E-580 in Isopar M	225
9. Air Force Corrosion Inhibitor Usage For JP-4 in FY85	230
10. Chromatogram of DCI-4A Using Preliminary RPHPLC Method	232
11. Carboxymethyl Column Separation of Dimer, Trimer and Monomer Linoleic Acids in Additive Free Sun Oil JP-4	235
12. Chromatogram of Resolved Monomer Acid Peak	235
13. Effect of Storage on CI Concentration: Stored 87 POSF-2605 Sample Versus New Blend	236
14. Effect of Connecting Tubing I.D. on Peak Broadening	237
D1. Effect of Apollo PRI-19 in Isopar M	259
D2. Effect of HITEC E-580 in Isopar M	260
D3. Effect of DCI-4A in Isopar M	261
D4. Effect of DCI-6A in Isopar M	262
D5. Effect of LUBRIZOL 541 in Isopar M	263
D6. Effect of NALCO 5403 in Isopar M	264
D7. Effect of TOLAD 245 in Isopar M	265
D8. Effect of UNICOR -J in Isopar	266
D9. Effect of IPC-4410 in Isopar M	267
D10. Effect of MOBILAD F-800 in Isopar M	268
D11. Effect of NALCO 5405 in Isopar M	269
D12. Effect of TOLAD 249 in Isopar M	270
D13. Effect of P-3305 in Isopar M	271
D14. Effect of IPC-4445 in Isopar M	272
D15. Effect of WELCHEM 91120 in Isopar M	273
D16. Effect of NUCHEM PCI-105 in Isopar M	274
D17. Effect of Apollo PRI-19 in Clay Treated JP-4	275
D18. Effect of HITEC E-580 in Clay Treated JP-4	276
D19. Effect of DCI-4A in Clay Treated JP-4	277
D20. Effect of DCI-6A in Clay Treated JP-4	278
D21. Effect of LUBRIZOL 541 in Clay Treated JP-4	279
D22. Effect of NALCO 5403 in Clay Treated JP-4	280
D23. Effect of TOLAD 245 in Clay Treated JP-4	281
D24. Effect of UNICOR-J in Clay Treated JP-4	282
D25. Effect of IPC-4410 in Clay Treated JP-4	283
D26. Effect of MOBILAD F-800 in Clay Treated JP-4	284
D27. Effect of NALCO-5405 in Clay Treated JP-4	285
D28. Effect of TOLAD 249 in Clay Treated JP-4	286
D29. Effect of P-3305 in Clay Treated JP-4	287
D30. Effect of IPC-4445 in Clay Treated JP-4	288
D31. Effect of WELCHEM 91120 in Clay Treated JP-4	289
D32. Effect of NUCHEM PCI-105 in Clay Treated JP-4	290
D33. Effect of Apollo PRI-19 in Clay Treated JP-8	291
D34. Effect of HITEC E-580 in Clay Treated JP-8	292
D35. Effect of DCI-4A in Clay Treated JP-8	293
D36. Effect of DCI-6A in Clay Treated JP-8	294
D37. Effect of LUBRIZOL in Clay Treated JP-8	295
D38. Effect of NALCO 5403 in Clay Treated JP-8	296

D39. Effect of TOLAD 245 in Clay Treated JP-8	297
D40. Effect of UNICOR-J in Clay Treated JP-8	298
D41. Effect of IPC 4410 in Clay Treated JP-8	299
D42. Effect of MOBILAD F-800 in Clay Treated JP-8	300
D43. Effect of NALCO 5405 in Clay Treated JP-8	301
D44. Effect of TOLAD 249 in Clay Treated JP-8	302
D45. Effect of P-3305 in Clay Treated JP-8	303
D46. Effect of IPR-4445 in Clay Treated JP-8	304
D47. Effect of WELCHEM 91120 in Clay Treated JP-8	305
D48. Effect of NUCHEM in Clay Treated JP-8	306
D49. Effect of Apollo PRI-19 in Clay Treated JP-8	307
D50. Effect of HITEC E-580 in Clay Treated JP-5	308
D51. Effect of DCI-4A in Clay Treated JP-5	309
D52. Effect of DCI-6A in Clay Treated JP-5	310
D53. Effect of LUBRIZOL 541 in Clay Treated JP-5	311
D54. Effect of NALCO 5403 in Clay Treated JP-5	312
D55. Effect of TOLAD 245 in Clay Treated JP-5	313
D56. Effect of UNICOR-J in Clay Treated JP-5	314
D57. Effect of IPC-4410 in Clay Treated JP-5	315
D58. Effect of MOBILAD F-800 in Clay Treated JP-5	316
D59. Effect of NALCO 5405 in Clay Treated JP-5	317
D60. Effect of TOLAD 249 in Clay Treated JP-5	318
D61. Effect of P-3305 in Clay Treated JP-5	319
D62. Effect of IPC-4445 in Clay Treated JP-5	320
D63. Effect of WELCHEM 91120 in Clay Treated JP-5	321
D64. Effect of NUCHEM PCI-105 in Clay Treated JP-5	322
F-1. RPHPLC Chromatogram of DCI-4A	338
F-2. RPHPLC Chromatogram of DCI-6A	339
F-3. RPHPLC Chromatogram of Hitec E-580	340
F-4. RPHPLC Chromatogram of IPC 4410	341
F-5. RPHPLC Chromatogram of IPC 4445	342
F-6. RPHPLC Chromatogram of Nalco 5403	343
F-7. RPHPLC Chromatogram of Nalco 5405	344
F-8. RPHPLC Chromatogram of Nuchem PCI 105	345
F-9. RPHPLC Chromatogram of PRI-19	346
F-10. RPHPLC Chromatogram of Tolad 245	347
F-11. RPHPLC Chromatogram of Tolad 249	348
F-12. RPHPLC Chromatogram of Unicor J	349
F-13. RPHPLC Chromatogram of Lubrizol 541	350
F-14. RPHPLC Chromatogram of Welchem 91120	351
F-15. RPHPLC Chromatogram of Mobilad F800	352
F-16. RPHPLC Chromatogram of Clay Treated JP-4 and Additive Free JP-4	353
F-17. RPHPLC Chromatogram of Trimer, Dimer, and Monomer Linoleic Acids	354

Determination of Corrosion Inhibitor Content In Aviation Fuels

1. Composite Calibration Chromatograms of DLA in Isopar M	360
2. Composite Calibration Chromatograms of DLA in Additive Free JP-4	360
3. Linear Regression Analysis of Data From Figure 1	361
4. Linear Regression Analysis of Data From Figure 2	361
5. RPHPLC Chromatograms of (a) DCI-4A, (b) Nalco, (c) Tolad 245 and (d) Tolad 249	362

Assessment of the Fiber Optic Modified Jet Fuel Thermal Oxidation Tester

1. Jet Fuel Thermal Oxidation Tester.....	376
2. Configuration of Fiber Optic JFTOT	377
3. Cross Section of FOM-JFTOT Heater Tube.....	378
4. Real Time CRT Display For Fiber Optic JFTOT	380
5. Fiber Optic JFTOT Theory	381
6. Effect of Film Thickness On Reflected Light.....	382
7. Linearity of Deposit Rate	383
8. Thickness vs Tube Position for NAPC FF-3.....	384
9. Fiber Optic Break Point Temperature	391
10. Arrhenius Plot for FF-3 JP-5.....	393
11. Arrhenius Plot for FF-8 JP-5.....	394
12. Arrhenius Plot for NAPC 17 (DFM)	395
13. Arrhenius Plot for FF-3 JP-5 - Repeatability of Measurements	396
14. Arrhenius Plot for NAPC 17 (DFM) - All Runs	397
15. Repeatability of Fiber Optic Break Point Derived From Arrhenius Plot.....	398
16. Fiber Optic Break Point Derived from Arrhenius Plot For Three Fuels	399
17. Real Time Display of Interferogram for NAPC FF-3 at 550°F Test Temperature.....	400
18. Real Time Display of Interferogram for NAPC FF-3 at 500°F Test Temperature.....	401
19. Real Time Display of Interferogram for NAPC FF-3 at 450°F Test Temperature.....	402
20. Real Time Display of Interferogram for NAPC FF-8 at 550°F Test Temperature.....	403
21. Real Time Display of Interferogram for NAPC FF-8 at 500°F Test Temperature.....	404
22. Real Time Display of Interferogram for P&W JP-5 at 550°F Test Temperature.....	405
23. Real Time Display of Interferogram for P&W JP-5 at 575°F Test Temperature.....	406
24. FOM-JFTOT Heater Tube Deposits.....	407

Thermal Oxidation Closed Cell Experiments

1. Arrhenius Plot of 3/8 Stainless Steel Total Carbon	419
2. Arrhenius Plot of 3/8 Aluminum Total Carbon	420
3. Arrhenius Plot of 3/16 Stainless Steel Total Carbon.....	421
4. Arrhenius Plot of 3/16 Aluminum Total Carbon	422
5. Arrhenius Plot of Composite TOCC	423
6. Normalized Total Carbon Comparison of 3/8	424
7. Normalized Total Carbon Comparison of 3/8	425
8. Arrhenius Plot of Filterable Carbon	426

High Temperature Fuel Requirements and Payoffs Study

1.2-1. P&W IHPTET Turbofan/Turbojet Goals	465
1.2-2. Cooling Capacity of Fuels Defines Thermal Barrier at High Speed	466
1.3-1. High Temperature Fuel Requirements and Payoffs Study Approach.....	467
2.1-1. Air Superiority (Mach 2.5) Mission Profile.....	470
2.1-2. Lightweight Fighter (Mach 1.5) Mission Profile	470
2.2-1. Increasing Heat Sink Demand On Fuel From Airframe Heat Loads (Per Engine)	471
3.1-1. Fuel System Model Used in The High Temperature Fuel Requirements and Payoffs Study	473
3.1-2. Fuel System Model Baseline - Current Airframe/Engine Fuel System Model	475
3.2-1. Typical Hot Tank Lubrication System	476
4.1-1. HPTET Phase I ATF Mission - Heat Load vs. Heat Sink	480
4.1-2. IHPTET Phase I ATF Mission - Fuel and Oil Temperatures Without Fuel Recirculation.....	481
4.1-3. IHPTET Phase II ASF Mission - Heat Load vs. Heat Sink.....	482
4.1-4. IHPTET Phase II ASF Mission - Fuel and Oil Temperature Without Fuel Recirculation	482
4.1-5. IHPTET Phase III LWF Mission - Heat Load vs. Heat Sink	483

4.1-6. IHPTET Phase III LWF Mission - Fuel and Oil Temperature Without Fuel Recirculation.....	484
4.1-7. Maximum Fuel Temperature for Idle Descent Flight Condition Without Fuel Recirculation.....	485
4.1-8. Maximum Fuel Temperature for Ground Idle Flight Condition Without Fuel Recirculation	485
4.2-1. IHPTET Phase I Fuel Recirculation Requirements For Advanced Tactical Fighter Mission.....	487
4.2-2. IHPTET Phase II Fuel Recirculation Requirements For Advanced Navy Fighter Mission.....	488
4.2-3. Fuel Recirculation Requirements For IHPTET Phase II Air Superiority Fighter Mission	488
4.2-4. Fuel Recirculation Requirements For IHPTET Phase II Lightweight Fighter Mission.....	489
4.2-5. IHPTET Phase III Fuel Recirculation Requirements for Air Superiority Fighter Mission.....	489
4.2-6. IHPTET Phase III Fuel Recirculation Requirements for Lightweight Fighter Mission	490
4.2-7. IHPTET Phase II ASF Heat Exchanger Wgt. Payoff-Based on Reduced Recirc. Requirements ...	492

LIST OF TABLES

<i>Table</i>	<i>Page</i>
Development of an Improved Method For High-Temperature Vapor Pressure Determinations	
ASTM D86 Distillation Data for AF Samples.....	4
ASTM D2887 Simulated Distillation Data For Sample No. DODX 1422-1	7
ASTM D2887 Simulated Distillation Data For Sample No. 84-POSF-2038	8
ASTM D2887 Simulated Distillation Data For Sample No. 85-POSF-1758	9
Vapor Pressure Data For Sample No. DODX 1422-1 (JP-7).....	9
Vapor Pressure Data For Sample No. 84-POSF-2038 (JP-8)	10
Vapor Pressure Data For Sample No.85-POSF-1758.....	11
Determination of Fuel Properties and General Analysis	
Hydrocarbon Type Analyses Of Candidate High Density	38
Heat Of Combustion For Candidate High Density Fuels Produced From Light Cycle Gas Oil.....	39
Kinematic Viscosity For Candidate High Density Fuels Produced From Light Cycle Gas Oil.....	39
Simulated Distillation For AF Foreign Division Field Samples.....	40
Determination of Thermal Conductivity of Aircraft/Missile Fuels	
Measured Thermal Conductivity, W/M/K.....	45
Two Way Analysis Of Variance To Determine If Fuel Type Affects Thermal Conductivity	46
Calculated Thermal Conductivity, W/M/K*	47
Characterization of Candidate High Density Fuels	
Hydrocarbon Types of Jet Fuel Samples by ASTM D2789 and ASTM D1319.....	69
Simulated Distillation of Various Combustion Test Fuels.....	70
Heats of Combustion For Various Combustion Test Fuels	71
Specific Heat As A Function of Temperature	71
Kinematic Viscosity As A Function of Temperature.....	72
Density As A Function of Temperature	72
Dielectric Constant AS a Function of Temperature.....	73
True Vapor Pressure As A Function of Temperature.....	73
Surface Tension AS a Function of Temperature.....	74
Thermal Conductivity As a Function of Temperature	74
Best Fit Line Equations For Measured Specific Heat and Viscosity	75
Best Fit Line Equations For Measured Density and Dielectric Constant	76
Best Fit Line Equations For Measured Vapor Pressure and Surface Tension.....	77
Best Fit Line Equations For Measured Thermal Conductivity.....	78
Characterization of Experimental Coal Tars	
Infrared And Proton Nmr Spectroscopic Data From The Light And Heavy Tar Oil Fractions	105
Elemental Analysis And LC + MS Compound Type Analysis Tar Oil Light And Heavy Distillate Fractions	106
Liquid Products Evaluation	109
Spectroscopic Characterization Of The Crude Phenol Stream.....	111
RJ-7 High Density Fuel Development	
Properties Of Cotrimers Of CPD And MCPD	120
Cotrimer And JP-10 Blend Data	120
Cotrimer And JP-10 Blend Data	121
Properties Of Perhydro And Dihydro Cpd/Indene Adducts With CPD/MCPD Cotrimer And JP-10	122

Properties Of Ternary Blends JP-10, CPD Trimer And Dihydro Cpd/Indene	123
Prototype Fuel Blends	124
Purification of RJ-5 and JP-10 Fuels For Use As Standards	
JP-10 Purification By Vacuum Distillation	128
RJ-5 Purification By Vacuum Distillation.....	129
Alternate High Flash Point Calibration Fluid	
High Flash Point Replacement Calibration Fluid Candidates	133
Properties Of Dodecane And Dioctryphthalate	134
JP-10 Fuel Discolorization Investigation	
List Of Samples	137
Integrated Area Values Of 4 Bulk Component (Total = 100%)	143
Minor GC/MS Peaks Of Field Sample And Control Samples With Proposed Structure Identities	149
Evaluation of The Shell Premixed Burner	
Shell Thornton Premixed Burner Test Fuels	172
Premixed Burner Numbers For Shell Thornton Fuel Samples	174
Standardization of Lubricity Test	
BOCLE Data For Candidate Reference Fluids	187
Differentiation Between Groups Of Cylinders	188
Precision of candidate reference fluids	189
Effect Of Cylinder Surface Finish--Part I.....	190
Verification Of Cylinder Surface Finish	191
Effect Of Cylinder Surface Finish--Part II	192
Effect Of Cylinder Surface Finish--Part III	194
Preliminary Falex Ring Evaluation.....	195
Reproducibility Between Falex Lots.....	197
Reproducibility Between Falex Lots (Continued)	198
Falex Ring Round Robin Results For JP-4	200
Falex Ring Round Robin Results For Isopar M.....	200
Falex Ring Round Robin Results For Clay Treated Shale JP-4	201
Falex Ring Lubricity Values For Typical Jet Fuels	203
Test Ball Source Evaluation	205
Skf Test Ball Composition.....	205
Evaluation of Corrosion Inhibitors As Lubricity Improvers	
Effective Corrosion Inhibitor Concentrations For Lubricity Improvement	222
Grouping Of Corrosion Inhibitor Performance.....	223
Effect Of Redefining Relative Effective Concentration In JP-4	229
Column Wash Gradient Program	237
Linear Regression Statistics For CI Calibration Standards	238
Effect Of Corrosion Inhibitors In Isopar M	253
Effect Of Corrosion Inhibitors In Clay Treated JP-4	254
Effect Of Corrosion Inhibitors In Clay Treated JP-8	255
Effect Of Corrosion Inhibitors In Clay Treated JP-5	256
Assessment of The Fiber Optic Modified Jet Fuel Thermal Oxidation Tester	
Temperature Profile Of Aluminum Tubes Corresponding To FOM-JFTOT Probes.....	379
FF-3 JP-5 (470°F BP) Test Data - All Runs	385
NAPC 17 DFM (470°F BP) Test Data - All Runs	386

FF-8 JP-5 (500°F BP) Test Data - All Runs	387
Summary Of Fiber Optic JFTOT Test Results	388
Repeatability Of Fiber Optic JFTOT Test Results.....	389
Reproducibility Of Fiber Optic JFTOT Test Results	390
Need For Correlating Fiber Optic And JFTOT Break Point	392

Thermal Oxidation Closed Cell Experiments

Data Set 1- Normalized Values For Total Filterable Carbon, Total Wall Carbon, & Total Carbon.....	414
Data Set 2- Normalized And Averaged Carbon Values.....	415
Data Sets 1 & 2 Statistical Analysis And Activation Energies (Ea) For Total Carbon	415
Statistical Analysis And Activation Energies For Total Filterable Carbon	416
Total Carbon And Total Carbon To Total Volume Ratios.....	417
Total Carbon And Total Wall Carbon To Total Carbon Ratios	418

Design Requirements For a Laboratory Scale Thermal Oxidation Stability Test

Typical Current Engine Thermal Management System Maximum Fuel Temperatures.....	439
Near-Term Advanced Engine Thermal Management System Fuel Temperatures.....	439
Near-Term Advanced Engine Thermal Management System Component Residence Times	440
Hot Section For Near-Term Advanced Engine Over Entire Envelope	440
Hot Section For Near-Term Advanced Engine At Critical Flight Points	441

High Temperature Fuel Requirements and Payoffs Study

P&W High Temperature Fluid Development Goals.....	465
Advanced Missions Selected For High Temperature Study.....	469
Estimated Fuel Recirculation System Component Weights.....	477
Summary Of Fuel Heat Loads (Btu/Min) For The Supercruise Flight Condition.....	479
Maximum Fuel Temperatures Relative To IHPTET Fluid Development Goals.....	486
Summary Of The Recirculation Flow Requirements Parametric Study	490

DEVELOPMENT OF AN IMPROVED METHOD FOR HIGH-TEMPERATURE VAPOR PRESSURE DETERMINATIONS

Period of Performance

8 July 1985 through 8 October 1985

Reference

Task Order No. 1, Topical Report No. 1, December 1985, FR-19032-1, W.H. Edwards, R.J. Meehan, P.A. Warner

Abstract

Mathematical models were developed to describe the correlation between ASTM D86 distillation data and ASTM D2887 simulated distillation data for three fuel samples: (1) JP-7, (2) JP-8, and (3) an experimental high-density fuel. In addition, a mathematical model was developed describing the correlation between simulated distillation data and vapor pressure data for these fuel samples. Recommendations for future studies to test and modify the models for general use in predicting ASTM D86 distillation data and vapor pressure from simulated distillation data are discussed.

SECTION 1.0

INTRODUCTION

1.1 BACKGROUND

During the 1960's, P&W and WRDC/POSF were instrumental in developing several low volatility fuels such as PWA 535, now identified as JP-7 (MIL-T-38219). This fuel was needed for high-Mach number, high-altitude aircraft to provide the required high thermal stability, low smoke and low volatility. Aircraft flying at high altitudes and high speeds subject the fuel to elevated temperatures and reduced pressure. Concerns regarding the vapor pressure of the fuel under these conditions led to the cooperative development of the vapor reflux method (VRM) for determining true vapor pressure of low-volatility fuels at elevated temperatures (Appendix C of MIL-T-38219A).

Vapor pressure is one measure of the volatility characteristics of a fuel. Fuels typically are used in many types of engines with large variations in operating conditions and operating temperatures. Fuels which have high vapor pressures may vaporize too quickly in a fuel system, resulting in vapor lock and reduced fuel flow. Fuels which have low-vapor pressure may not readily vaporize and could cause poor ground start or reduced ability for at-altitude relight.

1.2 OVERVIEW

There are several methods available for determining the true vapor pressure of complex hydrocarbon mixtures, including both empirical correlation techniques and experimental techniques. The empirical correlation techniques are more commonly used. For example, Appendix A2 of ASTM D3710, entitled "A Technique for Simulated Distillation Using Gas Chromatography," provides equations for calculating Reid Vapor Pressure and predicting ASTM D86 distillation curves from the simulated distillation (SIMDIST) data generated. However, ASTM D3710 and other techniques such as ASTM D323 are not directly applicable to low volatility JP-7, JP-8, and experimental high-density fuels. ASTM D86 distillation data and ASTM D93 flash point temperatures are currently used to measure volatility of fuels such as JP-7. Vapor pressure for JP-7 has been predicted at elevated temperatures using ASTM D86

distillation data (20% recovered point) in conjunction with a nomograph, or determined directly by the VRM described in Appendix C of MIL-T-38219A. A method is needed for determining the high-temperature vapor pressures of all low volatility fuels.

Recently, SIMDIST techniques have demonstrated excellent potential for assessing the volatility characteristics of less volatile gas turbine fuels. The gas chromatographic procedure defined by ASTM D2887 separates components of low volatility fuels into a wider spectrum of hydrocarbons than does ASTM D86. This separation is accomplished in a manner similar to ASTM D2892, a 15-plate distillation column apparatus. For this reason, ASTM D2887 is a more precise method than ASTM D86, while offering greater ease of operation than ASTM D2892. However, because the method described in ASTM D86 has been the industry standard for many years, a good correlation formula was needed to relate ASTM D86 and ASTM D2887 distillation data. In addition, since the VRM is very tedious and labor intensive relative to SIMDIST, a method for predicting vapor pressure from SIMDIST data was needed.

Based on these considerations, the technical work described in the following sections was directed toward developing an empirical correlation technique, similar to that included in Appendix A2 of ASTM D3710, for predicting vapor pressure of low-volatility fuels from distillation data performed using ASTM D2887. Further, a means for predicting ASTM D86 distillation data from ASTM D2887 SIMDIST data is discussed.

SECTION 2.0

EXPERIMENTAL

2.1 DISTILLATION AND VAPOR PRESSURE METHODS

Distillations using ASTM D86, "Distillation of Petroleum Products" and ASTM D2887, "Boiling Range Distribution of Petroleum Fractions By Gas Chromatography," were used to obtain distillation data for the three fuels supplied by the Air Force Program Monitor.

2.1.1 ASTM D2887 Simulated Distillation

ASTM D2887 analyses were conducted using an Antek Model Series 300 gas chromatograph with a flame ionization detector. Data acquisition and reduction were done with a Nelson Analytical 3000 Series Chromatography Data System with SIMDIST software for ASTM D2887 on an IBM PC AT mini-computer. The column was stainless steel, 3.0-meters long by 0.318-cm outside diameter (OD) and 0.174-cm inside diameter (ID). The solid support packing material was Chromasorb WHP, 80 to 100 mesh, with 10% SE-30 liquid phase. The carrier gas was helium at a flow rate of 30 cc/min. Injector and detector temperatures were 350°C (662°F). The column temperature was ramped at 8°C/minute, from an initial temperature of 70°C (158°F) to an end temperature of 280°C (536°F). The calibration standard consisted of the following: 8.9% hexane, 13.5% octene, 11.6% decane, 10.8% dodecane, 11.6% tetradecane, 13.5% pentadecane, 16.6% hexadecane, and 13.5% heptadecane (percent by weight). The resolution standard consisted of 1.0% hexadecane, and 1.0% octadecane in decane by weight. The calibration and resolution standards were analyzed frequently to ensure that ASTM D2887 resolution (R) and repeatability criteria were met. Resolution values averaged 5.1 with ASTM D2887 requiring R to be between 3.0 and 8.0.

2.1.2 ASTM D86 Distributions

ASTM D86 analyses were conducted with temperatures recorded for the initial boiling point, for every 5.0% recovered from 5 to 95%, and for the end point. No emergent stem corrections were used consistent with ASTM Committee D2 recommendations.

2.1.3 Vapor Pressure Determinations

The VRM, described in Appendix C of MIL-T-38219A, was used to determine vapor pressure as a function of temperature for the three fuels supplied by the Air Force Program Monitor. The basic test procedure was followed; however, the following minor modifications were made to upgrade the test apparatus.

1. The mercury manometer system was replaced by a pressure transducer with a range of 0 to 15 psia and a sensitivity of 0.01 psia. This transducer, complete with an Anadex digital display, eliminated the need for cumbersome mercury-filled pressure readout manometers.
2. The mercury thermometers were replaced by two calibrated chromel/alumel thermocouples using a Doric Model 412A digital display for temperature observations of the bulk fuel and refluxing fuel vapors.
3. A Whitey micrometer valve was used in the vacuum bleed system to provide trouble-free fine tuning of the system pressure.
4. A Nes-Lab CFT-33 Coolflow Refrigerated Circulator was used to maintain the condenser water at 15°C (60°F). This modification was made to preclude variations in the reflux height caused by changes in temperature in the condenser cooling water.

To ensure valid statistical analysis of vapor reflux data, each test fuel was evaluated in duplicate. Vapor pressures were determined at a minimum of 10 temperatures between 1.5 psia (10% of the range of pressure transducer) and atmospheric pressure. Vapor pressures below 1.5 psia and above atmospheric pressure were extrapolated from the linear function expressing the logarithm of vapor pressure versus the reciprocal of absolute temperature. Appendix A provides a detailed description of the improved VRM used in this investigation.

SECTION 3.0

RESULTS AND DISCUSSION

3.1 DISTILLATIONS AND VAPOR PRESSURE DETERMINATIONS

ASTM distillations were conducted to provide experimental data for correlation of ASTM D2887 to ASTM D86 and vapor pressure data from the VRM.

3.1.1 ASTM D86 Distillation

ASTM D86 analyses of sample numbers 84-POSF-2038 (JP-8) and DODX 1422-1 (JP-7) produced expected data. These data are presented in Table 1.

TABLE 1
ASTM D86 DISTILLATION DATA

Temperature (°C)						
°	<u>84-POSF-2038</u>		<u>86-POSF-1758</u>		<u>DODX 1422-1</u>	
Recovered	Run 1	Run 2	Run 1	Run 2	Run 1	Run 2
IBP	145.6	146.1	188.3	189.4	198.9	197.8
5	162.8	159.4	202.2	205.0	205.0	203.9
10	170.0	167.2	206.1	208.3	206.1	205.6
16	174.4	172.2	208.9	210.6	206.7	206.7
20	178.3	176.1	210.6	212.2	207.8	207.2
25	181.7	180.0	212.8	214.4	208.3	207.8
30	185.0	182.8	214.4	216.1	208.9	208.3
36	187.8	186.1	215.6	217.8	209.4	208.9
40	190.6	188.3	217.2	219.4	210.0	210.0
45	193.3	191.7	218.9	221.1	211.1	210.6
50	196.7	194.4	220.6	222.8	211.7	211.7
55	199.4	197.2	222.8	225.0	212.8	212.2
60	202.2	200.6	225.0	227.2	213.9	213.9
65	205.6	203.3	227.2	229.4	215.0	214.4
70	208.9	207.8	230.6	232.2	216.7	216.1
75	213.3	211.7	233.9	236.1	218.3	218.3
80	217.8	216.7	238.9	240.6	221.1	220.6
85	223.3	221.1	244.4	246.1	224.4	223.9
90	230.0	227.8	252.2	253.9	230.0	228.9
95	241.1	237.2	270.0	270.6	241.7	238.9
FBP	255.6	255.0	290.0	298.3	257.8	256.7

Sample number 85-POSF-1758 (light pyrolysis fuel) was found to have a distillation range of 105°C (190°F) similar to the JP-8 type fuel, but was higher boiling, similar to a JP-7 fuel. Additionally, the light pyrolysis fuel had an initial boiling point (IBP) lower than the JP-7 sample and had a considerably higher final boiling point (FBP).

3.1.2 ASTM D2887 Simulated Distillation

Simulated distillations by ASTM D2887 of the three samples were performed once each day for five consecutive days. Simulated distillation analyses of samples 84-POSF-2038 and DODX 1422-1 produced expected results. However, sample 85-POSF-1758, while easily chromatographed under the conditions given in Section 2.0, did provide an interesting chromatogram when compared to the other two samples. The existence of low boiling material at 78°C (172.4°F), although less than approximately 0.1 weight percent, was not expected for this sample. Figure 1 (a, b, and c) presents typical chromatograms for the three fuel samples for comparison. Tables 2, 3, and 4 present the raw data for the five separate simulated distillation runs for each fuel.

3.1.3 Vapor Pressure Determinations

Vapor pressure data for the three fuels were obtained using the VRM described in Section 2.0 and Appendix A of this report. Tables 5, 6, and 7 list specific data for the three fuels.

As shown in Tables 6 and 7, the vapor temperature differed from the liquid temperature by more than the specified 4.0°C for fuel samples 84-POSF-2038 and 85-POSF-1758. Both fuels have at least 100°C (180°F) boiling ranges as compared to JP-7's 106°C (190°F) boiling range. These facts led to concerns

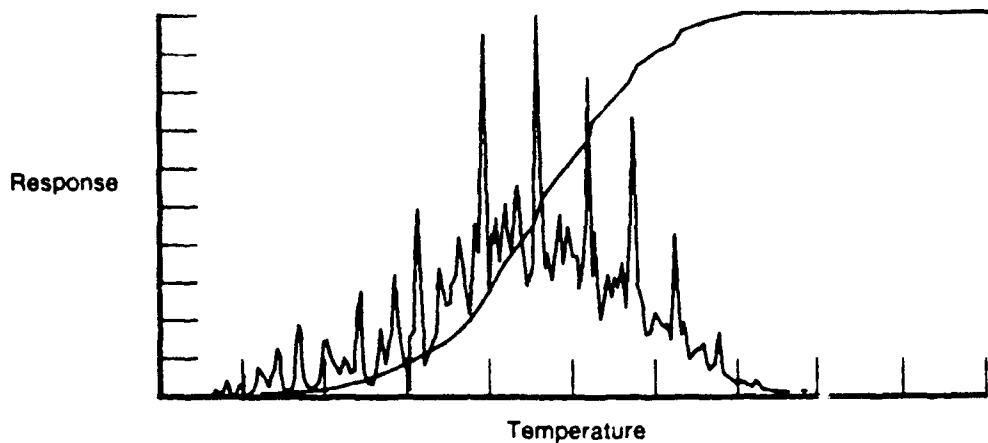
over loss of light ends during the degassing procedure and the selection of which temperature to use for vapor pressure determinations: the vapor temperature, the liquid temperature, or the average temperature. These questions were addressed through a model compound study.

Reagent grade 2,2,4-trimethylpentane (isooctane) and n-dodecane were chosen as model compounds because of their physical properties and the availability of accurate data in the literature. Two experiments were conducted using isooctane, dodecane, and a 50-volume percent mixture of the two. First, VRM data were obtained for the three test fluids as discussed in Appendix A, with no pretreatment of the test fluids. Second, a fresh aliquot of each fuel was chilled to -50°C , transferred to the VRM apparatus, and vacuum applied to degas as the sample thawed. Vapor reflux method data were then obtained as before.

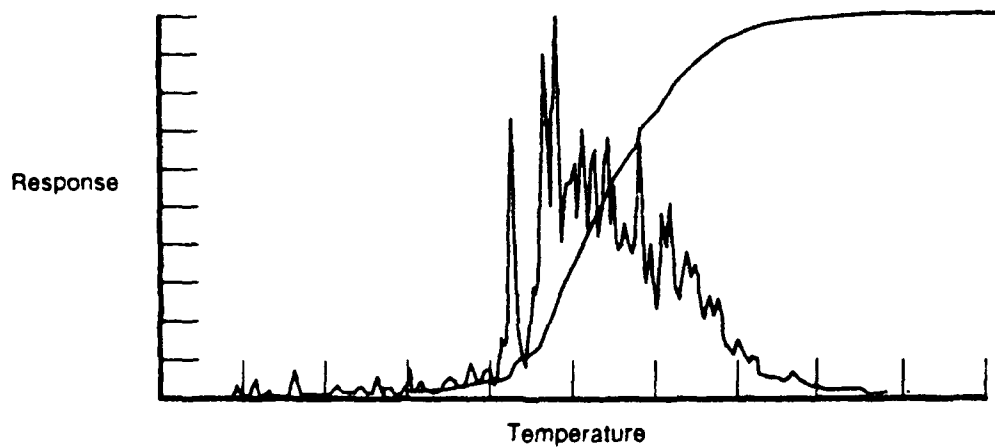
Using linear regression analysis, vapor pressures were calculated for liquid temperature, vapor temperature, and the average temperature. A comparison of these results to theoretical vapor pressure values obtained from the literature and calculated using Antoine's and Raoult's equations was then made.

Comparing chilled and degassed pure compound vapor pressures to those of the room temperature degassed vapor pressures indicated less than 1% absolute difference over the range of 50 to 300°C (122 to 572°F), well within the experimental error. In addition, the vapor and liquid temperature varied by less than 1°C throughout the series of vapor pressure determinations. This is consistent with the design capabilities of the VRM apparatus for pure compounds and narrow boiling mixtures.

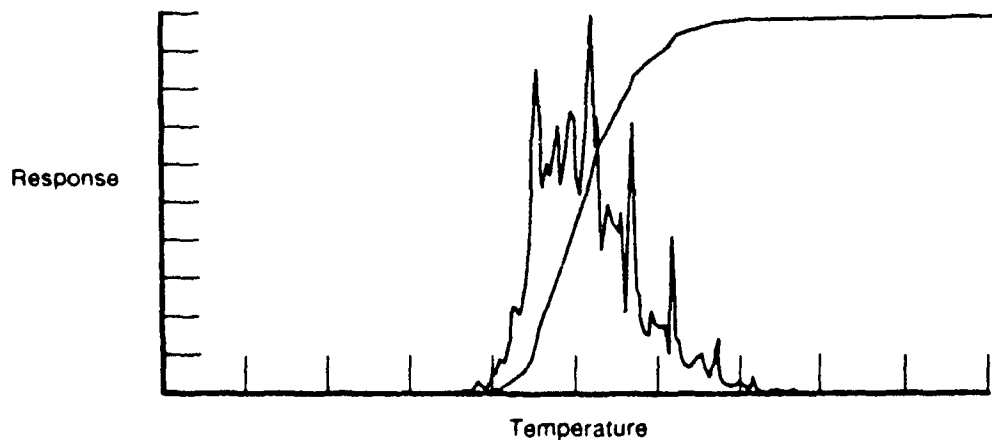
In contrast, the vapor and liquid temperatures differed by as much as 20°C during VRM evaluations on the 50% blend of isooctane and n-dodecane. When the 50% blend data are analyzed and compared with Raoult's Law calculations of vapor pressures using VRM data from pure compound determinations and data from the literature, two conclusions can be stated: 1.) for fuels with low IBP chilling the sample to less than -40°C before degassing appears to be necessary to preclude losses of lower boiling constituents; 2.) for wide boiling mixtures where the vapor and liquid temperatures vary more than 4.0°C , the VRM may still be used, but with reduced accuracy; the greater the difference, the more significant the loss in accuracy.



a) 84-POSF-2038 (JP-8)



b) 85-POSF-1758 (Light Pyrolysis Fuel)



c) DODX-1422-1 (JP-7)

FDA 303708

Figure 1. Comparison of Representative Chromatographs from ASTM D2887 Analyses

TABLE 2
ASTM D2887 SIMULATED DISTILLATION DATA FOR
SAMPLE NO. DODX 1422-1
(JP-7)

% Recovered	<i>Temperature (°C)</i>				
	Run 1	Run 2	Run 3	Run 4	Run 5
IBP	176.0	176.2	1 -6.6	176.0	176.0
5.00	188.5	188.4	188.9	188.2	188.3
10.00	193.4	193.3	193.7	193.4	193.5
15.00	195.1	195.1	195.5	195.5	196.6
20.00	197.7	197.7	198.1	198.0	198.2
25.00	200.8	200.7	201.1	200.9	201.1
30.00	203.2	203.1	203.6	203.5	203.7
35.00	206.1	206.0	206.4	206.3	206.5
40.00	208.3	208.2	208.6	208.8	208.9
45.00	210.7	210.6	211.0	211.3	211.4
50.00	213.9	213.7	214.1	214.3	214.4
55.00	215.7	215.5	215.9	216.4	216.4
60.00	217.0	216.8	217.2	217.9	218.1
65.00	218.9	218.7	219.1	220.2	220.6
70.00	222.4	222.2	222.5	224.0	224.3
75.00	226.2	226.1	226.3	227.7	227.9
80.00	231.0	230.9	231.1	232.5	232.6
85.00	234.2	234.0	234.3	235.6	235.8
90.00	242.7	242.5	242.7	244.2	244.4
95.00	252.0	251.7	251.9	253.5	254.0
FBP	281.5	281.4	281.5	282.8	285.7

TABLE 3
ASTM D2887 SIMULATED DISTILLATION DATA FOR
SAMPLE NO. 84-POSF-2038
(JP-8)

% Recovered	Temperature (°C)				
	Run 1	Run 2	Run 3	Run 4	Run 5
IBP	87.9	86.6	89.6	87.8	87.2
5.00	134.1	133.1	134.5	133.7	133.1
10.00	148.5	147.3	148.4	147.7	146.9
15.00	161.9	160.8	161.5	160.9	160.3
20.00	170.2	169.1	169.6	169.0	168.4
25.00	174.9	173.9	174.3	173.8	173.2
30.00	179.3	178.4	178.7	178.3	178.0
35.00	184.1	183.2	183.3	183.0	182.7
40.00	188.7	187.8	187.9	187.5	187.3
45.00	194.5	193.6	193.5	193.2	193.0
50.00	197.1	196.1	196.1	195.8	195.6
55.00	202.7	202.0	201.8	201.5	201.6
60.00	207.9	207.1	206.9	206.6	206.6
65.00	213.8	213.0	212.7	212.4	212.5
70.00	217.2	216.4	216.1	215.8	216.0
75.00	223.7	223.0	222.7	222.4	222.7
80.00	230.5	229.7	229.4	229.1	229.5
85.00	235.2	234.3	233.9	233.5	233.8
90.00	244.3	243.5	243.1	242.8	243.4
95.00	254.2	253.1	252.7	252.2	252.8
FBP	279.6	278.0	278.0	277.6	278.8

TABLE 4
ASTM D2887 SIMULATED DISTILLATION DATA FOR
SAMPLE NO. 85-POSF-1758
(LIGHT PYROLYSIS FUEL)

% Recovered	Temperature (°C)				
	Run 1	Run 2	Run 3	Run 4	Run 5
IBP	120.6	120.1	120.8	119.6	120.5
5.00	184.8	185.5	186.1	185.3	185.0
10.00	192.8	193.5	193.9	193.1	193.1
15.00	198.3	199.2	199.7	198.9	198.7
20.00	201.2	202.2	202.7	202.0	201.6
25.00	203.5	204.7	205.3	204.7	204.0
30.00	207.0	208.5	209.1	208.6	207.7
35.00	210.7	212.1	212.7	212.2	211.4
40.00	214.2	215.7	216.3	215.9	215.0
45.00	218.0	219.4	219.9	219.5	218.7
50.00	221.7	223.1	223.6	223.2	222.5
55.00	225.0	226.4	226.9	226.6	225.9
60.00	229.3	230.8	231.3	231.0	230.3
65.00	234.3	235.6	236.1	235.6	235.2
70.00	237.7	239.0	239.5	239.4	238.7
75.00	244.1	245.4	245.9	245.6	245.3
80.00	248.8	249.9	250.3	249.9	249.8
85.00	254.9	256.1	256.6	256.2	256.2
90.00	262.9	264.0	264.4	264.0	264.3
95.00	274.6	275.5	275.9	275.6	276.4
FBP	306.6	308.5	309.1	309.8	314.0

TABLE 5
VAPOR PRESSURE DATA FOR SAMPLE NO. DODX 1422-1 (JP-7)

Vapor Pressure (psia)	Vapor Temperature (°C)			Liquid Temperature (°C)			Average Temperature (°C)		
	Run 1	Run 2	Run 3	Run 1	Run 2	Run 3	Run 1	Run 2	Run 3
1.50		128.5			132.4			130.4	
2.00	138.0		138.3	141.5		141.5	139.8		139.9
3.00		150.1	150.4		153.3	153.7		151.7	152.0
4.00	159.1		159.7	162.6		162.9	160.8		161.3
5.00		166.9	167.1		170.2	170.4		168.6	168.8
6.00	173.8		173.5	176.8		176.8	175.3		175.2
7.00		178.8	179.2		182.0	182.4		180.4	180.8
8.00	183.9		184.2	187.4		187.4	185.6		185.8
9.00		188.6	189.0		191.8	192.1		190.2	190.6
10.00	192.6		192.9	196.0		196.2	194.3		194.6
11.00	196.4	196.6	197.0	199.8	199.9	200.0	198.1	198.2	198.5
12.00	200.1		200.7	203.5		203.6	201.8		202.2
13.00	203.8	203.6	204.8	207.0	206.7	207.2	205.4	205.2	206.0
14.00	206.8		207.2	210.0		210.3	208.4		208.8
14.74	209.1	209.2	209.6	212.1	212.2	212.6	210.6	210.7	211.1

TABLE 6
VAPOR PRESSURE DATA FOR SAMPLE NO. 84-POSF-2038 (JP-8)

Vapor Pressure (psia)	Vapor Temperature (°C)		Liquid Temperature (°C)		Average Temperature (°C)	
	Run 1	Run 2	Run 1	Run 2	Run 1	Run 2
2.00	92.0	88.0	105.0	105.1	98.5	96.6
2.97		101.5		117.6		109.6
3.00	103.3		117.7		110.5	
4.00	113.2	112.6	127.3	127.5	120.2	120.0
5.00	121.2	120.5	135.3	135.2	128.2	127.8
6.00	127.8	126.8	142.0	142.0	134.9	134.4
7.00	134.0	133.4	147.6	147.8	140.8	140.6
8.00	140.1		153.0		146.6	
8.01		139.5		153.0		146.2
8.96		144.7		157.3		151.0
9.00	145.0		157.5		151.2	
9.98		148.7		161.6		155.2
10.00	148.8		161.7		155.2	
10.97		153.0		165.5		159.2
11.00	153.2		165.6		159.4	
12.00	157.3	156.6	169.3	169.3	163.3	163.0
12.97		160.4		172.5		166.4
12.98	160.2		172.7		166.4	
13.95		163.8		176.0		169.9
13.98	164.0		176.0		170.0	
14.70		165.3		178.2		171.8
14.71	166.4		178.2		174.2	

TABLE 7
VAPOR PRESSURE DATA FOR SAMPLE NO.85-POSF-1758
(LIGHT PYROLYSIS FUEL)

Vapor Pressure (psia)	Vapor Temperature (°C)		Liquid Temperature (°C)		Average Temperature (°C)	
	Run 1	Run 2	Run 2	Run 2	Run 1	Run 2
1.99	--	123.0	--	138.6	--	130.8
2.00	124.6	--	139.7	--	132.2	--
2.94	--	140.0	--	151.9	--	146.0
3.00	139.3	--	153.1	--	146.2	--
4.00	149.8	--	163.2	--	156.5	--
4.04	--	152.0	--	162.9	--	157.4
4.97	157.7	--	171.5	--	164.6	--
5.04	--	158.6	--	171.0	--	164.8
6.00	--	166.3	--	177.8	--	172.0
6.02	166.8	--	178.8	--	172.8	--
7.00	173.2	--	184.8	--	179.0	--
7.05	--	173.8	--	184.2	--	179.0
7.97	--	179.2	--	189.3	--	184.2
8.04	180.0	--	190.5	--	185.2	--
8.97	185.0	--	195.1	--	190.0	--
9.00	--	185.0	--	194.5	--	189.8
9.96	189.4	--	199.6	--	194.5	--
10.04	--	190.4	--	199.1	--	194.8
10.95	--	194.4	--	203.0	--	198.7
11.06	194.0	--	204.2	--	199.1	--
11.96	--	198.4	--	206.9	--	202.6
12.01	198.3	--	208.0	--	203.2	--
12.91	--	202.0	--	210.5	--	206.2
13.00	201.5	--	211.4	--	206.4	--
13.90	--	205.5	--	213.8	--	209.6
13.97	205.0	--	214.8	--	209.9	--
14.70	--	207.9	--	216.4	--	212.2
14.71	207.5	--	217.2	--	212.4	--

Clearly, the model compound study raised more questions than it answered concerning the applicability of the VRM to fuels other than JP-7. From the preliminary data generated with the model compound study, it is difficult to discern which is the most accurate temperature to use for vapor pressure determinations: the liquid temperature, the vapor temperature, or the average temperature. For the purposes of this investigation, the average of the vapor and liquid temperatures was used. Additionally, the broader boiling range and lower IBP fuel, 84-POSF2038, was subjected to the chill and thaw degassing procedure, while fuel samples 85-POSF-1758 and DODX 1422-1 were not.

3.2 DATA ANALYSIS AND CORRELATIONS

Data generated in the aforementioned tests were analyzed to produce mathematical models which described the correlations between distillation and vapor pressure data. After generating data files of

distillation and vapor pressure data, a computer program (FORTRAN) was developed which reads the data files then evaluates the data using the models discussed below. The computer program then calculated the model fitting parameters, writes a TELAGRAF data set to plot actual data and calculated data, and provides a statistical analysis of the goodness of fit. This subsection discusses the development of the correlation models and the resultant data analyses for the three fuel samples evaluated.

3.2.1 Percent Recovered Versus Temperature Modeling for ASTM D2887 and ASTM D86 Data

Percent recovered versus temperature data from ASTM D86 distillations and ASTM D2887 SIMDIST for the three fuels were plotted. Because of the sigmoidal shape of the resulting curves, several models were then investigated, including fifth degree (and lower) polynomial models, a lognormal model (percent recovered was treated as cumulative percent), a Weibull model (treated similarly), and a hyperbolic sine model (SINH). Standard regression techniques were used to fit the linear models (polynomial, lognormal, and Weibull), while the nonlinear SINH was fitted using a version of the Simplex Algorithm.

Goodness of fit parameters R^2 (coefficient of multiple determination) and standard error of the estimate (SEE) were used to evaluate the quality of the various models. R^2 merely indicates what proportion of the total variation in the response Y is explained by the fitted model. The square root of R^2 is called the multiple correlation coefficient. Standard error of the estimate is the standard deviation between the fitted values and the actual values and is a measure of the total scatter of the curve fit.

The SINH was found to provide the best fit for both ASTM D86 and ASTM D2887 distillation data. In order to provide a significant improvement in the accuracy of the model, the IBP was not included in the expression. The SINH fits the equation:

$$Y = C_1 * \text{SINH}(C_2 * (X + C_3)) + C_4 \quad (1)$$

where Y = temperature ($^{\circ}\text{C}$), X = % recovered/100, and C_1 through C_4 are the fitting parameters. All R^2 values were greater than 0.99 (99% of the variation was explained by the model), while SEE ranged from a high of 3.5 to a low of 1.5 ($^{\circ}\text{C}$), indicating very good fits.

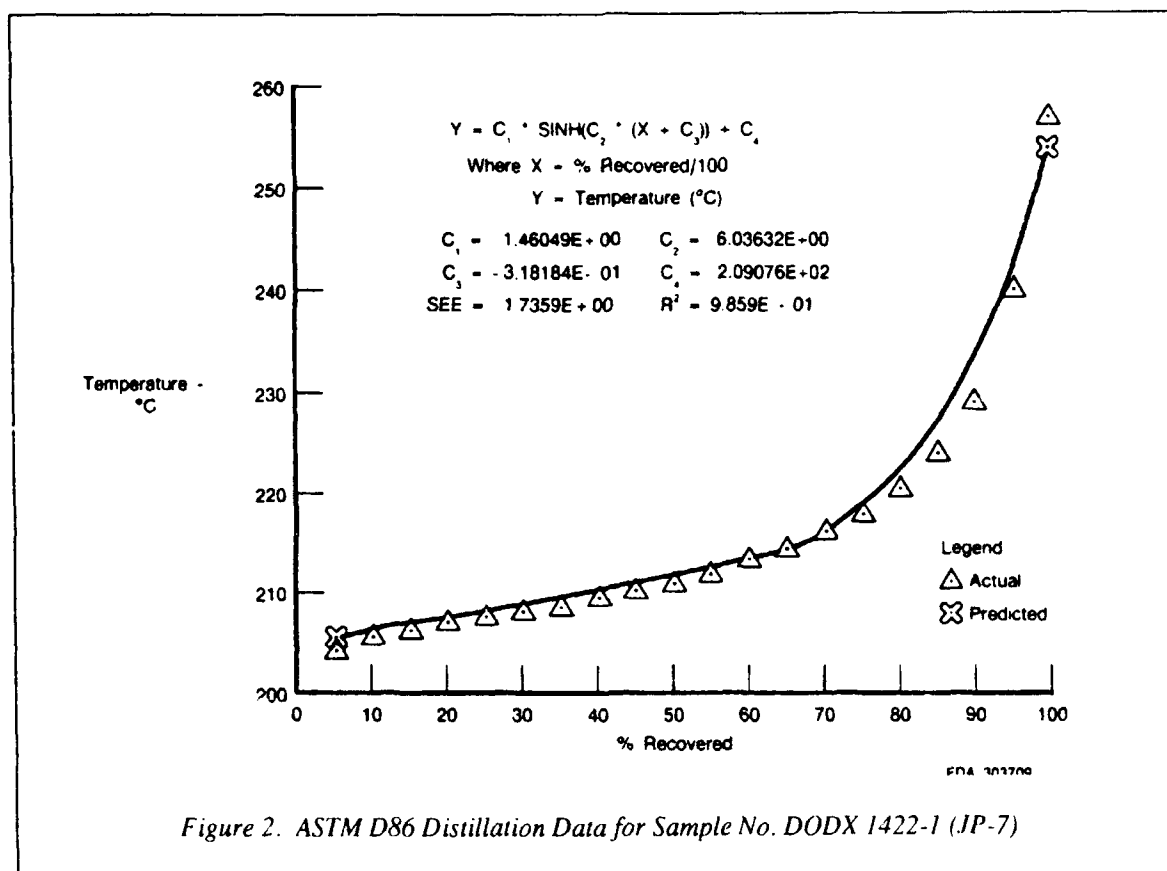
Figures 2, 3, and 4 summarize ASTM D86 distillation data and Figures 5, 6, and 7 summarize ASTM D2887 SIMDIST data for the three fuel types. These figures are composites showing all data generated in duplicate runs for each fuel for ASTM D86 distillations and five runs on each fuel for ASTM D2887 SIMDIST. The legend describes actual data points, those predicted by the mathematical model (the solid curve), the equation and coefficients describing the curve, the SEE, and the "goodness of fit" (R^2) value.

3.2.2 Vapor Reflux Modeling

The logarithm (log) of vapor pressure (psia) was plotted as a function of the reciprocal of absolute temperatures (1/K). The linearity of the resulting plots justified fitting this data with the equation:

$$\log \text{ Vapor Pressure} = K_1 + K_2/T \quad (2)$$

where T is the temperature in degrees Kelvin and K_1 and K_2 are fitting parameters. Again, R^2 and SEE were calculated. Resulting values of R^2 were greater than 0.99, while SEE values varied from 0.0145 to 0.0064, indicating excellent curve fits.



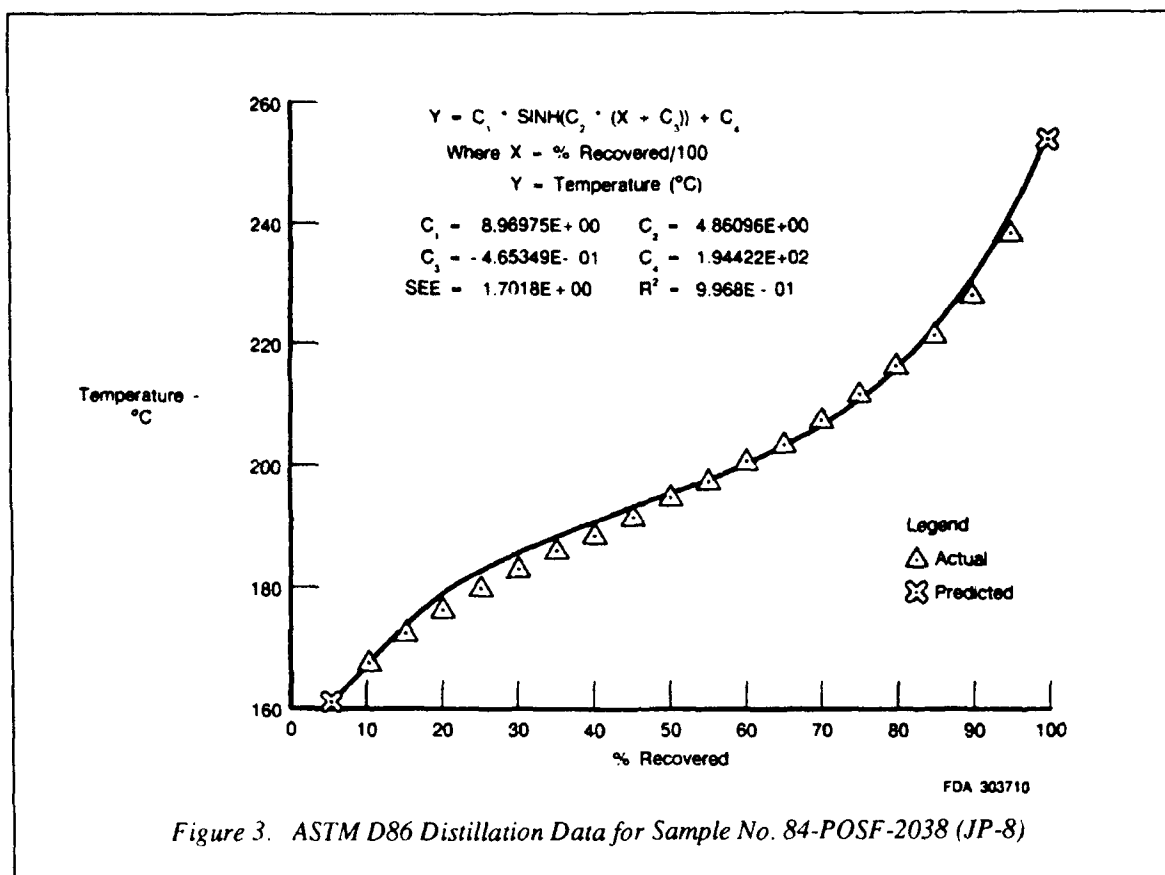
Figures 8, 9, and 10 are composite plots showing VRM data for duplicate tests on each of the three fuels. The legend describes the actual data and calculated values from the model for which the equation with coefficients is given for each fuel sample. Standard error of the estimate and R^2 values are also given.

3.2.3 Vapor Pressure Versus Percent Recovered Modeling

Figures 11, 12, and 13 illustrate the correlation model for predicting vapor pressure values from ASTM D2887 SIMDIST analyses of the three fuels. The mathematical model that describes the correlation between vapor pressure and SIMDIST data for the fuels tested was generated by combining equations (1) and (2) to get the new equation:

$$\log_{10} \text{Vapor Pressure}_t = K_1 + \left[\frac{K_2}{C1(\sinh(C2(X_t + C3))) + C4 + 273} \right]$$

Where X_t = the percent recovered at a given temperature $t(^{\circ}\text{C})$, divided by 100.



The fitting parameters C_1 through C_4 are the same values determined in equation (1), while K_1 and K_2 were determined from vapor reflux data evaluated with equation (2). The 273 that appears in the denominator of equation (3) is used to convert °C to °Kelvin. Values for SEE and R^2 are not reported because much of the data used for these correlations (vapor pressures greater than 14.7 psia) were extrapolated values. However, when vapor pressure are calculated using the model developed for sample DODX 1422-1 (JP-7) and compared to measured and extrapolated results from VRM test, the agreement is excellent (within 1.0%).

When the calculated vapor pressures for sample DODX 1422-1 (JP-7) from the prediction equation are compared to predicted values from the MIL-T-38219 Appendix C nomograph for 149°C (300°F) and 260°C (500°F), the agreement is excellent. These values are for the nomograph: 149°C, 2.85 psia and 260°C, 43.0 psia and for the prediction equation: 149°C, 2.74 psia and 260°C, 43.02 psia. On the other hand, while the experimental high-density fuel meets the criteria specified for applicability of the nomograph (for example, no more than 28°C (50°F) difference between IBP and 20% recovered temperature, and no greater than 93°C (200°F) difference between the 5% and the 95% recovered temperatures), the nomograph is not accurate for predicting the vapor pressure of high-density fuel. The vapor pressures at 149 and 260°C (300° and 500°F) derived from: (1) measured/extrapolated values, (2) values predicted based on the mathematical model developed in this program, and (3) values predicted from the MIL-T-38219 nomograph are 3.25 and 35.91; 3.26 and 35.90; and 4.9 and 66, respectively.

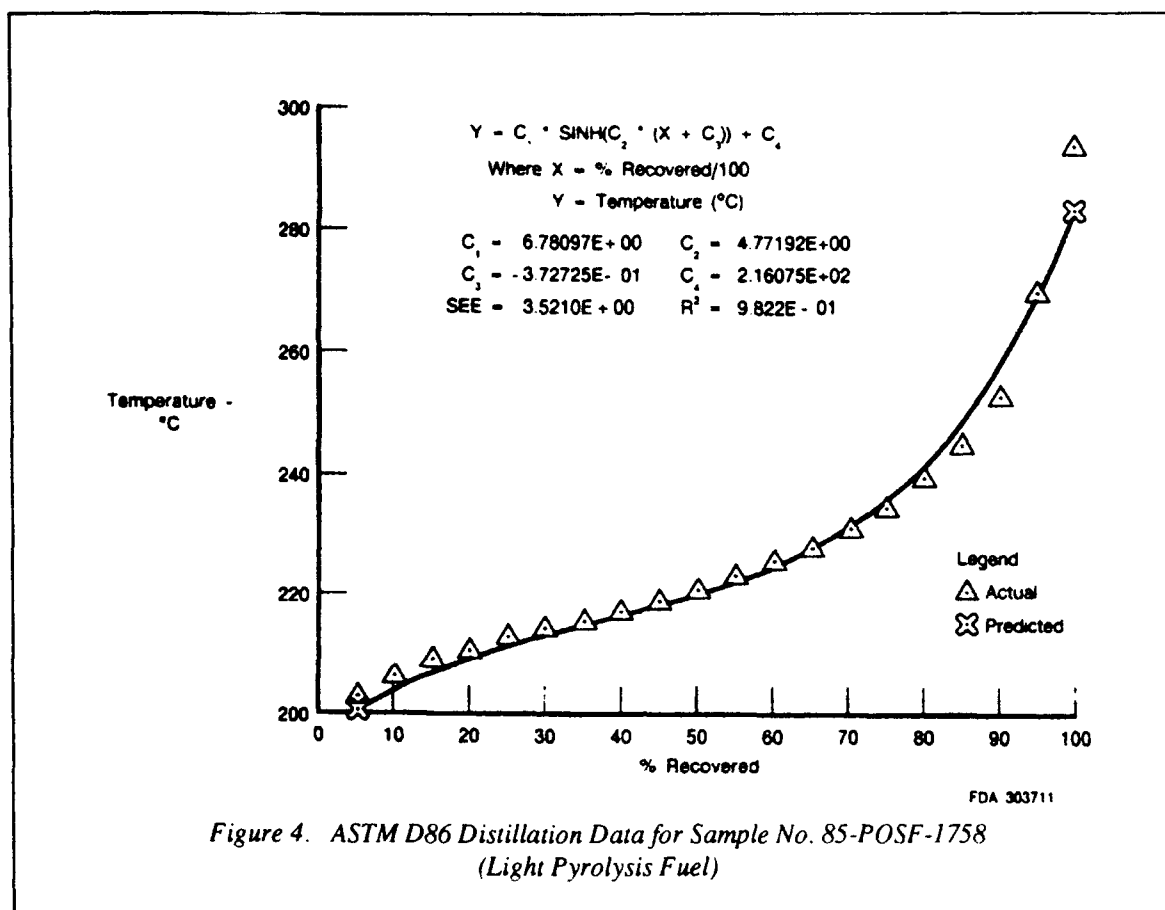


Figure 4. ASTM D86 Distillation Data for Sample No. 85-POSF-1758 (Light Pyrolysis Fuel)

Currently, because of limitations in vapor pressure and distillation data, the model shown in equation 3 is only applicable to the three fuel samples tested and cannot be applied to other fuel samples of the same type. While the model shown in equation 1 can be used to determine new fitting parameters C_1 through C_4 from a SIMDIST analysis on a test fuel, there is presently no way to determine K_1 and K_2 without vapor pressure data. However, given sufficient SIMDIST and vapor pressure data for a representative cross section of fuel samples within each fuel type, it should be possible to predict K_1 and K_2 from simulated data or determine a value for K_1 and/or K_2 that is representative of a given fuel type.

Two alternatives are available for developing a vapor pressure prediction method. The first and least accurate method would be to generate a nomograph for each fuel similar to that described in Appendix C of MIL-T-38219A. The reduced accuracy of this method is a result of using only one data point from a distillation; in that case the 20% recovered temperature. The second method would involve the development of computer software, based upon the initial program developed in this investigation; that can be combined with the SIMDIST software. The goal would be to (1) develop new software that would use the SIMDIST data file consisting of numerous coordinate pairs of percent recovered versus temperature, (2) produce a simulated distillation curve as shown in Figures 5, 6, and 7, (3) produce a table or figure of predicted ASTM D86 distillation data, and (4) produce a table or figure of predicted vapor pressure versus temperature.

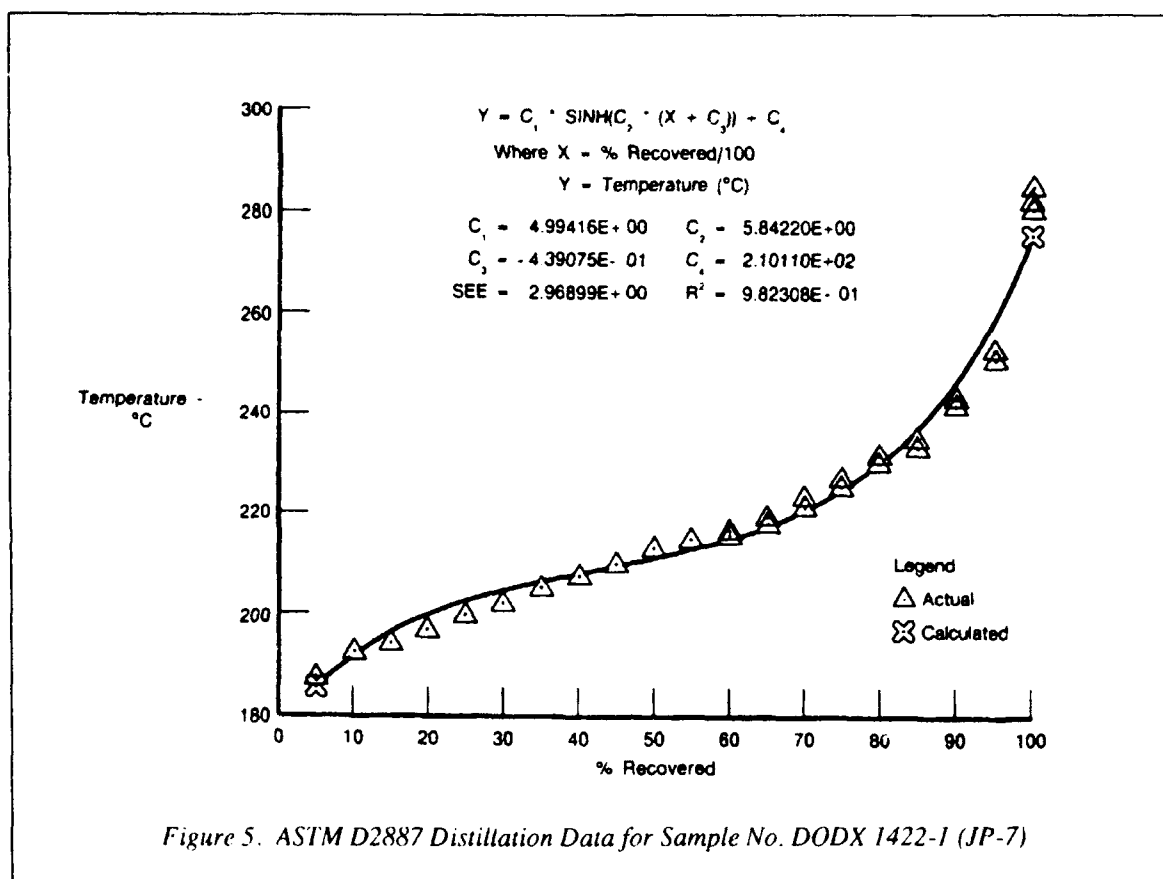


Figure 5. ASTM D2887 Distillation Data for Sample No. DODX 1422-1 (JP-7)

3.2.4 ASTM D86 Versus ASTM D2887 Modeling

Figures 14, 15, and 16 describe the correlation of ASTM D2887 to ASTM D86 data for the three fuels. Temperature values at each 5 percent recovered point for ASTM D86 were plotted against temperatures for the same percent recovered points from ASTM D2887. The resulting parabolic curve shapes were modeled using a second-degree polynomial of the form:

$$Y = C_1 + C_2 * X + C_3 * X^2 \quad (4)$$

where Y is the ASTM D86 temperature corresponding to the ASTM D2887 temperature (X) for a given percent recovered. A higher (third) degree polynomial model was fitted with only slight improvements in R^2 and SEE. These improvements were not considered worth the additional complexity of the third-degree model. If additional data for both distillations were available between 95% recovered and the FBP, the third-degree model might have been justified. The additional data would serve to fix the shape of the top end of the curve. Very good agreement was observed for the second degree fits in the 90% recovered and below region.

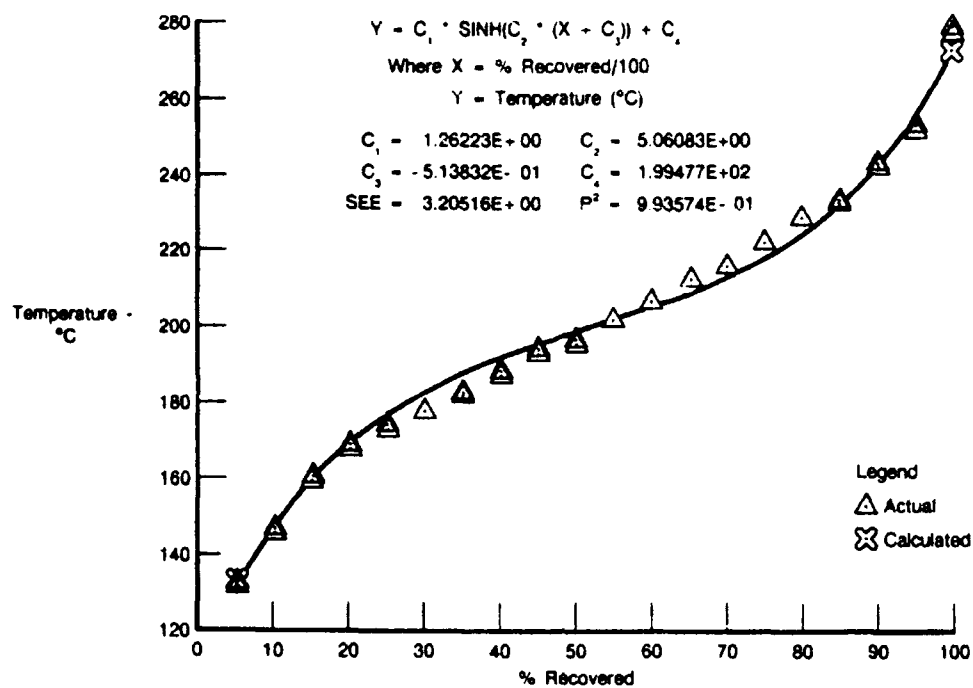
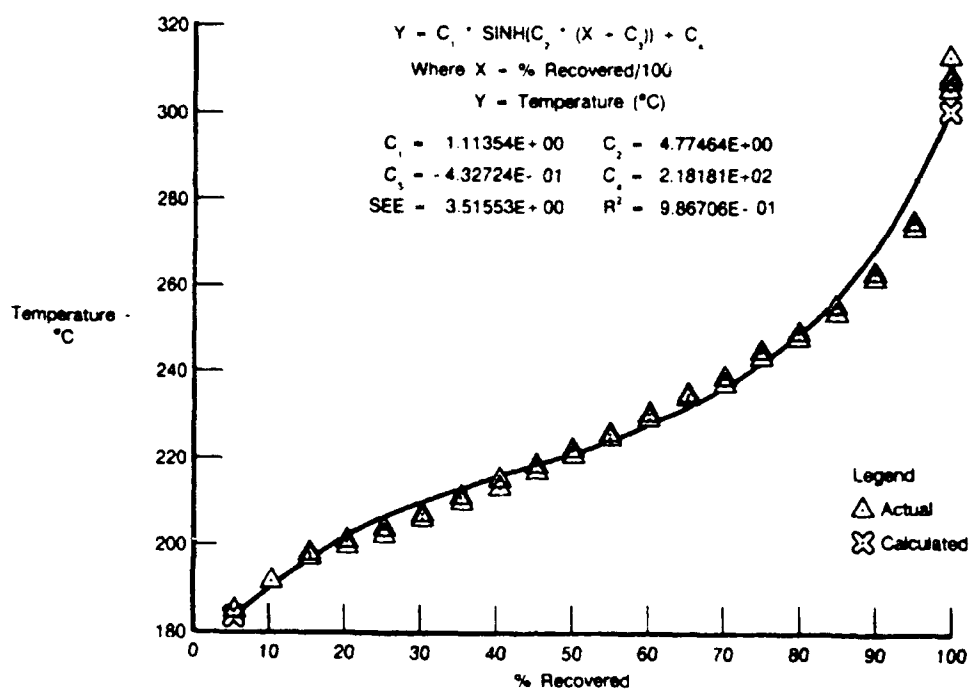


Figure 6. ASTM D2887 Simulated Distillation Data for Sample No. 84-POSF-2038



FDA 303714

Figure 7. ASTM D2887 Simulated Distillation Data for Sample No. 85-POSF-1758 (Light Pyrolysis Fuel)

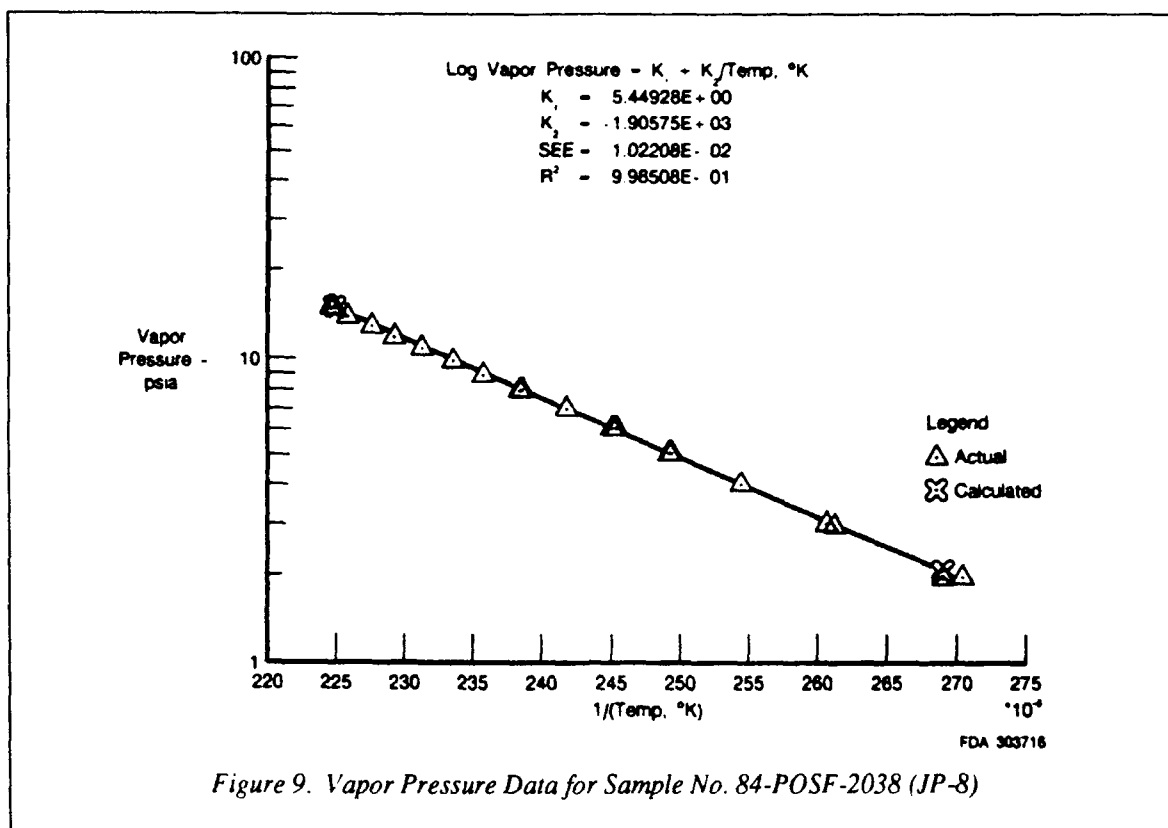


Figure 9. Vapor Pressure Data for Sample No. 84-POSF-2038 (JP-8)

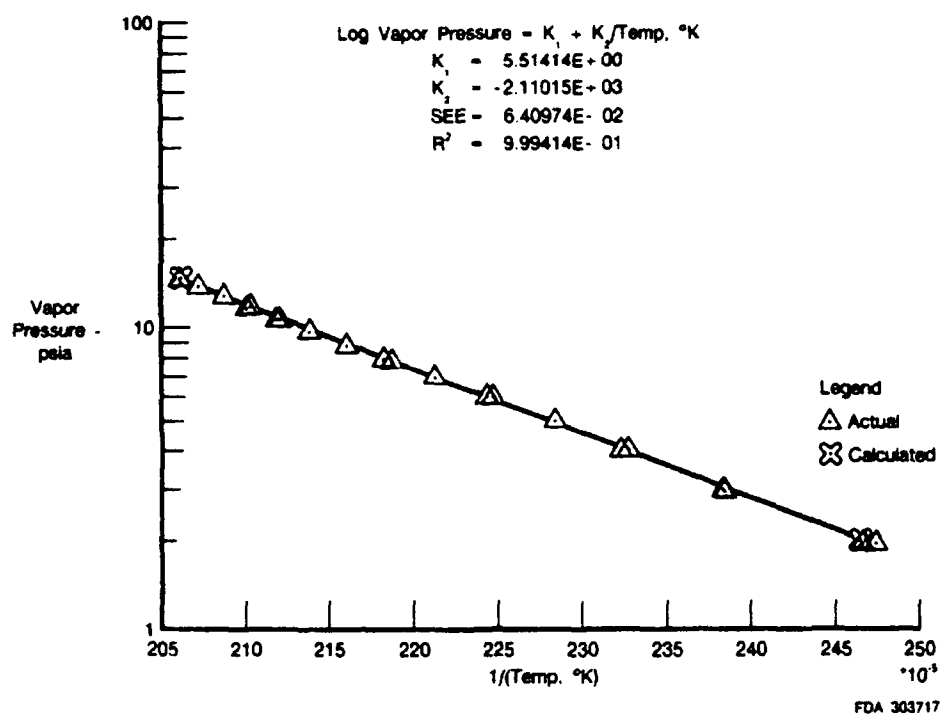
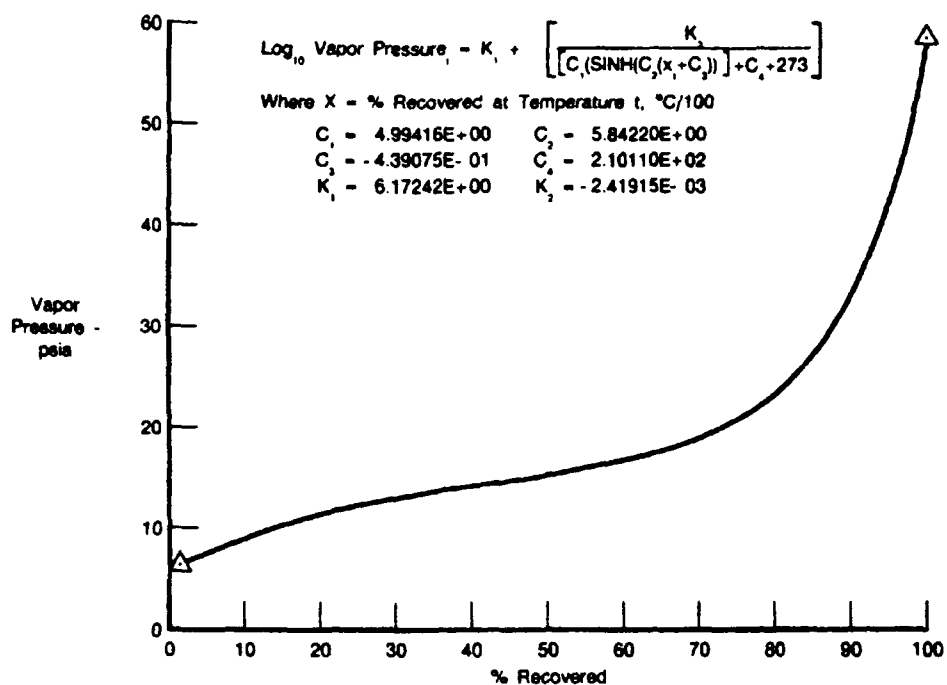
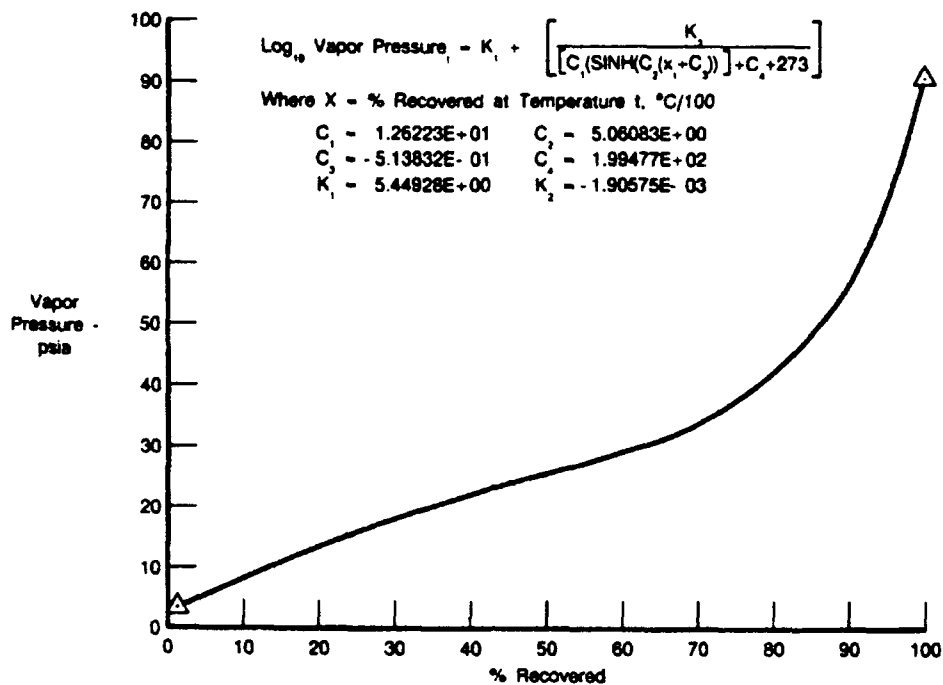


Figure 10. Vapor Pressure Data for Sample No. 85-POSF-1758 (Light Pyrolysis Fuel)



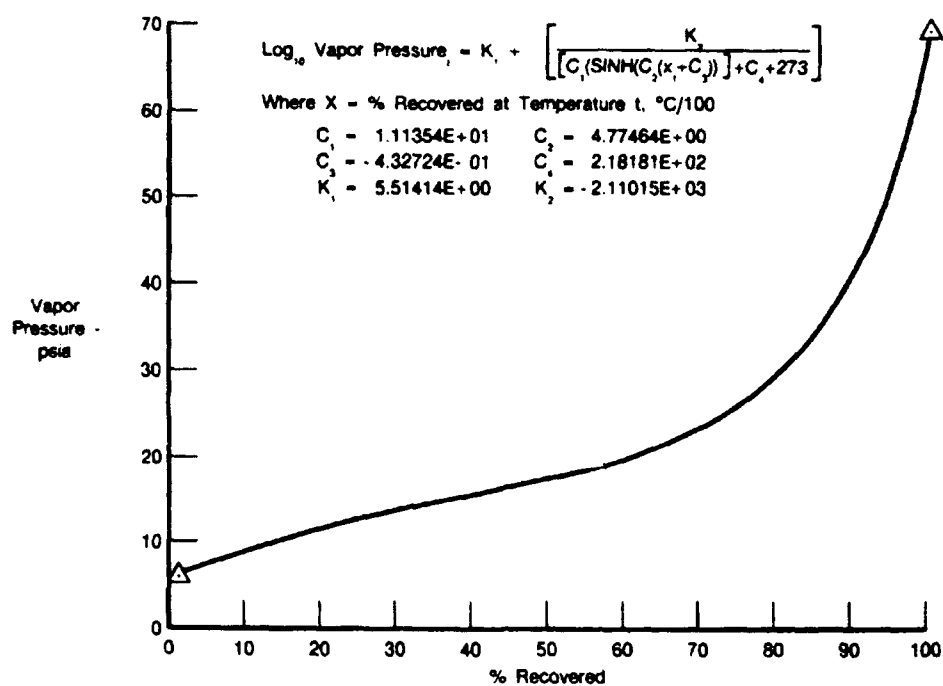
FDA 303718

Figure 11. Correlation Model for Predicting Vapor Pressure from ASTM D2887 Simulated Distillation Data for Sample No. DODX 1422-1 (JP-7)



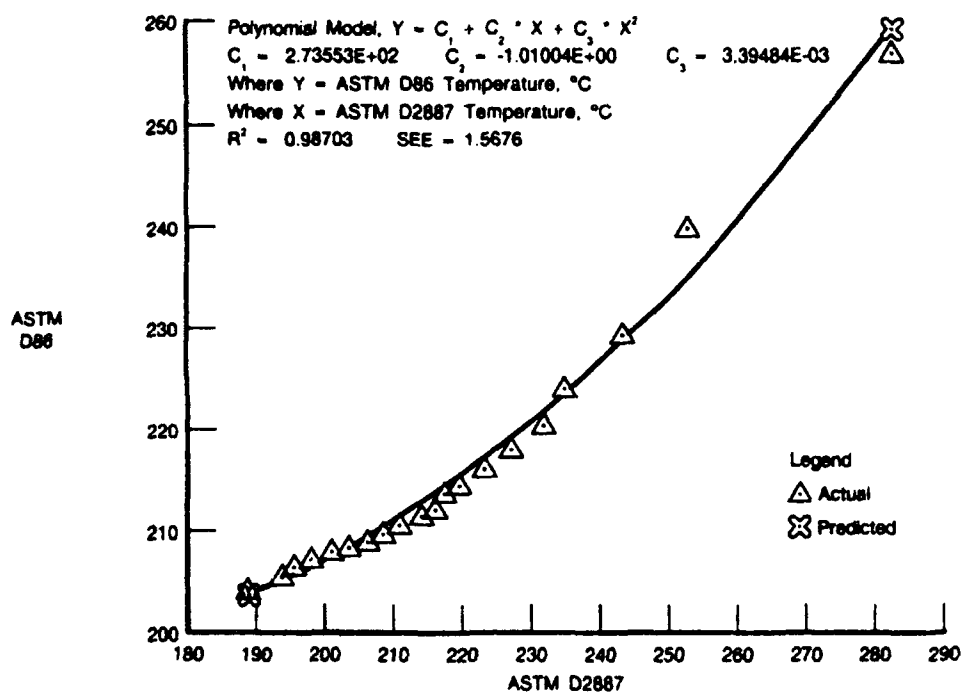
FDA 303719

Figure 12. Correlation Model for Predicting Vapor Pressure from ASTM D2887 Simulated Distillation Data for Sample No. 84-POSF-2038 (JP-8)



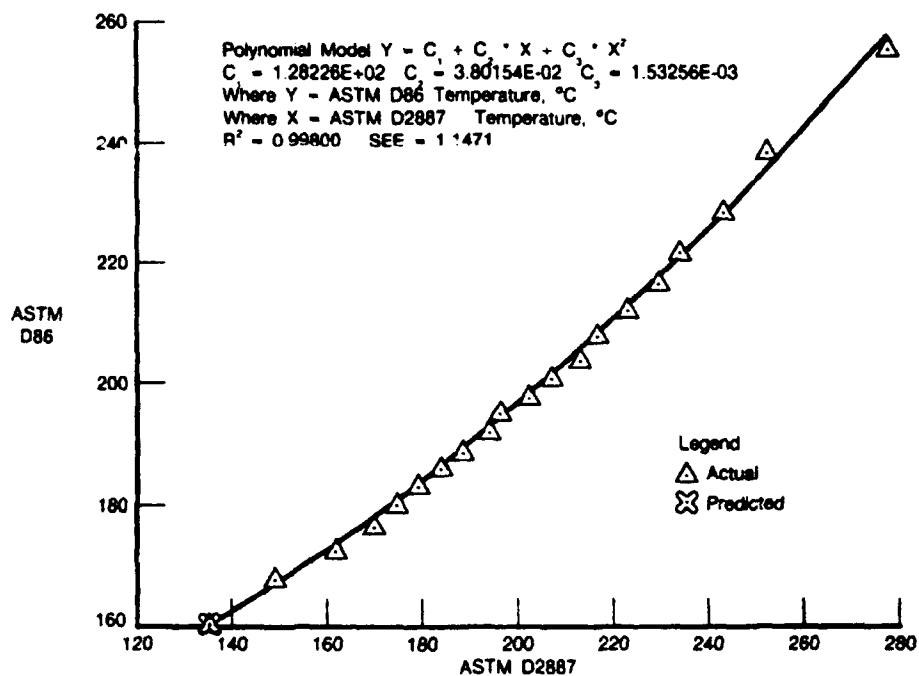
FDA 303720

Figure 13. Correlation Model for Predicting Vapor Pressure from ASTM D2887 Simulated Distillation Data for Sample No. 85-POSF-1758 (Light Pyrolysis Fuel)



FDA 303721

Figure 14. Correlation Model for Predicting ASTM D86 Distillation Results from ASTM D2887 Simulated Distillation Data for Sample No. DODX 1422-1 (JP-7)



FDA 303722

Figure 15. Correlation Model for Predicting ASTM D86 Distillation Results from ASTM D2887 Simulated Distillation Data for Sample No. 84-POSF-2038 (JP-8)

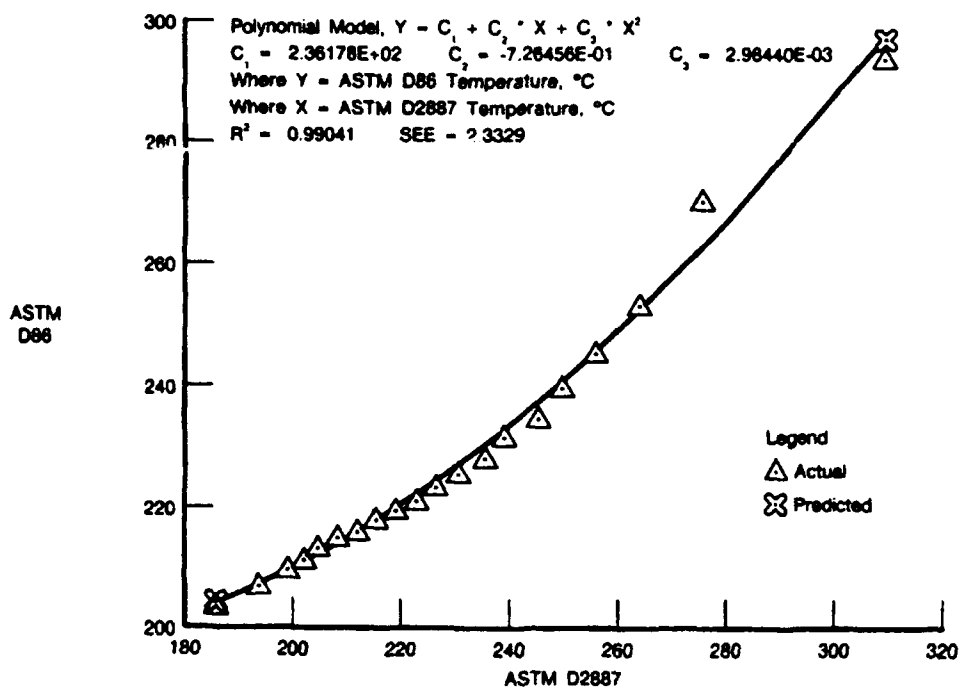


Figure 16. Correlation Model for Predicting ASTM D86 Distillation Results from ASTM D2887 Simulated Distillation Data for Sample No. 85-POSF-1758 (Light Pyrolysis Fuel)

SECTION 4.0

CONCLUSIONS AND RECOMMENDATIONS

Mathematical models were developed which describe the correlations between (1) ASTM D2887 SIMDIST data and ASTM D86 distillation data and (2) ASTM D2887 SIMDIST data and vapor pressures determined using the VRM described in Appendix C of MIL-T-38219A. In addition, a computer program was developed which uses the mathematical model to analyze distillation and vapor pressure data to calculate model fitting parameters, and predict ASTM D86 distillation data and vapor pressure data from SIMDIST data. These correlation models were developed on the basis of data generated for only one fuel of each type: JP-7, JP-8, and an experimental high-density fuel. While the mathematical models were found to provide accurate predictions for the fuels tested, it is necessary to test the applicability of the models to other fuel samples of the same specification types.

An updated version of the VRM described in Appendix C of MIL-T-38219A was shown to provide accurate vapor pressure data for pure compounds based on comparison with literature values. The VRM was also shown to be applicable for vapor pressure determinations for very narrow boiling mixtures such as JP-7 fuels. However, because of the wide boiling ranges of jet fuels such as JP-8, Jet A and the experimental high-density fuel, a significant variation exists between the vapor and liquid temperatures under equilibrium conditions of the VRM; thereby, reducing the accuracy of vapor pressure determination. This observation raises concern regarding the applicability of the VRM to fuels other than narrow boiling range fuels such as JP-7.

It is recommended that an investigation be conducted (literature search and/or laboratory tests using compounds and mixtures of pure compounds) to determine which vapor pressure method is most applicable to jet fuel analysis. Several methods are currently used for vapor pressure determinations on low-volatility fuels, including the isoteniscope method (ASTM D2879), the micro-vapor pressure method (ASTM D2551), and the VRM (MIL-T-38219A). The vapor pressure method selected should provide accurate (expected) results on pure compounds and mixtures of pure compounds, should have acceptable precision, should be applicable to narrow and wide boiling range fuels, and hopefully will not change the current data base for jet fuel vapor pressures.

Based on the findings of the recommended investigation, the mathematical models presented in this document should be modified to incorporate vapor pressure data from the selected method. Subsequent fuels evaluated during the program will then provide simulated distillation and vapor pressure data to test and modify the model to fit the variability of fuels within a given specification fuel type. This should then make possible the development of computer software to read the data file created by ASTM D2887 SIMDIST software, then predict ASTM D86 distillation data and vapor pressure data for a fuel based on the SIMDIST evaluation.

APPENDIX A

REFLUX VAPOR PRESSURE TEST

1. SCOPE

This procedure is applicable for pure compounds and narrow boiling range hydrocarbon liquids. It is recommended the test be limited to fluids exhibiting no greater than 70°C difference between the ASTM D86 IBP and FBP.

2. APPLICABLE DOCUMENTS

- MIL-T-38219A, Appendix C, "Vapor Pressure Test"

3. SUMMARY OF METHOD

Three hundred mL of material are heated in a 500-mL Pyrex flask that is constructed to provide magnetic stirring, liquid and vapor temperature observation, and ground glass fitting for attachment to a condenser. The fuel is outgassed by vacuum at ambient temperature for a minimum of 10 minutes. Pressure of the system is set by means of the Whitey micro bleed valve while maintaining vacuum on the system. Heat is applied to the Pyrex fuel container while maintaining constant pressure and magnetic stirring of the fuel. After the fuel begins boiling, the height of the fuel reflux in the condenser is observed and care taken to maintain a constant reflux height during the entire test procedure. The reflux rate is considered to be at equilibrium when the vapor temperature and the liquid temperature agree within 4°C. The pressure and the indicated temperatures of liquid and vapor are recorded at each pressure point selected during the run. Higher pressure determinations are made by opening the bleed valve in selected increments and increasing the applied heat. A minimum of four stable reflux conditions (boiling points) are obtained and plotted on semilog paper--the reciprocal of absolute temperature on the abscissa versus the logarithm of vapor pressure in psi on the ordinate for each boiling point.

4. REAGENTS AND MATERIALS

The following are reagents and materials used to perform the reflux vapor pressure test:

- Vacuum grease for sealing ground glass joints and seating rubber stoppers.
Note: Silicone grease has been shown to cause foaming during post test distillations of some fuels
- Acetone, reagent grade, for cleaning glassware.

5. APPARATUS

The following apparatus are used to perform the reflux vapor pressure test:

- Vacuum system capable of attaining 0.01 psia
- Variable AC voltage transformer, VWR Catalog No. 62546-251 or equivalent
- Magnetic stirrer, Teflon-coated magnetic stirring bar, 0.5-inch StarHead magnetic stir bars are satisfactory
- Heating mantle, Glas-Col 500 mL or equivalent

- Flask, 500 mL, Pyrex round bottom, short neck standard taper joint 24/40 with thermometer well, VWR Catalog No. 29129-428 or equivalent
- Tube, connecting, three way, joints 24/40. Upper ends have outer joints and bottom has inner member joint. VWR Catalog No. 62960-024 or equivalent
- Condenser, Liebig, Pyrex, 41-mm OD x 300-mm long with 24/40 joint at bottom. VWR Catalog No. 23122-000 or equivalent
- Rubber tubing, vacuum and medium wall
- Bleed valve, 1/4-inch, Whitey Micro Metering, Catalog No. 22RS4 or equivalent
- Trap, vacuum, separable, joint 29/42; VWR Catalog No. 55096-100 or equivalent
- Dewar flask, vacuum, flask to be large enough to accommodate the vacuum trap and cooling medium
- Neoprene stoppers, green, solid No. 5 and No. 4, VWR Catalog No. 59589-212 and 59589-198 or equivalent. The No. 5 and the No. 4 neoprene stoppers must be drilled with holes to permit passage of 3/32-inch OD probe through the No. 5 stopper and 1/4 inch OD tubing through the No. 4 stopper
- Thermocouples, Chromel-Alumel, calibrated, 3/32-inch diameter, SS sheathed, closed end. Thermocouple probe 10-inch long with 6-foot lead wire
- Omega Digicator or equivalent, for thermocouple temperature read out
- Transducer, 0 to 15 psia, transducer housing to be equipped with threaded fitting compatible with 1/4-inch Swagelok hardware
- Digital pressure readout system, Anadex Model DPM-735-VI-A115, or equivalent
- Refrigerated cooling bath, Endocal Model RTE-5B or equivalent.

6. SAMPLE

The sample will be prepared as follows:

1. Transfer 600 mL of the sample into a clean 1000-mL separatory funnel, cap the funnel top, then shake the funnel for 1 to 2 minutes and allow contents to settle for 15 to 20 minutes.
2. Draw off lower 100 mL of fuel and discard.

7. PREPARATION OF APPARATUS

Preparation of the apparatus includes the following steps:

1. Assemble the apparatus as shown in Figure A-1.
2. Place 300 mL of the prepared sample and a magnetic stir bar in the 500-mL flask.

3. Place ice around the vacuum trap in the dewar flask.
4. Position the vapor phase thermocouple through the No. 5 stopper in a manner that the probe tip is centered and even with the top rim of the 24/40 joint of the 500-mL flask.
5. Place the liquid phase thermocouple in the flask thermometer well and add 5 mL of high flash point oil to the well.
6. Begin the stirring action with the magnetic stirrer set at a high speed. Open the micrometer bleed valve and slowly engage the vacuum. If the vacuum system is opened too rapidly, the fuel may bump up into the condenser. As the system pressure decreases, start closing the bleed valve. When the bleed valve is completely closed, continue the fuel outgassing for a period of 10 minutes.

8. PROCEDURE

The following steps are to be performed for the reflux vapor pressure test:

1. Decrease the magnetic stirrer speed to a rate such that only a small vortex is noted in the fuel.
2. Slowly raise the system pressure to 21.5 psia using the micrometer bleed valve and the flask temperature by use of the variable transformer control.
3. Adjust the heat input and stirring speed to preclude violent boiling of the fuel which would cause bumping.
4. Verify pressure and temperature are properly adjusted; this ensures a steady reflux action of the fuel. The height of the reflux can be noted in the bottom section of the condenser. Condenser temperature of 15°C (60°F) has been found to be satisfactory. Condenser temperature is controlled by adjusting the refrigerated cooling bath temperature controller.
5. When refluxing is equilibrated, observe the liquid and vapor phase temperatures displayed by the Omega Digicator and the pressure reading displayed by the Anadex pressure module.
6. If the two temperatures do not agree within 4°C, change the system pressure by means of the bleed valve, increase the temperature, and repeat temperature-pressure measurements until stable reflux conditions are reached.
7. Ensure that stable reflux conditions are such that the temperature, pressure, and fuel reflux height do not change on three successive readings at 3-minute intervals.
8. Raise the system pressure, increase the temperature, and repeat the temperature-pressure measurements over the entire pressure range up to atmospheric pressure. A minimum of four stable reflux conditions (boiling points) will be obtained.
9. Record the temperature of the liquid, temperature of the vapor, and pressure of the system at stable reflux conditions.
10. Allow the fuel to cool to ambient temperature and pressure.
11. Remove sufficient fuel from the flask and run a distillation test as specified by ASTM D86. Results will agree within the prescribed limits with those obtained previous to the run or the test results will be discarded. If a significant increase in the IBP is observed between pretest and post-test distillations, this indicates the probability that some loss in lighter ends has occurred,

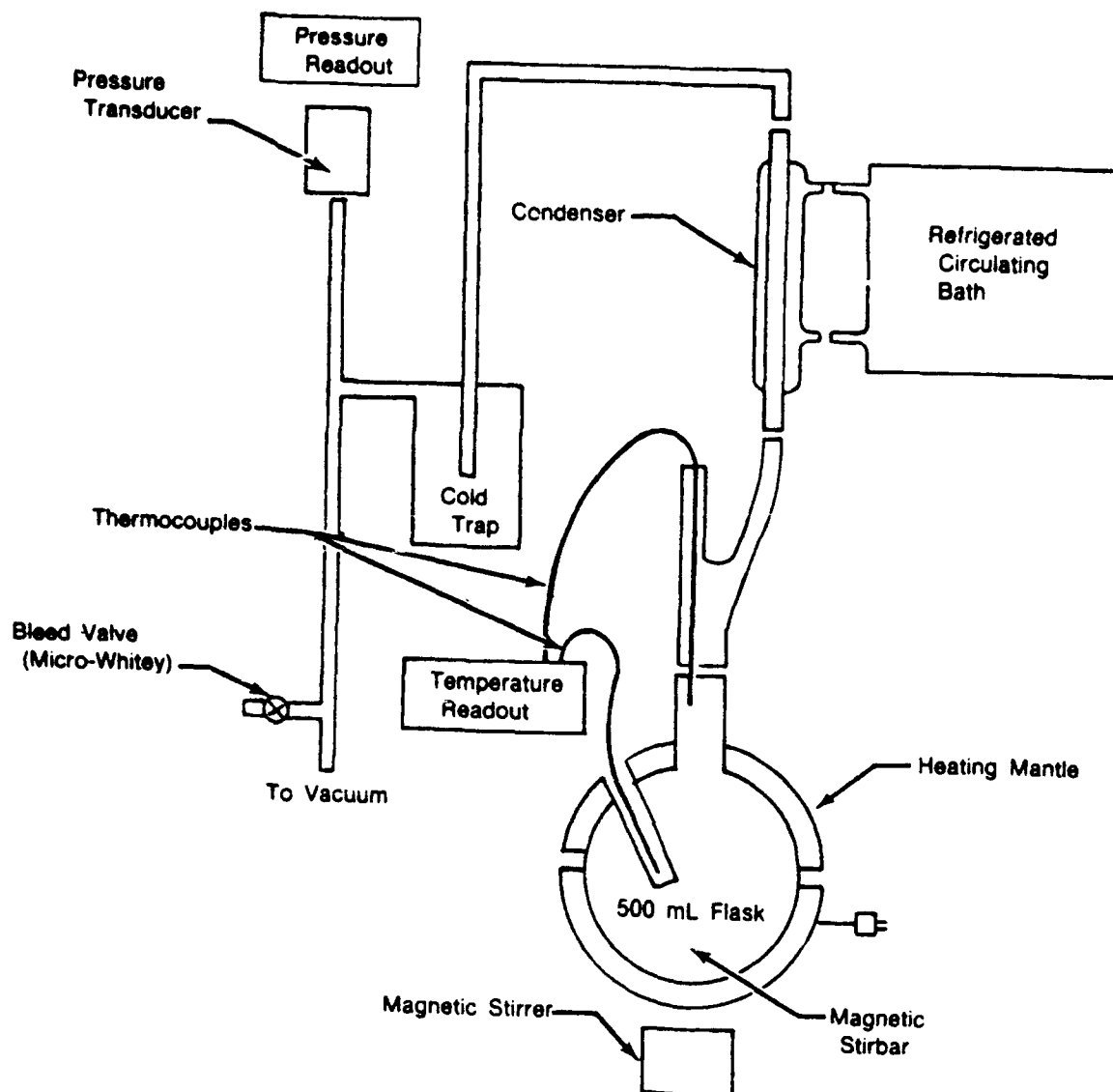
causing errors in vapor pressure determinations.

9. CALCULATIONS

Calculations are to be performed as follows:

1. Plot on semilog paper the reciprocal of absolute temperature on the abscissa versus the logarithm of vapor pressure in psi on the ordinate for each boiling point.
2. Draw a smooth curve through the boiling points obtained, extending the lines slightly at each end.
3. Report the results of vapor pressure as determined by the vapor reflux method from the prepared graph at desired temperatures.

Note: An alternate method of plotting the vapor pressure as a function of temperature has been found to be satisfactory. Using three-cycle semilog paper, plot the temperature ($^{\circ}\text{F}$) on the abscissa and the logarithm of pressure (psia) on the ordinate for each boiling point. A smooth curve can be drawn through these points.



FD 303707

Figure A-1. Vapor Pressure Apparatus Reflux Method

DETERMINATION OF FUEL PROPERTIES AND GENERAL ANALYSIS

Period of Performance

15 November 1985 through 30 October 1986

Reference

Task Order No. 2, Topical Report No. 5, October 1986, FR 19032-5, T.B. Biddle, W.H. Edwards, S.J. Guisinger, R.J. Meehan, P.A. Warner

Abstract

The technical work performed under this task order was directed toward responding to the Air Force's requirements for rapid analysis and short term investigations of fuels and fuel system components to identify the cause of fuel-related problems or anomalies that exhibit the potential to adversely affect aircraft performance. Additionally, experimental fuels and fuels with unique properties were analyzed to ascertain as precisely and accurately as practical the experimental value of the property measured. A specified number of these tests were conducted as a function of temperature over a range of -60 to 75°C (-76 to 167°F).

SECTION 1.0

INTRODUCTION

The necessity of an adequate supply of dependable fuels for operational use demands in-depth knowledge and insight into the concerns affecting fuel availability and the potential consequences or tradeoffs resulting from the use of fuels from alternate sources and broadened specification fuels. This is being emphasized by the current effort initiated by the United States Air Force to use a higher-density, lower-volatility fuel to bolster the volumetric energy value and increase the range of volume-limited aircraft.

Independent Research and Development (IR&D) programs and government-funded investigations conducted at the P&W Engineering Division-South have played a fundamental role in establishing a data base in broad areas of fuel technology. These areas include fuel production and availability, fuel storage and transportation, fuel contamination, fuel composition, fuel development, additive effectiveness, fuel and material compatibility, fuel performance, and test method development for evaluating fuel properties. Many of these efforts have been exerted in response to identifying and resolving problems experienced in the field and on engine test stands.

Performance and durability problems experienced in the field can often be attributed to a number of causes, some of which involve fuel handling and storage, and the effects of fuel property changes. In an attempt to define the cause of possible fuel-related problems that might be anticipated in the field, cognizance of fuel properties which have the most significant impact on engine performance and life, the specific components affected, and the nature of the effect is of consequence.

Based on these considerations, the technical work described in the following sections was directed toward responding to the Air Force's requirements for rapid analysis and short term investigations of fuels and fuel system components to identify the cause of fuel-related problems or anomalies that exhibit the potential to adversely affect aircraft performance. Additionally, experimental fuels and fuels with unique properties were analyzed to ascertain as precisely and accurately as practical the experimental value of the property measured. A specified number of these tests were conducted as a function of temperature over a range of -60 to 75°C (-76 to 167°F).

SECTION 2.0

EXPERIMENTAL

2.1 DETERMINATION OF FUEL PROPERTIES AND GENERAL ANALYSIS

Six Exxon produced experimental high density fuels, refined from light cycle gas oil (LCGO), were received for determinations of hydrocarbon type by mass spectroscopy, gross and net heat of combustion and kinematic viscosity as a function of temperature. These candidate JP-8X samples were identified as 85-POSF-2263, 85-POSF-2264, 85-POSF-2265, 85-POSF-2266, 85-POSF-2267 and 85-POSF-2268, respectively.

Two field samples of unknown origin, 85-POSF-2378 and 85-POSF-2379, were received for determination of hydrocarbon type by mass spectroscopy and simulated distillation. These samples were acquired by AFWAL/POSF through the Air Force Technology Division and were originally suspected to be gasoline.

2.1.1 Hydrocarbon Type by Mass Spectroscopy and FIA

Determination of hydrocarbon types by mass spectroscopy was accomplished using ASTM D2789 under the direction of Dr. Gene Sturm at the National Institute of Petroleum & Energy Research (NIPER). The mass spectrometer used in the hydrocarbon type analysis was a Consolidated Electrodynamics Corporation, Type 21-103, with a heated inlet system. The analyses consisted of determining a matrix of equations relating each of the hydrocarbon types to a summation of characteristic mass spectral lines. Average carbon numbers were determined for the paraffinic and aromatic fractions and used in setting up a series of simultaneous equations. The simultaneous equations were then solved to provide a relative measure of each compound type present. The paraffins, monocycloparaffins, dicycloparaffins, alkylbenzenes, indans and tetralins, and naphthalenes were calculated in volume percents.

The olefin content of the fuel samples was determined by P&W using the Fluorescent Indicator Adsorption (FIA) liquid chromatography method described in ASTM D1319. Since ASTM D2789 includes the olefins in the monocycloparaffin volume percentage, the olefin volume percent as determined by ASTM D1319 was subtracted from the monocycloparaffin content given by ASTM D2789 to reflect accurately both the monocycloparaffin and olefin volume percentages.

2.1.2 Gross and Net Heats of Combustion

The gross heat of combustion at 25°C (77°F) was determined using a procedure similar to ASTM D2387, "Heat of Combustion of Hydrocarbon Fuels by Bomb Calorimeter, High Precision Method", utilizing a Parr Model 1720 Calorimeter Controller and Model 1241 Calorimeter. The Parr system utilizes thermistor controller/temperature monitors as opposed to platinum resistance thermometry and has been found, in this laboratory, to provide accuracy and precision equivalent to ASTM D2382. Gross heats of combustion were calculated using the correction for the heat of formation of the sulfuric and nitric acids produced during combustion. Determination of the sulfur contents were performed using the ASTM D3120 Method, "Trace Quantities of Sulfur by Oxidative Microcoulometry." The sulfur contents were reported in weight percent.

The net heats of combustion were calculated using the hydrogen content determined by ASTM D3701, "Hydrogen Content By Low Resolution Nuclear Magnetic Resonance Spectrometry Method." Hydrogen contents were also reported in weight percent.

2.1.3 Kinematic Viscosity as a Function of Temperature

Viscosities were determined using ASTM D445, "Kinematic Viscosity of Transparent and Opaque Liquids." Thermometers were calibrated with an NBS-certified platinum resistance thermometer and conformed to ASTM E-77, "Verification and Calibration of Liquid-in-Glass Thermometers." Viscosity tests performed below 25°C

(77°F) used a NESLAB refrigerated viscosity bath with a temperature variation of less than 0.03°C (0.05°F). At these low temperatures, drying tubes were placed on the open ends of the viscometers which prevented water condensation inside the viscometer. Kinematic viscosities were performed at -40°C (-40°F), -20°C (-4°F), 25°C (77°F), and 40°C (104°F).

2.1.4 Simulated Distillation

Simulated distillation by gas chromatography was performed at Pratt & Whitney per ASTM D2887, "Boiling Range Distribution of Petroleum Fractions by Gas Chromatography," using a Packard Model 439 gas chromatograph with a Flame Ionization Detector (FID). Data acquisition and reduction were accomplished with a Nelson analytical 3000 Series Chromatography Data System with software interfaced to an IBM PC AT Minicomputer. The column was a packed type with Chromasorb WHP, 80 to 100 mesh, and liquid phase of SE-30, 10% loading. Temperature readings were taken after every 5% volatilized from the initial to the final boiling points of the samples.

SECTION 3.0

RESULTS AND DISCUSSIONS

3.1 DETERMINATION OF FUEL PROPERTIES AND GENERAL ANALYSIS

3.1.1 Hydrocarbon Type Analysis by Mass Spectroscopy and FIA

Hydrocarbon group-type analyses is a widely used procedure for obtaining information needed to evaluate feedstocks and products in the petroleum industry. The performance and specifications of jet fuels are inherently dependent upon the types of hydrocarbons present.

The fuel samples received for hydrocarbon type analysis consisted of the six candidate high density JP-8X fuels and the two Air Force Foreign Technology Division field samples. As shown in Table 1, straight and branched chain paraffins are present at much lower concentrations in the JP-8X fuels than are apparent in the field samples. Saturates making up the JP-8X fuels are predominantly in the cyclic forms, as the "highly naphthenic" description for candidate JP-8X fuels would imply. Consequently, it could be predicted that these JP-8X fuels would exhibit higher densities, lower gravimetric heats of combustion, lower hydrogen content and increased smoke point as compared to conventional fuels. The field samples were comprised largely of straight and branched chain saturates followed by monocycloparaffins. Unlike the high density fuels, the field samples contained only small concentrations of dicycloparaffins.

3.1.2 Gross and Net Heats of Combustion

Heat of combustion is a measure of the energy available from a fuel. Specific fuel types have characteristic heats of combustion. A knowledge of this value is essential when considering the thermal efficiency of equipment for producing either power or heat. The heat of combustion per unit mass of fuel is particularly important to weight-limited aircraft as the distance an aircraft can travel on a given weight of fuel is a direct function of the fuel's mass heat of combustion and its density. The volumetric heat of combustion is important to volume-limited aircraft as it is directly related to the distance traveled between refuelings.

Gross and net heats of combustion were determined for the six JP-8X high density candidate fuels along with the percentage by weight hydrogen and sulfur content, and the percentage by volume aromatic content. As shown in Table 2, the heats of combustion correlate with the hydrocarbon types present in the six high density fuels. In general, the fuels which were more paraffinic in nature with lower aromatic and bicyclic components exhibit the higher heats of combustion. This is most evident when comparing the first two fuels tabulated (85-POSF-2263 and 85-POSF-2264) with the last four fuels shown (85-FOSF-2265 through 85-POSF-2768). It should be noted that for all but one exception; the higher gravimetric heats of combustion were directly related to the lower indan,

tetralin and naphthalene content of the JP-8X candidate fuels. As shown in Table 2, higher gravimetric heats of combustion correlate well with increases in hydrogen content, while volumetric heats of combustion tend to decrease with increasing hydrogen content as a result of decreases in density.

3.1.3 Kinematic Viscosity as a Function of Temperature

Aviation fuels must have acceptable low-temperature fluid characteristics to insure adequate fuel flow to the engine during long missions at high altitudes. The fuel's viscosity is used in the fuel fluidity calculations and affects spray atomization within the combustor, engine starting characteristics, low power combustion efficiency and pattern factor. Reduced ignition capability can occur with the more viscous fuels along with reduced flow during low temperature start transients and reduced augmentor functional suitability.

Kinematic viscosity results over a temperature range of -40° to $+40^{\circ}\text{C}$ are shown for the six JP-8X high density fuels in Table 3 and Figure 1. As shown in Figure 1, kinematic viscosity decreases logarithmically with increasing temperature. Sample No. 85-POSF-2266, containing the greatest concentration of straight and branch chain paraffins and lowest concentration of dicycloparaffins is shown somewhat lower than the remaining JP-8X fuels on the viscosity-temperature curve.

3.1.4 Simulated Distillation

Distillation characteristics are a measure of volatility and give a broad indication of fuel type. Aircraft engine fuels must be easily convertible from storage in the liquid form to the vapor phase, which allows the formation of the combustible air/fuel vapor mixture. In gas turbine engines, fuel volatility influences the rate at which the fuel spray vaporizes, thereby influencing ignition, combustion efficiency and combustor exhaust temperature profile (pattern factor). Ignition characteristics are affected primarily by lower boiling fractions (i.e. the 10% distillation temperature) while combustion efficiency and pattern factor are believed to be controlled by the heavier fuel fractions (i.e. the 90% distillation temperature).

Table 4 is a tabulation of the simulated distillation data for the two Air Force Technology Division fuels designated as sample numbers 85-POSF-2378 and 85-POSF-2379. Although these samples were originally identified as gasoline-type fuels, the distillation characteristics shown in Table 4 would suggest a Jet A, Jet A-1, or JP-8 rather than a gasoline, or a gasolene which was severely weathered. The two samples were of unknown origin. For comparative purposes, a typical simulated distillation range for JP-4 would approximate an initial boiling point of 25°C (77°F) and a final boiling point of 275°C (527°F).

TABLE 1
HYDROCARBON TYPE ANALYSES OF CANDIDATE HIGH DENSITY

	Fuel Samples						
	2263	2264	2265	2266	2267	2268	2378 2379
<i>NIPER Results Using ASTM D2789 (Mass Spec)</i>							
Paraffins	11.7	10.7	9.3	30.3	9.6	5.3	54.3 63.6
Monocycloparaffins ¹	19.7	18.5	27.1	25.4	28.5	41.5	30.5 24.4
Dicycloparaffins	27.7	26.4	43.5	18.2	46.7	50.6	3.5 0.7
Alkylbenzenes	16.8	11.4	6.0	15.3	6.2	2.0	9.3 8.9
Indans and tetralins	21.3	28.5	12.0	9.5	7.8	0.6	1.4 1.4
Naphthalenes	2.3	3.9	1.5	0.8	0.7	BDL ²	0.5 0.5
Olefins ¹	0.6	0.6	0.5	0.5	0.5	BDL ²	0.5 0.4
<i>Pratt & Whitney Results Using ASTM D1319 (FIA)</i>							
Saturates	52.4	45.9	74.7	71.6	80.9	95.1	84.4 85.2
Aromatics	47.0	53.5	24.8	27.9	18.6	4.9	15.1 14.4
Olefins	0.6	0.6	0.5	0.5	0.5	BDL ²	0.5 0.4
<i>Average Carbon Number from NIPER Results Using ASTM D2789 (Mass Spec)</i>							
Paraffin	9.19	9.27	8.72	9.65	9.11	12.00	9.45 9.64
Aromatic	8.86	8.83	9.14	9.20	8.65	6.04	8.82 8.72
¹ Olefin values taken from the ASTM D1319 results, subtracted from ASTM D2789 matrix inverse results for monocycloparaffins							
² Below detectable limits							

TABLE 2
HEAT OF COMBUSTION DATA FOR CANDIDATE HIGH DENSITY
FUELS PRODUCED FROM LIGHT CYCLE GAS OIL

POSF No.	H Wt. %	S Wt. %	Gross Heat of Combustion MJ/kg (Btu/lb)	Net Heat of Combustion MJ/kg (Btu/lb)	Volumetric Heat of Combustion MJL (Btu/gal)
85-2263	12.18	0.004	44.743 (19236)	42.158 (18125)	37.054 (132942)
85-2264	11.89	<.002	44.485 (19125)	41.962 (18040)	37.724 (135345)
85-2265	12.89	<.002	45.236 (19448)	42.501 (18272)	37.422 (134264)
85-2266	13.19	0.004	45.513 (19567)	42.714 (18364)	36.063 (129393)
85-2267	13.08	<.002	45.229 (19445)	42.453 (18252)	37.083 (133051)
85-2268	13.55	<.002	45.655 (19628)	42.642 (18333)	36.996 (132739)

TABLE 3
KINEMATIC VISCOSITY FOR CANDIDATE HIGH DENSITY
FUELS PRODUCED FROM LIGHT CYCLE GAS OIL

Sample No.	Kinematic Viscosity			
	-40°C (-40°F)	-20°C (-4°F)	25°C (77°F)	40°C (104°F)
85 POSF 2263	20.83	7.97	2.31	1.76
85 POSF 2264	35.40	11.19	2.75	2.05
85 POSF 2265	34.96	11.79	2.95	2.19
85 POSF 2266	10.78	5.02	1.77	1.40
85 POSF 2267	27.16	9.94	2.69	2.05
85 POSF 2268	30.65	11.07	2.93	2.19

TABLE 4
SIMULATED DISTILLATION FOR AF FOREIGN DIVISION
FIELD SAMPLES

Fuel Sample No.	<i>Temperature °C (°F)</i>	
	T-1 (802) Fuel	Fuel 102
IBP	96.5 (205)	105.5 (222)
5 %	133.0 (271)	134.0 (273)
10 %	138.0 (280)	140.0 (284)
15 %	142.5 (289)	146.0 (295)
20 %	150.0 (302)	151.5 (304)
25 %	152.5 (306)	157.0 (314)
30 %	160.0 (320)	162.0 (323)
35 %	164.0 (327)	166.5 (332)
40 %	168.5 (336)	172.0 (342)
45 %	174.5 (346)	175.5 (348)
50 %	177.0 (351)	180.0 (356)
55 %	183.5 (362)	186.0 (367)
60 %	189.5 (373)	192.0 (378)
65 %	196.0 (385)	197.0 (386)
70 %	198.0 (388)	200.0 (392)
75 %	205.5 (402)	207.5 (405)
80 %	212.0 (414)	214.0 (417)
85 %	217.0 (423)	217.5 (423)
90 %	222.0 (432)	223.5 (434)
95 %	231.5 (449)	232.5 (451)
FBP	249.0 (480)	250.5 (483)

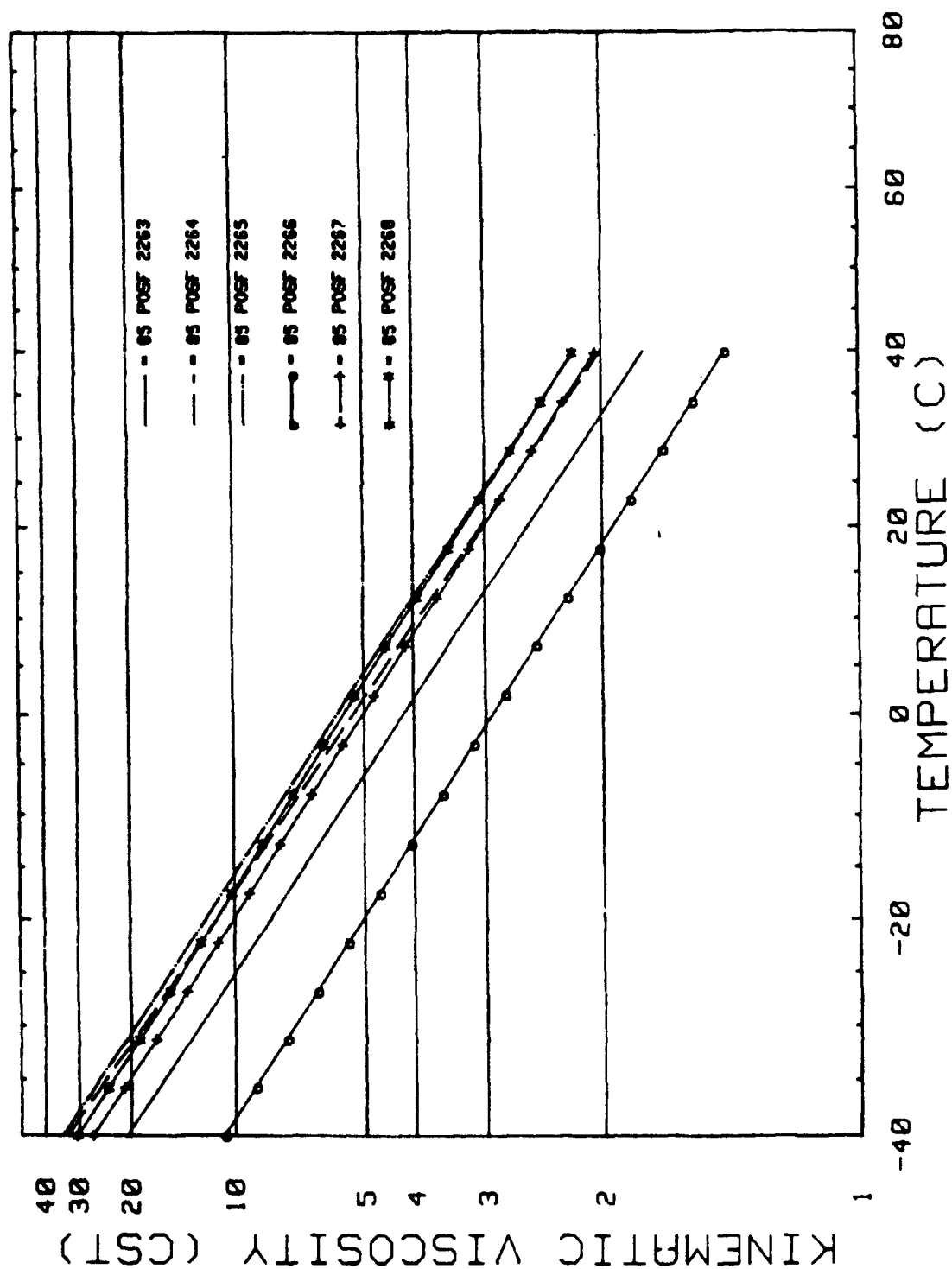


Figure 1. Kinematic Viscosity As a Function of Temperature For Candidate High Density JP-8X Fuels

SECTION 4.0

CONCLUSIONS

Straight and branched chain paraffins were found to be present in much lower concentrations in the candidate JP-8X fuels than were apparent in the field samples. Saturates making up the JP-8X fuels were found to be predominantly the cyclic form. in contrast to the high density fuels, the field samples contained only small concentrations of dicycloparaffins. Heats of combustion correlated well with the hydrocarbon types present in the six high density fuels. Higher gravimetric heats of combustion were exhibited by those fuels which were highly paraffinic and lower in aromatic and bicyclic compounds. Simulated distillation data for the 2 Air Force Foreign Technology Division samples of unknown origin and fuel type, indicate a Jet A, Jet A-I, or JP-8 type fuel.

DETERMINATION OF THERMAL CONDUCTIVITY OF AIRCRAFT/MISSILE FUELS

Period of Performance

15 December 1985 through 1 April 1986

Reference

Task Order No. 5, Topical Report No. 2, FR 19032-2, April 1986, S.J. Guisinger, T.B. Biddle, P.A. Warner

Abstract

Six fuels were evaluated to determine thermal conductivity as a function of temperature: JP-4, JP-7, JP-8, JP-10, RJ-6 and JP-TS. The fuel samples were evaluated in duplicate along with two standards over the temperature range from 0°C to 75°C.

SECTION 1.0

INTRODUCTION

Aircraft and missile fuels have an important secondary use as a heat sink, cooling the aircraft electronic equipment, hydraulic fluids and lubricants. The rate at which heat energy is transferred through the fuel is called its thermal conductivity.

In the "Handbook of Aviation Fuel Properties" compiled by the Coordinating Research Council (CRC) Aviation Handbook Advisory Group, the thermal conductivities for all hydrocarbon based aircraft and missile fuels are represented as one straight line function dependent on temperature. The objective of this investigation was to determine whether these fuels do, in fact, possess the same thermal conductivity/temperature relationship or if thermal conductivity is dependent upon fuel type.

Six fuels were evaluated to determine thermal conductivity as a function of temperature in this task: JP-4, JP-7, JP-8, JP-10, RJ-6 and JP-TS. The fuel samples were evaluated in duplicate along with two standards over the temperature range from 0°C to 75°C.

SECTION 2.0

EXPERIMENTAL

Determination of thermal conductivity was accomplished in accordance with ASTM D2717, "Test for Thermal Conductivity of Liquids" at Phoenix Chemical Laboratory in Chicago, Ill. This method is applicable to liquids that are chemically compatible with borosilicate glass and platinum, moderately transparent or absorbent to infrared radiation, and have a vapor pressure less than 27 kPa (3.9 psia) at the test temperature. Materials that have vapor pressures of up to 395 kPa (50 psia), such as JP-4, are also tested provided that adequate measures are taken to repress volatilization of the sample of pressurizing the thermal conductivity cell. All the fuels investigated in this task order had these characteristics

making this a valid method for determining thermal conductivity.

The thermal conductivity measurement cell consisted of a straight, four-lead, platinum resistance thermometer element located concentrically in a long, small-diameter, precision-bore borosilicate glass tube. The thermal conductivity was then determined by measurement of the temperature gradient across the fuel which was generated from a known amount of energy introduced into the test cell by an electrically heated platinum element.

The conductivity of the glass cell body was obtained from the manufacturer's literature, with additional calibration accomplished by using a standard. The temperature-resistance relationship of the cell filament was determined by measurement of its resistance at various temperatures with the cell filled with freshly boiled distilled water or the sample.

Measurements at 30, 50 and 75°C used a specially designed oil bath to achieve and maintain temperature to within $\pm 0.001^\circ\text{C}$. A thermopile was used to control the bath temperature while monitoring of thermal conductivity measurements at 0°C relied on the freeze point of a carefully maintained ice/water bath. The values for thermal conductivities below 0°C were determined by an appropriate linear function.

SECTION 3.0

RESULTS AND DISCUSSION

Table 1 shows the thermal conductivity data for duplicate analysis of the six fuels and a single analysis for each reference standard. Preliminary review of the table indicates good repeatability between the blind duplicates at any given temperature and there appears to be evidence of differentiation between fuel types. However, a rigid data analysis was needed to substantiate any correlations or interactions.

A statistical evaluation using two way analysis of variance with replication was conducted to determine whether the data showed with statistical certainty that fuel type affects thermal conductivity. Table 2 shows the statistical tests rejecting the hypothesis that fuel type does not affect thermal conductivity. The computed F value uses the fuel type as the source of variation and is calculated using equations found in Reference 1. This value is smaller than the critical F value which is found in Reference 2 at 5 and 24 degrees of freedom and a 0.5% level of significance. This indicates that the original hypothesis is rejected and therefore fuel type does influence thermal conductivity at a 99.5% confidence level.

Figures 1 through 11 show the data with a least square fit regression line drawn through the raw data points. With the inherent limitations of the present method precision (ASTM D2717 estimates repeatability at 10%), these curve fits are considered to be more accurate than the raw data over the range of test temperatures at which the values were measured. Also included on each plot is the correlation coefficient, which is a measure of how well the regression equation fits the raw data and the standard error of the estimate, which is a measure of the deviations about the regression line. The regression line parameters of slope and y-intercept are given for ease in determining values at any given temperature. Table 3 shows the values calculated from the regression line for each of the sample fuels and the two standards.

Figures 1 and 3 show the toluene and dimethyl phthalate standard regression lines and correlation parameters while Figures 2 and 4 compare these regression lines to the literature values. As shown, the toluene data is within approximately 4 to 7% of literature values, while the dimethyl phthalate is within 0.7 to 5% of the ASTM values. Figures 5 through 10 show the individual fuel regression line plots. Figure 11 is a comparison of all the fuels showing that the fuel types vary not only in the magnitude of

thermal conductivity, but also vary in thermal coefficients as shown by the difference in slopes.

TABLE 1				
MEASURED THERMAL CONDUCTIVITY, W/M/K				
Fuel Description	0°C	30°C	50°C	75°C
81 POSF 078 (JP-10)	.122	.120	.115	.112
	.122	.121	.115	.113
82 POSF 0562 (JP-8)	.125	.124	.118	.116
	.129	.129	.120	.119
83 POSF 0708 (JP-4)	.124	.125	.116	.119
	.125	.126	.116	.115
83 POSF 0878 (JP-7)	.123	.123	.115	.118
	.127	.120	.116	.116
84 POSF 1688 (RJ-6)	.117	.115	.111	.112
	.119	.115	.109	.112
84 POSF 2075 (JP-TS)	.122	.122	.114	.113
	.124	.122	.115	.112
Standards				
Toluene	.148	.140	.133	.133
Dimethyl Phthalate	.159	.150	.142	.145

TABLE 2

**TWO WAY ANALYSIS OF VARIANCE WITH REPLICATION
TO DETERMINE IF FUEL TYPE AFFECTS THERMAL CONDUCTIVITY**

Hypothesis:	Fuel type does not affect thermal conductivity.
Source of variation:	Fuel Type
Sum of squares:	3.6942×10^{-4}
Degrees of freedom:	5 (6 fuels - 1)
Mean square:	1.8471×10^{-4}
Calculated F:*	30.05
Critical F value:** (0.5% level of significance)	4.49

Conclusion:

Calculated F > Critical F at 0.5% level of significance.

Therefore, there is a 99.5% level of confidence that fuel type affects thermal conductivity.

*Calculated F obtained using equations from Reference 1.

**Critical F obtained from Reference 2 at k-1 degrees of freedom for the variation source, nk(r-1) degrees of freedom for the error and 0.5% significance level.

k = number of treatments or fuel types (6)

n = number of temperatures (4)

r = number of replicate runs (2)

TABLE 3				
CALCULATED THERMAL CONDUCTIVITY, W/M/K*				
Fuel Description	0°C	30°C	50°C	75°C
81 POSF 078 (JP-10)	.123	.119	.116	.113
82 POSF 0562 (JP-8)	.128	.124	.121	.117
83 POSF 0708 (JP-4)	.126	.122	.119	.116
83 POSF 0878 (JP-7)	.125	.121	.118	.115
84 POSF 1688 (RJ-6)	.117	.115	.113	.110
84 POSF 2075 (JP-TS)	.124	.119	.116	.112
CRC Data	.119	.114	.110	.106
Standards				
Toluene	.147	.140	.136	.131
CRC Data	.141	.133	.128	.122
Dimethyl Phthalate	.157	.151	.147	.142
ASTM D2717 Data	.150	.147	.144	.141
* Calculated using least squares fit of measured data				

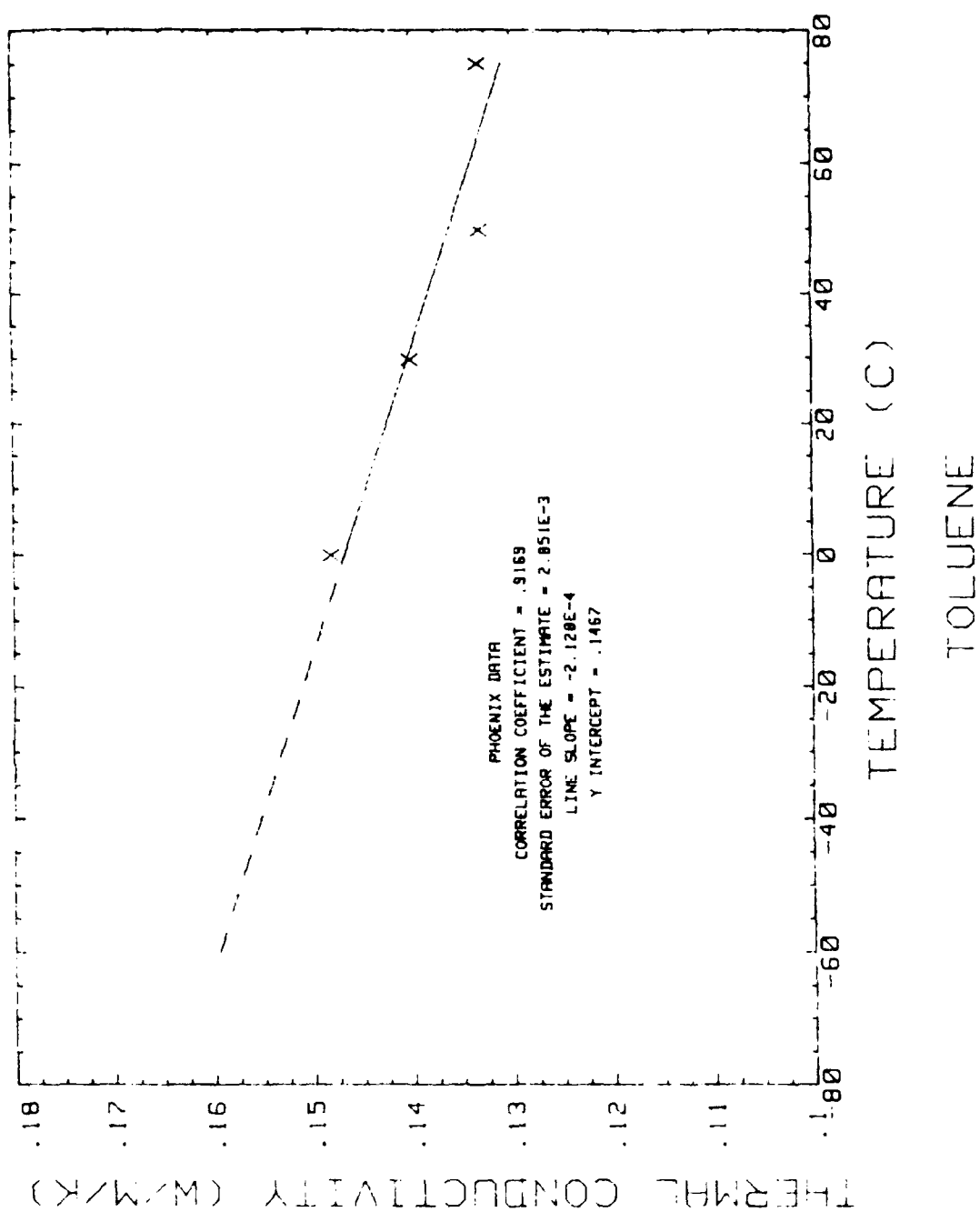


Figure 1. Thermal Conductivity Data Fit for Toluene

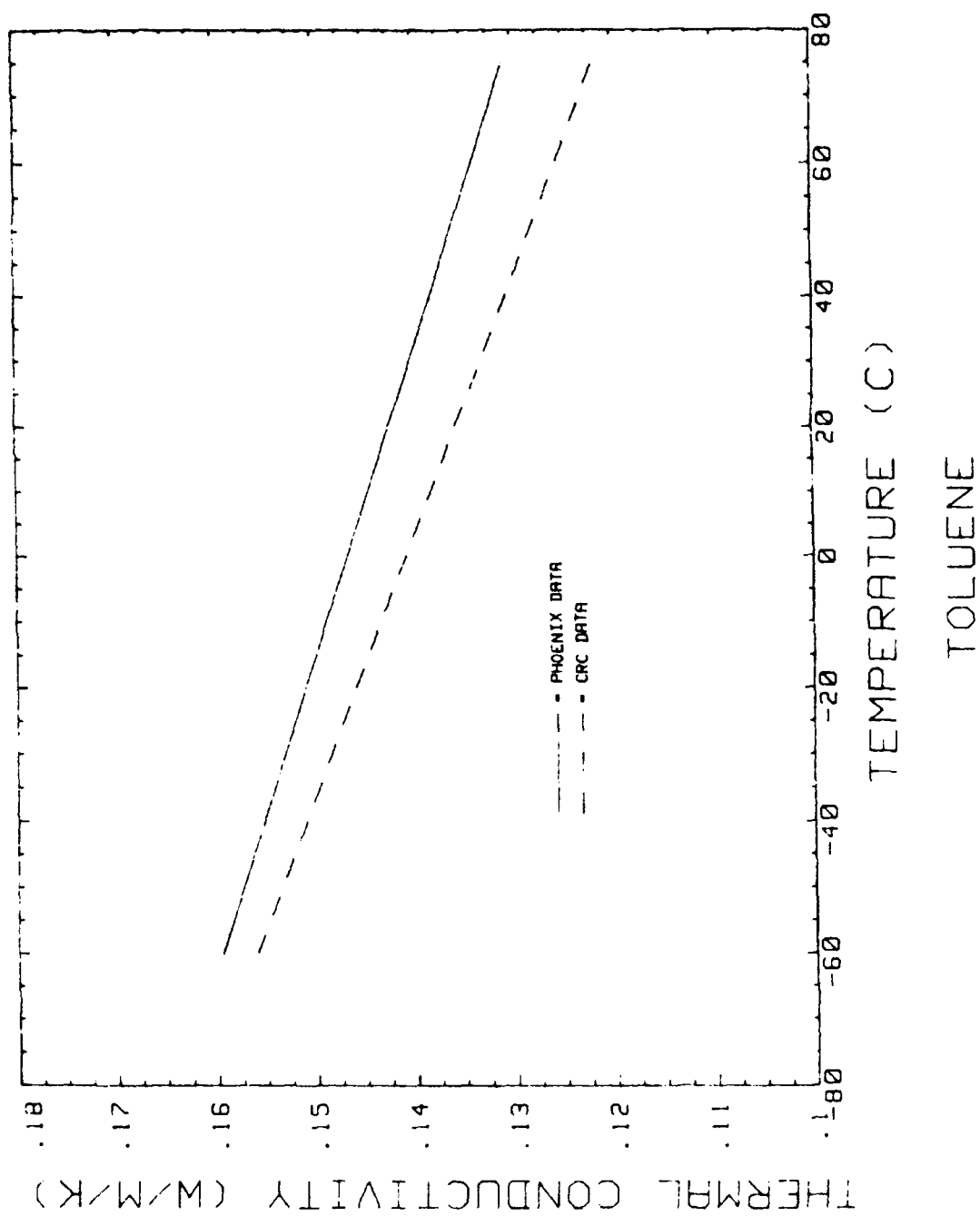


Figure 2. Comparison of Measured Toluene Thermal Conductivity to Literature Values

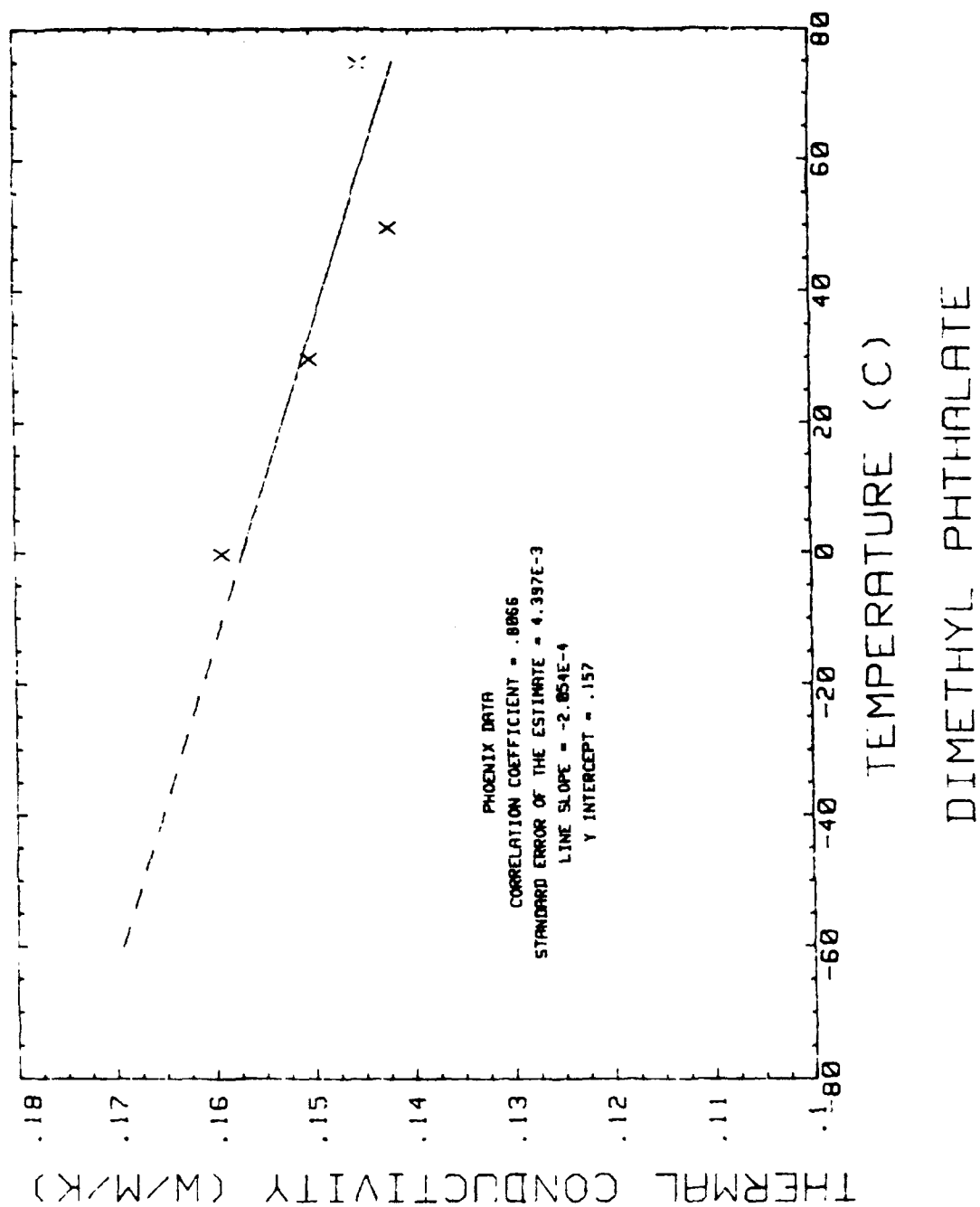


Figure 3. Thermal Conductivity Data Fit for Dimethyl Phthalate

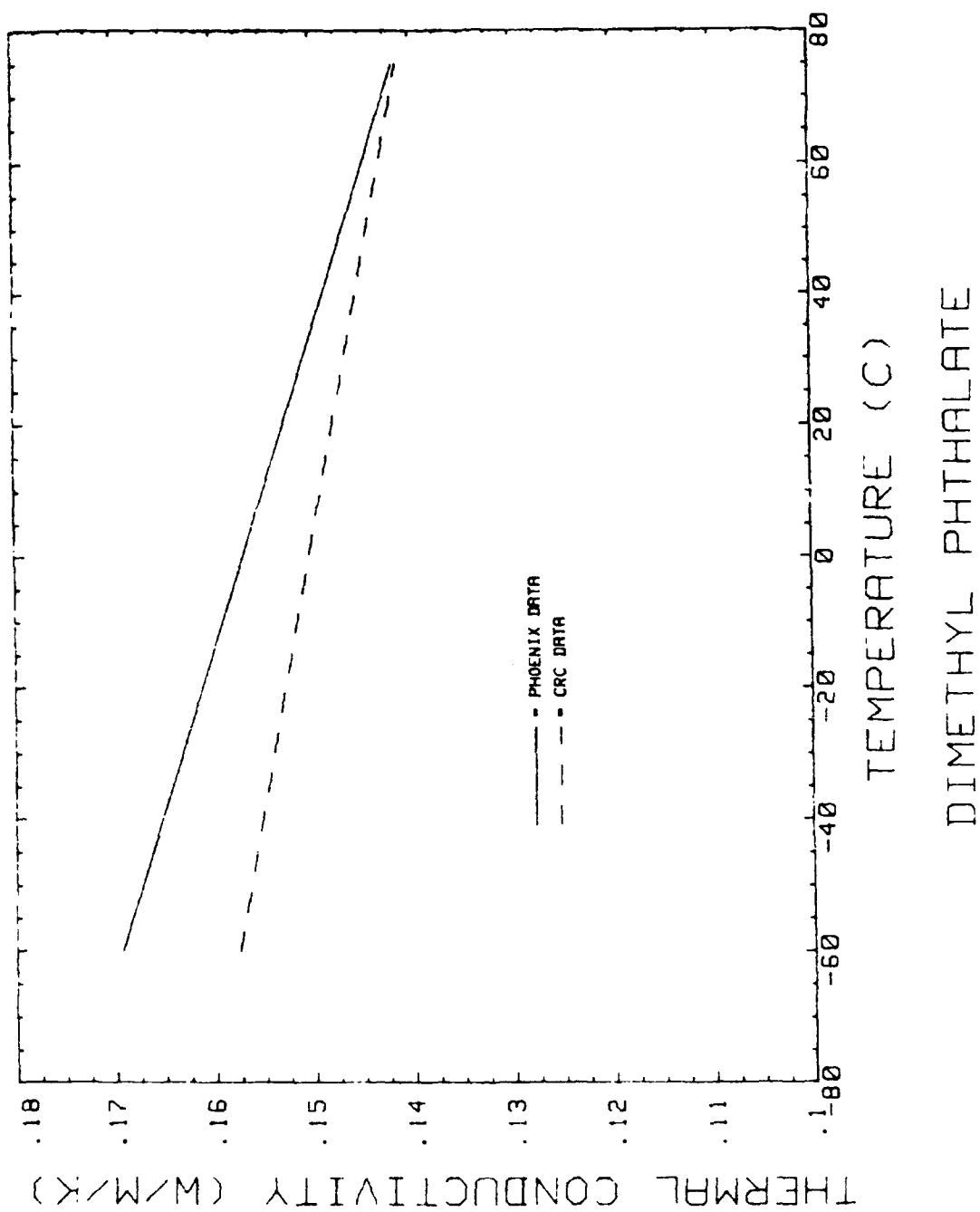


Figure 4. Comparison of Measured Dimethyl Phthalate Thermal Conductivity to Literature Values

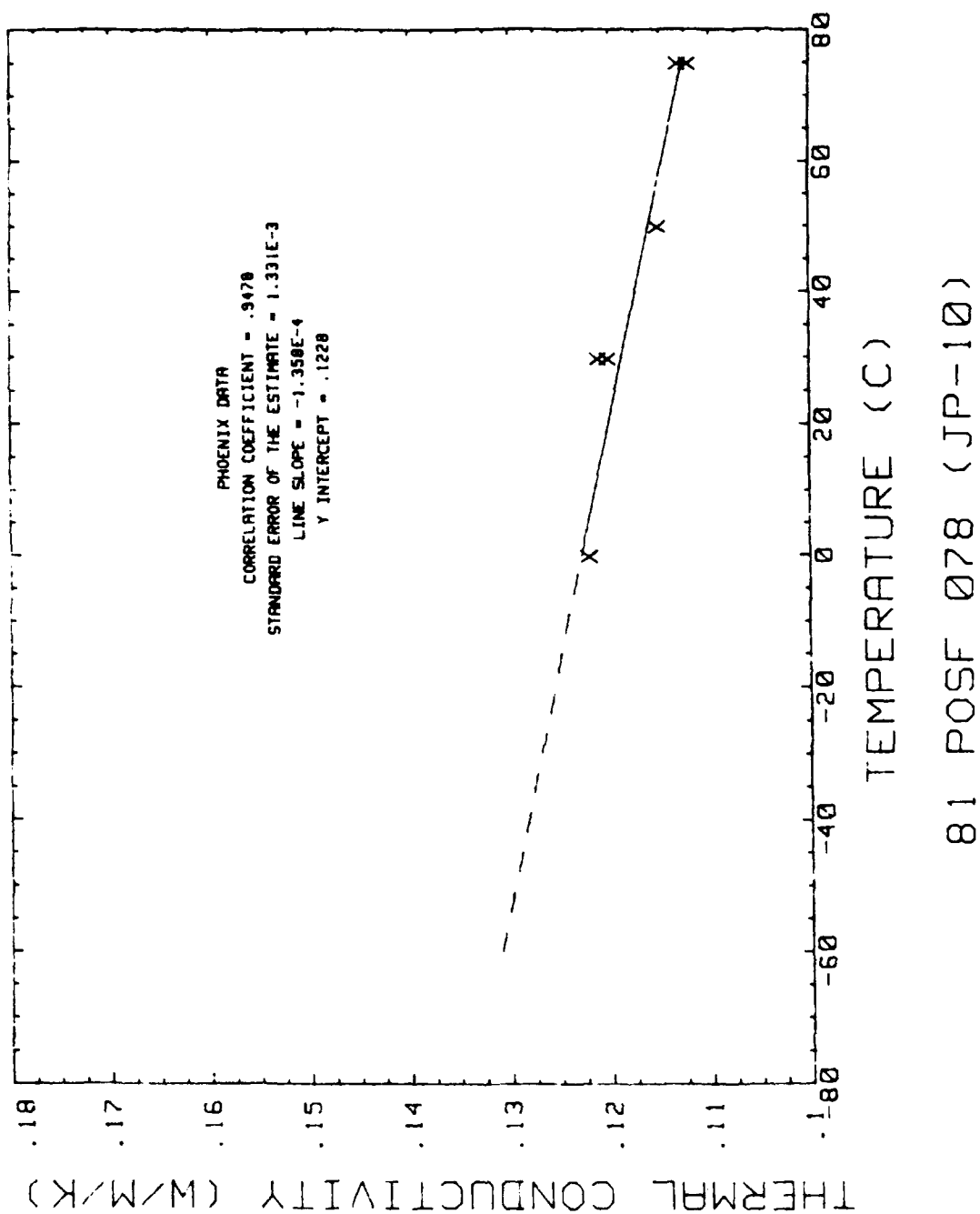
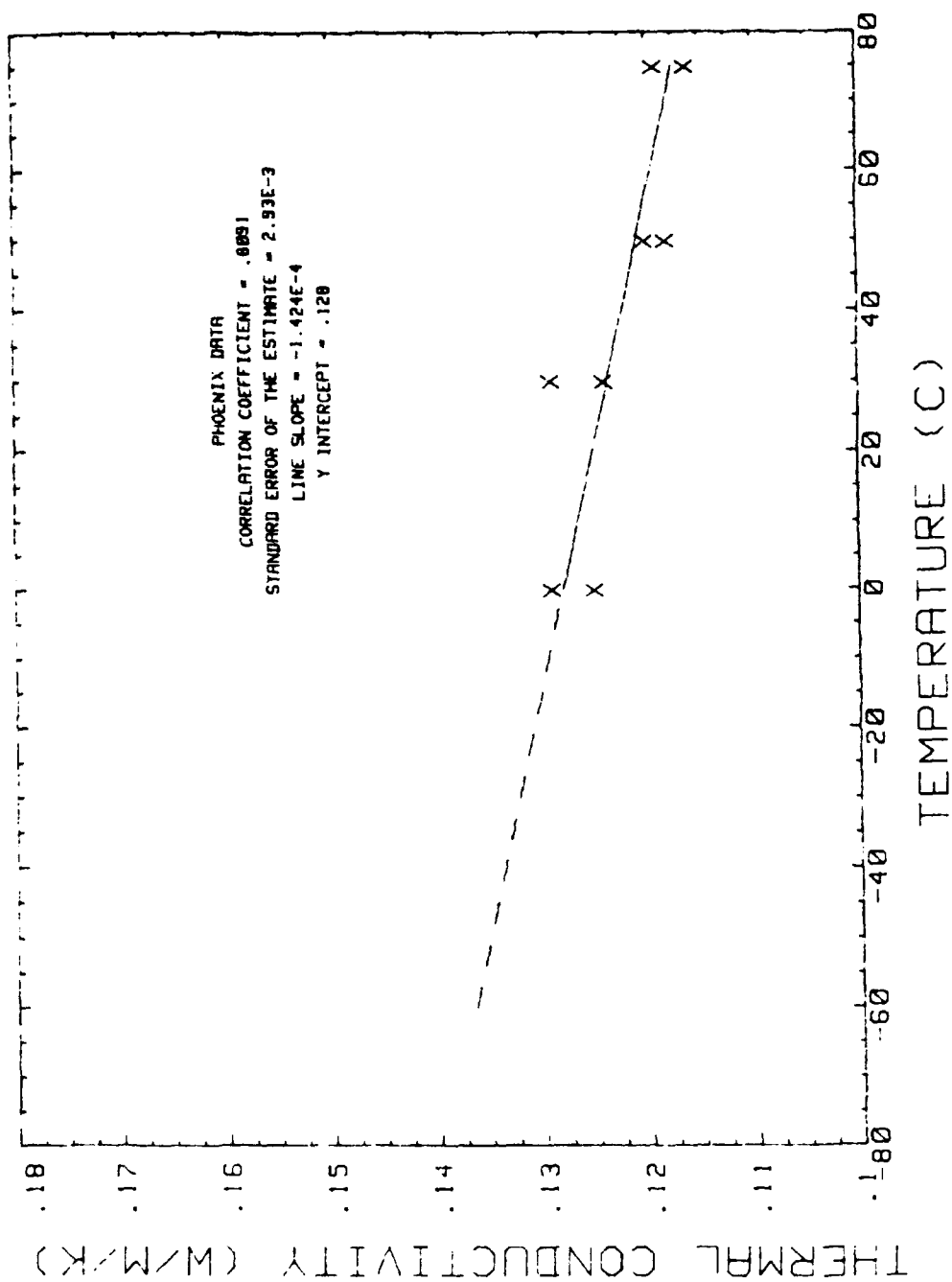
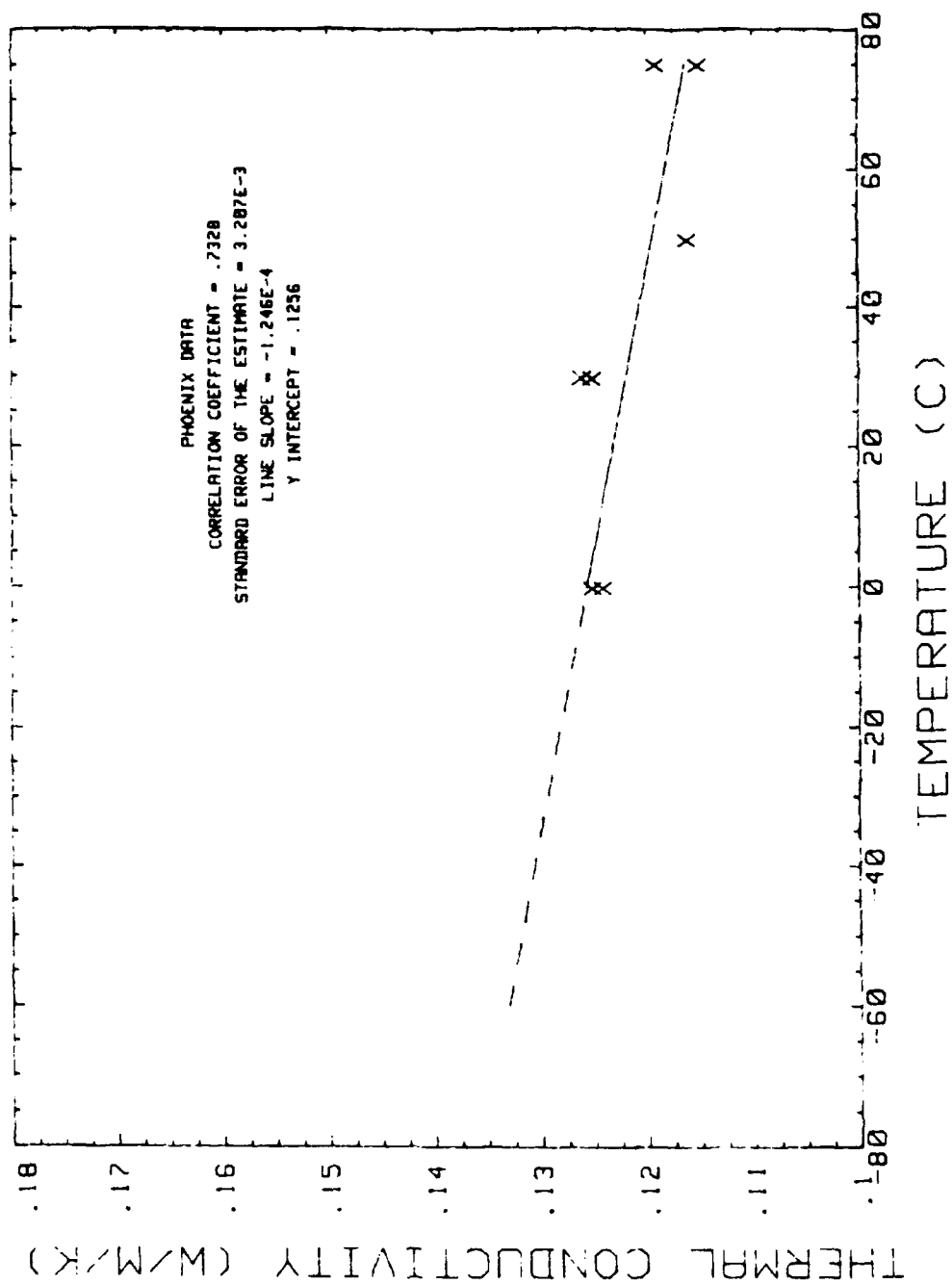


Figure 5. Thermal Conductivity Data Fit for JP-10



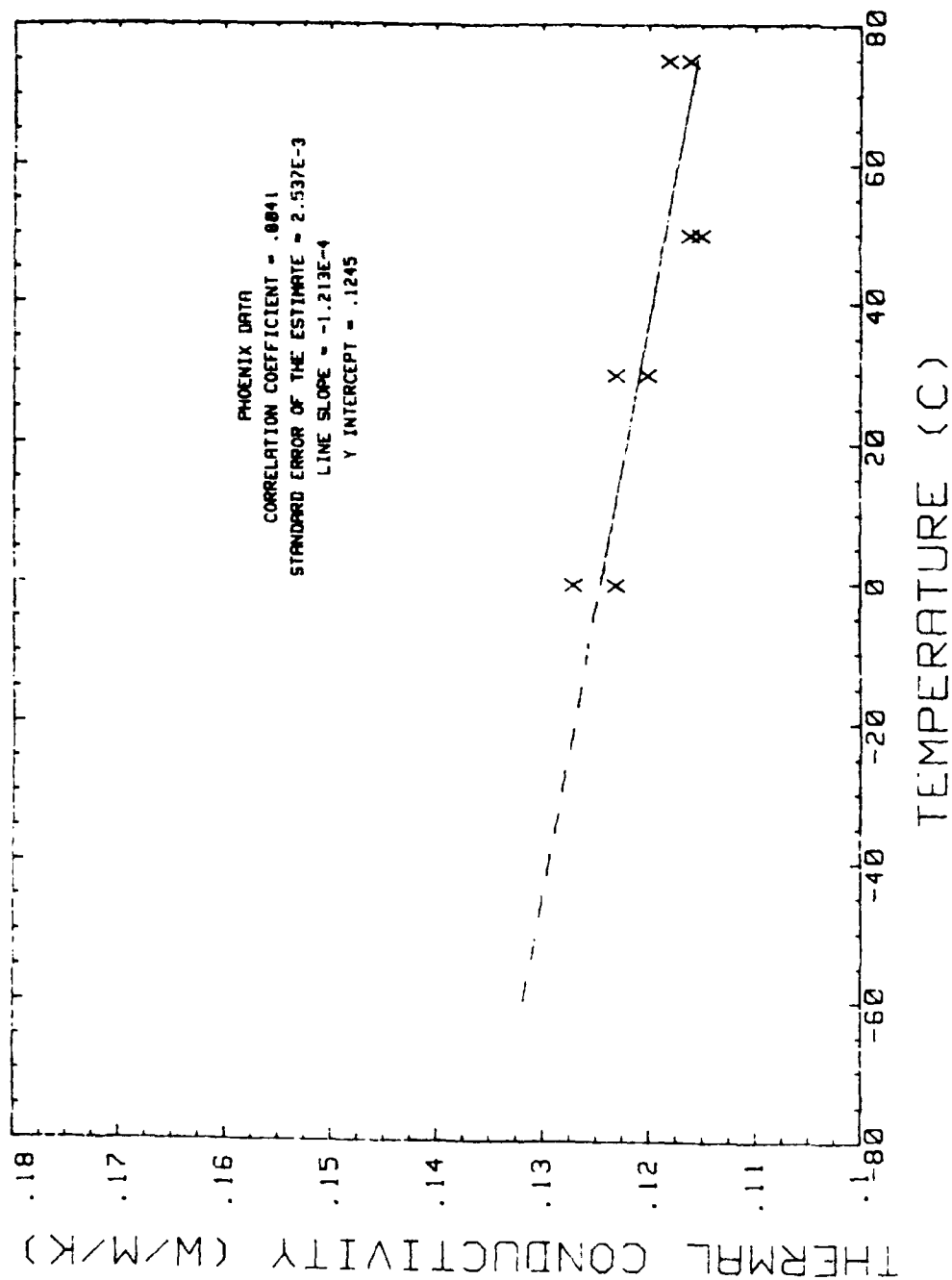
82 POSF 0562 (JP-8)

Figure 6. Thermal Conductivity Data Fit for JP-8



83 POSF 0708 (JP-4)

Figure 7. Thermal Conductivity Data Fit for JP-4



83 POSF 0878 (JP-7)

Figure 8. Thermal Conductivity Data Fit for JP-7

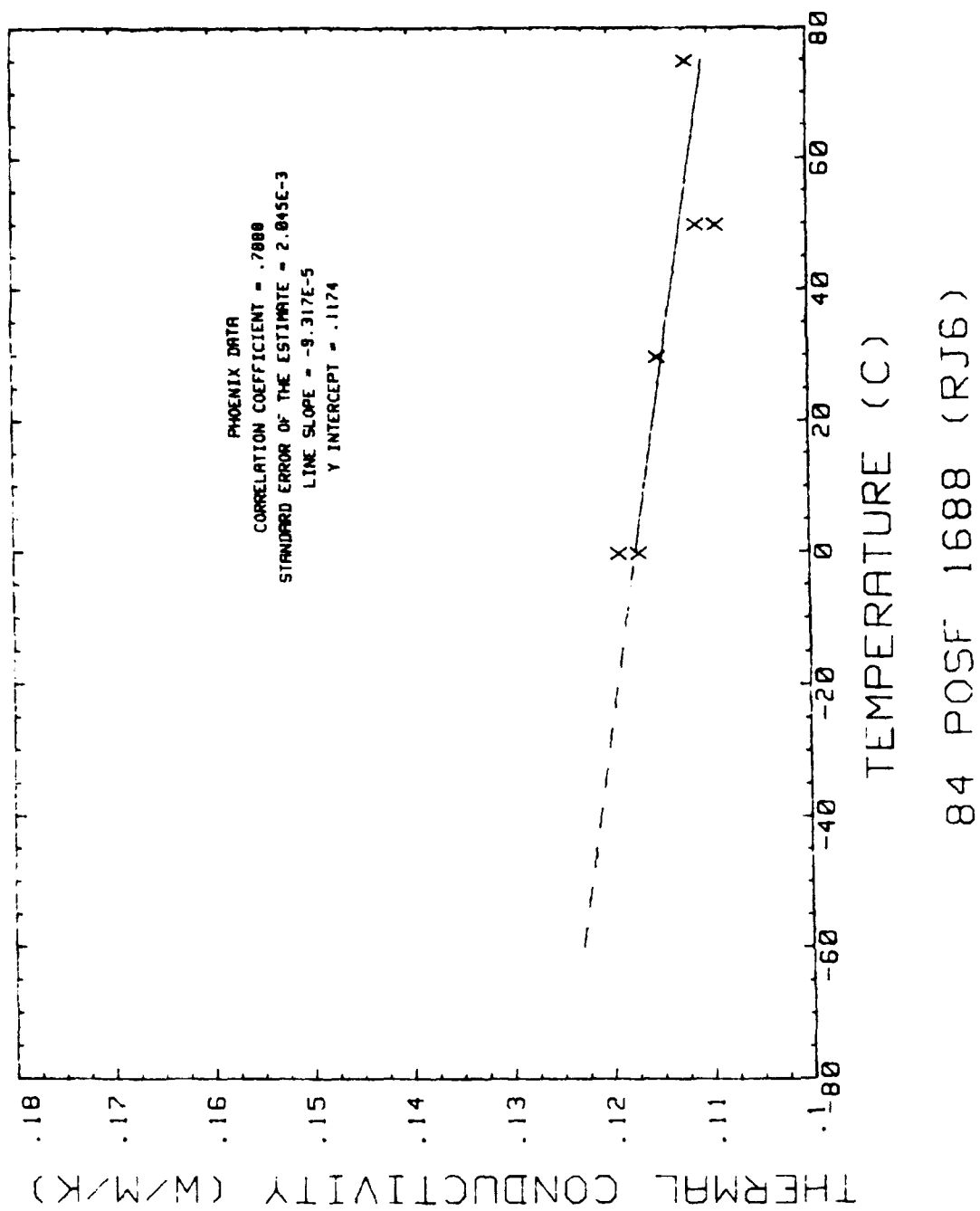
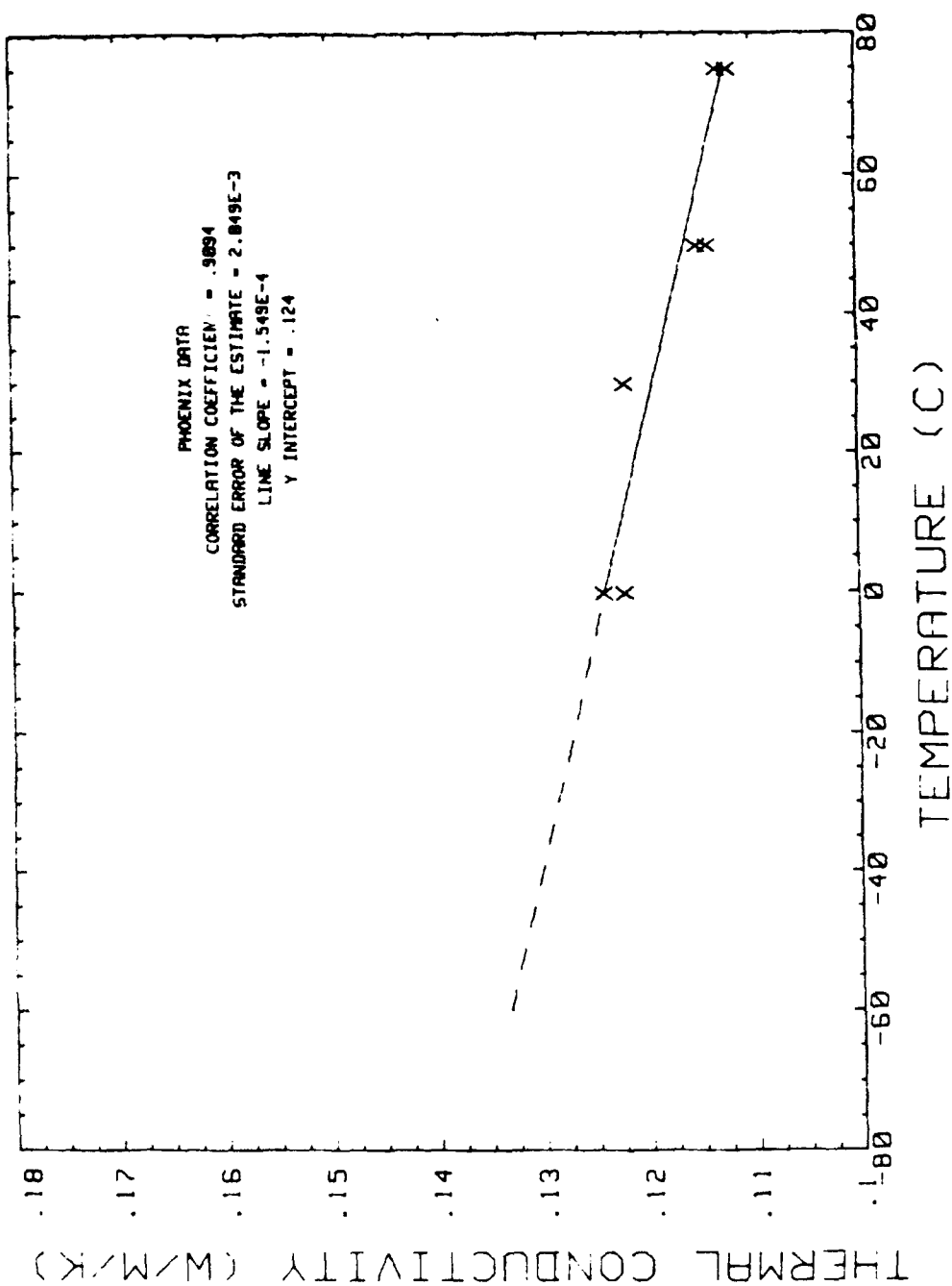
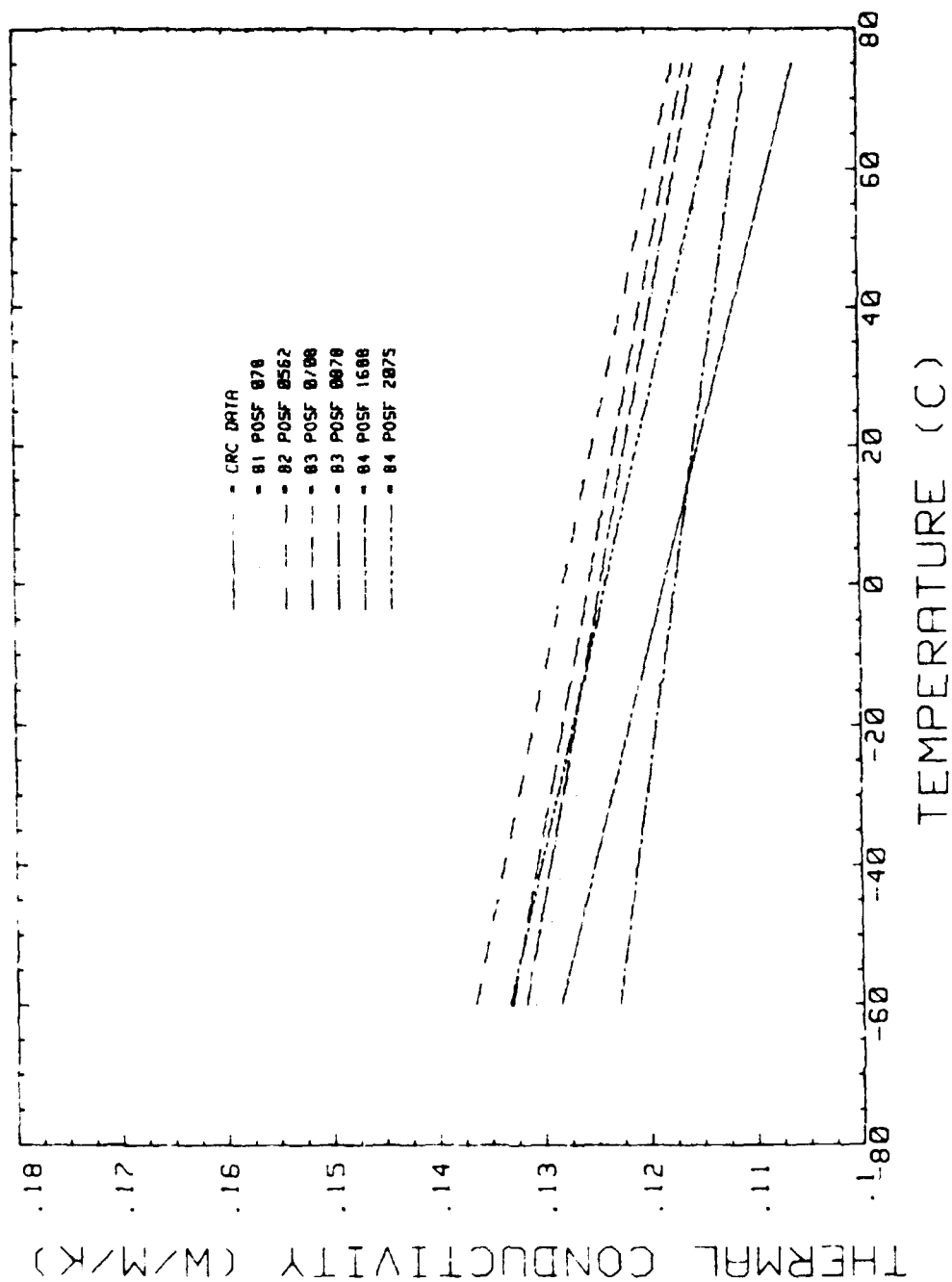


Figure 9. Thermal Conductivity Data Fit for RJ6



84 POSF 2075 (JP-TS)

Figure 10. Thermal Conductivity Data Fit for JP-TS



TASK ORDER NO. 5 AIRCRAFT/MISSILE FUELS

Figure 11. Comparison of Thermal Conductivity and Thermal Coefficients (slope) For All Fuel Types

SECTION 4.0

CONCLUSIONS AND RECOMMENDATIONS

The following conclusions have been ascertained through the statistical analysis of the raw data.

- Due to the inherent limitations in the precision of ASTM D2717, the thermal conductivities of hydrocarbon based fuels calculated from regression line equations produced from measured values are considered more accurate than the raw data.
- Fuel types vary in both magnitude of thermal conductivity and in thermal coefficients. Two way analysis of variance shows that there is a 99.5% confidence level that fuel type affects thermal conductivity and the fuels would be better represented by individual line functions.

It is recommended that a motion containing a proposed change to the "Handbook of Aviation Fuel Properties" be submitted to the CRC for consideration. The change would involve using unique line functions to better represent the individual fuel thermal conductivities in place of the existing single line representation.

REFERENCES

1. "Probability and Statistics for Engineers and Scientists", R. E. Walpole and R. H. Meycr, 2nd ed., 1978.
2. "Statistical Methods for Engineers and Scientists", R. M. Bethea, B.S. Duran, T. L. Boullion, 2nd ed., 1985.

CHARACTERIZATION OF CANDIDATE HIGH DENSITY FUELS

Period of Performance

15 December 1985 through 15 September 1986

Reference

Task Order No. 4, Topical Report No. 3, FR-19032-3, September 1986

Abstract

The Air Force is currently conducting programs designed to obtain demonstration batches of fuels from sources other than petroleum, from petroleum refinery by-product sources, and from novel refining streams. The JP-8X experimental high density fuels currently being investigated have a volatility more proportionate with heavier refinery feedstocks. A kerosene fuel of this type, besides being denser and more viscous, would tend to be more naphthenic (cyclic paraffins), higher in aromatic content, and lower in hydrogen content. The technical effort conducted under this task order was directed at characterizing the properties and composition of several naphthenic/aromatic based JP-8X jet fuels relative to conventional jet fuels.

SECTION 1.0

INTRODUCTION AND BACKGROUND

Worldwide shortages of conventional high quality crude oils have dramatically reduced the availability of aircraft fuels in past years. More recently, the refinery industry has gone through a severe transitory period where a shift to lower quality crudes and syncrudes from alternate sources, such as oil shale, tar sands, coal liquids and heavy oils has caused increased processing costs and uncertain market fluctuations. Additionally, there is a trend toward the increased conversion of heavy residual oils to transportation fuels, with reduced consumption as coker fluids and boiler fuels. Refineries are applying more severe processing conditions to the refining of syncrudes and residual materials. A combined effect of these trends is a gradual shift in the average properties and composition of jet fuels consumed by the Air Force.

In order to assure that the Air Force has an adequate supply of jet fuel in a crude-short world, it is compulsory that the Air Force investigate both the near-term and long-term prospects for fuels from alternate sources and state-of-the-art processing methods. The chemistry and combustion behavior of such fuels must be carefully defined. The Air Force is currently conducting programs designed to obtain demonstration batches of fuels from sources other than petroleum, from petroleum refinery by-product sources, and from novel refining streams. Sizable quantities of these demonstration batches are being produced for combustion rig tests. The JP-8X experimental high density fuels currently being investigated have a volatility more proportionate with heavier refinery feedstocks. A kerosene fuel of this type, besides being denser and more viscous, would tend to be more naphthenic (cyclic paraffins), higher in aromatic content, and lower in hydrogen content. The technical effort conducted under this task order was directed at characterizing the properties and composition of several naphthenic/aromatic based JP-8X jet fuels relative to conventional jet fuels. These characteristics will be used in correlating results from combustion testing ongoing under other Air Force Programs.

The first set of samples were received on 2 January 1986 and contained three conventional combustor test fuels: 85-POSF-2366 (JET A), 85-POSF-2367 (JP-4), and 85-POSF-2368 (Diesel Fuel #2). The second

set of fuel samples consisting of three Sun Oil Company Light Cycle Gas Oil (LCGO) candidate JP-8X fuels, 86-POSF-2383 (20% aromatics), 86-POSF-2398 (30% aromatics), and 86-POSF-2414 (45% aromatics) were received 28 January 1986. A third set of two samples arrived 4 April 1986 and consisted of an Allison Turbine combustor test fuel, 86-POSF-2415 (JP-4), and a Sun Oil Company Light Pyrolysis Fuel Oil (LPFO) candidate JP-8X fuel, 86-POSF-2429 (30% aromatics).

The eight fuels were characterized by determining their hydrocarbon types of mass spectrometry and fluorescent indicator adsorption (FIA) methods, simulated distillation, gross and net heats of combustion, sulfur and hydrogen content, and density, true vapor pressure, surface tension, dielectric constant, specific heat, kinematic viscosity and thermal conductivity as functions of temperature.

SECTION 2.0

EXPERIMENTAL

This section describes the equipment and procedures used in evaluating the experimental high density fuels and selected conventional fuels.

2.1 HYDROCARBON TYPES BY MASS SPECTROMETRY AND FIA

Determination of hydrocarbon types by mass spectroscopy was accomplished using ASTM D2789 under the direction of Dr. Gene Sturm at the National Institute of Petroleum Energy Research (NIPER). The mass spectrometer used in the hydrocarbon type analysis was a Consolidated Electrodynamics Corporation Type 21-103 with a heated inlet system. This was the system used during the development phase of the ASTM D2789 procedure making it the most directly applicable instrument for this procedure. The analysis consisted of determining a matrix of equations relating each of the hydrocarbon types to a summation of characteristic mass spectral lines. The paraffin and aromatic average carbon numbers were determined from the summations and used in setting up a series of simultaneous equations. These equations were then solved to provide a relative measure of each compound type present. The paraffins, monocycloparaffins, dicycloparaffins, alkylbenzenes, indans and tetralins, and naphthalenes were measured in volume percents.

The Fluorescent Indicator Adsorption (FIA) liquid chromatography procedure described by ASTM D1319 "Hydrocarbon Types in Liquid Petroleum Products by Fluorescent Indicator Adsorption" was performed by Pratt & Whitney and used to determine the olefin content in the fuel samples. Since ASTM D2789 includes the olefins in the monocycloparaffin volume percentage, the olefin percentage was then subtracted from the monocycloparaffin content to give the complete fuel compound volume percentages.

2.2 SIMULATED DISTILLATION

The simulated distillation by gas chromatography gave an indication of the volatility of the fuel samples. This measurement was performed at Pratt & Whitney per ASTM D2887 "Boiling Range Distribution of Petroleum Fractions by Gas Chromatography" using a Packard Model 439 gas chromatograph with a Flame Ionization Detector (FID). Data acquisition and reduction were accomplished with a Nelson Analytical 3000 Series Chromatography Data System with software interfaced to an IBM PC AT minicomputer. The column was a packed type with Chromosorb WHP, 80 to 100 mesh, and liquid phase of SE-30 10% loading. Temperature readings were taken after every 5% volatilized from the initial to the final boiling points of the samples.

2.3 GROSS AND NET HEATS OF COMBUSTION

The gross heat of combustion at 25° (77°F) was determined using a procedure similar to ASTM D2382, "Heat of Combustion of Hydrocarbon Fuels by Bomb Calorimeter, High-Precision Method," utilizing a Parr Model 1720 Calorimeter Controller and Model 1241 Calorimeter. The Parr system utilizes thermister controller/temperature monitors as opposed to platinum resistance thermometry and has been found in this laboratory to provide accuracy and precision equivalent to ASTM D2382.

Gross heats of combustion were calculated using the correction for the heat of formation of the sulfuric and nitric acids produced during combustion. Determination of the sulfur contents were performed using the ASTM D3120 method, "Trace Quantities of Sulfur by Oxidative Microcoulometry." The sulfur contents were reported in weight percent.

The net heats of combustion were calculated using the hydrogen content determined by ASTM D3701, "Hydrogen Content by Low Resolution Nuclear Magnetic Resonance Spectrometry Method." The hydrogen contents were also reported in weight percent.

2.4 SPECIFIC HEAT AS A FUNCTION OF TEMPERATURE

Specific heat measurements were determined using the Differential Scanning Calorimetry (DSC) technique described by Hodgson, et al in "Analysis of Aircraft Fuels and Related Materials," AFWAL-TR-82-2082. The analyses were conducted on a DuPont Model 910 DSC with a DuPont 1090 Thermal Analyzer Station. The samples were run in stainless steel O-ring sealed pans in a nitrogen-purged environment. A DuPont DSC Cooling Accessory was used to achieve the required subambient temperature range of 0C (32°F) to 75°C (167°F). Continuous scans were made while heating the sample at a given rate. The amount of heat required to raise the temperature of the fuel was then compared to the heat required to raise the temperature of the heptane external standard over the same range. The specific heats of the fuel sample were then calculated from the known specific heat of heptane.

2.5 KINEMATIC VISCOSITY AS A FUNCTION OF TEMPERATURE

Viscosities were determined using ASTM D445, "Kinematic Viscosity of Transparent and Opaque Liquids." Thermometers were calibrated with an NBS-certified platinum resistance thermometer and conformed to ASTM E-77, "Verification and Calibration of Liquid-in-Glass Thermometers." Viscosity tests performed below 25°C (77°F) used a NESLAB refrigerated viscosity bath with a temperature variation of less than 0.03°C (0.05°F). At these low temperatures, drying tubes were placed on the open ends of the viscometers which prevented water condensation inside the viscometer. At least three viscosity points were determined for each fuel sample from -40°C (-40°F) to 40°C (104°F).

2.6 DENSITY AS A FUNCTION OF TEMPERATURE

Densities were determined using a Mettler DMA 55 SI densitometer with a DMA 602 HT remote cell. The procedure followed was ASTM D4052, "Density and Relative Density of Liquids by Digital Density Meter." The instrument consisted of a U-tube which was placed in a constant temperature bath maintained within 0.01°C (0.02°F). The U-tube was completely filled with the sample and then vibrated in the bath. The sample mass was then determined on the basis of the tube's oscillation relative to an instrument calibration curve. The density was then calculated automatically using the tube volume, sample mass and instrument calibration curve. The JP-4 samples, because of their higher volatility, were measured under a 5 psig nitrogen head for higher temperatures to preclude volatilization. At least 4 measurements were taken for each sample between -30°C (-22°F) and 75°C (167°F).

Calibration of the densitometer was performed using 2 standards of known densities at the test

temperature. The densities of distilled water (nonane at the lower temperatures) and air were used for calibration of the instrument. The calibration curve was then calculated as a straight line between these two points. The precision of the densitometer was found to be within 0.00003 g/mL. An NBS traceable isooctane standard was found to be within 0.00002 g/mL of the published value.

2.7 DIELECTRIC CONSTANT AS A FUNCTION OF TEMPERATURE

The dielectric constant measurements were conducted at the United States Testing Company, Inc. (UST) under the direction of Frank Savino, Supervisor in the Materials Engineering Section. UST determined the dielectric constant by the method described in ASTM D924-92b, "A-C Loss Characteristics and Relative Permittivity (Dielectric Constant) of Electrical Insulating Liquids." The basic dielectric constant apparatus specified by this method consisted of a controller, a 3-electrode test cell, and a glass test vial.

The dielectric constant was calculated from the ratio of the capacitance of the test cell with the fuel sample as the dielectric and the capacitance of the test cell with air as the dielectric. The accuracy of the method is at least as good as the accuracy of the capacitance measurements involved, which approaches 0.1%. Dielectric constant was measured at temperatures of 0°C (32°F), 30°C (86°F), 50°C (122°F), and 75°C (167°F) for all fuel samples.

2.8 TRUE VAPOR PRESSURE AS A FUNCTION OF TEMPERATURE

Phoenix Chemical Company measured the fuel sample vapor pressures under the direction of Dr. Arthur Krawetz. The true vapor pressure was determined using ASTM D2879, "Vapor Pressure-Temperature Relationship and Initial Decomposition Temperature of Liquids by Isoteniscope." This method determined the pressure exerted by the fuel in a closed vessel at 40% ullage. The sample in the isoteniscope was subjected to a reduced pressure environment which removed the dissolved and entrained gases. The isoteniscope was placed in a constant-temperature bath. Dry nitrogen was added to the gas sampling system until its pressure equaled that of the sample at temperature equilibrium. The liquid levels of the manometer arms were balanced, and the nitrogen pressure was measured by a McLeod vacuum gauge for pressures below 2 kilo-Pascals (kPa) and a mercury manometer for pressures above 2 kPa to 101 kPa. The tests below 25°C (77°F) were performed in a refrigerated bath and those above 25°C (77°F) in a resistance-heated dewar. The true vapor pressure was the pressure measured after equilibrium was established. Vapor pressure measurements were taken at 10 to 12 equilibrated temperatures over the pressure range from 0 to 101 kPa. Measurements were reported at temperatures of -30°C (-22°F), 0°C (32°F), 40°C (104°F), and 75°C (167°F).

2.9 SURFACE TENSION AS A FUNCTION OF TEMPERATURE

Surface tensions were determined using a tensiometer that used the DuNouy principle for measuring interfacial and surface tension, as described in ASTM D971, "Interfacial Tension of Oil Against Water by the Ring Method." Measurements were made at temperatures of -10°C (14°F), 0°C (32°F), 40°C (104°F), and 75°C (167°F).

2.10 THERMAL CONDUCTIVITY AS A FUNCTION OF TEMPERATURE

Thermal conductivity measurements were performed under the direction of Dr. Arthur Krawetz of Phoenix Chemical Company. These measurements were accomplished in accordance with ASTM D2717, "Test for Thermal Conductivity of Liquids." Thermal conductivity was determined by measurement of the temperature gradient across the fuel sample generated from a known amount of energy introduced into the test cell by an electrically heated platinum element. Conductivity of the glass cell body was obtained from the manufacturer's literature, with additional calibration accomplished by using a standard such as dimethyl phthalate. The temperature-resistance relationship of the cell filament

is determined by measurement of its resistance at various temperatures with the cell filled with freshly boiled distilled water or the sample. Measurements were made at 0°C (32°F), 30°C (86°F), 50°C (122°F), and 75°C (167°F).

SECTION 3.0

RESULTS AND DISCUSSION

3.1 FUEL PROPERTIES

A summary of the properties discussed herein are organized by fuel type and can be found in Tables 1 through 10 with the corresponding plots in Figures 1 through 7. Tables 11 through 14 provide the best fit equations for quick calculations of the fluid properties at specified temperatures. The best fit lines were determined by least squares fit approximations from the raw data. The individual fuel property tabulations and plots, which include the statistical data for the least square fit approximations for each fuel, are included in Reference report FR-19032-3.

3.1.1 Hydrocarbon Types by Mass Spectrometry and FIA

Hydrocarbon group-type analysis is a widely used procedure for obtaining information needed to evaluate feedstocks and products in the petroleum industry. The performance and specifications of jet fuels are inherently dependent upon the types of hydrocarbons present.

As can be seen in Table 1, the hydrocarbon type analyses show trends dependent upon the fuel type. Straight and branched chain paraffins are present at much lower concentrations in the JP-8X fuels. Saturates making up the JP-8X fuels are predominantly in the cyclic forms (naphthenic). Predictions based upon this compositional information include higher densities, lower gravimetric heats of combustions, lower hydrogen content and increased smoke point for the JP-8X fuels as compared to conventional fuels.

The three LCGO fuels (2383, 2398, and 2414) represent varying levels of hydrotreatment on two separate feedstocks. These feedstocks were hydrotreated separately to high density fuels with target aromatic contents of 20%, 30%, and 45%. Each set of two hydrotreated fuels with similar aromatic content were then blended to produce the combustion test fuels used in these analyses. The paraffins, unaffected by hydrotreatment, are essentially equal for all three of these fuels. The effect of hydrotreatment is evident in comparisons of the aromatic and saturate contents for the 3 LCGO fuels. Varying hydrotreatment levels from the target values of 45% to 20% aromatics show that the decrease in concentration of alkylbenzenes corresponds to the increase in concentration of monocycloparaffins. Likewise, the decreasing levels of naphthalenes, tetralins and indans with further hydrotreatment corresponds to increasing levels of dicycloparaffins. The LPFO fuel (2429) had considerably less normal and branched paraffins and a significantly higher concentration of dicycloparaffins, indans and tetralins than the other JP-8X fuels. The effect of this compositional difference was exhibited in most all fuel properties measured.

3.1.2 Simulated Distillation

Distillation characteristics are a measure of volatility and give a broad indication of fuel type. Aircraft engine fuels must be easily convertible from storage in the liquid form to the vapor phase which allows the formation of the combustible air/fuel vapor mixture. (Ref. 1) In gas turbine engines, the fuel volatility influences the rate at which the fuel spray vaporizes, thereby influencing ignition, combustion efficiency and combustor exhaust temperature profile (pattern factor). Ignition characteristics are affected primarily by lower boiling fractions (i.e. the 10% distillation temperature) while combustion

efficiency and pattern factor are believed to be controlled by heavier fractions (i.e. the 90% distillation temperature).

Table 2 shows the simulated distillation comparisons. As can be seen by comparing distillation ranges, the JP-8X fuels are significantly lower in volatility than conventional JP-4 fuels. This was reflected in higher densities and viscosities and lower vapor pressures of these fuels. Also, referencing Table 1, these higher boiling fuels correlate with lower saturate contents. In comparison, the higher concentration of two ring hydrocarbons in the LPFO fuel result in comparatively fewer light ends.

3.1.3 Gross and Net Heats of Combustion

The heats of combustion are the quantities of heat liberated by the combustion of a unit quantity of fuel with oxygen and can affect the economics of engine performance along with the range of the aircraft. The energy demand (Btu/sec) is determined by the aircraft configuration and the thrust requirements of the mission. Fuel flow rates are set to meet this energy demand, and are therefore dependent on the heat of combustion of the fuel.

The heats of combustion correlate with the hydrocarbon types present. As is shown in Table 3, JP-4 fuels have the highest heats of combustion and are more paraffinic (higher hydrogen content), with low aromatic and bicyclic components. The Jet A sample ranked next in both heats of combustion and saturate percentage. The LCGO fuels showed increasing heats of combustion and hydrogen percentage with increased hydrotreatment. The LPFO fuel, because of the high concentration of dicycloparraffins, indans, and tetralins, exhibited significantly lower gravimetric gross and net heats of combustion.

3.1.4 Specific Heat as a Function of Temperature

The specific heat of a fuel is an important parameter in the heat transfer equations of jet aircraft. Based on the energy demand (Btu/sec) for the specific mission segments, the specific heat determines the temperature rise in components such as heat exchangers, fuel manifolds, and fuel nozzles. Due to the increased speeds, reduced cooling air and increased combustor temperature of advanced aircraft, the specific heat, along with thermal conductivity and heat of combustion, is becoming very important in thermal management calculations.

The specific heat analyses results are found in Table 4 and Figure 1 and show specific heat increasing with temperature. As shown, the JP-8X fuels have measurably lower specific heats than the conventional jet fuels, JP-4 and Jet A. Sample 85-POSF-2367, a JP-4 fuel, exhibited a non-reproducible base line anomaly between 30 and 60C during the DSC programmed temperature runs. This anomaly was only observed with this sample. New samples of the fuel were analyzed with similar results, thereby making it impossible to get reliable specific heat data. Evaluation of other physical and chemical data for this sample, relative to other JP-4 fuels, revealed no obvious differences which would lead to such an anomaly.

3.1.5 Kinematic Viscosity as a Function of Temperature

Aviation fuels must have acceptable low-temperature fluid characteristics to insure adequate fuel flow to the engine during long missions at high altitudes. The fuel's viscosity is used in the fuel fluidity calculations and affects spray atomization within the combustor, engine starting characteristics, low power combustion efficiency, and pattern factor. Reduced ignition capability can occur with the more viscous fuels along with reduced flow during low temperature start transients and reduced augmentor functional suitability.

Kinematic viscosity results are shown in Table 5 and Figure 2. As illustrated, kinematic viscosity decreases logarithmically with increasing temperature. The lower volatility fuels (JP-4's) have the lower

viscosities corresponding to their lower aromatic contents. The Jet A fuel sample ranks next in both viscosity and aromatic content. The LCGO JP-8X fuels are grouped together next and have essentially the same viscosity-temperature relationship. The LPFO is slightly higher showing a differentiation in the basestock composition. As expected, the highly aromatic DF-2 fuel was the most viscous.

3.1.6 Density as a Function of Temperature

The fuel load calculations need accurate density measurements to predict aircraft or flight pattern dictated weight and volume limitations. As previously mentioned, high density fuels provide the greater heating value per volume of fuel, thereby increasing the range of the aircraft. (Ref. 1)

The density as a function of temperature results are shown in Table 6 and Figure 3. As shown, the JP-8X fuels are significantly higher in density than conventional JP-4 and Jet A fuels. Figure 3 illustrates the effect of hydrotreatment on density with density decreasing for the 3 LCGO fuels in order of greater hydrotreatment (i.e. lower aromatic content). The LPFO fuel has the highest density which can be attributed to the higher concentration of dicycloparaffins.

3.1.7 Dielectric Constant as a Function of Temperature

The dielectric constant measurement is used in the electrostatic calculations of aviation fuel systems along with the electrical conductivity. These calculations help in predicting the sparking tendencies of a fuel. This sparking tendency dissipates the electric charge faster in the higher density fuels. (Ref. 2) The dielectric constant measurement is also used in the calibration of the fuel gauges. The dielectric properties relate to the way a fluid varies the capacitive reactance of a pair of parallel electrodes, and is the key to the design of fuel gauges. (Ref. 3) Any variation in the dielectric constant versus density from conventional fuels should be considered to assure that the accuracy of the gauging systems is not seriously affected. (Ref. 4)

The dielectric constant ranking, Table 7 and Figure 4, followed the same pattern as that of the density measurements both in response to temperature and fuel type. This could be predicted by the fact that the higher density fuels are known to dissipate electrical charges faster than conventional fuels.

3.1.8 Vapor Pressure as a Function of Temperature

Vapor pressure is an indication of the extent of vapor loss likely during fuel storage in vented tanks or during high speed, high altitude flight where fuel temperature increases and ambient pressure decreases. It also is an indication of the tendencies of possible "vapor lock" in fuel pump lines. (Ref. 2)

Results for vapor pressure determinations are found in Table 8 and Figure 5. As could be predicted on the basis of distillation data, all the JP-8X fuels exhibited similar vapor pressures, significantly lower than conventional JP-4 fuels.

3.1.9 Surface Tension as a Function of Temperature

Surface tension measurements give an indication of the rapid vaporization rate which is used in the calculations performed on the combustor section. These rates affect the atomization and ignition of the fuel droplets allowing predictions of fuel consumption.

Surface tension decreases with increasing temperature as can be seen in Table 9 and Figure 6. The higher density, higher aromatic fuels (i.e. JP-8X's and Diesel Fuel #2) have higher surface tensions than the conventional Jet A and JP-4's. The LCGO fuels had surface tensions which decreased with increasing level of hydrotreatment. The LPFO fuel, however, had a surface tension higher than any of these values. This suggests that surface tension is a function of both hydrotreatment and basestock composition.

3.1.10 Thermal Conductivity as a Function of Temperature

Aircraft fuels have an important secondary use as heat sinks, cooling the aircraft electronic equipment, hydraulic fluids and lubricants. The rate at which heat energy is transferred through the fuel is called thermal conductivity. Similar to specific heat, thermal conductivity is used in heat transfer and thermal management calculations.

Thermal conductivity, as shown in Table 10 and Figure 7, appears to only slightly decrease with temperature. As shown, the JP-8X fuels have lower thermal conductivities than the JP-4 and Jet A fuels. The LPFO fuel had the lowest thermal conductivity with the LCGO fuels next in ascending aromatic content. The highest aromatic content LCGO fuel appeared to be less dependent on temperature. The slope of the curve is similar to that of DF-2, which also has a similar aromatic content.

3.2 POTENTIAL FUEL EFFECTS ON ENGINE PERFORMANCE AND LIFE

Mission studies have shown that the use of JP-8X type fuels will produce a significant increase in aircraft range, particularly in typical fighter aircraft applications. This could prove to be a major advantage for JP-8X if the minimum density were held to a value well above conventional fuels. However, some trade offs are anticipated through the use of these fuels in conventional engines.

Since the JP-8X fuel is being seriously considered as an alternate fuel, a discussion of some potential effects on the operation and life of a typical gas turbine engine is appropriate. The fuel effects discussed are predicated on the use of JP-8X fuels in engines/aircraft designed for conventional JP-4, Jet A., and JP-8 fuels.

As discussed in the previous section (see Tables 5, 6, and 8), the JP-8X fuels have higher viscosity and density, coupled with lower volatility than conventional JP-4 and Jet A fuels. Reduced engine ignition characteristics are typical of the higher density JP-8X fuels. The lower fluidity, as predicted by the higher viscosities and surface tensions, and the lower volatility affect the spray atomization and vaporization rates which in turn affect the engine starting capabilities. As a result, altitude relight limits are reduced and minimum ground-start fuel flow and temperature limits are affected. Fuels with lower vapor pressures may have difficulty vaporizing and, therefore, hinder engine ignition.

Fuel volatility, viscosity, and surface tension all are physical properties which influence combustion efficiency through fuel atomization and vaporization. The JP-8X fuels, because of their higher viscosity and surface tension coupled with lower volatility, are expected to reduce combustion efficiency at lower power settings. At power levels above idle, efficiency losses should be negligible for any modern engine using JP-8X. It is anticipated that at idle the losses would be measurable and at sub-idle the losses could be significant.

Combustor exit pattern factor is determined by the spatial heat release in the combustor and is influenced by the same physical properties which influence combustion efficiency. Increases in pattern factor at high power levels could reduce turbine life.

As shown in Table 3, the hydrogen contents of the JP-8X fuels ranged from 12.3 weight % to 13.3%. Smoke and combustor flame radiation are both strongly influenced by the hydrogen content of the fuel being burned. Fuel effect data from current production engines indicate that smoke number could nearly double in changing from a fuel of 14% hydrogen (typical for JP-4) to a fuel with only 12% hydrogen. On that basis, an increase of 30% to 100% in smoke number is anticipated for the JP-8X fuels analyzed.

As smoke in the combustor primary zone increases, flame radiation to the combustor liner also increases. Analysis of current production engines shows a 24% to 50% reduction in liner life when changing from a

fuel hydrogen content of 14% to 12%. The increased flame radiation will also reduce turbine life (particularly first vane life), but probably to a smaller degree.

Fouling of fuel spray nozzles, flow divider valves, fuel heat exchangers and fuel manifolds exposed to heated fuels has been noted in several production engines. Even a small increase in fuel temperature can greatly increase this tendency. In general, heavy fuels such as JP-8X tend to be less thermally stable than JP-4. Preliminary thermal stability and gum tests conducted at AFWAL/POSF indicated potential problems with the JP-8X fuels evaluated in this program. Assuming a constant energy demand (Btu/sec) for an existing engine, the lower specific heat of JP-8X is expected to increase the fuel temperature rise in the engine heat exchangers and injection system, further compounding the problem.

SECTION 4.0

CONCLUSIONS

The JP-4 and Jet A fuels were composed of higher saturate contents which led to higher gravimetric heats of combustions, specific heats, vapor pressures, and thermal conductivities. The JP-8X and Diesel fuels had the higher aromatic and naphthene contents, volumetric heats of combustion, viscosities, densities, dielectric constants, and surface tensions. All the properties appeared to be dependent upon both the feedstock composition and the effect of hydrotreatment. Looking at the LCGO fuels, which had the same basestocks with different hydroprocessing, the heats of combustion, density, dielectric constant, surface tension, and thermal conductivity were obviously dependent on the extent of hydroprocessing (hydrogen content).

The use of JP-8X has significant payoffs in expanding the availability of feedstocks for Air Force fuels and extending the range of volume limited aircraft. However, significant operational problems and reduction in component life could be encountered from the arbitrary use of JP-8X. If JP-8X is to be used as an alternative fuel, the experimental evaluation should be continued followed by component development in critical areas. If JP-8X will provide significant improvements in future fuel availability or improved range, such a development program may well be desirable. Based on preliminary data generated in this program, it appears that the most desirable fuel, with the least impact on performance and life of current engines, is the 20% aromatic LCGO JP-8X fuel.

TABLE 1
HYDROCARBON TYPES OF JET FUEL SAMPLES
BY ASTM D2789 AND ASTM D1319

Jet A Fuel	JP-4 Fuels	JP-8X Fuels Diesel Fuel #2	Target Aromatic Content			
			LCGO	LCGO	LPFO	LCGO
2366	2367 2415	2368	20%	30%	30%	45%
			2383	2398	2429	2414

NIPER Results in Volume Percent
Using ASTM D2789 (Mass Spec)

Paraffins	46.6	69.8	64.0	48.8	14.5	14.2	1.3	14.2
Monocycloparaffins ¹	32.4	17.8	23.6	29.3	35.9	30.6	20.8	26.3
Dicycloparaffins	5.5	2.8	2.7	3.8	35.6	34.3	56.0	26.6
Alkylbenzenes	8.4	7.8	7.3	7.1	8.2	10.8	7.2	15.3
Indans and tetralins	4.5	1.3	1.0	5.5	4.7	8.4	13.1	14.5
Naphthalenes	2.3	0.1	0.8	5.2	0.6	0.9	0.9	2.3
Olefins ¹	0.4	0.5	0.7	0.4	0.4	0.8	0.7	0.7

Pratt & Whitney Results in Volume Percent
Using ASTM D1319 (FIA)

Saturates	79.1	88.2	89.1	65.8	82.7	73.0	74.1	62.3
Aromatics	20.5	11.3	10.2	33.8	16.9	26.2	25.2	37.0
Olefins	0.4	0.5	0.7	0.4	0.4	0.8	0.7	0.7

Average Carbon Number from NIPER Results
Using ASTM D2789 (Mass Spec)

Paraffin	9.98	8.07	8.20	10.39	9.20	9.01	8.91	9.46
Aromatic	9.12	8.59	8.22	9.04	9.10	9.14	8.14	9.18

¹Olefin values taken from the ASTM D1319 results, subtracted from ASTM 2789 matrix inverse results for monocycloparaffins.

TABLE 2
SIMULATED DISTILLATION OF VARIOUS COMBUSTION TEST FUELS

	Temperatures in Celsius							
	2366 Jet A	2367 JP-4	2415 JP-4	2368 DF-2	2383 LOGO 20% Arom.	2398 LOGO 30% Arom.	2429 LPFO 30% Arom.	2414 LOGO 45% Arom.
IBP	116.5	26.5	28.5	132.5	112.0	118.0	131.5	115.0
5%	160.0	62.0	59.0	183.5	152.5	158.5	183.0	161.0
10%	174.0	75.0	69.0	204.0	169.0	171.5	186.0	173.5
15%	183.5	88.5	87.5	216.5	181.0	183.5	187.5	184.5
20%	191.0	91.0	93.0	228.5	186.5	189.0	195.0	191.0
25%	197.0	97.5	97.5	236.0	194.0	197.5	198.0	198.5
30%	202.5	105.5	104.0	245.5	199.0	201.5	201.5	203.0
35%	208.0	116.0	114.5	253.5	203.0	206.0	204.0	207.5
40%	213.5	120.0	120.5	259.0	208.5	211.5	207.5	213.0
45%	217.0	132.0	124.5	267.0	213.0	215.5	211.0	217.5
50%	221.5	141.5	136.0	273.5	217.0	221.0	216.5	223.5
55%	227.5	151.0	143.5	281.5	222.5	226.0	221.0	228.5
60%	232.0	165.0	149.5	288.0	227.5	232.0	226.0	235.0
65%	236.0	174.0	163.0	297.0	233.5	238.0	232.0	241.0
70%	239.5	187.0	171.5	304.5	241.0	246.0	235.5	249.0
75%	246.0	197.5	186.5	313.0	249.0	253.5	237.0	256.5
80%	252.0	211.5	196.5	322.0	258.0	263.0	244.0	265.5
85%	256.5	221.5	211.0	333.0	269.0	273.5	249.0	276.5
90%	264.0	234.5	227.5	346.0	282.0	285.5	258.5	289.0
95%	273.0	250.0	245.0	364.5	303.5	308.5	277.5	312.5
FBP	303.0	279.0	289.5	410.5	346.5	355.0	407.5	395.0

TABLE 3

HEATS OF COMBUSTION FOR VARIOUS COMBUSTION TEST FUELS

POSF #	H Wt %	S Wt %	Gross Heat of Combustion MJ/kg (Btu/lb)	Net Heat of Combustion MJ/kg (Btu/lb)	Volumetric Heat of Combustion MJ/L (Btu/gal)
85-2366 Jet A	13.58	0.053	45.935 (19748)	43.051 (18508)	35.297 (126637)
85-2367 JP-4	14.54	0.008	46.787 (20115)	43.702 (18788)	32.964 (118269)
86-2415 JP-4	14.62	0.026	46.790 (20116)	43.688 (18782)	32.928 (118138)
85-2368 DF-2	12.91	0.289	45.173 (19421)	42.433 (18243)	36.331 (130350)
86-2383 LOGO 20% Arom.	13.31	0.006	45.485 (19555)	42.661 (18341)	36.508 (130984)
86-2398 LOGO 30% Arom.	13.01	0.007	45.287 (19470)	42.526 (18283)	36.711 (131714)
86-2429 LPFO 30% Arom.	12.47	0.004	44.887 (19298)	42.241 (18160)	37.754 (135454)
86-2414 LOGO 45% Arom.	12.35	0.022	44.927 (19316)	42.307 (18188)	36.931 (132498)

TABLE 4

SPECIFIC HEAT AS A FUNCTION OF TEMPERATURE

	Specific Heat (kJ/kg/K) at					
	0C (32F)	15C (59F)	30C (86F)	45C (113F)	60C (140F)	75C (167F)
85-POSF-2366 Jet A	1.87	1.97	2.04	2.10	2.16	2.19
86-POSF-2415 JP-4	1.85	1.95	2.03	2.13	2.19	2.25
85-POSF-2368 DF-2	1.93	1.95	2.00	2.05	2.08	2.11
86-POSF-2383 LOGO 20% Arom.	1.58	1.67	1.74	1.81	1.90	1.92
86-POSF-2398 LOGO 30% Arom.	1.53	1.70	1.76	1.84	1.90	1.96
86-POSF-2429 LPFO 30% Arom.	1.56	1.65	1.72	1.78	1.83	1.89
86-POSF-2414 LOGO 45% Arom.	1.57	1.66	1.73	1.81	1.87	1.93

TABLE 5
KINEMATIC VISCOSITY AS A FUNCTION OF TEMPERATURE

	Kinematic Viscosity (cSt) at				
	40C (-40F)	-20C (-4F)	0C (32F)	25C (77F)	40C (104F)
85-POSEF-2366 Jet A	13.08	5.78		1.96	1.54
85-POSEF-2367 JP-4	2.62	1.69		0.87	0.75
86-POSEF-2415 JP-4	2.49	1.64		0.86	0.73
85-POSEF-2368 DF-2			7.80	1.78	2.73
86-POSEF-2383 LOGO 20% Arom.	17.50	7.29		2.27	1.76
86-POSEF-2398 LOGO 30% Arom.	19.18	7.57		2.33	1.77
86-POSEF-2429 LPEO 30% Arom.	21.61	8.85		2.63	2.01
86-POSEF-2414 LOGO 45% Arom.	19.64	7.60		2.28	1.75

TABLE 6
DENSITY AS A FUNCTION OF TEMPERATURE

	Density (g/mL) at					
	-30C (-22F)	-20C (-4F)	0C (32F)	15.5C (60F)	40C (104F)	75C (167F)
85-POSEF-2366 Jet A	85.149		.82970	.81989	.80161	.76002
85-POSEF-2367 JP-4	.79024		.76479	.75430	.73400	.70538
86-POSEF-2415 JP-4		.78158		.75371	.73358	.70436
85-POSEF-2368 DF-2			.86574	.85619	.83856	.81407
86-POSEF-2383 LOGO 20% Arom.	.88904			.85576	.83812	.81252
86-POSEF-2398 LOGO 30% Arom.	.89590			.86325	.84579	.82016
86-POSEF-2429 LPEO 30% Arom		.82012		.89378	.87589	.85014
86-POSEF-2414 LOGO 45% Arom.	.89568			.87293	.85529	.82944

TABLE 7

DIELECTRIC CONSTANT AS A FUNCTION OF TEMPERATURE

	Dielectric Constant at			
	0C (32F)	30C (86F)	50C (122F)	75C (167F)
85-POSF-2366 Jet A	2.17	2.13	2.10	2.08
85-POSF-2367 JP-4	2.06	2.03	2.01	1.98
86-POSF-2415 JP-4	2.06	2.01	1.99	1.97
85-POSF-2368 DF-2	2.28	2.24	2.21	2.19
86-POSF-2383 LUGO 20% Aram.	2.19	2.15	2.14	2.11
86-POSF-2398 LUGO 30% Aram.	2.23	2.18	2.16	2.14
86-POSF-2429 LPEO 30% Aram.	2.27	2.22	2.20	2.18
86-POSF-2414 LUGO 45% Aram.	2.27	2.23	2.20	2.17

TABLE 8

TRUE VAPOR PRESSURE AS A FUNCTION OF TEMPERATURE

	True Vapor Pressure (kPa) at			
	-30C (-22F)	0C (32F)	40C (104F)	75C (167F)
85-POSF-2366 Jet A	0.069	0.063	0.63	2.8
85-POSF-2367 JP-4	0.63	2.8	15	41
86-POSF-2415 JP-4	0.73	2.7	16	51
85-POSF-2368 DF-2		0.041	0.40	1.8
86-POSF-2383 LUGO 20% Aram.	0.0053	0.056	0.56	2.7
86-POSF-2398 LUGO 30% Aram.	0.0060	0.047	0.47	2.3
86-POSF-2429 LPEO 30% Aram.	0.0053	0.049	0.49	2.3
86-POSF-2414 LUGO 45% Aram.	0.0059	0.056	0.53	2.5

TABLE 9

SURFACE TENSION AS A FUNCTION OF TEMPERATURE

	Surface Tension (dynes/cm) at			
	-100° (144°)	0° (32°)	40° (104°)	75° (167°)
85-POSE-2366 Jet A	25.9	25.4	22.7	19.3
85-POSE-2367 JP-4	22.7	22.4	18.6	15.8
86-POSE-2415 JP-4	22.7	22.0	18.1	15.2
85-POSE-2368 DF-2	27.7	27.2	24.2	20.1
86-POSE-2383 LOGO 20% Arom.	28.1	27.5	24.0	20.5
86-POSE-2398 LOGO 30% Arom.	28.6	27.5	24.2	20.8
86-POSE-2429 LPFO 30% Arom.	29.2	27.9	25.1	22.4
86-POSE-2414 LOGO 45% Arom.	28.8	27.2	24.4	21.7

TABLE 10

THERMAL CONDUCTIVITY AS A FUNCTION OF TEMPERATURE

	Thermal Conductivity (W/m/K) at			
	0° (32°)	30° (86°)	50° (122°)	75° (167°)
85-POSE-2366 Jet A	.125	.123	.121	.119
85-POSE-2367 JP-4	.127	.122	.119	.116
86-POSE-2415 JP-4	.124	.120	.118	.115
85-POSE-2368 DF-2	.123	.122	.122	.121
86-POSE-2383 LOGO 20% Arom.	.118	.115	.112	.109
86-POSE-2398 LOGO 30% Arom.	.119	.115	.113	.110
86-POSE-2429 LPFO 30% Arom.	.113	.109	.107	.105
86-POSE-2414 LOGO 45% Arom.	.116	.114	.113	.111

TABLE 11

BEST FIT LINE EQUATIONS FOR THE MEASURED PROPERTIES
OF SPECIFIC HEAT AND VISCOSITY

	Specific Heat		Viscosity	
	A*10 ³	B	A	B
85-POSF-2366 Jet A	4.248	1.896	-3.983	9.485
85-POSF-2367 JP-4			-3.733	8.551
86-POSF-2415 JP-4	5.371	1.865	-3.704	8.471
85-POSF-2368 DF-2	2.533	1.923	-4.040	9.811
86-POSF-2383 LCGO 70% Arom.	4.686	1.594	-3.966	9.488
86-POSF-2398 LCGO 30% Arom.	5.390	1.580	-4.029	9.649
86-POSF-2429 LPFO 10% Arom.	4.286	1.578	-3.850	9.245
86-POSF-2414 LCGO 45% Arom.	4.781	1.582	-4.098	9.815

BEST FIT EQUATIONS:

$$\text{Specific Heat (kJ/kg/K)} = A * T + B$$

$$\text{LOG (LOG (Z))} = A * \text{LOG (T + 273.15)} + B$$

$$\text{Viscosity (cSt)} = Z - 0.7$$

A = Slope

T = Temperature in C

TABLE 12

**BEST FIT LINE EQUATIONS FOR THE MEASURED PROPERTIES
OF DENSITY AND DIELECTRIC CONSTANT**

	Density		Dielectric Constant	
	A*10 ⁴	B	A*10 ³	B
85-POSF-2366 Jet A	7.333	.8309	-1.226	2.167
85-POSF-2367 JP-4	-8.309	.7659	-1.060	2.061
86-POSF-2415 JP-4	-8.133	.7658	1.197	2.054
85-POSF-2368 DF-2	-6.941	.8663	-1.226	2.277
86-POSF-2383 LCCO 20% Arom.	-7.283	.8672	-1.031	2.187
86-POSF-2398 LCCO 30% Arom.	-7.301	.8749	-1.197	2.224
86-POSF-2429 LIFO 30% Arom.	-7.357	.9053	-1.197	2.264
86-POSF-2414 LCCO 45% Arom.	-7.345	.8846	-1.346	2.270

BEST FIT EQUATIONS:

Density (g/mL) = A * T + B

Dielectric Constant = A * T + B

A = Slope

T = Temperature in C

TABLE 13

**BEST FIT LINE EQUATIONS FOR THE MEASURED PROPERTIES
OF VAPOR PRESSURE AND SURFACE TENSION**

	Vapor Pressure		Surface Tension	
	A	B	A*10 ²	B
85-POSF-2366 Jet A	-.090	10 ⁻⁶ .453	-7.869	25.27
85-POSF-2367 JP-4	-.470	10 ⁻⁵ .834	-8.424	22.09
86-POSF-2415 JP-4	-.562	10 ⁻⁶ .183	-8.985	21.86
85-POSF-2368 DF-2	-.062	10 ⁻⁶ .182	8.876	27.13
86-POSF-2383 LOGO 20% Arom.	-.135	10 ⁻⁶ .549	-8.999	27.39
86-POSF-2398 LOGO 30% Arom.	-.114	10 ⁻⁶ .428	-9.015	27.64
86-POSF-2429 LPFO 10% Arom.	-.111	10 ⁻⁶ .427	-7.743	28.18
86-POSF-2414 LOGO 45% Arom.	-.088	10 ⁻⁶ .389	-7.981	27.62

BEST FIT EQUATIONS:

$$\text{LOG (Vapor Pressure (kPa))} = A / (T + 273.15) + B$$

$$\text{Surface Tension (Dynes/cm)} = A * T + B$$

A = Slope

T = Temperature in C

TABLE 14

**BEST FIT LINE EQUATIONS FOR THE MEASURED PROPERTY
OF THERMAL CONDUCTIVITY**

	Thermal Conductivity	
	$A \times 10^5$	B
85-POSF-2366 Jet A	-7.288	.1248
85-POSF-2367 JP-4	-14.41	.1266
86-POSF-2415 JP-4	-11.55	.1237
85-POSF-2362 DF-2	-3.147	.1232
86-POSF-2383 LCGO 20% Arom.	-12.17	.1182
86-POSF-2398 LCGO 10% Arom.	-12.38	.1190
86-POSF-2429 LPFO 30% Arom.	-8.282	.1112
86-POSF-2414 LCGO 45% Arom.	-6.708	.1161

BEST FIT EQUATION:

Thermal Conductivity (W/m/K) = $A * T + B$

A = Slope

T = Temperature in C

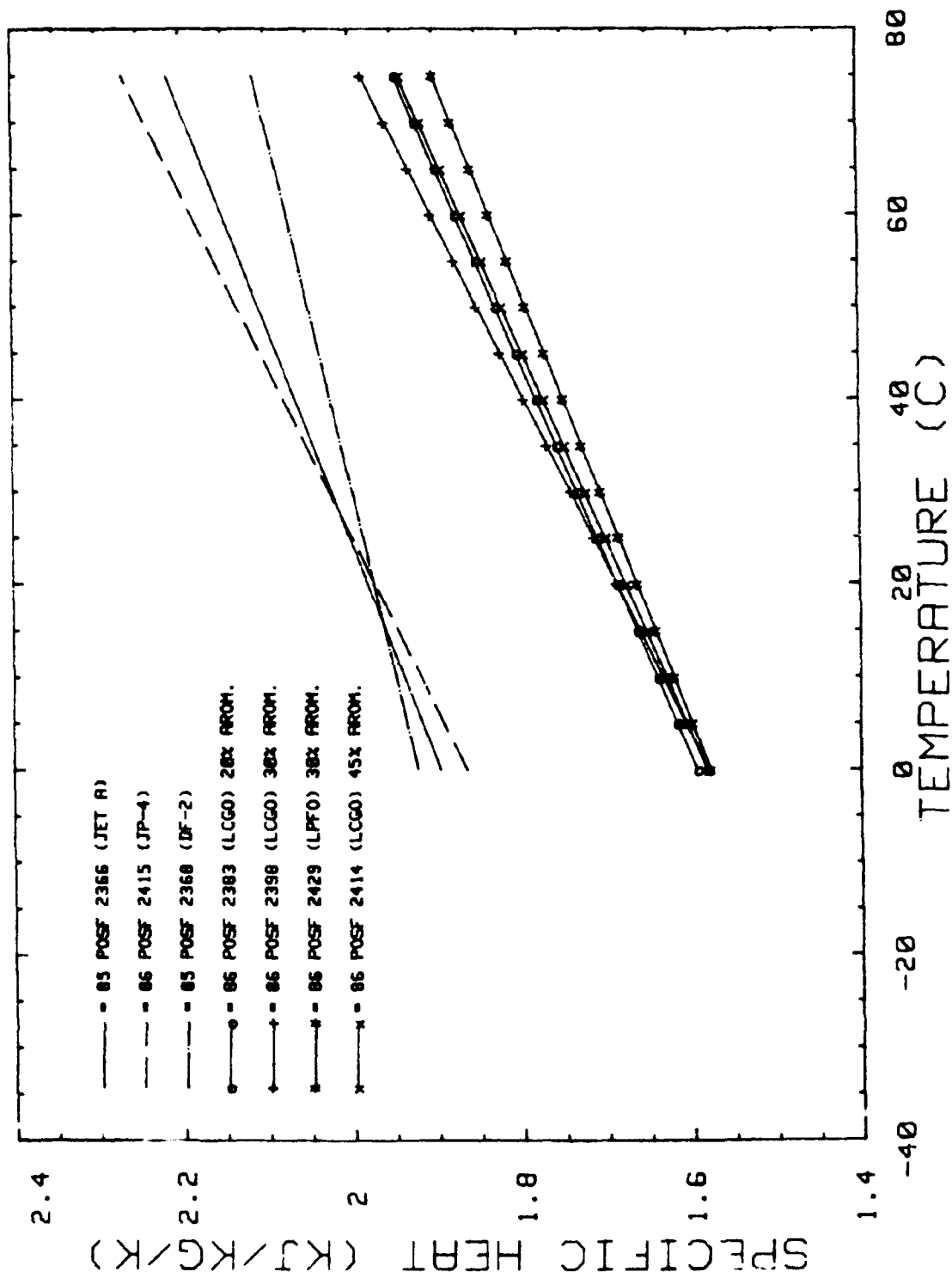


FIGURE 1 SPECIFIC HEAT AS A FUNCTION OF TEMPERATURE
FOR VARIOUS COMBUSTION TEST FUELS

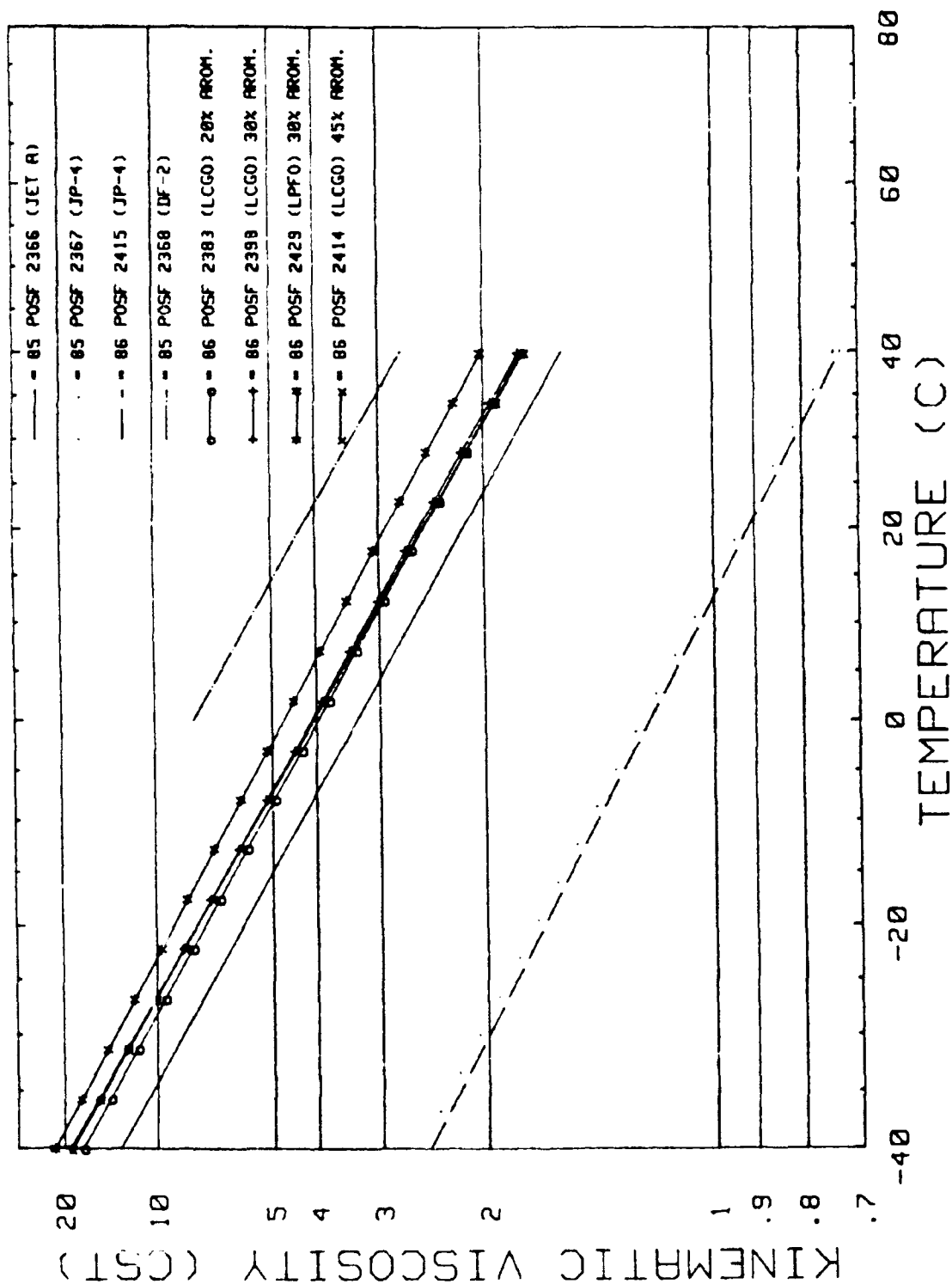


FIGURE 2 KINEMATIC VISCOSITY AS A FUNCTION OF TEMPERATURE
FOR VARIOUS COMBUSTION TEST FUELS

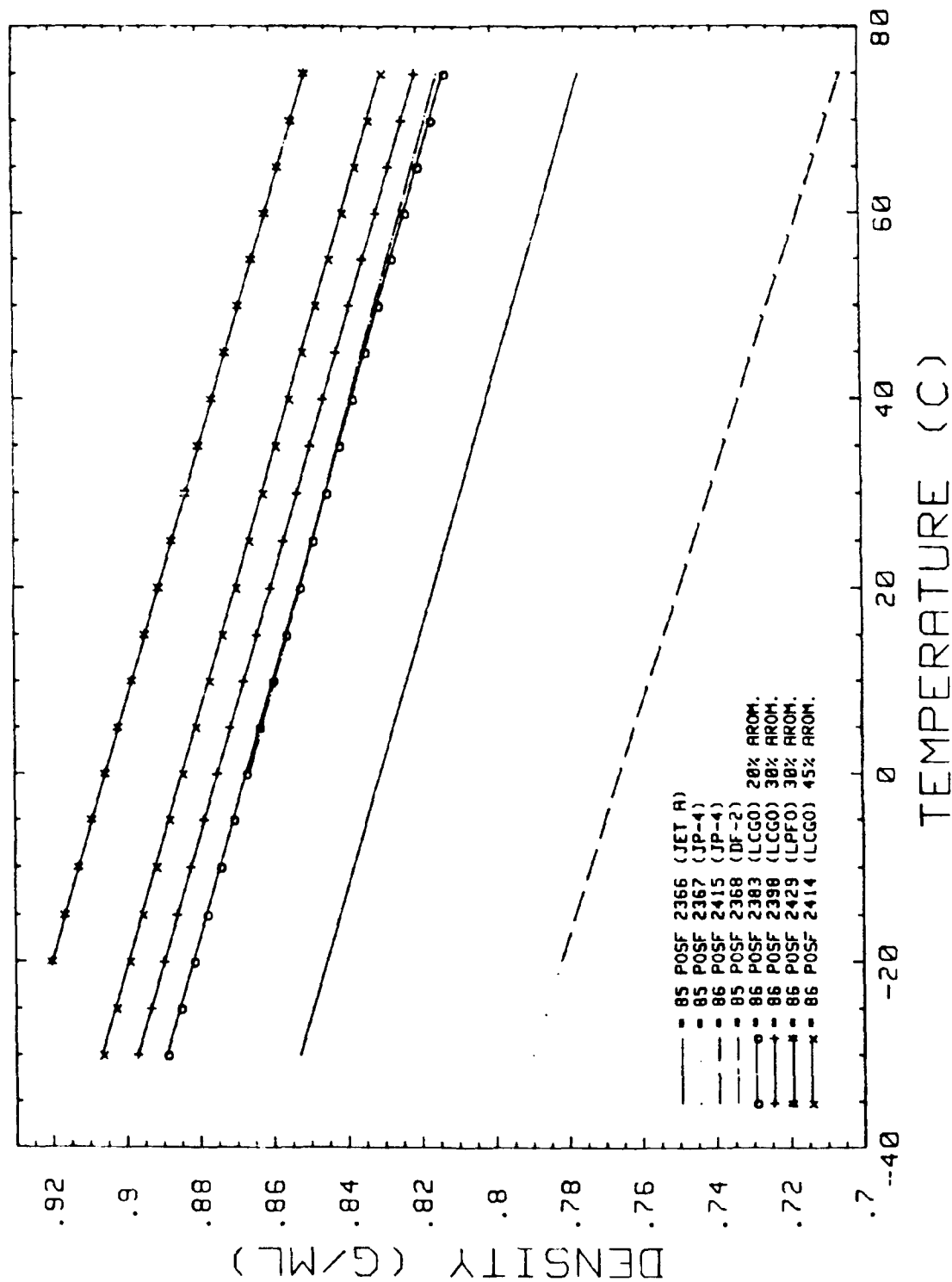


FIGURE 3 DENSITY AS A FUNCTION OF TEMPERATURE
FOR VARIOUS COMBUSTION TEST FUELS

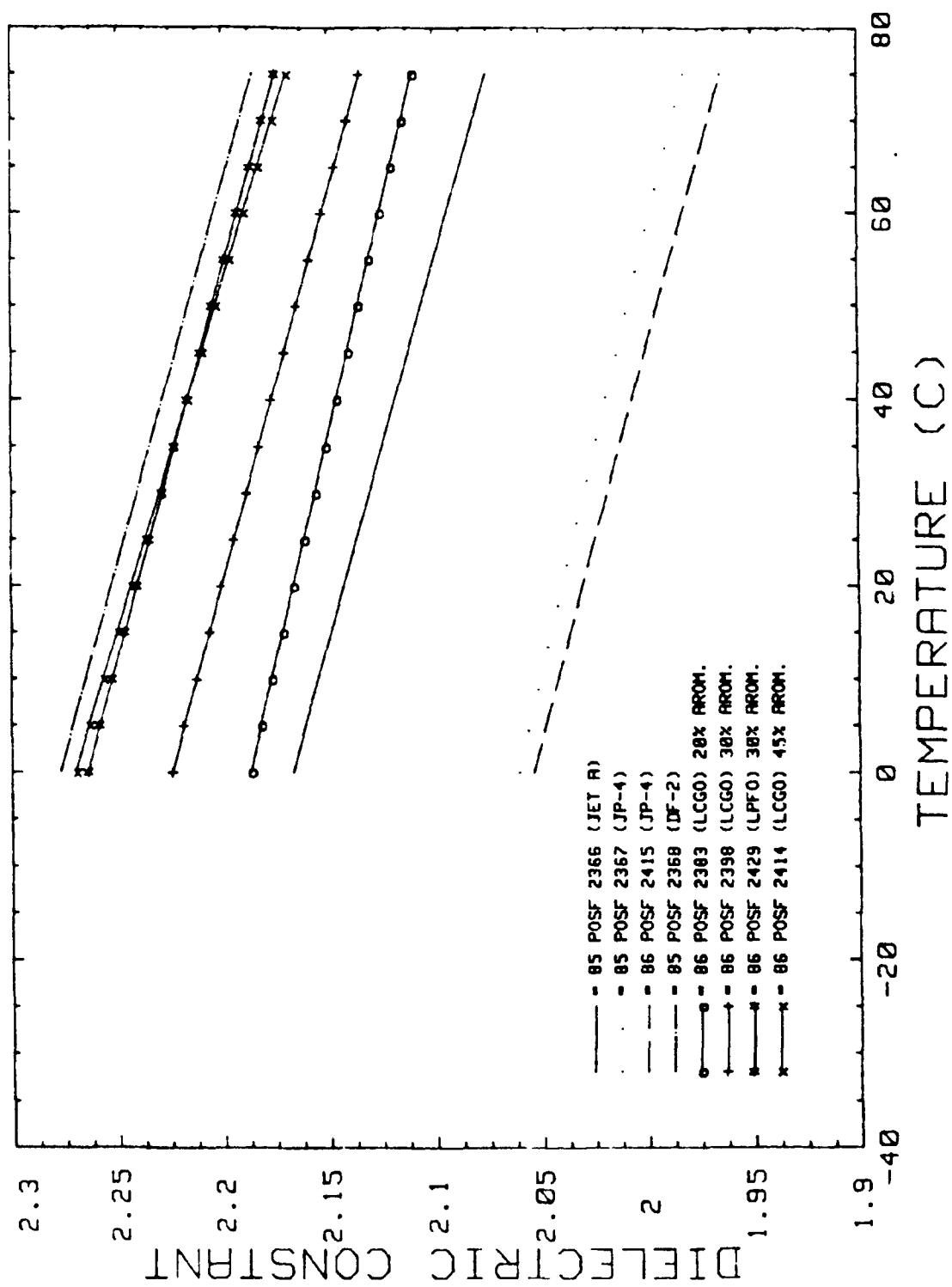


FIGURE 4 DIELECTRIC CONSTANT AS A FUNCTION OF TEMPERATURE
FOR VARIOUS COMBUSTION TEST FUELS

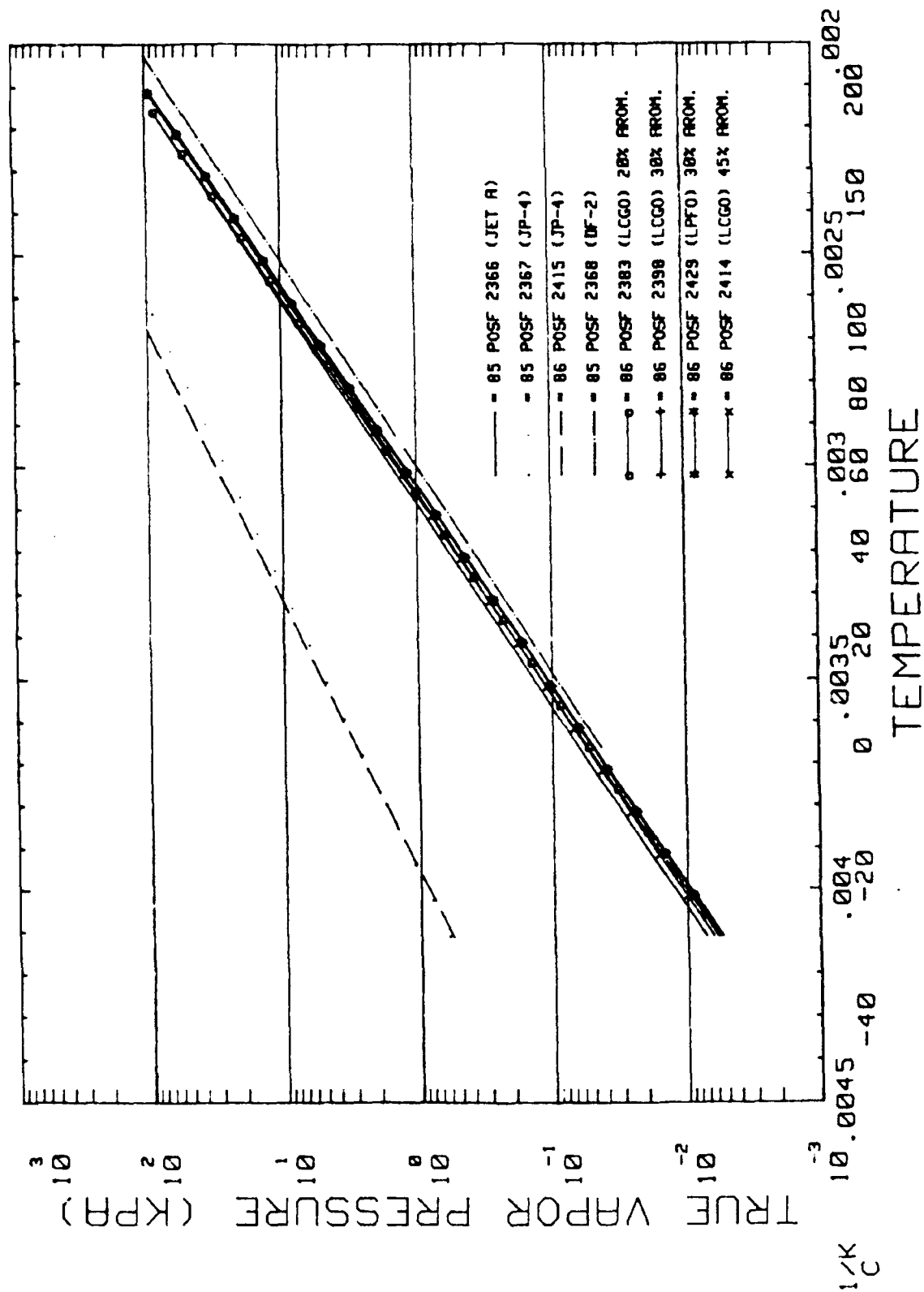


FIGURE 5 TRUE VAPOR PRESSURE AS A FUNCTION OF TEMPERATURE
FOR VARIOUS COMBUSTION TEST FUELS

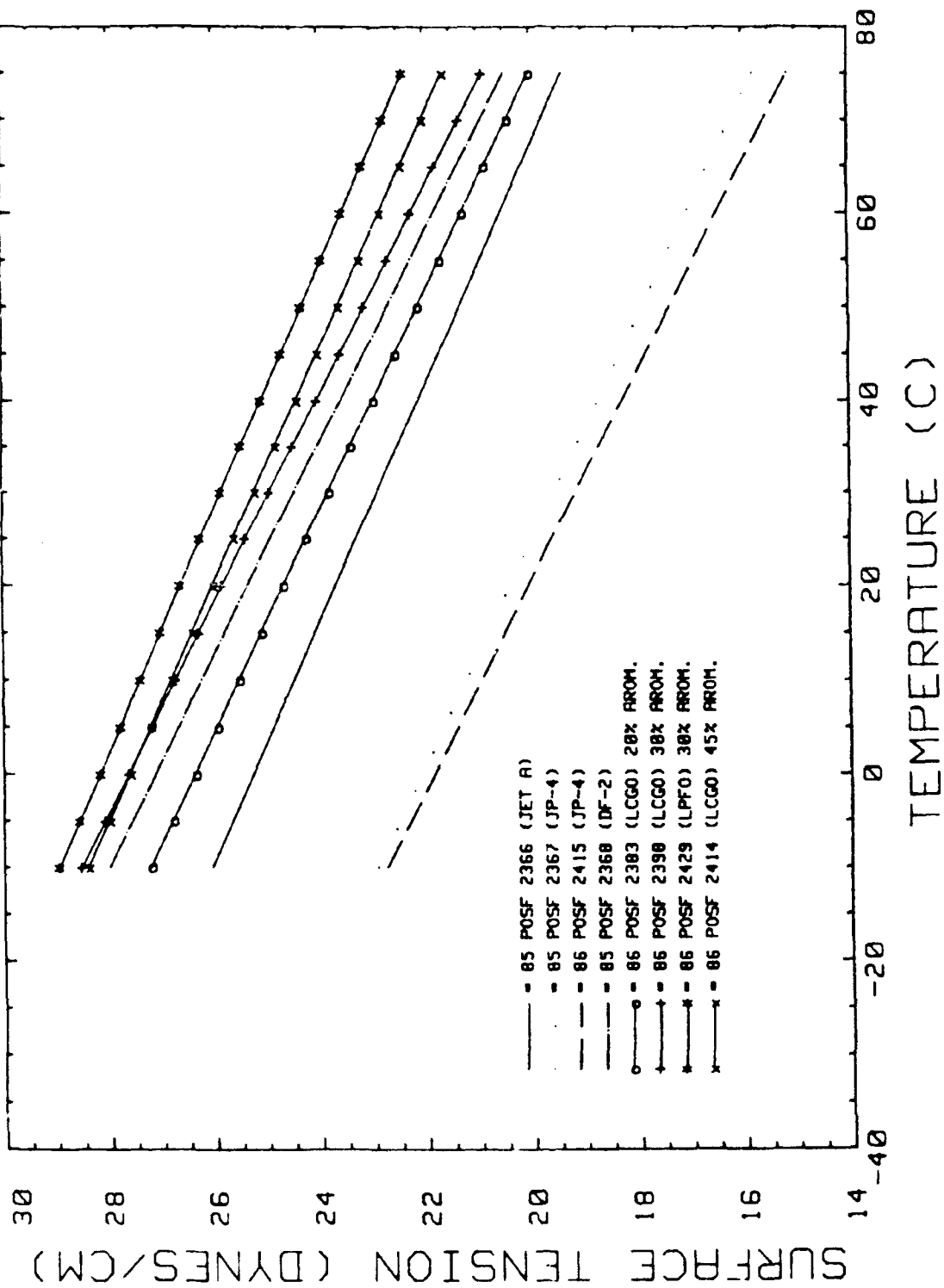


FIGURE 6 SURFACE TENSION AS A FUNCTION OF TEMPERATURE
FOR VARIOUS COMBUSTION TEST FUELS

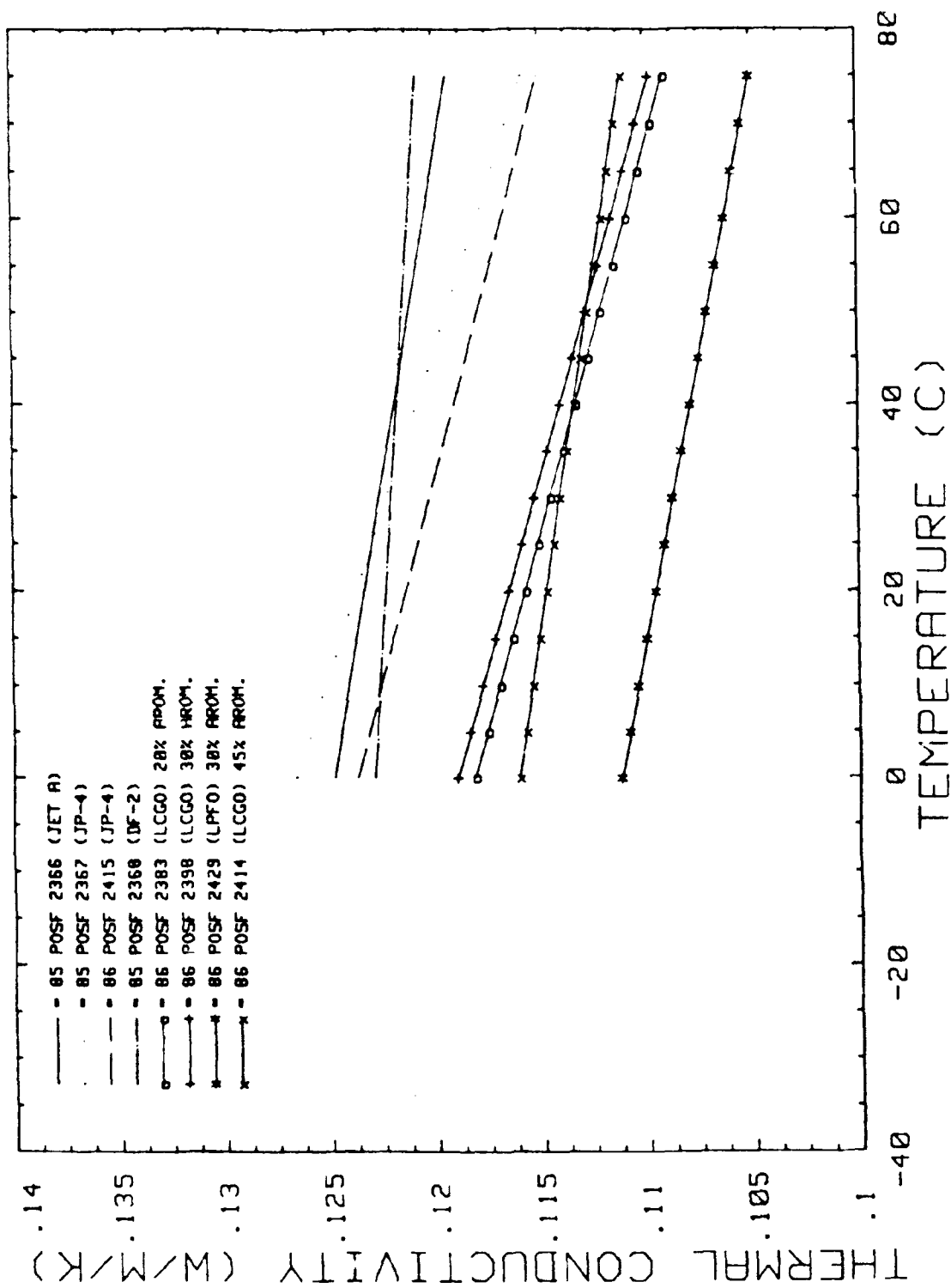


FIGURE 7 THERMAL CONDUCTIVITY AS A FUNCTION OF TEMPERATURE FOR VARIOUS COMBUSTION TEST FUELS

REFERENCES

1. R. Boldt and B. Hall, Editors, Significance of Tests for Petroleum Products, American Society for Testing and Materials, Pennsylvania, 1977.
2. E. M. Goodger, Hydrocarbon Fuels, Halsted Press, New York, 1975.
3. Handbook of Aviation Fuel Properties, Coordinating Research Council, Inc., Georgia 1983.
4. G. Beal, B. McCallum, and F. Grenich, Fuel-Engine-Airframe Optimization Study, Air Force Aero Propulsion Laboratory, Wright-Patterson Air Force Base, Ohio 45433, AFWAL TR-84-2028, April, 1984.

CHARACTERIZATION OF EXPERIMENTAL COAL TAR S

Period of Performance

1 May 1986 through 15 September 1986

Reference

Task Order No. 9, Topical Report No. 4, FR 196.2-4, September 1986, H.L.C. Meuzelaar, B.L. Hoesterey, M.Y. Wen

Abstract

Renewed interest in domestic supplies of nonpetroleum based liquid fuel feedstocks, e.g., as a strategic source of jet fuels led to this study directed at evaluating the composition and stability of the liquid streams from the Great Plains Gasification plant. In addition, suitability for use in transportation fuels was assessed. The study was performed under the auspices of this program by the University of Utah Biomaterials Profiling Center (UUBPC). The three main liquid product streams produced by the Great Plains Gasifier consist of a light naphtha, a tar oil, and a crude phenols fraction. The high oxygen content of the tar oil stream (approx. 50% of all molecules contain oxygen) was seen as the major hurdle in producing transportation fuels in general and aviation fuels in particular. Only after removal of the oxygen moieties (e.g. by hydrodeoxygenation) can the resulting syncrude be compared with petroleum and oil shale-derived crudes of similar aromaticity. Moreover, unless average ring size is reduced (e.g., by hydrocracking) the tar oil derived syncrude is likely to yield primarily diesel grade transportation fuels with relatively small amounts of JP4 - JP8 grade aviation fuels.

SECTION 1.0

INTRODUCTION

1.1 HISTORICAL BACKGROUND

Coal gasification can provide two different routes to liquid fuels, namely directly by upgrading of the tars formed during the initial devolatilization steps and indirectly by synthesis from the main gaseous products. Producing liquid fuels from coal gasification processes is not a new concept. From 1920's thru WWII, Germany produced gasoline from coal by hydrogenation of coal tar as well as by Fischer Tropsch synthesis [1]. Coal gasification and processes to convert coal to methanol were in use in the USA in the 1950's but use dwindled due to increased availability of petroleum and natural gas [2]. In South Africa, the oldest SASOL plant has been in operation for more than 20 years, producing gasoline by indirect liquefaction, and several other gasifiers are used in parts of Europe.

Increased attention on nonpetroleum energy resources in the last decades rekindled interest in coal gasification in America. Several types of gasifiers and processes have been evaluated in the last 15 years as to economical operation conditions and health issues, including Lurgi, Koppers-Tozek, Winkler and Texaco [3], Texaco, British Gas/Lurgi and Combustion Engineering [4], and Wellman Galusha [5]. There are two currently operational coal gasification plants in the US, the Great Plains Gasification Project using Lurgi gasifiers [6] and the Cool Water plant [7] using a proprietary Texaco process. The Great Plains plant, operated by ANG Coal Gasification Company (ANG), produces synthetic natural gas. The objective of the Cool Water project is to use gas to power a combustion turbine generator for electricity production.

In general, the primary purpose of gasification is to convert coal to a synthesis gas consisting of CO and H₂ using steam and oxygen. The gas can be upgraded to methane, or used for syntheses of other organics or electricity generation. All gasification processes generate by-products such as ash (or slag, depending on temperature), sulfur, and ammonia. Fixed bed gasifiers such as the Wellman Galusha and Lurgi retorts generate significant amounts of tar, due to relatively mild operating conditions compared to other processes [2]. In a previous study of gasifier tars sponsored by EPRI it was shown that coal tar yields from a pilot plant scale (30 tpd) Wellman Galusha gasifier operated by Black Sivalis & Bryson for MIFGA in Minneapolis produced up to 1 barrel of tar distillate per dry ton of feed coal, depending on coal rank and type [8]. Preliminary comparison of a Wellman Galusha tar with coal tar produced by the Great Plains Gasification plant from the same coal (Beulah Gap lignite) revealed major differences in composition due to the more severe operating conditions of the latter, resulting in reduced heteroatomic content and a higher degree of condensation [9].

1.2. THE GREAT PLAINS COAL GASIFICATION PLANT

The largest Lurgi type coal gasification plant in the U.S. is the Great Plains Gasification plant in Mercer County, North Dakota which began operation in 1984. A simplified flow diagram of this plant is shown in Figure 1. The following description of the process was taken from references 6, 10 and 11. Approximately 22,000 ton per day (tpd) of lignite is crushed to -8" in the primary crushers. It is further crushed to -2" in secondary crushers and fed to a storage pile with a holding capacity of several days. Coal is reclaimed from storage and screened. Approximately 14,000 tpd of 2 to 1/4" coal is fed to the gasification plant, with the remaining 8000 tons of -1/4" sent to Basin Electric for boiler fuel.

The gasification plant contains 14 Lurgi Mark IV counter current fixed bed gasifiers, of which 12 are in use at one time. Each gasifier is equipped with an automatic coal lock chamber which feeds coal from a coal storage bunker. Through a revolving grate at the bottom of the reactor, steam and oxygen are injected and distributed upward through the coal bed. An ash lock chamber below the reactor discharges the ash from the reactor. Gasifier operation is controlled by regulating the flows of steam and oxygen, while the coal flow is adjusted accordingly to keep the gasifier full. The heat necessary for the endothermic gasification reaction is supplied by the rising gas, which upon leaving the combustion zone has a temperature of approximately 2200°F. The main reaction is that of steam with carbon to produce hydrogen and carbon monoxide. Heat is absorbed in this reaction and the hot gas eventually cools to a temperature less than 1300°F. Much of the remaining heat is used for carbonization, drying and preheating of the coal. The gasifier shell is surrounded by a cooling water jacket which generates 500 psig steam. The raw gas produced is sent from the gasification area to gas cooling units with about 30% of the gas going first to a shift conversion unit. Liquid is removed in the gas/liquid separation area and tar, tar oil, crude phenols, water and ammonia are subsequently removed from the liquid stream. The gas stream itself is further purified to remove a product termed naphtha, containing hydrocarbons, CO₂ and S. The synthesis gas then goes to methanation units which use a reduced Ni catalyst to convert the gas to a high BTU (977 btu/ft³) pipeline gas. Thus, there are two process streams, the gas stream from which naphtha is removed, indicated as stream A in Figure 1, and the liquid byproduct stream from which tar (+ coal dust), tar oil, and crude phenols are removed. The tar is recycled into the reactor. The tar oil is stored in holding tanks, and can be burned as fuel. It is designated stream B in Figure 1. The crude phenols are designated stream C. The remaining liquid consists of ammonia and water, both of which are recovered. Relative amounts of the liquids are naphtha: 120,000 to 145,000 lb per day, tar oil: 120,000 to 140,000 gal per day (approx. 1 million lb per day), and crude phenols: 220,000 lb per day. This translates into some 650 to 700 tons of distillate liquids per day, representing a total liquid yield of approximately 5% of the (wet) feed coal or 8.5% on a daf coal basis.

1.3 STUDY OBJECTIVES

Renewed interest in domestic supplies of nonpetroleum based liquid fuel feedstocks, e.g., as a strategic source of jet fuels has led to the present study aimed at evaluating the composition and stability of the liquid streams from the Great Plains Gasification plant against the perspective of potential commercial use. Specific objectives of this study carried out at the University of Utah Biomaterials Profiling Center (UUBPC) were:

- obtain representative samples of selected liquid product streams from the Great Plains Coal Gasification Plant in Beulah, N. Dakota;
- transport and store these liquid samples and to prepare suitable aliquots for further studies with minimal change in physical and chemical properties;
- determine the elemental and molecular composition of these coal liquids by means of a comprehensive analytical approach involving elemental (CHNOS) analysis, trace element analysis, LC fractionation, MS analysis, FTIR analysis and ¹H NMR analysis techniques;
- integrate, reduce and interpret the analytical data;
- determine the stability of the Great Plains coal liquids (i.e., tar oil), by exposing representative aliquots to oxygen containing atmospheres at elevated temperature conditions followed by careful analysis of any changes in elemental and/or molecular composition using low voltage MS and computerized multivariate analysis techniques; and
- provide conventional fuel characterization parameters on fractions of the tar oil stream and crude phenols stream for determination by others of the suitability of these streams as feedstock for general transportation or special aviation fuels.

SECTION 2.0

EXPERIMENTAL

2.1 SAMPLE COLLECTION

Tar oil samples were obtained from the Great Plains Coal Gasification plant at Beulah, North Dakota by ANG Coal Gasification Company personnel. Two on-stream tar oil samples were determined to be representative samples at different stages of the process. The first on-stream tar oil sample was taken from the midstream holding tank (between the reactor and the final tar oil holding tank). This tar oil had been stored in the holding tank at 60°C for less than 8 hours and therefore, was considered the freshest tar sample. The second on-stream tar oil sample was taken from the final holding tank. This is a 30 day capacity holding tank which had been drained out a week before the tar oil was collected. Therefore, the second tar oil sample was considered a 7-day old, possibly partially oxidized, tar oil sample. Later, a third tar oil sample was obtained from the laboratory of the Great Plains plant, where the tar oil had been stored at room temperature in a closed container for 6 months. Therefore, this tar oil sample should be considered as possibly severely oxidized. The first two samples were drained from the holding tanks into 250 ml polyethylene containers (7 containers for each sample) in a nitrogen environment and immediately frozen in dry ice and shipped to UUBPC Salt Lake City, Utah. The third tar oil sample was simply filled into a one liter glass bottle without a nitrogen purge or dry ice environment and sent to UUBPC. Besides tar oil samples, additional naphtha and crude phenols samples were also received in

one liter bottles without oxidation protection. Long term storage for the first two tar oil samples was carried out under -90°C in a freezer, while the third oil sample as well as the naphtha and crude phenols samples were stored in a regular freezer at -30°C.

2.2 SAMPLE CHARACTERIZATION

The fresh tar oil sample was first separated into two fractions (approximately 50:50 by wt.) by a simple laboratory distillation at ambient pressure (640 torr) with nitrogen flow introduced into the system to prevent oxidation. The cut point for light and heavy fractions was 200°C. These two fractions along with other samples were analyzed by various analytical methods.

2.2.1 Thermogravimetry

TG analyses were performed on a Mettler I thermoanalyzer system. Typical ambient pressure (= 650 mm Hg) analysis conditions were: sample weight 10 mg, helium flow rate 100 ml/min, heating rate 6°C/min, maximum temperature 200°C for light fraction tar oil and 300°C for heavy fraction tar oil and crude phenols. The TG data were used to generate simulated distillation curves for the samples.

2.2.2 Liquid Chromatography

Open column LC was performed on a 19 mm I.D. x 400 mm length glass column packed with activated silica gel using a procedure reported by McClennen, *et al.* [12]. The samples were separated into four fractions by gravity elution from the silica gel column using solvent mixtures of increasing polarity and strength. Between 17 and 20 g of 120/200 mesh (74-125 µm) silica gel (Baker Analyzed Reagent), which was dried at 200°C overnight were used per gram of sample. The sample (1.5-1.8 g) was placed on the silica gel column and successively eluted with 150 ml each of pentane, 8:1 pentane/benzene, 4:1 benzene/ethylether, and 1:1 benzene/methanol, all solvents rated HPLC grade. The solvent mixtures were adapted from Rubin, *et al.* [13] who applied them to the neutral fraction (insoluble in aqueous base and acid solutions) of coal-derived liquids rather than to the whole sample.

2.2.3 Low Voltage Mass Spectrometry

Low voltage MS analyses were carried on the Extranuclear 5000-1 system with Curie-point inlet as shown in Figure 2. A detailed description of the system can be found in reference 14. For liquid samples of low volatility, 5 µg samples were coated on ferromagnetic wires. The wires were then inserted into borosilicate glass reaction tubes and introduced into the vacuum system of the mass spectrometer. The ferromagnetic wires were inductively heated at a rate of approximately 100°C/s to an equilibrium temperature of 610°C (as determined by the Curie-point temperature of the wire). Total scanning time was 20 seconds. For liquid samples of moderate and high volatility, a special introduction method was used [15]. This method involves the use of a glass capillary tube (micro caps, Drummond Scientific) sealed on one end and capable of holding up to .25 µl liquid. A detailed schematic of capillary sample introduction system is shown in Figure 3. After introducing into the vacuum system the capillary tube was inductively heated by a tightly wound ferromagnetic spring. This ensured complete evaporation of most samples within approximately 2 minutes. Typical operating conditions were as follows: electron energy 12 eV, scanning rate 1000 amu/s, mass range 20-280 amu. All spectra were recorded by an IBM 9000 computer and summed into a single time-integrated spectrum.

2.2.4 Fourier Transform Infrared Spectrometry

FTIR spectra of the light and heavy fractions of fresh tar oil and crude phenols were run on an IBM Instruments Model 32 FTIR system with IBM 9000 computer. Neat tar oil and crude phenols samples were placed between salt plates and 256 scans of the 4000 to 600 cm⁻¹ region were summed for each sample.

2.2.5 Elemental Analysis

Elemental analysis of the light and heavy fraction of fresh tar oil and crude phenols were carried out by Standard Laboratories at Huntington, Utah. C, H, N contents were determined by a Leco CHN 600 analyzer. A specially designed tin capsule was used for liquid samples to prevent evaporation prior to analysis. The measurement of total sulfur contents were performed on a Leco SC-12 sulfur analyzer. The oxygen contents of the samples were obtained by difference.

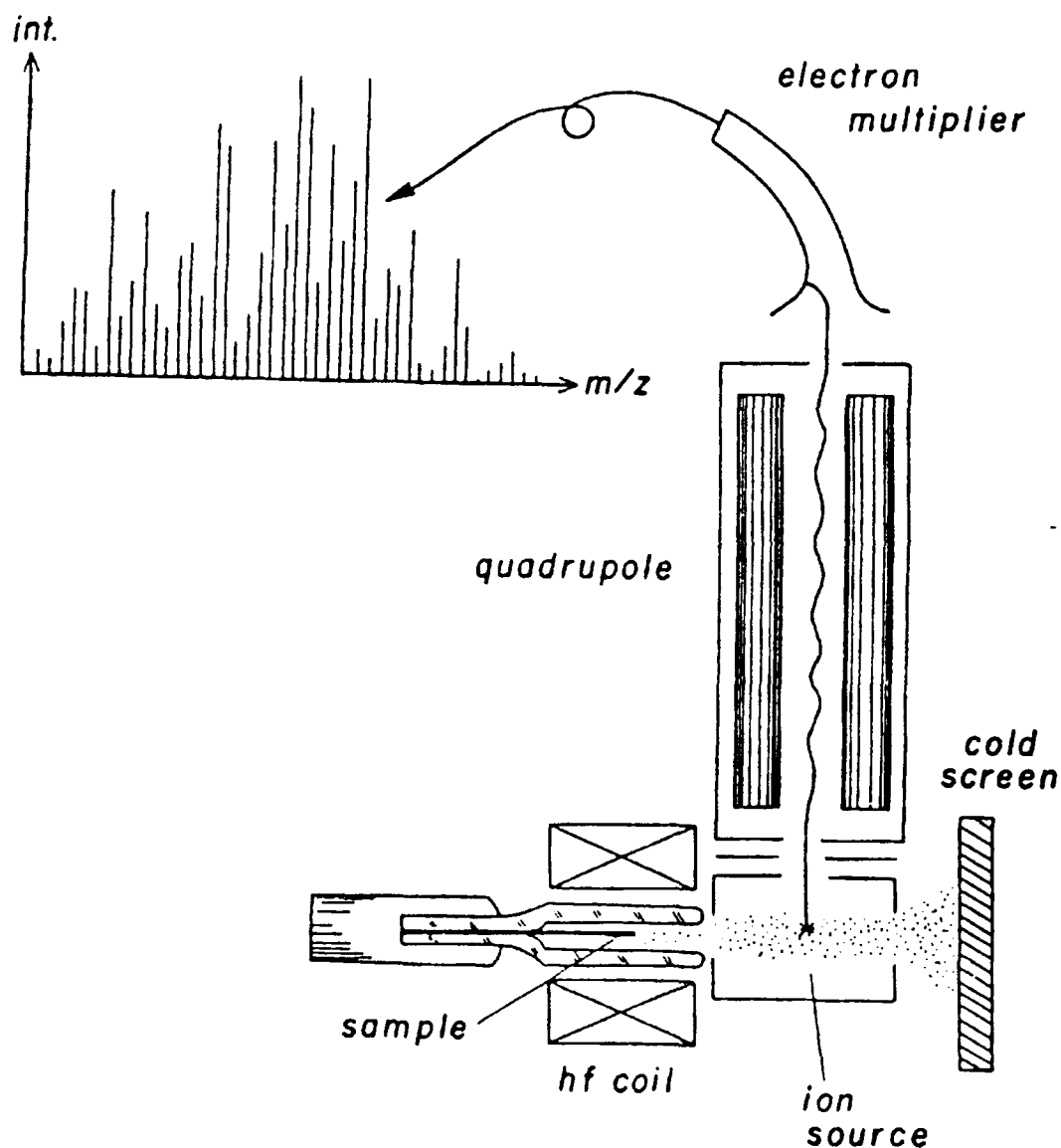


Figure 2. Low voltage mass spectrometry system with special system inlet for low volatile liquids and/or solids using hf inductive heating

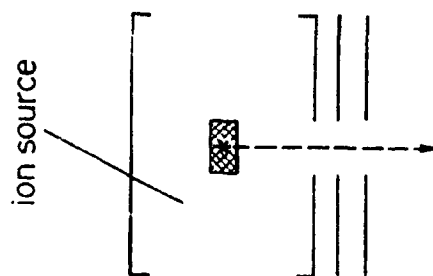
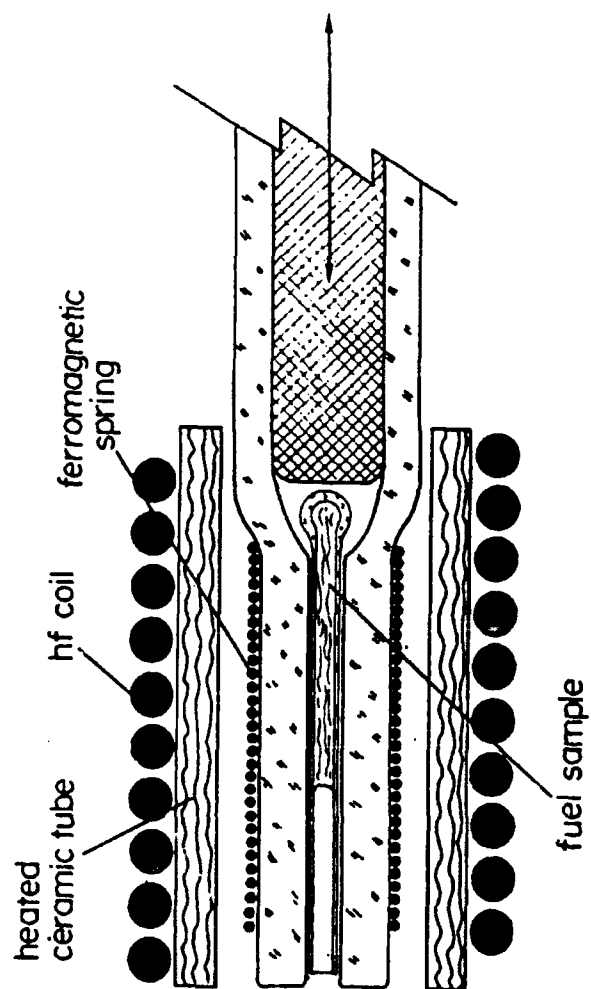


Figure 3. Schematic of capillary sample introduction system

2.2.6 Trace Metals Analysis

The light and heavy fractions of fresh tar oil and crude phenols samples were sent to Pratt & Whitney, W. Palm Beach, Florida for trace metal analysis, performed on an ICP emission spectrometer. The metal contents of Zn, Cd, Ba, B, Mg, Si, Fe, Ni, and V were determined. For the crude phenol stream, Ni and V content were measured using atomic absorption.

2.2.7 Simulated Distillation

Simulated distillation of the light fraction of fresh tar oil and crude phenols were carried out on an HP-5730A gas chromatograph at the U of U Fuels Engineering Department. A 1/4" x 18" stainless steel U tube, packed with Dexsil 400 on 90/100 mesh Anakrom Q was used as GC column. Data were collected every 12 seconds with an HP-26488 computer. The computer program used ASLC method D2887 (corresponding to ASTM method D2887-73), in which paraffins were used for calibration. Typical operating conditions were as follows: injection temp. 250°C before injection and increasing to 350°C after injection, detector temp. 499°C, oven temp. -30 to 350°C, heating rate 11°C/min, final holding time 4 min., carrier gas helium.

2.2.8 Proton Nuclear Magnetic Resonance Spectrometry

Proton NMR spectra of the light and heavy fractions of fresh tar oil and crude phenols were run on a Varian SC 500 superconducting instrument at the U of U Chemistry Department. Samples were dissolved in CDCl₃ with TMS as reference. Spectra were taken of the 0 to 10 ppm region and the integrated peak intensities were tabulated for those samples.

2.2.9 Conventional Analyses

Samples of the light and heavy fractions of fresh tar oils and crude phenols were sent to the Fuels Characterization Laboratory (U of U, Fuels Engineering Department) to determine conventional fuel characterization parameters, including pour point, density and viscosity. Pour points (°C) were measured by ASTM method D-97. Densities (g/cc) were measured using a DMA 40 Digital Density Meter. Viscosities (cp) were determined at two different temperatures: 25°C for the fresh tar oil light fraction and crude phenols and 37°C for the fresh tar oil heavy fraction, using a Wells-Brookfield Micro Viscometer Model LVT-C/P.

2.2.10 Data Analysis

Low voltage mass spectrometry data were first calibrated using the CALEB program, with subsequent normalization and multivariate factor and discriminate analysis by means of the SIGMA program. Both programs were specially developed at UUBPC for the IBM 9000 computer and are written in Fortran 77. From all the low voltage MS data obtained, only the tar stability/weathering data sets were large enough to enable multivariate statistical analysis. First of all, factor analysis was performed on a matrix consisting of all individual mass spectra. Subsequently, discriminate analysis was carried out on all factors with eigenvalues >1.0. Numerical extraction of major chemical components were done by means of the Variance Diagram (VARDIA) method [16]. Finally, factor and discriminate scores as well as discriminate spectra (standardized co-variance plots) were plotted.

SECTION 3.0

RESULTS AND DISCUSSION

Low voltage mass spectra of whole tar oil, naphtha and crude phenols stream samples are shown in Figure 4. The naphtha stream was found to consist of relatively low molecular weight compounds, e.g., short chain alkanes, olefins and alicyclics, many containing heteroatoms such as sulfur, nitrogen and oxygen. The whole tar oil sample is a complex mixture of (alkyl) aromatic compounds including oxygen containing aromatics such as phenols and naphthols, and 2- and 4-ring fused aromatic systems, as indicated in the figure. The crude phenol stream contained primarily mono- and dihydroxyaromatic compounds.

3.1 NAPHTHA STREAM

A full spectroscopic characterization of the naphtha stream was not accomplished, since it is not, per se, a liquid stream sample and is not currently of interest as a potential feedstock for conversion to liquid fuels. Reference 6 states that the stream typically contained 1.5% sulfur and 0.2% nitrogen.

3.2 TAR OIL STREAM

By far the largest (approx. 75% of total distillable liquids) stream is the tar oil stream, produced at a rate of 120,000 to 140,000 gal per day. It also appears to be the richest in (alkyl) aromatic hydrocarbons, principally as 2- to 4-ring compounds. Consequently the tar oil stream was given the most attention in our spectroscopic evaluation. Tar oil samples were obtained from two holding tanks in the process stream, one that was emptied every shift (designated an "8 hour" collection point) and another from the large 30 day holding tank after seven days of collecting (designated by a "7 day" collection point). Another large holding tank was not being used at the time of sample collection.

Seven 125 ml samples of tar were obtained at each collection point. During transport to UUBPC under dry ice, several paper labels designating the collection point came off the bottles. However, the inked numbers on the bottles themselves had remained readable. Consequently, the identities of the unlabeled containers were inferred from the remaining labels and subsequently confirmed in a telephone conversation with ANG personnel.

Furthermore, aliquots from each of the labelled containers as well as two of the unlabeled containers were subjected to low voltage mass spectrometry with subsequent factor and discriminate analysis, to evaluate possible differences among the collection points. Categories for discriminate analysis were defined as replicates from sample containers, so as to treat the data in a relatively unsupervised way. Figure 5 shows the D1 vs. D2 discriminate space which contained 16% of the total variance. It is obvious that the differences among the samples were not well explained by collection point. From a comparison of the variances involved and the average relative s.d. between replicate analyses we concluded that tars from the 8 hr and 7 day collections were very similar with overall differences in composition amounting to less than 2% of the total sample.

3.3 TAR OIL FRACTIONS: LIGHT AND HEAVY

The Air Force requested conventional characterization of two distillate fractions of the whole tar oil in addition to the spectrometric analysis to present to potential contractors for a process development project. Spectrometric analysis was also done on two tar oil fractions obtained by a laboratory distillation of an 8 hour collection point sample into a sample distilling below 200°C (designated "light") and a sample of remaining liquid (designated "heavy"). Distillation yields were 47% for the light fraction and 54% for the heavy fraction. Spectroscopic analysis of the light and heavy fractions included low voltage mass spectrometry, infrared spectroscopy and proton NMR spectrometry.

Low voltage mass spectra of the light and heavy fractions appear in Figure 6. The light fraction has ion series such as alkyl substituted phenols/quinones, naphthalenes and indanes/tetralins. The heavy fraction contains peaks characteristic of generally higher molecular weight compounds, e.g., alkyl naphthalenes, naphthols, biphenyls/acenaphthenes, fluorenes and phenanthrenes/anthracenes. The peak at m/z 178, thought to represent primarily unsubstituted phenanthrene, was the highest peak in the spectrum of the heavy fraction.

When comparing the various low voltage mass spectra it should be kept in mind that aliphatic compounds give relatively weak ion signals under low voltage electron ionization conditions and therefore may well be underrepresented in the spectra. Moreover, the identification of most peak series is tentative and generally these interpretations are based on previous studies of coal pyrolysis products by GC/MS [17] and MS/MS [18] techniques or using numerical extraction of direct MS data [19] as well as on correlations with IR and NMR data [9, 20].

Infrared spectra of the light and heavy fractions of the tar oil are shown in Figure 7. Strong peaks include the $3300\text{--}2800\text{ cm}^{-1}$ region characteristic of aliphatic CH stretching modes, 3048 and 1600 cm^{-1} , from aromatic CH and C=C stretches and the broad absorption at 3400 to 3300 cm^{-1} from hydroxy groups. The spectra show that oxygen in the fractions occurs predominantly in hydroxyl form, e.g., as alcohols or hydroxyaromatic compounds, thus supporting the assignment of the mass spectra peaks as phenols in the light fraction and naphthols and indanols in the heavy fraction.

Attempts to gain quantitative information the IR data are hampered by overlapping peaks of finite band width which ideally should be deconvoluted and then subjected to peak area calculations. Unfortunately, these procedures are neither trivial nor unambiguous. Instead, a simple approach is to measure peak height in absorbance and use that as a semiquantitative yardstick. Relative differences among the light and heavy fractions can be seen from the scaled absorbances in Table 1. The light fraction has more absorbance in the hydroxyl region (3370 cm^{-1}) and the heavy fraction shows higher methylene absorption (2850 cm^{-1}). Absorbances from the aromatic C=C and C-H functional groups (1600 and 3048 cm^{-1}) are fairly similar for the light and heavy fractions. This implies that the light fraction has more hydroxyl substituents on aromatic rings than the heavy.

The significance of the larger aliphatic methylene signal in the heavy fraction can be better elucidated from proton NMR data. The NMR appear in Figure 8. Tabulated proton NMR data for the light and heavy tar oil fractions also appear in Table 1. For complex mixtures such as these tar fractions, NMR can give average structure parameters. We used a system for classifying the regions of the proton NMR spectrum taken from Pugmire [21] on shale oil data.

The overall distribution of the protons in the light and heavy fractions shows that the heavy fraction is less abundant in aromatic protons. Clearly, the heavy fraction distribution of aromatic protons shows most of these to be in 2- and 3-ring aromatic structures, whereas the light fraction has a higher proportion of protons in 1-ring structures. This is in agreement with the mass spectrum in Figure 6b which shows higher molecular weight polynuclear aromatics dominating the heavy fraction.

Interestingly, the heavy fraction also contains a relatively higher proportion of aliphatic proton signals. A more detailed inspection of the aliphatic region for both the fractions reveals that the light fraction contains large numbers of protons in the alpha methyl region (i.e., methyl groups directly attached to aromatic rings) as well as in the beta and gamma CH_2 regions, with the majority of these methylenes in acyclic structures, defined by reference 22 as $1.0\text{--}1.4\text{ ppm}$. This implies that long chain aliphatic structures are present either as side chains or as aliphatic hydrocarbon compounds. The heavy fraction also shows a large signal for beta and gamma CH_2 , principally in acyclic structures.

Finally, the heavy fraction does not show a distinct signal for alpha methyls, rather there is a broad peak

with some structure in the 1.9 to 2.9 ppm region which contains both alpha methyl and alpha methylene signals. A comparison of all alpha types of protons shows that the aromatic rings in the light fraction are more heavily substituted with methyls and methylenes than in the heavy fraction, which appears to have less highly substituted aromatic rings. Hydroxyl protons on phenolic compounds can be found in the 4.0 to 7.5 ppm region, depending on concentration, solvents and temperature [23]. The shape of the hydroxyl peak is usually a sharp singlet. It was not apparent which singlet was due to phenolic hydroxyl protons when examining the spectra of the light and heavy fractions, even when expanding the low intensity 4.4 to 6.4 ppm region.

Elemental analysis and compound type were also measured for the light and heavy fractions. Elemental analysis data for the fractions appear in Table 2. The light fraction contains about 1.5% more oxygen than the heavy fraction. The H/C ratio of the light fraction is slightly higher than the heavy fraction.

Liquid chromatography fractionation results and mass spectra of the fractions appear in Table 2 and Figures 9 and 10, respectively. For the light fraction total hydrocarbon content is higher than for the heavy fraction. The heavy fraction, contains a larger proportion of polycyclic aromatic hydrocarbons, as reflected in LC fraction 2. Looking at total heteroatomic containing compounds, the results at first appear to contradict the assertion from the infrared data that the light fraction contains more hydroxyl groups than the heavy. Note however that these data are presented as weight percent. The mass spectra of the fractions revealed that LC fraction 3 of the light oil contains principally phenolics (at m/z 108, 122, etc.) whereas the heavy fraction contains naphthols (m/z 144, 158, 172). Equimolar amounts of cresol and methyl naphthol have a weight ratio of 0.7. A better comparison of these LC fractionation results is possible by estimating the percentage of oxygen from the compounds contained in the polar fractions. The estimated oxygen percentages based on LC plus MS data can then be compared with the elemental analysis results for the light and heavy oils.

Oxygen Content Estimation for the Light Tar Oil Fraction

The two highest peaks in the mass spectrum of the hydroxyaromatic fraction:

m/z 122 C ₈ H ₁₀ O	13.1% oxygen
m/z 108 C ₇ H ₈ O	<u>14.8% oxygen</u>
	13.95 average oxygen content

Multiplying the average oxygen content of this fraction by its weight %
 $13.95 \times 42.0 = 5.8\%$

The highest peak in the mass spectrum of the polyfunctional fraction:

m/z 138 C ₈ H ₁₀ O ₂	23.2% oxygen
---	--------------

Multiplying by the weight of the fraction:

$$23.2 \times 3.9 = 0.9\%$$

Total oxygen content:

$$5.8\% + 0.9\% = 6.7\% \text{ oxygen in the light fraction}$$

Oxygen Content Estimation for the Heavy Tar Oil Fraction

The two highest peaks in the mass spectrum of the hydroxyaromatic fraction:

m/z 158 C ₁₁ H ₁₀ O	10.1% oxygen
---	--------------

m/z 172 C ₁₂ H ₁₂ O	<u>9.3% oxygen</u>
	9.7% average oxygen content

Multiplying the oxygen content by the weight of the fraction:

$$9.7 \times 49.6 = 4.97\%$$

The two highest peaks in the mass spectrum of the polyfunctional fraction:

m/z 144 C ₁₀ H ₈ O	11.1%
m/z 158 C ₁₁ H ₁₀ O	<u>10.1%</u>
	10.6% average oxygen content

Multiplying as before:

$$10.6 \times 9.5 = 1.01\%$$

Total: 9.7 + 1.01 = 5.98% oxygen in the heavy fraction

The rough estimate from compound type using LC and MS data is comparable results to the elemental analysis data in Table 2. The LC + MS method, however, also shows compound type and provides a much more complete picture of the mixture.

Conventional parameters from both the light and heavy oils appear in Table 3. The simulated distillation data in Table 3 need some comment. Since we were concerned that ASTM simulated distillation methods (developed for hydrocarbon mixtures only) might give inaccurate boiling point distributions due to the polarity of the hydroxy containing compounds, we chose to estimate the distillation curve of these tar oil fractions by thermogravimetry. Thermogravimetry gives a type of flash distillation curve, due to the lack of theoretical plates in the device. In the case of the light fraction, simulated distillation data were obtained by gas chromatography as well. A comparison of the two types of simulated distillation for the light oil reveals the typical differences between types of distillation information, e.g., the boiling range determined by thermogravimetry was 25 to 200°C and by gas chromatography as -30 to 400°C. To estimate the actual range of boiling temperatures in the mixture, the boiling points of compounds assigned from mass spectral data were obtained [24]. For example, m/z 156, C₂ naphthalenes, have boiling points of 250°C (ethyl naphthalene) and 263°C (dimethylnaphthalene) at 760 torr (211 and 221°C at 640 torr in Salt Lake City). It was obvious that higher than 200°C boiling compounds are present in the light oil. The gas chromatography was not done at UUBPC we could not phenolic standards to estimate the effect of polar compounds on the simulated distillation data.

3.4 CRUDE PHENOLS STREAM SAMPLES

Data from the mass spectrum (Figure 4), infrared spectrum and proton NMR spectrum (Figure 11) of the crude phenols stream are shown in Table 4. In the mass spectrum, ion series are present that are characteristic of phenols, dihydroxybenzenes, naphthols and indanols, all hydroxy substituted aromatics. The infrared spectrum contains peaks characteristic of hydroxyl, aromatic and ether or alcohol functional groups, in agreement with the mass spectrum. Low intensity peaks from the aliphatic region on the spectrum are also present. The proton NMR spectrum shows a broad unstructured peak centered at 4.65 ppm which is probably due to water contained in the sample, since phenolic peaks are usually sharper [23]. In the NMR spectrum the largest group of protons are found to be associated with the aromatic region. Protons from alpha methyl groups are also present in high concentration.

All the data indicate that methyl substituted hydroxyaromatics dominate the crude phenols stream, which is not surprising. Compound type analysis by LC fractionation gave 91.1% hydroxyaromatic compounds, and the elemental analysis showed almost 20% oxygen by weight. This oxygen value may be a little high, however, due to the inferred presence of some water in the sample. Conventional parameters are shown in Table 3.

3.5 WEATHERING AND LONG TERM STABILITY STUDIES OF THE TAR OIL

3.5.1 Laboratory Weathering

An 8 hr collection point tar oil sample was weathered for 60 days in a 60°C oven with subaliquots taken at 30 days and 60 days. These aliquots were compared by low voltage MS to a fresh sample stored at -90°C. Figure 12 shows the score plot of factor 1 versus factor 2 which contains 90% of the total variance, with the superimposed weathering direction marked with an arrow. The fresh sample was well differentiated from the 30 day and 60 day samples along the weathering direction. When projected on the proposed weathering axis, the 30 day and 60 day samples appear quite similar. Thus, the main oxidation reactions are probably more or less complete within the first 30 days.

Figure 13 shows the factor spectra along the weathering direction, revealing which compounds changed in the weathering process. Naphthols and phenanthrenes are the dominant ion series which decreased in the weathered samples. Alkyl fragment ions are more pronounced in this direction, indicating that some types of alkyl substitution appear to predispose alkylaromatic molecules to weathering changes.

Only a few compound types show a relative increase upon weathering, e.g., phenols/quinones and C₁ and C₂ substituted naphthalenes. These are perhaps the more stable components of the tar, thus becoming relatively enriched over time. An alternative explanation is that these compounds represent pyrolysis products of oligomers formed during weathering. The most reactive components in self coupling reactions during liquefaction are dihydroxybenzenes [25] which are much reduced in this tar oil due to processing. However, both dihydroxybenzenes (m/z 110, 124, 152) and naphthols or naphthoquinones (m/z 158, 172, 186) decreased during the weathering experiment whereas quinones (and/or phenols, m/z 108, 122...) and naphthalenes (m/z 128, 142, 156) increased.

Conceivably, oligomeric or even polymeric substances might be formed by a coupling reaction of dihydroxybenzene + naphthol with loss of water to form an ether bridged aromatic with further reaction possible at the remaining hydroxy group. Pyrolytic fragmentation of the oligomer in the Curie-point inlet of the MS is likely to favor two stable subunits, e.g., quinone and naphthalene.

3.5.2 Long-Term Stability

Tar oil samples from the 8 hr and 7 day collection points were compared to an "old" sample stored at room temperature for 6 months at the ANG laboratory using low voltage mass spectrometry. Due caution needs to be exercised in interpreting these results, since many sources of variation including compositional differences between feedstock coals (e.g., due to seam heterogeneity or coal weathering) as well differences in storage conditions (e.g., temperature, container type, oxygen levels) may be contributing to the observed differences between tar oil samples.

Discriminate analysis results from the long term storage experiment are shown in Figure 14. Three samples of 8 hr tar oil, two samples of 7 day tar oil and one sample of "old" tar oil were given separate category designations. Figure 14 shows a projection of the samples into a (D1 + D2) versus D3 space which allowed optimum correlation with an imaginary storage time axis as indicated in the Figure. Numerically extracted discriminate spectra corresponding to this axis (Figure 15) indicate that the "old" sample and the 7 day sample contain more phenols and what appear to be short chain acids and H₂S. The 8 hour sample has relatively more dihydroxybenzenes and indane/tetralin series. These trends do not appear to be fully explainable by tar weathering effects alone, as can be surmised from a comparison with the laboratory weathering data in Figures 12 and 13 as well as earlier tar weathering studies. A rough estimate of the variance in the "storage time axis" direction shows that storage time accounts for, at most, 17% of the total variance in the system. This corresponds to an estimated maximum variation in relative tar composition of only a few percent. Apparently, long term storage at ambient conditions is not

especially deleterious to this tar oil.

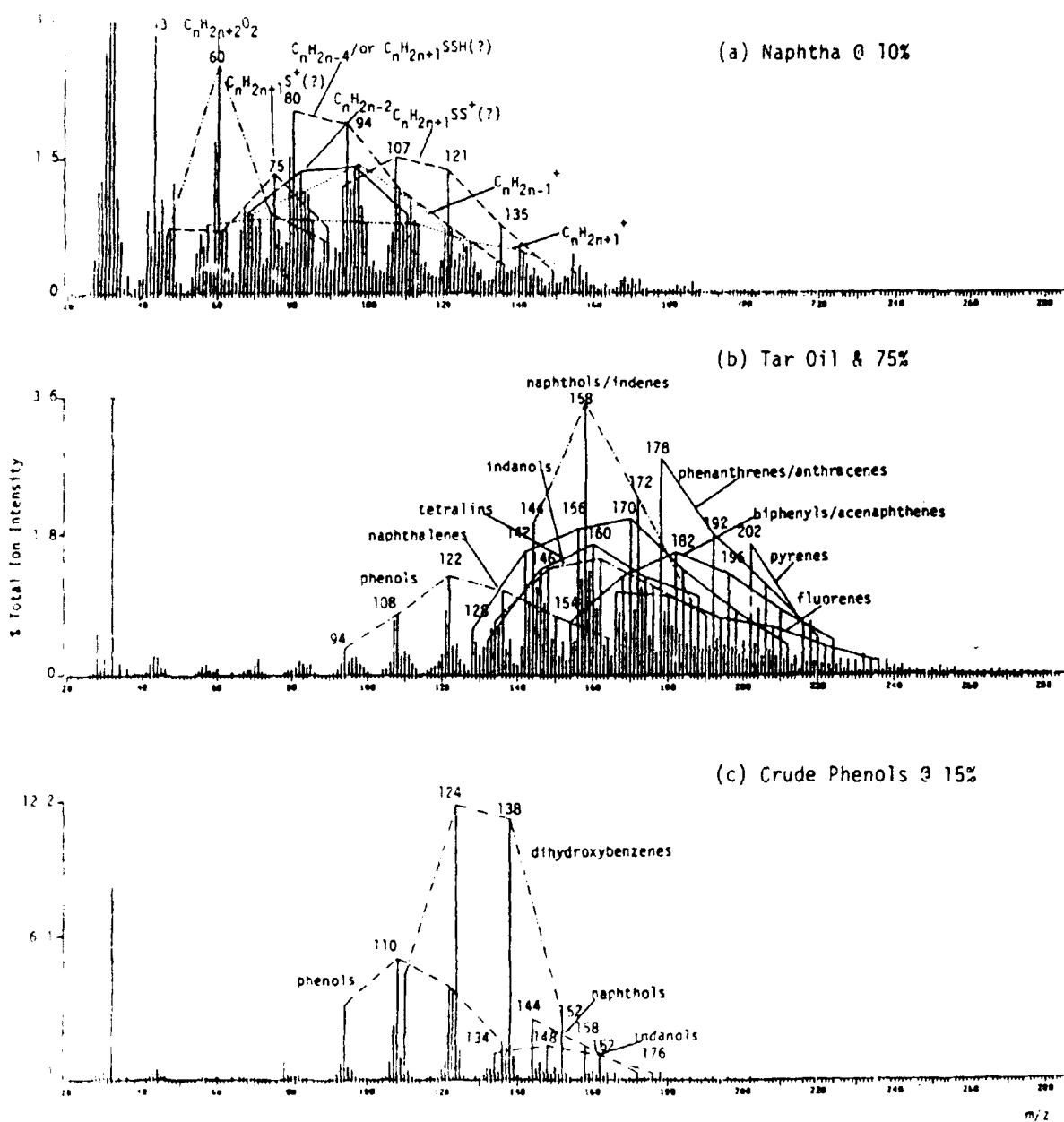


Figure 4 Low voltage mass spectra of the three main product streams obtained from the ANG coal gasification plant

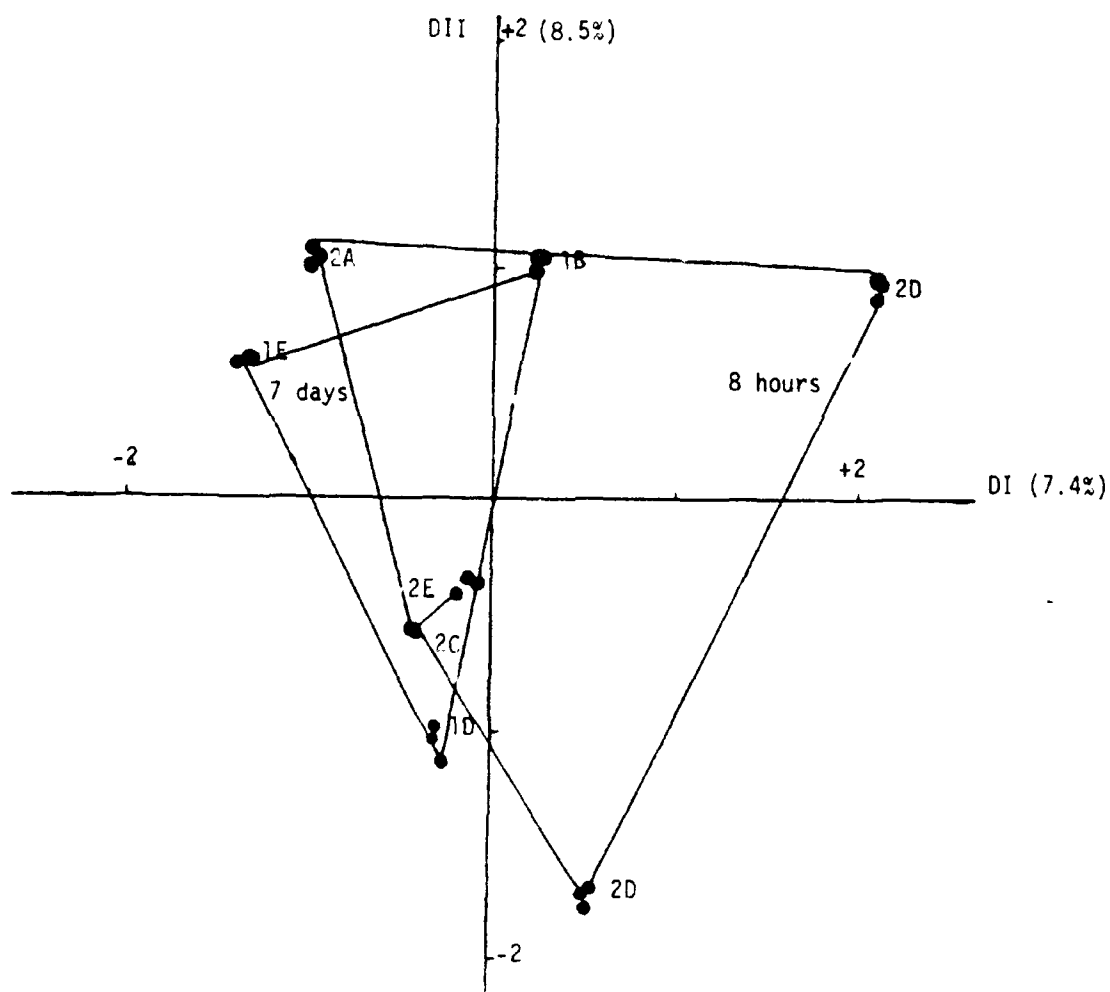


Figure 5. Score plot of the first two discriminant functions obtained on a set of 24 low voltage mass spectra of ANG tar oil representing two collection points. Samples labeled "2" were taken from the midstream holding tank (8 hours storage time) and samples taken labeled "1" were taken from the final holding tank (7 days storage time). A-E describe the samples taken from different bottles. Note that each sample was analyzed in triplicate.

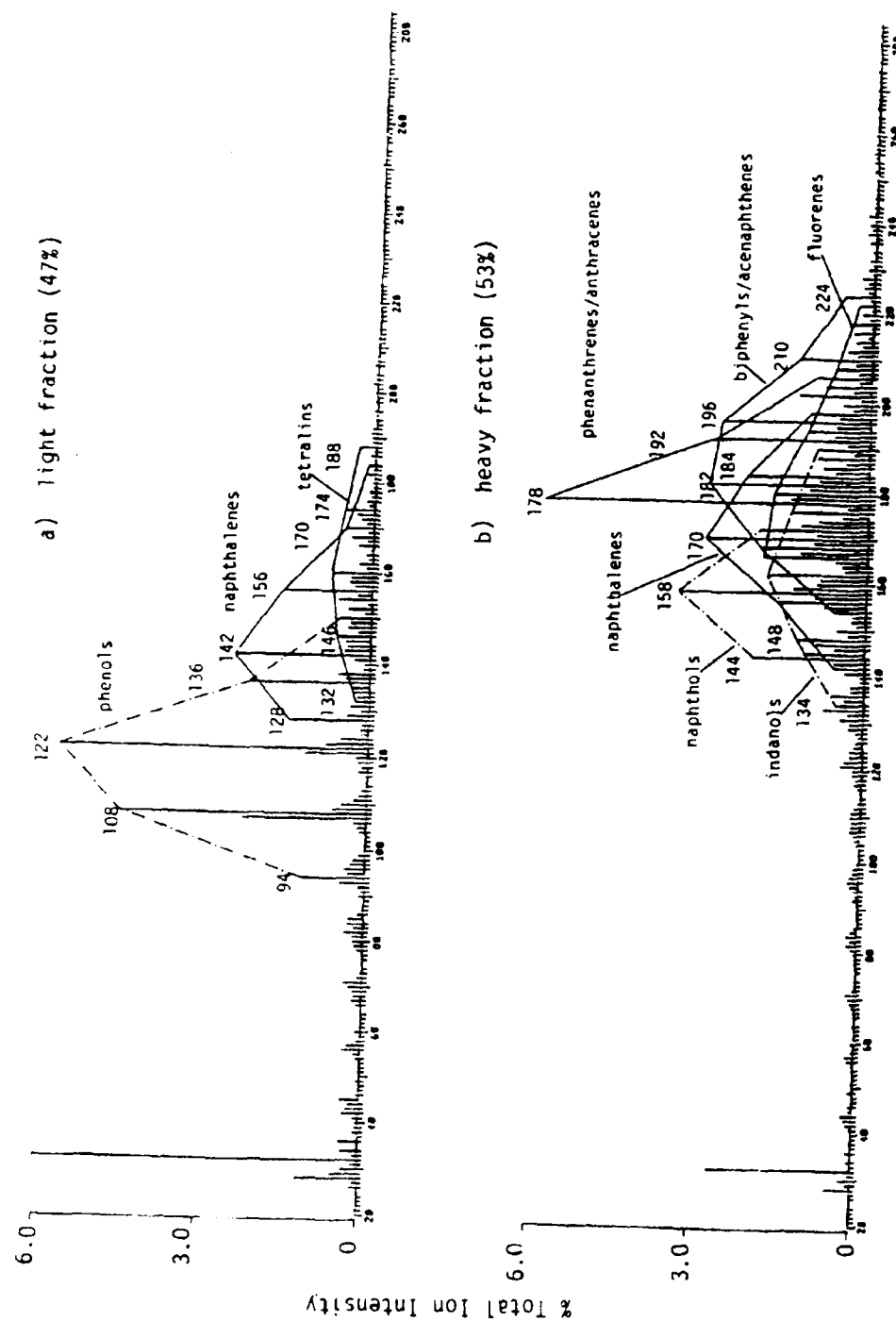


Figure 6. Low voltage mass spectra of the light ($<200^{\circ}\text{C}$) and heavy ($>200^{\circ}\text{C}$) fractions of tar oil obtained from the ANG gasification plant.

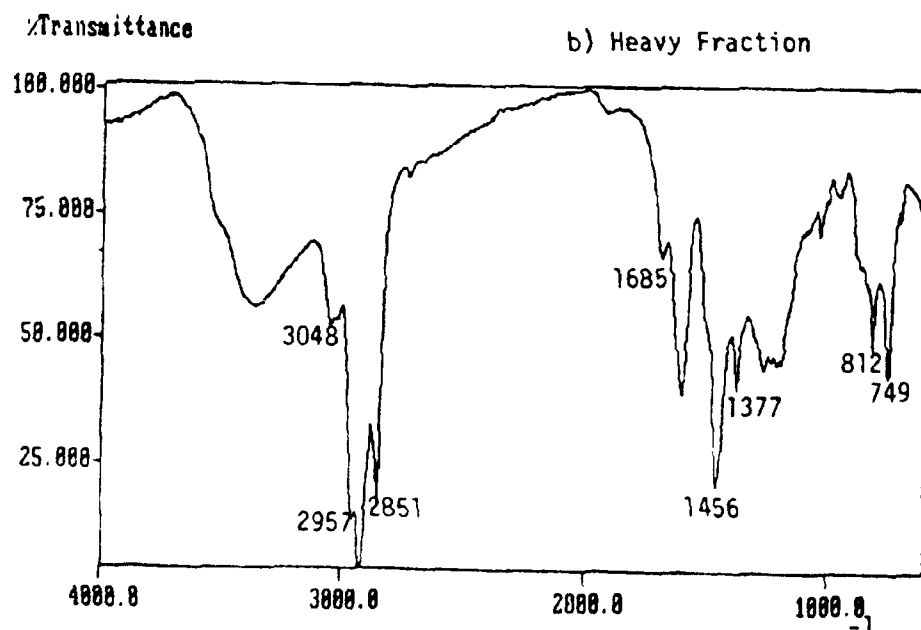
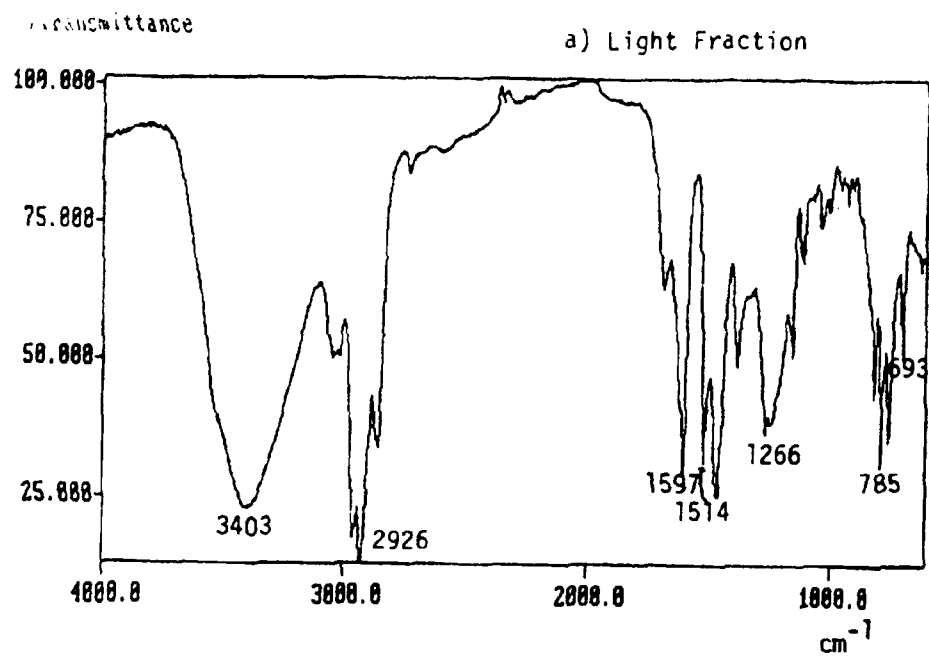


Figure 7. Fourier transform infrared (FTIR) spectra of the light and heavy fractions of tar oil

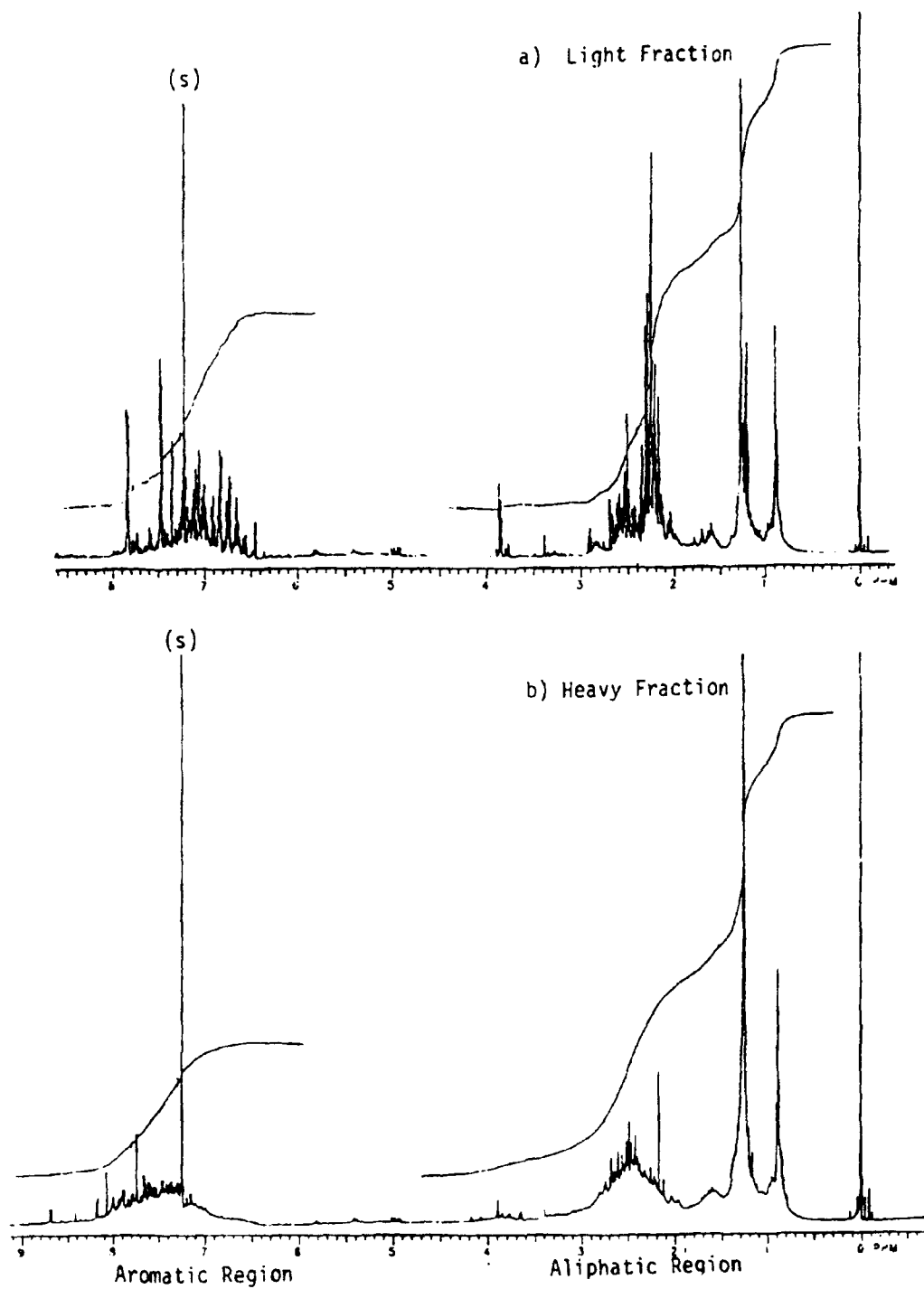


Figure 8. High resolution ^1H -NMR spectra of the light and heavy fractions of tar oil with CDCl_3 as solvent and TMS as reference

TABLE 1

INFRARED AND PROTON NMR SPECTROSCOPIC DATA FROM THE LIGHT AND HEAVY TAR OIL FRACTIONS

Summary of Scaled Infrared Absorbances

Position (cm ⁻¹)	Assignment	Light	Heavy
3370	hydroxy	0.16	0.06
3048	aromatic	0.07	0.07
2957	methyl	0.19	0.22
2850	methylene	0.12	0.20
1685	olefin	0.05	0.05
1600	aromatic	0.13	0.10
1456	aliphatic	0.15	0.17
1265	C-O or O-H	0.11	0.09
1036	C-O	<u>0.03</u>	<u>0.04</u>
		1.00	1.00

Summary of Proton NMR Integrated Intensities

Position (ppm)	Assignment	Light	Heavy
9.0-5.8	aromatic H	0.30	0.22
4.4-0.2	aliphatic H	0.70	0.78
4.4-5.8	olefinic H	<u><0.01</u>	<u><0.01</u>
		1.0	1.0
2-5/5-9	aliphatic H/aromatic H	2.33	3.545

Type of Aromatic

6.0-7.3	1-ring	0.64	0.25
7.3-7.8	2-ring	0.28	0.50
7.8-9.0	3-ring	<u>0.08</u>	<u>0.25</u>
		1.0	1.0

Type of Aliphatic

0.5-1.0	β and γ CH ₃	0.13	0.13
1.9-2.3	α CH ₃	0.35	*
1.9-1.9	β and γ CH ₂	0.36	0.48
(1.0-1.4)	(alkyl CH ₂)	(0.28)	(0.40)
(1.4-1.9)	(cyclic CH ₂)	(0.08)	(0.08)
2.3-4.0	α CH ₂	<u>0.17</u>	<u>*</u>
		1.0	1.0

* one broad peak in the 1.9 to 4.0 region - .40 intensity

TABLE 2

**ELEMENTAL ANALYSIS AND LC + MS COMPOUND TYPE ANALYSIS FOR THE TAR
OIL LIGHT AND HEAVY DISTILLATE FRACTIONS**

<u>Elemental Analysis</u>			
<u>Element</u>	<u>Light</u>	<u>Heavy</u>	
C	82.2	84.61	
H	8.72	7.92	
N	0.47	0.62	
O (by difference)	8.15	6.56	
S	0.46	0.29	
	<u>100.00</u>	<u>100.00</u>	
<u>Molar ratios</u>			
H/C	1.27	1.12	
O/C	0.07	0.06	
<u>LC Fraction</u>			
hydrocarbons	38.5	13.3	(11.9)
PAH	15.6	27.6	(25.7)
hydroxyaromatic	42.0	49.6	(52.9)
polyfunctional	3.9	9.5	(9.5)
	<u>100.0</u>	<u>100.0</u>	<u>100.0</u>
Total hydrocarbons	54.1	40.9	(37.6)
Total heteroatomics	45.9	59.1	(62.4)

() duplicate analysis results for heavy fraction

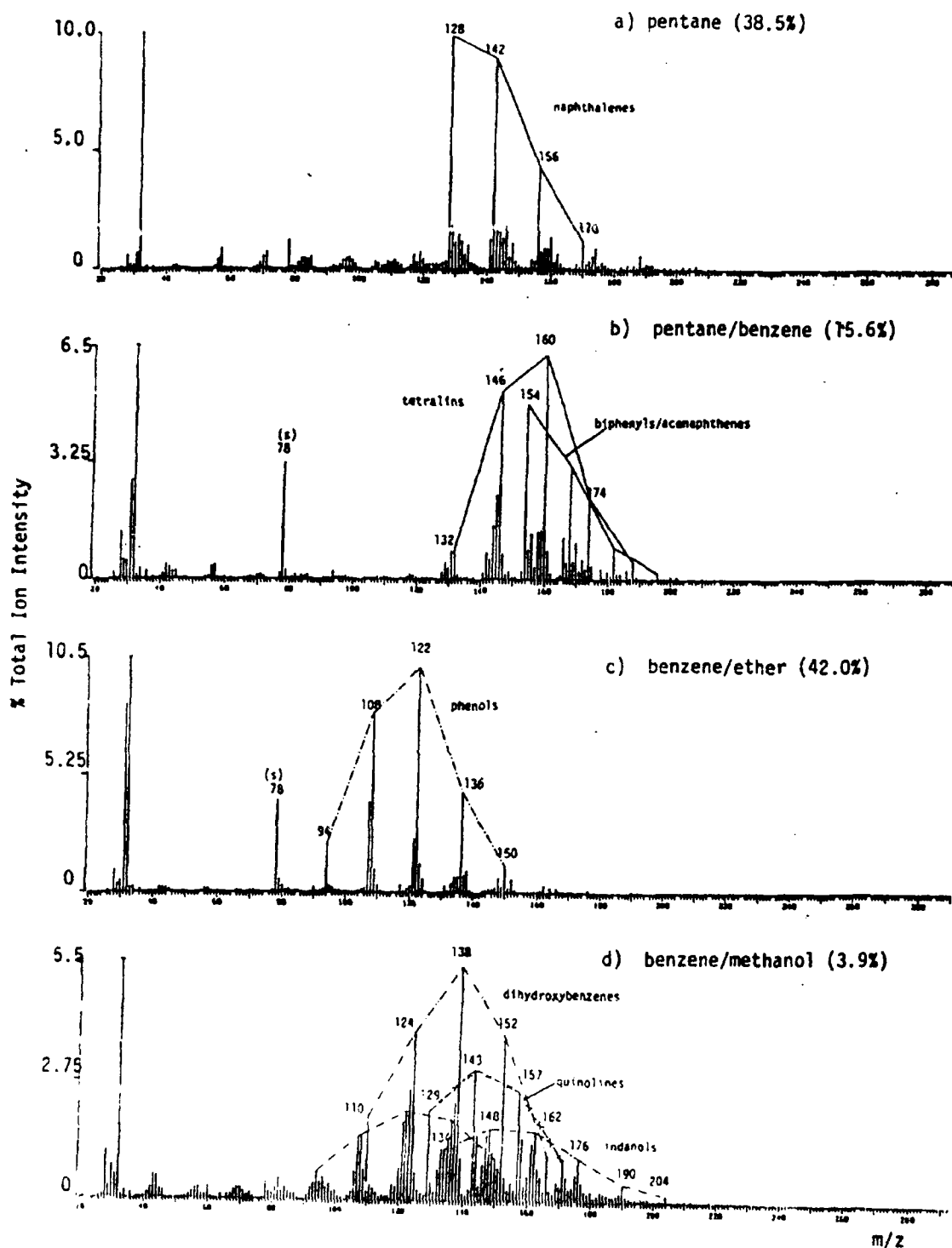


Figure 9. Low voltage mass spectra of four ANG light tar oil fractions obtained by open column silica gel chromatography with increasing polar solvents. Note hydrocarbon character of (a) and (b) as opposed to heteroatomic nature of (c) and (d). (s) indicates solvent peaks. Compare with heavy tar oil fractions in Figure 10.

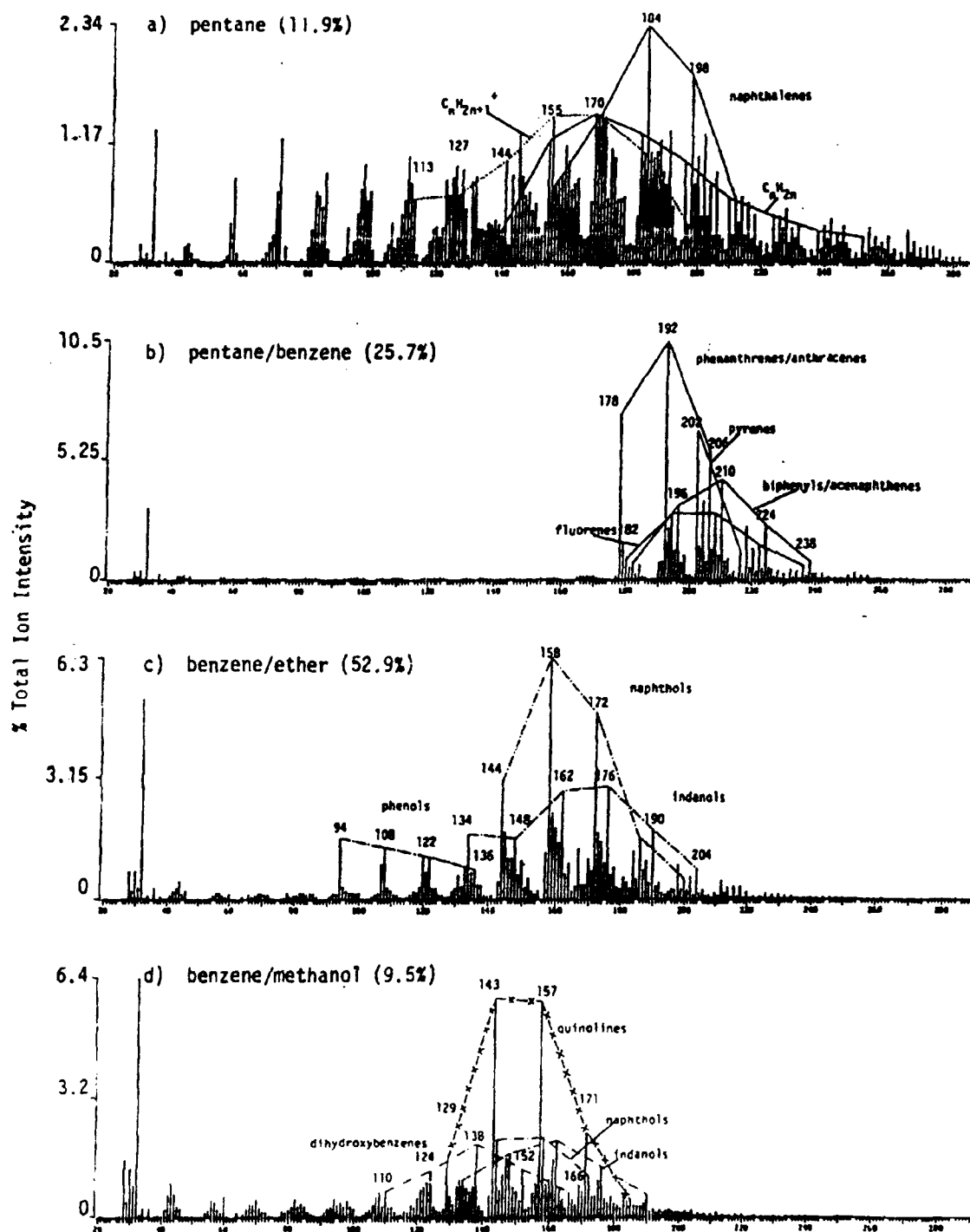


Figure 10. Low voltage mass spectra of four heavy tar oil fractions obtained by open column silica gel chromatography with increasingly polar solvents. Note hydrocarbon character of (a) and (b) as opposed to heteroatomic nature of (c) and (d). Compare with light tar oil fractions in Figure 9.

TABLE 3
LIQUID PRODUCTS EVALUATION

<u>Properties</u>	<u>Tar Oil</u>		<u>Crude Phenols</u>
	<u>Light Fraction</u>	<u>Heavy Fraction</u>	
b.p. range (°C)	82-200	200-388	75-139 ^b
Yield (wt %)	46.8	53.2	-
Density (g/cc) @25°C	0.963	1.007	1.059
Viscosity (cp) @25°C	3.75	1300 ^a	14.78
Pour point (°C)	-35	34	-29.5
<u>Elemental (%)</u>			
C	82.20	84.61	71.83
H	8.72	7.92	7.31
N	0.47	0.62	0.55
O (by difference)	8.15	6.56	19.69
S	0.46	0.29	0.62
<u>Metals (ppm)</u>			
Zn	0.1	0.6	n.d.
Cd	0.1	0.3	n.d.
Ba	0.2	1.4	n.d.
B	0.2	0.9	n.d.
Mg	<0.1	4.0	n.d.
Si	<0.5	12.5	n.d.
Fe	<0.1	11.0	n.d.
Ni	<0.1	<0.1	35
V	<0.1	<0.1	0
<u>Hydrocarbon type by LC (%)</u>			
aliphatics and aromatics	38.5	11.9	0.7
polycyclic aromatics	15.6	25.7	1.4
hydroxy aromatics	42.0	52.9	91.1
polyfunctionals	3.9	9.5	6.8
<u>Simulated distillation by GC (%)</u>			
gasoline (<200°C)	19.7	n.a.	28.58
kerosene (200-275°C)	58.5		59.4
gas oil (275-325°C)	17.9		9.3
heavy gas oil (325-400°C)	3.4		3.5
vacuum gas oil (>400°C)	0.6		-
<u>Simulated distillation by TG (°C)</u>			
10%	63	122	75
20%	79	172	87
30%	88	188	95
40%	98	203	100
50%	103	221	104
60%	110	242	111
70%	117	267	117
80%	125	297	125
90%	132	352	139
FBP	200	452 ^c	278

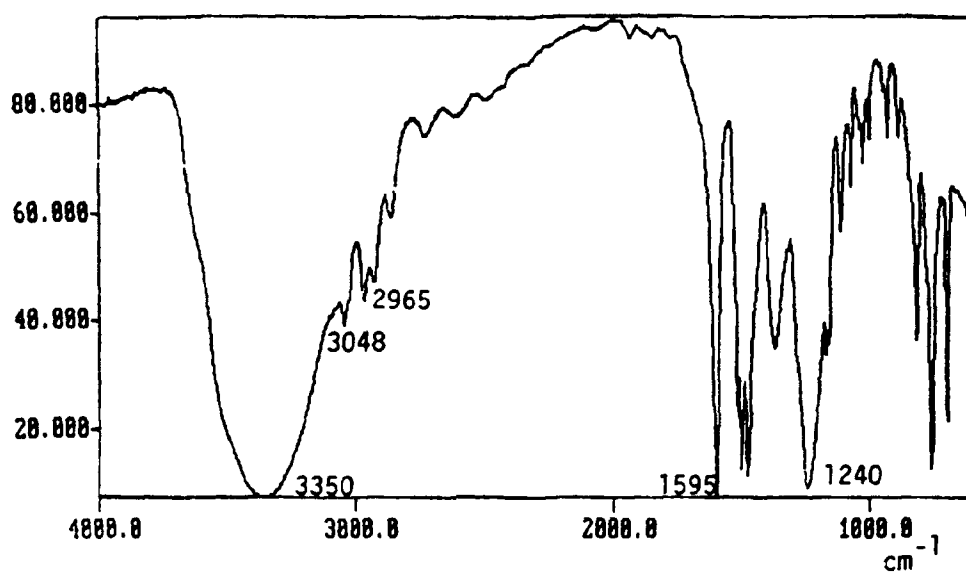
a - measured at 37°C

b - from TG data

c - 4.65% residue left

%Transmittance

(a) Infrared Spectrum



(b) Proton NMR Spectrum

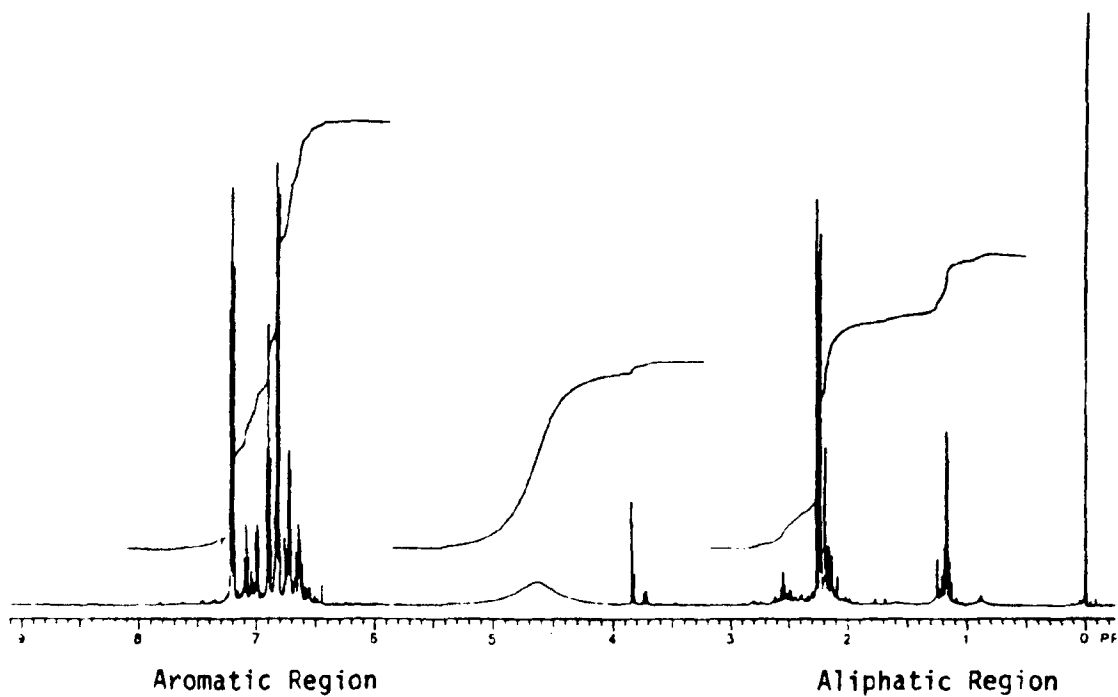


Figure 11. Infrared and ¹H-NMR spectra of crude phenols (stream c) obtained from ANG gasification plant

TABLE 4.
SPECTROSCOPIC CHARACTERIZATION OF THE CRUDE PHENOL STREAM

<u>Mass Spectral Data</u>		
<u>Ion Series</u>	<u>Assignment</u>	
94, 108, 122, 136	alkyl phenols (and/or quinones)	
110, 124, 138, 152	dihydroxybenzenes (and/or methoxyphenols)	
134, 148, 162	indanols (and/or hydroxyindanes)	
144, 158, 172	naphthols (and/or naphthoquinones)	
<u>Infrared Absorbances</u>		
<u>Position</u>	<u>Assignment</u>	<u>Absorbance</u>
3348.8	hydroxy	1.134
1595.3	aromatic	1.115
1240.4	C-O or O-H	1.03
2965.0	aliphatic CH ₃	0.359
<u>Proton NMR</u>		
<u>Position</u>	<u>Assignment</u>	<u>Intensity</u>
9.0-5.8	aromatic	2.294
4.0-0.2	aliphatic	1.568
5.8-4.0	olefinic and OH	1.00
.2-4.0/6.0-9.0	aliphatic H/aromatic H ratio	0.685
<u>Type_of Aromatic</u>		
6.0-7.3	1-ring	0.97
7.3-7.8	2-ring	0.02
7.8-9.0	3-ring	0.01
<u>Type_of Aliphatic</u>		
0.5-1.0	β and γCH ₃	0.02
1.9-2.3	α CH ₃	0.59
1.0-1.9	β and γCH ₂	0.21
2.3-4.0	α CH ₂	0.18

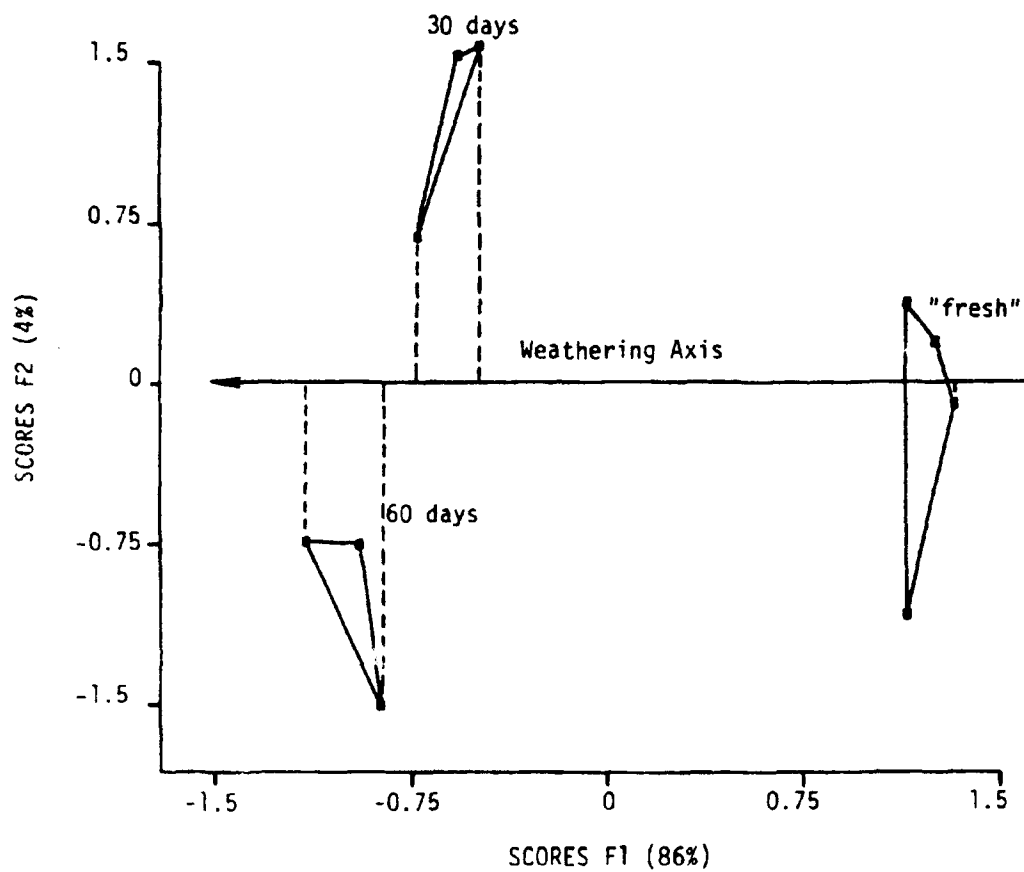


Figure 12. Score plot of the first two factors obtained on a set of 10 low voltage mass spectra of ANG tar oil representing three weathering categories (fresh, 30 days at 60°C and 60 days at 60°C). Each triplicate analysis is connected by lines. Note the weathering axis.

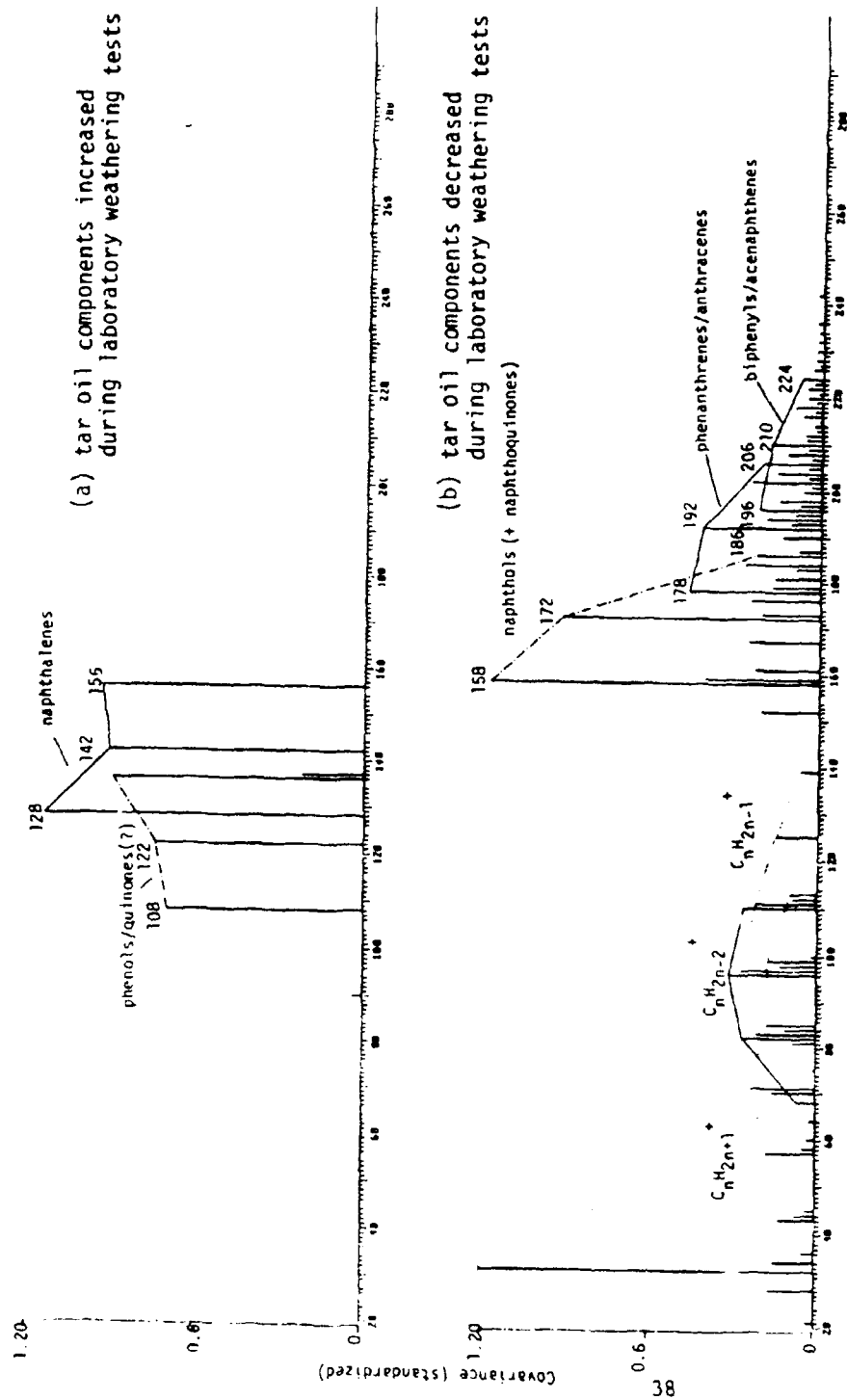


Figure 13. Factor spectrum of the weathering axis (see Figure 12) showing the effect of oxygen exposure on ANG tar oil

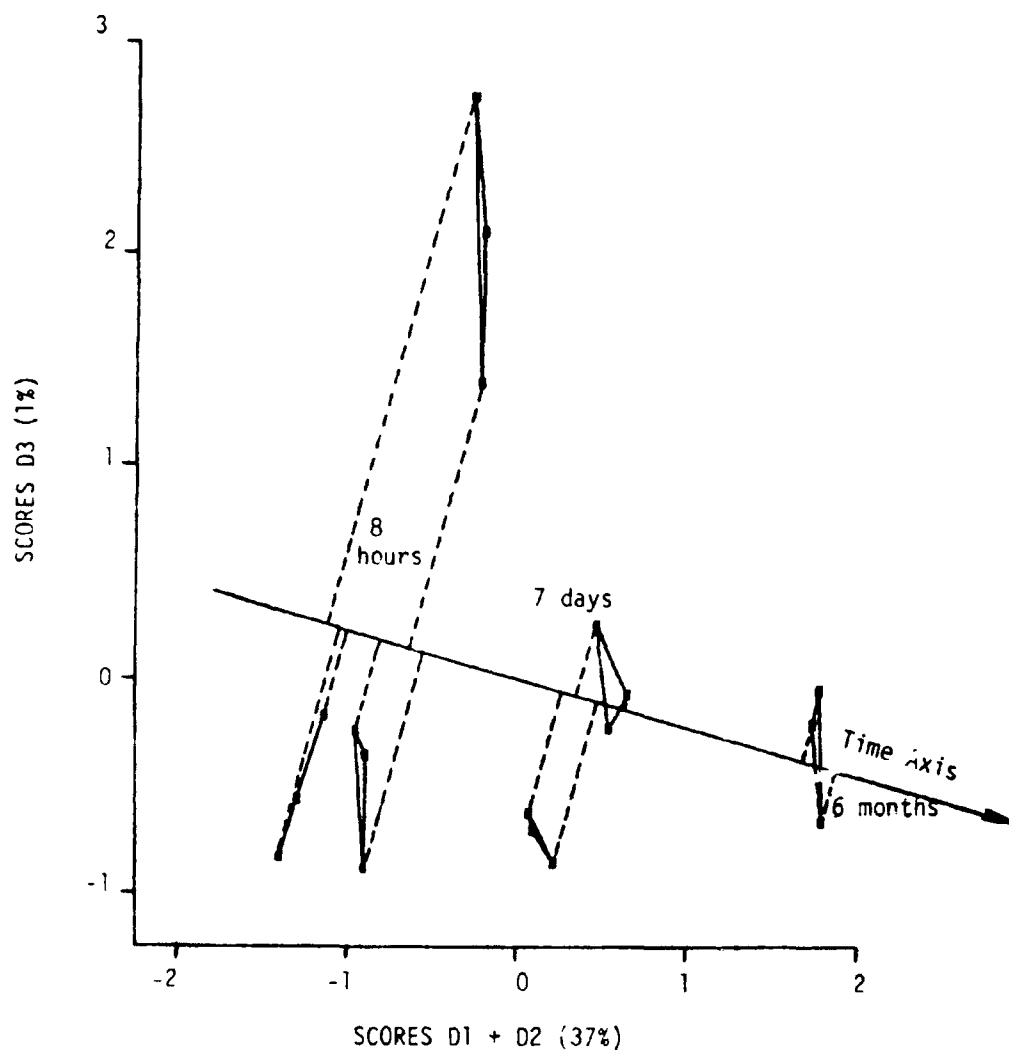


Figure 14. Score plot of the first three functions obtained on a set of 18 low voltage mass spectra of ANG tar oil representing three storage times (8 hours, 7 days and 6 months). Each triplicate analysis is connected by lines. Note the time axis.

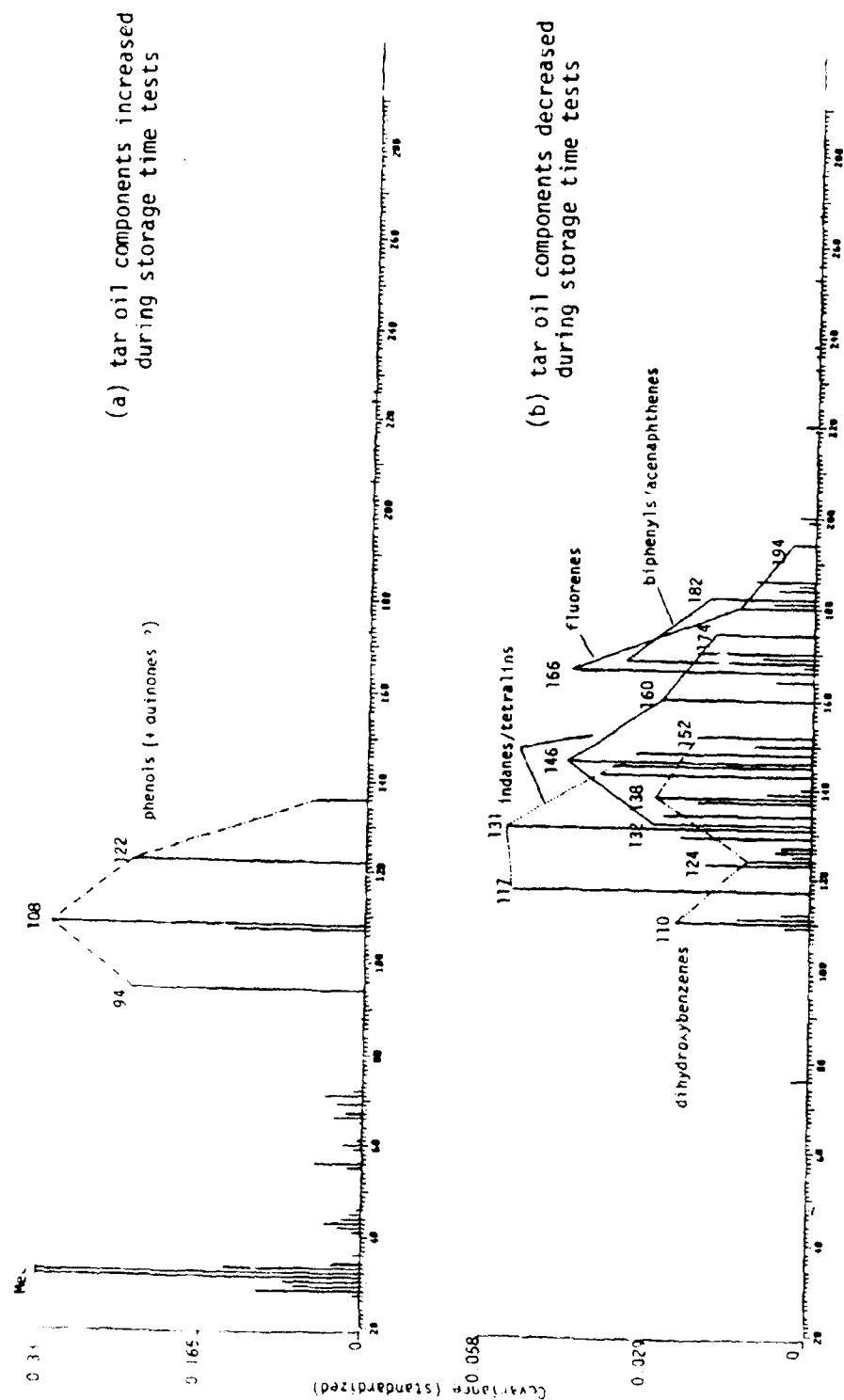


Figure 15. Discriminate spectrum of the time axis (see Figure 14) showing the effect of storage time on ANG tar oil.

SECTION 4.0

CONCLUSIONS

4.1 LIQUID YIELDS

The total yield of distillable liquids produced by the Great Plains Gasifier is approx. 8.5% w/w/ (d.a.f. coal), or close to 1/2 barrel/tone d.a.f. lignite. The three main liquid product streams consist of a light naphtha (approx. 10%) a tar oil (approx. 75%) and a crude phenols fraction (approx. 15%). Fresh samples of all three streams are completely distillable. Approximately 50% of the main tar oil stream distills below 200°C.

4.2 COMPOSITION

Separation of tar oil samples into compound classes by open column LC gives roughly equal amounts of hydrocarbon and heteroatomic (primarily oxygen containing) compounds. Tar oil hydrocarbons were found to be dominated by naphthalenes, tetralins, biphenyl/acenaphthenes and phenanthrenes/anthracenes in addition to significant concentrations of long chain ($> C_{10}$) aliphatic hydrocarbons. Tar oil heteroatomic compounds consist primarily of hydroxyaromatics such as phenols, indanols and naphthols in addition to polyfunctionals (e.g., dihydroxybenzenes) and nitrogen heterocyclics (e.g., quinolines). The crude phenols stream consists primarily of C_0 - C_3 alkylsubstituted phenols, dihydroxybenzenes, indanols and naphthols.

4.3 STABILITY

Tar oil oxidation ("weathering") tests at 60°C in air for up to 60 days indicate good stability with overall sample composition changing by less than 5%. Especially naphthols (and/or naphthoquinones) appear to be involved in regressive ("retrograde") reactions, apparently leading to the formation of a polyphenolic gum through condensation reactions. Tar oil stream samples stored for up to 8 days in the main holding tank or up to 6 months exposure to atmospheric conditions in the ANG laboratory show little or no compositional changes which can be attributed to these exposure conditions.

4.4 SUITABILITY FOR TRANSPORTATION FUELS

The high oxygen content of the tar oil stream (approx. 50% of all molecules contain oxygen) would seem to be the major hurdle in producing transportation fuels in general and aviation fuels in particular. Only after removal of the oxygen moieties (e.g. by hydrodeoxygenation) can the resulting syncrude be compared with petroleum and oil shale-derived crudes of similar aromaticity. Moreover, unless average ring size is reduced (e.g., by hydrocracking) the tar oil derived syncrude is likely to yield primarily diesel grade transportation fuels with relatively small amounts of JP4 - JP8 grade aviation fuels.

Because of the highly aromatic nature of the cyclic compounds in the tar oil, extensive hydrotreatment would be necessary to produce "high density/decalin type") jet fuels. Approximately 20-30% of the tar oil could perhaps be regarded as a possible precursor for such fuels. The very high oxygen content of the crude phenols stream (1-2 oxygen atoms per molecule) appears to make this liquid an unattractive feedstock for transportation fuels. Moreover, although the storage stability of the crude phenols samples was not specifically investigated, previous experience with similar coal-derived liquids predicts a high reactivity towards condensation reactions, thereby causing serious storage stability problems.

REFERENCES

1. D. Crabbe, R. McBride, The World Energy Book. MIT Press, 1979.
2. N.B. Munko, R.J.M. Fry, R.B. Gammage, W.M. Haschek, E.E. Calle, J.A. Klein, T.W. Schultz, "Indirect Coal Liquefaction: A Review of Potential Health Effects and Worker Exposure during Gasification and Synthesis", ORNL-5938, contract W7405-eng-26, 1983.
3. D.B. Howard, W.A. Peters, M.A. Serio, "Coal Devolatilization Information for Reactor Modelling", EPRI AP 1803, Research Project 986-5, April 1981.
4. R.M. Parsons *et al.* "Evaluation of the British Gas Corporation/Lurgi Slagging Gasifier in Gasification Combined Cycle Power Generation", EPRI AP-3980 Research Project 2029-5 and 2029-6, 1985.
5. Black, Sivals, and Bryson, "Fixed Bed Gasification Research Using US Coals" vol. 1. Program and Facility Description. USBOM, contract HO222001, October 1984.
6. A.K. Kuhn, "The Great Plains Gasification Project" Chem. Eng. Progress, (1982) 64-68.
7. D.F. Spenser, S.B. Alpert, H.H. Gilman, Science, 232, #4750 (1986), 609-612.
8. Black, Sivals and Bryson, "Fixed Bed Gasification Research Using US Coals", Vol. 17, Gasification and Liquids Recovery of Four US Coals, U.S. Bureau of Mines, Dec. 1985, contract HO222001.
9. G.R. Hill, H.L.C. Meuzelaar, B.L. Hoesterey, "Characterization of Coal Pyrolysis Liquids" Final Report to Electric Power Research Institute, July 1986.
10. D.L. Imler, D.C. Pollock, A.K. Kuhn, "Progress Report from the Great Plains Gasification Project" 20th IECEC, Miami, SAE Technical Paper Series (1985).
11. Report from ANG Coal Gasification Company, reference not noted, unpublished.
12. W.H. McClennen, H.L.C. Meuzelaar, G.S. Metcalf, G.R. Hill, Fuel, 62 (1983), 1422-1429.
13. I.B. Rubin, M.R. Guerin, A.A. Hardigree, J.L. Epler, Environ. Res. 12, (1976) 358.
14. H.L.C. Meuzelaar, J. Haverkamp, F.D. Hileman, Pyrolysis Mass Spectrometry of Recent and Fossil Biomaterials Elsevier Scientific Publishing Company, 1982.
15. H.L.C. Meuzelaar, W.H. McClennen, "Tandem Mass Spectrometric Analysis (MS/MS) of Jet Fuels, Part II: Quantitative Aspects of Direct MS Analysis" Final Report to Air Force Wright Aeronautical Laboratories, AFWAL-TR-85-2047, July 1985.
16. W. Windig, H.L.C. Meuzelaar, Anal. Chem., 56 (1984) 2297-2303.
17. G. Van Graas, J.W. DeLeeuw, P.A. Schenck, in Advances in Organic Geochemistry Pergamon Press, Oxford, 1979, pp. 485-494.
18. G.R. Hill, W.H. McClennen, G.S. Metcalf, W. Koah-Hsing, H.L.C. Meuzelaar, "The Direct Determination of Oxygen Components in Coal Derived Liquids", Proc. Int. Conf. on Coal Science, Dusseldorf, 1981, pp. 477-481.

19. W. Windig, W.H. McClennen, H. Stolk, H.L.C. Meuzelaar, Optical Engineering, 25 (1986) 117-122.
20. B.L. Hoesterey, W.H. McClennen, W. Windig, H.L.C. Meuzelaar, "Computer Enhanced Separation of Compound Classes in Fuel Mixtures Using a Combined LC/MS Approach", ACS Preprint, Fuel Division, Vol. 30, No. 4, Chicago, 1985, 85-92.
21. D.K. Dalling, B.K. Bailey, R.J. Pugmire, "Carbon-13 and Proton Nuclear Magnetic Resonance Analysis of Shale-Derived Refinery Products and Jet Fuels and of Experimental Referee Broadened-specification Jet Fuels", NASA Contractor Report 174761 under contract NAG3-27, Sept. 1984.
22. R.A. Winschel, and F.P. Burke "Process and Product Oil Characterization in Two Stage Coal Liquefaction" Proceedings of the 8th Annual EPRI Contractors Conference on Coal Liquefaction, Feb. 1984.
23. R.M. Silverstein, G. Clayton Bassler and T.C. Morrill, Spectrometric Identification of Organic Compounds, 4th Ed. 1981, New York, John Wiley and Sons.
24. The Aldrich Catalog Handbook of Fine Chemicals, 1986-1987. The Aldrich Chemical Company, Milwaukee, Wis.
25. D.F. McMillen, R. Malhotra, S. Chang, S.E. Nigenda and G. St. John "The Nature of Oxygen Functions in Coals and their Potential Impact on Co Processing" Proceedings of the 10th Annual EPRI Contractors Conference on Liquid and Solid Fuels, October 1985.

RJ-7 HIGH DENSITY FUEL DEVELOPMENT

Period of Performance

31 December 1989 through 20 June 1990

Reference

Task Order No. 19, Topical Report No. 15, FR 19032-15, Lewis W. Hall, Sun Refining and Marketing Co., June 1990

Abstract

The use of RJ-5 as a component for high density fuel has become less desirable due to high cost and the fact that continued production of the raw material, norbornadiene, needed for production has become very tenuous. The objective of this work was the preparation and characterization of cyclopentadiene/methylcyclopentadiene (CPD/MCPD) cotrimers and of the CPD/Indene adduct such that properties of blends with JP-10 can be characterized and evaluated.

SECTION 1.0

INTRODUCTION

The use of RJ-5 as a component for high density fuel has become less desirable due to high cost and the fact that continued production of the raw material, norbornadiene, needed for production has become very tenuous. Previous work⁽¹⁾ carried out under Contract F33615-88-C-2835 served to identify two potentially attractive high density fuel components that can be blended with JP-10 to produce an advanced fuel substantially equivalent in properties to RJ-6. These components are: (1) a cotrimer of cyclopentadiene (CPD) and methylcyclopentadiene (MCPD) and (2) an adduct of CPD and Indene both of which can serve as a substitute for the RJ-5 component of RJ-6.

The objective of this work is the preparation and characterization of CPD/MCPD cotrimers and of the CPD/Indene adduct such that properties of blends with JP-10 can be characterized and evaluated. Target properties of potential fuel blends are: a maximum freezing point of -65°F, a minimum heating value of 150,000 Btu/gal and a viscosity in the region of 400 cSt at -65 ° F.

SECTION 2.0

EXPERIMENTAL

2.1 COTRIMER FUEL COMPONENT

Previous work⁽¹⁾ had shown that cotrimers produced by heating mixtures of cyclopentadiene (CPD) and methylcyclopentadiene (MCPD) dimers ranging from 16 to 100 mole percent of the latter component resulted in a cotrimer which exhibited a freezing point on the order of 40 degrees lower than CPD trimer. Further work was carried out under this program to prepare and characterize cotrimers between 0 and 16 mole percent in an effort to establish the optimum cotrimer composition required to attain maximum freezing point lowering and minimum viscosity.

Table 1 contains a compilation of cotrimer properties containing 0.06, 0.08 and 0.16 mole fraction MCPD as well as data for cotrimers containing 16 to 100 mole percent MCPD previously⁽¹⁾ determined.

TABLE 1
PROPERTIES OF COTRIMERS
OF CPD AND MCPD

<u>Mole Fraction</u> <u>CPD</u> <u>MCPD</u>	<u>Density 20/4</u> <u>g/cm³</u>	<u>Heating Value</u> <u>Btu/Gal X10³</u>	<u>Melting</u> <u>Point, °C</u>	<u>Glass</u> <u>Transition, °C</u>
1.0 0	1.03	155.4	11	-21
0.94 0.06	1.04	155.6	-2	-89.5
0.92 0.08	1.04	154.8	-12	-88.0
0.84 0.16	1.03	155.5	-28, -35	-
0.84 0.16	1.04	154.8	-28	-84.5
0.74 0.26	1.03	154.3	-29	-84
0 1.0	0.994	150.2	-28	-78

It appears that the optimum cotrimer composition with respect to freezing point occurs at CPD/MCPD ratio of 0.84/0.16.

Properties of blends of the 0.84/0.16 CPD/MCPD cotrimer with JP-10 are tabulated in Table 2. Somewhat surprising is the fact that the cotrimer in JP-10 exhibits a freezing point (-17.5°C) at 40% cotrimer concentration and at 70% (-6.0°C) suggesting a eutectic in the region of 40-70% cotrimer.

TABLE 2
COTRIMER AND JP-10
BLEND DATA

<u>Cotrimer</u> <u>Wt%</u>	<u>JP-10</u> <u>Wt%</u>	<u>Density</u> <u>g/cm³</u>	<u>Heating Value</u> <u>Btu/Gal X10³</u>	<u>Freeze Point</u> <u>°C</u>	<u>Viscosity, cSt</u>	
					<u>-40°F</u>	<u>-65°F</u>
40	60	0.9725	146.9	-17.5		
50	50	0.9820	148.4	-	168.9	599.0
60	40	0.9917	149.6	-	302.7	1304.2
70	30	1.0015	150.9	-6.0	536.7	2984.0
80	20	1.0115	152.2	-15.5, -4.5	-	-

The freezing point observations were confirmed by preparing identical cotrimer/JP-10 blends with an alternate batch of cotrimer. Density and thermal data for the resulting blends are compared in Table 3.

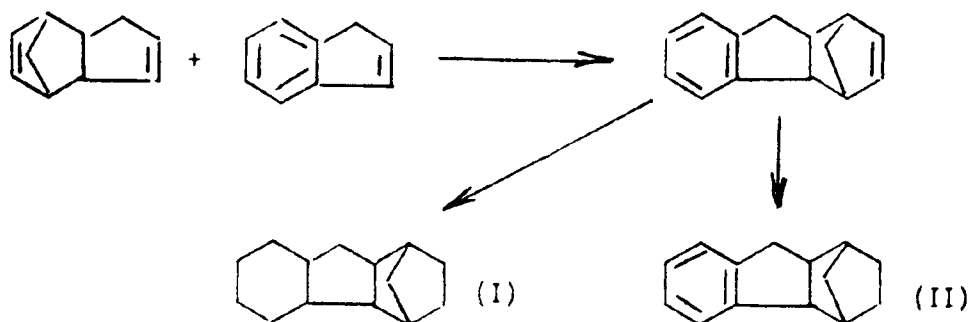
These data would further suggest a eutectic in the range of 40 to 70 weight percent cotrimer in JP-10. Discrepancies in the observed melting points are attributable to thermal history of the sample since in past work, annealing has been shown to affect melting behavior.

TABLE 3
COTRIMER AND JP-10
BLEND DATA

<u>Cotrimer</u> <u>Wt%</u>	<u>JP-10</u> <u>Wt%</u>	<u>Density 20/4</u>		<u>Melting Point, °C</u>	
		Blend		Blend	
		<u>825</u>	<u>832</u>	<u>825</u>	<u>832</u>
40	60	0.9725	0.9731	-17.5	-8.5
50	50	0.9820	0.9829	-	-
60	40	0.9926	0.9917	-	-
70	30	1.0026	1.0015	-6.0	-36.0
82	20	1.0115	1.0127	-15.5	-38.0

2.2 CYCLOPENTADIENE COTRIMER/INDENE ADDUCT

The Diels Alder reaction of Indene and CPD dimer produces an adduct containing of olefinic bond and aromatic ring:



In previous work⁽¹⁾, the CPD/Indene adduct was hydrogenated under severe conditions (Harshaw 5132P Catalyst, 200-235°C, 500 psi hydrogen) to produce the fully saturated molecule I. This compound when blended with CPD trimer and JP-10 produced an attractive fuel blend which has a heating value greater than can be achieved by blending CPD trimer or CPD/MCPD cotrimer with JP-10 within the confines of a -65°F freezing point, but viscosities at -65°F are in excess of the target of 400 cSt at -65°F.

Under milder hydrogenation conditions (5132P catalyst, 100-125°C, 100 psi hydrogen) saturation of the olefinic bond occurs to produce the Dihydro Adduct II in which the aromatic ring remains intact.

Properties of this compound are:

Heating Value Net	151,981 Btu/gal 17,451 Btu/lb
Density	1.0446 g/cm ³
Sp Gr	1.0483
Hydrogen (calc'd)	8.6%

Blends of the Dihydro Adduct II and the Perhydro Adduct I with CPD/MCPD cotrimer and JP-10 were prepared and characterized with respect to target properties shown in Table 4.

TABLE 4
PROPERTIES OF PERHYDRO AND DIHYDRO
CPD/INDENE ADDUCTS WITH CPD/MCPD COTRIMER AND JP-10

Composition, Wt %				Density	Heating Value	Viscosity, cSt	
<u>JP-10</u>	<u>Cotrimer</u>	<u>Perhydro</u>	<u>Dihydro</u>	<u>g/cm³</u>	<u>Btu/Gal X10³</u>	<u>-40°F</u>	<u>-65°F</u>
23.8	52.4	23.8	-	0.9975	151.0	708	3750
20.0	40.0	40.0	-	0.9944	150.5	733	2668
23.8	52.4	-	23.8	1.0101	150.5	*	*
20.0	40.0	-	40.0	1.0151	150.5	516	4100

* Blend exhibited a melting point at -18°C.

SECTION 3.0

DISCUSSION

The data in Table 2 suggest that a binary blend of cotrimer in JP-10 containing 60 weight percent of the cotrimer would achieve the target heating value of approximately 150,000 Btu/gallon which was not achieved with a binary blend of CPD trimer in JP-10. However, the blend viscosity is significantly higher than the target value of 400 cSt at -65°F and generally it appears that CPD/MCPD cotrimer contributes to a greater degree to blend viscosity than does CPD trimer.

Table 4 contains blend data for ternary blends of cotrimer, JP-10 and both dihydro and perhydro indene adducts. In general, the ternary blends provide greater flexibility in achieving heating values in excess of 150,000 Btu/gallon which is not possible with binary blends of either CPD trimer or CPD/MCPD cotrimer. Viscosity, however, is still in excess of the target value of 400 cSt at -65° F.

It is also apparent from the data in Table 4 that the blend viscosity of cotrimer with JP-10 and perhydro

CPD/Indene adduct is significantly higher than a comparable blend using CPD trimer⁽³⁾. As a ternary blend with JP-10 and the CPD/Indene adduct, there appears to be little advantage to using cotrimer as a blend component since it contributes to higher viscosity but not to higher energy values. Freezing points of such blends are within the required -65°F range.

Overall, it appears that blend viscosity at -65° F will be the limiting factor in maximizing fuel energy content. With this in mind, the following blends shown in Table 5 were prepared using the dihydro CPD/Indene adduct, CPD trimer and JP-10.

TABLE 5
PROPERTIES OF TERNARY BLENDS
JP-10, CPD TRIMER AND DIHYDRO CPD/INDENE

Composition, Wt %			Density	Heating Value	Viscosity, cSt	
<u>JP-10</u>	<u>CPD Trimer</u>	<u>CPD/Indene</u>	<u>g/cm³</u>	<u>Btu/Gal X10³</u>	<u>-40°F</u>	<u>-65°F</u>
9.1	63.6	27.3	1.025	152.5	1853	*
16.7	58.3	25.0	1.017	151.6	680	5150
22.9	53.4	23.6	1.011	151.0	385	2861

* Crystallization occurred during measurement.

The data in Table 5 demonstrate a rather wide range of flexibility in blending with respect to energy content and viscosity and also provide significant increases in heating value over the binary CPD/MCPD cotrimer and JP-10 blends shown in Table 2.

SECTION 4.0

CONCLUSIONS AND RECOMMENDATIONS

Based on the data in Table 5, it is apparent that significant flexibility in fuel component blending is available to accommodate some trade-off between fuel heating value and viscosity. Overall it appears that blend viscosity will be the limiting factor relative to maximizing fuel energy content and to the extent that the fuel viscosity requirements are not well defined at this time. The prototype fuel blends shown in Table 6 are suggested for further consideration.

Blend #1 would have the advantage of being the least costly fuel to produce, but would be limited (depending upon fuel viscosity at -65°) to a maximum energy content in the range of 148,000 to 149,000 Btu/gallon or an increase of 4.6 to 5.3 percent over JP-10.

Blend #2 would be a more costly fuel to produce, but would have the advantage of a potential energy

increase of 6 to 7 percent greater than JP-10, depending upon the low temperature viscosity requirements.

TABLE 6
PROTOTYPE FUEL BLENDS

BLEND #1

CPD/MCPD Cotrimer	60 - 65 Wt %
JP-10	40 - 35 Wt %
Heating Value	150,000 Btu/Gallon
Density	0.992 - 0.996 g/cm ³
Viscosity @ -65°F	1300 - 1500 cSt
@ -40°F	300 - 400 cSt
Freezing Point	Below -65°F

BLEND #2

CPD Trimer	53 - 55 Wt %
Dihydro CPD/Indene	23 - 25 Wt %
JP-10	20 - 23 Wt %
Heating Value	151,000 Btu/Gallon
Density	1.01 - 1.02 g/cm ³
Viscosity @ -65°F	2500 - 2800 cSt
@ -40°F	350 - 400 cSt
Freezing Point	Below -65°F

REFERENCES

1. Lewis W. Hall, Jr. "High Density Fuel/Lower Cost RJ-6" WRDC-TR-89-2140
2. Ibid, Table 2.
3. Ibid, Table 3.

PURIFICATION OF RJ-5 AND JP-10 FUELS FOR USE AS STANDARDS

Period Of Performance

01 April 1986 through 17 June 1986

Reference

Task Order No. 8, Letter Report No. 1, 17 June 1986, FR 19372-1, Richard Meehan, Tedd Biddle

Abstract

RJ-5 and JP-10 were purified by vacuum distillation for use as standards by the Air Force in gas chromatography analyses of jet fuels. Purities obtained for RJ-5 and JP-10 were 99.86 % and 99.72 %, respectively.

SECTION 1.0

INTRODUCTION

A 1-quart sample each of JP-10 and RJ-5 fuels, labeled 85-POSF-2361 and 83-POSF-1108, respectively, was received on 17 April, 1986 from AFWAL/POSF for purification by vacuum distillation. The objective of this effort was to provide pure reference standards for use by both users and suppliers of JP-10 and RJ-5 fuels. The standards are used in gas chromatographic analyses to verify composition of the fuels.

SECTION 2.0

EXPERIMENTAL

2.1 DISTILLATION OF JP-10 AND RJ-5 FUELS

Vacuum distillation the JP-10 fuel sample was performed at a vapor temperature of approximately 98°C (208°F) at a pressure of 50 millimeters (mm) Hg. Successive one milliliter (mL) fractions were collected and monitored according to refractive index. Two fractions were collected and retained upon achieving optimum refractive index and agreement to within + 0.0001 of at least three adjacent cuts. Several runs using 100-mL charges were performed to ensure optimum conditions for separation of gross contaminants. Percent purity of the retained fraction was analyzed by gas chromatography. Table 1 shows the distillation parameters and the refractive indices of the distillate fractions collected.

Purification of the as-received RJ-5 sample was accomplished by vacuum distillation at a vapor temperature of approximately 173°C (343°F) at a pressure of 50 mm Hg. Five-mL fractions were collected and monitored for optimum refractive index. The first 3 fractions collected were immediately discarded. The first 2 of these fractions were cloudy in appearance, the third was clear. The retained fractions of 1.5415 or greater refractive index were blended together in order to retain existing isomer ratios. Determination of final purity was accomplished by gas chromatography. Table 2 shows the distillation parameters and refractive indices of the distillate fractions collected.

2.2 GAS CHROMATOGRAPHIC ANALYSES OF DISTILLED FUELS

Gas chromatographic (GC) analyses were performed on the purified JP-10 and RJ-5 fuels to determine purity by weight percent. The work was performed using a Varian Model 3740 chromatograph equipped with a flame ionization detector (FID) and a Nelson Analytical Data System.

Instrument parameters for GC analysis

Column:	Dimethyl-polysiloxane (Hewlett Packard PONA) 0.50 micrometer film thickness 50 meter X 0.025 cm I.D. fused silica capillary
Carrier Gas:	helium, 2.5 cc/minutes
Column Temperature:	150°C to 250°C at 10 C/minute, isothermal for 20 minutes
Injector Temperature:	280°C
Detector Temperature:	280°C
Sample Size:	1.0 microliter, 1:10 Dilution with pentane

SECTION 3.0

RESULTS AND DISCUSSION

The calculated percent purity values for the distilled fuels are:

JP-10 (C-10): 99.72 %

RJ-5 (C-14): 99.86 %

Assuming a linear detector response to mass, these values are based on peak area percents as computed by the Nelson Analytical Data System. The chromatographic conditions used were dictated by the resolution criteria of paragraph 50.2 and Note 9 of Appendix A of Mil-P-87107B for JP-10 and Mil-P-Draft for RJ-5. The gas chromatograph for distilled JP-10 is shown in Figure 1. The chromatograph for RJ-5 is shown in Figure 2.

Ten fractions each of the purified JP-10 and RJ-5 fuels were sealed in 2-mL septum-capped vials. The caps were screw type with Teflon lined replaceable septa. In addition, two 5-mL fractions of each purified fuel were sealed in glass Teflon lined crimp cap type vials. All vials were appropriately labeled and dated. A remaining 25 mL of purified JP-10 and 7mL of purified RJ-5 fuel was sealed in Teflon lined screw cap glass vials, blanketed with nitrogen, and placed in cold storage for future reference. The ten 2-mL and two 5-mL vials of JP-10 and RJ-5 were transported to the Air Force Program Monitor for distribution.

TABLE 1
JP-10 PURIFICATION BY VACUUM DISTILLATION

<i>Fraction Number</i>	<i>Fraction Size, mL</i>	<i>Liquid Temp.(°C)</i>	<i>Vapor Temp.(°C)</i>	<i>Refractive Index N_D^{25}</i>	<i>Disposition</i>
1	1	106.0	98.4	1.4866	discarded
2	1	106.0	98.4	1.4864	discarded
3	1	106.0	98.4	1.4864	discarded
4	1	106.0	98.4	1.4870	discarded
5	1	105.9	98.4	1.4870	discarded
6	1	-----	-----	1.4869	discarded
7	1	105.7	98.4	1.4869	discarded
8	1	105.8	98.6	1.4869	discarded
9	1	105.8	98.6	1.4869	discarded
10	45	-----	-----	1.4870	retained
11	20	112.8	98.8	1.4870	retained
12	1	-----	----	1.4869	discarded

Distillation Parameters

- Charge: 100 mL
- Pressure: 50 mm Hg

Refractive Index N_D^{25}

- As received: 1.4865
- Maximum achieved: 1.4870

GC Analysis For Purity

- 99.72 wt %

TABLE 2
RJ-5 PURIFICATION BY VACUUM DISTILLATION

<i>Fraction Number</i>	<i>Fraction Size, mL</i>	<i>Liquid Temp. (°C)</i>	<i>Vapor Temp. (°C)</i>	<i>Refractive Index n_d^{25}</i>	<i>Disposition</i>
1	2.5				discarded
2	2.5			1.5386	discarded
3	2.5	174.6	172.2	1.5400	discarded
4	5.0	174.6	172.2	1.5400	discarded
5	5.0	174.8	173.0	1.5406	discarded
6	5.0	174.7	173.0	1.5410	discarded
7	5.0	174.8	173.0	1.5411	discarded
8	5.0	174.8	173.0	1.5411	discarded
9	5.0	174.8	173.4	1.5413	discarded
10	5.0	174.8	173.4	1.5415	retained
11	5.0	174.8	173.4	1.5415	retained
12	5.0	174.8	173.4	1.5415	retained
13	5.0	174.8	173.7	1.5415	retained
14	5.0	175.0	173.7	1.5419	retained
15	5.0	175.2	173.8	1.5419	retained
16	5.0	175.6	174.4	1.5420	retained
17	5.0	176.6	174.4	1.5424	retained
18	3.0	177.5	172.4	1.5425	retained

Distillation Parameters

- Charge: 100mL
- Pressure: 50 mm Hg

Refractive Index, n_d^{25}

- As received: 1.5401
- Maximum achieved: 1.5425
- Fractions retained & mixed for GC analysis: > 1.5415

Gc Analysis For Purity

- 99.86 wt %

Pk No.	Ret Time	Peak Area	Area %	B L	Peak Ht.	Normalized %	Area/ Height
1	10.25	1562668	94.0945	2	102208	100.000	12.8
2	10.70	92517	5.6274	2	10259	5.981	8.9
3	11.75	2127	0.1280	2	219	0.176	9.7
4	12.10	2475	0.1501	2	259	0.160	9.6
Total Area:		1561306	Area Reject:		0 One sample per 1.000 sec.		

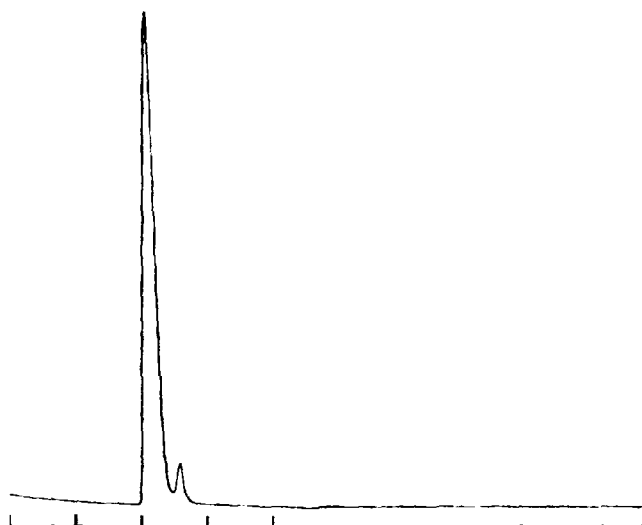


Figure 1. Gas Chromatogram of Distilled JP-10

Pk No.	Ret Time	Peak Area	Area %	B L	Peak Ht.	Normalized %	Area/ Height
1	11.52	1849	0.0483	1	153	0.065	12.1
2	13.07	388	0.0124	2	51	0.021	11.5
3	13.75	943	0.0247	2	65	0.033	14.6
4	16.08	521287	13.6513	2	18886	18.221	27.6
5	16.42	407194	10.6478	2	18274	14.233	22.3
6	17.82	2860881	74.8099	2	67695	100.000	42.3
7	18.83	22664	0.5926	2	1982	0.792	11.4
8	19.35	6696	0.1731	2	559	0.254	12.0
9	21.73	1006	0.0263	1	65	0.035	15.4
10	28.57	1093	0.0286	1	68	0.038	16.0
Total Area:		3824201	Area Reject:		0 One sample per 1.000 sec.		

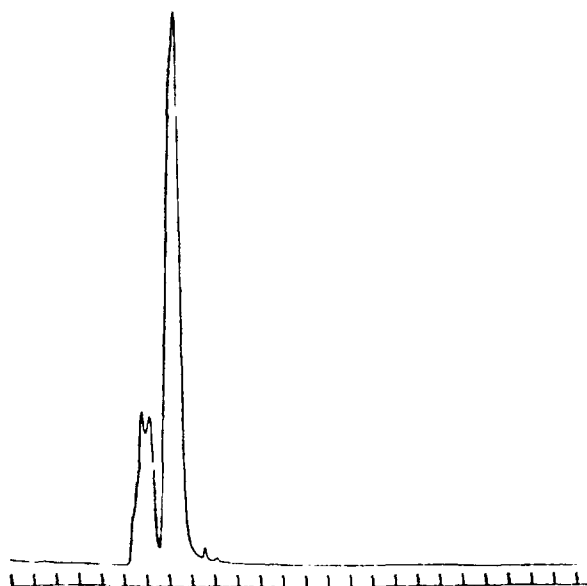


Figure 2. Gas Chromatogram of Distilled JP-10

ALTERNATE HIGH FLASH POINT CALIBRATION FLUID

Period of Performance

June 1987

Reference

Task Order No. 12, Letter Report No. 2, FR 19372-2, June 1987, Susan Guisinger

Abstract

A literature search was performed to identify a high flash point alternative to Mil-C-7024B Type II calibration fluid. Candidate fluids were evaluated for flash point, density, kinematic viscosity, freeze point, and cost.

SECTION 1.0

INTRODUCTION

The ongoing investigation of candidate high flash point fuel component calibration fluid is detailed in this report. This effort is in response to the ASD/EN "Technical Need" (TN-ASD-AFWAL / PO-2104-87-61) entitled "Nonhazardous Methods of Testing Aircraft Fuel System Components."

This document states that the aircraft fuel system components should be tested under similar conditions as those experienced in service. The current test fluid MIL-C-7024B, Type II, has a flash point of 38°C (100°F) which severely restricts testing of aircraft components that operate at higher temperatures. In addition, safety limitations on the use of this fluid are imposed by NFPA (Class I, Division I, Groups C and D). The equipment and facilities required include: explosion proofing, air purging or complete air exchange on a frequent basis, venting, special heaters, fire suppression and sprinkler systems, air conditioning, automation, and personnel hazard preventive measures.

To reduce these safety requirements, the flash point of the calibration fluid needs to be at least 80°C (176°F). This is the primary target property. Fluid density and viscosity are both vital to calibration calculations according to Pratt & Whitney engine control groups. Therefore, it is important to match these two properties with typical fuel values. The freeze point is included to insure that the fluid can be pumped at lower temperatures. A summary of these target properties can be found on the following page in Table 1. Cost is also important as the estimated amount of calibration fluid usage by the government and industry appears to be relatively high. Pratt & Whitney uses around 20,000 gallons of MIL-C-7024B, Type II per year. The Air Force is the largest user at approximately 765,000 gallons per year for Tinker and Kelly Air Force Bases.

SECTION 2.0

DISCUSSION

In an initial literature search using the Dialog Computer Database, a patent for a high flash point fuel calibration fluid was found. This patent (Reference 1) was issued in April 1986 to Roscoe Pike of United Technologies Research Center (UTRC) which is a division of United Technologies Corporation (UTC). This work had been done in the period from February 24 to May 9, 1975 in response to a request from

Hamilton Standard, another UTC division. See Reference 2. This fluid matched all the requirements for flash point, density, viscosity, and freeze point.

Isopar M, a high boiling isoparaffinic solvent, was suggested as an alternate calibration fluid. Exxon and Phillips Petroleum were contacted for information. Exxon produces Isopar M and Phillips produces an equivalent fluid called Soltrol 170. Dow Corning 200 silicone fluids were also suggested. A 2.0-centistoke fluid was selected for the best viscosity and flash point match.

A summary of the fluids, pertinent properties, and 1986 costs is found in Table 1. The UTRC fluid patented by Mr. Pike (90% dodecane / 10% dioctyl phthalate) matches all the required properties. The Phillips Soltrol 170 matched all the properties except viscosity which was high. Exxon Isopar M had a low flash point and high viscosity values. The Dow 200 fluid matched all properties except density which had a value of 0.873 g/mL at 25°C (77°F). This is greater than the target limits of 0.74 to 0.78 g/mL at 15.5°C (60°F).

In the cost analysis, the current MIL-C-7024B fluid appears the most desirable. The next candidate was Soltrol 170, however, viscosity was not within limits. Similarly, Isopar M is viscosity limited. The UTRC fluid is expensive based on limited quantities but reducing certain safety applications and ordering in bulk might make this a viable alternative. In addition, because of the simple matrix, it may be possible to develop simple low cost reclamation procedures to lower the cost of the fluid. The price of the Dow fluid is extreme at \$8,100 per 55 gallons, making only small scale testing reasonable.

TABLE 1
HIGH FLASH POINT REPLACEMENT CALIBRATION FLUID CANDIDATES

TABLE 1 HIGH FLASH POINT REPLACEMENT CALIBRATION FLUID CANDIDATES							
Fluid Type	Flash Point, °C	Density 60°F g/mL	-20°C	Kinematic Viscosity 25°C	40°C	Freeze Point, °C	Cost \$/55 gal.
Target Req.	80	.74 - .78	1.5 - 6.0		0.5 - 2.0	< -46	
JP-4, Typical	-23	0.762	1.72	0.89	0.755	< -62	55
JP-8, Typical	53	0.818	4.40	1.50	1.18	< -54	34
Mil-C-7024, II	38			1.165-1.175			91
UTRC Fluid	83	0.76	06.09	2.11	1.66	< -54	510
Isopar M	77	0.783	15.51	3.39	2.45	< -60	179
Soltrol 170	85	0.776	14.57	3.22	2.33		146
Dow 200	87	>0.873	4.94	2.0	1.61	< -100	8100

SECTION 3.0

CONCLUSION AND RECOMMENDATIONS

Further work should include a formal industry search and consider both property and cost restrictions. Considering the need to meet safety requirements, cut costs, and meet all property requirements the UTRC fluid appears to be the most viable candidate investigated. Component calibration tests are recommended to ensure compatibility before actual implementation. The cost reducing possibility of reclamation of the UTRC fluid by filtration and distillation should also be examined. Table 2 shows the boiling point differences between the two components.

TABLE 2
PROPERTIES OF DODECANE AND DIOCTYLPHTHALATE

Property	Dodecane	Dioctylphthalate
Molecular Weight	170	391
Boiling Point, °C	216	384
Freezing Point, °C	-10	-50
Flash Point, °C	71	207
Density at 15.5°C, g/mL	0.749	0.961

REFERENCES

1. Pike, Roscoe A., United States Patent, Number 4,582,631 "High Flash Point Fuel Control Calibration Fluid" April 15, 1986.
2. Pike, Roscoe A., UTRC Report R75-313035-1, "High Flash Point Fuel Control Calibration Fluids", May 1975.

JP-10 FUEL DISCOLORIZATION INVESTIGATION

Period of Performance

15 November 1985 through 30 October 1986

Reference

Task Order No. 2, Topical Report No. 5, October 1986, FR 19032-5, H.L.C. Meuzelaar, W.H. McClennen, B.L. Hoesterey, J.A. Bunker

Abstract

In response to an Air Force field report of fuel discoloration during pumping operations, a short term investigation was conducted at the University of Utah Biomaterials Profiling Center (UUBPC). The objective of the investigation was to determine the cause of the discoloration and evaluate the possible consequences on fuel properties and material compatibility. This effort was performed under the direction of Dr. Henk Meuzelaar of UUBPC, Dr. H.R. Lander of AFWAL/POSF and monitored by P&W.

SECTION 1.0

BACKGROUND

1.1 JP-10 PROBLEMS EXPERIENCED BY THE AIR FORCE

The studies reported here were undertaken after a sample of JP-10 fuel was submitted by the Air Force because yellowish discoloration was observed during aircraft fuel pump tests. The tests involved recycling of JP-10 which had been stored in relatively small fuel tanks for periods of up to several years.

In addition to the discoloration, metallic (copper?) particulates had been noticed by Air Force personnel at the bottom of JP-10 containers after recycle pumping tests. Moreover, subsequent conventional fuel characterization methods carried out by an outside laboratory showed the discolored JP-10 samples to be "out of spec" for flash point (low) specific gravity (low), color (yellow) and gum content (high).

Since electrical fuel pumps used in the recycle tests were thought to be possibly responsible for the observed JP-10 changes by Air Force personnel, several used as well as new pumps were received for testing along with a number of JP-10 "control" samples which had not undergone recycle tests and were known to represent JP-10 batches derived from different drums or even refineries. Moreover, Air Force personnel had undertaken several fuel stability and compatibility tests involving exposure of different fuel system components (whole pumps, pump armatures and selected polymers) to JP-10 at temperatures up to 60°C and periods up to several months or even years. JP-10 samples from these tests, some which had shown evidence of possible JP-10 degradation (discoloration, resin formation) were also made available to us.

Finally, towards the end of the study a JP-10 sample showing yellowish discoloration upon retrieval from a large storage tank and which had failed the JFTOT (Jet Fuel Thermal Oxidation Test) was submitted for analysis.

1.2 JP-10 PRODUCTION PROCESS INFORMATION

JP-10 is an Air Force fuel Meeting the -53C (-65F) operational requirement for use in the Air-Launched Cruise Missile (LCM). JP-10 in its purest form has the single chemical structure exo-tetrahydrodi(cyclopentadiene). Commercial JP-10 is made by a multistep process from cyclopentadiene. The cyclopentadiene is generally isolated from refinery hydrocracker products and separated by distillation from the methyl substituted isomers. The cyclopentadiene is dimerized to form the compound dicyclopentadiene which is then hydrogenated over a nickel catalyst to give the endo-isomer of tetrahydrodi(cyclopentadiene). The endo-isomer is not suitable for use as a jet fuel because of its high freezing point so that it is isomerized over an aluminum chloride catalyst to form the exo-isomer which only freezes below -70°C. This product is washed to neutralize it and purified by a narrow distillation cut with a 3-4°C boiling point range. Finally, 2-methoxyethanol is added as an icing inhibitor and dibutylhydroxytoluene (BHT) is added as an antioxidant.

1.3 AVAILABLE LITERATURE DATA ON JP-10 COMPOSITION AND STABILITY

A previous Air Force report [2] examined the purity of JP-10 samples and showed that at least two isomers are present in low concentration and are not readily removed even by very narrow fractional distillation cuts. One of these is some residual endo-isomer which is actually considered advantageous at concentrations up to 4% in order to increase overall specific gravity [1]. JP-10 oxidation products have also been examined [3] although the fuel is normally considered very stable due to the fact that virtually no aromatics or unsaturated compounds can survive the aluminum chloride isomerization step [1].

SECTION 2.0

EXPERIMENTAL

2.1 SAMPLE DESCRIPTION

Table 1 lists the JP-10 samples delivered by Air Force personnel for analysis. V-39 was one of the first yellow samples taken from an aircraft refueling operation. ALS is the field sample received from another Air Force Base storage tank where fuel yellowing was observed near the end of our project. Control CA consisted of 4 gallons of JP-10 batch 84-1-B which we obtained from Hill Air Force Base to use in our own accelerated aging tests. The control CB includes a collection of several separate samples intended to represent the starting material for the V-39 fuel and subsequent accelerated aging tests performed by Air Force personnel. Controls CC and CD were taken from two other separate sources to help us examine the range of variation between different JP-10 batches. CC was produced in 1985 and obtained as a relatively fresh sample directly from the Koch refinery. Sample CD was produced in 1977 and has been stored in covered outdoor ambient conditions at Wright Patterson AFB since then. The rest of the JP-10 samples in Table 1 are the result of one dynamic fuel pump test and several static accelerated aging tests performed by Air Force personnel.

**TABLE I.
LIST OF SAMPLES**

Sample Code	Description
(Field Samples)	
V39, V40, PFP	first yellow samples of JP-10 V39 and V40 taken from vehicles. PFP from process fuel panel
ALS	later yellow sample of JP-10 from Allison AFB became discolored after storage in fuel tank
(Control Samples)	
CA	JP-10 batch 84-1-EB stored at -30°C at UUBPC in glass containers
CB	a) presumed JP-10 control for V39, V40, and PFP obtained and stored in polyethylene containers b) JP-10 control for T2-T4, S2-S4 samples
CC	JP-10 from Koch refinery, batch 85-9
CD	JP-10 batch labelled "received Aug. 1977" stored by A.F. personnel since 1977
(Samples Obtained from Air Force Laboratory Tests)	
S1	2.5 year extraction of 2 fuel pumps kept at ambient temperature
S2	extraction of urethane tubing kept for 2 months at 60°C formed brown gum deposits that looked like the tubing material
S3, T3	extraction of whole armature kept for 2 months at 60°C which formed an obvious brown gum deposit
S4	extraction of Torlon rod kept for 1 month at 60°C with no obvious residue formation
T2	extraction of metal pump ring kept for 1 month at 60°C and which yellowed quickly
T4	extraction of fish paper kept for 1 month at 60°C which formed brown gum deposit

2.2 DYNAMIC AND STATIC TEST PROCEDURES

Since the Walbro electric fuel pump was initially strongly suspected in the fuel problems, our first tests were designed to isolate it and its effects from all other fuel system components. Thus the apparatus shown in Figure 1 was constructed to allow only fuel contact with Teflon and borosilicate glass surfaces outside the pump itself. A volume of 0.5 to 2 liters could be recirculated for extended periods of time to increase the concentration of any reaction products while simulating the fuel recycling performed in the Air Force refueling process. The fuel reservoir flask was submerged in a constant temperature bath to minimize fuel heating from the pump operation. The apparatus was also designed to allow siphon priming of the pump with fuel to minimize reactions of fuel liquid and vapor with gaseous air inside the pump. This was originally intended to aid the removal of air for operation of the system under N₂ but was routinely done even for all the experiments under air.

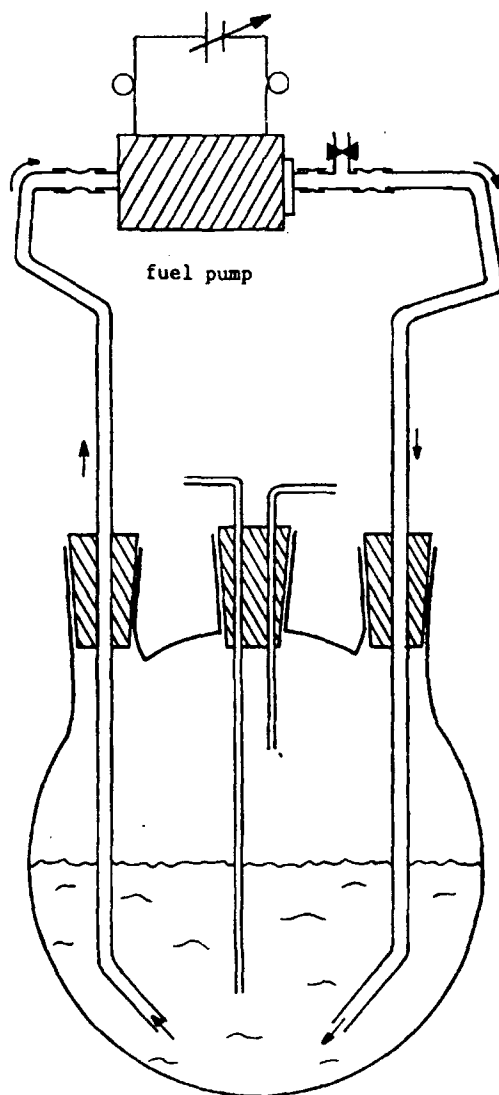


Figure 1. Apparatus for Dynamic JP-10 Tests

Most of our static tests were performed by placing samples of JP-10 in capped test tubes (or vials) along with various parts of a disassembled armature from a fuel pump in a 60°C oven. Visual inspections of samples and low voltage direct MS were performed periodically after several days and several weeks of aging. These experiments were done primarily using our JP-10 control CA with a few tests started using CB and CD.

One static test was performed using a round bottom flask, heating mantle and condenser system. JP-10 control CA and fish paper were added to the flask and the sample was kept at 60°C for 8 weeks, with visual inspection daily for the first month, and weekly thereafter. In this case, the fuel was in constant equilibrium with the atmosphere rather than just the limited headspace of closed vials. Although the condenser minimized evaporation losses of the fuel, it allowed ambient air to react both with vapor and condensed liquid which was essentially separated from the less volatile antioxidant BHT in the main volume of liquid. This experiment was initiated to duplicate conditions of the Air Force static tests which had generated marked amounts of gum.

2.3 LIQUID CHROMATOGRAPHY (LC)

Several samples were fractionated by open column LC to separate several different classes of impurities from each other and the bulk components of the fuel. The open column LC was performed using a 5 mL graduated pipette packed with 80-120 mesh Florisil (Mg Silicate) approximately 0.5 g sea sand was used at both ends of the column to physically stabilize the dry Florisil bed. The sample (0.5 to 0.8 g) was diluted in approximately 0.5 mL n-hexane and the resulting solution (approximately 1 mL) was then placed on the column and successively eluted with 3 mL n-hexane, 2 mL 10% dichloromethane in n-hexane, 2 mL dichloromethane, and 2 to 4 mL 10% methanol in dichloromethane; all solvents rated HPLC grade. The sample was separated into volumetric fractions by gravity elution. Fractions 1 through 4 contained 1/2 mL each. Fraction 5 contained 1 mL, fraction 6 contained 1.5 mL, and fractions 7 and 8 contained 2 mL each. Fraction 9 ranged between .5 mL and 1 mL and consisted of the remaining solvent forced off the column through the use of a pipette bulb. The small volume of fraction 9 was attributed to column holdup and the evaporation of solvent at the tip of the column.

A thorough cleanup of JP-10 was attempted using an open LC column of activated charcoal and Florisil. A 2.2 cm inside diameter x 43 cm long column was packed in the bottom half (ca. 75 mL) with 60-100 mesh activated Florisil (Aldrich 22,075-2) and in the top half with a mixture of ca. 19% by weight activated charcoal powder (MCB CX 660) and activated Florisil. An 800 mL sample of control CA was added to 50 g of activated Florisil as a preadsorption treatment to remove the most polar impurities. When this adsorbent developed a light pink color in less than 30 minutes, the fuel was decanted to a second 50 g of activated Florisil which also turned a slightly darker salmon pink color. The fuel was then decanted over several hours onto the dry packed column. The JP-10 flowed very slowly through the very fine particles of the charcoal bed and required more than 10 hours to elute four major sequential fractions of ca. 20 mL, 50 mL, 90 mL and 35 mL with 1.5-2mL analytical fractions after each.

2.4 FTIR ANALYSIS

Fourier transform infrared spectroscopy was performed using an IBM IR 32 controlled by an IBM 9000 computer. Samples were run as neat liquids on salt plates or in the case of the S3 residue as a semi-solid mass smeared on a salt plate. Resolution was 4 cm⁻¹ and 256 scans were taken of each sample. Spectra were stored on the computer for subsequent data workup.

2.5 LOW VOLTAGE DIRECT MASS SPECTROMETRY

Low voltage MS analyses were carried out on the Extranuclear 5000-1 Curie-point Py-MS system. A detailed description of the system shown in Figure 2a can be found elsewhere [4]. For residue analysis of

the JP-10 samples, 5 μg samples were coated on ferromagnetic wires. The wires were then inserted into borosilicate glass reaction tubes and introduced into the vacuum system of the mass spectrometer. The ferromagnetic wires were inductively heated at a rate of approximately 100°C/s to an equilibrium temperature of 610°C (as determined by the Curie-point temperature of the wire). The total scanning time was 20 seconds. For liquid samples of moderate and high volatility (i.e. JP-10 itself), a special introduction method was applied. This method involves the use of a glass capillary tube (micro caps, Drummond Scientific) sealed on one end and capable of holding up to .5 μl liquid. A detailed schematic of the capillary sample introduction system is shown in Figure 2b [5]. After introducing into the vacuum system the capillary tube was inductively heated up by a tightly wound ferromagnetic spring. This ensured complete evaporation of most samples within approximately 2 minutes.

Typical operating conditions were as follows: electron energy 12 eV, scanning rate 1000 amu/S, mass range 20-280 amu. All spectra were recorded on an IBM 9000 computer and summed into a single time-integrated spectrum of 100 scans for residue analysis and 800 scans for capillary analysis.

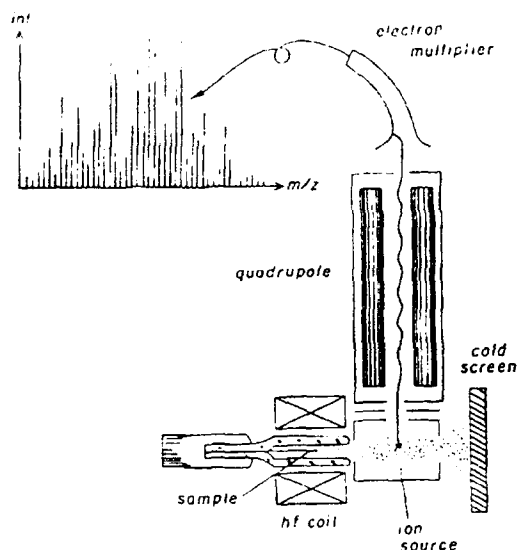


Figure 2a. Low voltage mass spectrometry system with special inlet for low volatile liquids and/or solids using hf induction heating (Curie-point) evaporation/desorption pyrolysis principles.

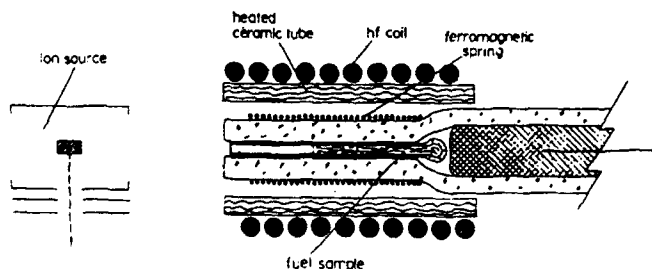


Figure 2b. Detailed schematic of capillary sample introduction system which adapts a conventional Curie-point pyrolysis inlet for use with high volatile liquid samples (low volatile samples were introduced on a ferromagnetic filament). Small inside diameter (0.1 mm) and long length (1.5 cm) minimize sample evaporation prior to heating.

2.6 GAS CHROMATOGRAPHY / MASS SPECTROMETRY (GC/MS)

GC/MS analyses were performed using a Tracor 560 gas chromatograph interfaced to a Finnigan Ion Trap Detector with an IBM PC-XT data system. Preliminary data were taken on a packed column of 5% Dexsil 300 GC on Chromosorb G HP, 100/120 mesh in an 118 in. x 8 ft. stainless steel tube. These columns were run with a 25 mL/min He carrier gas flow with one fifth split to the mass spectrometer and the rest to a flame ionization detector. The main column used was a 15 m x 0.32 mm i.d. fused silica capillary column coated with a 0.25 μ m bonded film of 5% phenyl methyl silicone (J&W Scientific, Inc., DB-5). The column was operated with a head pressure of He carrier gas at 5 psig to give an average linear flow of ca. 0.5 m/s. For analysis of neat JP-10 samples for low concentration impurities an on-column injector (J&W Scientific, Inc.) was used to place the liquid samples directly inside the capillary column by means of a fused silica syringe needle. The outlet of the column was connected to an open-split interface which carried ca. 1.5 mL/min of the column flow through a heated, DB-5 coated fused silica transfer line into the vacuum of the mass spectrometer.

For analysis of the major JP-10 components, samples were dissolved at 1 mg / mL in HPLC grade n-hexane and 0.1 μ L injected on-column with temperature programming from 30 to 270°C at 20°C / min. The low concentration impurities were analyzed by treating the JP-10 main compound as the solvent and injecting ca. 0.05 μ L with a temperature program from 80 to 300°C at 10°C / min. The upper temperature limits were only necessary for high boiling contaminants and cleaner samples, e.g., control samples, were often terminated below 300°C. LC fractions were also often analyzed by GC/MS to aid peak identifications in the neat samples. Fractions in solvents were injected on-column into a cool portion of capillary outside the chromatograph oven before pushing the capillary back into the 80°C oven and then programming identical to the neat samples at 10°C / min.

The ion trap detector (ITD) mass spectrometer was operated both in electron ionization (EI) and chemical ionization (CI) modes for different samples. The EI mode (using new dynamic range enhancement software, version 2.03) was used for identification and quantitation of the main JP-10 components. It was also used to give the fingerprint fragmentation patterns and true molecular ions when present to identify the low concentration impurities. The CI mode was used to simplify the data by reducing the amount of compound fragmentation; in many cases giving primarily a single "pseudo- molecular" ion peak. The CI was operated using H₂O vapor as the reagent gas at an operational pressure selected to give an m/z 19 to 18 ratio of 10 to 1 with an ionization time of 200 μ s to form the water ions and a reaction time with sample molecules of 100 ms. The mass spectrometer scan rate depended both on ionization mode and mass range and was generally 4 scans/s from m/z 50 to 240 for the EI bulk component analysis and 2 scans/s from m/z 40 to 300 for the low concentration impurities analysis.

Quantitation of the bulk components was done simply by integration of the total ion chromatogram (TIC) for the four main peaks and normalization to 100% total. However, the concentrations of the many low level impurities were only approximated for the CI data using specific ion peak heights relative to two internal standards. Neat JP-10 samples were spiked with 10 μ L/mL of a standard solution in n-hexane to give final concentrations of 40 ppm (μ g/mL) acenaphthene and 60 ppm n-heptadecane. For unknowns such as aromatics which gave mainly a single ion, their concentration was simply estimated as the ratio of that ion peak height to the added acenaphthene pseudomolecular ion (m/z 155) peak height times the 40 ppm standard concentration. For compounds such as the aliphatics, which still showed significant fragmentation in the CI mode, the peak height of a major fragment ion was ratioed to that of m/z 57 of the heptadecane and multiplied by 60 ppm. The internal standard peak heights were corrected for the relative amounts of acenaphthene and heptadecane in the original samples by comparison to analyses without the standards added.

SECTION 3.0

RESULTS AND DISCUSSION

3.1 ANALYSIS OF JP-10 BULK COMPONENTS

In order to check for possible gross differences between problem sample V39 and JP-10 control samples gas chromatography combined with mass spectrometry (GC/MS) was used to measure and identify the major bulk components. As shown in Figure 3, four major components were found: JP-10 exo-isomer (MW 136, 95.5%), JP-10 endo-isomer with an identical mass spectrum to the exo-isomer (MW 136, 1.88%), a more symmetrical isomer, probably adamantane (MW 136, 1.07%); and an analog with two additional hydrogens and therefore one less ring than the other tricyclic JP-10 isomers (MW 138, 1.53%). Compared to the three control samples (Figure 4) the relative concentrations of these four components do not seem to differ by more than fractional percentage points as shown in Table 2. The official JP-10 specifications leave considerable room for quantitative, or even qualitative, variations in the compositions of bulk components (since extra peaks which are within plus or minus ten percent of the retention time for the exo-isomer peak are allowed to comprise up to 20% of the exo-isomer area to give the required minimum content of at least 98.5% of the total GC signal), the relatively small differences between Figures 3 and 4 do not appear to provide cause for concern.

Another approach to rapid "fingerprinting" of the bulk composition of JP-10 as well as some of the most prominent trace components is by direct low voltage MS using the capillary tube sample introduction technique illustrated in Figure 2. The capillary tube spectra of V39 and two control samples (A&B) are shown in Figure 5. Due to the large dynamic range of the signal-averaged mass spectra obtained by the capillary tube introduction method it is possible to blow the intensity scales of the spectra up by a factor 20 or so and still maintain good signal-to-noise ratios. This enables a quick look at trace components such as aromatic compound series (see Figures 5d, e, f). A disadvantage of the capillary tube method is that less volatile components such as BHT (dibutylhydroxytoluene) are not easily detected. Therefore, it remains to be determined whether the typical silicone oil (m/z 207) and dioctylphthalate (m/z 251) fragment ion peaks seen in the V39 sample and some of the controls are derived from actual fuel components or may have come from the outside of the capillary tube (thus representing contaminants introduced during the sample preparation procedure). From the low voltage MS patterns in Figure 5 it can be concluded that the overall composition of JP-10 bulk components is very similar (as also indicated by the GC data in Figures 3 and 4) but that significant differences appear to exist at the trace component level. These differences in trace organic components will be analyzed and discussed in greater detail in the next few paragraphs.

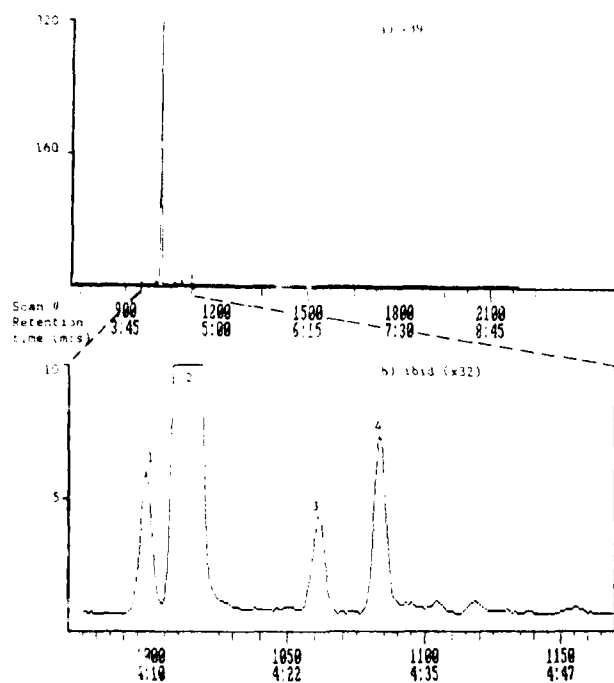


Figure 3. Gas chromatogram of sample V39 showing major components. Trace b) is an expansion of the scan #970 to 1170 region, showing the four major components in the sample. Components were tentatively identified by mass spectrometry and are listed in Table 2.

TABLE 2
INTEGRATED AREA VALUES OF 4 BULK COMPONENT (TOTAL = 100%)

Peak Assignment Sample	1 Bicyclic m/z 138 (%)	2 EXO-isomer (%)	3 Adamantane (%)	4 Endo-isomer (%)
CA	1.59	95.5	1.21	1.69
CB	1.44	95.2	1.25	2.08
CB*	1.52	94.8	1.28	2.44
CC (C85)	0.97	94.8	0.85	3.39
V39	1.53	95.5	1.07	1.88
S3	0.48	97.4	0.71	1.46
S3*	0.50	97.1	0.68	1.74

* duplicate runs

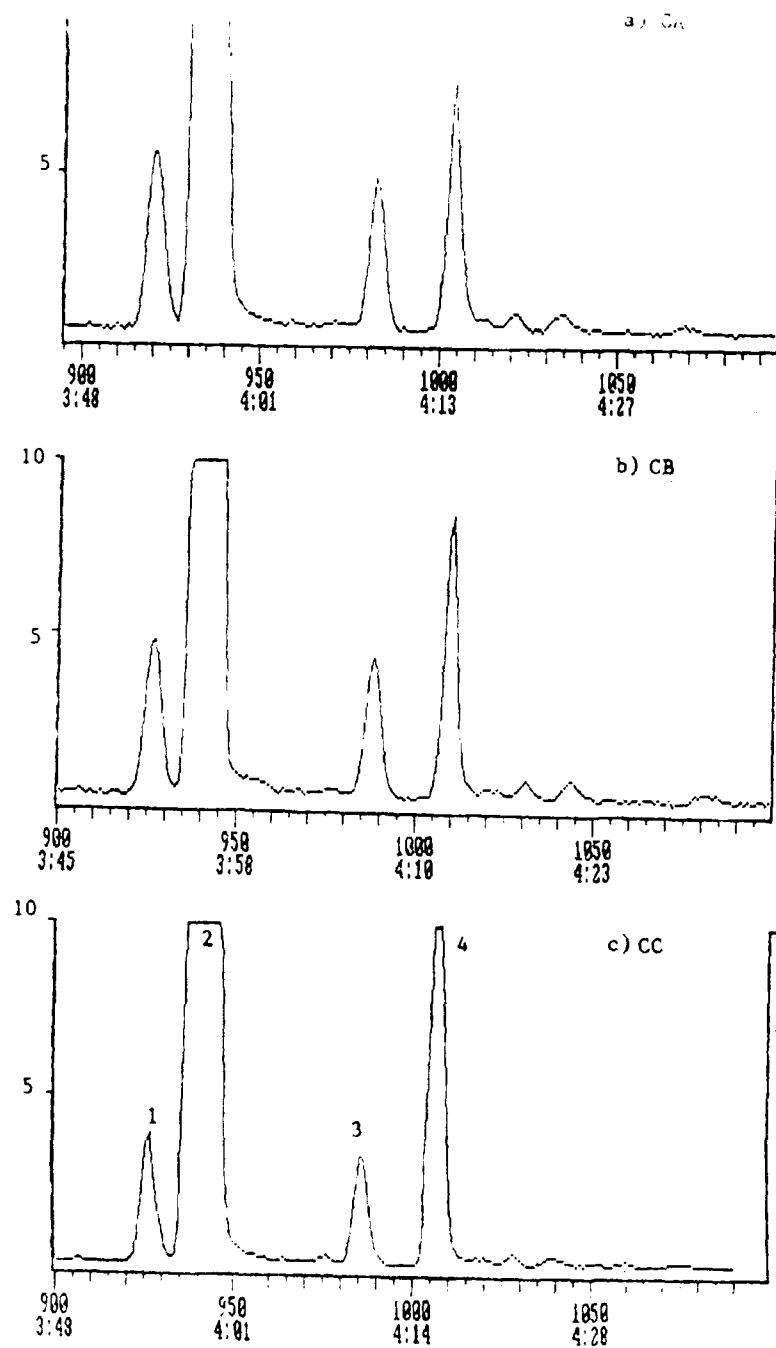


Figure 4. Gas chromatograms of control samples A, B and C showing the four major components of JP-10.

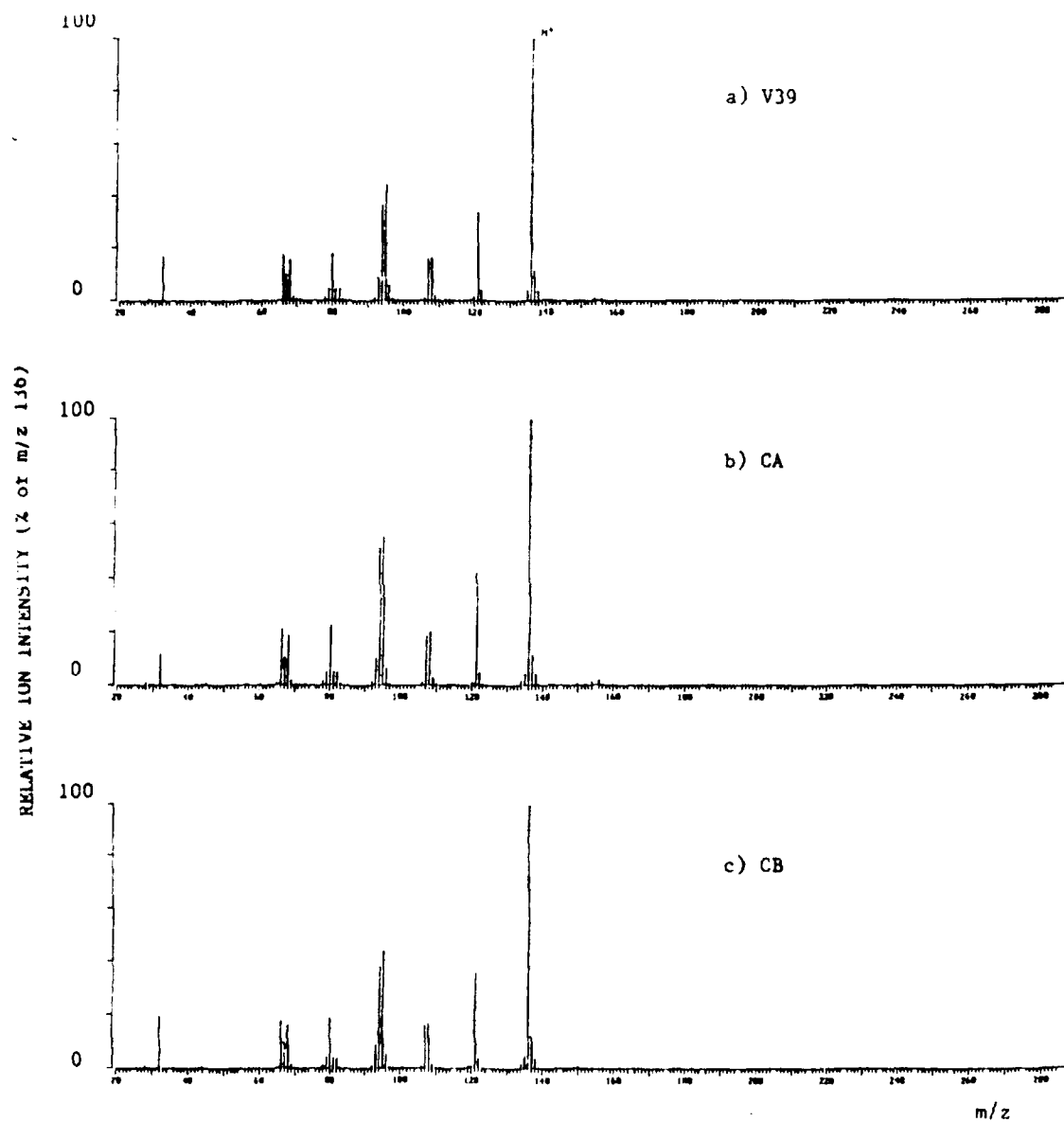


Figure 5 a,b,c. Low voltage mass spectra of V39 and two control samples (A & B) performed using the capillary introduction technique. 5a-5c show that the bulk compositions of these samples are very similar (the differences in trace components among these samples is shown in Figure 5d-f with 20 x expanded spectra)

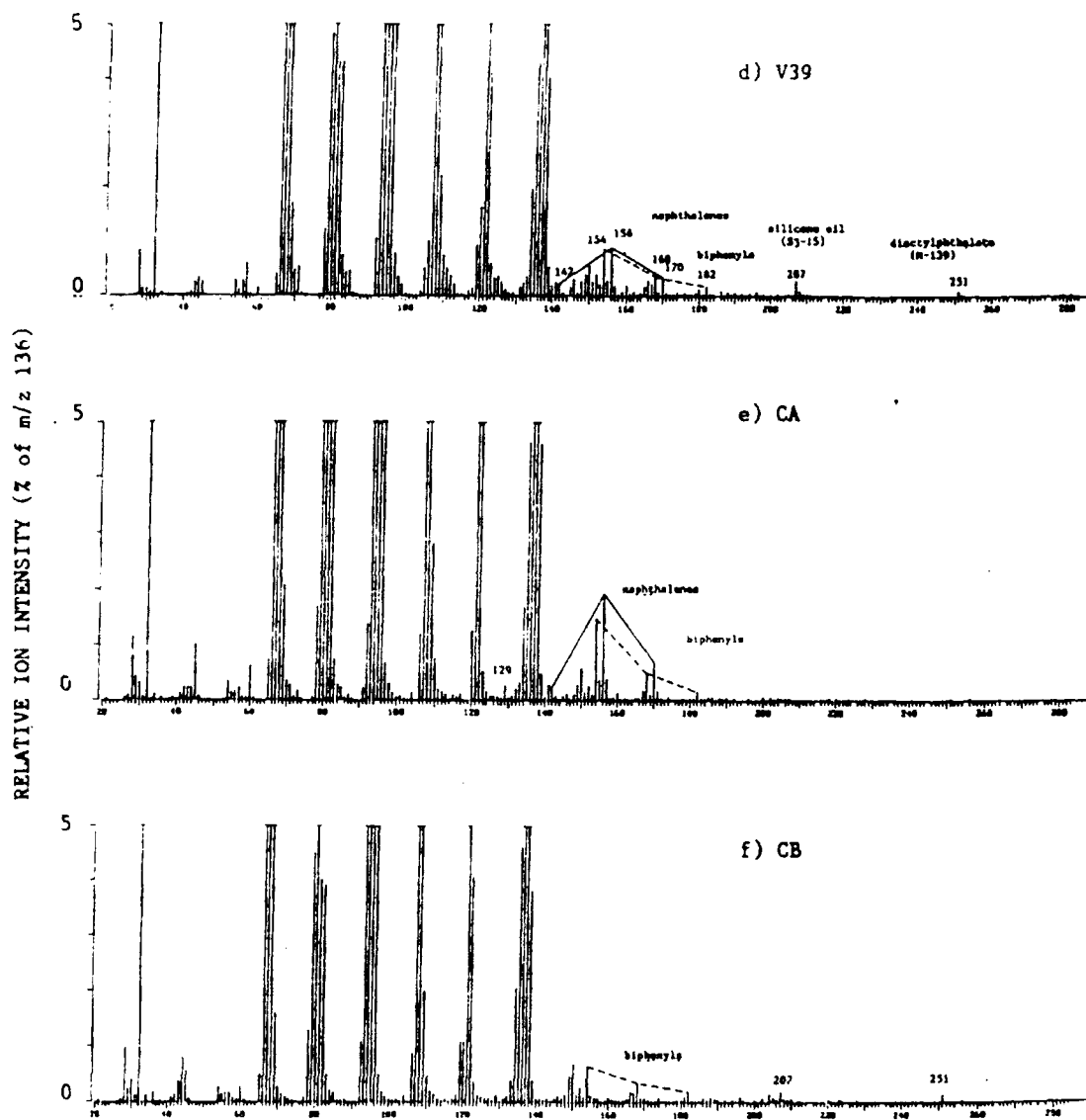


Figure 5 d.e.f. Low voltage mass spectra of V39 and two control samples (A & B) performed using the capillary introduction technique. 5d - 5f show the difference of trace components among these samples. Note the spectra are expanded 20 times (bulk compositions of these samples are shown in Figure 5 a,b,c)

3.2 ANALYSIS OF JP-10 TRACE COMPONENTS

In order to determine the nature, relative abundance, and possible significance of trace components further GC/MS analyses were performed in such a way as to focus on relatively small peaks while letting the bulk component peaks go off scale (in effect saturating the MS detector system). Moreover, direct (low voltage) mass spectrometry and FTIR spectroscopy were performed on the residue obtained after evaporating most of the JP-10. Finally, several fuel samples were separated into 6 to 9 subfractions by open column LC before being submitted to further direct MS analysis.

The highly complex nature of the organic trace components in JP-10 is illustrated by the GC/MS total ion current (TIC) and ion chromatogram profiles of the V39 sample in Figure 6. As can be seen in Figure 6b and 6c, the aromatic compounds are represented in the CI spectra primarily by pseudomolecular ions of m/z $M+1$ due to simple protonation. However, the m/z 203 trace (6d) for the oligomers indicates sesquimers both of molecular weight 202 ($C_{15}H_{22}$) and 204 ($C_{15}H_{24}$) with the latter compounds experiencing neutral H_2 loss after the initial protonation to give an $M+1-2$ ion. Other aliphatic compounds showed significant fragmentation even in the low energy chemical ionization as shown in Figure 6e by peaks of the butyl ion at m/z 57 from the alkanes. Besides aromatic and aliphatic hydrocarbons, intriguing JP-10 oligomer (sesquimer and dimer) signals were found in many samples, as well as heteroatomic components such as BHT, DOP (dioctylphthalate) and silicone oil.

Although some 7 classes of organic trace components (most in the 1-100 ppm range) were found to occur in V39 as well as in the control samples, none of these compounds or compound classes were found to be unique to the V39 sample. In fact, all JP-10 samples analyzed thus far (see Table 1) contain most of these compound series as evidenced by the lists of approximate impurity concentrations in Table 3. The data in Table 3 represent a preliminary effort to identify and roughly quantitate some of the low concentration impurities. Peak numbers correspond to major single ion chromatogram peaks as labeled in Figures 6 and 7. The Kovats index is a retention index in which peak times are linearly interpolated between the n -alkanes when the GC analysis uses a linear temperature program. Compound types were determined from both EI and CI ionization modes on both neat samples and LC fractions but are still somewhat uncertain for some oligomers and other aliphatics which did not show clear molecular ions. The carbon number indicates the total number of carbons in the compounds. The "Z" number is a measure of the number of hydrogens according to the formula C_nH_{2n+Z} and is a useful guide to compound types: e.g. +2 for an alkane, -4 for the JP-10 exo- and endo-isomers, -12 for naphthalenes and -6 or -8 for some of the oligomers. The internal standards are indicated as peak 66 for acenaphthene and peak 100 for the heptadecane. An outside limit for the accuracy of concentrations is suggested by the values for BHT which has an unusual CI fragmentation and results in errors of a factor of 3 or more. More careful estimates by other techniques showed the BHT to be within 20% of its specification 100 ppm value for each of the 3 samples.

This brings up the important questions of what the origin is of all these trace components and what role, if any, each of these compounds or compound classes might play in causing the observed discoloration and gum formation problems. In order to provide plausible answers to these questions, each of the trace component types will be discussed separately.

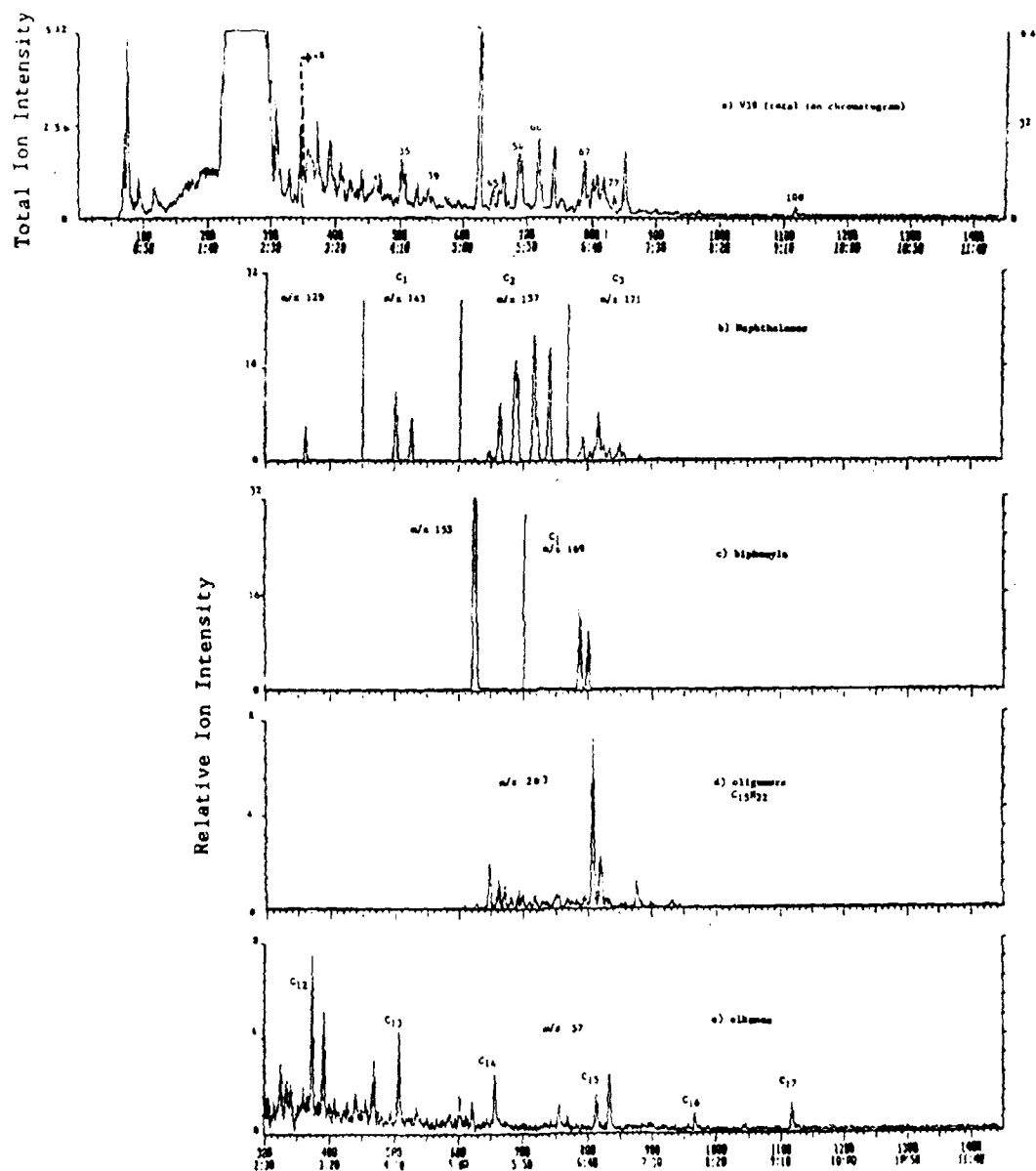


Figure 6. Gas chromatogram of sample V39, showing a) the total ion chromatogram and b-e) ion chromatograms of four compound types present as trace components in sample V39. Note that the intensities of the ion chromatograms are each expanded relative to the total ion chromatogram in (a).

TABLE 3.
MINOR GC/MS PEAKS IN THE V39 FIELD SAMPLE AND IN THE CA, CB, CD CONTROL
SAMPLES WITH PROPOSED STRUCTURE IDENTITIES

Pk #	Ret. Index	Compound Type	# Carbons	Z-No.	Concentration (ppm) V39 CA CB CC	Pk #	Ret. Index	Compound Type	# Carbons	Z-No.	Concentration (ppm) V39 CA CB CC
5	1145	JP-10 homolog	C11	-4	2870 1180 1920 1970	53	1408	oligomer	C15	-6	43 49 51 43
6	1151	bicyclo	C11	-2	115 53 140 190	54	1417	naphthalene	C12	-12	190 290 23 2.0
7	1152	tetralin or indane	C10	-8	68 11 29 40	55	1420	naphthalene	C12	-12	124 220 16 -
8	1157	tetralin or indane	C10	-8	320 150 510 510	56	1421	naphthalene	C12	-12	31 - 24 -
9	1160	JP-10 homolog	C11	-8	116 27 37 52	57	1422	naphthalene	C12	-12	23 - 10 85 -
10	1163	JP-10 homolog	C11	-4	1250 1000 1570 1140	58	1428	naphthalene	C12	-12	240 312 680 120
11	1171	tetralin or indane	C10	-8	108 70 37 108	59	1429	naphthalene	C12	-12	84 130 15 0.8
12	1171	JP-10 homolog	C11	-4	812 540 600 624	60	1434	naphthalene	C12	-12	220 270 18 -
13	1174	bicyclo	C12	-4	220 81 280 190	61	1436	naphthalene	C12	-12	- 17 110 -
14	1188	naphthalene unsub.	C10	-12	68 160 40 236	62	1449	naphthalene	C12	-12	39 - - -
15	1191	naphthalene unsub.	C10	-12	5.2 - 19 6.4	63	1466	acenaphthene	Internal stan.	-	Internal standard
16	1194	n-alkane	C12	+2	370 - - -	64	1472	biphenyl	C13	-14	39 206 57 44
17	1200	aliphatic	C12	-4	390 - - -	65	1473	naphthalene	C13	-12	11 90 1.6 0.3
18	1212	aliphatic	C11	-4	203 - - -	66	1476	biphenyl	C13	-14	29 180 41 20
19	1212	JP-10 homolog	C11	-4	80 97 100 104	67	1477	naphthalene	C13	-14	11 59 - 13
20	1213	JP-10 homolog	C11	-4	160 190 220 280	68	1482	biphenyl	C13	-14	7.9 - 270 129
21	1215	JP-10 homolog	C11	-4	87 - - -	69	1485	oligomer	C15	-6	313 230 450 280
22	1215	(tetralin or indane)	C11	-8	202 290 240 -	70	1488	naphthalene	C13	-12	115 160 330 234
23	1226	bicyclo	C12	-2	32 28 21 717	71	1489	oligomer	C13	-12	8.2 33 1.4 0.1
24	1227	JP-10 homolog	C12	-4	26 14 - 9.8 217	72	1490	naphthalene	C14	-14	78 82 62 -
25	1229	aliphatic	C11	-8	64 - - -	73	1495	biphenyl	C15	-6	50 39 190 34
26	1236	JP-10 homolog	C11	-4	71 - - -	74	1496	oligomer	C15	-6	30 61 -
27	1238	aliphatic	C11	-8	39 - - -	75	1497	naphthalene	C15	-6	- 3.7 63 0.4
28	1241	aliphatic	C11	-8	44 43 16 6.8	76	1501	oligomer	C15	-6	- 8.6 83 17
29	1245	tetralin or indane	C12	-4	22 290 27 -	77	1507	fluorene	C14	-16	1.2 5.2 200 6.3
30	1251	JP-10 homolog	C11	-4	68 47 20 11	78	1518	biphenyl	C14	-14	- - 4.8 -
31	1266	tetralin or indane	C11	-8	170 - 15 -	79	1520	naphthalene	C15	-14	- 230 -
32	1267	aliphatic	C11	-8	136 156 18 6	80	1522	oligomer	C16	-14	39 6.6 -
33	1271	naphthalene	C11	-12	210 12 20 -	81	1538	biphenyl	C16	-14	- - 2.1 -
34	1285	n-alkane	C13	+2	88 75 11 2.0	82	1553	oligomer	C16	-14	- - 37 -
35	1296	naphthalene	C13	-12	31 14 7.6 0.96	83	1563	biphenyl	C16	-14	- - 11 11
36	1300	naphthalene	C12	-8	240 230 300 -	84	1575	oligomer	C16	-14	- - 49 -
37	1313	tetralin or indane	C12	-8	12 - 3.2 -	85	1578	fluorene	C16	-14	- - 39 -
38	1320	tetralin or indane	C12	-8	85 98 120 -	86	1580	biphenyl	C16	-14	- 0.8 2.8 -
39	1324	bicyclo	C13	-2	18 - 48 19 -	87	1590	biphenyl	C16	-14	- 9.2 57 10
40	1328	tetralin or indane	C12	-8	18 19 18 23	88	1594	naphthalene	C16	-14	- - 25 -
41	1330	JP-10 homolog	C13	-4	680 580 560 592	89	1596	oligomer	C16	-14	- - 7.0 -
42	1340	biphenyl unsub.	C12	-14	8.8 11 8.8 9.2	90	1596	biphenyl	C16	-14	- - -
43	1357	tetralin or indane	C12	-8	24 22 - 4.0	91	1600	oligomer	C16	-14	- - -
44	1369	naphthalene	C12	-12	21 25 28 28	92	1601	biphenyl	C16	-14	- - -
45	1386	naphthalene	C15	-6	120 8.0 6.1 11	93	1610	oligomer	C16	-14	- - -
46	1393	n-alkane	C13	+2	490 530 590 -	94	1613	biphenyl	C16	-14	- - -
47	1394	biphenyl	C13	-14	- - -	95	1620	oligomer	C16	-14	- - -
48	1395	oligomer	C13	-14	- - -	96	1621	biphenyl	C16	-14	- - -
49	1395	oligomer	C13	-14	- - -	97	1628	biphenyl	C16	-14	- - -
50	1400	oligomer	C13	-14	- - -	98	1638	oligomer	C16	-14	- - -
51	1400	oligomer	C13	-14	- - -	99	1663	biphenyl	C16	-14	- - -
52	1404	oligomer	C13	-14	- - -	100	1700	biphenyl	C16	-14	- - -
						101	1711	biphenyl	C16	-14	- - -

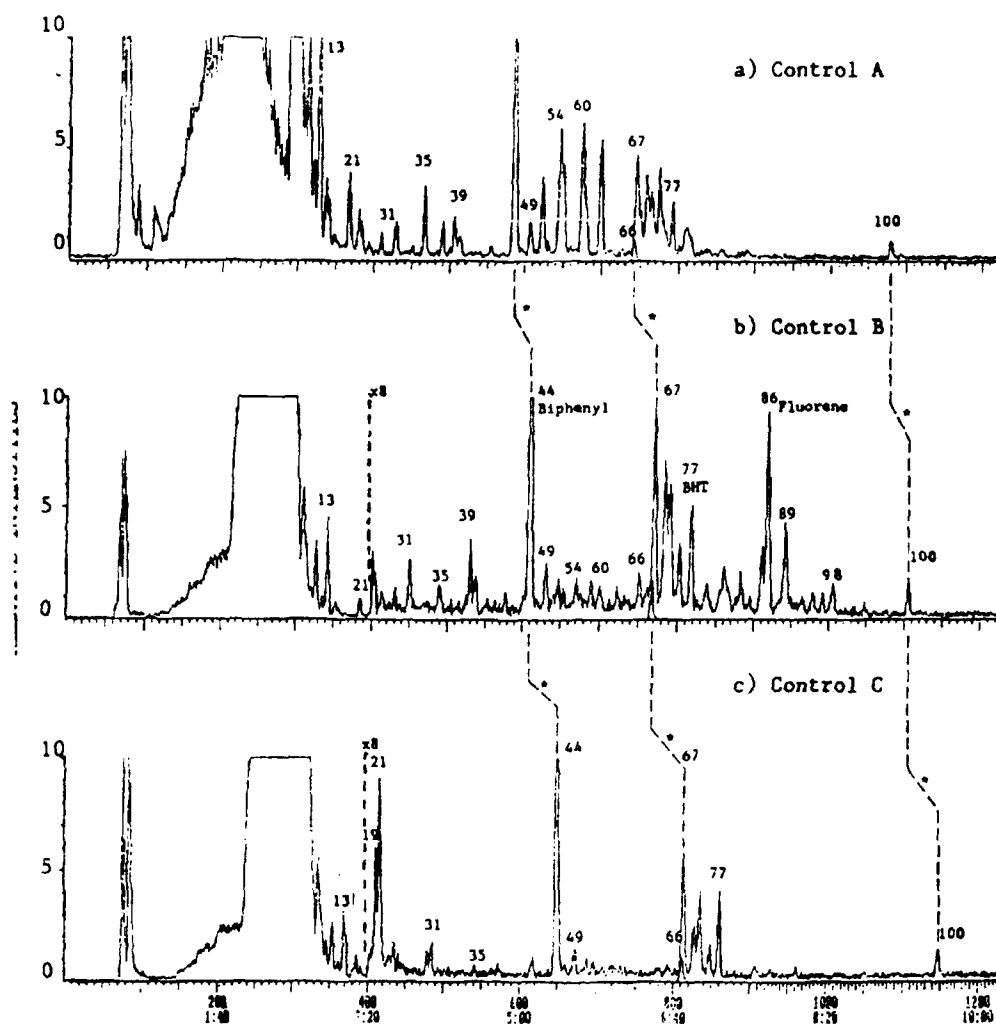


Figure 7. Gas chromatography/mass spectrometry of the three control samples A, B, and C showing trace components. Many of the peaks have been identified on Table 3. * = The dashed lines between chromatograms connect several common peaks between analyses with differing carrier gas flows.

3.2.1 (Alkylsubstituted) Aromatic Hydrocarbons

Type and relative abundance of aromatic hydrocarbon trace components are found to vary considerably between different sample batches as shown in Figures 7 and 8. The GC/MS and low voltage MS profiles of three different control samples in Figures 7 and 8, respectively, illustrate the three main aromatic patterns encountered in this study. Sample A reveals dominant series of (alkyl) naphthalenes and (alkyl) biphenyls. Sample B shows a prominent fluorene peak and higher biphenyl homologs while lacking significant naphthalene signals. Sample C on the contrary has by far the lowest concentrations of alkylaromatics and the most significant of these are (alkyl) biphenyls.

The origins of the aromatic hydrocarbon components in JP-10 may well be multiplex. None of the aromatic series is likely to be a direct by-product of the JP-10 production process since aromatic

compounds would not survive the aluminum chloride endo- to exo-isomerization step. The alkylbenzenes and alkylnaphthalenes appear to show the greatest variation among different sample batches. In view of the fact that most fuel distribution, transportation and storage systems have probably been in contact with common jet fuels and other transportation fuels, the alkylbenzenes and alkylnaphthalenes are likely to represent cross contamination with such fuels.

However, the biphenyls which appear in all three recent controls (but not the 1977 sample discussed below) are not as common to normal commercial fuels. According to conversations with refinery personnel [1] the biphenyls may represent bottoms from a process such as the demethylation of toluene. Since this process is not very common among large refineries, the biphenyl impurities may possibly represent a signature of the Koch refinery which may alternate between use of a distillation column for JP-10 production and bottoms recovery. The fluorene in control sample B is also a likely byproduct of toluene demethylation and in this scheme would simply suggest a wider range bottoms distillation to leave it and the C2 and higher biphenyls as refinery contaminants to the batch from which control sample B was obtained.

With regard to the possible role of alkylaromatic compounds in the chemical degradation of JP-10 the following observations may have some relevance. First of all, alkylaromatic content appears to be relatively low in JP-10 samples exposed to long term atmospheric conditions (e.g., the 1977 batch sample shown in Figure 9a,b) or accelerated laboratory conditions (e.g., the sample S4 exposed to air at 60°C for 1 month, shown in Figure 9c). This may indicate a direct involvement of alkylaromatic components. Secondly, accelerated weathering tests in our laboratory with control sample A (which contains a relatively high abundance of alkylnaphthalenes) failed to produce visible changes whereas similar weathering tests with control sample B (performed by Air Force laboratories) caused extensive discoloration and gum formation. Assuming that oxidative processes do play an important role and that the relatively low concentration (approximately 100 ppm) of BHT (dibutylhydroxytoluene) is insufficient to prevent these processes then the question could be asked whether alkylnaphthalenes and/or other aromatic compound series might perhaps offer added protection against oxidation, e.g., by scavenging reactive radicals or by promoting hydrogen transfer reactions. If so, then complete removal of naphthalenes and other aromatic trace components from JP-10 batches might actually result in a less stable fuel. This assumption should be tested carefully in future JP-10 experiments.

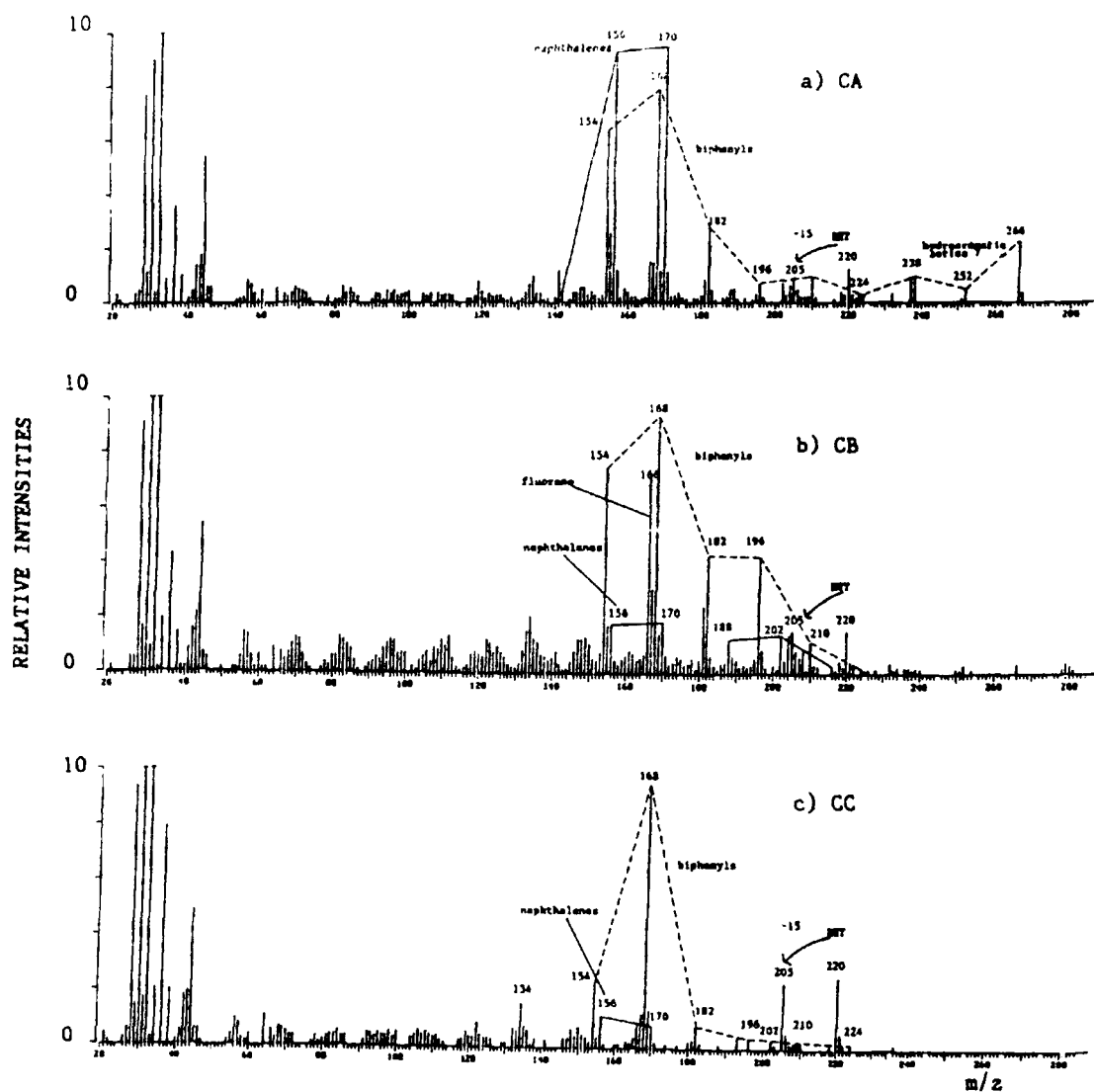


Figure 8. Low voltage mass spectra of three control samples of JP-10 using Curie point wires. Batch variation among the control samples is apparent.

3.2.2 JP-10 Related Oligomers, Homologs and Analogs

As illustrated in Figure 9 considerable quantities of JP-10 sesquimers (or cyclopentadiene trimers) and dimers are found in weathered samples whereas only minimal abundances are observed in the "fresh" control samples in Figures 7 and 8. GC/MS analysis reveals that the sesquimers at m/z 202/204 as well as the dimers at m/z 270/272 consist of a complex mixture of isomers. This is in line with a mechanism by which JP-10 radicals are formed in different positions, e.g., through peroxide intermediates, which subsequently recombine to form stable dimers. Sesquimer formation would require decomposition of JP-10 (or one of its analogs) into two C₅ fragments with one of these fragments subsequently combining with an intact JP-10 molecule.

Whether one or more of the various JP-10 isomers and/or analogs (e.g., shown in Figures 3 and 4) are relatively reactive and responsible for most of the oligomer formation or whether the main JP-10 exo-isomer is directly involved is uncertain at this point. However, the relative abundances of the bulk components shown in Figures 3 and 4 have been observed to change during accelerated laboratory weathering tests, suggesting that the dicyclic analog (MW 138) and adamantane may be slightly more reactive under some conditions. The large relative reduction in the amounts of these two peaks for sample S3 is seen in the data of Table 2 as compared to the CB starting fuel.

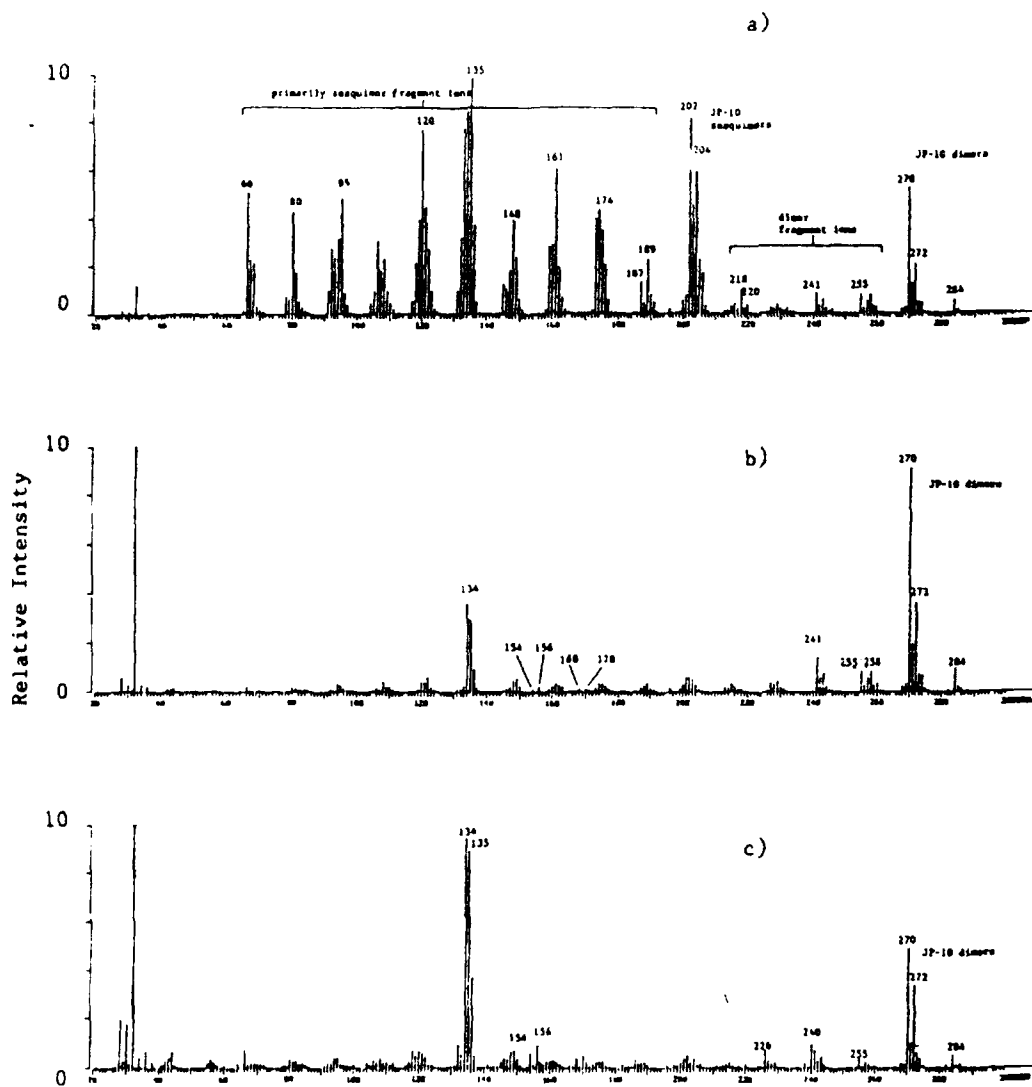


Figure 9. Low voltage mass spectra of a) and b) Control D and c) sample S4. Sample a) was analyzed more quickly with less time for evaporation of the moderately volatile sesquimers at m/z 202 and 204 than the samples in b) and c).

Besides JP-10 oligomers, various homologs (e.g., at m/z 150) and analogs (e.g., representing different degrees of ring formation and saturation at m/z 134 and 138 or indicating the presence of hydroxy and/or keto-substituted moieties, e.g., at m/z 152, 166, 184) can be observed by GC/MS and, especially, LC/MS techniques. Oxygen substituted JP-10 forms are primarily found in polar LC fractions of JP-10 samples obtained from accelerated weathering tests, as shown in Figure 10.

That JP-10 oligomers and analogs might play an important role in JP-10 stability problems is not difficult to imagine. However, it should be noted that the 1977 (CD) sample in Figure 6a was still within current specs in November of 1985. In other words, oligomer formation does not necessarily lead to significant increases in gum formation. Perhaps the dimers at m/z 270/272 represent fairly stable end products. The oxygen substituted JP-10 forms as indicated in Figure 10 are obviously likely candidates for condensation reactions, potentially forming oligomeric and polymeric fragments, as well as for the formation of hydrogen-bonded gels.

3.2.3 Long Chain Paraffins

Although encountered in most JP-10 samples, long chain paraffins appear to be especially abundant in the two discolored samples V39 and ALS (see Figures 6a and 11a). The most likely origin of these paraffinic compounds must be sought in oils and greases used to lubricate fuel pumps as well as used as cutting and quenching oils during the machining of fuel pump parts or other fuel system components.

Static extraction tests of fuel pumps with JP-10 revealed that a single pump held enough grease-like material to cause yellowish discoloration of relatively large quantities of JP-10. Extraction of a sintered (?) fuel pump ring with JP-10 produced strong aliphatic hydrocarbon patterns, as shown in Figure 11b. In conclusion, contamination with oils and greases from fuel distribution systems appears to be the main cause of yellowish discoloration. Moreover, although completely saturated paraffins tend to be quite stable at higher temperatures, occasional branching, unsaturated bonds and/or oxygen substitutions are likely to cause thermal degradation under JFTOT conditions, thus explaining the problems encountered with the ALS sample during JFTOT testing.

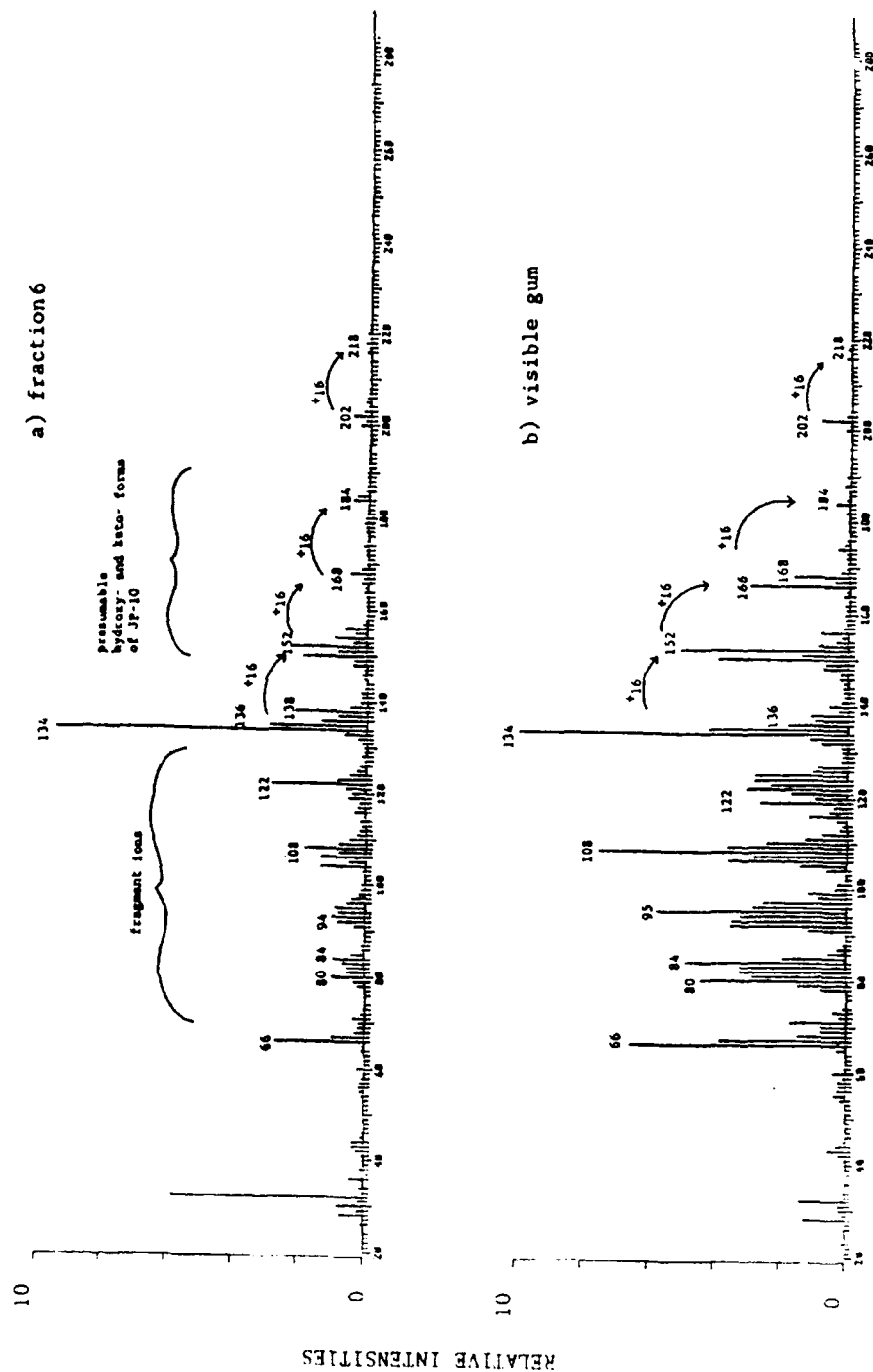


Figure 10. Low voltage mass spectra of apolar (late eluting) liquid chromatography fraction and a visible gum sample from the S3 accelerated laboratory weathering test showing oxygen substituted forms of JP-10.

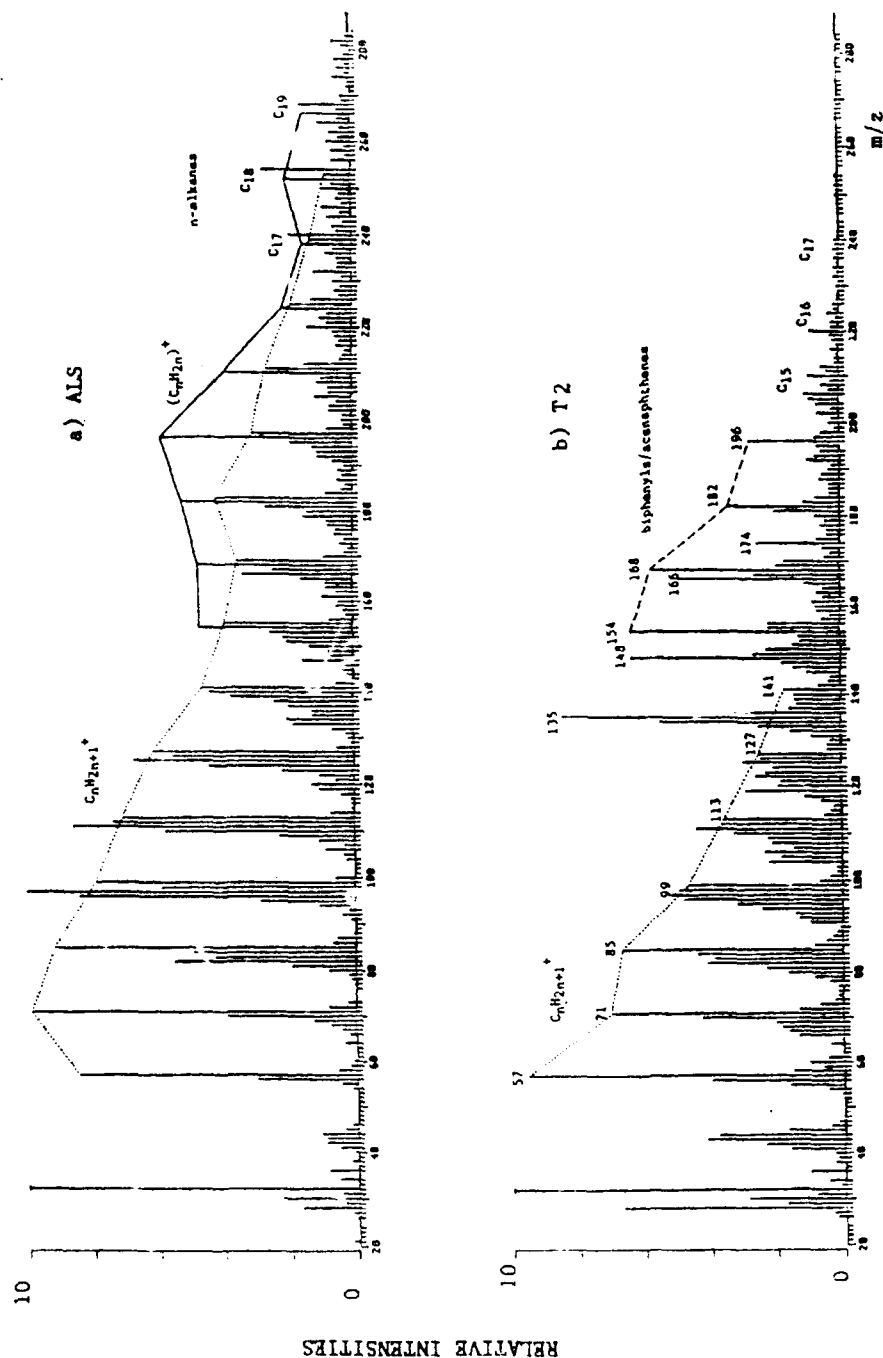


Figure 11. Low Voltage Mass Spectra Of Discolored Field Samples ALS And Extracted Fuel Pump Ring Sample T2 Showing Series Of Long Chain Paraffins.

3.2.4 Additives (methoxyethanol and dibutylhydroxy toluene)

The methoxyethanol de-icing additive which is present in relatively large amounts (approximately 1000 ppm) is relatively volatile and therefore tends to be obscured in the early portions of the chromatograms

or to be lost by evaporation in the direct low voltage MS procedures. No attempt was made to make this additive the focus of special analysis since it was not expected to have a major effect on JP-10 stability. The widely used BHT antioxidant is clearly seen at m/z 220 and 205 in the low voltage mass spectra of the control samples in Figure 8. On the contrary, little if any trace of BHT is left in the two "weathered" samples shown in Figure 9. However, the behavior of BHT during exposure of JP-10 to oxidative conditions is not easily predicted. In fact, some severely oxidized samples still contained most of the BHT, thus casting doubt on its efficacy in preventing oxidative degradation of JP-10. In fact, other organic trace components such as naphthalenes could perhaps play a significant role in protecting JP-10 against oxidative environments.

3.2.5 Dioctylphthalate (DOP)

DOP was detected and identified in the FTIR spectrum of the V39 residue as shown in Figures 12 and 13. In contrast, however, DOP is not seen in the FTIR spectrum of the control A sample in Figure 2b. The origin of DOP, primarily a vacuum pump oil (Octoil) is not immediately clear. However, its presence in several of the samples received from Air Force personnel was also confirmed by low voltage MS. Therefore, accidental contamination outside our laboratory cannot be ruled out and the presence of DOP in the V39 sample is of doubtful significance.

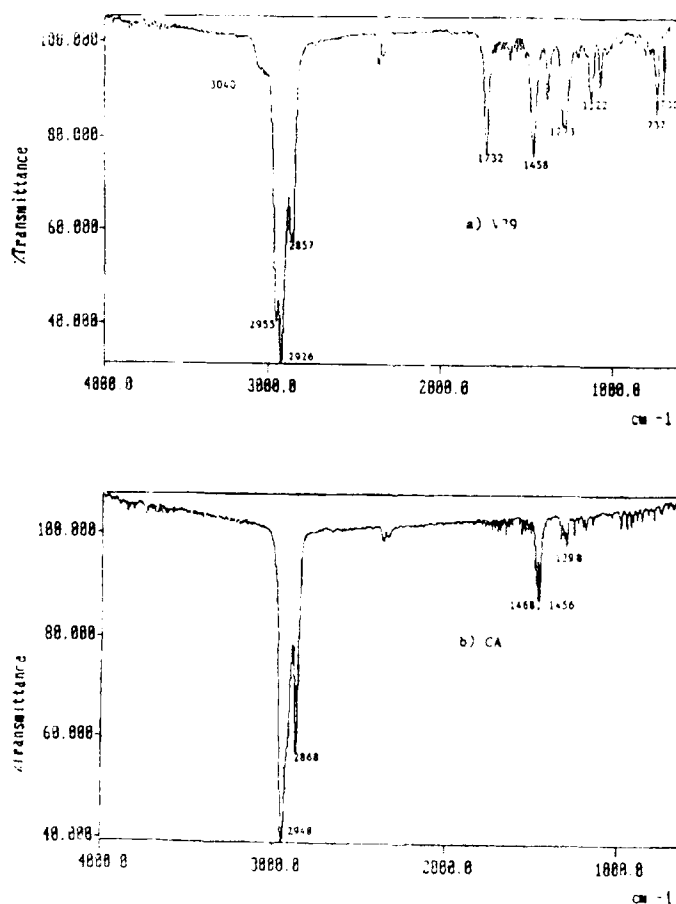


Figure 12. Fourier transform infrared spectra of samples V39 and control A as neat liquids on salt plates. V39 contains aliphatic, aromatic and carbonyl functional groups whereas control A contains only aliphatic methylene functional groups.

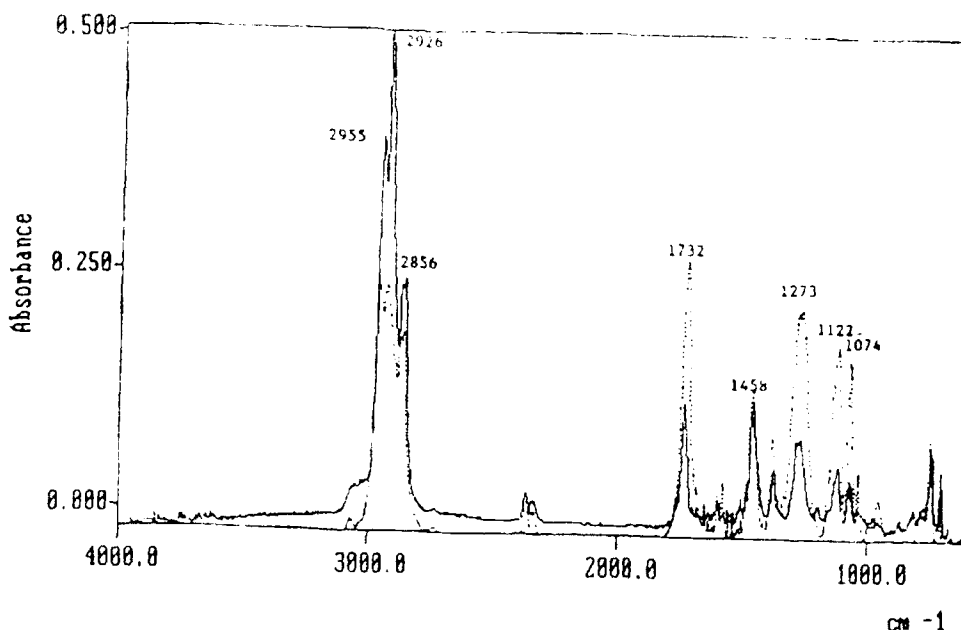


Figure 13. Fourier transform infrared spectrum of V39 (solid line) with superimposed spectrum of dioctyl phthalate (dashed line) plotted in absorbance versus wavenumber. Note the similarity between many of the peaks in the spectra.

3.2.6 Unknown Peak Series at m/z 210, 238, 266

The identity of these peaks is incompletely understood and will require additional GC/MS (and/or MS/MS) analyses. The relative abundance of this peak series appears to correlate positively with the relative abundance of alkylnaphthalenes. Perhaps we are dealing with a hydroaromatic compound. If so, then this compound series may play a role in protecting JP-10 against oxidative phenomena.

3.2.7 Miscellaneous Compounds (e.g., silicone oil)

These are especially abundant in the GC/MS and low voltage MS data in Figures 6, 7 and 8 some miscellaneous trace organic components can be found in the list of GC/MS peaks in Table 3.

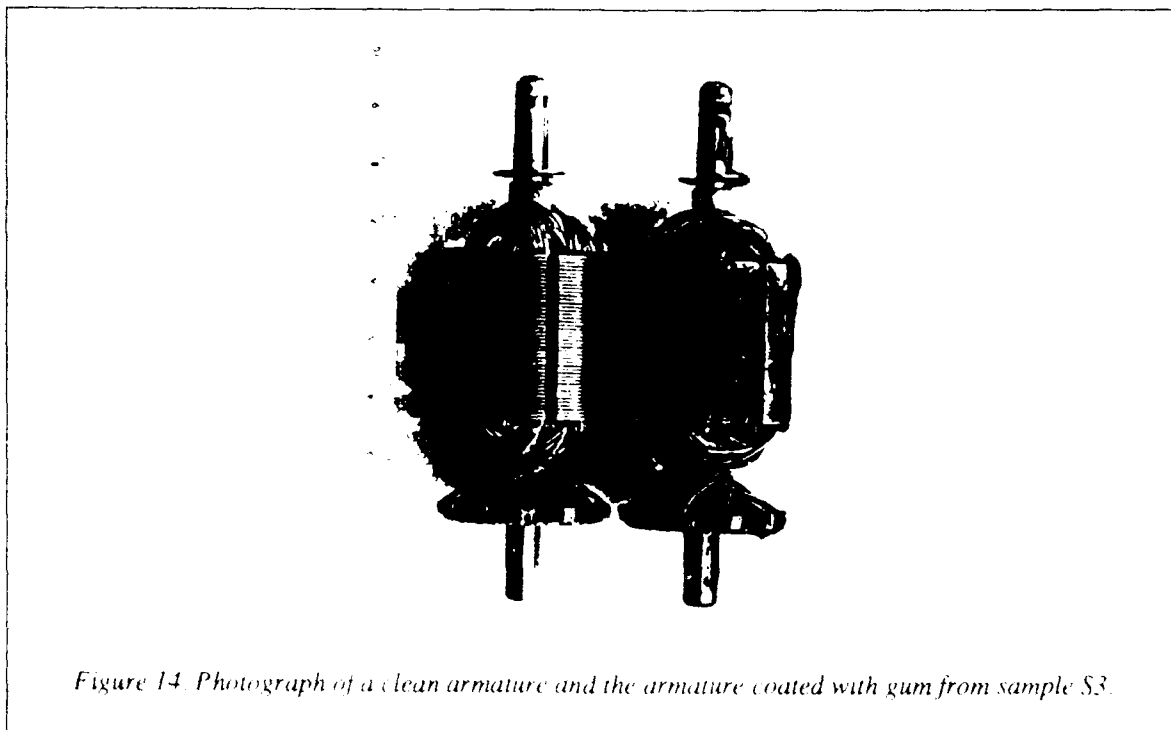
3.3 FTIR AND PYROLYSIS MS ANALYSIS OF GUM COMPONENTS

Since the low voltage mass spectra in Figures 8 and 9 were obtained by heating JP-10 residues to 610°C (heating rate 100°C/s) directly in front of the ion source, these spectra contain low volatile JP-10 components as well as the pyrolysis products of completely nonvolatile residues such as gum. However, JP-10 samples which are within specifications contain less than 50 ppm gum. Therefore, rigorous evaporation of JP-10 residues can help to remove low volatile organic residues thus obtaining a sample enriched in gum components. An example of this trend can be seen by comparing Figures 9a and b. Prolonged evaporation of the CD (1977) control sample removes most of the JP-10 sesquimers but leaves the dimer signal intact. Thus, JP-10 dimers appear to represent borderline components of the gum fraction.

In order to obtain a more direct impression of the composition and nature of JP-10 gum components a sample of the visible gum (resin) precipitate seen on the fuel pump armature (Figure 14) during one of the static exposure tests performed by Air Force personnel at 60°C was directly analyzed by FTIR and

Curie-point pyrolysis MS. This gum sample corresponds to fuel samples S3 (Table 1) and, thus, should be compared to the LC samples in Figure 10. The FTIR spectrum in Figure 15a shows the residue obtained by room temperature evaporation of the S3 sample. It undoubtedly contains some JP-10, since it was not evaporated to dryness. The methylene stretches were at 2948 and 2867 cm^{-1} , identical to those of JP-10 itself. A carbonyl absorption is also present, at 1734 cm^{-1} and probable C-O peaks at 1253 and 1181 cm^{-1} . No pronounced OH peak was seen in this spectrum suggesting ester linkages or a combination of ketones and ethers. A small peak at 3030 cm^{-1} is probable evidence of unsaturation. No peaks were seen at 1600 and 1516 cm^{-1} , ruling out significant aromatic functionalities. An olefinic peak at $1680\text{--}1660$ might be obscured by the carbonyl. In contrast, the spectrum of the visible gum coating the S3 glass container (Figure 15b) shows a strong, broad hydroxy peak at $3400\text{--}2600\text{ cm}^{-1}$, a carbonyl at 1732 cm^{-1} (shoulder at 1768 cm^{-1}) and two C-O peaks at 1172 and 1043 cm^{-1} . This spectrum is consistent with a carboxylic acid. The aliphatic stretches are those of JP-10, at 2948 and 2867 cm^{-1} . The lack of methyl and acyclic methylene stretches in both of these spectra make it likely that oxygen functionalities have been incorporated into JP-10 molecules.

The Curie-point pyrolysis MS pattern of the visible gum in Figure 10b supports the impression that we are dealing with a highly functionalized,



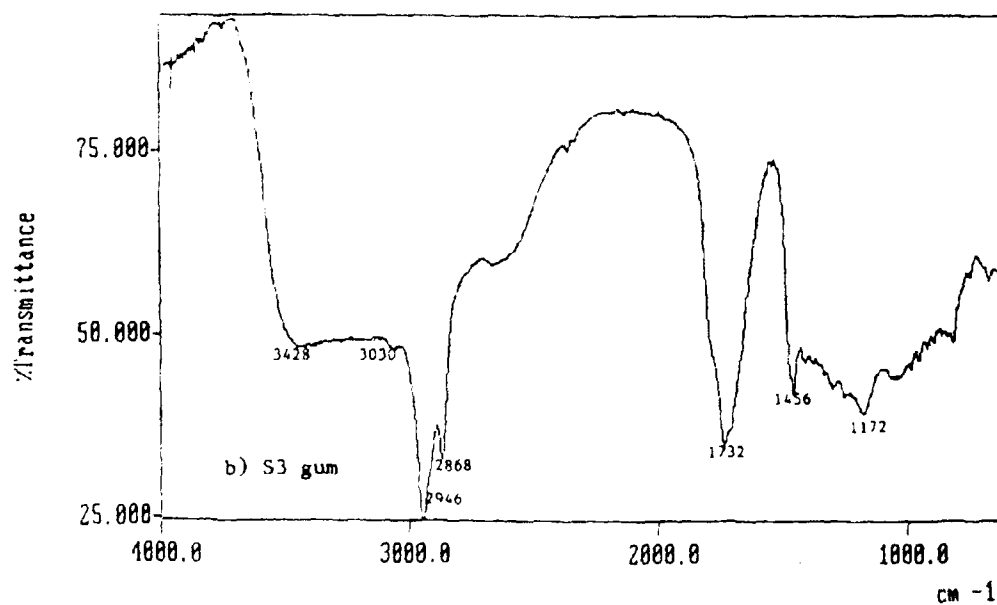
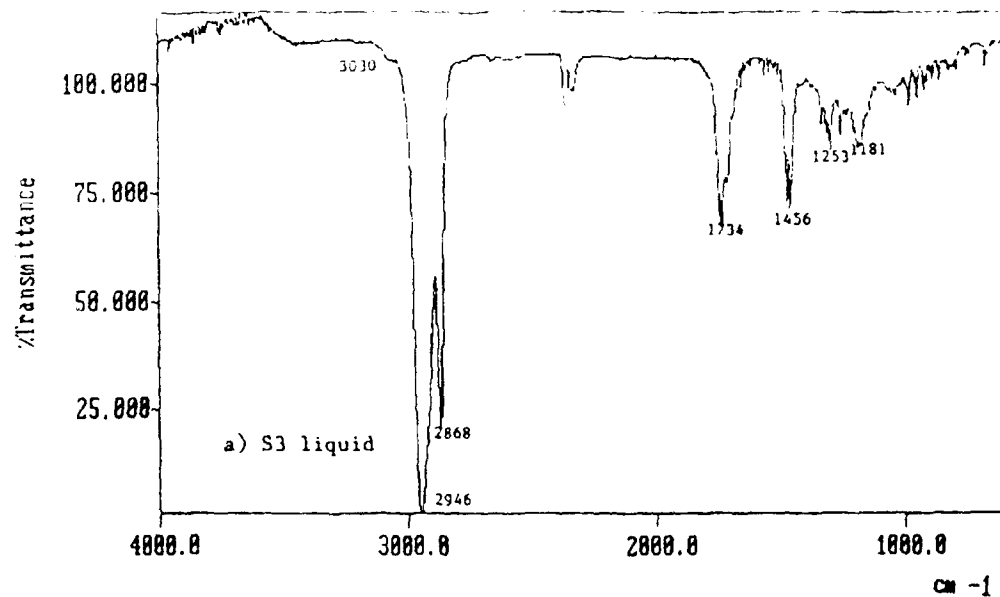


Figure 15. Fourier transform infrared spectra of sample S3 and the gum precipitate from S3.

(carbonyl, hydroxyl) JP-10, like material. Whether this gum has a truly covalently bonded polymeric structure or, rather, should be regarded as a hydrogen-bonded gel-like material cannot be decided from these observations and will require further studies, e.g. using quantitative LC techniques.

3.4 STATIC AND DYNAMIC EXPOSURE TESTS RESULTS

The static test samples were surveyed after ca. 3 months and 5 months by visually observing for gross color changes and by direct MS analysis of residues on bare wires. None of the samples in closed vials showed significant change from their respective starting materials during storage at 60-70°C in our lab. This includes previously weathered samples from Air Force accelerated aging tests and the control D from 1977 which both had high oligomer concentrations when we received them; their impurities showed no obvious change. The separate static test of our control A fuel in a flask with a condenser open to the air also showed no change in impurities by packed column GC for the bulk liquid sample after 2 months. However, the same analysis of a drop of the condensate above the flask showed a strong reduction in the aromatic impurities, thus confirming that the head space vapors were in a position to react with the air without the protection of the BHT or other effective antioxidants though no such reaction products were observed. Finally, the one 60°C static test of a complete armature extraction which did develop an obvious yellow color after just 2 days showed no obvious difference in the GC/MS total ion chromatogram from the control A fuel except for the addition of several alkane and phthalate related peaks.

The bulk of the dynamic test fuels were stored at -90°C until such time as a weathering scheme could be developed. Since our static test showed virtually no changes other than simple extraction effects, these samples are still present in the freezer. Small 6-8 mL aliquots of each of these as well as one half of one of first dynamic test fuels have been stored in the ambient lab environment without detectable change aside from the settling out of fine copper particles in the first few days. GC/MS analysis of one of these samples also showed no apparent change in the total ion chromatogram of the starting material (our control A) except for slightly increased alkane and phthalate peaks similar to the above mentioned extraction experiment.

SECTION 4.0

CONCLUSIONS

4.1 CHEMICAL COMPOSITIONAL CHANGES

Fresh JP-10 control samples from different batches contain 4 bulk components (JP-10 exo- and endo-isomers, ring-opened JP-10 and adamantane-like JP-10) as well as hundreds of trace components. Trace components can be divided into: (a) alkylsubstituted aromatic hydrocarbons (benzenes, naphthalenes, biphenyls, fluorene); (b) JP-10 homologs, analogs and oligomers; (c) long chain paraffins; (d) additives (e.g., diethylhydroxy toluene antioxidant); (e) dioctylphthalate; (f) unknown (hydroaromatic?) peak series at m/z 266, 238, 210; and (g) miscellaneous trace compounds. Considerable variation exists between the compositions of the trace organic compound fractions of different JP-10 batches. Fresh JP-10 samples show at least 3 different aromatic hydrocarbon patterns, whereas weathered samples tend to show significant quantities of JP-10 oligomers (sesquimers and dimers) combined with diminished abundances of aromatic hydrocarbons, BHT antioxidant and an unknown compound series at m/z 266, 238 and 210.

Two discolored (yellow) field samples of JP-10 submitted by the Air Force were found to have increased levels of paraffinic hydrocarbons up to C20 presumably derived from oil and grease in fuel pumps or other fuel distribution systems. Similar discolorations were observed when rinsing new fuel pumps with

JP-10. Moreover, the unusually high levels of paraffins may have been responsible for the JFTOT failure of one of the samples (labelled "ALS"). Increased gum content noted in the other sample (labeled "V39") appears to correlate with the presence of significant quantities of DOP (dioctyl phthalate) as well as increased JP-10 oligomer levels.

Some JP-10 samples (derived from a single batch) exhibited severe resin formation tendencies when exposed to different fuel pump components (whole armature and fish paper) at 60°C for periods up to two months in an Air Force laboratory. LC/MS analysis of the supernatant indicated the formation of marked quantities of hydroxy- and/or keto-substituted analogs of JP-10 and its oligomers. When exposed to a relatively inert polyimide rod under the same conditions for 1 month the concentration of oxygen substituted JP-10 analogs was found to be much lower. However, significant oligomer formation was still observed. FTIR and pyrolysis MS analysis of the resin fraction formed during JP-10 exposure to a fuel pump armature indicated a polymeric structure, probably involving oxidized (carbonyl and hydroxy substituted) JP-10 building blocks. Attempts to reproduce these phenomena in our laboratory using a different JP-10 batch failed. This JP-10 batch contained higher levels of alkylnaphthalenes and (possible) hydroaromatic compound series which may have had a protective effect against oxidation. In addition however, all samples produced in the Air Force experiments were found by low voltage MS to contain some DOP (dioctylphthalate) which might have promoted the observed resin formation.

The formation of marked quantities of JP-10 oligomers (sesquimers and dimers) in a naturally weathered JP-10 batch produced in 1977 would seem to warn against prolonged (e.g., >10 years) JP-10 storage. Moreover, at higher temperatures (e.g., 60°C) similar oligomerization processes have been observed to take place within a few months. Although several JP-10 samples with relatively high oligomer content still were found to be within specification (e.g., with regard to gum content), the observed oligomerization processes may well lead to eventual polymerization. The resinous gum precipitate observed in the static exposure tests performed by the Air Force was found to consist of a highly functionalized (carbonyl + hydroxyl groups) JP-10 like material. Whether this gum represents a truly polymeric material or a gel consisting of hydrogen bonded low MW components could not be determined from the available data. Oligomerization products observed in naturally aged ("weathered") JP-10 samples kept at ambient temperature since 1977 should be investigated in order to determine the likelihood of further polymerization, as well as to determine the effect of various possible chemical inhibitors.

A more detailed set of specifications should be developed in order to control the composition of bulk components as well as trace organic components in JP-10. Development of reliable specifications will require a better understanding of the stability of the various JP-10 bulk and trace components under a variety of different conditions (temperature, oxygen, W, moisture, catalytic surfaces) as well as of their possible roles in promoting or inhibiting oxidation and polymerization processes in JP-10 fuel. Care should be taken to avoid contamination with paraffinic hydrocarbons as well as phthalates during all stages of transportation, distribution and storage of JP-10 fuels.

Until the above proposed investigations have been undertaken and completed any JP-10 batches undergoing long term storage should be monitored on a regular (e.g., yearly) basis using suitable chromatographic and spectroscopic techniques. Samples stored at above-ambient temperature or pressure conditions should preferably be monitored on a semi-annual or quarterly basis. Fresh aliquots of newly produced JP-10 batches leaving the refinery should be analyzed by suitable chromatographic and spectroscopic methods in order to monitor fluctuations in the composition of bulk and trace components. The remainder of these aliquots should be stored at low temperatures under inert atmospheric conditions for future reference purposes, until the recently observed stability problems have been more fully investigated and explained.

4.2 SUSPECTED CAUSE OF FIELD PROBLEM

Contamination with oils and greases from fuel distribution systems appears to be the primary cause of the

yellow discoloration of JP-10 reported during pumping operation. The increased levels of paraffinic hydrocarbons, noted in the discolored samples, were presumably derived from oil and grease in fuel pumps. Although completely saturated paraffins tend to be quite stable at higher temperatures, occasional branching, unsaturated bonds and/or oxygen substitutions are likely to cause thermal degradation as measured by the Jet Fuel Thermal Oxidation Tester (JFTOT). These conditions are suspected to have contributed to the JFTOT failure of one of the discolored JP-10 samples. Increased gum content appears to correlate with the presence of significant quantities of DOP (dioctyl phthalate) as well as increased JP-10 oligomer levels. Resin formation in some weathered JP-10 samples, when exposed to specific fuel pump components, are suspected to be a result of the formation of significant amounts of hydroxy or keto substituted analogs of JP-10 and its oligomers.

REFERENCES

Telephone communication with Dr. Lou Hall, Sun Refining and Marketing Company, Pennsylvania.

F.N. Hodgson, E.A. Steinmetz, J.D. Tobias, B.B. Bowles, C.D. Fritsch, Analysis of Aircraft Fuels and Related Materials, Air Force, Aero Propulsion Laboratory, Wright-Patterson AFB, Ohio, AFWAL-TR-82-2082, December 1981.

F.N. Hodgson and J.D. Tobias, Analysis of Aircraft Fuels and Related Materials, Air Force Aero Propulsion Laboratory, Wright-Patterson Air Force Base, Ohio AFAPL-TR-79-2016, March 1979.

H.L.C. Meuzelaar, J. Haverkamp, F.D. Hileman, Pyrolysis Mass Spectrometry of Recent and Fossil Biomaterials; Compendium and Atlas, Elsevier Publishing, Amsterdam, 1982.

H.L.C. Meuzelaar, W.H. McClennen, Tandem Mass Spectrometric Analysis (MS/MS) of Jet Fuels, Part I and II, Air Force Aero Propulsion Laboratory, Wright-Patterson Air Force, Base, Ohio, AFWAL-TR-85-2047, Parts I and II, 1985.

EVALUATION OF PARTICULATE MATTER

Period of performance

September 1987

Reference

Task Order No. 12, Topical Report No. 8, FR 19032-6, September 1987, Marc Rippen

Abstract

Particulate matter collected from field components experiencing problems was identified using an electron scanning microscope, X-ray energy spectroscopy techniques, and direct insertion probe mass spectroscopy.

SECTION 1.0

INTRODUCTION

Four samples of particulate matter were submitted by the Fuels Branch of the Air Force Wright Aeronautical Laboratories (AFWAL/POSF) for composition analysis. Other than the fact that the particulate was collected from fuel in a fuel control system, no information was available regarding the fuel type, the system type of materials, or the history of the sample. The information supplied with each sample, along with Codes assigned by Pratt & Whitney, are as follows:

<i>P&W Code</i>	<i>AFWAL/POSF Sample Nomenclature</i>
Sample A:	7/1/87 SN-0014 Inlet Filter
Sample B:	7/2/87 SN-0014 From Filters & Orifice Packs
Sample C:	7/1/87 SN-0014 System A-63
Sample D:	7/20/87 SN-062040 S/B Control
Sample E:	Blank Filter (Millipore MF type-mixed Ester of Cellulose)

SECTION 2.0

EXPERIMENTAL

All samples were received as residue on 47-mm Millipore MF-type filters (mixed ester of cellulose). Each sample was visually examined and the observations documented. An ETEC Autoscan Scanning Electron Microscope was used to examine each sample for its elemental contents using X-ray Energy Spectroscopy techniques (XES). XES is a rapid, simultaneous method of conducting elemental analysis of materials with elements of atomic masses down to sodium. It utilizes an electron energy beam to excite surface atom electrons from their ground states to higher transient energy states. When these electrons drop back to their ground state, photons in the x-ray energy band are emitted. The wavelengths of the photons emitted are characteristic of the element analyzed. The XES detector (typically a lithium drifted silicon detector) acts to measure the x-ray photons emitted by the sample as a function of their energy. As the detector counts the number of photons of different energies, a computer integrates these and then generates an XES spectrum with intensity as the Y axis and energy or wavelength as the X axis.

The relative intensities observed at the elemental wavelengths provide for a direct measurement of the relative quantities of the elements observed in the sample analyzed.

Direct Insertion Probe Mass Spectroscopy (DIP-MS) was utilized for analysis of some of the samples. This work was conducted on a Hewlett Packard Model 5995C Quadrapole Mass Spectrometer equipped with a Gas Chromatograph (GC) and a DIP interface. Samples were collected into capillary tubes and then placed into the DIP for analysis. The following experimental parameters were utilized.

DIP Temperature Program:

Initial Time:	0 minutes
Initial Temperature:	50°C
Temperature Increase Rate:	30°C/minute
Final Temperature:	300°C
Final Time:	5 minutes
Total Run Time:	4 minutes

Mass Spectrometer Parameters:

Mass Analyzer Temperature:	220°C
Ion Source Temperature:	220°C
Electron Impact Source Beam Energy:	70 eV
Masses Scanned:	17 amu to 550 amu at 0.84 scans/second
Scan Threshold:	20

The NBS Data Base was utilized for identification through the standard Hewlett Packard ten major mass peak computer search algorithm.

Samples were also analyzed by Fourier Transform Infrared (FTIR) spectrometry on an IBM series 98 FTIR system. Samples were prepared in KBr pellets and their absorbance spectra recorded from 4000-500 cm^{-1} . A Sadtler Research Laboratories data base was utilized for component identification searches.

SECTION 3.0

DISCUSSION

Sample A

Sample A consisted of a thin layer of gray material with small finely dispersed shiny particles. XES analysis revealed four material types:

Type 1

Type 1 was a 300 series stainless steel, defined by the Fe, Cr, Ni peaks in the "overall" XES spectra.

Type 3

Type 3 was a material composed of Sn and some Pb.

Type 4

Type 4 was composed of Al with traces of Si, S, Fe and Cu. No DIP/MS analysis of Sample A was conducted for lack of adequate amounts of sample. FTIR analysis was conducted. A manual search was conducted using the Standard Infrared Spectra Collection from Sadtler Research Laboratories. No match was found. This was probably due to the fact that the sample was a mixture of several organic materials. The bands in the 3500 cm^{-1} region indicate possible O-H stretching and N-H stretching. Those in the 2900 cm^{-1} region are probably due to C-H stretching. In the 1600 cm^{-1} region there is evidence of N-H deformation while in the 1400 cm^{-1} there may be C-H deformation. The 1037 cm^{-1} peak is possibly due to Si-O stretching. Looking at this spectrum one would suspect that phenols, amines, aliphatic hydrocarbons and possibly some silicates moieties could be present.

Sample B

There was a large amount of particulate residue present in this sample. It appeared gray with patches of brownish-red. XES of this sample showed its composition to be primarily Pb with traces of Si, Al, Sn, Fe and Cu. When the sample was run with the DIP/MS nothing was evolved until the probe passed 200°C . A DIP total ion profile was generated. Three areas seemed to be differentiated in this profile. Average spectra were taken with background interference. The first area averaged showed a typical aliphatic hydrocarbon spectrum with correlation to NBS reference library components such as nonane at 97%. The spectrum is obviously not of a pure component but is typical of aliphatic profile. The second average generated a spectrum which was similar to that expected for amines or possibly phenols (92%), plus other lesser components. No positive identification was possible due to the number of components in the sample.

FTIR analysis of the sample yields a similar spectrum to that of the first one. O-H and N-H stretching is evident in the peak in the 3500 cm^{-1} region. C-H stretching can be already seen in the 2900 cm^{-1} region. N-H deformation appears in the 1600 cm^{-1} region. This sample appears to consist of amines, phenols and aliphatic hydrocarbons. A manual spectral search was inconclusive due to the presence of several components.

Sample C

This sample consisted of brownish-red crystals. XES analysis of this sample showed high Pb with Si, Al, Ca, Fe and Cu traces. Organic components appeared to be present as indicated by the high background. DIP/MS produced the same spectrum as that of Sample B. FTIR Analysis also produced a spectrum similar to that of Sample B.

Sample D

This sample appeared to be full of sand, dirt, fibers, and shiny particles. XES showed presence of low alloy steel plus Al, Si, S, Cl, K, Ca and Cu. DIP/MS showed mostly water with some evidence of hydrocarbons with very mixed mass spectra. FTIR analysis showed the same general spectrum as seen in the three previous spectra.

SECTION 4.0

CONCLUSION

The bulk of the debris in the filtrates supplied are inorganic. The organic components present in these samples seemed to be of the same chemical makeup. DIP/MS and FTIR indicated the possible presence of amines, phenols and aliphatic hydrocarbons which could not be positively identified due to number and types of components present in the material. Samples B and C were unusual because they showed a high amount of Pb in their particles. As there is little known of the origin of these samples, no possible explanations can be made of their nature or origin of the materials observed.

EVALUATION OF THE SHELL PREMIXED BURNER

Period of Performance

22 March 1989 through 22 March 1990

Reference

Task Order No. 16, Topical Report No. 14, FR 19032-14, May 1990, Tedd Biddle

Abstract

The Shell Premixed Burner, developed by Shell Thornton Research Center, has been presented as a novel approach for discriminating between fuels of varying quality based on their burning characteristics. The Shell Premixed Burner is based on the concept that a vaporized fuel sample added at a controlled flow rate to the methane/air supply of a Bunsen-type flame will reduce the air/fuel ratio. As the fuel supply is increased and the air/fuel ratio decreases, the sooting point is reached. The rate of flow is a direct correlation to the combustion quality of the fuel. Based on Shell Thornton's preliminary results, a cooperative effort was initiated among several independent laboratories to evaluate proof-of-concept. The laboratories participating in this effort were unable to reproduce Shell Thornton's results. It was concluded that at its current stage of development, the Shell Premixed Burner requires considerable development work to resolve problems associated with both the test equipment and the test procedure. Efforts should be directed at improving fuel atomization, detecting changes in flame illumination, and addressing high volatility fuels.

SECTION 1.0

INTRODUCTION

The Shell Premixed Burner, developed by Shell Thornton Research Center, has been presented as a novel approach for discriminating between fuels of varying quality based on their burning characteristics. Comparisons by Shell Thornton with full-scale combustor tests indicated that the technique provided a better correlation and more realistic index of combustion quality than smoke point or hydrogen content. Shell's preliminary results indicated that the premixed burner was able to discriminate between fuels in a qualitative or ranking-order fashion.

Based on Shell Thornton's preliminary results, a cooperative effort was initiated among several independent laboratories to evaluate proof-of-concept. The laboratories participating in this effort included Rolls Royce, the Naval Research Laboratory (NRL), and Pratt & Whitney (P&W). P&W's effort was performed under the auspices of T.O. No. 16. The technical effort described in the following sections was directed at the following objectives: 1.) Set up and evaluate the Shell Premixed Burner; 2.) reproduce data set previously generated by Shell; 3.) identify system strengths and limitations; 4.) determine potential for further development; and 5.) generate a data base for elucidating the relationship between chemical composition and the premixed burner number.

SECTION 2.0

EXPERIMENTAL

The Shell Premixed Burner is based on the concept that a vaporized fuel sample added at a controlled flow rate to the methane/air supply of a Bunsen-type flame will reduce the air/fuel ratio. As the fuel supply is increased and the air/fuel ratio decreases, the sooting point is reached. The rate of flow is a direct correlation to the combustion quality of the fuel. Luminosity at the sooting point is measured using a photodetector which permits comparisons between samples that could not be achieved visually. The sooting point was established as the change in luminosity of the methane/air flame when Shellsol T is added at a flow rate of 10 grams/hour (g/hr) (0.5 g/180 seconds). Shellsol T is a proprietary solvent that is almost exclusively a mixture of dodecane isomers. The Premixed Burner Number (PMBN) is the number of seconds required to inject 0.5 g of the fuel sample into the methane/air flame at a rate which produces the same change in luminosity as the Shellsol T.

The Shell Premixed Burner was set up using equipment that met the specifications given in Shell report No. TNER.87.007 and subsequent updates. The Premixed Burner configuration is shown in Figure 1. The premixed burner assembly, i.e., burner globe, mixing chamber and injector capillary glassware, and fiber optic light guide were supplied by Shell Thornton. Blending of the methane and air for the flame was accomplished using a Matheson Modular Dyna-Blender Model 8210. Sample was supplied to the system with a Sage Model 341A syringe pump. The hot plate for heating the mixing chamber was a Barnstead/Thermolyne Cimarec 2. Two different photodetectors were used during the course of the investigation to convert the luminous output to a measurable current. A Mettler PC220 balance was used for weighing the sample. A Hewlett Packard 7132A Recorder was used for recording the output from the photodetector.

The Matheson Modular Dyna-Blender Model 8210 was capable of maintaining the required methane/air supply to the burner at 3.0 +/- 0.2 liter/minute with the methane concentration at 14.5 +/- 1.0 volume percent. The Cimarec 2 hot plate was one of the few hot plates commercially available that could maintain the 500°C (932°F) temperature needed to vaporize the sample being injected. The two photodetectors used were an OSD 50-5 and an OSD 50-E available through Centronic, Inc. The OSD 50-5 detector has a range from 400 to 1000 nanometers (nm). The OSD 50-E has a range of 400 to 700 nm and is designed for use where a response is required that approximates the human eye. The premixed burner assembly was enclosed in a box to eliminate as much background light as possible. An exhaust vent was provided to the hole in the top of the box to create enough flow to remove combustion gasses without causing a turbulence which would affect the flame.

Alignment of the light guide was one of the most critical elements to producing meaningful data. The light guide was positioned perpendicular to the flame by way of a side arm, or sleeve, incorporated into the globe structure. However, fixed reproducible positioning of the light guide between runs was not possible due to loose tolerances in the design of the side arm. Careful adjustment of the light guide was necessary to ensure that readings were from the portion of the flame most affected when sample was introduced into the system. It would even be possible to be looking above the flame. Since it was necessary to determine the amplitude of the trace produced at the recorder, any condition causing fluctuations had to be eliminated or minimized. Areas of concern included pulses caused by the pump, air bubbles in the sample injection tube, bubbles produce in the injection tube by volatilization of the sample, and noise inherent in the optics and electronics.

In preparation for running samples, the vaporization chamber was heated to 500°C (932°F). The air flow through the Dyna-Blender and glassware was initiated when the hot plate was turned on to prevent distortions in the glassware due to overheating. When the temperature approached 500°C (932°F), the methane flow was started and the burner lit. The recorder was then turned on and adjusted to establish a

baseline or zero reading. Subsequent to filling the syringe with the Shellsol T reference fluid, the syringe pump was turned on and the flow to the burner adjusted to deliver 0.5 grams (g) per 180 seconds. Flow was discontinued when a stable strip chart trace was achieved. The system was purged of the Shellsol T, rinsed with hexane, and air dried. The test sample was then introduced via the syringe pump. Flow of the test sample was begun and adjusted until the amplitude of the trace produced was the same as that produced with Shellsol T. The time in seconds required to deliver 0.5 g of sample to the burner was calculated and reported as the PMBN.

Ten fuel samples were received from Shell Thornton Research Center for use in evaluating Premixed Burner proof-of-concept. Smoke point, hydrogen, aromatic and naphthalene content for these fuels were generated by Shell Thornton and are shown in Table 1. Aliquots of these samples were forwarded to WRDC and the Air Force Academy as requested by the Air Force Project Scientist. In addition, ten pseudo fuels formulated by WRDC were received for evaluation using the Shell Premixed Burner.

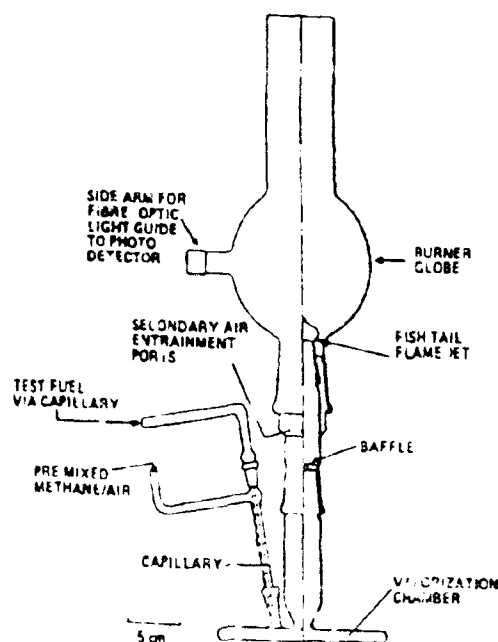


Figure 1. Shell Premixed Burner

**TABLE 1.
SHELL THORNTON PREMIXED BURNER TEST FUELS**

Fuel Sample	IP Smoke Point (mm)	Hydrogen Content (%w)	Aromatic Content (%v)	Naphthalene Content (%v)
Shellsol T	45	15.17	<1	0
HC2 (1)	28	14.08	12.6	0.40
HT3 (2)	26	13.95	16.4	0.87
JET A-1	24	13.80	19.0	3.00
AVCAT	23	13.80	19.0	2.02
HIGH NAPH KERO	22	13.62	20.5	5.02
HC27 (1)	21	13.49	15.4	0.40
NORTH SEA MGO	19	13.48	23.9	8.05
HC29 (1)	16	12.99	29.7	2.41
ERBS2 (3)	14	12.85	27.6	11.76

Note: (1) Hydrocracked Kerosine
(2) Hydrotreated Kerosine
(3) NASA Experimental Referee Broad Specification Fuel

SECTION 3.0

RESULTS AND DISCUSSION

Preliminary test runs resulted in erratic strip chart recorder traces. Responses were intermittently very high and very low, which made it difficult to establish sooting point. Examination of the fuel injection segment of the glassware revealed that fuel droplets were forming on the end of the fuel injection capillary. The droplets would then fall onto the bottom of the vaporization chamber where they were volatilized rather than undergoing the continual atomizing action intended. Upon disassembly, it was determined that the inner fuel injection capillary was warped and touched the wall of the gas delivery tube. Shell Thornton was consulted and agreed to send an injector tube that was correctly fabricated. Repeatability problems and erratic traces, however, persisted even after installation of the new injector tube.

Since NRL was also having difficulties obtaining meaningful, repeatable data, Shell Thornton was contacted for direct technical assistance. Peter Wolveridge acting on behalf of Shell Thornton Research management graciously volunteered to send a technical representative to assist both NRL and P&W. Richard Heins of Shell Thornton visited NRL and spent one week working with their system. Don Yost of P&W visited NRL for the last two days of that week to observe the NRL system and procedures and to discuss problems they were experiencing.

Richard Heins spent the first three days of the following week at P&W. Based on his experience, the light guide was realigned and several changes were made to the system and test procedure. Although the methane/air flow rate had been predetermined by Shell after the glassware was fabricated, it was found that additional adjustments were required based on a visual check of the flame geometry. The light guide, which fits into the side arm of the burner globe, was realigned so that the tip of the light guide

extended to the plane of the globe. The glassware, including the vaporization chamber, lower stem and some of the upper stem, was covered with insulating material. This was done to minimize condensing or coking out of the vaporized fuel on the glassware before reaching the burner. The insulating material was kept away from the secondary air entrainment ports so as to not restrict the supply of air to the flame.

A Simplex mini-pump and pulse damper had been procured from LDC Milton Roy to supply sample to the system. The required sample flow could not be maintained pulse free using the pump and pulse damper. In addition to the pulsating flow, changing to a different sample proved to be a problem as it was difficult to determine if the pump, pulse damper and lines had been cleared of the previous sample before collecting data on a new sample. Use of a Sage Model 341A syringe pump with a 50 milliliters (mL) syringe resolved both problems. A continuous, nonpulsing, flow was attained using the syringe/pump in a spill return mode. The syringe was used to clear the lines and then cleaned before adding a new sample. Valves were added to the fuel delivery system tubing that could be used to reduce or eliminate fuel flow to the burner when required. A resistor and capacitor were added to the recorder input to dampen out the signal enough that the trace could be read. Subsequent to implementing these refinements to the system, the unit was checked out using Shellsol T reference fluid. Fuel testing was then initiated.

After successfully determining PMBN's on the nine fuel samples supplied by Shell, the burner was dismantled due to the formation of coke on the upper stem and areas around the secondary air entrainment ports. The coke was removed from the upper stem and gas mixing baffle by heating in a muffle furnace at 570°C (1058°F) for several hours and then slowly returning to room temperature. The system was then reassembled to its original configuration.

An attempt was made to determine the PMBN of ten pseudo fuels supplied by WRDC. The volatility of components used for these fuel blends precluded analysis using the Shell Premixed Burner as bubbles formed in the injection tube. The momentary interruption of fuel being injected into the vaporization chamber was recorded as a deflection toward the baseline. The hot plate/vaporization chamber temperature was reduced from 500°C to 350°C (932°F to 662°F) in an effort to prevent premature volatilization. This approach was unsuccessful as bubbles continued to form in the fuel injection capillary. Lower hot plate/vaporization chamber temperatures were not attempted because of the high probability of fuel constituents condensing out before reaching the burner. This was especially a concern for the Shellsol T. After making runs at the reduced temperature, coke had again formed on the upper stem and areas around the secondary air entrainment ports. The Premixed Burner glassware was again dismantled, the coke removed by heating to 570°C (1058°F), and reassembled.

The ten fuel samples supplied by Shell were tested a second time to establish repeatability of the test. The initial traces produced were so erratic that comparison of the test samples (change in luminosity) to the sooting point established for the Shellsol T reference fluid was difficult and extremely subjective. A number of possible causes were investigated to determine why the traces were so different from the first set of results. Alignment of the light guide, leaks in the fuel supply, a possible change in the hot plate/vaporization chamber temperature, and numerous other variables were scrutinized. As a last resort, the photodetector was changed from the OSD 50-5 to the OSD 50-E eye response detector. The traces produced using the OSD-50E eye response detector resulted in considerably less noise, but a proportionate decrease in the amplitude of the trace was also realized. Attempts to obtain a traces with greater amplitude and low noise were unsuccessful. Under these conditions, the nine fuels were run a second time and results calculated. NRL also reran the samples using the OSD 50-E eye response detector because they were unable to reproduce their first set of runs using the OSD 50-5 detector.

PMBN's for the ten fuels supplied by Shell Thornton are shown in Table 2. Included in this table are duplicate runs performed by P&W, NRL, and Shell Thornton Research Center. NRL results are those presented to the Coordinating Research Council (CRC) in April, 1990. The OSD 50-5 detector was used for Run No. 1 by both P&W and NRL. The OSD 50-E eye response detector was used for Run Number 2 by both labs.

As shown in Table 2 and Figure 2, Shell Thornton experienced good repeatability between duplicate runs. The P&W and NRL laboratories were unable to achieve acceptable repeatability between duplicate runs as illustrated in Figures 3 and 4. The scatter between duplicate runs was greater than the difference observed by Shell between fuel types. Reproducibility of PMBN between the three laboratories was poor and there was general disagreement in the ranking of fuels. Figure 5 compares the order in which the three laboratories ranked the fuel samples using the OSD 50-5 photodetector. Figure 6 compares the order in which the three laboratories ranked the fuel samples using the OSD 50-E eye response detector.

TABLE 2.
PREMIXED BURNER NUMBERS FOR SHELL THORNTON FUEL SAMPLES

Fuel Sample	Shell Thornton Run No.1	Run No.2	P&W Run No.1	P&W Run No.2*	NRL Run No.1	NRL Run No.2*
Shellsol T	180	180	180	180	180	180
HT3	191	190	200	191	177	199
HC2	191	190	220	194	177	198
JET A	192	191	190	197	179	201
AVCAT	192	193	201	199	178	202
HIGH NAPH KERO	197	196	202	203	**	213
				196		
				197		
HC27	201	203	208	207	191	221
NORTH SEA MGO	207	203	202	201	186	214
HC29	218	219	222	217	**	227
ERBS2	232	225	235	220	208	237
* OSD 50-E Eye Response Detector ** Undetermined						

Fuel Ranking By Premixed Burner Number

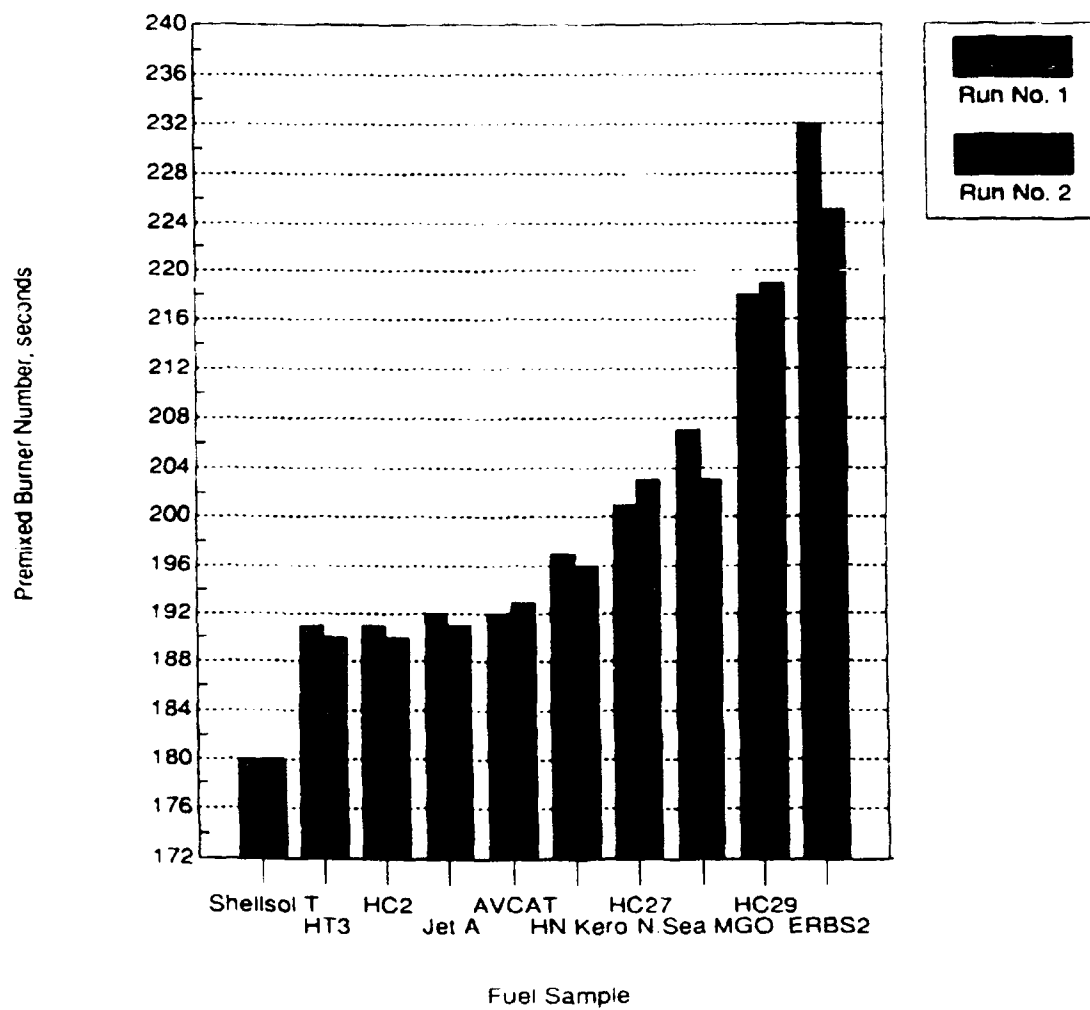


Figure 2. Repeatability of Shell Thornton Measurements

Fuel Ranking By Premixed Burner Number

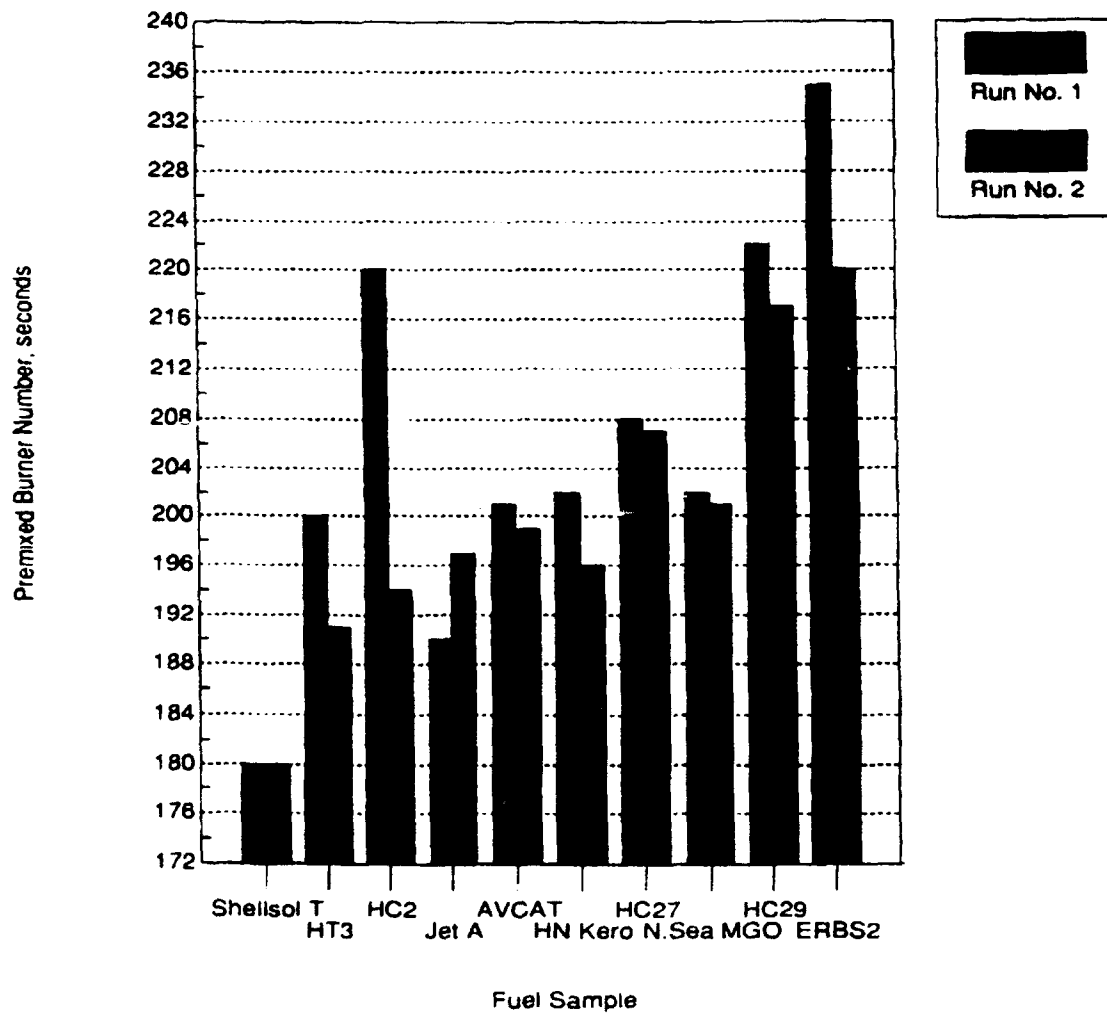


Figure 3. Repeatability of P&W Measurements

Fuel Ranking By Premixed Burner Number

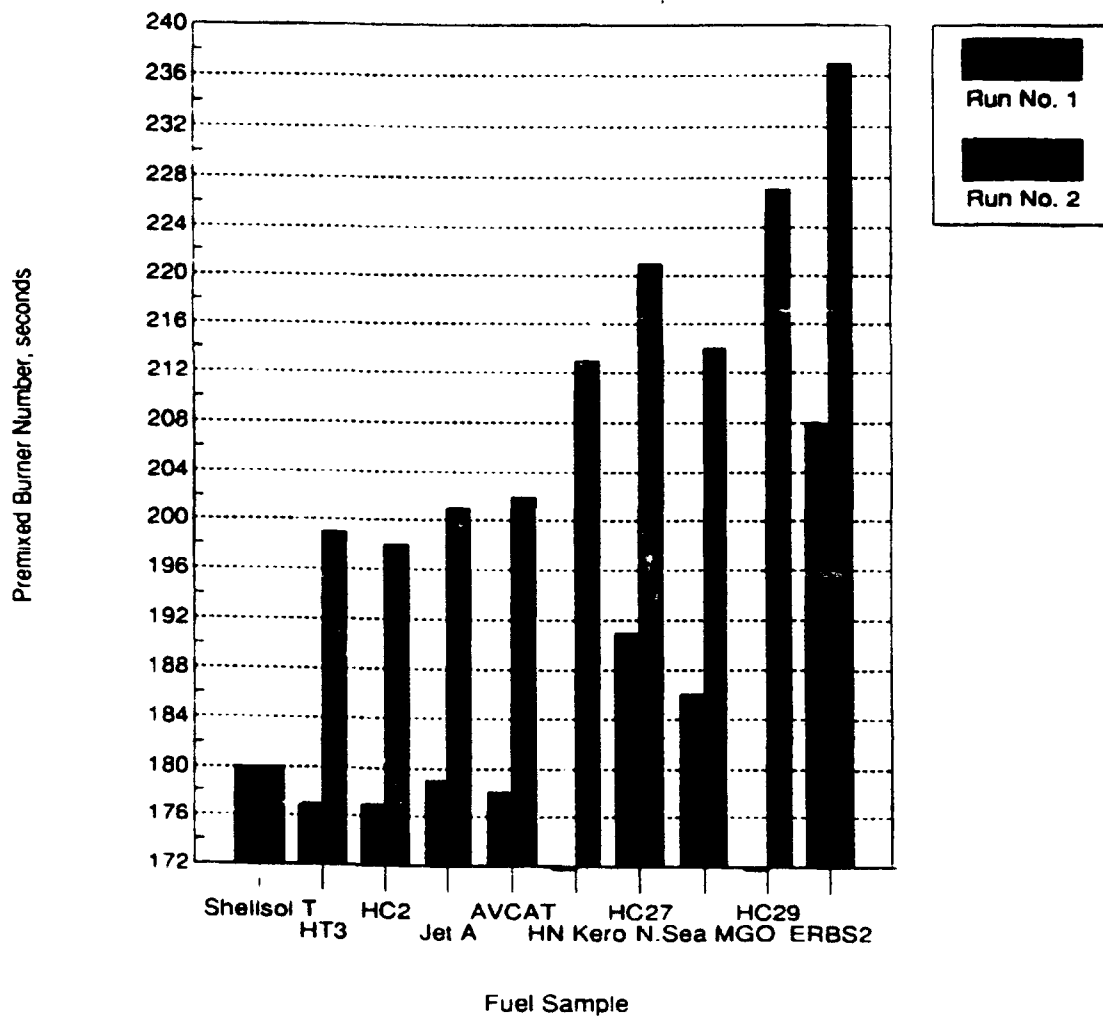


Figure 4. Repeatability of the Naval Research Laboratory Measurements

Fuel Ranking By Premixed Burner Number

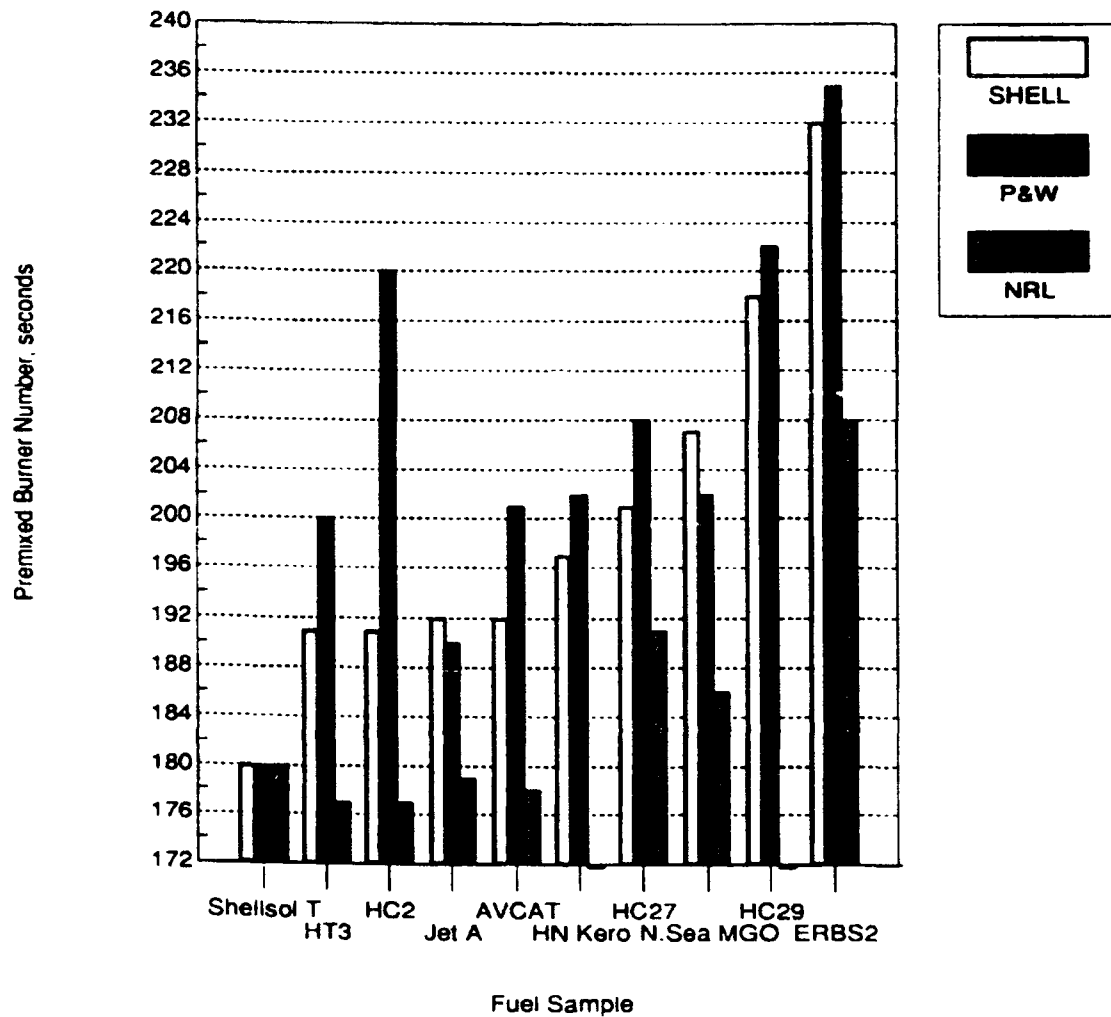


Figure 5. Reproducibility Between Laboratories Using the OSD 50-5 Detector

Fuel Ranking By Premixed Burner Number

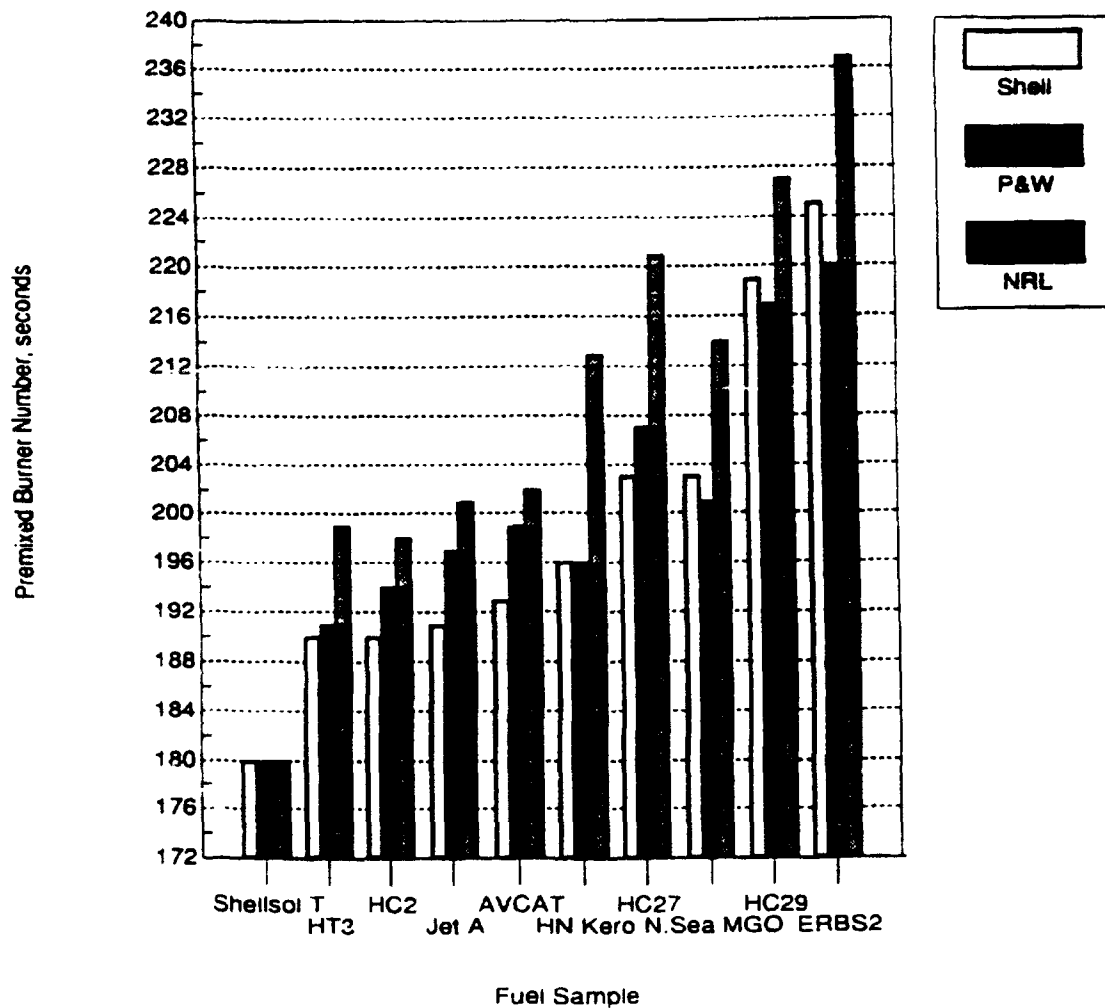


Figure 6. Reproducibility Between Laboratories Using the OSD 50-E Eye Response Detector

SECTION 4.0

CONCLUSIONS

At its current stage of development, the Shell Premixed Burner requires considerable development work to resolve problems associated with both the test equipment and the test procedure. Efforts should be directed at improving fuel atomization, detecting changes in flame illumination, and addressing high volatility fuels.

STANDARDIZATION OF LUBRICITY TEST

Period of Performance

30 November 1985 through 01 November 1986

Reference

Task Order No. 3, First Interim Report, August 1987, AFWAL-TR-87-2041, T.B. Biddle, R.J. Meehan, P.A. Warner

Abstract

The technical effort described herein was directed at refining and standardizing the Ball-On-Cylinder Lubricity Evaluator (BOCLE) test. The thrust of the effort focused on identifying variables suspected of affecting test method precision. Recommendations based on the conclusions of this study were submitted to the Air Force Project Engineer for consideration and review by the Coordinating Research Council (CRC) BOCLE Operators' Task Force and Fuel Lubricity Panel. The Falex Ring was shown to significantly enhance BOCLE test precision and eliminate many of the problems associated with the conventional AMS 6444 test cylinder. Test results showed that the source of the test ball can have a significant effect on BOCLE results. SKF Swedish precision balls were found to provide optimum batch to batch consistency. Isopar M + 30 ppm DuPont DCI-4A was shown to be a reproducible fluid suitable for use as a standard reference fluid for BOCLE testing.

SECTION 1.0

INTRODUCTION

Lubricity may be the most critical fuel property likely to be degraded by refining methods. Future fuels will be refined from high sulfur and high aromatic crudes, as well as from shale oil and coal syncrudes with equally high sulfur and aromatic concentrations. Low quality feedstocks will necessitate the use of severe hydrotreating. This refinery process removes or reduces the lubricity enhancing polar molecules that naturally occur in crudes and provide the boundary lubrication necessary for engine fuel system components.

Lubricity related fuel system component problems first surfaced in the early 1960's. Catastrophic failure and extreme reduction in component life have been associated with low lubricity fuel of all types used by both military and commercial aircraft. Typical problems include severe bore wear, ball joint wear, and complete piston failure of piston type pumps. Gear type fuel pumps operating on low lubricity fuels have encountered journal bearing seizure, drive shaft failure, wear of gear teeth flanks, and flaking of the contact area of the teeth in the main stage drive gear. Most recently, incidents of F-111 aircraft hydraulic pump housing fractures have been reported by Cannon AFB, New Mexico; Plattsburgh AFB, New York; and Tinker AFB, Oklahoma.

A significant level of effort has been expended in the study of low lubricity fuels: chemical properties, lubricity enhancing additives, and test method development. Since the early 1960's, the Ball-On-Cylinder Lubricity Evaluator (BOCLE) has been recognized as the best available method for providing a relative system of measurement of the lubricity properties of jet fuels. A variety of ball-on-cylinder machines, test procedures, test cylinders, and reference fluids exist in the military and throughout industry. This lack of standardization serves to severely restrict test repeatability and reproducibility of data among different laboratories.

Standardization of the BOCLE test method is of fundamental importance in order that conventional and experimental fuels can be accurately characterized to predict potential problems or to determine the cause and mechanism of lubricity-related fuel system failures. Of equal importance is the ability to compare and interpret data from various laboratories. This can be accomplished only if test apparatus and procedures are standardized and variables affecting precision are minimized by way of definitive specifications.

The technical effort described in the following sections was directed toward refining and standardizing the BOCLE test. The thrust of the effort focused on identifying variables suspected of reducing test method precision. Recommendations based on the conclusions of this study are herein submitted to the Air Force Project Engineer for consideration and review by the Coordinating Research Council (CRC) BOCLE Operators' Task Force and Fuel Lubricity Panel.

SECTION 2.0

EXPERIMENTAL

In order to accomplish the goals set forth in this investigation, the technical approach followed a step-like progression in identifying the primary variables suspected of affecting BOCLE test precision. Once identified, these critical parameters were evaluated within the constraints of the operating conditions of the BOCLE test. Based on the assessment, optimum conditions and material specifications were defined.

Technical effort included determination of an appropriate standard reference fluid to permit test cylinder calibration and interlaboratory comparison of data. Cylinders, which were fabricated by different vendors to selected surface finishes, were evaluated. This was done to assess the effect of surface finish on test precision. These tests also served to appraise vendor quality control in providing a source for repeatable and reproducible test cylinders. An alternative test specimen to that of the problem-laden conventional test cylinder, currently used in the BOCLE test, was investigated. A further investigation focused on test ball to determine whether there was a measurable effect on test precision between ball manufacturers. Work was concluded with an interlaboratory evaluation of the Falex Timken Ring. This cooperative effort assessed the ability of the Falex Ring to meet the criteria required for a standard specification test, enhance test precision, and resolve existing problems associated with the conventional BOCLE cylinder. Five laboratories participated in the mini-round robin.

All BOCLE tests were performed on an InterAv BOC-100 lubricity tester. With the exception of the variable or material specimen under test, the test procedure throughout the course of the program closely adhered to the CRC recommended BOCLE test method outlined in Draft #9, "Standard Test Method for Measurement of Lubricity of Liquid Hydrocarbon Fuels By the Ball-On-Cylinder Lubricity Evaluator".

2.1 REFERENCE FLUID INVESTIGATION

Determination of appropriate or desired properties for a candidate reference fluid was made by surveying the chemical and physical properties of various hydrocarbon type fluids in a range of carbon numbers from C6 to C12. Storage stability, long term availability, and the level of fluid harshness were among the criteria examined. It was considered desirable that the degree of fluid harshness permit sensitivity to exceptionally high lubricity fuels. It was also desirable to retain the precision which is sometimes lost as a result of larger BOCLE wear scar diameters (WSD). Pure hydrocarbon fluids and formulations of hydrocarbon fluids were considered along with additive blends and "neat" fuels. The merit of multiple fluids for purposes of cylinder calibration, quantitative lubricity references, and contamination detection was also examined.

Among the pure hydrocarbon solvents considered was Isopar M which is produced by the Exxon

Company and used extensively in industry as a calibration fluid. Isopar M is an odorless, relatively high boiling, narrow cut isoparaffinic solvent of high purity. It is synthesized by a catalytic process from petroleum fractions. A table of physical and chemical properties characterizing Isopar M is presented in Appendix A. Reference fluid candidates included straight chain hydrocarbons (C6 to C12); a cycloparaffin, cyclohexane; naphthalene derivatives, decalin and tetralin; neat Isopar M; Isopar M with additive (DuPont DCI-4A); and blends of Isopar M and tetralin.

Candidate reference fluids were selected and evaluated by way of a series of BOCLE tests. The test matrix consisted of three cylinders of known and proven good quality and three cylinders of known inferior quality. Determination of "good" and "bad" cylinder quality was based on P&W experience and current standards as defined by the existing BOCLE test procedure. All good cylinders were fabricated to specifications defined by CRC recommended guidelines: 4 to 9 microinch (min.) surface finish, 20 to 22 Rockwell C (Rc) hardness, and AMS 6444 alloy. Cylinders determined to be of poor quality varied in surface finish, hardness, and alloy. These cylinders were fabricated from an AMS 6440 alloy. The surface finish of the cylinders varied from 10 to 40 min. Hardness varied from 22 to 24 Rc.

The candidate reference fluids were run in quadruplicate on each of the three good and three bad cylinders. The initial test run on a cylinder was spaced 1.0 millimeter (mm) from the edge of the hub-side of the cylinder. Succeeding runs were spaced in increments of 0.75 mm. The candidate fluids were tested in an alternating sequence across the face of each cylinder.

Selection of a standard specification reference fluid was based on the following criteria:

- Repeatability across the cylinder running surface
- Reproducibility from cylinder to cylinder
- Differentiation between cylinders of known good quality and cylinders of questionable or inferior quality
- Maintainability of a constant lubricity value over extended periods of storage
- Storage stability and availability in future years

2.2 TEST CYLINDER SURFACE FINISH INVESTIGATION

The fluid selected as the most promising standard at the conclusion of the reference fluid investigation was used to provide a baseline for assessing and comparing cylinder variables, and for quantifying their effect on test repeatability and reproducibility. The effect of surface finish on test cylinder repeatability, both across the running surface and from cylinder to cylinder, was examined in three separate phases. These three phases of investigation were necessitated by anomalies encountered during the first and second phases of surface finish testing.

The effect of surface finish was determined for two different surface finishes which had been previously verified by profilometer measurements. The two different manufacturers supplying test cylinders were assigned the codes "J" and "FV," respectively. Surface finishes evaluated consisted of FV fabricated cylinders ground to a 4 to 9 min. surface and J fabricated cylinders ground to a 16 to 22 min. surface finish. Material alloy and cylinder hardness, also considered to be important cylinder variables, were held constant. The specified material was an AMS 6444 alloy, tempered to a Rockwell hardness of 20-22 Rc. Three cylinders of each surface finish were evaluated. BOCLE tests were performed in quadruplicate and included the following fluids: (1) Isopar M + 30 parts per million (ppm) DCI-4A, as the most promising candidate reference fluid; (2) JP-4, which is highly volatile and typically produces a relatively small wear scar; (3) clay-treated (CT) JP-4, which generates a relatively large wear scar; and (4) JP-7, which is of

low volatility and typically produces a wear scar diameter between that of an as-received JP-4 and a CT JP-4.

2.3. FALEX RING INVESTIGATION

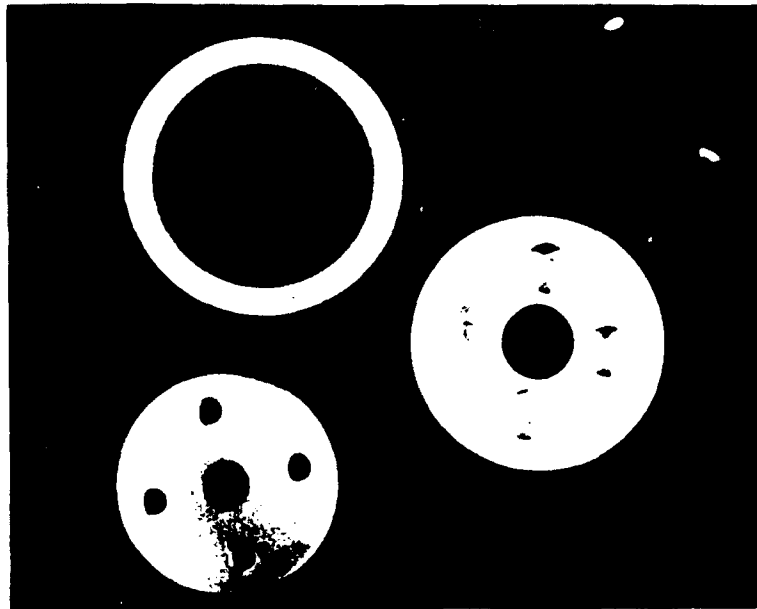
The Falex Ring is currently sanctioned by ASTM in two test methods which assess lubricating properties of oils (D2782 and D2509). The Falex Ring differs from the conventional solid BOCLE cylinder in alloy material, hardness, and surface finish. The alloy is an SAE 8720 modified steel, tempered to a hardness of 58 to 62 Rc, and ground to a 20-30 μ in. surface finish. It has a 50 mm (1.97 inch) outside diameter (OD) and a 39 mm (1.54 inch) inside diameter (ID). The Falex Ring, fabricated by the Falex Corporation, is a readily available, low cost stock item.

Relatively minor special test conditions were necessary for use of the Falex Ring in place of the conventional AMS 6444 solid cylinder. A mandrel, also manufactured by the Falex Corporation, permitted installation of the Falex Ring on the standard InterAv cylinder shaft. Figure 1 shows the Falex Ring, mandrel, and the manner of installation. Because the Falex Ring is 5.55 mm (0.21 in.) larger in diameter than a conventional BOCLE cylinder, a minor modification to the BOCLE apparatus itself was necessary to permit leveling of the load arm. The modification consisted of inserting a 38.1 x 76.2 mm (1-1/2 X 3 in.) shim, made from a piece of 2.28 to 2.79 mm (0.090 to 0.110 in.) sheet metal shim stock, between the load pedestal and the top base plate. It was also necessary to attach a 19.0 X 19.0 mm (3/4 X 3/4 in.) shim to the underside of the load beam in such a manner that the hydraulic lift plunger met the shim when the plunger was fully extended in the "up" position. This was required to compensate for the plunger's limited length of travel. Appendix B contains a diagram with instructions to assist in modifying the BOCLE apparatus for use with Falex Rings.

A reduction in applied load from 1000 grams (g) to 500 g represented the only change in the actual test conditions. The harder ring material was found to generate a larger wear scar than the conventional cylinder. After a series of trial runs with harsher test fluids, it was determined that a 500 g applied load was more suitable for maintaining a wear scar within the limits of the 1-mm graduated reticle of the microscope.

A preliminary investigation was performed to evaluate the potential of the Falex Ring to enhance BOCLE test precision. The test matrix consisted of three runs performed on each of three rings from the same material lot. Evaluations were conducted using five different fuel types. A total of 45 runs were performed.

As a result of the promise shown in the initial phase of the Falex Ring evaluation, a more extensive investigation was performed. This investigation consisted of 180 runs and was designed to determine repeatability of the Falex Ring in a variety of fuel types, degree of differentiation between fuel types of varying known lubricity, reproducibility of data from ring to ring within a given production lot, and reproducibility of data from the manufacturer's lot to lot production. Three rings were evaluated from each of four different production lots in five different fuel and fluid types. The test fluids and fuel types included the selected BOCLE reference fluid (Isopar M + 30 ppm DCI-4A), JP-4, JP-8, JP-7 and CT JP-4. Tests were performed in triplicate on each test ring. This generated a total of 36 data points for each fuel sample.



(a) Falex Ring, Right and Left Halves of Mandrel Assembly

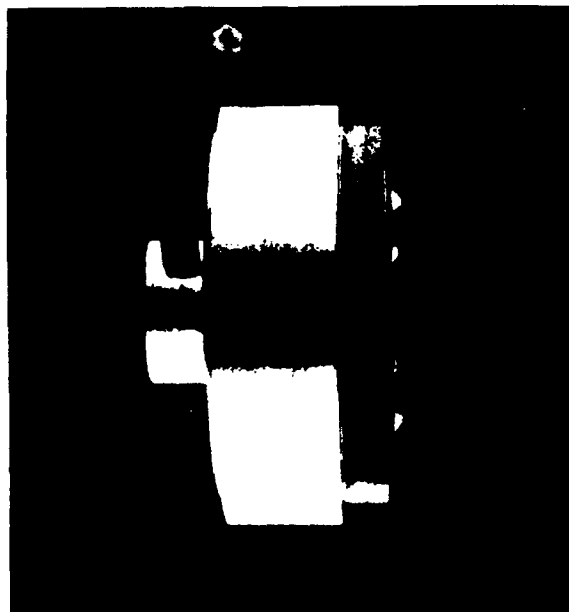


Figure 1. Falex Ring and Mandrel Assembly

2.4 INTERLABORATORY EVALUATION OF THE FALEX RING

An interlaboratory cooperative effort was organized to confirm the potential shown by the Falex Ring to enhance test precision. The intent of the mini-round robin was to generate a preliminary precision statement before recommending a full-scale round robin sponsored by the CRC. Five laboratories participated in the cooperative effort. A summary sheet was forwarded to each facility outlining the objectives, special test conditions, test matrix, and special instructions for the performance of the test program.

The test matrix was designed to evaluate the Falex Ring on the basis of the following criteria:

- Differentiation between fuel types
- Repeatability across the running surface
- Repeatability from ring to ring
- Reproducibility from lot to lot
- Objectivity of wear scar interpretation

All necessary hardware was supplied to the participating independent laboratories by P&W and AFWAL/POSF. The required hardware included a mandrel fabricated by the Falex Corporation for use in mounting the Falex Ring to the standard BOCLE cylinder shaft, six Falex test rings (two each from three different lots), shims for BOCLE machine modification to enable leveling of the load arm and extension of hydraulic plunger, and 100 Falex test balls.

Two of the four fluid samples to be tested, Isopar M and an Isopar M + 30 ppm DCI-4A blend, were supplied by P&W. The remaining two test fluids, consisting of a petroleum based JP-4 and a shale derived CT JP-4, were supplied by AFWAL/POSF. The latter samples were test fluids which had been used in the December 1984 CRC BOCLE Task Force Round Robin. The samples had been in refrigerated storage since the completion of that program. The four test fuels were selected based on their range of wear scars, volatility extremes and availability of historical data generated using conventional BOCLE cylinders. All test fuels were evaluated in triplicate on each of the six Falex Rings.

2.5 TEST BALL INVESTIGATION

The final effort conducted under this task was an investigation of the effect of the test balls on BOCLE test results. This study focused on the dependence of wear scar size and repeatability on the source from which the ball was procured. A number of suppliers of 0.5 in., AISI 52100, Rc 64-66, Grade 25 EP ball bearings were contacted to determine the origin of the test balls traditionally used in conjunction with the BOCLE test apparatus.

SKF, a major distributor of ball bearings, advised that test balls acquired from SKF were manufactured both domestically and in Sweden. SKF manufactures their own ball bearings in Sweden. These are considered precision balls, and are produced under tight tolerances, with little or no variation from batch to batch. The balls are furnished with a Grade 5 to 10 EP polished finish, as opposed to the 25 EP standard equated with balls produced in the United States. Balls originating from SKF Sweden will always carry the designation "RB12.7" on the box in which they are packaged. The "12.7" part of the Swedish designation represents the diameter of the ball in millimeters.

Balls obtained domestically for distribution by SKF are procured from three different manufacturers and sold by SKF's Atlas Ball Division. Manufacturers which produce balls for Atlas include N.N. & Roller Co. of Erwin, New Jersey; Hoover Group, also of Erwin, New Jersey; and Winstead Precision Ball Co., located in Colebrook, Connecticut. Consequently, Atlas Balls would be expected to show slight batch to batch variations. The Falex Corporation, a major manufacturer of wear type equipment and supplier of

0.5 in. BOCLE balls, purchase their balls for resale from SKF's Atlas Ball Division. Another variety of ball, somewhat inaccurately referred to as "German Balls," although distributed in Germany, were found to be produced in SKF's plant in Sweden.

Test balls received from Falex, SKF Atlas, SKF Sweden, and Winstead were evaluated in BOCLE tests in four fuel types. The test fuels consisted of a petroleum based JP-4, JP-7, CT JP-4, and Isopar M + DCI-4A (BOCLE calibration/ reference fluid). Tests were performed in triplicate using the Falex Ring at a 500 g applied load.

SECTION 3.0

RESULTS AND DISCUSSION

3.1 REFERENCE FLUID SELECTION

Preliminary screening of n-paraffins, cycloparaffins, and hydrocarbon mixtures resulted in the elimination of the C6 through C12 n-paraffins and cycloparaffins from further consideration. In these preliminary tests, abrasive wear (scuffing) was exhibited which in most cases resulted in premature termination of the test. Four of the more promising candidate fluids, which produced acceptable wear scars, were selected for in-depth evaluations. Those candidates shown to merit further investigation included neat Isopar M, an Isopar M + 30 ppm DCI-4A additive blend, tetralin, and a mixture of 15 volume percent (vol %) tetralin in Isopar M.

Table 1 shows BOCLE test results for the four candidate reference fluids (CRF). Cylinders identified by a "J" prefix were of known poor quality. Those labeled with a prefix of "FV" were previously qualified at 0.30 ± 0.02 mm WSD and were determined to be acceptable P&W control cylinders.

TABLE 1
BOCLE DATA FOR CANDIDATE REFERENCE FLUIDS

<i>Candidate Fluid</i>	<i>Run No.</i>	Wear Scar Diameter, mm					
		<i>Cyl.</i> <i>J14</i>	<i>Cyl.</i> <i>J01</i>	<i>Cyl.</i> <i>J27</i>	<i>Cyl.</i> <i>FV5</i>	<i>Cyl.</i> <i>FV6</i>	<i>Cyl.</i> <i>FV7</i>
Isopar M/DCI-4A	1	0.595	0.420	0.520	0.305	0.270	0.340
	2	0.590	0.465	0.535	0.305	0.290	0.310
	3	0.550	0.455	0.510	0.275	0.295	0.325
	4	0.530	0.430	0.505	0.320	0.235	0.320
Tetralin	1	0.395	0.320	0.365	0.285	0.280	0.295
	2	0.365	0.335	0.375	0.275	0.275	0.280
	3	0.375	0.505	0.365	0.260	0.285	0.290
	4	0.440	0.325	0.420	0.325	0.285	0.290
85 % Vol Isopar M/ 15 Vol % Tetralin	1	0.690	0.600	0.675	0.690	0.560	0.665
	2	0.580	0.565	0.675	0.645	0.595	0.660
	3	0.705	0.555	0.700	0.665	0.590	0.655
	4	0.650	0.540	0.635	0.650	0.640	0.645
Isopar M	1	> 1.00	0.920	1.02	0.945	0.930	0.945
	2	0.865*	1.01	0.805	0.925	0.895	0.905
	3	0.875	0.935	0.925	0.930	0.910	0.935
	4	0.950	0.920	0.965	0.895	0.940	0.910

*Scuffed
Note: Cylinders prefixed by 'J' are of known poor quality
Cylinders prefixed by 'FV' are of proven good quality

3.1.1 Ability to Discern Cylinder Quality

As a method of assessing the data to determine which fluids were capable of differentiating between cylinders, the average WSD of the group of three good cylinders and the group of three bad cylinders were calculated for each fluid. These are shown in Table 2. As indicated, both tetralin and Isopar M + DCI-4A were able to differentiate between good cylinders and bad cylinders. Those fluids which were unable to discern between the cylinders, and as such, rated both groups similarly, included the 85/15 vol % Isopar M/tetralin blend and neat Isopar M. Similar results for individual cylinder ratings for the CRF are shown in Table 3. Table 3 summarizes the data generated during the BOCLE tests by providing the average and standard deviation of the four runs performed on each of the three good and three bad cylinders for each CRF.

TABLE 2
DIFFERENTIATION BETWEEN GROUPS OF CYLINDERS

<i>Candidate Fluid</i>	<i>Bad Cylinders</i> WSD		<i>Good Cylinders</i> WSD	
	Avg.	sd	Avg.	sd
Isopar M/DCI-4A	0.509	0.057	0.299	0.029
Tetralin	0.382	0.053	0.285	0.015
85/15 Vol % Isopar M/ Tetralin	0.631	0.060	0.638	0.037
Isopar M	0.936	0.068	0.922	0.018

3.1.2 Reproducibility of Candidate Fluid

In addition to the average WSD and standard deviation calculated for the CRF for each of the good and bad cylinders, Table 3 also shows the maximum spread in WSD for each of the test fluids. In this manner, the reproducibility from cylinder to cylinder of the candidate fluids can be assessed for good cylinders. Data scatter is anticipated on those cylinders which are of poor quality and as such cannot be used to assess the reproducibility of the CRF. Table 3 would indicate that tetralin and neat Isopar M, followed by Isopar M + DCI-4A, are the most reproducible CRF from cylinder to cylinder. Although neat Isopar M is shown to be a reproducible fluid by its minimal spread in WSD, the data shown in Table 2 suggest that it may not discriminate between cylinders of good and poor quality. The most objective evaluation of repeatability must consider primarily the "good" cylinders. The bad cylinders would be expected to show scatter. However, if very little or no spread is observed in the case of the bad cylinders by a CRF, then it is possible that the CRF is not sensitive to surface irregularities and variations in hardness. If a large spread is noted in the bad cylinders by a CRF, then the assumption can be made that the CRF is sensitive to differences across the cylinder surface.

3.1.3. Repeatability Across Running Surface

A review of standard deviations reported in Table 3 indicates that repeatability is good for all CRF on each of the three good cylinders. With the exception of Isopar M + DCI-4A, the repeatability of the fluids evaluated on poor cylinders declined dramatically. Since the scatter did not occur on the good cylinders, it is apparently not due to increasing fluid harshness. Isopar M + 30 ppm DCI-4A and technical grade tetralin were selected as the two most promising candidates for use as a standard BOCLE reference fluid. Selection was made on the basis of the best combination of cylinder differentiation, repeatability across the running surface, and reproducibility from cylinder to cylinder. Because tetralin is a known producer of peroxides, a short investigation was conducted to determine the effect of peroxides on lubricity.

TABLE 3
PRECISION OF CANDIDATE REFERENCE FLUIDS

<i>Candidate Fluid</i>		Bad Cylinders			
		Wear Scar Diameter, mm			
		<i>J14</i>	<i>J01</i>	<i>J27</i>	<i>Max. Δ</i>
Isopar M/DCI-4A	\bar{x}	0.566	0.443	0.518	0.123
	<i>sd</i>	0.031	0.021	0.013	
Tetralin	\bar{x}	0.394	0.371	0.381	0.023
	<i>sd</i>	0.033	0.089	0.026	
85/15 Vol % Isopar M/Tetralin	\bar{x}	0.656	0.565	0.671	0.106
	<i>sd</i>	0.056	0.025	0.027	
Isopar M	\bar{x}	0.922	0.946	0.924	0.024
	<i>sd</i>	0.064	0.043	0.085	

<i>Candidate Fluid</i>		Good Cylinders			
		Wear Scar Diameter, mm			
		<i>FV5</i>	<i>FV6</i>	<i>FV7</i>	<i>Max. Δ</i>
Isopar M/DCI-4A	\bar{x}	0.301	0.273	0.324	0.051
	<i>sd</i>	0.019	0.027	0.012	
Tetralin	\bar{x}	0.286	0.281	0.289	0.008
	<i>sd</i>	0.028	0.005	0.006	
85/15 Vol % Isopar M/Tetralin	\bar{x}	0.663	0.596	0.656	0.067
	<i>sd</i>	0.020	0.023	0.008	
Isopar M	\bar{x}	0.924	0.919	0.923	0.005
	<i>sd</i>	0.021	0.020	0.019	

* \bar{x} and *sd* based on 4 runs

5038C

Preliminary results showed that peroxides have a significant effect on fuel lubricity. A dramatic increase in WSD was observed when the peroxide content of a stressed reagent grade tetralin was lowered from 100 ppm to 40 ppm. Lowering the peroxide content from 40 ppm to less than 1 ppm, by percolating the tetralin through activated silica, had no significant affect on lubricity. Tetralin used during CRF testing was determined to contain 100 ppm peroxides. Typically, 40 to 50 ppm peroxide were measured from new, previously unopened, bottles and 100 ppm from opened bottles after minimal shelf storage. A BOCLE test was performed on tetralin containing peroxides below detectable levels to determine if peroxides were generated during testing. Samples taken after 15 minutes and after 30 minutes showed no peroxide formation. Based on the poor storage stability and unpredictable effects of peroxide formation, tetralin was rejected as a CRF. Isopar M + 30 ppm DCI-4A was selected as the recommended standard reference fluid and was used throughout the remainder of the program effort.

3.2 TEST CYLINDER SURFACE FINISH INVESTIGATION

The test cylinder investigation was directed at defining material hardness and surface finish specifications for standardizing BOCLE test cylinders. The effect of cylinder surface finish on data precision is discussed in the following paragraphs.

After one-third of the planned BOCLE tests had been completed, a number of anomalies were noted. Testing was temporarily suspended and the data critically reviewed. As shown in Table 4, the average

WSD for JP-7 closely approximated the WSD for the CT JP-4 sample on the J-A1 cylinder. Typically, there is good differentiation between these two fuel types, JP-7 being considerably less harsh than a CT fuel. Since this was not reflected in the measurements, the data were considered suspect. Significantly higher WSDs than expected were exhibited by both the reference fluid (Isopar M DCI-4A) and JP-4 on the 4 to 9 min. J-A1 cylinder. The nominal WSD indicative of these fluids is 0.30 to 0.33 mm. The WSD measured for the reference fluid was inconsistent with the WSD measured for JP-4 on the FV9 4 to 9 min. cylinder in that the reference fluid was formulated to approximate a high lubricity JP-4. Conflicting WSD were reported for all but the CT JP-4 sample when comparing the two sources of 4 to 9 min. cylinders. The source of the 4 to 9 min. cylinders appeared to be contributing more to variations in reproducibility than the surface finish.

TABLE 4
EFFECT OF CYLINDER SURFACE FINISH--PART I

Cyl No.	SF (μ in.)	Run No.	Wear Scar Diameter, mm			
			ISOPAR M			
			+DCI-4A	JP-4	JP-7	CT JP-4
J-A1	4-9*	1	0.465	0.550	0.855	0.860
		2	0.460	0.560	0.840	0.895
		3	0.475	0.650	0.840	0.800
		4	0.475	0.530	0.845	0.970
		\bar{x}	0.469	0.572	0.845	0.881
		sd	0.008	0.053	0.007	0.071
		Δ	0.015	0.120	0.015	0.170
J-F1	20-30*	1	0.525	0.645	0.805	0.885
		2	0.505	0.570	0.780	0.765
		3	0.490	0.580	0.800	0.885
		4	0.485	0.630	0.795	0.895
		\bar{x}	0.501	0.606	0.795	0.858
		sd	0.018	0.037	0.011	0.062
		Δ	0.040	0.075	0.025	0.130
FV9	4-9	1	0.290	0.405	0.555	0.835
		2	0.305	0.445	0.610	0.860
		3	0.295	0.390	0.575	0.940
		4	0.275	0.380	0.575	0.900
		\bar{x}	0.291	0.405	0.579	0.884
		sd	0.012	0.028	0.023	0.046
		Δ	0.030	0.065	0.055	0.105

All Fuels
Repeatability
(Avg. Spread)

		Cal Fluid	
		Δ	\bar{x}
J-A1	4-9	0.080	0.469
J-F1	20-30	0.068	0.501
FV9	4-9	0.064	0.291

*Note: Post test Profilometer traces showed surface finish of cylinders fabricated by J inconsistent with specification.

J-A1 = 18.5 μ in. J-F1 = 27 μ in.

5038C

The average data spread and the average standard deviation were calculated to assess the effect of both the source and the two different surface finishes on repeatability. This calculation is presented in Table 4 and is inclusive of all fuel types. This approach, in effect, gives insight into the average error that could be anticipated during a BOCLE test on any given fuel within the confines of those tested. The average potential error (Δ) is shown to be as great between the two different sources of the same surface finish, as it is between the two distinctive surface finishes evaluated. This is also true of the average WSD shown for the calibration fluid for each of the three cylinders. The difference in the average WSD for the calibration fluid is as great between the two different 4 to 9 min. cylinder sources as it is between the 4 to 9 min. and 20 to 30 min. finishes.

Surface finish and hardness measurements were performed on the above cylinders to verify that they had been fabricated to specification by the two different vendors. While cylinder hardness proved to be within specification limits, profilometer measurements indicated that the majority of the J manufactured cylinders failed to meet specification for surface finish. As shown in Table 5, only four were found to be within the specification limits. Surface finish varied from 11 to 40 min. on the remaining J cylinders fabricated to a 4 to 9 min. specification. The surface finishes of the FV cylinders, fabricated and ground to a 4 to 9 min. specification were also verified by profilometer measurements. All FV cylinders were found to be within specification limits.

TABLE 5
VERIFICATION OF CYLINDER SURFACE FINISH

Source:	FV	J	
Purchased			
Specification:	4-9 μ in.	4-9 μ in.	20-30 μ in.
	(Number of Cylinders)		
Surfanalyzer			
Ra* Results, μ in.			
1-10	10	0	
11-20		14	2
21-30		9	8
30-40		2	5

*Ra — Roughness Average
Average of 2 Ra values taken at 90 degrees

SONAC

The results of the profilometer measurements for each set of cylinders shown in Table 5 are based on an average of two readings across the cylinder surface. Two locations were measured, the second at a 90 degree rotation from the first. Twelve of the 40 J cylinders had a difference in Ra (roughness average) value of greater than 5 min. This indicates a significant difference in the surface finish around the cylinder. In contrast, the FV cylinders had a maximum difference of 2 min. (1 of the 10 cylinders), with 7 of the 10 cylinders having a difference of 1 min.

Based on these findings, the previously performed tests were considered invalid for the purpose of evaluating surface finish. They did demonstrate, however, the importance of vendor quality control. Testing was resumed and was restricted to assessing the effects of two different verified surface finishes on test repeatability. The second set of BOCLE tests which followed compared three FV fabricated

cylinders with verified surface finishes of 4 to 9 min. to that of three J fabricated cylinders with verified 16 to 22 min. surface finishes. The same test fluids were used as in the previous analyses. The results are shown in Table 6.

TABLE 6
EFFECT OF CYLINDER SURFACE FINISH--PART II

Wear Scar Diameter, mm							
Cyl No	SF (μ in)	Run No	ISOPAR M				
			+DCI 4A	JP-4	JP-7	CT JP-4	
FV22	4-9	1	0.235	0.470	0.530	1.03	
		2	0.245	0.420	0.600	0.840	
		3	0.275	0.475	0.595	0.960	
		4	0.270	0.460	0.575	0.935	
		\bar{x}	0.256	0.456	0.575	0.941	
		st	0.098	0.025	0.032	0.078	
		Δ	0.040	0.055	0.070	0.190	
FV23	4-9	1	0.285	0.610	0.835	0.905	
		2	0.300	0.470	0.675	1.010	
		3	0.340	0.445	0.590	0.980	
		4	0.315	0.510	0.675	0.945	
		\bar{x}	0.310	0.509	0.694	0.960	
		st	0.023	0.073	0.102	0.045	
		Δ	0.055	0.165	0.245	0.106	
FV25	4-9	1	0.335	0.525	0.825	1.050	
		2	0.315	0.490	0.740	0.830	
		3	0.325	0.495	0.750	0.995	
		4	0.265	0.505	0.760	0.940	
		\bar{x}	0.310	0.502	0.769	0.954	
		sd	0.031	0.016	0.038	0.094	
		Δ	0.070	0.035	0.085	0.220	
J-F2	16-22	1	0.600	0.755	0.805	0.970	
		2	0.560	0.835	0.800	0.880	
		3	0.525	0.645	0.775	0.865	
		4	0.445	0.680	0.785	0.950	
		\bar{x}	0.532	0.679	0.791	0.916	
		st	0.066	0.054	0.014	0.052	
		Δ	0.155	0.120	0.030	0.105	
J-F3	16-22	1	0.550	0.690	0.795	0.975	
		2	0.530	0.635	0.820	0.935	
		3	0.555	0.565	0.815	0.900	
		4	0.510	0.570	0.840	0.930	
		\bar{x}	0.536	0.615	0.818	0.935	
		st	0.021	0.059	0.018	0.031	
		Δ	0.045	0.120	0.045	0.075	
J-F5	16-22	1	0.510	0.600	0.765	0.930	
		2	0.480	0.595	0.750	0.940	
		3	0.465	0.585	0.800	0.990	
		4	0.465	0.560	0.815	0.975	
		\bar{x}	0.480	0.585	0.782	0.950	
		sd	0.021	0.018	0.030	0.028	
		Δ	0.045	0.040	0.065	0.060	
Repeatability (avg. spread)			Reproducibility between 3 cylinders (Max Δ between avg. cylinder value)				
Δ sd							
All Fuels			Cal Fl	JP-4	JP-7	CT JP-4	\bar{x} Max Δ
FV	4-9	0.111 0.048	0.054	0.053	0.194	0.013	0.078
J	16-22	0.075 0.034	0.056	0.094	0.036	0.043	0.057

1018C

To summarize and provide an overview of the test data, such that a quick comparison of the two surface finishes could be made, average spread and maximum differences between average cylinder WSD were calculated for each fuel type. Average spread was determined by averaging the deltas (highest WSD - lowest WSD) from each of the four BOCLE runs performed on each fuel for each of the three 4 to 9 min. cylinders. This average spread was then compared to that calculated for the 16 to 22 min. cylinders. This summary is shown at the bottom of Table 6. Average spread was used as a means of assessing repeatability across the running surface of the test cylinders. The maximum difference between the average cylinder WSD was used to evaluate reproducibility between cylinders of the same surface finish. Although the test results indicated that the 4 to 9 min. FV cylinders were somewhat superior to that of the 16 to 22 min. J cylinders, the desired precision was not achieved by either surface finish. The overall repeatability of this series of tests was, in fact, worse than the preceding series of tests whereby the surface finish specifications had not been met. The data was, therefore, once more considered inconclusive.

A tighter controlled test plan was devised in an effort to eliminate any unknown variables which may have contributed to the data scatter encountered in the former series of BOCLE tests. In the subsequent third set of tests, two FV 4 to 9 min. cylinders were compared to two J 16 to 22 min. cylinders. In contrast to the former surface finish evaluations, the same operator performed all test runs. Periods of interruption in the completion of the test matrix were minimized. All runs were restricted to a single BOCLE unit, whereas previous testing had been conducted simultaneously on two separate InterAv BOCLE units. Spacing of run tracks was also a concern. The previous series of tests were characterized by relatively close spacing (0.5 mm) between run tracks on the test cylinder. There was some concern that localized heating and surface deformation caused by a previous run may have some effect on a succeeding run. The follow-up series of tests used 0.75 mm spacing between tracks. These tests were performed in triplicate using three of the four original test fluids. The results of this third series of tests are shown in Table 7.

Repeatability was again related to the average spread observed inclusive of all fuels. In a similar manner, reproducibility from cylinder to cylinder was related to the maximum difference calculated between average cylinder WSD. Table 7 shows that there was some improvement in repeatability of the 4 to 9 min. cylinders based on the average spread. Reproducibility also showed improvement. However, in this case only two cylinders of each surface finish were evaluated which inherently biases comparison. The conclusions afforded by the test results were disappointing in that the desired repeatability required for selection of an optimum surface finish still had not been achieved.

3.3 FALEX RING INVESTIGATION

A comprehensive investigation of the Falex Ring resulted from the inability to identify an optimum surface finish or a source for reliable repeatable conventional BOCLE test cylinders. The results of this investigation are discussed in the following paragraphs.

Table 8 shows data generated in a preliminary investigation of the Falex Ring. The purpose of this preliminary investigation was to determine the merit of conducting a full-scale evaluation of the Falex Ring as a potential candidate for replacing the conventional test cylinder. As shown in Table 8, the test data were very promising. Repeatability across the running surface was excellent. Little variation from ring to ring was observed for the three rings tested. The desired differentiation between fuel types was apparent and the size of the wear scar exhibited little influence on data scatter.

TABLE 7
EFFECT OF CYLINDER SURFACE FINISH--PART III

			Wear Scar Diameter, mm					
Cyl No.	SF (μ in.)	Run No.	Isopar M					
			DCI-4A	JP-4	JP-7			
FV25	4-9	1	0.315	0.495	0.595			
		2	0.355	0.470	0.670			
		3	0.320	0.460	0.665			
		\bar{x}	0.330	0.475	0.643			
		st	0.022	0.018	0.042			
		Δ	0.040	0.035	0.075			
FV13	4-9	1	0.330	0.570	0.720			
		2	0.295	0.460	0.730			
		3	0.310	0.415	0.620			
		\bar{x}	0.312	0.480	0.690			
		st	0.018	0.082	0.061			
		Δ	0.035	0.160	0.110			
J-F2	16-22	1	0.460	0.625	0.800			
		2	0.470	0.680	0.785			
		3	0.455	0.670	0.760			
		\bar{x}	0.462	0.658	0.782			
		sd	0.008	0.029	0.020			
		Δ	0.015	0.055	0.040			
J-F3	16-22	1	0.440	0.505	0.785			
		2	0.465	0.855	0.775			
		3	0.450	0.485	0.820			
		\bar{x}	0.452	0.615	0.793			
		st	0.013	0.208	0.024			
		Δ	0.025	0.370	0.045			
			Repeatability (avg. spread)			Reproducibility between 2 cylinders (Max. Δ between avg. cylinder value)		
			Δ sd					
			All Fuels	Cal Fluid	JP-4	JP-7		
FV	4-9	0.078 0.041	0.018	0.005	0.047			
J	16-22	0.092 0.050	0.010	0.043	0.011			

3038C

The wear scar generated on the Falex Ring was found to be well-defined. Measurement of the wear scar was considerably less subjective than that of the conventional BOCLE cylinder. Figure 2 illustrates the irregular and jagged wear scars produced by the conventional cylinders for three typical jet fuels. Unlike these ill-defined scars, the Falex Ring scars were well-defined, symmetrical ellipses. Harsh fluids, which in the past were found to be nonreproducible as a result of the scatter induced by large wear scars, were found to show excellent repeatability. Based on these preliminary results, it was concluded that the Falex Ring appeared to enhance test precision and merited a full-scale investigation.

TABLE 8
PRELIMINARY FALEX RING EVALUATION

Ring No.	Run No.	Wear Scar Diameter, mm				
		JP-7 Tank 2	Isopar M DCI-4A	JP-4 Tank 1	CT JP-4	JP-8 WPAFB
3	1	0.680	0.520	0.545	0.935	0.550
	2	0.680	0.515	0.550	0.905	0.560
	3	0.685	0.520	0.545	0.880	0.540
	\bar{x}	0.682	0.518	0.547	0.907	0.550
	sd	0.003	0.003	0.003	0.028	0.010
	Δ	0.005	0.005	0.005	0.055	0.020
4	1	0.680	0.520	0.565	0.905	0.560
	2	0.685	0.530	0.555	0.915	0.555
	3	0.685	0.505	0.550	0.895	0.555
	\bar{x}	0.683	0.518	0.557	0.905	0.557
	sd	0.003	0.013	0.008	0.010	0.003
	Δ	0.005	0.025	0.015	0.020	0.005
5	1	0.680	0.515	0.565	0.935	0.560
	2	0.675	0.510	0.565	0.945	0.555
	3	0.680	0.510	0.550	0.930	0.545
	\bar{x}	0.678	0.512	0.560	0.937	0.553
	sd	0.003	0.003	0.009	0.008	0.008
	Δ	0.005	0.005	0.015	0.015	0.015
Repeatability (avg. spread)		Reproducibility between 3 rings (Max. Δ between avg. ring value)				
Δ	sd					
All Fuels		JP-7	Cal Fluid	JP-4	CT JP-4	JP-8
0.014	0.009	0.005	0.006	0.013	0.032	0.007

Applied Load — 500 g

Falex Ring Specification

Material: SAE 8720

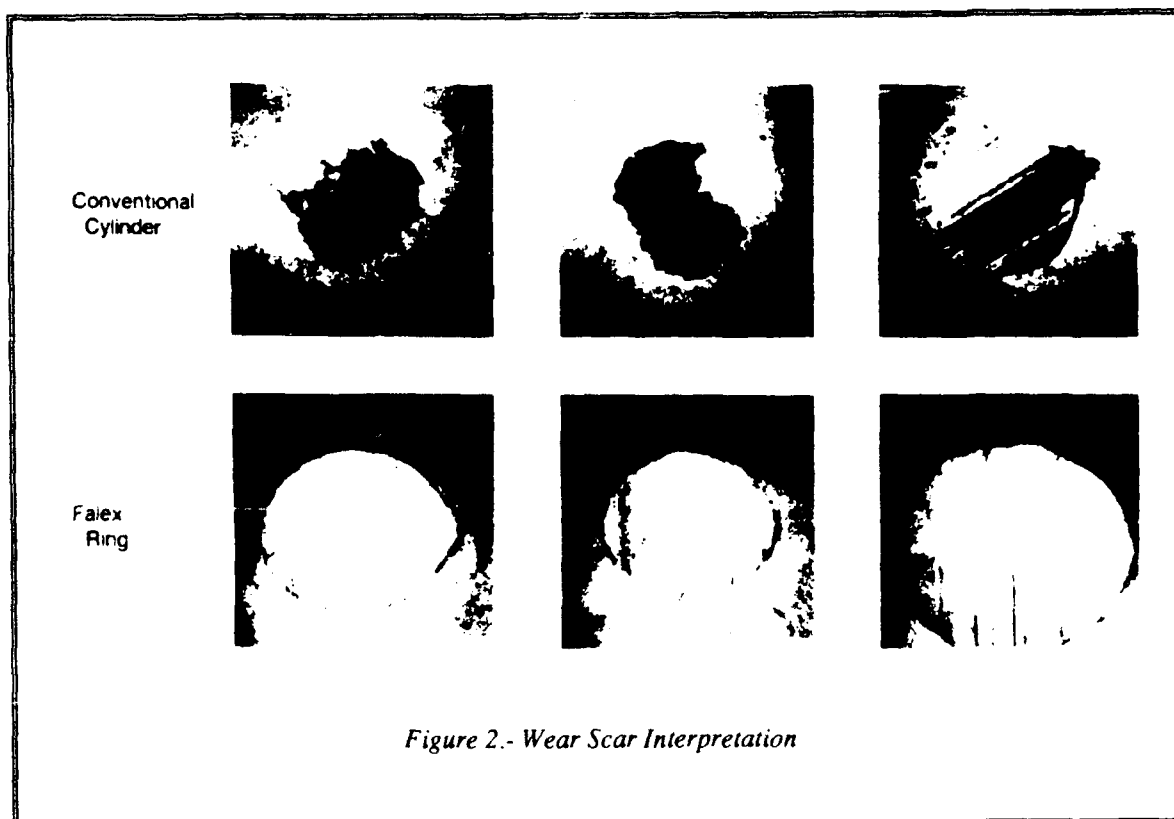
Hardness: 58-62 Rc

Surface Finish: 20-30 μ in.

5038C

Table 9 lists the data from BOCLE tests performed on four different production lots of Falex Rings. The data summarized at the bottom of Table 9 present an assessment of the Falex Ring in terms of both repeatability and reproducibility between material lots. The data generated exhibited excellent repeatability across the running surface of any given test ring, within any given lot, for all fuel types tested. The loss of repeatability and introduction of data scatter with increasing fuel harshness, as typically experienced with conventional BOCLE cylinders, was not exhibited by the Falex Ring.

The Falex Ring also exhibited excellent lot to lot reproducibility. Figure 3 illustrates the minimal variation in Falex lots. In this plot, the average WSD for each lot is shown as a function of fuel type. The average WSD for the four lots differed by a maximum of only 0.006 to 0.020 mm for the four high-to-intermediate lubricity level fluids. The maximum variation between averages of the four lots was only 0.028 mm for the harshest of the test fluids (CT JP-4). Small standard deviations, calculated for all runs performed on each test fluid, indicate a very close grouping about the means.



Based on the average WSD for the 36 runs made on each of the test fluids, the fluids shown in Table 9 were grouped in order of descending lubricity levels. The relative ranking of the fluids in terms of decreasing fuel lubricity (increasing WSD) were as follows: Isopar M + 30 ppm DCI-4A (0.504) > JP-4 (0.552) / JP-8 (0.556) > JP-7 (0.684) > CT JP-4 (0.917). Discrimination between JP-4 and JP-8 was not obvious. WSD differed by only 0.006 mm, which is well within the repeatability of the test. There is no data bank currently available which characterizes the lubricity properties of JP-8. However, the data bank generated for the remaining test fluids indicates that the Falex Ring provides good differentiation between fuel types of known lubricity levels.

As a cursory check on quality control, six Falex Rings were analyzed to confirm that specification limits had been met during production. Surface finishes and hardness all fell within a tight tolerance band conforming to specification.

3.4 INTERLABORATORY EVALUATION OF THE FALEX RING

Results from the five laboratories completing the Falex Ring Round Robin are shown in Tables 10 through 13. One laboratory, due to a shortage in available manpower, was able to evaluate only one ring per material lot for each of the three different lots. The remaining laboratories evaluated two rings from each lot. The mean, standard deviation, and range are shown, as a function of fuel type, for each laboratory. This serves to provide a cursory assessment of repeatability and reproducibility among laboratories.

TABLE 9
REPRODUCIBILITY BETWEEN FALEX LOTS

Ring No.	Run No.	Wear Scar Diameter, mm				
		Isopar M +DCI-4A	JP-4	JP-8	JP-7	CT JP-4
K-1	1	0.490	0.525	0.535	0.670	0.885
	2	0.475	0.523	0.535	0.665	0.905
	3	0.470	0.530	0.540	0.675	0.910
	\bar{x}	0.478	0.527	0.537	0.670	0.900
	sd	0.010	0.003	0.003	0.005	0.013
	max. Δ	0.020	0.005	0.005	0.010	0.025
K-2	1	0.500	0.540	0.555	0.675	0.890
	2	0.505	0.550	0.555	0.695	0.895
	3	0.510	0.555	0.550	0.695	0.930
	\bar{x}	0.505	0.548	0.553	0.688	0.905
	sd	0.005	0.008	0.003	0.012	0.022
	max. Δ	0.010	0.015	0.005	0.020	0.040
K-3	1	0.485	0.565	0.545	0.680	0.910
	2	0.510	0.570	0.575	0.695	0.920
	3	0.515	0.565	0.570	0.695	0.900
	\bar{x}	0.503	0.567	0.563	0.690	0.910
	sd	0.016	0.003	0.016	0.009	0.010
	max. Δ	0.030	0.005	0.030	0.015	0.020
L-1	1	0.510	0.550	0.555	0.670	0.895
	2	0.485	0.550	0.545	0.675	0.910
	3	0.505	0.555	0.565	0.665	0.920
	\bar{x}	0.500	0.552	0.555	0.670	0.908
	sd	0.013	0.003	0.010	0.005	0.013
	max. Δ	0.025	0.005	0.020	0.010	0.025
L-2	1	0.500	0.540	0.555	0.680	0.900
	2	0.500	0.560	0.565	0.700	0.900
	3	0.490	0.560	0.555	0.690	0.930
	\bar{x}	0.497	0.553	0.558	0.690	0.910
	sd	0.006	0.012	0.006	0.010	0.017
	max. Δ	0.010	0.020	0.010	0.020	0.030
L-3	1	0.500	0.540	0.565	0.685	0.925
	2	0.495	0.550	0.565	0.710	0.910
	3	0.505	0.550	0.565	0.690	0.930
	\bar{x}	0.500	0.547	0.565	0.695	0.922
	sd	0.005	0.006	0.000	0.013	0.010
	max. Δ	0.010	0.010	0.000	0.025	0.020
M-1	1	0.525	0.550	0.545	0.680	0.915
	2	0.480	0.555	0.580	0.680	0.905
	3	0.505	0.545	0.550	0.670	0.905
	\bar{x}	0.503	0.550	0.558	0.677	0.908
	sd	0.023	0.005	0.019	0.006	0.006
	max. Δ	0.045	0.010	0.035	0.010	0.010
M-2	1	0.500	0.555	0.550	0.675	0.925
	2	0.530	0.580	0.555	0.690	0.950
	3	0.520	0.565	0.560	0.690	0.935
	\bar{x}	0.517	0.567	0.555	0.685	0.937
	sd	0.015	0.013	0.005	0.009	0.013
	max. Δ	0.030	0.025	0.010	0.015	0.025

TABLE 9
REPRODUCIBILITY BETWEEN FALEX LOTS (CONTINUED)

Ring No.	Run No.	Wear Scar Diameter, mm				
		Isopar M +DCI-4A	JP-4	JP-8	JP-7	CT JP-4
M-3	1	0.500	0.555	0.580	0.695	0.945
	2	0.490	0.545	0.550	0.695	0.980
	3	0.505	0.555	0.565	0.705	0.935
	\bar{x}	0.498	0.552	0.565	0.698	0.953
	sd	0.008	0.006	0.015	0.006	0.024
	max. Δ	0.015	0.010	0.030	0.010	0.045
MX-3	1	0.520	0.545	0.550	0.680	0.935
	2	0.515	0.550	0.560	0.680	0.905
	3	0.520	0.545	0.540	0.685	0.880
	\bar{x}	0.518	0.547	0.550	0.682	0.907
	sd	0.003	0.003	0.010	0.003	0.028
	max. Δ	0.005	0.005	0.020	0.005	0.055
MX-4	1	0.520	0.565	0.560	0.680	0.905
	2	0.530	0.555	0.555	0.685	0.915
	3	0.505	0.550	0.555	0.685	0.895
	\bar{x}	0.518	0.557	0.557	0.683	0.905
	sd	0.013	0.008	0.003	0.003	0.010
	max. Δ	0.025	0.015	0.005	0.005	0.020
MX-5	1	0.515	0.565	0.560	0.680	0.935
	2	0.510	0.565	0.555	0.675	0.945
	3	0.510	0.550	0.545	0.680	0.930
	\bar{x}	0.512	0.560	0.553	0.678	0.937
	sd	0.003	0.009	0.008	0.003	0.008
	max. Δ	0.005	0.015	0.015	0.005	0.015
Lot avg.						
K		0.496	0.547	0.551	0.683	0.905
L		0.499	0.551	0.559	0.685	0.913
M		0.506	0.556	0.559	0.687	0.933
MX		0.516	0.553	0.553	0.681	0.916
All runs \bar{x}		0.504	0.552	0.556	0.684	0.917
All runs sd		0.015	0.012	0.011	0.011	0.021
Lot-Lot max. Δ *		0.020	0.009	0.008	0.006	0.028

* Calculated on average value for each lot.

Summary of Test Matrix

No. of lots evaluated: 4
 No. of rings/lot: 3
 No. of fuel samples: 5
 No. of runs/fuel sample: 36
 No. of total runs: 180

Special Test Conditions

Applied load: 500 g

Falex Ring Specification

Material: SAE 8720
 Hardness: 58-62 Rc
 Surface finish: 20-30 μ in.

5038C

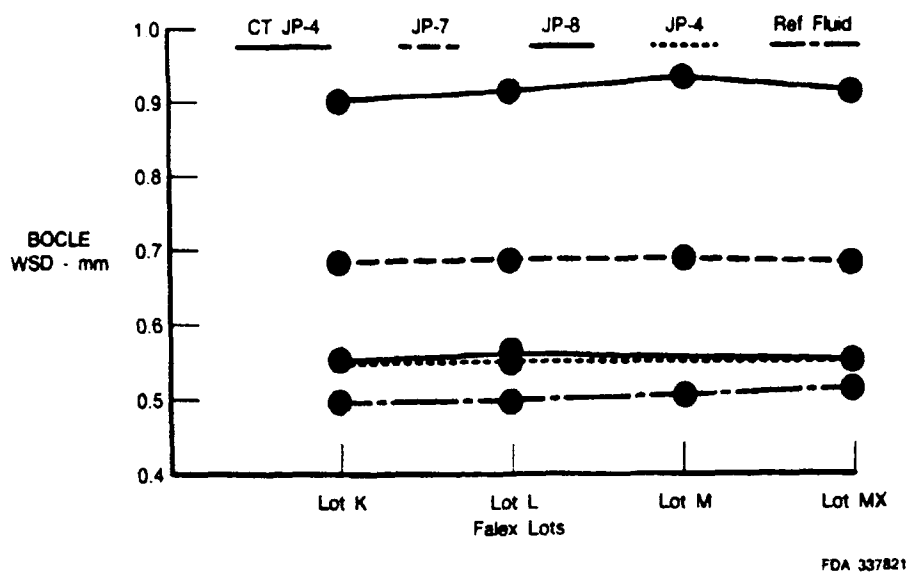


Figure 3. — Variation in Falex Lots

TABLE 10.
FALEX RING ROUND ROBIN RESULTS FOR ISOPAR M +30 PPM DCI-4A

Lot Desig.	Ring No.	Run No.	Pratt & Whitney	Woodward Governor	Chevron	Rolls Royce	WPAFB
K	1	1	0.510	0.510	0.510	0.496	0.500
		2	0.485	0.520	0.510	0.510	0.505
		3	0.485	0.520	0.530	0.507	0.505
	2	1	0.490	0.520		0.504	0.500
		2	0.495	0.530		0.481	0.510
		3	0.490	0.530		0.511	0.520
KX	1	1	0.500	0.530	0.510	0.499	0.510
		2	0.510	0.540	0.500	0.506	0.530
		3	0.520	0.520	0.520	0.488	0.510
	2	1	0.490	0.510		0.479	0.525
		2	0.506	0.510		0.501	0.490
		3	0.515	0.520		0.473	0.515
L	1	1	0.475	0.530	0.510	0.476	0.530
		2	0.485	0.530	0.520	0.500	0.510
		3	0.485	0.540	0.540	0.515	0.525
	2	1	0.520	0.530		0.477	0.515
		2	0.525	0.540		0.521	0.490
		3	0.515	0.520		0.501	0.525
Mean			0.500	0.525	0.517	0.497	0.512
Standard Deviation			0.015	0.010	0.012	0.015	0.012
Range			0.050	0.030	0.040	0.048	0.040

3098C

TABLE 11

FALEX RING ROUND ROBIN RESULTS FOR JP-4

Lot Design	Ring No	Run No.	Pratt & Whitney	Woodward Governor	Chevron	Rolls Royce	WPAFB
K	1	1	0.585	0.570	0.590	0.586	0.585
		2	0.565	0.570	0.580	0.595	0.560
		3	0.565	0.580	0.570	0.597	0.555
	2	1	0.560	0.570		0.564	0.560
		2	0.575	0.570		0.568	0.570
		3	0.570	0.570		0.585	0.575
KX	1	1	0.555	0.600	0.580	0.616	0.575
		2	0.565	0.580	0.570	0.553	0.565
		3	0.555	0.600	0.590	0.593	0.560
	2	1	0.575	0.590		0.580	0.540
		2	0.560	0.590		0.570	0.565
		3	0.560	0.590		0.588	0.555
L	1	1	0.545	0.590	0.590	0.582	0.585
		2	0.555	0.580	0.580	0.577	0.565
		3	0.565	0.570	0.580	0.561	0.565
	2	1	0.570	0.570		0.584	0.570
		2	0.570	0.580		0.567	0.555
		3	0.575	0.580		0.581	0.575
Mean			0.564	0.581	0.581	0.580	0.564
Standard Deviation			0.008	0.011	0.008	0.015	0.010
Range			0.030	0.030	0.020	0.063	0.045

8028C

TABLE 12

FALEX RING ROUND ROBIN RESULTS FOR ISOPAR M

Lot Desig	Ring No.	Run No.	Pratt & Whitney	Woodward Governor	Chevron	Rolls Royce	WPAFB
K	1	1	0.840	0.840	0.820	0.804	0.790
		2	0.820	0.860	0.800	0.824	0.805
		3	0.845	0.850	0.820	0.808	0.820
	2	1	0.825	0.830		0.827	0.790
		2	0.835	0.840		0.823	0.825
		3	0.830	0.830		0.814	0.795
KX	1	1	0.860	0.840	0.800	0.862	0.820
		2	0.840	0.860	0.800	0.803	0.810
		3	0.845	0.860	0.810	0.855	0.790
	2	1	0.850	0.840		0.829	0.795
		2	0.845	0.840		0.800	0.810
		3	0.840	0.840		0.833	0.830
L	1	1	0.840	0.840	0.830	0.826	0.815
		2	0.855	0.850	0.820	0.812	0.790
		3	0.855	0.850	0.820	0.824	0.795
	2	1	0.810	0.850		0.812	0.800
		2	0.810	0.850		0.817	0.820
		3	0.830	0.860		0.820	0.790
Mean			0.838	0.846	0.813	0.822	0.805
Standard Deviation			0.014	0.010	0.011	0.016	0.014
Range			0.050	0.030	0.030	0.062	0.040

8028C

TABLE 13
FALEX RING ROUND ROBIN RESULTS FOR CLAY TREATED SHALE JP-4

<i>Lot Desig.</i>	<i>Ring No.</i>	<i>Run No.</i>	<i>Pratt & Whitney</i>	<i>Woodward Governor</i>	<i>Chevron</i>	<i>Rolls Royce</i>	<i>WPAFB</i>
K	1	1	0.855	0.900	0.930	0.777	0.800
		2	0.855	0.910	0.900	0.815	0.795
		3	0.835	0.920	0.890	0.847	0.785
	2	1	0.865	0.930		0.844	0.740
		2	0.835	0.910		0.823	0.790
		3	0.825	0.930		0.773	0.775
KX	1	1	0.860	0.920		0.844	0.775
		2	0.830	0.890	0.880	0.815	0.765
		3	0.825	0.920	0.880	0.851	0.760
	2	1	0.870	0.930		0.833	0.740
		2	0.850	0.920		0.854	0.735
		3	0.845	0.910		0.839	0.745
L	1	1	0.855	0.920	0.930	0.819	0.730
		2	0.845	0.910	0.860	0.810	0.715
		3	0.845	0.920	0.940	0.840	0.710
	2	1	0.820	0.900		0.822	0.760
		2	0.830	0.910		0.812	0.760
		3	0.830	0.910		0.856	0.750
Mean			0.843	0.914	0.901	0.826	0.757
Standard Deviation			0.015	0.011	0.029	0.024	0.026
Range			0.050	0.040	0.080	0.083	0.090

5038C

A statistical analysis was performed on the raw test data using a Statistical Analysis System (SAS) computer software package and the general linear models procedure. The procedure used in the statistical analysis was as outlined in the "Manual On Determining Precision Data for ASTM Methods on Petroleum Products and Lubricants (RR-D-2-1007)." Statistically, a model was designed to assess the effect of the Falex Ring on test method precision. The model considered all effects (independent variables) encountered in the performance of the interlaboratory round robin. Construction of the model considered primary effects (labs, fuels, lots, rings) and indirect effects or interactions (lab*fuel, lab*lot, etc.).

Therefore,

Falex Ring Lubricity Model Primary Effects + Interactions

- Labs + Lots + (Lab*Lot) + Rings + (Lab*Ring) + Fuels + (Lab*Fuel)
+ (Lot*Fuel) + (Ring*Fuel) + (Lab*Lot*Fuel) + (Lab*Ring*Fuel)

The general linear models procedure was used to determine deviations from the model. This process is based on laboratory observations and model-predicted values. From these deviations, differences in the levels of the effects (both primary and interactions) were analyzed. Null and alternative hypotheses were formulated to evaluate the performance of the Falex Ring. Probability testing involved comparison by

SAS of a calculated F value to that of a critical F value. If the probability of observing the calculated F value was small, or F itself was large, then the null hypothesis was rejected. It was, therefore, concluded that a statistically significant difference existed to support the alternative hypothesis. Conclusions, based on statistical analysis of the raw data, are discussed in the following paragraphs.

There appeared to be no significant difference between Falex Ring material lots, nor any interactions between lot and other independent variables. Since all lot effects and interactions appeared to have no significant contribution to the model, all lots were considered identical, and the lot effect and lot interaction terms were dropped from the model. The model, consequently, was reduced to:

$$\text{Falex Ring Lubricity Model} = \text{Labs} + \text{Rings} + (\text{Lab} * \text{Ring}) + \text{Fuels} + (\text{Lab} * \text{Fuel}) \\ + (\text{Ring} * \text{Fuel}) + (\text{Lab} * \text{Ring} * \text{Fuel})$$

From the reduced model, an analysis of variance using the general linear models procedure in SAS was performed. Based on this test, it was concluded that: (1) there was a statistically significant difference in the four fuels as measured by the Falex Ring, (2) there was a significant difference between at least two laboratories measuring the CT JP-4 sample, and (3) there was no apparent difference in rings from ring to ring.

The aforementioned statistical tests were directed at the primary effects influencing the Falex Ring Lubricity Model. Interaction terms were evaluated similarly and were concluded to be insignificant. Hence, secondary effects involving interactions between rings and fuels and between rings and laboratories were also eliminated from the equation. Since there was shown to be no significant difference in rings, the ring term was eliminated from the Falex model along with the ring interaction terms. As a consequence, the model was reduced to:

$$\text{Falex Ring Lubricity Model} = \text{Labs} + \text{Fuels} + (\text{Lab} * \text{Fuel})$$

Examination of data dispersion showed that CT JP-4 occurred at three distinct levels, as opposed to one unique level. As a result of this inconsistency, the entire statistical analysis was repeated considering only the three remaining fuel types. The F values for tests which yielded significant F values previously, were still significant after removal of the CT JP-4 data. Therefore, after elimination of the CT JP-4 data, the previous conclusions were unchanged.

A further analysis was performed to provide additional information on the effect of fuel type on reproducibility of data between laboratories. In this analysis, the mean WSD was determined for all runs as a function of fuel type, rings, and lots for each laboratory. The mean WSD as shown in Tables 10 through 13 for each laboratory were used in calculating the interlaboratory range for specific fuel types. This range was used to determine if there was an interaction between laboratory and fuel type. It was already determined statistically that an interaction between laboratory and fuel type was apparent with the CT JP-4 sample. This was supported by concern voiced by the supplier of the CT sample during the course of the round robin. Because the five CT samples were drawn from the bottom of a 55- gallon drum on different days over a period of 4 to 6 weeks, there was considerable doubt that the samples had identical compositions. Based on the range of WSD exhibited by the remaining fuels, little interaction between fuel type and laboratory were noted. Differences in average values for fuel types between all laboratories were as follows: Isopar M + DCI-4A, 0.028; JP-4, 0.017; neat Isopar M, 0.041; and CT JP-4, 0.157.

Elimination of the CT sample data, and a determination that an interlaboratory range of up to 0.041 was acceptable, would further reduce the practical model to:

$$\text{Falex Ring Lubricity Model} = \text{Fuel}$$

The statistical model, therefore, indicates that in theory, the Falex Ring measurement is a direct function of fuel lubricity.

A precision statement was calculated using the equations set forth for repeatability and reproducibility in "Manual On Determining Precision Data For ASTM Methods On Petroleum Products and Lubricants (RR D-2-1007)." The procedure consists of estimating variance components from a two-way analysis of variance. It is performed with regard for substitutions made for missing or outlying values. These components are then combined to provide estimates of repeatability and reproducibility variances. These terms provide a measure from which no two successive data points should differ within a laboratory, in the case of repeatability, or between laboratories when referencing reproducibility.

For lubricity measurements inclusive of all fuel types:

Repeatability, $r = 0.042$

Reproducibility, $R = 0.262$

For lubricity measurements excluding the CT JP-4 sample:

Repeatability, $r = 0.035$

Reproducibility, $R = 0.108$

3.5 FALEX RING LUBRICITY VALUES FOR TYPICAL JET FUELS

Commencing with the preliminary investigation and maintained throughout the remainder of this test program, all incoming fuel samples to the P&W facilities were monitored using the Falex Ring. Fuel samples were obtained from on-going engine tests and weekly sampling of on-site fuel storage tanks, and from a number of fuels of varying origin and types from foreign and domestic air bases. These data were used to initiate a data base for establishing Falex Ring lubricity values for typical jet fuels. This limited data bank also encompasses the data generated during the mini-round robin and is considered representative of expected values. Nominal WSD and those WSD which are speculated to be marginal for typical jet fuels are shown in Table 14 and Figure 4.

TABLE 14
FALEX RING LUBRICITY VALUES FOR TYPICAL JET FUELS

<i>Fuel Type</i>	<i>Nominal WSD, mm</i>	<i>Marginal WSD, mm</i>
JP-4	0.550	0.600
JP-5	0.510	0.600
JP-7	0.690	0.740
Jet A	0.510	0.600
*JP-8	0.560	0.600
CT JP-4	0.920	

Calibrating Fluid: Isopar M +30 ppm DCI-4A
Falex Ring Deemed Acceptable With a Generated WSD of
0.500 \pm 0.020 mm.

*JP-8 Nominal WSD values based on limited data

5038C

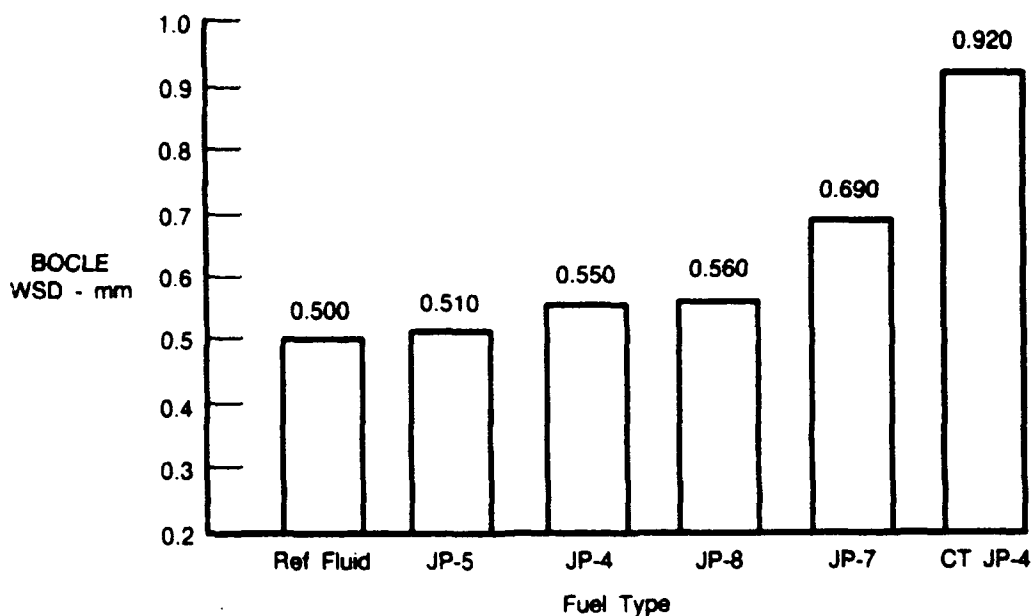


Figure 4. -- Nominal Falex Ring Lubricity Values for Typical Jet Fuels

3.6 TEST BALL INVESTIGATION

The data in Table 15 show the influence that the source of the test ball can have on the size and repeatability of the BOCLE wear scar. BOCLE tests indicated that: (1) the Winstead ball was unable to differentiate between JP-4 and JP-7, and only marginally between JP-7 and the Isopar M / DCI-4A reference fluid; (2) the Winstead ball consistently produced lower WSD for all fluids; (3) the Falex, Atlas, and Swedish balls produced essentially the same average WSD for each specific fuel type; and (4) the ball source had no measurable effect on repeatability. Table 16 compares the composition of the SKF Swedish and SKF domestically produced 0.5 inch O.D. test balls.

The test results show that the source of the test ball can have a significant effect on the data generated during BOCLE operation. Material lots can vary as a consequence of the three different suppliers of balls to the Atlas Division of SKF. The balls produced by Winstead Precision Ball Co., one of the three potential Atlas suppliers, were shown to produce WSD inconsistent with those of the other two SKF suppliers.

TABLE 15
TEST BALL SOURCE EVALUATION

<i>Fuel Type</i>	<i>Run No.</i>	<i>Wear Scar Diameter, mm</i>			
		<i>Falex</i>	<i>Atlas</i>	<i>Swedish</i>	<i>Winstead</i>
JP-4	1	0.560	0.560	0.560	0.445
	2	0.565	0.545	0.550	0.435
	3	0.560	0.570	0.535	0.460
	\bar{x}	0.562	0.558	0.548	0.447
	sd	0.003	0.013	0.013	0.013
JP-7	1	0.690	0.675	0.685	0.440
	2	0.695	0.690	0.675	0.460
	3	0.695	0.690	0.690	0.450
	\bar{x}	0.693	0.685	0.683	0.450
	sd	0.003	0.009	0.008	0.010
CT JP-4	1	0.905	0.900	0.925	0.700
	2	0.950	0.925	0.915	0.725
	3	0.910	0.905	0.920	0.705
	\bar{x}	0.922	0.910	0.920	0.710
	sd	0.025	0.013	0.005	0.013
Isopar M/DCI-4A	1	0.510	0.510	0.505	0.375
	2	0.500	0.510	0.500	0.415
	3	0.510	0.510	0.445*	0.385
	\bar{x}	0.507	0.510	0.483	0.392
	sd	0.006	0.000	0.033	0.021

Note: (1) All BOCLE runs performed using Falex Ring.
 (2) Winstead balls consistently lower WSD values.
 (3) Winstead balls could not differentiate between JP-4 and JP-7.

*Run suspect

5038C

TABLE 16
SKF TEST BALL COMPOSITION

	<i>SKF (Swedish)*</i>	<i>SKF (U.S.)**</i>
Carbon	0.92 — 1.02	0.95 — 1.10
Manganese	0.95 — 1.25	0.25 — 0.45
Silicon	0.50 — 0.70	0.20 — 0.30
Chromium	0.90 — 1.15	1.30 — 1.60

*% Composition obtained from SKF R&D (U.S.)

**% Composition obtained from Handbook
 MIL-H1-2 and verified by SKF R&D (U.S.)

5038C

SECTION 4.0

CONCLUSIONS AND RECOMMENDATIONS

The Falex Ring was shown to significantly enhance BOCLE test precision. Concurrent studies conducted by Rolls Royce, Ltd. in the United Kingdom also produced superior test results. Statistical analysis, performed on data generated by a five member interlaboratory round robin, confirmed a marked improvement in test method repeatability and reproducibility over that realized by the conventional AMS 6444 BOCLE cylinder.

A source for a reliable reproducible AMS 6444 cylinder, yielding the desired precision, does not appear obtainable despite vast effort and expenditure on the part of the lubricity community. It is, therefore, recommended that the CRC be urged to further evaluate the Falex Ring as an alternative to the AMS 6444 material. Advantages for incorporating the Falex Ring into the BOCLE test procedure as the standard test specimen include: definitive, less subjective interpretation of the wear scar; enhanced test precision; and availability at a low cost.

It was shown that the source of the test ball can have a significant effect on BOCLE test results. Most distributors of balls represent a composite of manufacturing sources which is not conducive to the goal of standardization of the lubricity test method. SKF precision balls produced in Sweden are manufactured under tight tolerances exhibiting little or no variation from batch to batch. It is recommended that SKF Swedish 12.7 mm (0.5 in.) ball bearings be incorporated into the standard test method. Standardization of all critical test parts and operating parameters is essential in eliminating extraneous variables suspected, or known, to affect test repeatability or reproducibility.

Isopar M + 30 ppm DuPont DCI-4A was shown to be a reproducible fluid suitable for use as a standard reference fluid in the calibration of Falex Rings.

APPENDIX A

ISOPAR M PROPERTY DATA SHEET

TYPICAL PROPERTIES

The values shown here are representative of current production. Some are controlled by manufacturing specifications, while others are not. All of them may vary within modest ranges.

Solvency		Test Method	General Properties (cont.)	Test Method
Aniline point, C(F)	89 (192)	ASTM D611	320-329m	<0.08
Solubility parameter	7.3	Calculated	330-350m	<0.05
Kauri-butanol value	27	ASTM D1133	Color, Saybolt	+30
			Color stability, 16 hr at 100C (212F)	+30
Volatility				
Flash point, PM, C (F)	80 (176)	ASTM D93	Gravity, API	49.2
Fire point, CXC, C (F)	93 (200)	ASTM D92	Specific gravity @ 15.6/15.6C	0.784
			kg/m ³	784
Auto-ignition temperature, C (F)	338 (640)	ASTM D286	lb/gal	6.53
Flammability limits in air, vol% at 21C (70F)	0.8-6.5	Calculated	Refractive Index, 20C	1.4362
Distillation, C (F)		ASTM D86	Viscosity	ASTM D445
IRP	207 (406)		cp at 25C	2.46
5%	212 (413)		cp at 100C	0.72
10%	213 (415)		cSt at 0C	6.80
50%	223 (434)		cSt at 25C	3.35
90%	241 (466)		Odor, bulk	very slight
95%	247 (476)		Odor, residual	none
Dry point	254 (490)		Odor stability	excellent
FBP	260 (500)		Freezing point, C (F) <-60 (<-76)	
Vapor pressure, kPa at 38C	4.1	ASTM D2551	Specific heat, liquid, kJ/kg/C (Btu/lb/F)	
Vapor pressure, psia at 100F	0.6		at 18C (60F)	205 (0.49)
			at 66C (150F)	2.26 (0.54)
			at 93C (200F)	2.39 (0.57)
Composition			Heat of vaporization, kJ/kg (Btu/lb)	
Hydrocarbon type, mass %			at 100C (212F)	307 (132)
Total saturates	99.5	Mass spectrometer	at BP	24 (105)
Aromatics	0.4	UV Analysis		
Trace compounds				
Sulfur				
Doctor test	pass	ASTM D484		
Total sulfur, ppm	1	Microcoulometer		
Peroxides, ppm	<1	Exxon Method		
General Properties			Surface Properties	
Average molecular weight	191	Cryogenic	Demulsibility	excellent
Bromine index (1)	230	ASTM D2710	Interfacial tension, dynes/cm at 25C	51.0
Copper corr., 1/2 hr at BP	2	ASTM D130	Surface tension, dynes/cm at 25C	24.8
Unsulfoxated residue, wt%	99+	ASTM D483		
UV absorbance		FDA Method		
260-319 m	<1.5	21 CFR 172.862		

(1) Bromine index = Bromine number \times 1000

(2) TLV is a registered trademark of the American Conference of Governmental Industrial Hygienists. It is the threshold limit value or occupational exposure limit: the time weighted average concentration for a normal 8-hour workday, 40-hour workweek, to which nearly all workers may be exposed repeatedly without adverse effect. Refer to the most recent Material Safety Data Sheet for the latest recommended maximum exposure limit.

(3) A TLV has not been established for this product. The value shown has been recommended by Exxon Corporation Medical Research based on consideration of available toxicological data. Additional data are being obtained to help define a recommended occupational exposure limit more conclusively.

APPENDIX B

BOCLE MODIFICATION FOR USE WITH FALEX RING

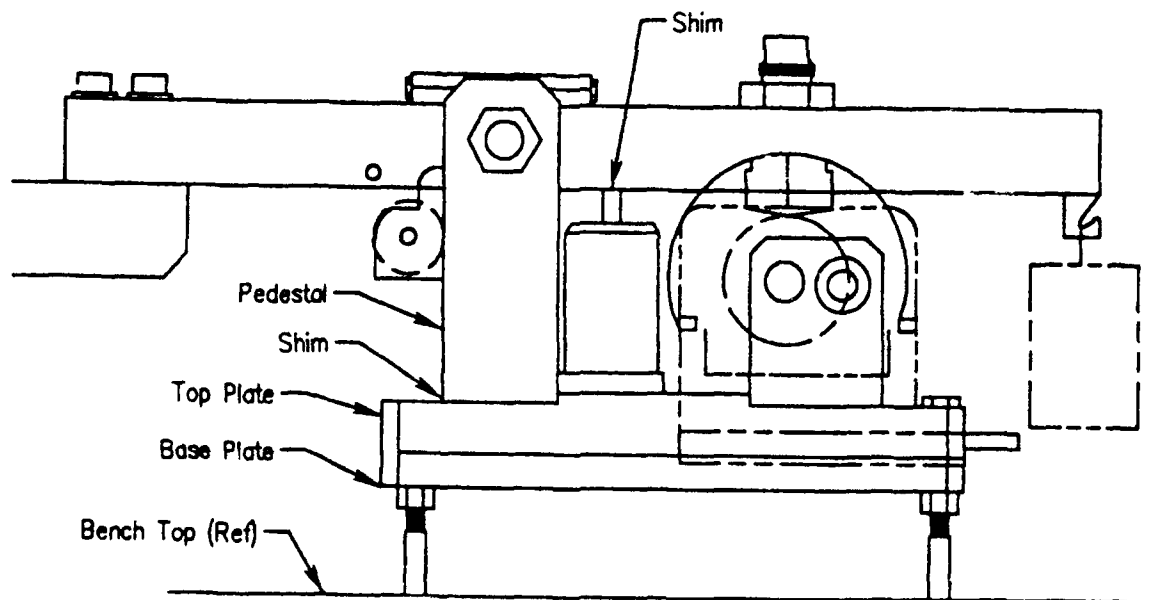
Refer to Figure B-1 when performing the following steps:

1. Remove the six Allen screws that secure the base plate to the top plate.
2. Remove the four Allen screws that secure the load beam pedestal to the top plate.
3. Insert the 1 1/2 X 3 in. shim between the load beam and the top plate. Replace the four Allen securing screws.
4. Reattach the top plate to the base plate.
5. Attach the 3/4 X 3/4 in. shim to the underside of the load beam in such a position that the hydraulic lift plunger meets the shim when in the 'up' position.

NOTE:

Contact cement has been found to be satisfactory for attachment of the shim to the load beam.

6. Check the load beam balance and adjust if required.



FD 337823

Figure B-1. — BOCLE Modification

EVALUATION OF CORROSION INHIBITORS AS LUBRICITY IMPROVERS

Period of Performance

16 February 1987 through 15 February 1988

Reference

Task Order No. 13, Second Interim Report, AFWAL-TR-88-2036, T.B. Biddle, W.H. Edwards

Abstract

The thrust of technical effort described in the following report was directed at evaluation of the currently approved QPL CI in terms of lubricity enhancement; establishment of minimum effective concentrations for approved CI; generation of working curves to profile CI performance in jet fuels; development of an approach for incorporating a lubricity requirement into MIL-I-25017 for the purpose of qualifying candidate CI; refinement of the RPHPLC method for determining CI content in jet fuels; determination of applicability of the RPHPLC method to QPL CI; and generation of an RPHPLC spectral library of QPL CI in JP-4.

SECTION 1.0

INTRODUCTION

At present, the mechanisms associated with fuel lubricity are not well understood. However, it became apparent in the mid 1960s that corrosion inhibiting additives are responsible for imparting good lubricity characteristics to the fuel. The requirement for a corrosion inhibitor (CI) was rescinded at that time, resulting in numerous lubricity problems. The requirement for a CI was reinstated, and lubricity incidents were dramatically reduced. It is now generally accepted that the primary role of a CI is lubricity enhancement and not corrosion inhibition.

Fuel lubricity continues to receive considerable attention and concern in response to reports of lubricity related incidents. During the first eight months of 1986 alone, the U.S. Air Force experienced operational problems with 30 TF30 engine hydraulic fuel pumps in F-111 aircraft flying out of Cannon Air Force Base. The Oklahoma City Air Logistics Center (OC-ALC) investigated the incidents and determined that the problem was due to sensitivity of the pump to the lubricity of the fuel. The investigation also revealed that the same CI was used in each case. Addition of a different CI at the fuel terminal resulted in preventing further occurrences of excessive wear. No reports of pump failures have occurred since the change was made (Ref. 1).

Similar lubricity problems have been reported at other locations. In response to these incidents, the Air Force initiated a program to evaluate the CIs qualified under MIL-I-25017D for their effectiveness as lubricity enhancers in aviation turbine fuels. The intent of this effort was to modify the CI specification to include a requirement for lubricity. Currently, the use of fuel soluble CI is one solution to circumventing wear problems caused by fuels lacking natural lubricating agents.

1.1 BACKGROUND

An excellent historical background of the current requirement for the addition of CI in jet fuel was presented by Chuck Martel, et al in an Air Force Aero Propulsion Report published in July 1974 (Ref 2).

The technical report, entitled "Aircraft Turbine Engine Fuel Corrosion Inhibitors and Their Effects On Fuel Properties," outlines the initial specification requirements and the subsequent revisions that resulted in the required use of CI specifically for improving fuel lubricity.

The Air Force study reports that with the introduction of jet aircraft and kerosene type fuels in the mid 1940s, fuel contamination problems were experienced that were much more severe than previously experienced with aviation gasolines. The greater viscosity and density of jet fuels resulted in the entrainment of water and solid matter that often carried over into aircraft fuel systems. The addition of CI to jet fuels was begun in the early 1950s to combat excessive corrosion in ground fuel systems and subsequent carry over of corrosion products into the aircraft.

The first requirement for CI addition to JP-4 type fuels was by Amendment 1 to the MIL-F-5624B jet fuel specification in March of 1954. In October 1954, a specification for CI was issued as MIL-I-25017 and entitled "Inhibitor, Corrosion, for Aircraft Engine Fuels." Performance of a corrosion test was required by this specification to determine the effective level of CI to be added to a JP-4 fuel. The 20-hour test conducted at a bath temperature of 38°C (100°F) defined the minimum effective concentration required for each CI qualified to the specification.

The first QPL for CI was issued in September of 1956 as QPL-25017-1 and contained three approved inhibitors. The revisions to MIL-I-25017 that followed included Revision A in September 1959 that specified the corrosion test designation to be ASTM Method D665, Procedure B. In May 1955, and again in December 1957, revisions were made to MIL-F-5624 (Revisions C and D) that dictated that a CI "shall be" added to JP-4 and JP-5 fuels. Revision E, however, was issued in March 1960 that changed this wording to "may be" added. Revision F of this specification followed in September 1962 and stated that a CI "shall be added to JP-4," but "shall not be added to JP-5 unless approval is obtained."

Despite the early success of CI to alleviate lubricity related problems, it was immediately apparent that CI were not without potential shortcomings. In the late 1950s some CI caused severe fuel/water separation problems. In the presence of CI, fuel filter coalescer units failed to efficiently remove undissolved water from the fuel. The result was the removal of a number of CI from the QPL. A Water Separometer Index (WSI) limit was incorporated into the fuel specification to ensure acceptable fuel/water separation characteristics in the presence of additive. In the early 1960s, jet fuel filtration problems were associated with the use of CI. The formation of a gelatinous material that rapidly plugged filters resulted from a chemical reaction involving undissolved water, metal (aluminum, steel, magnesium, or zinc) and CI. Consequently, the requirement for a CI to be added to JP-4 was deleted in November 1965. The revised specification stated that a CI shall not be added to grade JP-4 or JP-5 without prior approval from the end user (Refs 3 and 4).

The repercussions caused by the elimination of CI were immediate and readily apparent. A number of occurrences of fuel control malfunctions were reported. Ultimately these were traced back to the removal of the CI that was functioning as a lubricity agent in gas turbine fuels. Because of the severity of the problems, the Air Force issued an operational Technical Order in March 1966 to blend CI into all JP-4 fuel at the base level. Amendment 1 to MIL-T-5624G was issued in November 1966 reinstating the requirement for CI conforming to MIL-I-25017 to be blended into JP-4 by the supplier. The use of CI in JP-5, however, was excluded. The requirement for the addition of CI to JP-5 type fuel was not adopted until revision 'L' of MIL-T-5624 was issued in January 1983. Although not entirely resolved, fuel lubricity problems both domestically and abroad are currently controlled by the mandatory use of CI.

The current QPL contains 15 approved CI. Among these, DCI-4A, Nalco 5403 and ARCO IPC 4445 tend to dominate in Air Force usage. DCI-4A and Nalco 5403 are also used, as well as Unicor J, extensively by the U.S. Navy. Any of the 15 CI presently qualified to MIL-I-25017 and listed on the QPL may be used, at the option of the supplier, in JP-4 and JP-5 type fuels.

Currently concentration requirements for the addition of CI in jet fuel are determined in accordance with

the 'Rusting Test Method' specified by MIL-I-25017D. The Rust Test is in keeping with the original purpose of CI to inhibit pipeline and ground system corrosion. However, since 1966 the addition of CI to jet fuels has been mandated primarily for the purpose of lubricity enhancement. The Ball-On-Cylinder Lubricity Evaluator (BOCLE) is recognized as the best available method for providing a relative system of measurement of fuel lubricity. A variety of Ball-On-Cylinder machines, test procedures, test cylinders and reference fluids have been investigated in past years. Recommendations to the Coordinating Research Council (CRC) based on results of an Air Force study completed in August of 1987 (Ref 5), resulted in standardization of the test apparatus and procedure. With the acceptance of a standard BOCLE test procedure, reevaluation of CI, based on their ability to impart lubricity to jet fuels, was the next step in the Air Force's plan for controlling the lubricity of fuels used in fleet aircraft.

1.2 QUANTIFICATION OF CORROSION INHIBITORS

Despite dependance on the mandatory use of fuel soluble CI to alleviate lubricity related fuel system wear problems, there is no accepted method for monitoring compliance. Nor is there a means of measuring CI levels at the point of use for detecting additive losses occurring during transportation.

In the past, labor intensive extraction techniques have been proposed for quantitative analysis (Refs. 6 and 7) of CI. These techniques have not been evaluated for broad application to all QPL CI or varying fuel matrices. A simple, direct fuel injection, analytical method to quantify low levels of CI was developed under Task Order No. 6, "Determination of Corrosion Inhibitor in Aviation Fuels" (Ref 8). This method, using Reverse Phase High Performance Liquid Chromatography (RPHPLC), appears to best satisfy the prerequisites of a reliable, effective, means for determining CI content in jet fuels. The RPHPLC methodology is based on detection of the dilinoleic acid active ingredient found in the most frequently used CI.

Additional refinement of the test method was, however, needed to extend its applicability to all QPL approved CI. A limited survey of QPL CI indicated that most are multi-component mixtures. Increased resolution of CI components was necessary to provide good precision and accuracy for quantification. Further, identification of the specific CI product added to the fuel was believed to be possible, but only if the product components yielded unique chromatograms.

1.3 PROGRAM OBJECTIVES

The thrust of technical effort described in the following sections was directed at accomplishing the following goals:

- Evaluation of the currently approved QPL CI in terms of lubricity enhancement
- Establishment of minimum effective concentrations for approved CI
- Generation of working curves to profile CI performance in jet fuels
- Development of an approach for incorporating a lubricity requirement into MIL-I-25017 for the purpose of qualifying candidate CI
- Refinement of the RPHPLC method for determining CI content in jet fuels
- Determination of applicability of the RPHPLC method to QPL CI
- Generation of an RPHPLC spectral library of QPL CI in JP-4

SECTION 2.0

EXPERIMENTAL

This investigation focused on two distinct but interrelated efforts. These efforts were conducted simultaneously and together provided an assessment of CI performance and a method to quantify them. The CI evaluations focused on the ability of each of the QPL CI to measurably improve fuel lubricity. The quantification of CI focused on refinement of the recently developed RPHPLC methodology for determining CI content in jet fuels. Applicability of the method to each of the 15 approved QPL CI was also investigated. The following paragraphs discuss test parameters, equipment set up, and experimental approaches used in this investigation.

2.1 CORROSION INHIBITOR EVALUATIONS

2.1.1 Ball-On-Cylinder Lubricity Evaluator (BOCLE)

An InterAv BOCLE was used to assess the ability of each CI to improve the lubricity properties of jet fuels. BOCLE tests were performed according to the standard test procedure approved by the CRC Ball-On-Cylinder Operators' Task Force, "Standard Test Method For Measurement of Lubricity of Liquid Hydrocarbon Fuels By the Ball-On-Cylinder Lubricity Evaluator." The method assesses the boundary lubrication properties of aviation fuels and similar hydrocarbon liquids on rubbing surfaces.

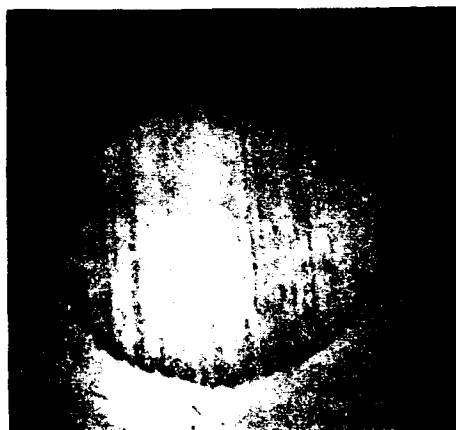
In this method, the test fluid is placed in a reservoir in which the air atmosphere is maintained at 10 percent relative humidity. The fuel temperature during a standard test is maintained at 25°C (77°F). A nonrotating loaded steel ball is held in a vertically mounted chuck and forced against an axially mounted steel test ring. The test ring is rotated at 240 revolutions per minute (rpm) and receives a momentary exposure to the test fluid upon each revolution. At the conclusion of the test, the wear scar generated on the test ball is viewed under a microscope at 100X magnification. A 1-millimeter (mm) graduated reticule permits the major and minor axis of the scar to be measured to the nearest 0.01 mm. The average of the two measurements is reported as the BOCLE wear scar diameter (WSD) and is a measure of the fluid lubricating properties. The smaller the WSD, the better the fuel lubricity. Typical wear scars produced by jet fuels are shown in Figure 1. For the purpose of evaluating lubricity effects at elevated temperatures, an auxiliary Neslab Exocal-100 DD Bath Circulator and a Neslab EN-150 Endocal Flow Through Cooler were interfaced with the existing system.

An overview of the InterAv BOCLE control panel is shown in Figure 2-a. The control panel permits control of test duration, temperature, relative humidity, and ring rotational speed. The base unit is shown in Figure 2-b and is comprised of a fuel reservoir, an axially mounted Falex Ring, a micrometer used for spacing the wear tracks of subsequent runs, and a load beam with test ball installed. The lines shown running to the fuel reservoir provide the means for circulating a fluid medium through the heat exchanger for controlling test temperature.

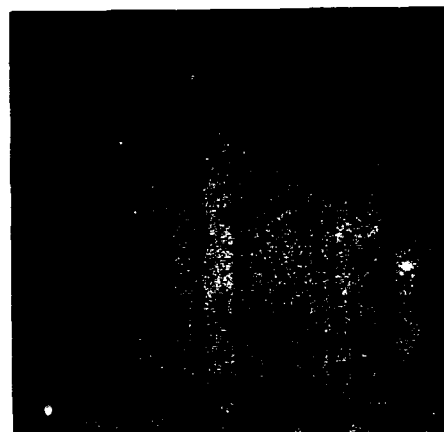
A reduction in applied load from 1000 to 500 grams represents the only change in test conditions from that described in Draft No. 10 of the CRC BOCLE test procedure. A previous Air Force investigation to standardize the BOCLE test resulted in replacing the AMS 6444 test cylinder with the Falex Ring (Ref 5). The harder Falex Ring material generated a significantly larger scar than the AMS 6444 cylinder. At a 1000 gram load, the WSD of clay treated fuels sometimes approached or exceeded 1 mm.

Reference fluid A was used specifically to qualify the test rings for use in BOCLE testing. A WSD of 0.50 ± 0.02 mm was used as the qualifying criteria. Reference Fluid B (neat Isopar M) is a considerably harsher fluid than that of the Isopar M/DCI-4A mixture and as a result produces a significantly larger

wear scar. It is, therefore, sensitive to ring contamination and so was used to ensure that proper cleaning precautions had been followed.



JP-4
wear scar



JP-7
wear scar

Figure 1. Typical BOCLE Wear Scars Produced by Jet Fuels

In addition to qualifying the test rings using the primary and secondary reference fluids, conformance to material specifications for surface finish and hardness was verified. These measurements also permitted the relationship between the specified material properties and the accepted reference fluid calibration value to be established. Verification of the 20 to 30 microinch (min) surface finish was accomplished using a Sheffield Model E-20A Surface Texture Measuring Instrument. Rockwell hardness was verified using a Wilson Mechanical Rockwell Superficial Hardness Tester.

2.1.2 Additives Evaluated

BOCLE tests were performed on each of the CI/Lubricity Improvers approved for use by the MIL-I-25017D QPL. The CI evaluated, manufacturer's designation, and specified relative effective, minimum effective, and maximum allowable concentrations are listed in QPL-25017-15 which is contained in Appendix B. During the course of the investigation, the most recent revision of the QPL, QPL-25017-15 issued in January 1987, resulted in the deletion of P-3305 (Unichema Chemie B.V., Netherlands) from the QPL. Two new CI were added to the revised QPL: Nuchem PCI-105 and Welchem 91120. Both the former and the latter CI were included in the investigation. Fresh samples of CI were procured from the manufacturers.

2.1.2 Test Fuels

CI performance was evaluated in four test fuels: neat Isopar M, JP-4, JP-8, and JP-5. The matrix fuels were stored in 55-gallon epoxy-lined drums. With the exception of Isopar M, 20 gallons of each fuel type were stripped of additives, naturally occurring lubricity enhancers (polar compounds), and contaminants by slow percolation through oven dried Attapulgus clay. Clay treating (CT) was performed according to Annex A of ASTM D2550. The degree of fluid harshness attained was verified by performing BOCLE tests upon completion of the clay treating. In instances where a BOCLE WSD of greater than 0.75 mm was not obtained, the fuel was subjected to additional passes through the clay. The harshness of the matrix fuels was verified a second time prior to preparation of each set of CI/fuel blends.

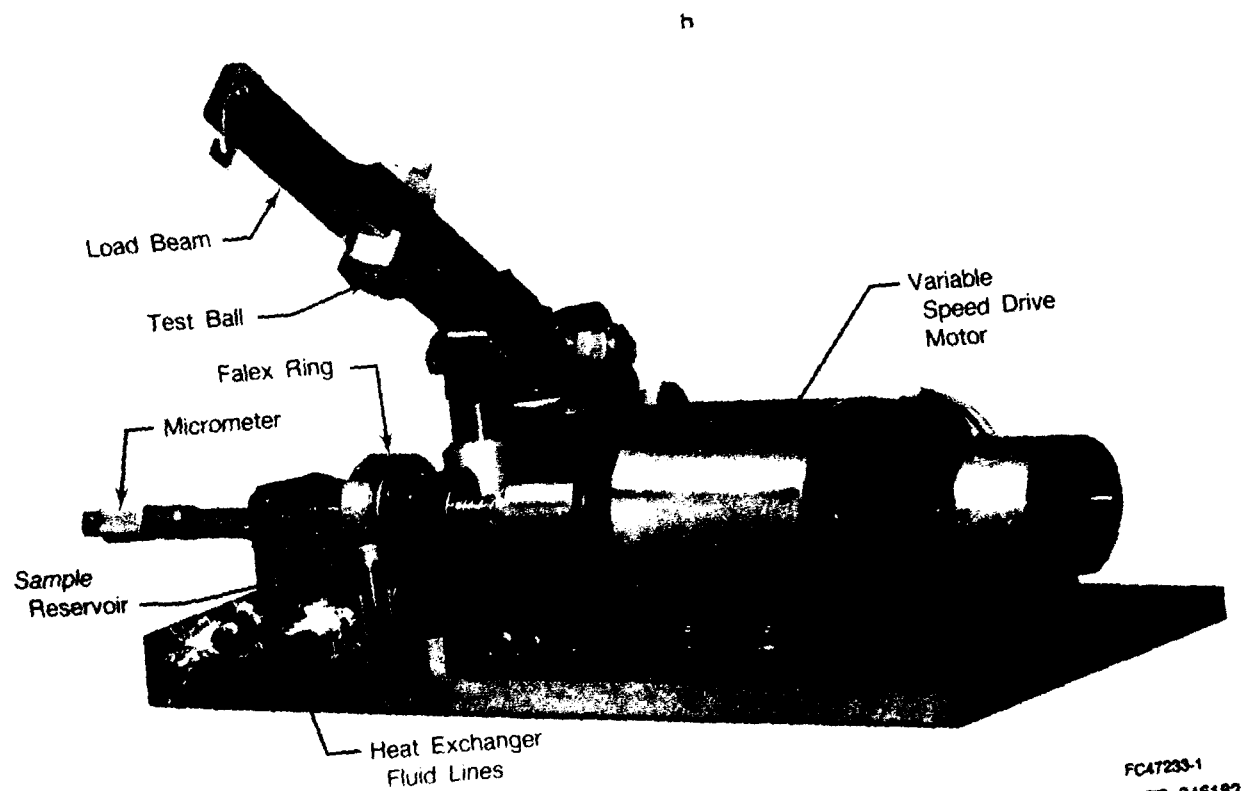
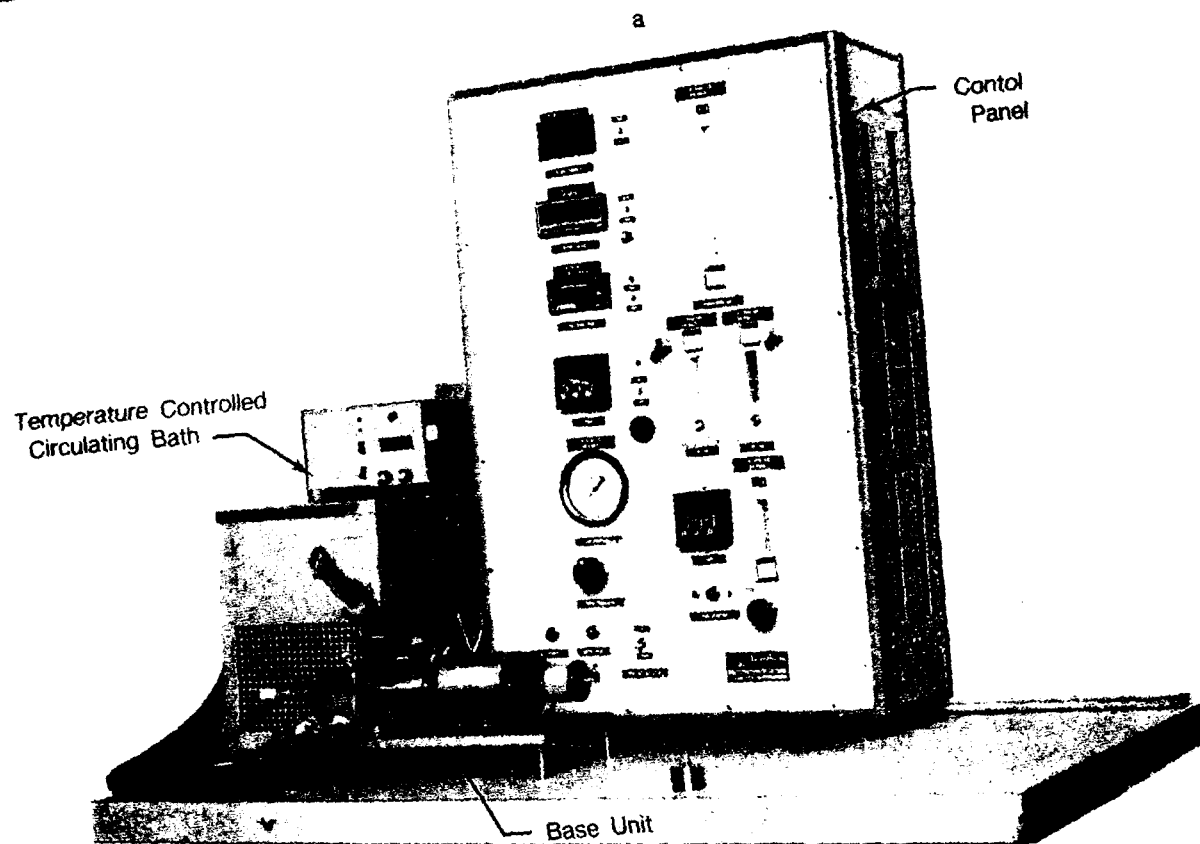
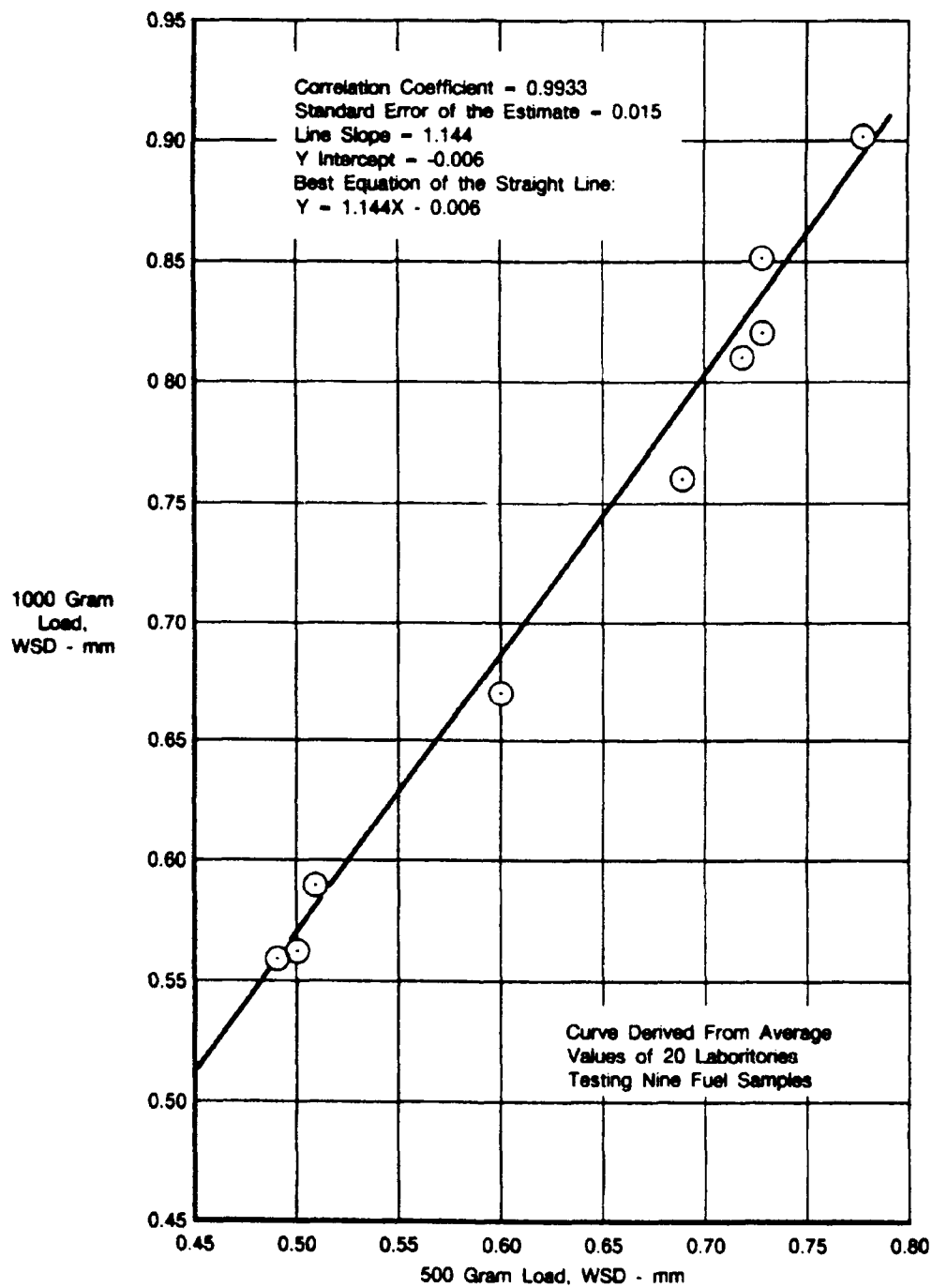


Figure 2. InterAv Ball-On-Cylinder Lubricity Evaluator



FDA 355194

Figure 3. BOCLE Load Correlation

2.1.4 Additive/Fuel Blends

To determine effective CI concentrations in each of the four test fuels, testing was performed at nine concentrations ranging from zero to the maximum allowable concentration permitted for each CI in QPL-25017-15. Additive/fuel blends were formulated from a 100-ppm concentrate at levels of 0, 1.5, 3, 6, 9, 12, 15, 20, and 30 ppm by weight. This range was extended for two of the CI having maximum allowable concentrations of 42 ppm. To provide a fair assessment of the effective concentration of the CI in each of the four different test fuels, the CI were blended at the various concentrations in ppm by weight rather than in grams per cubic meter (g/m^3). Depending on the density of the fuel, a maximum allowable concentration of 22.5 g/m^3 ranges from approximately 26 to 30 ppm.

2.1.5 Test Temperatures

BOCLE WSD as a function of CI concentration were generated at 25°C (77°F). In three of the four test fuels, CI were also evaluated at 75°C (167°F) to assess the effect of temperature on additive performance.

2.1.6 Summary of Test Matrix

A summary of the test materials, CI concentrations, and test temperatures is shown below:

BOCLE:	Falex Ring, 500g applied load
QPL CI/Lubricity Improvers:	16
CI Levels Evaluated (ppm):	0, 1.5, 3, 6, 9, 12, 15, 20, 30, 42
Test Fuels:	Neat Isopar M, CT JP-4, CT JP-8, CT JP-5
Test Temperatures:	25°C (77°F), 75°C (167°F)

2.2 REFINEMENT OF RPHPLC METHOD FOR DETERMINING CI CONTENT IN JET FUELS

2.2.1 Equipment and Instrumental Conditions

Based on previous research reported in Reference 6, the following equipment and instrumental conditions were used to begin the method optimization:

A Varian Model 5560 Ternary Liquid Chromatograph as shown in Figure 4 was used to perform all HPLC analyses in this study. It was equipped with a Varian Model UV200 variable wavelength ultraviolet-visible detector set to 202 nanometer (nm) with a 0.5-second response time, a Rheodyne Model 7125 injector valve with 50 microliter (mL) sample loop, and an electronic column heater. Quantification was accomplished using a Varian Model Vista 402 Chromatography Data System. Baseline treatment was performed automatically by the data system software. All calibrations were performed in the External Standard mode.

The following HPLC bonded phase columns were evaluated: cyano (Alltech Associates, Deerfield, IL); amino, cyano and phenyl (Brownlee Labs, Santa Clara, CA); carboxymethyl weak ion exchange (Toyo Sota, Japan); phenyl sulfonic acid strong cation exchange and quaternary amine strong anion exchange (Whatman, obtained from Alltech Associates).

The mobile phase compositions evaluated included blends of methanol, isopropanol, and aqueous buffers. Samples and standards were injected into the chromatograph, without any pretreatment, via a 50mL sample loop. After the additive compounds eluted, a column wash and reequilibration program was necessary to remove the residual fuel sample. The ternary (3 solvent) capability of the chromatograph was used to perform this function.

Standards were prepared in 125-milliliter (mL) Teflon bottles (Nalge Co., Rochester, NY).



2.2.2 Materials

- HPLC grade methanol, isopropanol and water were obtained from Burdick and Jackson (Muskegon, MI).
- Potassium phosphate, monobasic (KH_2PO_4) and sodium hydroxide (NaOH) were ACS Analytical Reagent grade and were obtained from Mallinckrodt, Inc. (Paris, KY).
- EMPOL 1010, a 97 percent pure dilinoleic acid, and EMPOL 1041, an 80 percent trilinoleic acid (20 percent dimer), were obtained from Emery Chemical Company (Cincinnati, OH).
- Purified linoleic acid was obtained from Fisher Scientific Company, (Fair Lawn, NJ).
- The 15 CI products listed in the QPL-25017 -15 were obtained from the respective suppliers.
- Clay treated JP-4 fuel was prepared by filtering JP-4 through a glass column packed with Attapulugus clay per ASTM D2550.
- Additive free JP-4 was obtained from Sun Oil Company (Philadelphia, PA).

SECTION 3.0 RESULTS AND DISCUSSION

The results and significance of the BOCLE tests performed on 16 corrosion inhibitors are discussed in the paragraphs that follow. Results and discussion of work directed at refining the RPHPLC method for determining CI content in jet fuels and applicability of the methodology to CI approved under MIL-I-25017D are also presented.

3.1 CORROSION INHIBITOR EVALUATIONS

3.1.1 Lubricity Test Data

Tables of the BOCLE data generated for each of the CI in each test fuel, over the range of concentration... at which they were tested, are included in Appendix C. Profiles of additive performance were generated for each CI in the form of polynomial curve fits plotted from the test data. These plots provide a means for determining the amount of additive required to provide sufficient lubricity properties to jet fuels. The plots also provide an avenue for tracking deterioration in fuel lubricity as levels of CI are depleted. These curve fits are presented in Appendix D, indexed by fuel type.

3.1.2 Criteria Used to Assess Performance

In order to assess the effectiveness of the CI, guidelines and criteria were established to permit comparison of the responsiveness of one CI to another. Among the criteria considered was the amount of additive required to provide relative effective lubricity enhancement. For the purpose of this discussion, the terminology 'relative effective concentration' is defined as the concentration of CI required to provide a BOCLE WSD equal to 0.60 mm. The 0.60 mm WSD is currently under consideration by the Air Force to describe minimum acceptable lubricity. This value was selected on the basis of an Air Force survey of hydraulic fuel pumps that had experienced problems when exposed to fuel having a WSD of greater than 0.60 mm. In rating CI performance, consideration was also given to the lubricity improvement that was attainable at maximum allowable concentration. Twenty-two and a half grams per cubic meter was the maximum allowable concentration permitted by QPL-25017 for all but two of the CI evaluated. The two exceptions are Unichema P-3305 (excluded from the QPL in the January 1987 revision) and Tolad 245. Both are permitted a maximum allowable concentration of 42 ppm (31.5 g/m³).

Therefore, examination of the BOCLE results considered (1) 'relative effective concentration', defined as the level of CI required to reduce the BOCLE WSD to 0.60 mm (2) 'maximum effective concentration', defined as that concentration at which no further reduction in WSD is apparent with continued increases in CI concentration; and (3) maximum lubricity achieved, i.e., WSD at the maximum allowable concentration.

3.1.3 Performance Profile

Computer software was developed to permit archiving and plotting of the BOCLE test data. Second, third, and fourth order polynomial curve fits best-fit the test data for plotting WSD as a function of concentration. The curve fits were used as a tool to establish relative effective concentrations for each CI and for determining the effect of fuel type and temperature on CI response. Figure 4 is an example of the curves produced by the software. For quick reference, a dashed line was drawn across the plot by the computer to represent the targeted 0.60 mm WSD lubricity value. The point at which the plotted curve crossed the dashed line was calculated from the polynomial equation and printed out on the plot as the "relative effective concentration." As shown in Figure 5, the concentration requirements per QPL-25017 the accuracy of the curve fit data (standard error of the estimate (SEE)), and correlation coefficient (R) are also documented on the plot. A complete set of curve fits, profiling additive performance for each QPL CI, are contained in Appendix D, indexed by fuel type.

While interpreting the curves shown for each CI, consideration should be given to small variations in additive response that may appear unduly emphasized by the graph. In reality, the data fall within the established limits of test repeatability (0.03 mm). Although varying in profile, the curves for each CI assessed at 25°C (77°F) responded predictably to increasing CI concentrations. At maximum allowable concentration, WSD ranged from 0.47 to 0.61 mm for the 16 CI tested in the four fuel types. In at least three out of the four test fuels, all but four of the 16 CI had achieved maximum effectiveness upon reaching maximum allowable concentration. As shown by the plots in Appendix D, the majority of CI

exhibited a plateau between 20 and 30 ppm, showing no further reduction in WSD with increased concentration. Six of the CI, however, did show evidence of a continued reduction in WSD with increasing concentration.

Curve fits comparing IPC-4410 and Tolad 249 in CT JP-4 are shown in Figures 5 and 6, respectively. IPC-4410, as shown in Figure 5, exhibits outstanding lubricity improving properties with a 0.48 mm WSD achieved at maximum allowable concentration. Additive efficiency of IPC4410 in JP-4 is reflected by the small amount of CI required to meet the required 0.60 mm WSD. IPC-4410 performed equally well in CT JP-8 and CT JP-5. As shown by the curve in Figure 6, Tolad 249 failed to meet the 0.60-mm WSD criteria for lubricity enhancement even at its maximum allowable concentration. Field experience supports the test data, indicating that Tolad 249 is among the least effective CI currently on the approved QPL.

3.1.4 Effect of Fuel Type on Additive Performance

It was suspected during the early stages of this investigation that some additives would respond differently to different type fuels. In general, fuel type had little effect on additive performance. These were, however, clay treated fuels. It is possible that unique responses to additives could occur with fuels containing different polar compounds. In the clay treated samples, the BOCLE WSD at maximum allowable concentration, and the level of CI required to achieve a 0.60-mm WSD, were relatively consistent from fuel type to fuel type. Some variation, however, was observed. As shown in Table 1, the most significant variation was that of P-3305 (no longer an approved CI) in JP-5. This is apparent when comparing its performance in JP-5 to the other three test fuels. It was thought that the slight differences in the performance of an additive from one fuel type to another could be attributed to one, or a combination, of the following causes:

- CI depletion
- Unique CI response to the properties of a specific fuel type
- Small variations in CI active ingredient between stock solutions caused by vaporization of diluent during weighing/blending procedure
- Variations in volatility of the fuels that may cause concentration of CI during the BOCLE test
- Unknown test variable(s)

A brief study was conducted to investigate the effect of CI depletion on the test data. The effect of CI depletion on BOCLE results was considered in relation to the time between preparation of the 100 ppm concentrate and preparation of the subsequent blends. Also investigated was the effect of time between preparation of the individual blends and performance of the BOCLE tests. A series of CI profiles previously generated were repeated. BOCLE tests on the individual blends were performed within 24 hours of preparation of the initial 100 ppm concentrate. RPHPLC was used to monitor CI depletion rates. No evidence was found that the BOCLE results had been affected by depletion of CI or that significant plating out of additive had occurred during the 24-hour period. The newly generated curves were consistent with those previously reported for the other three test fuels.

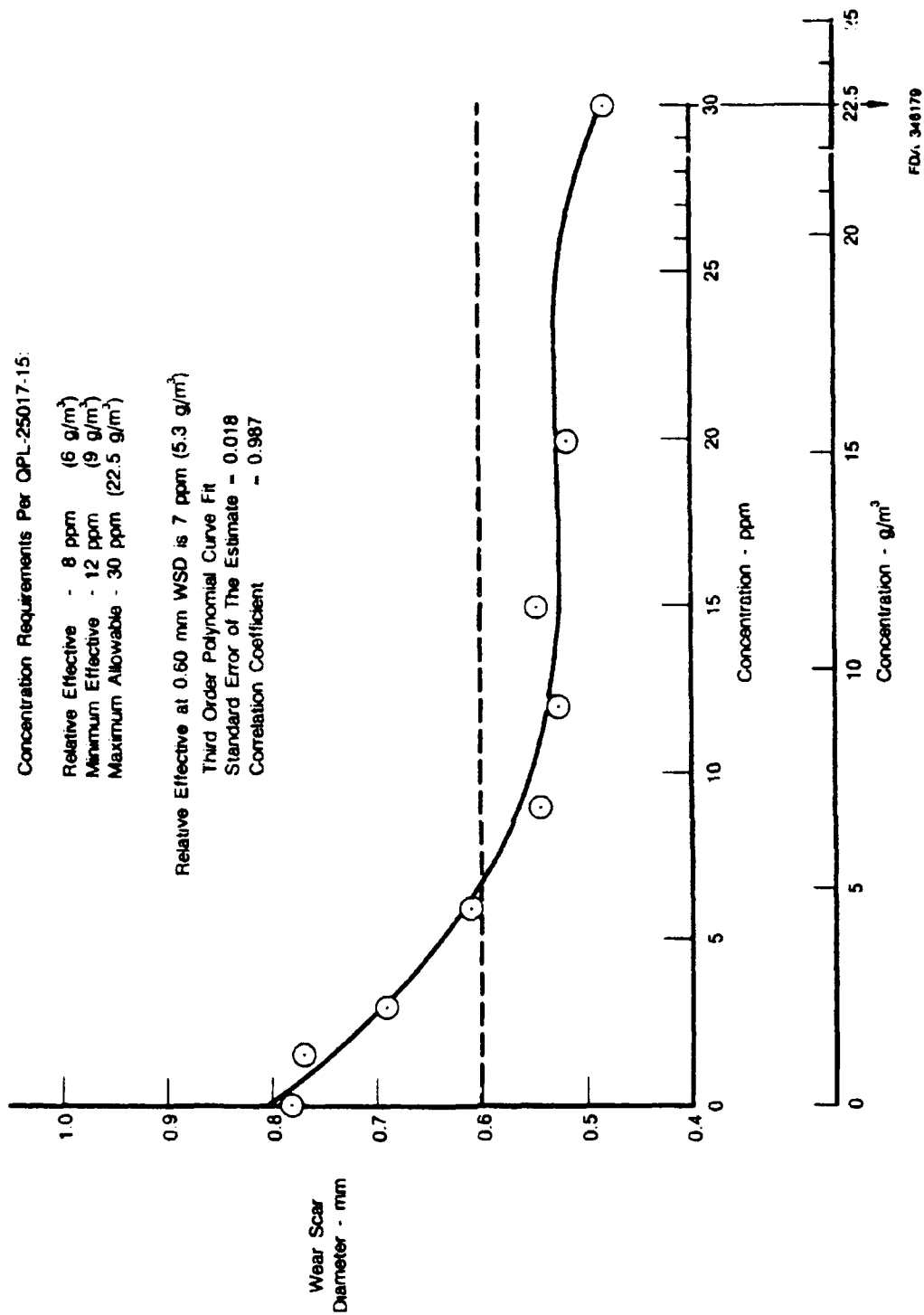


Figure 5. Effect of IPC-4410 in Clay Treated JP-4

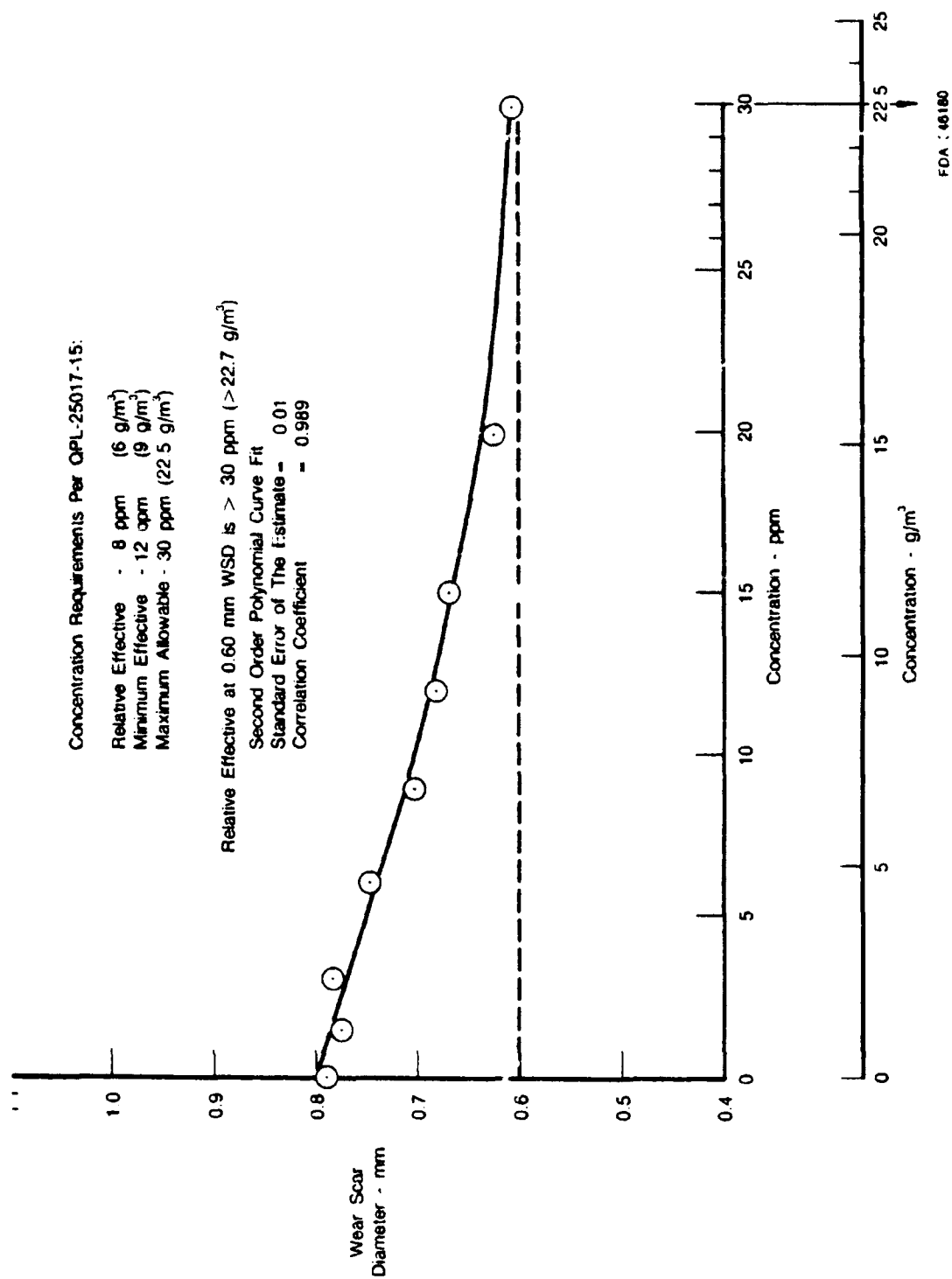


Figure 6. Effect of Tolad 249 in Clay Treated JP-4

TABLE 1
EFFECTIVE CORROSION INHIBITOR CONCENTRATIONS
FOR LUBRICITY IMPROVEMENT

Corrosion Inhibitor	Concentration Required to Achieve 0.60 mm BOCLE WSD g/m ³						BOCLE WSD at Maximum Allowable Concentration mm					
	Isopar M	CT JP-4	CT JP-5	CT JP-8	Range	Average Concentration Required	Isopar M	CT JP-4	CT JP-5	CT JP-8	Range	Average WSD
IPC-4410	8.3	5.3	6.5	6.4	3.0	6.6	0.51	0.48	0.48	0.48	0.03	0.49
NALCO 5405	9.8	6.8	8.1	7.9	3.0	8.2	0.48	0.50	0.52	0.48	0.04	0.50
ARCO IPC-4445	14.4	9.0	11.3	11.9	5.4	11.6	0.54	0.50	0.56	0.54	0.06	0.54
UNICHEM P-3305	7.6	8.3	18.9	9.5	11.3	11.1	0.47	0.52	0.51	0.52	0.05	0.50
NALCO 5403	10.8	9.0	8.9	9.5	1.7	9.5	0.53	0.53	0.50	0.50	0.03	0.52
UNICOR J	8.8	6.8	8.1	8.7	1.9	7.6	0.47	0.53	0.46	0.54	0.08	0.50
MOBILAD F-800	8.3	6.8	6.5	9.5	2.7	7.8	0.49	0.52	0.50	0.48	0.04	0.50
TOLAD 245	20.4	21.1	19.4	19.1	2.0	20.0	0.55	0.54	0.54	0.55	0.01	0.54
DCI-6A	9.1	8.3	6.5	8.7	2.6	8.2	0.48	0.54	0.48	0.52	0.06	0.50
LUBRIZOL 541	13.6	13.6	10.5	11.9	3.1	12.4	0.54	0.54	0.56	0.55	0.02	0.55
DCI-4A	8.8	9.0	6.5	7.2	2.5	7.4	0.48	0.55	0.48	0.50	0.07	0.50
HITEC E-580	12.1	8.3	11.3	11.1	3.8	10.7	0.52	0.55	0.51	0.54	0.04	0.53
APOLLO PRI-19	15.1	14.3	13.0	14.3	2.1	14.2	0.54	0.56	0.52	0.57	0.05	0.55
TOLAD 249	21.9	>22.6	23.5	23.1	1.6	>22.8*	0.59	0.61	0.60	0.60	0.02	0.60
WELCHEM 91120	12.1	8.3	11.3	12.7	4.4	11.1	0.56	0.52	0.54	0.54	0.04	0.54
NUCHEM PCI-105	13.6	12.8	13.8	11.9	1.9	13.0	0.55	0.54	0.54	0.52	0.03	0.54

*Exceeds Maximum Allowable Concentration per QPL-25017-15

RL0021-11

3.1.5 Effective Concentrations for Lubricity Improvement

The effective concentrations for lubricity improvement, based on the 0.60mm WSD criteria, are shown in Table 1 for each of the 16 CI in each of the four test fuels. Military specifications require the addition of CI to JP-4, JP-5, and JP-8. It is unlikely that a future revision to the military specification will call out varying relative, minimum, and maximum concentrations based on fuel type alone. Fuel type has been shown to have little effect on additive performance. Since there is a need to know how an additive will respond in general to any current JP fuel, much of the following discussion will focus on the average test results for all matrix fuels cumulatively as opposed to addressing each fuel type individually. Table 1 permits independent comparison of test fuels.

In addition to data for each specific fuel, the average concentration required in all test fuels to achieve minimum lubricity improvement is shown in Table 1. Only six of the CI evaluated exhibited a 0.60 mm WSD at concentration levels of 9 g/m³ or less. Nine g/m³ is the 'minimum effective concentration' defined by QPL-25017-15, while 0.60 mm WSD is the Air Force proposed value for determining minimum acceptable lubricity improvement. Of the remaining ten CI, eight met the 0.60-mm WSD criteria between 10 and 14 g/m³, one approached its maximum allowable concentration, and one CI (Tolad 249) exceeded maximum allowable concentration. Looking at the test fuels independently, only 5 CI in Isopar M, 5 in JP-8, 7 in JP-5, and 11 in JP-4 met the desired 0.60-mm WSD criteria for minimum effective lubricity improvement at the minimum effective concentration of 9 g/m³ designated by QPL-25017-15. The improved performance of many CI in JP-4 may be a result of evaporation of light ends during the BOCLE test, thereby concentrating CI. Maximum effective concentration (that in which no further reduction in WSD was realized) ranged from 9 to 31.5 g/m³.

3.1.6 Performance Ranking

Based on their performance as lubricity improvers, the 15 currently approved CI fell into three distinct groups. Grouping of CI performance was based on the average results of all test fuels. Each performance

group, as shown in Table 2, was distinctive in relation to both total reduction in WSD achieved at maximum allowable concentration as well as the concentration required to achieve 0.60 mm WSD.

Group No. 1 consisted of six CI in which similar maximum lubricity improvement of 0.49 to 0.50 mm WSD (essentially the same) was achieved. Concentrations required to achieve a 0.60 mm WSD ranged from 6.6 to 8.2 g/m³. This concentration range conformed to the 9 g/m³ minimum effective concentration requirement set forth by QPL-25017-15. The CI in Group No. 1 were extremely efficient in low level response to providing and maintaining excellent lubricity enhancement.

Group No. 2 consisted of eight CI providing a maximum lubricity improvement of 0.52 to 0.55 mm WSD. Concentrations required to achieve a 0.60 mm WSD ranged from 9.5 to 12.4 g/m³. With the exception of one CI, this group exceeded the QPL defined minimum effective concentration (Tolad 245 has a 22.5 g/m³ minimum effective concentration while the remaining CI have requirements of 9 g/m³). This group of CI exhibited good to fair lubricity enhancing properties.

Group No. 3 consisted of one CI (Tolad 249) that provided an average maximum lubricity improvement of 0.60 mm WSD. In three out of four test fuels, maximum allowable concentration was exceeded prior to achieving this value. Tolad 249 was shown to be the least effective CI in providing adequate lubricity enhancement of jet fuels.

TABLE 2
GROUPING OF CORROSION INHIBITOR PERFORMANCE

<i>Corrosion Inhibitor</i>	<i>Average, All Test Fuels</i>	
	<i>WSD at MAC</i> <i>mm</i>	<i>Concentration Required</i> <i>To Achieve</i> <i>0.60 mm WSD</i> <i>g/m³</i>
<i>Group No. 1</i>		
IPC 4410	0.49	6.6
NALCO 5405	0.50	8.2
UNICOR J	0.50	7.5
MOBILAD-F800	0.50	7.8
DCI-6A	0.50	8.2
DCI-4A	0.50	7.4
<i>Group No. 2</i>		
NALCO 5403	0.52	9.5
HITEC E-580	0.53	10.7
IPC 4445	0.54	11.6
TOLAD 245	0.54	20.0
WELCHEM 91120	0.54	11.1
NUCHEM PCI-105	0.54	13.0
APOLLO PRI-19	0.55	14.2
LUBRIZOL 541	0.55	12.4
<i>Group No. 3</i>		
TOLAD 249	0.60	>22.8

Note:

1. QPL — MIL-I-25017D Qualified Products List
2. Average WSD-Average Wear Scar Diameter of CI in Four Test Fuels
3. MAC — Maximum Allowable Concentration Per QPL-25017-15
4. QPL Minimum Effective Concentration 9 g/m³, Except TOLAD 245 22.5 g/m³

R19001/11

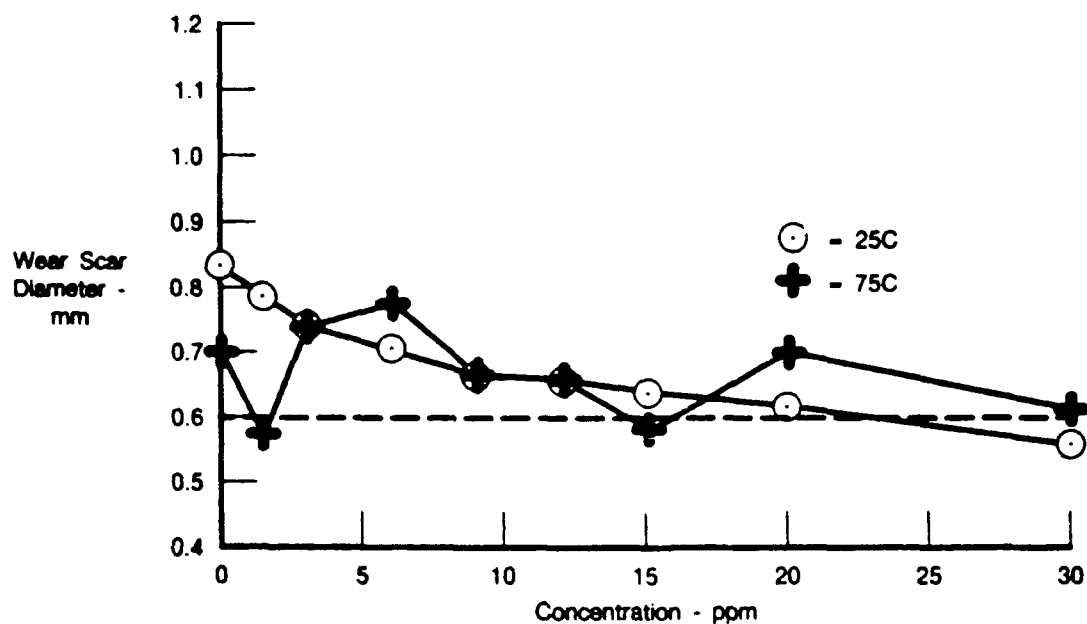
While the grouping of CI performance is subjective, the thought process in discerning between the three groups takes into consideration not only the total reduction in WSD but also the military specification

requirements for minimum effective concentration. Of those additives evaluated, IPC-4410 was among the most effective while Tolad 249 was shown to be the least effective.

3.1.7 Effect of Temperature

BOCLE tests at 75°C (167°F) were performed on the CI/fuel blends to assess the effect of temperature on CI performance. As predicted, wear scars generated at 75°C (167°F) were in most cases measurably larger than those produced for the same fuel blends at 25°C (77°F). This supported earlier work by the Naval Air Propulsion Center (NAPC) (Ref 9) and P&W (Ref. 10) indicating that temperature has a dramatic effect on fuel lubricity. Plots generated from the 75°C (167°F) runs, however, were shown to be extremely erratic. The predictable curves exhibited by the 25°C (77°F) data, showing enhanced lubricity as a function of concentration, were not apparent when testing at 75°C (167°F). Data scatter and lack of repeatability made valid interpretation of the test results difficult, if not impossible, at 75°C (167°F).

Figures 7 and 8 are representative of the phenomenon observed during the elevated temperature tests. To verify that the erratic data was the result of random, temperature-induced scatter, the entire series of BOCLE runs were repeated from 0 to 30 ppm at 75°C (167°F) for two CI. The resulting profiles were significantly different from the original plots. Both CIs continued to exhibit nonrepeating, random data scatter. It was concluded that the validity and usefulness of the data was questionable. With the concurrence of the Air Force Project Engineer, BOCLE testing at elevated temperature was terminated.



FDA 346195

Figure 7. Effect of Temperature on PRI-19 in Clay Treated JP-4

Temperature has an effect on the way CI function in different wear modes. Although not fully understood, it is suspected that more than one type of wear occurs during BOCLE operation. Wear mechanisms that occur in the boundary lubrication regime that could be applicable to BOCLE operation include (1) corrosive wear, (2) abrasive wear, and (3) adhesive wear.

Corrosive wear occurs when oxygen reacts with metal surfaces to form metal oxides. These oxides are

easily worn away providing fresh surfaces for further oxidation. CI function by adsorption of the CI polar carboxy group to the metal surface, thus forming a molecular boundary layer that acts as a barrier to oxygen and moisture. Adhesive and abrasive wear occurs when asperities of two metal surfaces come into contact. CI function to provide a molecular boundary layer between the two surfaces. In abrasive or adhesive wear, asperity contact area can grow due to the high normal and tangential stresses on the metal so that the trapped boundary film may be stretched until it ruptures. Local heating can weaken the adsorption forces of the surface film. Simple polar compounds desorb under high temperatures.

It is suspected that the data scatter observed at elevated temperature may be a result of opposing effects of the following increased wear rates, desorption of CI, and increased fuel oxidation rates. Temperature increases the rate of corrosive wear by accelerating the rate of corrosion reactions at the metal surface. In addition, temperature has been shown to increase the rates of adhesive and abrasive wear. The latter has been demonstrated by the increase in wear observed in an inert environment. An increase in temperature will also increase the rate of fuel oxidation reactions that has been shown to reduce wear rates. Fuel oxidation reactions form various oxygenated species (i.e., carboxylic acids, aldehydes, alcohols, etc.) that, because of their polarity, act as good lubricity agents. Fuel decomposition during BOCLE testing is evident from the brownish black residue observed on the test ball at the point of contact. Consequently, in any given test, there may be an ongoing competition between increased wear rates caused by higher temperatures and reduced wear rates due to fuel oxidation.

While not clearly understood, temperature does appear to have a significant effect on CI performance. However, it is apparent that under standard operating conditions, assessment of the effects of temperature on fuel lubricity is beyond the capabilities of the BOCLE.

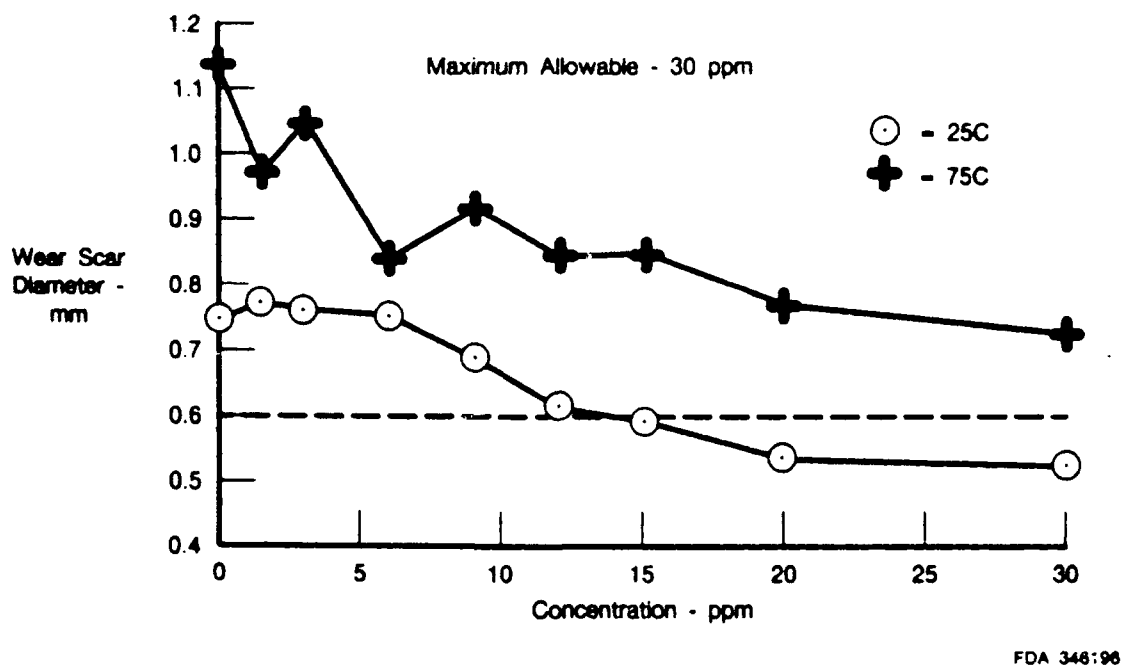


Figure 8. Effect of Temperature on Hitec E-580 in Isopar M

3.2 PROPOSED MIL-I-25017 LUBRICITY REQUIREMENT

A thorough review of MIL-I-25017D, which is included in Appendix E, was performed and the historical background of CIs researched. Current Air Force quality assurance and fleet support needs were

compared to those of the past. The review sought to determine how the current CI specification could be modified to address a product's ability to improve fuel lubricity, as well as inhibit pipeline and ground fuel system corrosion. We found that a requirement for lubricity enhancement could be easily incorporated into the current specification with no significant effect on other criteria used in qualifying a candidate CI.

There are 12 tests listed in the military specification used to qualify CIs. These tests are directed at controlling CI properties, minimizing the effect on fuel properties, and in establishing relative effective (REC), minimum effective (MEC), and maximum allowable (MAC) concentrations.

The twelve test criteria consist of the following:

- 1) Solubility - At MAC, there can be no precipitation, cloudiness or other evidence of insolubility.
- 2) Compatibility--At MAC, the CI must be compatible with all other CI currently qualified and with approved static dissipator additives.
- 3) Rust Test--Establishes REC, the lowest concentration yielding a passing result.
- 4) Water Separation Index, Modified (WSIM)--One of two primary criteria used in establishing MAC: the highest concentration giving a WSIM value of 70 or higher.
- 5) Electrical Conductivity -- The second of two primary criteria used in establishing MAC: the highest concentration giving less than a 40-percent change in electrical conductivity with fuel containing static dissipator additive.
- 6) Ash Content -- Shall not exceed 0.10 percent when determined in accordance with ASTM D482.
- 7) Pour Point--Shall not exceed--18°C when determined in accordance with ASTM D97.
- 8) Storage Stability -- Shall show no evidence of gross separation or degradation after storage for 12 months.
- 9) Induction System Deposits -- Applicable if CI to be qualified for motor gasolines.
- 10) Emulsification Tendency--Applicable if CI to be qualified for use in motor gasolines and diesel fuels.
- 11) Accelerated Stability--Applicable if CI to be qualified for use in diesel fuels. Determines formation of total insolubles in accordance with ASTM D2274 at MAC.
- 12) Engine Test--Must pass 100-hour engine test using JP-4 containing CI at 2 times the MAC. Shall indicate no excessive deposits, wear or corrosion attributed to the inhibitor.

Currently, CI effectiveness is evaluated in terms of corrosion inhibition and is assessed primarily on passing the rust test. The lowest concentration at which a CI passes the rust test is defined as the REC, and cannot be less than 6 g/m³. The "not less than 6 g/m³" requirement originates from early development work in which the rust test was shown to exhibit poor precision at low concentrations. The range of concentrations permissible for use in fuels is derived in part from the REC. MEC is specified as 1.5 times REC and cannot be less than 9 g/m³ (1.5 times 6 g/m³). MAC is governed by a number of considerations; the most significant are WSIM and electrical conductivity. MIL-I-25017D defines MAC as the lowest of the following:

- Fifty-four grams of inhibitor per cubic meter of fuel.
- Four times the REC.
- The highest concentration giving a WSIM value of 70 or greater.
- The highest concentration giving less than a 40-percent change in electrical conductivity with fuel containing static dissipator.

MIL-I-25017D also specifies that the MAC shall be equal to, or greater than, the MEC and shall be a value evenly divisible by 4.5 within a range of 9 to 54 g/m³.

Minimal changes to the current specification would be necessary to incorporate lubricity enhancement as an additional criteria for qualifying CI. Inclusion of a lubricity requirement can be most readily accomplished by redefining REC while leaving the requirements for MEC and MAC unchanged. Maintaining the MEC as 1.5 times the REC is recommended to compensate for (1) blending errors at the refinery, (2) losses during transport and storage, and (3) variations in performance between fuels. MAC would continue to define upper limits. In this way, the basic test requirements are unaffected by the modification. Redefining REC would entail incorporating a 0.60-mm BOCLE WSD lubricity requirement along with the rust test, as well as the following stipulations: (1) REC not exceed 36 g/m³ (if it did, then MAC would exceed the 54 g/m³ limit); (2) 1.5 times the REC not yield a WSIM value less than 70; and (3) 1.5 times the REC not yield greater than 40 percent change in electrical conductivity with fuel containing static dissipator additive.

The latter three stipulations act as a cutoff to prevent those CI that require large concentrations to meet a 0.60-mm BOCLE WSD from exceeding the current MAC requirements. Inclusion of the above restrictions would also permit a step-wise progression for qualifying a CI; eliminating the need for further testing of CI that did not meet the WSIM and electrical conductivity values ultimately required of them at MAC.

The following proposes a rewording of the current MIL-I-25017D specification based on the above discussion. Additional requirements for defining REC and those that have been modified for the current specification are denoted by an asterisk (*).

RELATIVE EFFECTIVE CONCENTRATION (SEC 3.5)

- 1) *Shall be defined as the lowest concentration giving both a passing result in the rust test (Sec 4.6.3) and a maximum BOCLE WSD of 0.60 mm.
- 2) The REC shall not be less than 6 g/m³.
- 3) *The REC shall not exceed 36 g/m³.
- 4) *One and a half times the REC shall not yield a WSIM value less than 70.
- 5) *One and a half times the REC shall not yield greater than 40 percent change in electrical conductivity with fuel containing static dissipator additive.

MINIMUM EFFECTIVE CONCENTRATION (SEC 3.6)

- 1) Shall be defined as 1.5 times the REC.

2) Shall not be less than 9 g/m^3 .

3)*Shall not exceed MAC.

MAXIMUM ALLOWABLE CONCENTRATION (SEC 3.7)

The MAC shall be equal to, or greater than, the MEC and shall be the lowest of the following:

1) Fifty-four g/m^3 .

2) Four times the REC.

3) The highest concentration giving a WSIM value of 70 or higher.

4) The highest concentration giving less than 40 percent change in electrical conductivity with fuel containing static dissipator additive.

The effect of redefining relative effective concentration, as shown in Table 3, indicates that MEC would be increased for all but two of the currently approved CI. Three CI would be disqualified based on the above revisions. Those CI failing to meet the new requirements are Tolad 249, Lubrizol 541, and Nuchem PCI-105.

Tolad 249 would fail to qualify on the basis of its limited lubricity improving properties. In determining its REC by the new guidelines, Tolad 249 was unable to achieve a BOCLE WSD of less than or equal to 0.60 mm at concentrations up to 22.5 g/m^3 . Since its MAC is 22.5 g/m^3 , Tolad 249 would be disqualified.

Although Lubrizol 541 meets the lubricity requirement at a REC of 13.6 g/m^3 , its MEC ($1.5 \times 13.6 \text{ g/m}^3 = 20.4 \text{ g/m}^3$) exceeds its current MAC, and as a result would fail to qualify. The same is true for Nuchem PCI-105, whose redefined REC exceeds its MAC. Since MAC for CIs are defined primarily by their effect on WSIM and changes in electrical conductivity, it is also unlikely that Lubrizol 541 and Nuchem PCI-105 would meet the requirements that 1.5 times the REC not give a WSIM value less than 70 nor result in a change greater than 40 percent in electrical conductivity of a fuel containing static dissipator additive.

One other CI, Tolad 245, only marginally meets the requirements of the proposed revision. The REC was determined to be 21.1 g/m^3 (highest, second only to Tolad 249) thus making its MEC 31.6 g/m^3 . MAC is set at 31.5 g/m^3 by QPL 25017-15. Of the three additives failing to meet the proposed lubricity requirement for MIL-I-25017D, only Tolad 249 is among those CI most commonly used by the AF according to a 1984-1985 survey shown in Figure 9.

An important aspect to be considered in incorporating a lubricity requirement into the current military specification is the need for a specific reference fluid. Under the suggested guidelines for a revised MIL-I-25017D specification, passing or failing a particular product may be dependent on the test fluid in which it is evaluated. Fuel properties are not likely to remain constant in future years. Therefore, for the purpose of approving a candidate CI for the QPL, the reference fluid should be a relatively pure hydrocarbon of a known, consistent, composition. Isopar M meets the above requirements. Its composition is well known and there is a considerable data base available for Isopar M in terms of lubricity testing. Currently, Isopar M containing 30 ppm DCI-4A is used as the primary reference fluid and neat Isopar M, containing no additive, is used as the secondary reference fluid in the standard BOCLE test procedure.

TABLE 3
EFFECT OF REDEFINING RELATIVE EFFECTIVE CONCENTRATION IN JP-4

<i>Corrosion Inhibitor</i>	<i>g/m³</i>					
	<i>Redefined REC (0.60 WSD)</i>	<i>QPL REC</i>	<i>Redefined MEC (1.5× REC)</i>	<i>QPL MEC</i>	<i>QPL MAC</i>	<i>WSD at MAC</i>
IPC-4410	5.3	6	8.0	9.0	22.5	0.48
NALCO 5405	6.8	6	10.2	9.0	22.5	0.50
IPC-4445	9.0	6	13.5	9.0	22.5	0.50
P-3305	8.3	9	12.4	13.5	31.5	0.52
NALCO 5403	9.0	6	13.5	9.0	22.5	0.53
UNICOR J	6.8	6	10.2	9.0	22.5	0.53
MOBILAD F-800	6.8	6	17.0	9.0	22.5	0.52
TOLAD 245	21.1	15	31.6	22.5	31.5	0.54
DCI-6A	8.3	6	12.4	9.0	22.5	0.54
LUBRIZOL 541	13.6	6	20.4	9.0	15.0	0.54
DCI-4A	9.0	6	13.5	9.0	22.5	0.55
HITEC E-580	8.3	6	12.4	9.0	22.5	0.55
PRI-19	14.3	6	21.4	9.0	22.5	0.56
TOLAD 249	> 22.6	6	> 33.9	9.0	22.5	0.61
WELCHEM 91120	8.3	6	13.5	9.0	22.5	0.52
NUCHEM PCI-105	12.8	12	19.2	18.0	18.0	0.54

Notes:

- (1) REC - Relative Effective Concentration
- (2) MEC - Minimum Effective Concentration
- (3) MAC - Maximum Allowable Concentration
- (4) 0.60 WSD - Maximum BOCLE WSD advocated by Air Force
- (5) QPL - QPL-25017-15

R10031/11

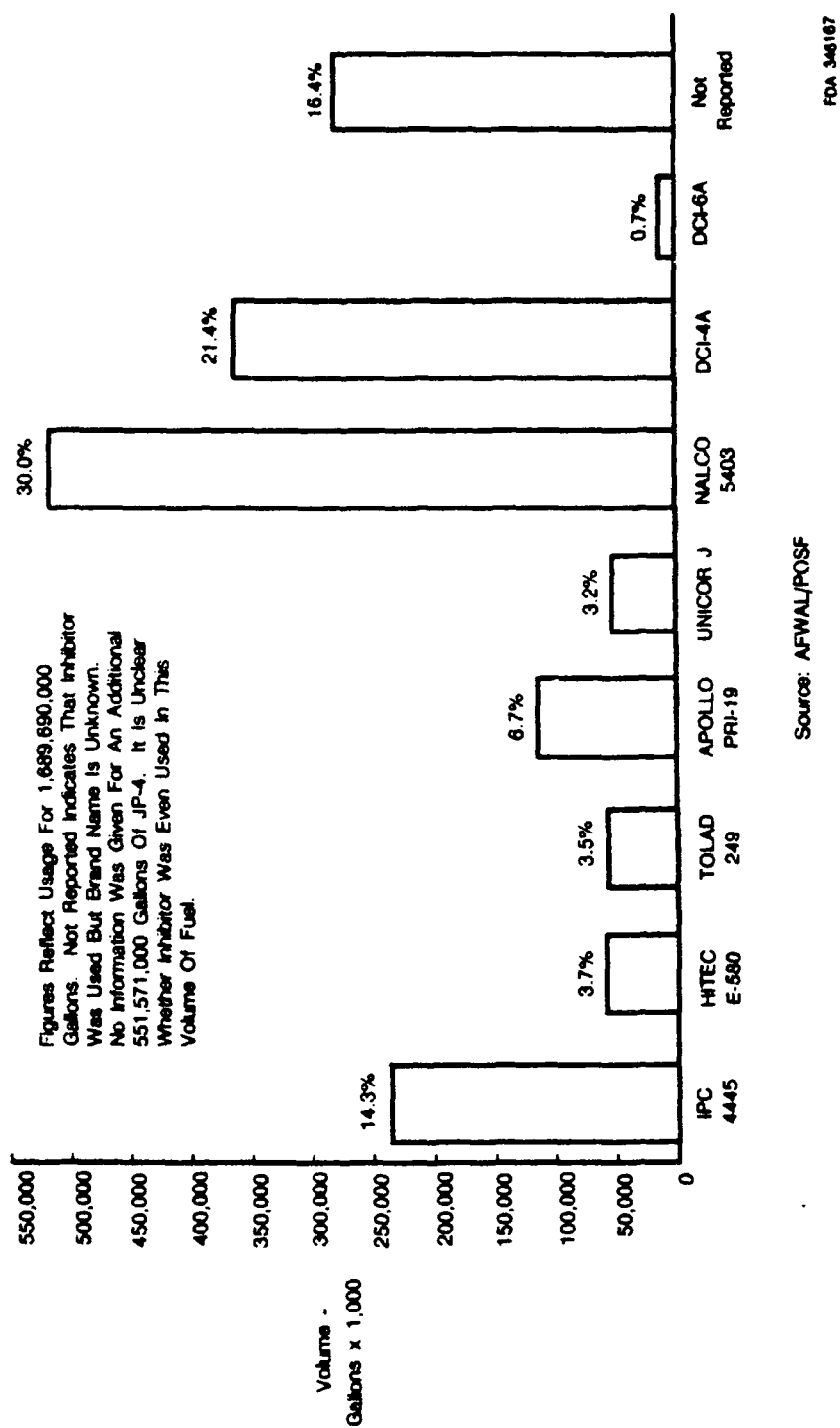


Figure 9. Air Force Corrosion Inhibitor Usage for JP-4 in FY85

3.3 REFINEMENT OF RPHPLC METHOD FOR DETERMINING CI CONTENT IN JET FUELS

3.3.1 Method Development Goals

The objective of this investigation was the development of a relatively simple method for quantifying CI content in jet fuels. The overall goal was the development of a method that could be setup and utilized by Air Force quality assurance laboratories and by refineries. Specific goals set for the method were:

- No sample pretreatment be required.
- Applicability to all approved CI.
- Good precision and accuracy.
- Instrumentation be moderate in cost, readily available and not require special expertise in data interpretation.

3.3.2 Preliminary Method Development - Theory and Mechanism

The theory upon which the current methodology was developed takes advantage of the unique properties of the CI components and the ability of RPHPLC to resolve those components. All of the approved CI use polar, surface-active organic compounds as active ingredients. Most are similar to the trimer, dimer, and monomer linoleic acids. The material safety data sheets for eleven CI describe active ingredients as high molecular weight organic acids or their derivatives. One exception was Tolad 245, which is described as "acylated glycols and alkanolamines." Four CI claim proprietary ingredients only.

The active ingredients used in CI do not lend themselves well to gas chromatography because of their low volatility and would require derivation prior to analysis. Other methods such as infrared spectrometry require extraction of the CI from the fuel matrix prior to detection. In addition, infrared spectroscopy requires expert data interpretation.

However, considering the ionic nature and the molecular size of the CI components, it appeared possible to use liquid chromatography for separation from the fuel matrix prior to detection. An ultraviolet detector was chosen because carboxylic acids absorb fairly well in the ultraviolet region of 200 to 210 nanometers. This type of detector is very stable, sensitive, and readily available.

The preliminary method, described in Reference 8, demonstrated that polar high molecular weight (MW) compounds such as the model compound dilinoleic acid, could be separated from a fuel matrix and quantified down to about one ppm. This was accomplished using a cyanopropyl bonded phase column and a mobile phase composed of 60 percent isopropanol and 40 percent buffer (pH 7.0, 0.396 M KH_2PO_4 /NaOH). This mode of HPLC analysis is termed reverse phase because the mobile phase is more polar in nature than the column stationary phase. Normal phase HPLC is just the opposite.

The apparent separation mechanism of the cyanopropyl column is size exclusion of ionically neutralized CI components. Size exclusion describes the mechanism by which sample molecules elute through a column stationary phase according to their MW, the largest molecules passing through the column first. The order of elution is trimer linoleic acid (MW 845), dimer linoleic acid (MW 565), and mono linoleic acid (MW 282) followed by the fuel matrix components (MW less than 225). The buffer ionically

neutralizes the acids at a pH of 7.0 causing them to elute as narrow zones that increases their detectability. This mechanism is termed ionization suppression (IS). IS is believed to control chromatographic retention by suppressing the ionization of the ionic sample with a mobile phase modifier such as a buffer. IS is most useful in the range of pH 3 to 8 and is normally performed using reversed phase columns (i.e., C-18 (octadecyl), C-8 (octyl), etc.). The result is the elution of compounds exhibiting sharper peaks than peaks produced without the buffer.

In support of this theory, the presence of the KH_2PO_4 /NaOH buffer was necessary as no peaks were observed when pure water was substituted. Further evidence is given by capacity factor (k') calculations that can be defined as a measure of chromatographic efficiency. Small k' values indicate that the solute is not well retained by the column packing. The k' for dilinoleic acid was 0.0 and that of linoleic acid was 0.14. This indicates that both compounds are essentially unretained by the column and implies a separation mechanism of size exclusion facilitated by IS. The result is an on-column separation of CI components from the fuel matrix. The sample with no pretreatment is simply injected directly into the chromatograph for analysis.

A limited survey of CI was conducted using the RPHPLC method. Figure 10 is a chromatogram of DCI-4A obtained by this method. The survey indicated that most CI were, in fact, multi-component and that greater chromatographic resolution between the components would be necessary to achieve good precision and accuracy.

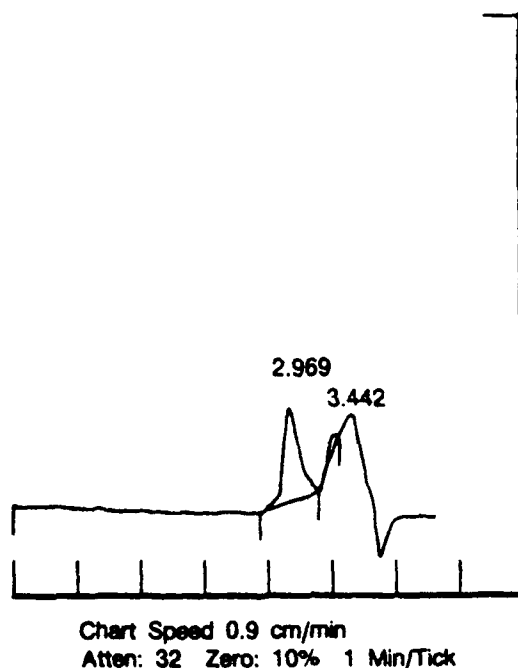


Figure 10. Chromatogram of DCI-4A Using Preliminary RPHPLC Method

3.3.3 Method Modification

This phase of the investigation focused upon modification of the preliminary method to improve the chromatographic resolution of the CI components. Building upon the previous research, it seemed obvious to evaluate the possibility of increasing resolution by increasing the analytical column length. It was found, however, that as column length was increased, the peak widths increased, but with no

improvement in resolution. Adjustments in the mobile phase also failed to provide the needed resolution.

Various other column types were coupled after the cyanopropyl column to evaluate their effect on CI peak resolution. Amino, phenyl, C-18 and C-8 bonded phases were rigorously evaluated, including ion pairing techniques, but no increase in CI component resolution was obtained. In fact, it became apparent that adjustments made to increase k' of the components by mobile phase or column-type changes either had no effect, or so dramatically increased k' that the CI components were lost in the fuel matrix peak.

Ion exchange chromatography (IEC) was also evaluated. Typically, IEC is difficult to use because of the many variables that can affect results. It does, however, offer the capability to precisely vary the chromatographic retention of ionic compounds. The first column investigated was a Particil 10 SAX strong anion exchange (Whatman). Use of this column resulted in too much retention of the CI compounds that caused them to be lost in the fuel matrix peak. Attempts to decrease retention by varying the mobile phase parameters proved unsuccessful. Results did indicate, however, that weak ion exchange columns could likely provide the desired resolution. Subsequently, a carboxymethyl weak ion exchange column (Toyo Sota Co.) was coupled to the cyanopropyl column. Mobile phase ionic strength, pH, and percent organic modifier were varied and evaluated for optimum conditions. DCI-4A in clay treated JP-4 was used to evaluate the test parameters. DCI-4A was chosen because of its complex nature. Information from DuPont Co. indicated that DCI-4A was about 16 percent high polymers or trimer acids, 53 percent dimer acids, 18 percent monomer acids, and 13 percent rosins. It is a byproduct of pine tree cellulose processing.

The low percentage of trimer acid in DCI-4A caused its peak to appear only as a leading shoulder on the dimer peak at a 32 ppm level of DCI-4A. However, a blend of 23 ppm trimer (TLA), 25 ppm dimer (DLA), and 21 ppm monomer linoleic acid (MLA) produced a very good separation. Figure 11-a shows the chromatogram of the additive-free JP-4 used to make the blend while Figure 11-b shows the separation achieved for the trimer, dimer, and monomer peaks. Very good resolution ($R=0.9$) of the trimer acid from the dimer acid was obtained. Previously, the trimer and dimer acids coeluted first, followed by coelution of the monomer acids plus the rosins and polar fuel components.

At this point, several observations were made that caused reconsideration of which additive components or peaks should be used for calibration. These observations are summarized below:

- (1) A review of chromatograms for fuels before and after storage suggested that dimer acid levels may diminish rapidly with time. It appeared that monomer acids, however, diminished at a much lesser rate and may more closely approximate the CI content of a fuel upon receipt of the sample.
- (2) BOCLE data indicated that MLA is an excellent fuel lubricity improver. BOCLE results on three neat JP-4 samples containing 10 ppm MLA, DLA, and TLA, respectively, showed the order of lubricity enhancement to be MLA (0.51mm WSD) greater than DLA (0.55 mm WSD) greater than TLA (0.56 mm WSD).
- (3) A high density fuel sample (87-POSF-2605) received from AFWAL/POSF for determination of fuel lubricity and CI content produced a BOCLE WSD of 0.51 mm. Using the BOCLE curves showing WSD vs CI concentration, a 0.51 mm WSD was indicative of approximately 24 ppm DCI-4A. When calibrating on the dimer peak, RPHPLC analysis indicated a CI content of 9.5 ppm. However, when calibrations were performed on the monomer peak, the CI content measured 22 ppm that agreed significantly better with the BOCLE/CI curves.

One point of concern was that some fuels displayed a small additional peak that coeluted close to the same retention time as the monomer acid peak, and this could be contributing to the integrated peak height of the monomer. The above findings indicated that further method development was necessary to separate the monomer acid peak from the fuel components.

Experience with strong cation exchange chromatography and the information gained with weak ion and strong anion columns, indicated that the use of a strong cation exchange bonded phase column, coupled after the cyanopropyl column, could be made to provide the desired separation. With small mobile phase modifications, the monomer acid peak was resolved from the fuel components as shown in Figure 12 at a retention time of 5.657.

Although complete resolution of the monomer peak was achieved, there was some loss in resolution between the trimer and dimer peaks. This loss, however, did not seem to affect quantitation results. Analysis of the 87-POSF-2605 sample was repeated using DCI-4A standards. As shown in Figure 13, calibration on the dimer peak produced a result of 9.2 ppm, while calibration on the monomer peak indicated 24.4 ppm DCI-4A. It was apparent that more than just the fuel peak (probably the rosins) was resolved from the monomer peak since the size of the resolved fuel peak was much greater with DCI-4A additive than without. Apparently, some minor DCI-4A constituents were included in the fuel peak. This peak will now be referred to as "others" to acknowledge this observation. The retention time differences were due to different flow rates (i.e. 0.5 vs 0.75 mL/min.) used during final method optimization. This affected retention times only.

The mechanism of this separation is a form of ionization suppression (IS) as described earlier. The phenylsulfonate bonded phase of the Particil 10 SCX strong cation exchange column acts to provide the reverse phase-like surface normally used in IS; except there is the cationically active sulfonate moiety present. We found that by adjusting the mobile phase pH to 5.5, the ionic strength of the buffer to 0.02 M, and using a methanol organic modifier at 90 volume percent, good separation of the CI components was obtained. We believed that under these conditions, the sulfonate moiety competes to some degree with the trimer, dimer, and monomer acids and the "other" components for the available sodium and potassium cations. This action tends to slightly increase retention of both the CI and "other" components on the phenyl phase, thus providing the desired separation.

In addition, we believed that only polar molecules and large molecules with molecular weights greater than about 200 are eluted ahead of the fuel matrix peak. As shown in Figure 11, peaks have been observed in additive free fuels with this method. These peaks could be naturally occurring lubricity compounds, auto-oxidation products or other contaminants. Therefore, the method may have applications in the isolation and identification of naturally occurring lubricity agents and in studies of fuel thermal stability.

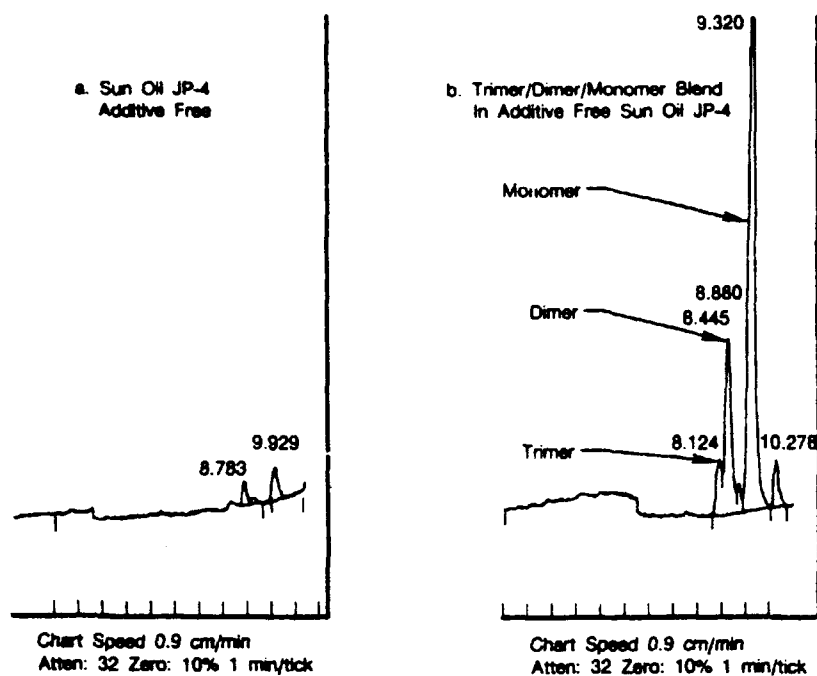


Figure 11. Carboxymethyl Column Separation of Dimer, Trimer and Monomer Linoleic Acids in Additive Free Sun Oil JP-4

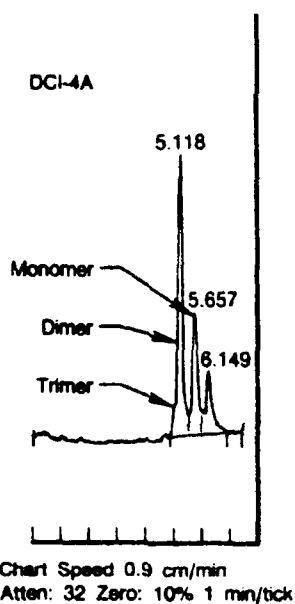


Figure 12. Chromatogram of Resolved Monomer Acid Peak

3.3.4 Finalized Test Method

The instrumentation described in Section II was used for all QPL CI evaluations with the exception of the substitution of the 50-mL sample loop for that of a 20-mL sample loop on the Rheodyne injector valve. The instrumental conditions used in the final method are given here:

A cyanopropyl bonded phase column (Brownlee Labs), 5 micron particle size, 22 cm X 4.6 mm with 3 cm cyanopropyl guard column, coupled to a Particil 10 SCX column, 25 cm x 4.6 mm (Whatman, Clifton, NJ) were used for the separations. It should be noted that the internal diameter of the column connecting tube will affect the CI peak shape as shown in Figure 14. Considerable peak broadening can occur when the tubing is increased from 0.007 inches to 0.01 inches.

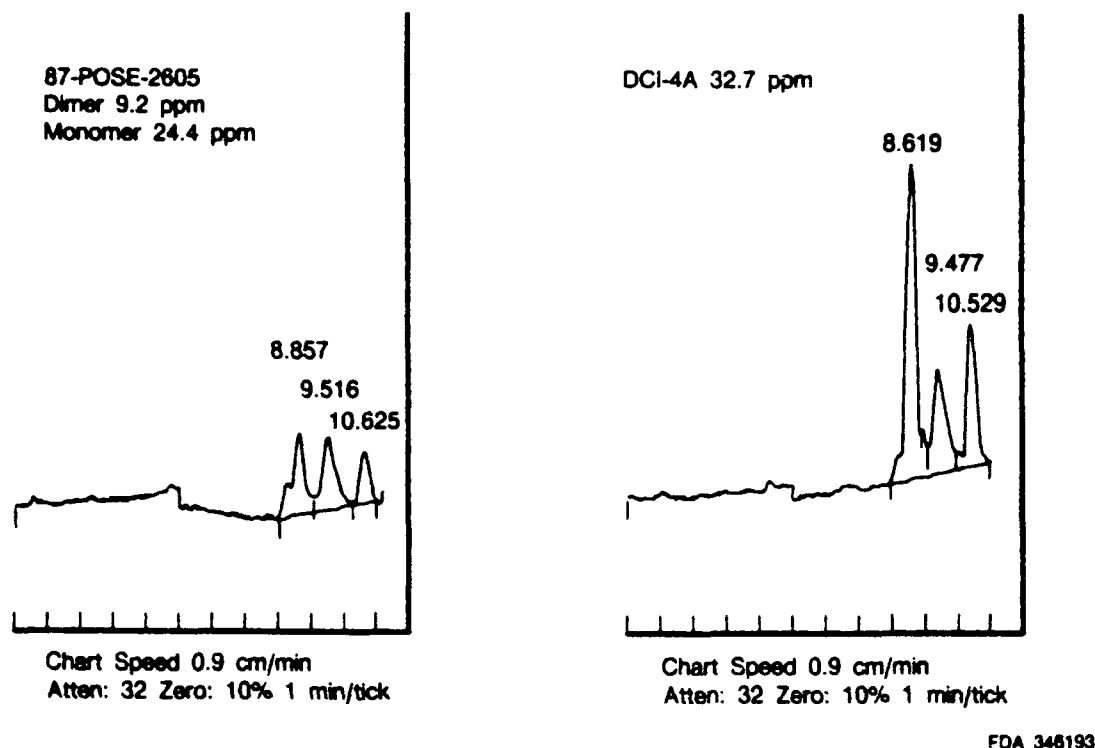


Figure 13. Effect of Storage on CI Concentration: Stored 87 POSF-2605 Sample Versus New Blend

The mobile phase consisted of 90 percent methanol and 10 percent buffer (pH 5.5, 0.02 M KH_2PO_4 /NaOH). The buffer solution was prepared by diluting 50 mL of 0.1 M KH_2PO_4 and 2.5 mL of 0.1 M NaOH to 250 mL with HPLC grade water. The column heater was set to 30-C (86°F) to eliminate the effect of temperature fluctuations on the chromatographic separation. We found that a 1°C column temperature change altered peak retention times. A temperature of 30°C (86°F) was sufficient to overcome this problem and yet not damage the column packing. In addition, baseline fluctuations and system reequilibration time were reduced with column temperature control.

The standards and samples were syringe injected directly into the HPLC system via the 20-mL sample loop. A 500-mL smooth bore glass and Teflon syringe was best for this purpose. The sample loop was first washed with a 500-mL aliquot of sample from the syringe. The second 500-mL aliquot was the analysis sample. This assured complete sample loop filling and that sample loss and cross contamination was minimized. Between samples, the syringe plunger was removed and the syringe was thoroughly cleaned with isopropyl alcohol and acetone. It was then dried with clean nitrogen.

During a chromatographic analysis, the additives eluted first, ahead of the fuel matrix. After the CI products and the bulk of the fuel had eluted, it was necessary to remove the rest of the fuel sample from the column prior to the next analysis. To accomplish this, a programmed wash cycle using the ternary reservoir capability of the chromatograph was used. Table 4 shows time, reservoir, percent, and flow rate

in mL/minute. Reservoirs A, B and C contained isopropanol, methanol/buffer solution, and HPLC grade water, respectively. Analysis time, including wash and reequilibration of the columns, was 35 minutes.

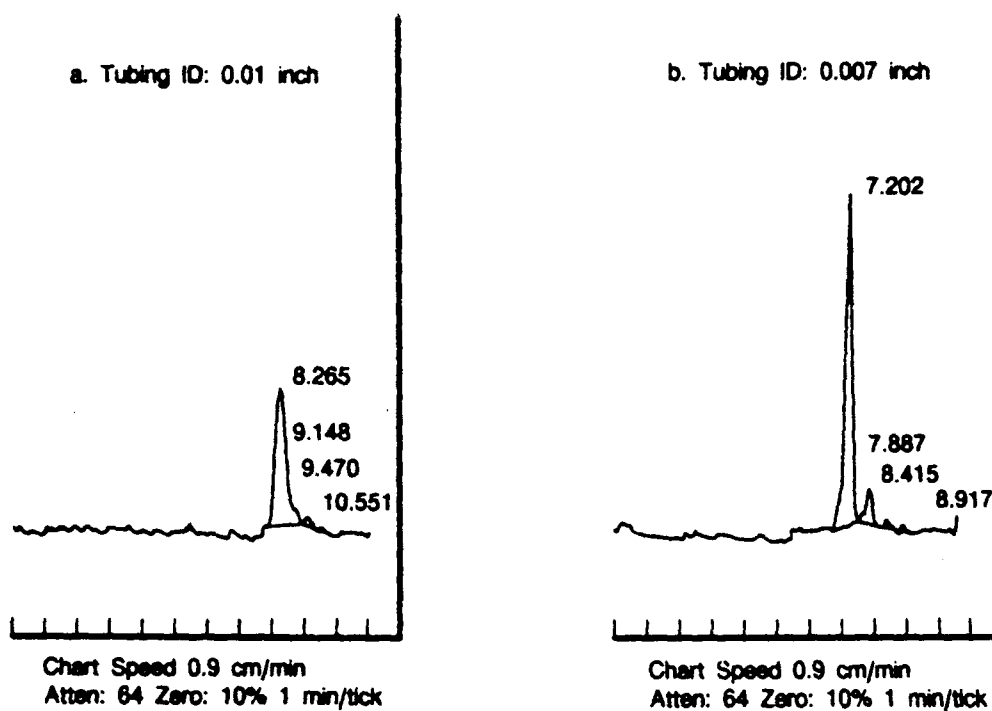


Figure 14. Effect of Connecting Tubing I.D. on Peak Broadening

TABLE 4.
COLUMN WASH GRADIENT PROGRAM

Time	Reservoir			Flow
	%A	%B	%C	
0.00	0	100	0	0.75
8.00	0	100	0	0.75
8.50	0	0	100	1.0
9.00	50	0	50	
9.50	50	0	50	
10.00	100	0	0	
16.00	100	0	0	
16.50	0	0	100	
17.00	0	0	100	
17.50	0	50	50	
18.00	0	100	0	
28.00	0	100	0	1.0
28.50	0	100	0	0.75
35.00	0	100	0	0.75

R19081/11

Prior to shutting the system down, pure water was pumped through the columns for at least five minutes at 0.75 mL/minute followed by 20 minutes of isopropanol at 0.75 mL/minute. This removed all buffer salts and preserved the system and columns against bacterial growth and corrosion.

3.3.5 Applicability to QPL-25017-15

Standards were prepared and analyzed at four different concentrations for each QPL CI. These results were subjected to linear regression analyses. Appendix F contains the calibration chromatograms for the 15 approved CI. With the exception of Lubrizol 541, Tolad 245, and Tolad 249 the principal ingredient seems to be dimer acids. Lubrizol 541 appears to contain mainly monomer acid types. Tolad 249 appears to contain a relatively high percentage of trimer acids at a retention time of 4.89 minutes. Tolad 245 peak shape and retention times do not correspond to trimer, dimer or monomer acids. This is because the active ingredients are not acids, but "acylated glycols and alkanolamines." It is interesting to note that the method is applicable to these compounds as well. Figures F-16 and F-17 of Appendix F show chromatograms of the CT JP-4 base fuel and of trimer linoleic, dimer linoleic, and monomer linoleic acids, respectively. Comparison of these retention times with those obtained for the various CI additives is helpful in their understanding.

Table 5 contains the SEE, correlation coefficient, and y-intercept for each CI. The worst correlation coefficient was that of IPC 4410 with a 0.993. The best was Tolad 245 at 1.00. SEE varied from a high of 2.0 ppm for IPC 4410 to a low of 0.12 ppm for Tolad 245.

TABLE 5
LINEAR REGRESSION STATISTICS FOR CI CALIBRATION STANDARDS

<i>CI Product Name</i>	<i>Correlation Coefficient</i>	<i>SEE</i>	<i>Y-Axis Intercept</i>
DCI-4A	0.997	1.17	-2.0
DCI-6A	0.995	1.87	-1.4
HITEC 580	0.999	0.81	-1.9
IPC 4410	0.993	2.00	-4.5
IPC 4445	0.999	0.24	-1.3
LUBRIZOL 541	0.998	0.98	-1.9
MOBILAD F800	0.999	0.64	0.1
NALCO 5403	0.994	1.68	-3.4
NALCO 5405	0.994	1.27	-5.4
PCI 105	0.999	0.74	-1.1
PRI 19	0.997	1.08	-1.8
TOLAD 245	1.000	0.12	-5.5
TOLAD 249	0.997	1.47	0.7
UNICOR J	0.998	1.05	-2.5
WELCHEM 91120	0.999	0.87	-2.7

R18031/11

Extreme care and good analytical technique were required when making up CI standards. The stock standard was prepared by weighing the additive concentrate to four decimal places in a clean Teflon bottle then volumetrically diluted with clay treated or additive free fuel. Serial dilutions into appropriate volumetrically pipetted quantities of fuel diluent, in Teflon, were then made. The pipets used were thoroughly cleaned and then rinsed several times with stock standard prior to making the working standards. It was found that failure to follow this procedure would yield either erroneously high results for unknowns if a single point external standard calibration was made, or a low correlation coefficient and SEE if a calibration line was used.

The type fuel used as diluent did not appear to matter. Good results were obtained using CT JP-4

standards to analyze JP-5 and JP-8X type fuels. However, until more experience is gained, the use of clay treated fuels of the type to be analyzed for standards preparation is recommended.

3.3.6 Chromatograms

Upon first inspection, the chromatograms in Appendix F appear to have unique fingerprints by which each additive might be identified. Close examination, however, reveals that many have essentially the same fingerprints, especially at lower concentration levels. Further, the spectra will probably be altered after the effects of storage and transport have acted upon the CI/fuel blend. The dramatic effect of CI depletion can be seen in Figure 13, which compares the chromatogram of a DCI-4A fuel blend subjected to short term storage to that of a freshly blended sample.

The use of a single compound such as dilinoleic acid to quantify these additives does not appear to be possible. The UV detector responses to different CI at the same concentration do not correlate well when calibrating on the DLA peak alone. There are a number of possible explanations for this lack of correlation:

- Differences in percent active ingredient between CI.
- Variability due to different isomeric forms of dimer linoleic acid. Emery Chemical Co. indicated that they could not verify the molecular structure of their 97 percent pure dilinoleic acid used in this study. The dimer linkage can, apparently, be very complex.
- Dimer acids, other than linoleic, could be used as active ingredients in CI. These dimer acids, differing in carbon number or placement of the double bonds could have similar chromatographic retention times, but produce different UV detector responses.

It is, therefore, necessary to know what additive was blended into a fuel in order to obtain the best analytical results. This would limit the accuracy of determinations made on co-mingled bulk storage tanks where several different CI may be present. However for quality assurance testing conducted by suppliers (i.e., refiners) and users (e.g., Air Force bases), this is not considered a severe limitation since, in most cases, the type of CI added to a fuel is known by the user.

SECTION 4.0

CONCLUSIONS AND RECOMMENDATIONS

The technical effort performed under this program fulfilled the need to reevaluate CI in terms of lubricity enhancement and refine the RPHPLC method for determining CI content in jet fuels. It also produced functional references, working curves and spectral fingerprints, to assist in predicting and circumventing potential lubricity related fuel system problems. The work resulted in the following accomplishments:

- Establishment of the concentration required for each QPL CI to provide minimum lubricity improvement based on a 0.60 mm WSD.
- Generation of polynomial curve fits profiling CI efficiency in jet fuels.
- Comparison of maximum lubricity improvement attainable for each CI at maximum allowable concentration.
- Approach for incorporating a lubricity requirement into MIL-I-25017.

- Refinement of the RPHPLC method and determination of its applicability to QPL CI.
- Generation of an RPHPLC spectral library of QPL CI.

4.1 CORROSION INHIBITOR EVALUATIONS

Conclusions drawn from lubricity evaluations of the CI approved under MIL-I-25017D included the following:

- In general, fuel type has little effect on CI performance.
- Temperature appears to have a significant effect on fuel lubricity. Under standard operating conditions, however, assessment of these effects are beyond the current capabilities of the BOCLE.
- CI have unique performance profiles in terms of the concentrations required to achieve acceptable lubricity and the maximum lubricity improvement attainable at maximum allowable concentrations.
- Effective CI concentrations for lubricity improvement range from 6.6 to greater than 22.8 g/m³.
- Maximum effective CI concentrations, at which no further reduction in WSD is realized, range from 9 to 31.5 g/m³.
- Only six of the CI evaluated exhibit acceptable lubricity improvement at the 'minimum effective concentration' levels defined by QPL-25017-15.
- CI fall into three distinctive performance groups in relation to total reduction in WSD achieved at maximum allowable concentration and concentration required to achieve a 0.60 mm WSD.
- IPC-4410 was found to be the most effective CI at improving the lubricity properties of jet fuels, while Tolad 249 was found to be the least effective.

Recommendations for further study include the selection of a specific reference fluid for the purpose of approving CI for the QPL. It is also recommended that future work evaluate the currently approved CI in the selected reference fluid at a 1000-g applied load in accordance with the latest CRC revision of the BOCLE test procedure. It is proposed that performance profiles be generated over a range of nine concentrations and the relative effective concentration be established. A correlation between previous work conducted at 500-g load and that performed at the 1000-g load should be presented.

4.2 PROPOSED MIL-I-25017 LUBRICITY REQUIREMENT

A thorough review of MIL-I-25017, current Air Force quality assurance requirements, and fleet support needs resulted in the following conclusions:

- A lubricity requirement can be easily incorporated into MIL-I-25017 with minimal changes to the current specification and no significant effect on other criteria used in qualifying candidate CI.
- Inclusion of the lubricity requirement can be most readily accomplished by redefining REC while leaving the requirements for MEC and MAC unchanged.
- The effect of redefining REC is that MEC would be increased for all but two of the currently approved CI.

- Three CI (Tolad 249, Lubrizol 541, and Nuchem PCI-105) would be disqualified based on the proposed MIL-I-25107 revision. A fourth CI, Tolad 245, exhibited marginal performance and should be closely scrutinized before requalifying.

4.3 REFINEMENT OF RPHPLC METHOD

The RPHPLC analytical method has been refined and can quantitatively determine all 15 approved CI in jet fuels. The method requires no sample pretreatment, allowing direct injection of the fuel to be analyzed. The method has been shown to provide good precision and accuracy. Readily available, moderate cost instrumentation is used. Expert data interpretation is not required and the method can be automated if desired. Additionally, the method may be used in quality control for detecting changes in CI concentrations due to losses during transportation and storage. Identification of an unknown CI based on its chromatogram alone, is currently not within scope of this method due to many CI exhibiting essentially the same spectral fingerprint. This is not considered a severe limitation since, in most cases, the specific CI added to a fuel is known by the user.

It is recommended that the RPHPLC test method for CI be evaluated in a second laboratory. This would allow for procedural "loop holes" to be closed, if found. After this, a round-robin evaluation of the method should be conducted prior to its general use.

REFERENCES

1. Bradley, R. P. Trip Report - Travel Order No. TA 1201 B, Fuel Lubricity Problems, TF 30 Problems Solving Conference, February 3, 1987.
2. Martel, C. R., R. P. Bradley, et al, "Aircraft Turbine Engine Fuel Corrosion Inhibitors and Their Effects on Fuel Properties," AF Aero Propulsion Laboratory Report, AFAPL-TR-74-20, July 1974.
3. Hayes, Paul C., "Development of an Improved Fuel Filtration-Time Test," AFAPL-TR-74-33, September 1974.
4. McLaren, G.W., J.A. Krynitsky, and R.N. Hazlett, "Effect of Corrosion Inhibitors on Jet Fuel Filtration," Naval Research Laboratory Memorandum Report No. 1660, November 1965.
5. Biddle, T. B., R. J. Meehan, P. A. Warner, "Standardization of Lubricity Test," First Interim Report, F33615-85-C-2508, August 1987.
6. "Determination of the Dilinoleic Acid Content of Aviation Turbine Fuels," NATO STANAG 3390, Addition No. 5, Annex C.
7. Wechter M. A., "Quantitative Determination of Corrosion Inhibitor Levels in Jet Fuels by HPLC," NRL Contract No. N00014-85-M-0248.
8. Edwards, W. H., T. B. Biddle, and P. A. Warner, "Determination of Corrosion Inhibitor Content in Aviation Fuels," Topical Report No. 7, F33615-85-C-2508, March 1987.
9. Grabel, L., "Lubricity Properties of High Temperature Jet Fuel," Naval Air Propulsion Test Center, AD/A-045 467, August 1977.
10. Masters, A. I., J. L. Weston, T. B. Biddle, J. A. Clark, M. Gratoon, C. B. Graves, G. M. Rone and C. D. Stone, "Additional Development of the Alternate Test Procedure for Navy Aircraft Fuels," Final Report for Period September 1984 to March 1986, Contract N00140-84-C-5533, March 1987.

APPENDIX A ISOPAR M PROPERTY DATA SHEET

TYPICAL PROPERTIES

The values shown here are representative of current production. Some are controlled by manufacturing specifications, while others are not. All of them may vary within modest ranges.

Solvency	Test Method	General Properties (cont.)	Test Method
Aniline point, C (F)	89 (192) ASTM D611	129-129m	+0.08
Solubility parameter	7.3 Calculated	130-150m	+0.05
Kauri butanol value	27 ASTM D1133	Color, Saybolt	+30 ASTM D156
		Color stability, 16 hr at 100C (212F)	+30
Volatility			
Flash point, FM, C (F)	80 (176) ASTM D93	Gravity, API	19.2 ASTM D287
Fire point, COC, C (F)	93 (200) ASTM D92	Specific gravity, 15.6/15.6C	0.84 Calculated
		kg/m ³	781
Auto-ignition temperature, C (F)	338 (640) ASTM D288	lb/gal	6.53 Calculated
Flammability limits in air, vol% at 21C (70F)	0.6-6.5 Calculated	Refractive Index, 20C	1.4362 ASTM D1218
Distillation, C (F)	ASTM D86	Viscosity	ASTM D445
1BP	207 (405)	cp at 25C	2.16
5%	212 (413)	cp at 100C	0.72
10%	213 (415)	cSt at 6C	6.60
50%	223 (434)	cSt at 25C	3.35
90%	241 (466)	Odor, bulk	very slight Exxon Method
95%	247 (476)	Odor, residual	none Exxon Method
Dry point	254 (490)	Odor, stability	excellent Exxon Method
FBP	260 (500)	Freezing point, C (F) < -60	
		(< -76)	
Vapor pressure, kPa at 18C	4.1 ASTM D2551	Specific heat, liquid,	
Vapor pressure, psia at 100F	0.6	kJ/kg/C (Btu/lb/F)	
		at 18C (60F)	205 (0.49) Calculated from
		at 56C (130F)	2.26 (0.54) enthalpy data
		at 94C (200F)	2.19 (0.57)
Composition		Heat of vaporization,	Est. from Maxwell's
Hydrocarbon type, mass %		kJ/kg (Btu/lb)	Data Book of
Total saturates	99.5 Mass spectrometer	at 100C (212F)	Hydrocarbons and
Aromatics	0.4 UV Analysis	at BP	report of API
Trace compounds			Project 44 (1954)
Sulfur			
Docu test	pass ASTM D484	Surface Properties	
Total sulfur, ppm	1 Microcoulometer	Demulsibility	excellent Exxon Method
Polymers, ppm	<1 Exxon Method	Interfacial tension,	
		dynes/cm at 25C	51.0 ASTM D471
General Properties		Surface tension	
Average molecular weight	191 Cryogenic	dynes/cm at 25C	21.8 du Noüy
Bromine index (1)	230 ASTM D2710		
Copper corrosion, 1/2 hr			
at BP	2 ASTM D150	Toxicological Data	
Unsulphated residue,		Inhalation, TLV(2) ppm	300(1)
wt%	99+ ASTM D483	Acute Oral LD50 (Rat), g/kg	>10
UV absorbance	FDA Method	Acute Dermal LD50 (Rabbit),	
260-319 m	<1.5 21 CFR 172.882	g/kg	<1.1

(1) Bromine index = Bromine number x 1000

(2) TLV is a registered trademark of the American Conference of Governmental Industrial Hygienists. It is the threshold limit value or occupational exposure limit: the time weighted average concentration for a normal 8 hour workday, 40 hour workweek, to which nearly all workers may be exposed repeatedly without adverse effect. Refer to the most recent Material Safety Data Sheet for the latest recommended maximum exposure limit.

(3) A TLV has not been established for this product. The value shown has been recommended by Exxon Corporation Medical Research based in consideration of available toxicological data. Additional data are being obtained to help define a recommended occupational exposure limit more conclusively.

Qualifications Certified
January 1987

APPENDIX B
QUALIFIED PRODUCTS LIST
OF
PRODUCTS QUALIFIED UNDER MILITARY SPECIFICATION
MIL-I-25017

QPL-25017-15
Superceding
QPL-25017-14
11 April 1984
FSC 6850

This list has been prepared for use by or for the Government in the acquisition of products covered by the subject specification and such listing of a product is not intended to and does not connote endorsement of the product by the Department of Defense. All products listed herein have been qualified under the requirements for the product as specified in the latest effective issue of the applicable specification. This list is subject to change without notice; revision or amendment of this list will be issued as necessary. The listing of a product does not release the supplier from compliance with the specification requirements.

The activity responsible for this qualified products list is the Air Force, ASD/ENES, Wright-Patterson AFB OH 45433-6503.

The qualified products are listed in the QPL in two categories.

Category 1 additives are approved for use in fuels conforming to VV-F-800, VV-G-1690, MIL-G-3056, MIL-T-5624, MIL-C-7024, MIL-T-25524, MIL-F-25558, and MIL-T-83133.

Category 2 additives are approved for use in fuels conforming to MIL-T-5624, MIL-C-7024, MIL-F-25558, and MIL-T-83133.

The QPL lists the Government designation, which is also the additive identification, the approving office and date of the letter of approval, the manufacturer's name and address, and additive specifications.

<u>Government Designation</u>	<u>Manufacturer's Designation</u>	<u>Test or Qualification Reference</u>	<u>Manufacturer's Name And Address</u>
<i>Category 1</i>			
<i>PRI-19</i>			
Relative effective conc (g/m)	6	AFWAL/POSF Ltr, 9 Apr 85	Apollo Technologies International Corp. 130 Speedwell Ave Morris Plains NJ 07950
Minimum effective conc (g/m)	9		
Maximum allowable conc (g/m)	22.5		
Density at 15°C (kg/)	0.88-0.92		Plant: c/o Kramer Chemical Inc. Atlantic Ave and Delaware River Camden NJ 08104
Viscosity (centistokes at 37.8°C)	80-120		
Flashpoint (0°C, minimum)	60		
Neutralization number	100-120		
Ash content (%, maximum)	0.10		
Pour point (°C, maximum)	-18		

Note: This page scanned into report. Error in concentration unit: g/m=g/m³

<u>Government Designation</u>	<u>Manufacturer's Designation</u>	<u>Test or Qualification Reference</u>	<u>Manufacturer's Name And Address</u>
DCI-4A			
Relative effective conc (g/m)	6	AFWAL/POSF Ltr, 15 Aug 83	E.I. duPont deNemours and Company C&P Dept Specialty Chemicals Div Wilmington DE 19898
Minimum effective conc (g,m)	9		
Maximum allowable conc (g/m)	22.5		
Density at 15°C (kg/L)	0.93-0.95		
Viscosity (centistokes at 37.8°C)	48-68		
Flashpoint (°C, minimum)	27		
Neutralization number	100-124		
Ash content (%, maximum)	0.10		
Pour point (°C, maximum)	-18		
DCI-6A			
Relative effective conc (g/m)	6	AFWAL/POSF Ltr, 15 Aug 83	
Minimum effective conc (g/m)	9		
Maximum allowable conc (g/m)	22.5		
Density at 15°C (kg/L)	0.93-0.95		
Viscosity (centistokes at 37.8°C)	40-60		
Flashpoint (°C, minimum)	27		
Neutralization number	120-150		
Ash content (%, maximum)	0.10		
Pour point (°C, maximum)	-18		

Note: This page scanned into report. Error in concentration unit: g/m=g/m³

<u>Government Designation</u>	<u>Manufacturer's Designation</u>	<u>Test or Qualification Reference</u>	<u>Manufacturer's Name And Address</u>
HITEC 580			
Relative effective conc (g/m)	6	AFWAL/POSF Ltr, 15 Aug 83	Ethyl Petroleum Additives Division 20 S. Fourth Street St Louis MO 63102-1886
Minimum effective conc (g/m)	9		
Maximum allowable conc (g/m)	22.5		
Density at 15°C (kg/L)	0.91-0.94		Plant: Route 3 Saugent IL 62201
Viscosity (centistokes at 37.8°C)	120-160		
Flashpoint (°C, minimum)	66		
Neutralization number	80-100		
Ash content (%, maximum)	0.10		
Pour point (°C, maximum)	-18		
LUBRIZOL 541'			
Relative effective conc (g/m)	6	AFWAL/POSF Ltr, 22 Mar 84	Lubrizol Corporation PO Box 428 Painesville OH 44077
Minimum effective conc (g/m)	9		
Maximum allowable conc (g/m)	15		
Density at 15°C (kg/L)	0.94-0.97		
Viscosity (centistokes at 37.8°C)	34-48		
Flashpoint (°C, minimum)	14		
Neutralization number	152-172		
Ash content (%, maximum)	0.10		
Pour point (°C, maximum)	-18		

Note: This page scanned into report. Error in concentration unit: g/m=g/m³

<u>Government Designation</u>	<u>Manufacturer's Designation</u>	<u>Test or Qualification Reference</u>	<u>Manufacturer's Name And Address</u>
NALCO 5403			
Relative effective conc (g/m)	6	AFWAL/POSF Ltr. 15 Aug 83	Nalco Chemical Company 77011 Highway 90A Sugar Land TX 77478
Minimum effective conc (g/m)	9		
Maximum allowable conc (g/m)	22.5		
Density at 15°C (kg/L)	0.92-0.94		
Viscosity (centistokes at 37.8°C)	25-50		
Flashpoint (°C, minimum)	38		
Neutralization number	70-100		
Ash content (%, maximum)	0.10		
Pour point (°C, maximum)	-18		
TOLAD 245			
Relative effective conc (g/m)	15	AFWAL/POSF Ltr. 15 Aug 83	Petrolium Corporation 369 Marshall Ave St Louis MO 63119
Minimum effective conc (g/m)	22.5		
Maximum allowable conc (g/m)	31.5		Plant: 369 Marshall Ave St Louis MO 63119
Density at 15°C (kg/L)	0.94-0.96		
Viscosity (centistokes at 37.8°C)	7-14		
Flashpoint (°C, minimum)	32		
Neutralization number	50-62		
Ash content (%, maximum)	0.10		
Pour point (°C, maximum)	-18		

Note: This page scanned into report. Error in concentration unit: g/m=g/m³

<u>Government Designation</u>	<u>Manufacturer's Designation</u>	<u>Test or Qualification Reference</u>	<u>Manufacturer's Name And Address</u>
<i>UNICOR J</i>			
Relative effective conc (g/m)	6	AFWAL/POSF Ltr, 15 Aug 83	UOP, Inc.
Minimum effective conc (g/m)	9		Box 5017
Maximum allowable conc (g/m)	22.5		20 Algonquin Road
Density at 15°C (kg/L)	0.93-0.94		Des Plaines IL 60017-5017
Viscosity (centistokes at 37.8°C)	65-85		and
Flashpoint (°C, minimum)	52		Universal-Matthey
Neutralization number	110-126		Products (France) S.A.
Ash content (%, maximum)	0.10		Rue D'epinal
Pour point (°C, maximum)	-18		Calais 62100 France

Category 2

<i>IPC 4410</i>			
Relative effective conc (g/m)	6	AFWAL/POSF Ltr, 15 Aug 83	ChemLink, Incorporated
Minimum effective conc (g/m)	9		16950 Wallisville Rd
Maximum allowable conc (g/m)	22.5		Houston TX 77049
Density at 15°C (kg/L)	0.94-0.96		
Viscosity (centistokes at 37.8°C)	220-270		
Flashpoint (°C, minimum)	60		
Neutralization number	130-155		
Ash content (%, maximum)	0.10		
Pour point (°C, maximum)	-18		

Note: This page scanned into report. Error in concentration unit: g/m=g/m³

<u>Government Designation</u>	<u>Manufacturer's Designation</u>	<u>Test or Qualification Reference</u>	<u>Manufacturer's Name And Address</u>
<i>IPC 4445</i>			
Relative effective conc (g/m)	6	AFWAL/POSF Ltr, 1 Dec 82	
Minimum effective conc (g/m)	9		
Maximum allowable conc (g/m)	22.5		
Density at 15°C (kg/L)	0.91-0.93		
Viscosity (centistokes at 37.8°C)	10-40		
Flashpoint (°C, minimum)	60		
Neutralization number	80-100		
Ash content (%, maximum)	0.10		
Pour point (°C, maximum)	-18		
<i>MOBILAD 7800</i>			
Relative effective conc (g/m)	6	AFWAL/POSF Ltr, 15 Aug 83	Mobil Chemical Company Chemical Products Div PO Box 250 Edison NJ 08816
Minimum effective conc (g/m)	9		
Maximum allowable conc (g/m)	22.5		
Density at 15°C (kg/L)	0.84-0.88		
Viscosity (centistokes at 37.8°C)	23-35		
Flashpoint (°C, minimum)	38		
Neutralization number	80-100		
Ash content (%, maximum)	0.10		
Pour point (°C, maximum)	-43		

Note: This page scanned into report. Error in concentration unit: g/m=g/m³

<u>Government Designation</u>	<u>Manufacturer's Designation</u>	<u>Test or Qualification Reference</u>	<u>Manufacturer's Name And Address</u>
<i>NALCO 5405</i>			
Relative effective conc (g/m)	6	AFWAL/POSF Ltr, 15 Aug 83	Nalco Chemical Company 7701 Highway 90A Sugar Land TX 77478
Minimum effective conc (g/m)	9		
Maximum allowable conc (g/m)	22.5		
Density at 15°C (kg/L)	0.91-0.95		
Viscosity (centistokes at 37.8°C)	40-70		
Flashpoint (°C, minimum)	60		
Neutralization number	115-145		
Ash content (%, maximum)	0.10		
Pour point (°C, maximum)	-29		
<i>NUCHEM PCI-105</i>			
Relative effective conc (g/m)	12	AFWAL/POSF Ltr, 12 Sep 86	NuChem Corp Maple Lane PO Box U Blairstown NJ 07825
Minimum effective conc (g/m)	18		
Maximum allowable conc (g/m)	18		
Density at 15°C (kg/L)	0.89-0.93		
Viscosity (centistokes at 37.8°C)	100-150		
Flashpoint (°C, minimum)	60		
Neutralization number	95-120		
Ash content (%, maximum)	0.10		
Pour point (°C, maximum)	-18		

Note: This page scanned into report. Error in concentration unit: g/m=g/m³

<u>Government Designation</u>	<u>Manufacturer's Designation</u>	<u>Test or Qualification Reference</u>	<u>Manufacturer's Name And Address</u>
TOLAD 249			
Relative effective conc (g/m)	6	AFWAL/POSF Ltr. 15 Aug 83	Petrolite Corporation Industrial chemicals Group 369 Marshall Ave St Louis MO 63119
Minimum effective conc (g/m)	9		
Maximum allowable conc (g/m)	22.5		
Density at 15°C (kg/L)	0.89-0.93		
Viscosity (centistokes at 37.8°C)	7-25		
Flashpoint (°C, minimum)	32		
Neutralization number	85-120		
Ash content (%, maximum)	0.10		
Pour point (°C, maximum)	-29		
WELCHEM 91120			
Relative effective conc (g/m)	6		Welchem, Inc. 11200 Bay Area Blvd Houston TX 77507
Minimum effective conc (g/m)	9		
Maximum allowable conc (g/m)	22.5		
Density at 15°C (kg/L)	0.93-0.96		
Viscosity (centistokes at 37.8°C)	50-70		
Flashpoint (°C, minimum)	65		
Neutralization number	90-110		
Ash content (%, maximum)	0.10		
Pour point (°C, maximum)	0°C		

Note: This page scanned into report. Error in concentration unit: g/m=g/m³

APPENDIX C
LUBRICITY TEST DATA
LIST OF TABLES

Table	Title
C-1	Effect of Corrosion Inhibitors in Isopar M
C-2	Effect of Corrosion Inhibitors in Clay Treated JP-4
C-3	Effect of Corrosion Inhibitors in Clay Treated JP-8
C-4	Effect of Corrosion Inhibitors in Clay Treated JP-5

Table C-1. Effect of Corrosion Inhibitors in ISCPAR M

Corrosion Inhibitor	Temperature °C	Base Fuel	15 ppm	30 ppm	60 ppm	90 ppm	120 ppm	150 ppm	200 ppm	300 ppm	420 ppm
PRI 19	25	0.80	0.76	0.76	0.4	0.71	0.66	0.62	0.61	0.54	
	75	1.12	1.05	1.03	0.96	0.91	0.88	0.86	0.82	0.76	
HITEC E-580	25	0.75	0.78	0.76	0.76	0.69	0.62	0.60	0.54	0.52	
	75	1.13	0.97	1.05	0.84	0.92	0.85	0.86	0.78	0.73	
ICI-4A	25	0.76	0.74	0.72	0.67	0.60	0.54	0.54	0.50	0.48	
	75	1.01	1.04	0.98	0.90	0.86	0.81	0.68	0.64	0.58	
ICI 6A	25	0.78	0.76	0.76	0.71	0.65	0.60	0.54	0.50	0.48	
	75	1.19	1.08	1.00	0.84	0.90	0.89	0.82	0.76	0.68	
LUBRIZOL 541	25	0.81	0.80	0.78	0.74	0.70	0.68	0.62	0.56	0.54	
	75	1.03	0.98	0.94	0.74	0.76	0.74	0.80	0.77	0.59	
NALCO 5403	25	0.80	0.80	0.72	0.74	0.74	0.61	0.56	0.52	0.52	
	75	1.14	1.08	1.06	0.80	0.81	0.68	0.84	0.73	0.66	
TOLAD 245	25	0.76	0.75	0.76	0.72	0.74	0.70	0.64	0.60	0.60	0.55
	75	1.08	1.13	0.90	0.81	0.83	0.90	0.86	0.66	0.66	0.68
UNICOR J	25	0.80	0.72	0.68	0.64	0.58	0.56	0.52	0.50	0.47	
	75	1.12	0.86	1.02	0.82	0.79	0.82	0.91	0.84	0.77	
IPC 4410	25	0.78	0.77	0.74	0.67	0.62	0.57	0.54	0.54	0.52	
	75	1.08	1.05	0.89	0.80	0.80	0.83	0.88	0.82	0.78	
MOBILAD F800	25	0.74	0.74	0.74	0.70	0.62	0.57	0.55	0.52	0.49	
	75	1.12	0.97	0.87	0.75	0.86	0.85	0.82	0.77	0.70	
NALCO 5405	25	0.76	0.78	0.76	0.72	0.67	0.60	0.56	0.52	0.48	
	75	1.06	0.99	0.97	0.82	0.80	0.84	0.83	0.82	0.69	
TOLAD 249	25	0.78	0.78	0.75	0.73	0.76	0.74	0.72	0.66	0.59	
	75	1.06	1.02	1.02	1.01	0.76	0.72	0.78	0.84	0.82	0.47
P 3305	25	0.74	0.76	0.76	0.68	0.66	0.56	0.54	0.52	0.47	
	75	1.09	1.06	0.86	0.90	0.86	0.82	0.78	0.77	0.66	0.60
IPC 445	25	0.81	0.78	0.76	0.75	0.72	0.68	0.63	0.58	0.54	
	75	0.94	1.08	1.09	1.07	0.92	1.02	0.92	0.88	0.79	
WELCHEM 91120	25	0.80	0.80	0.78	0.76	0.68	0.62	0.60	0.59	0.56	
NUCHEM PCT-105	25	0.79	0.77	0.77	0.72	0.68	0.66	0.64	0.58	0.55	

Table C-2. Effect of Corrosion Inhibitors in Clay Treated JP-4

Corrosion Inhibitor	Temperature °C	Base Fuel	1.5 ppm	3.0 ppm	6.0 ppm	9.0 ppm	12.0 ppm	15.0 ppm	20.0 ppm	30.0 ppm	42.0 ppm
PRI-19	25	0.84	0.79	0.74	0.71	0.66	0.66	0.64	0.62	0.56	
	75	0.70	0.57	0.74	0.78	0.66	0.66	0.58	0.70	0.62	
HITEC E 590	25	0.83	0.78	0.74	0.67	0.62	0.58	0.58	0.57	0.55	
	75	0.52	—	—	—	0.61	0.68	0.66	0.60	0.56	
IXT 4A	25	0.82	0.78	0.74	0.70	0.66	0.58	0.56	0.54	0.55	
	75	0.78	0.52	0.58	0.63	0.60	0.58	0.58	0.56	0.52	
IXT 6A	25	0.81	0.76	0.76	0.68	0.62	0.59	0.54	0.56	0.54	
	75	0.79	—	—	—	0.72	0.65	0.62	0.58	0.58	
LUBRIZOL 541	25	0.84	0.80	0.77	0.74	0.70	0.64	0.62	0.60	0.54	
	75	0.66	0.62	—	—	0.72	0.57	0.62	0.70	0.66	
NALCO 5403	25	0.78	0.78	0.74	0.65	0.64	0.61	0.60	0.54	0.53	
	75	0.84	—	—	—	0.73	0.69	0.64	0.60	0.56	
TOLAD 245	25	0.81	0.76	0.76	0.72	0.70	0.70	0.68	0.64	0.60	0.54
	75	0.70	—	—	—	0.65	0.52	0.52	0.47	0.60	0.50
UNICOR J	25	0.79	0.75	0.70	0.62	0.61	0.57	0.58	0.52	0.53	
	75	0.88	—	—	—	0.70	0.66	0.63	0.60	0.54	
IPC 4410	25	0.78	0.77	0.69	0.61	0.54	0.53	0.55	0.52	0.48	
	75	0.68	—	—	—	0.65	0.60	0.59	0.56	0.53	
MOBILAD F800	25	0.81	0.76	0.71	0.65	0.62	0.58	0.54	0.54	0.52	
	75	0.67	—	—	—	0.61	0.62	0.62	0.58	0.54	
NALCO 5405	25	0.78	0.78	0.74	0.66	0.60	0.53	0.56	0.51	0.50	
	75	0.70	—	—	—	0.60	0.57	0.59	0.56	0.55	
TOLAD 249	25	0.80	0.78	0.79	0.75	0.70	0.68	0.67	0.63	0.61	
	75	0.83	—	—	—	0.64	0.59	0.58	0.62	0.56	
P-3305	25	0.81	0.80	0.78	0.70	0.61	0.56	0.56	0.56	0.55	0.52
	75	0.60	—	—	—	0.70	0.61	0.58	0.54	0.52	0.52
IPC-4445	25	0.78	0.78	0.80	0.70	0.68	0.58	0.55	0.53	0.50	
	75	0.52	—	—	—	0.56	0.60	0.56	0.63	0.58	
WELCHEM 91120	25	0.81	0.78	0.74	0.68	0.63	0.59	0.56	0.52	0.52	
NUCHEM PCI-105	25	0.80	0.76	0.76	0.69	0.66	0.64	0.62	0.58	0.54	

cm/c

Table C-3. Effect of Corrosion Inhibitors in Clay Treated JP-8

Corrosion Inhibitor	Temperature °C	Base Fuel	1.5 ppm	3.0 ppm	6.0 ppm	9.0 ppm	12.0 ppm	15.0 ppm	20.0 ppm	30.0 ppm	42.0 ppm
PRI 19	25	0.83	0.80	0.80	0.74	0.70	0.66	0.61	0.59	0.57	
HITEC E-580	25	0.81	0.78	0.76	0.68	0.66	0.61	0.58	0.57	0.54	
DCL 4A	25	0.82	0.76	0.72	0.64	0.61	0.56	0.54	0.52	0.50	
DCL 6A	25	0.80	0.81	0.78	0.68	0.62	0.58	0.56	0.55	0.52	
LUHRIZOL 541	25	0.87	0.84	0.80	0.75	0.68	0.64	0.60	0.56	0.55	
NALCO 5403	25	0.82	0.78	0.75	0.68	0.62	0.61	0.56	0.54	0.50	
TOLAD 245	25	0.82	0.79	0.78	0.74	0.70	0.67	0.66	0.62	0.58	0.550
UNICOR J	25	0.82	0.79	0.76	0.68	0.62	0.59	0.54	0.54	0.54	
IPC 4410	25	0.83	0.78	0.70	0.66	0.58	0.56	0.52	0.50	0.48	
MORILAD F800	25	0.87	0.80	0.74	0.68	0.64	0.61	0.57	0.53	0.48	
NALCO 5405	25	0.82	0.77	0.74	0.66	0.62	0.58	0.54	0.53	0.48	
TOLAD 249	25	0.84	0.82	0.82	0.76	0.75	0.70	0.69	0.66	0.60	
P-3305	25	0.77	0.76	0.75	0.70	0.63	0.58	0.57	0.54	0.52	0.520
IPC 4445	25	0.78	0.76	0.75	0.68	0.67	0.62	0.60	0.57	0.54	
WELCHEM 91120	25	0.85	0.80	0.78	0.72	0.66	0.62	0.60	0.58	0.54	
NUCHEM PCT 105	25	0.80	0.80	0.77	0.72	0.65	0.63	0.60	0.57	0.52	

00194

Table C-4. Effect of Corrosion Inhibitors in Clay Treated JP-5

Corrosion Inhibitor	Temperature °C	Base Fuel	1.5 ppm	3.0 ppm	6.0 ppm	9.0 ppm	12.0 ppm	15.0 ppm	20.0 ppm	30.0 ppm	42.0 ppm
PRI-19	25	0.30	0.74	0.72	0.74	0.66	0.63	0.60	0.56	0.52	
	75	0.50	0.50	0.48	0.49	0.52	0.50	0.56	0.60	0.58	
HITEC E-580	25	0.76	0.71	0.70	0.70	0.64	0.62	0.59	0.55	0.51	
	75	0.54	0.53	0.51	0.52	0.52	0.51	0.56	0.52	0.55	
DCI-4A	25	0.76	0.72	0.68	0.64	0.60	0.52	0.51	0.50	0.48	
	75	0.49	—	—	—	0.50	0.66	0.54	0.62	0.56	
DCI-6A	25	0.74	0.70	0.68	0.62	0.58	0.54	0.52	0.49	0.48	
	75	0.50	—	—	—	0.54	0.55	0.52	0.56	0.59	
LUBRIZOL 541	25	0.77	0.76	0.73	0.68	0.63	0.62	0.58	0.57	0.56	
	75	0.54	—	—	—	0.52	0.54	0.53	0.52	0.53	
NALCO 5403	25	0.73	0.73	0.72	0.68	0.64	0.58	0.54	0.52	0.50	
	75	0.49	—	—	—	0.58	0.54	0.50	0.59	0.48	
TOLAD 245	25	0.76	0.73	0.73	0.69	0.70	0.66	0.63	0.63	0.58	0.54
	75	0.50	—	—	—	0.52	0.49	0.49	0.51	0.45	0.54
UNICOR J	25	0.78	0.78	0.74	0.66	0.66	0.57	0.50	0.48	0.46	
	75	0.54	—	—	—	0.54	0.54	0.62	0.60	0.59	
IPC 4410	25	0.77	0.74	0.70	0.61	0.60	0.53	0.54	0.52	0.48	
	75	0.50	—	—	—	0.54	0.53	0.53	0.54	0.52	
MOBILAD P800	25	0.81	0.76	0.70	0.66	0.57	0.54	0.52	0.52	0.50	
	75	0.51	—	—	—	0.56	0.59	0.58	0.56	0.53	
NALCO 5405	25	0.79	0.76	0.75	0.66	0.61	0.56	0.54	0.52	0.52	
	75	0.52	—	—	—	0.52	0.55	0.56	0.64	0.60	
TOLAD 249	25	0.80	0.80	0.78	0.72	0.74	0.71	0.66	0.64	0.60	
	75	0.82	—	—	—	0.58	0.61	0.56	0.50	0.55	
P-3305	25	0.78	0.74	0.76	0.66	0.60	0.60	0.56	0.56	0.52	0.51
	75	0.77	—	—	—	0.62	0.65	0.62	0.63	0.58	0.52
IPC-4445	25	0.78	0.78	0.74	0.70	0.64	0.61	0.59	0.58	0.56	
	75	0.74	—	—	—	0.58	0.60	0.57	0.54	0.54	
WELCHEM 91120	25	0.78	0.77	0.76	0.70	0.66	0.61	0.58	0.56	0.54	
NUCHEM PCI-105	25	0.80	0.75	0.74	0.72	0.68	0.63	0.60	0.59	0.54	

**APPENDIX D
PERFORMANCE PLOTS**

LIST OF ILLUSTRATIONS

Figure

D-1	Effect of Apollo PRI-19 in ISOPAR-M
D-2	Effect of HITEC E-580 in ISOPAR-M
D-3	Effect of DCI-4A in ISOPAR-M
D-4	Effect of DCI-6A in ISOPAR-M
D-5	Effect of LUBRIZOL 541 in ISOPAR-M
D-6	Effect of NALCO 5403 in ISOPAR-M
D-7	Effect of TOLAD 245 in ISOPAR-M
D-8	Effect of UNICOR-J in ISOPAR-M
D-9	Effect of IPC-4410 in ISOPAR-M
D-10	Effect of MOBILAD F-800 in ISOPAR-M
D-11	Effect of NALCO 5405 in ISOPAR-M
D-12	Effect of TOLAD 249 in ISOPAR-M
D-13	Effect of P-3305 in ISOPAR-M
D-14	Effect of IPC-4445 in ISOPAR-M
D-15	Effect of WELCHEM 91120 in ISOPAR-M
D-16	Effect of NUCHEM PCI-105 in ISOPAR-M
D-17	Effect of Apollo PRI-19 in Clay Treated JP-4
D-18	Effect of HITEC E-580 in Clay Treated JP-4
D-19	Effect of DCI-4A in Clay Treated JP-4
D-20	Effect of DCI-6A in Clay Treated JP-4
D-21	Effect of LUBRIZOL 541 in Clay Treated JP-4
D-22	Effect of NALCO 5403 in Clay Treated JP-4
D-23	Effect of TOLAD 245 in Clay Treated JP-4
D-24	Effect of UNICOR-J in Clay Treated JP-4
D-25	Effect of IPC-4410 in Clay Treated JP-4
D-26	Effect of MOBILAD F-800 in Clay Treated JP-4
D-27	Effect of NALCO-5405 in Clay Treated JP-4
D-28	Effect of TOLAD 249 in Clay Treated JP-4
D-29	Effect of P-3305 in Clay Treated JP-4
D-30	Effect of IPC-4445 in Clay Treated JP-4
D-31	Effect of WELCHEM 91120 in Clay Treated JP-4
D-32	Effect of NUCHEM PCI-105 in Clay Treated JP-4
D-33	Effect of Apollo PRI-19 in Clay Treated JP-8
D-34	Effect of HITEC E-580 in Clay Treated JP-8
D-35	Effect of DCI-4A in Clay Treated JP-8
D-36	Effect of DCI-6A in Clay Treated JP-8
D-37	Effect of LUBRIZOL 541 in Clay Treated JP-8
D-38	Effect of NALCO 5403 in Clay Treated JP-8
D-39	Effect of TOLAD 245 in Clay Treated JP-8
D-40	Effect of UNICOR-J in Clay Treated JP-8
D-41	Effect of IPC 4410 in Clay Treated JP-8
D-42	Effect of MOBILAD F-800 in Clay Treated JP-8
D-43	Effect of NALCO 5405 in Clay Treated JP-8
D-44	Effect of TOLAD 249 in Clay Treated JP-8
D-45	Effect of P-3305 in Clay Treated JP-8
D-46	Effect of IPR-4445 in Clay Treated JP-8
D-47	Effect of WELCHEM 91120 in Clay Treated JP-8

LIST OF ILLUSTRATIONS (Continued)

Figure

- D-48 Effect of NUCHEM PCI-105 in Clay Treated JP-8
- D-49 Effect of Apollo PRI-19 in Clay Treated JP-5
- D-50 Effect of HITEC E-580 in Clay Treated JP-5
- D-51 Effect of DCI-4A in Clay Treated JP-5
- D-52 Effect of DCI-6A in Clay Treated JP-5
- D-53 Effect of LUBRIZOL 541 in Clay Treated JP-5
- D-54 Effect of NALCO 5403 in Clay Treated JP-5
- D-55 Effect of TOLAD 245 in Clay Treated JP-5
- D-56 Effect of UNICOR-J in Clay Treated JP-5
- D-57 Effect of IPC-4410 in Clay Treated JP-5
- D-58 Effect of MOBILAD F-800 in Clay Treated JP-5
- D-59 Effect of NALCO 5405 in Clay Treated JP-5
- D-60 Effect of TOLAD 249 in Clay Treated JP-5
- D-61 Effect of P-3305 in Clay Treated JP-5
- D-62 Effect of IPC-4445 in Clay Treated JP-5
- D-63 Effect of WELCHEM 91120 in Clay Treated JP-5
- D-64 Effect of NUCHEM PCI-105 in Clay Treated JP-5

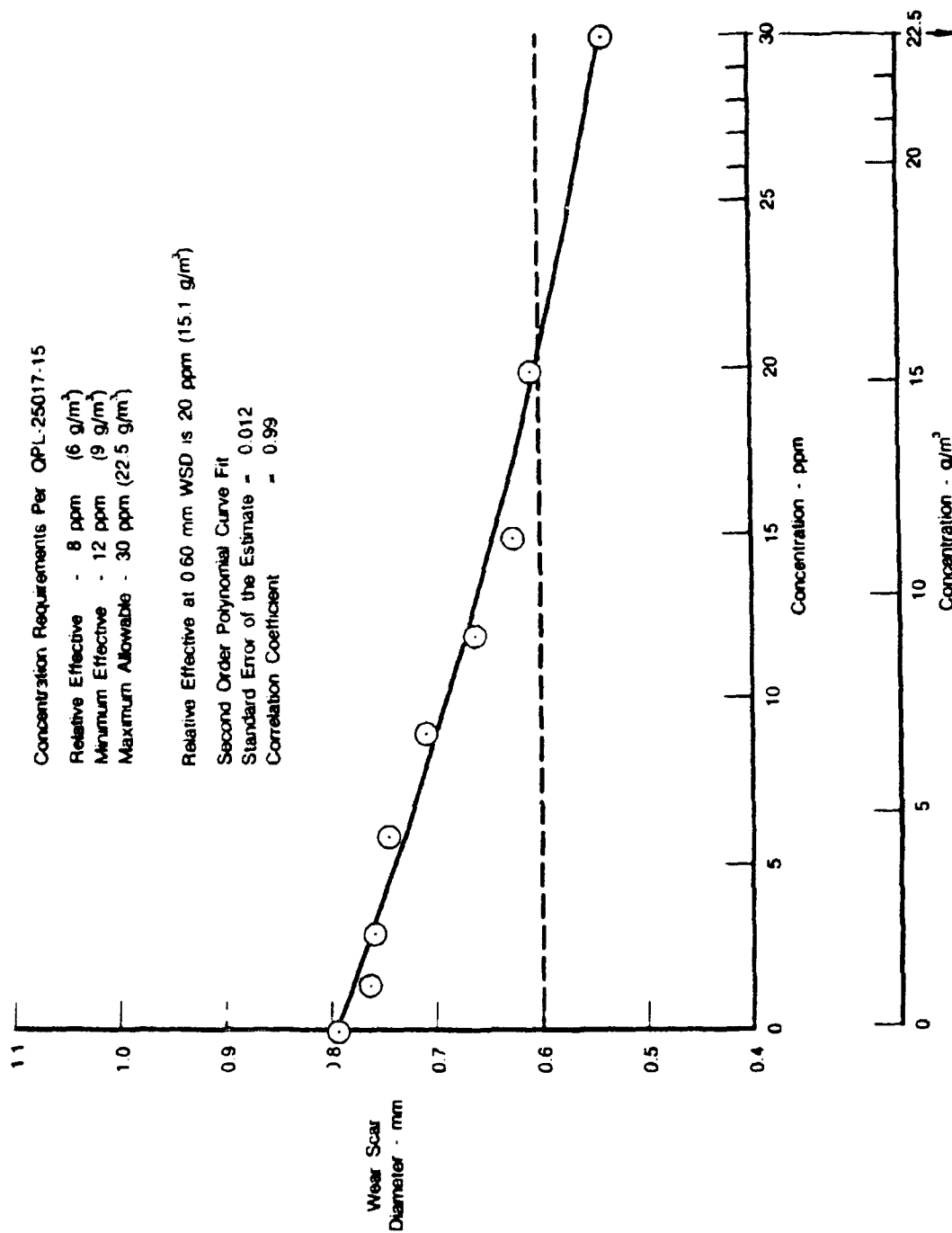


Figure D-1. Effect of Apollo PRI-19 in Isopar M

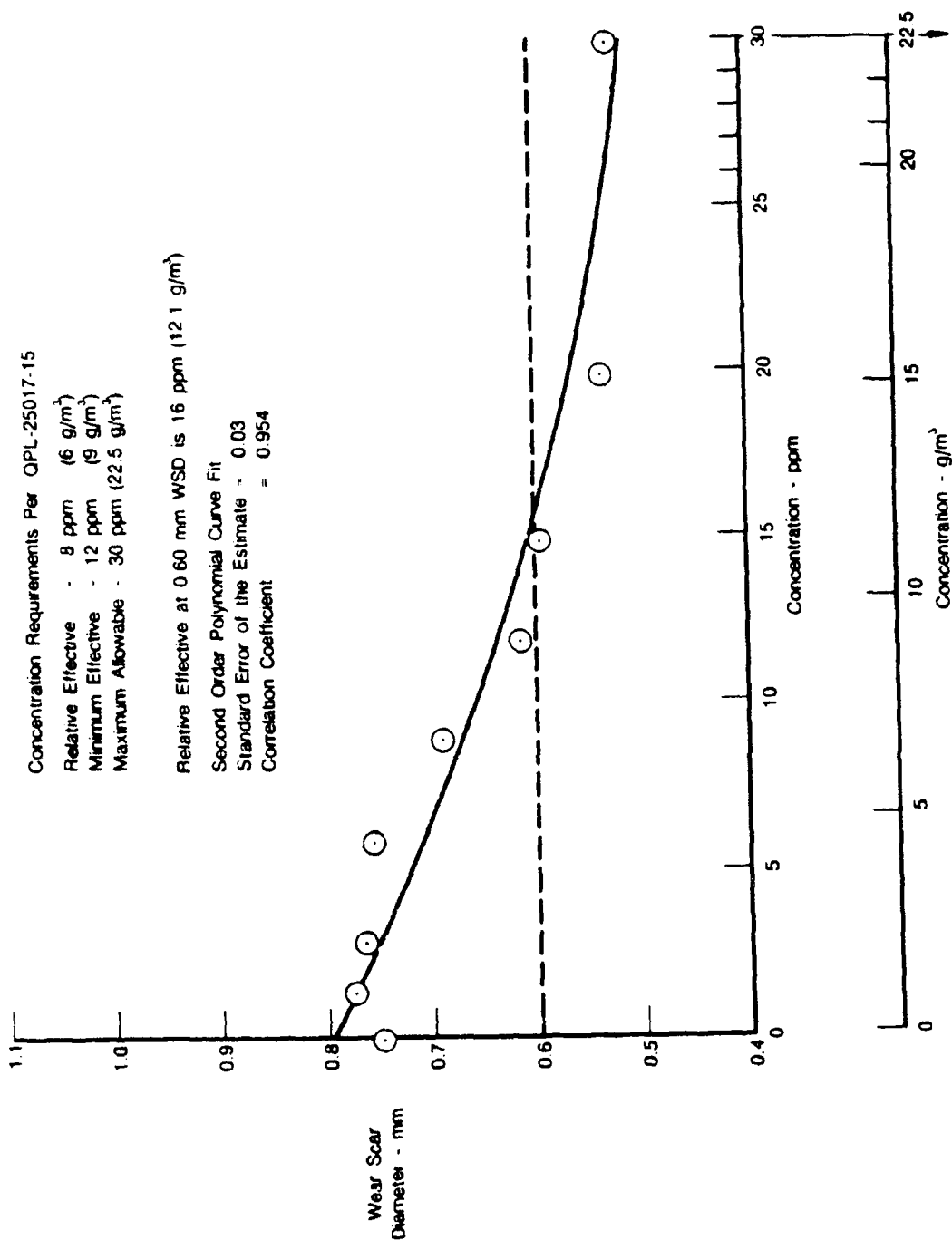


Figure D-2. Effect of HITEC E-580 in Isopar M

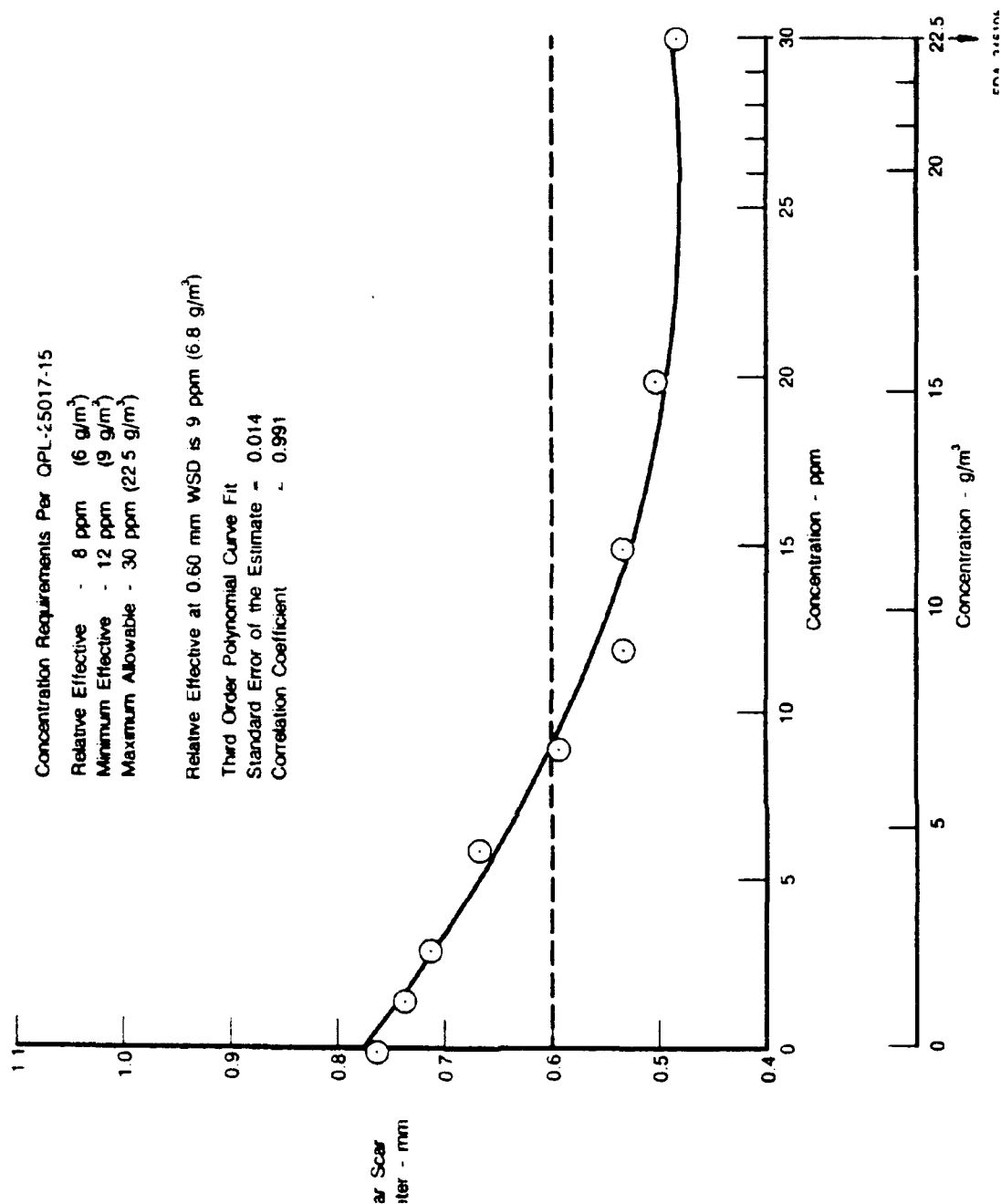


Figure D-3. Effect of DCI-4A in Isopar M

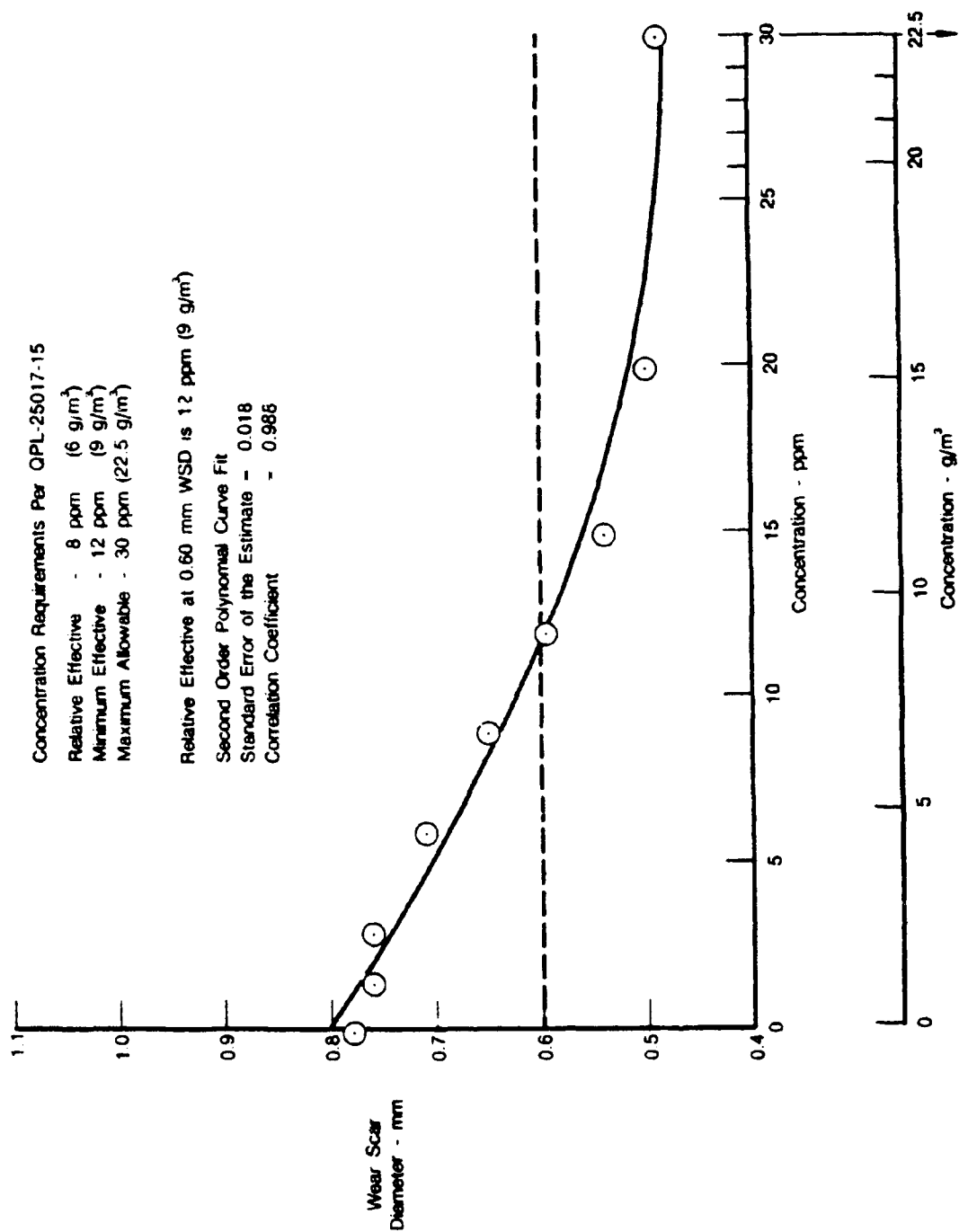


Figure D-4. Effect of DCI-6A in Isopar M

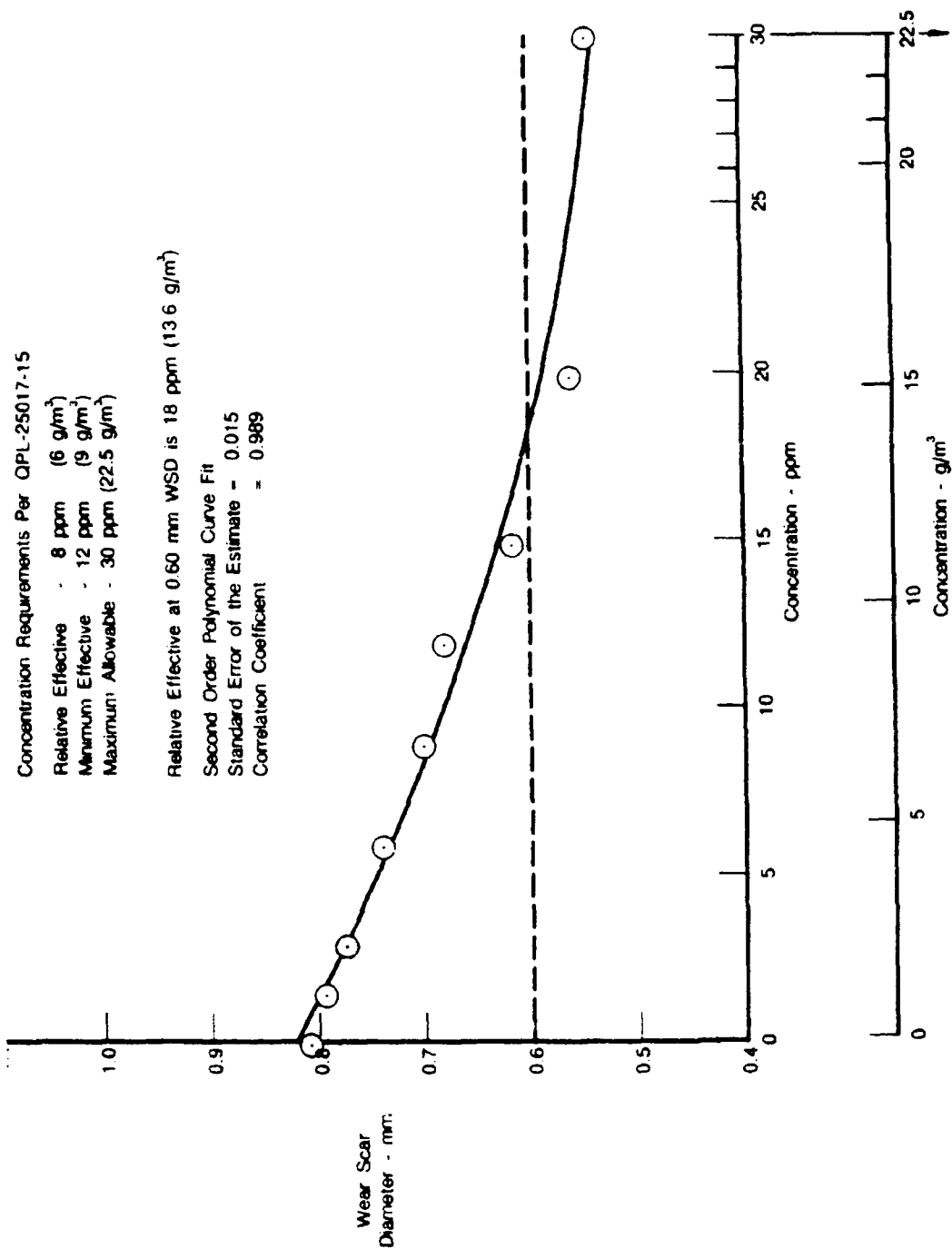


Figure D-5. Effect of LUBRIZOL 541 in Isopar M

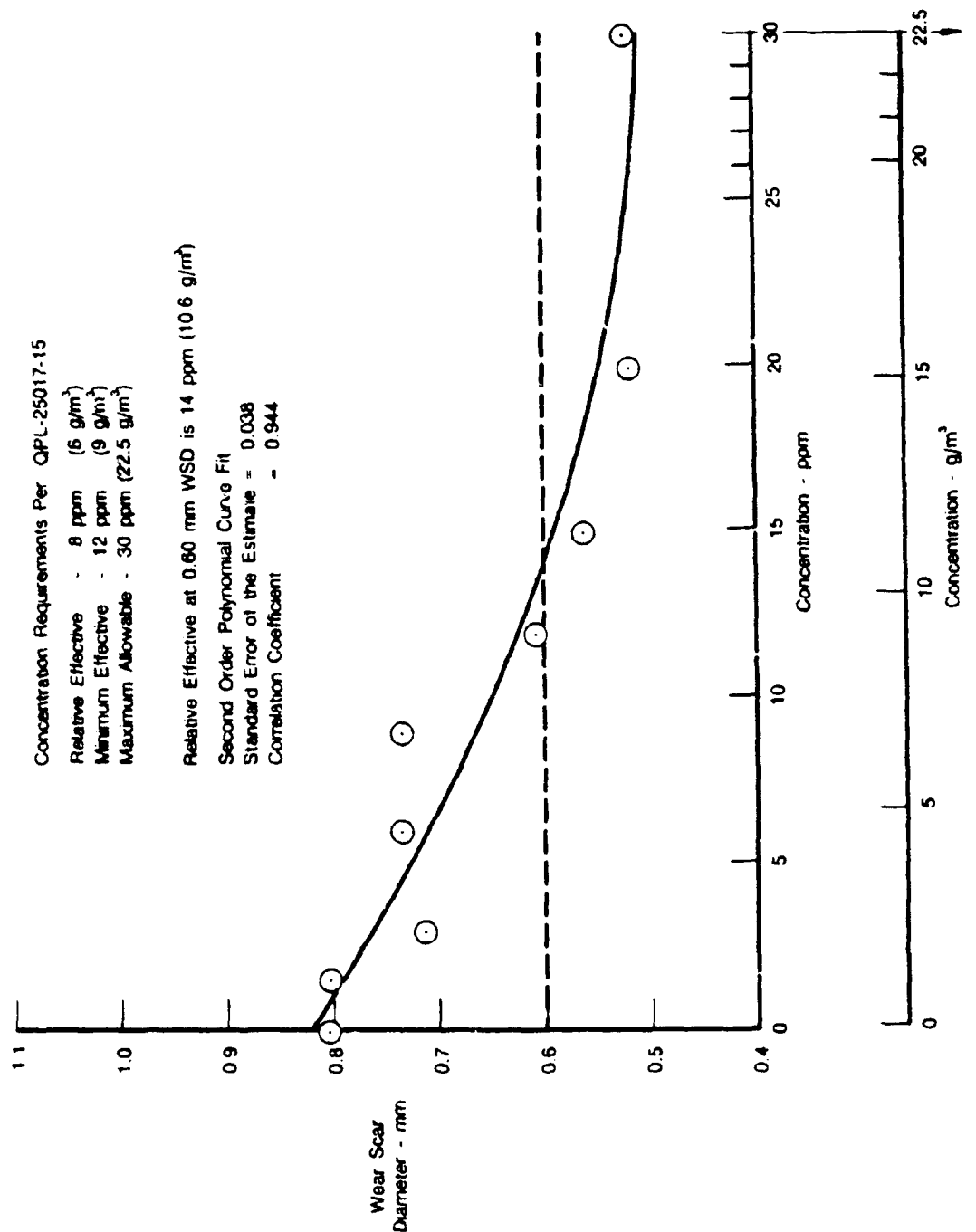


Figure D-6. Effect of NALCO 5403 in Isopar M

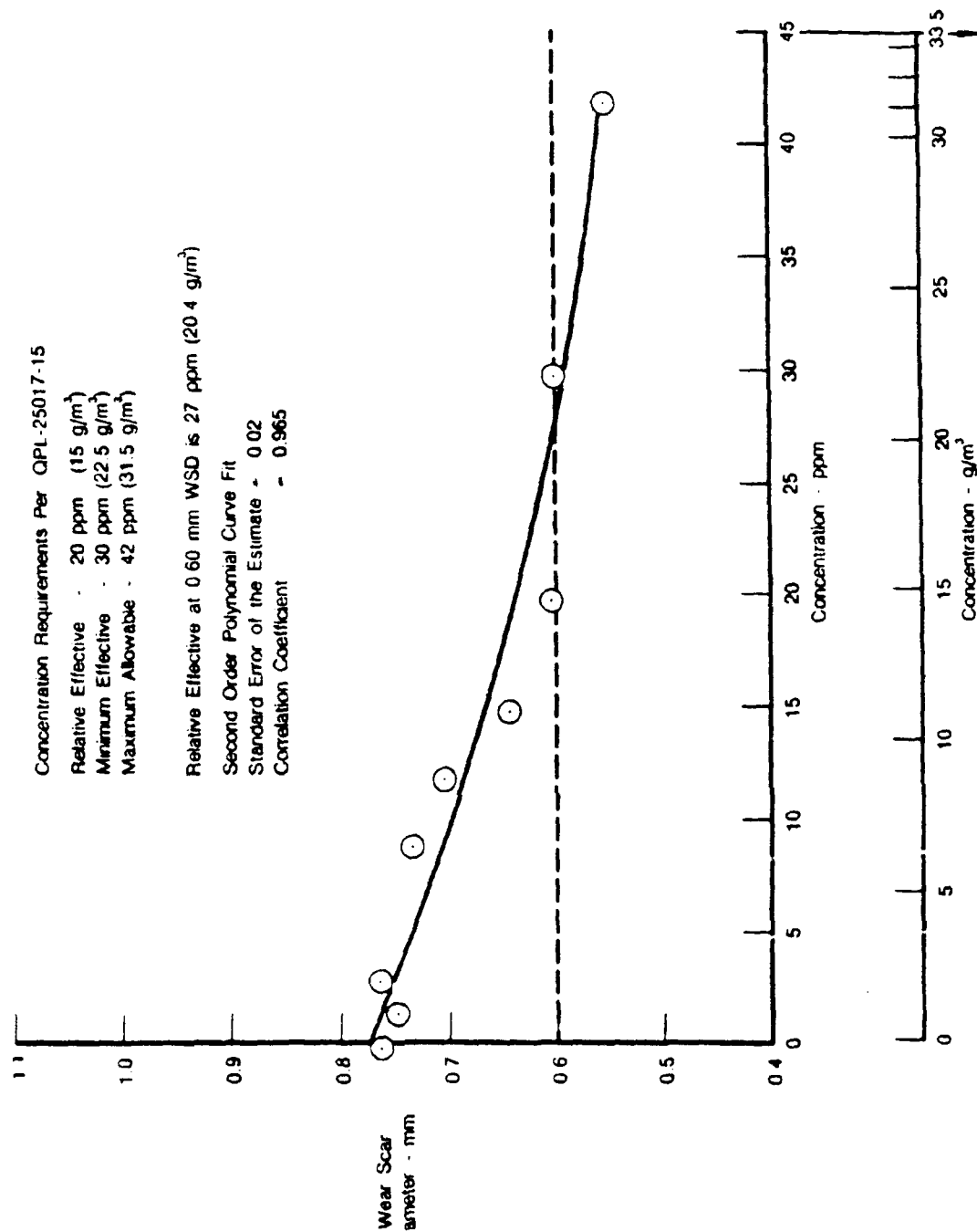


Figure D-7 Effect of TOLAD 245 in Isopar M

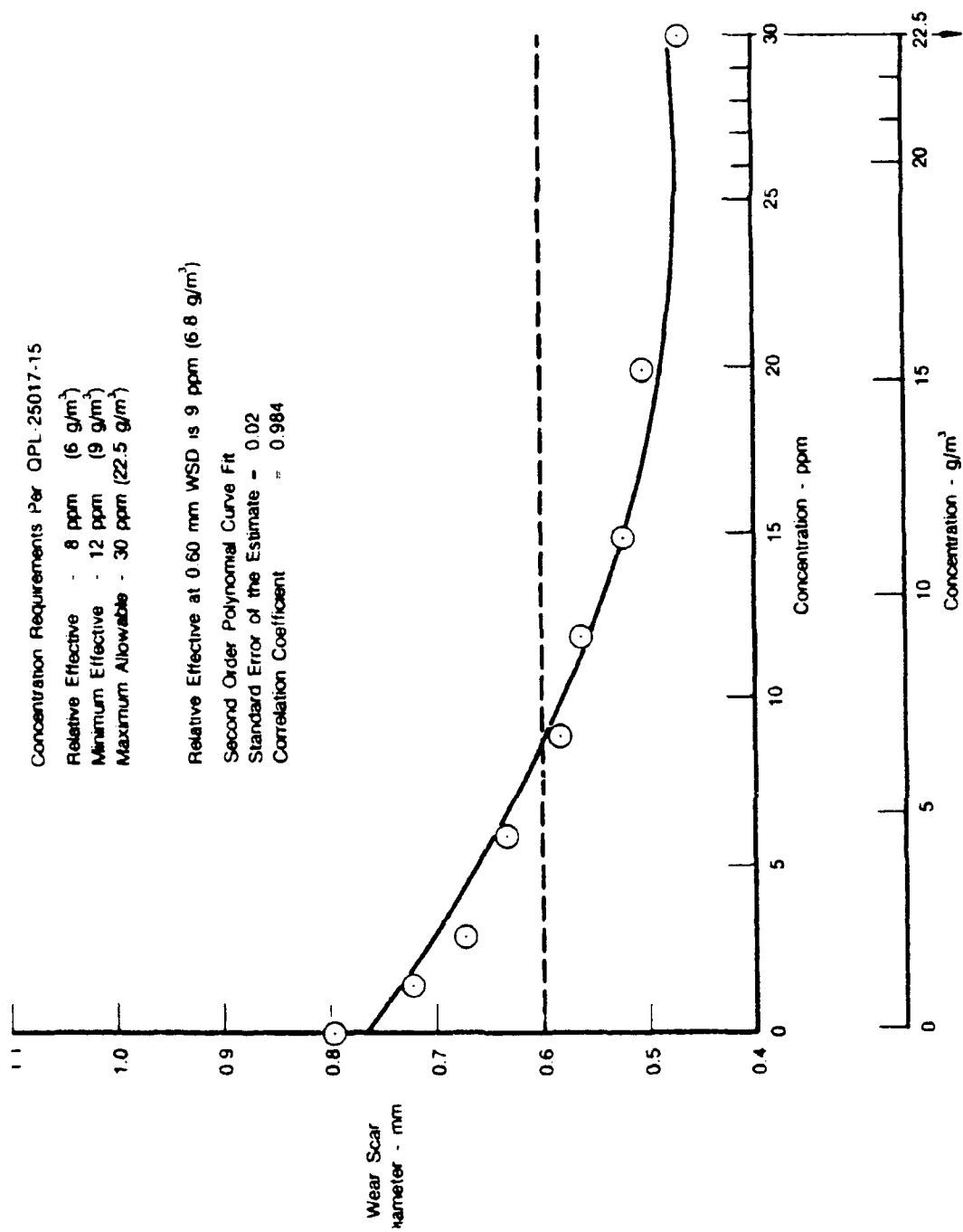


Figure D-8. Effect of UNICOR-J in Isopar M

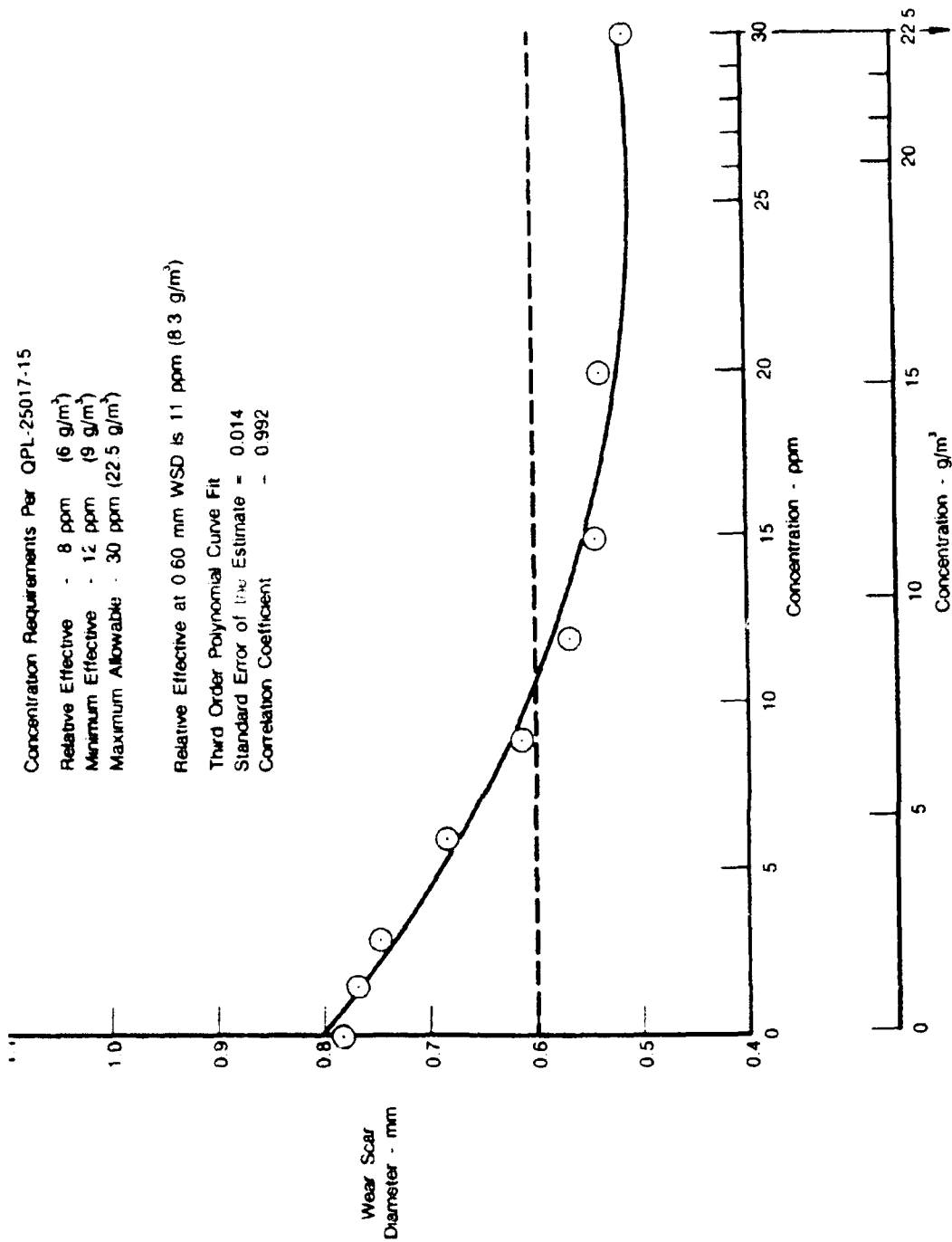


Figure D-9. Effect of IPC-4410 in Isopar M

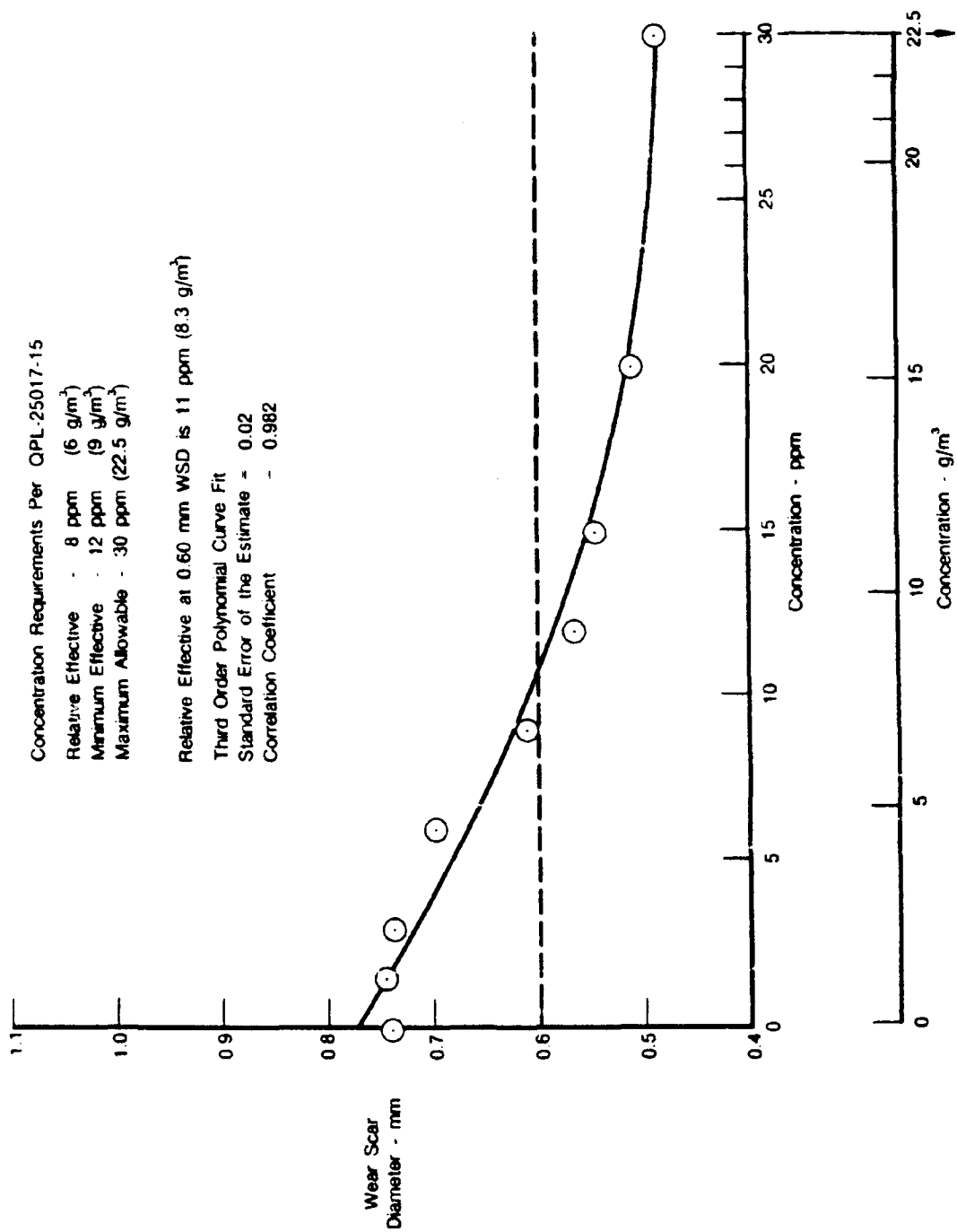


Figure D-10. Effect of MOBILAD F-800 in Isopar M

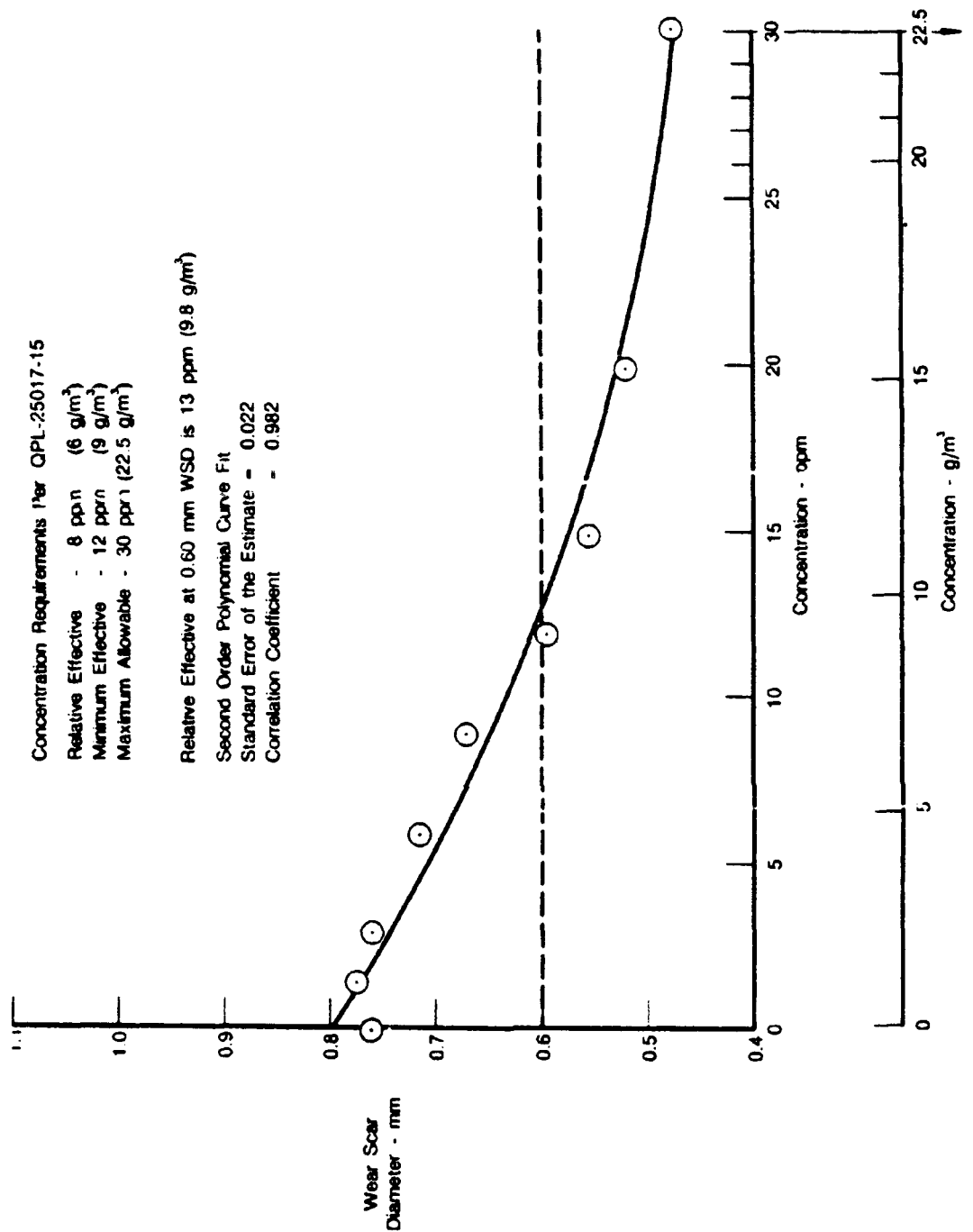


Figure D-11. Effect of NALCO 5405 in Isopar M

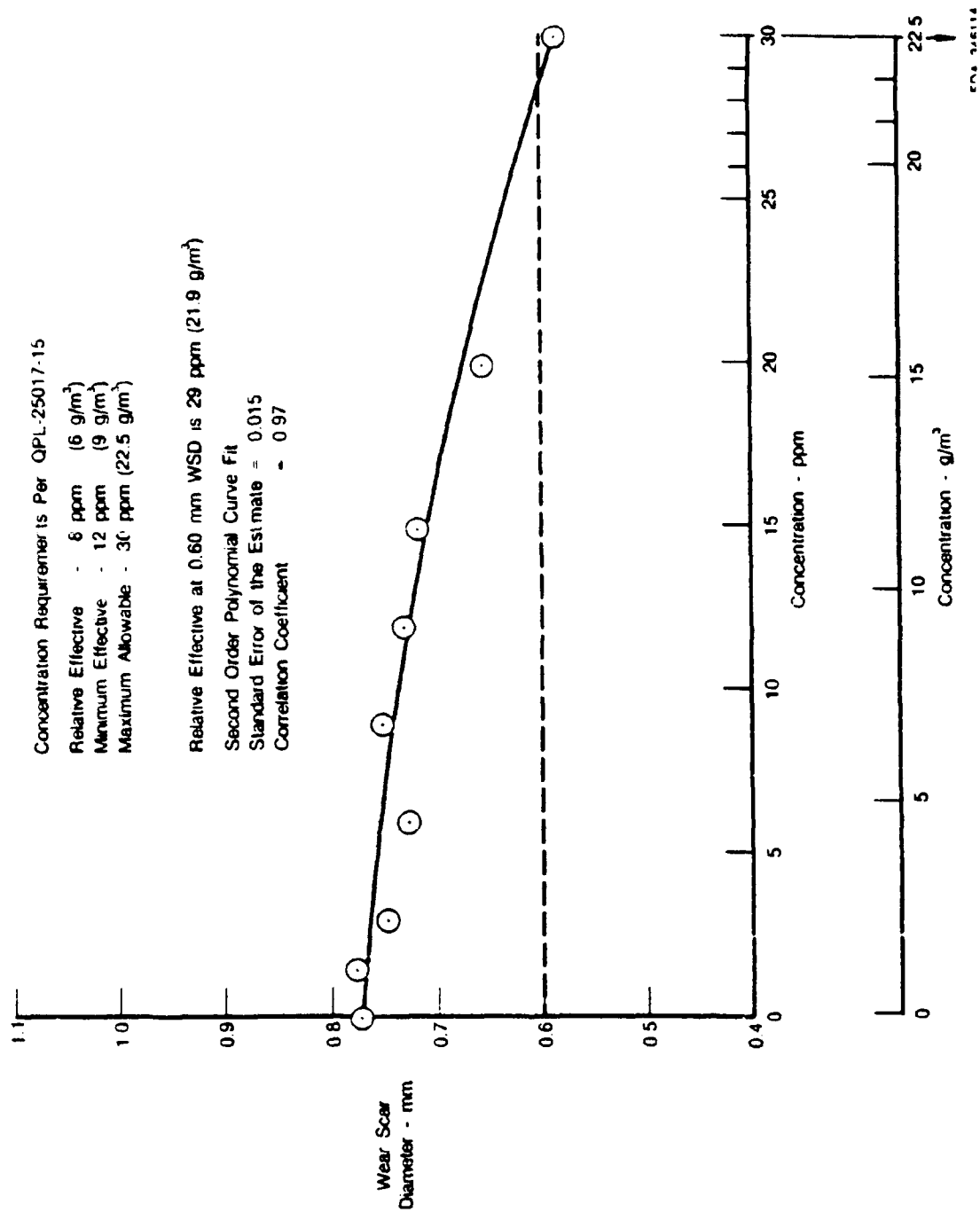


Figure D-12. Effect of TOLAD 249 in Isopar M

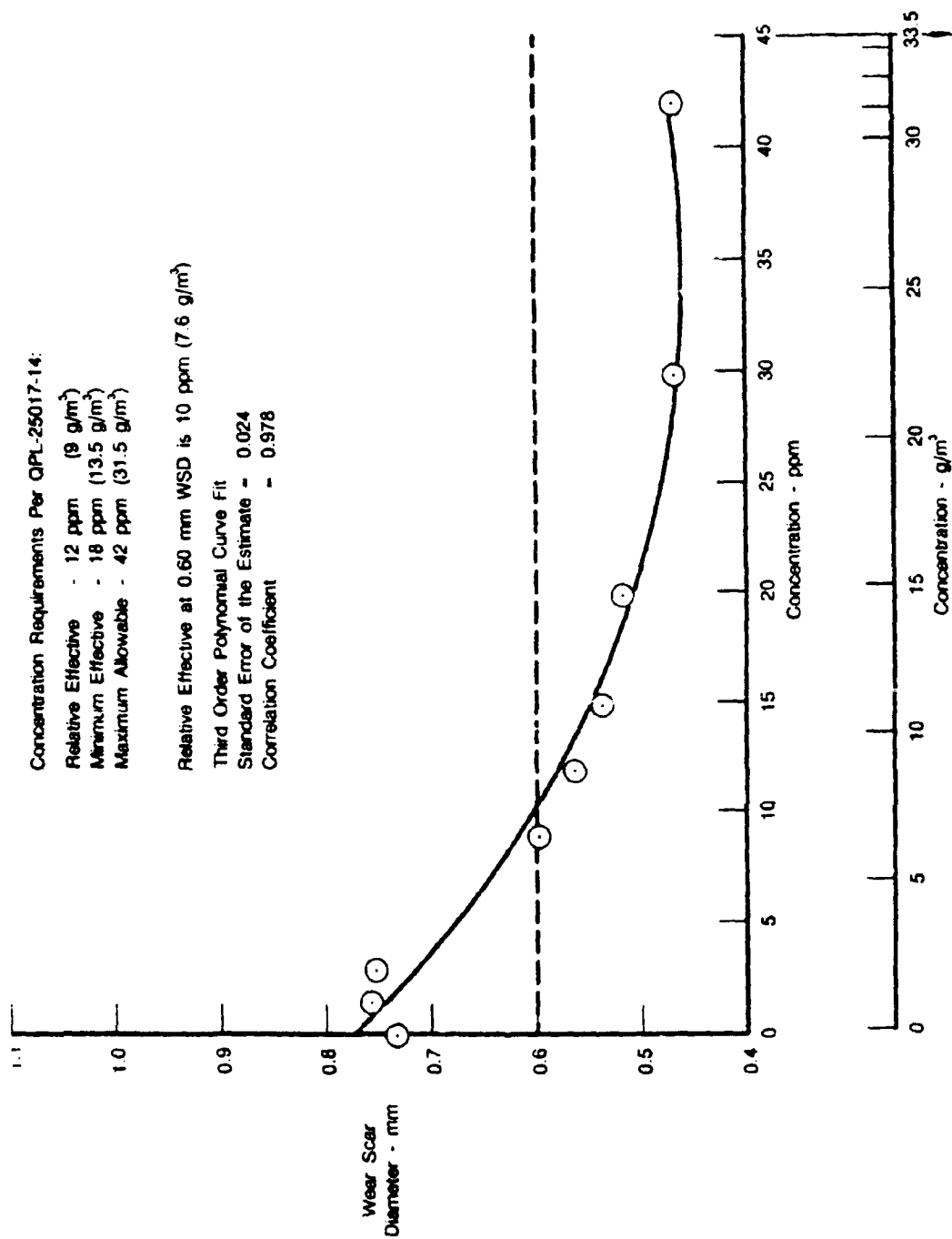


Figure D-13 Effect of P-3305 in Isopar M

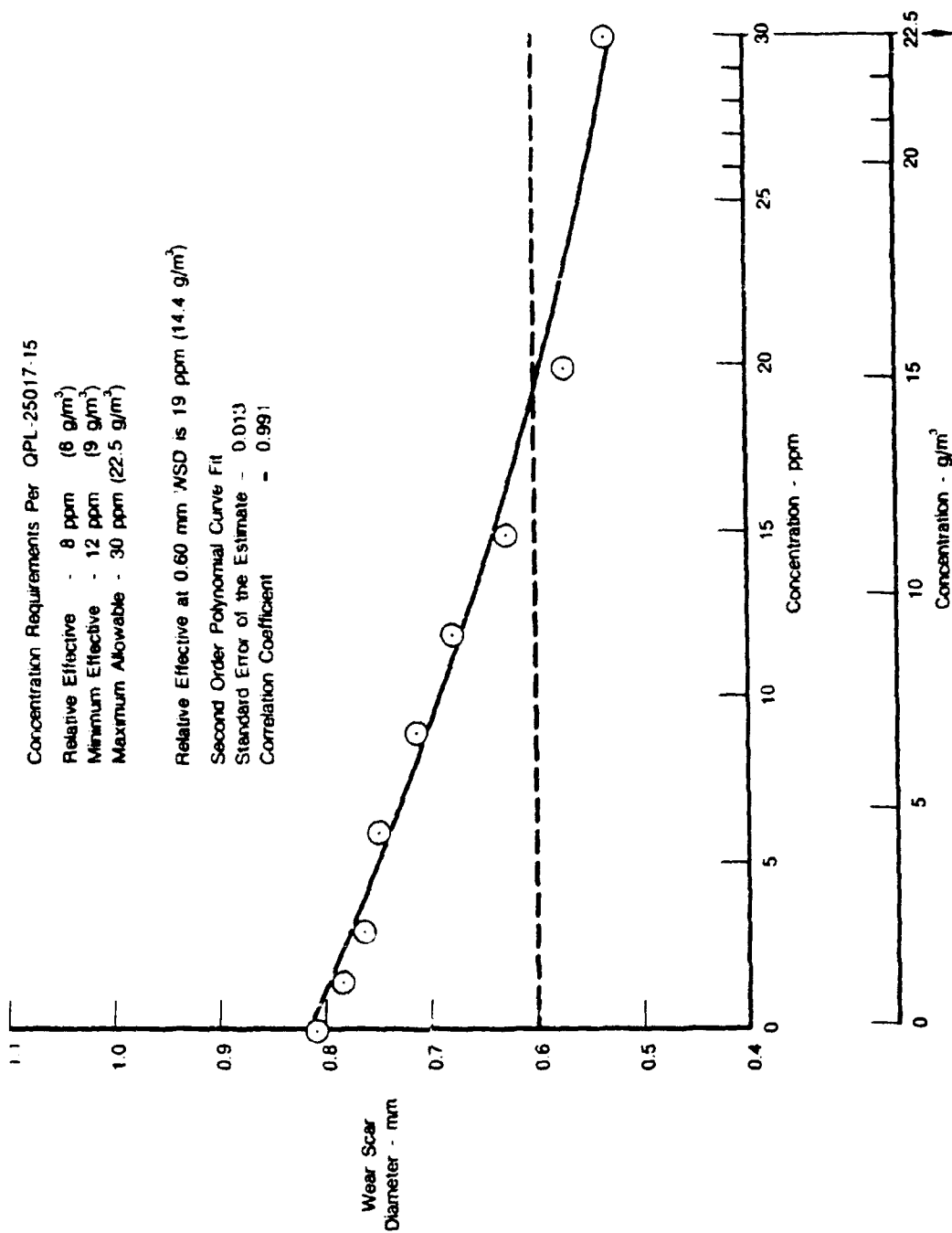


Figure D-14. Effect of IPC-4445 in Isopar M

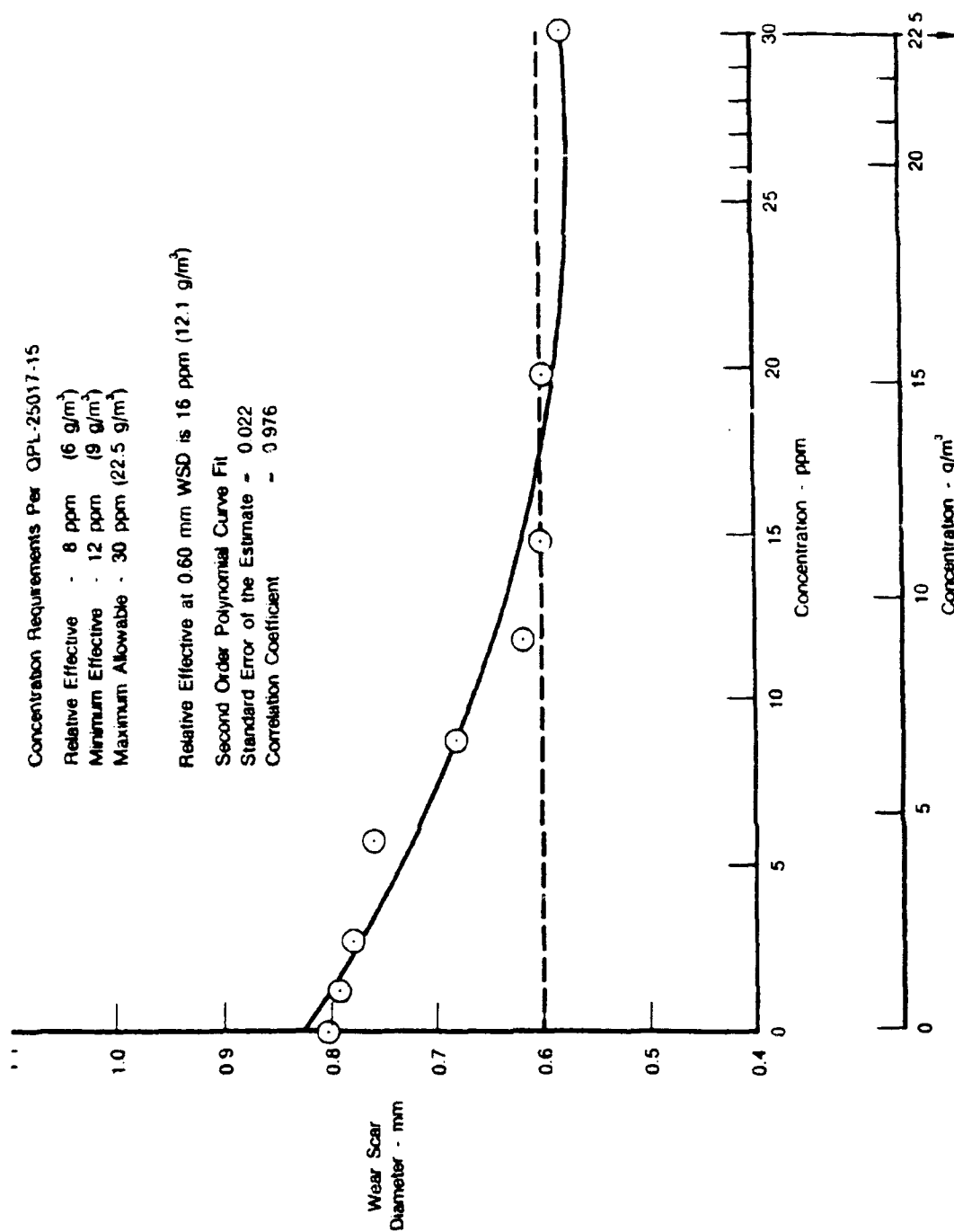


Figure D-15. Effect of WELCHEM 91120 in Isopar M

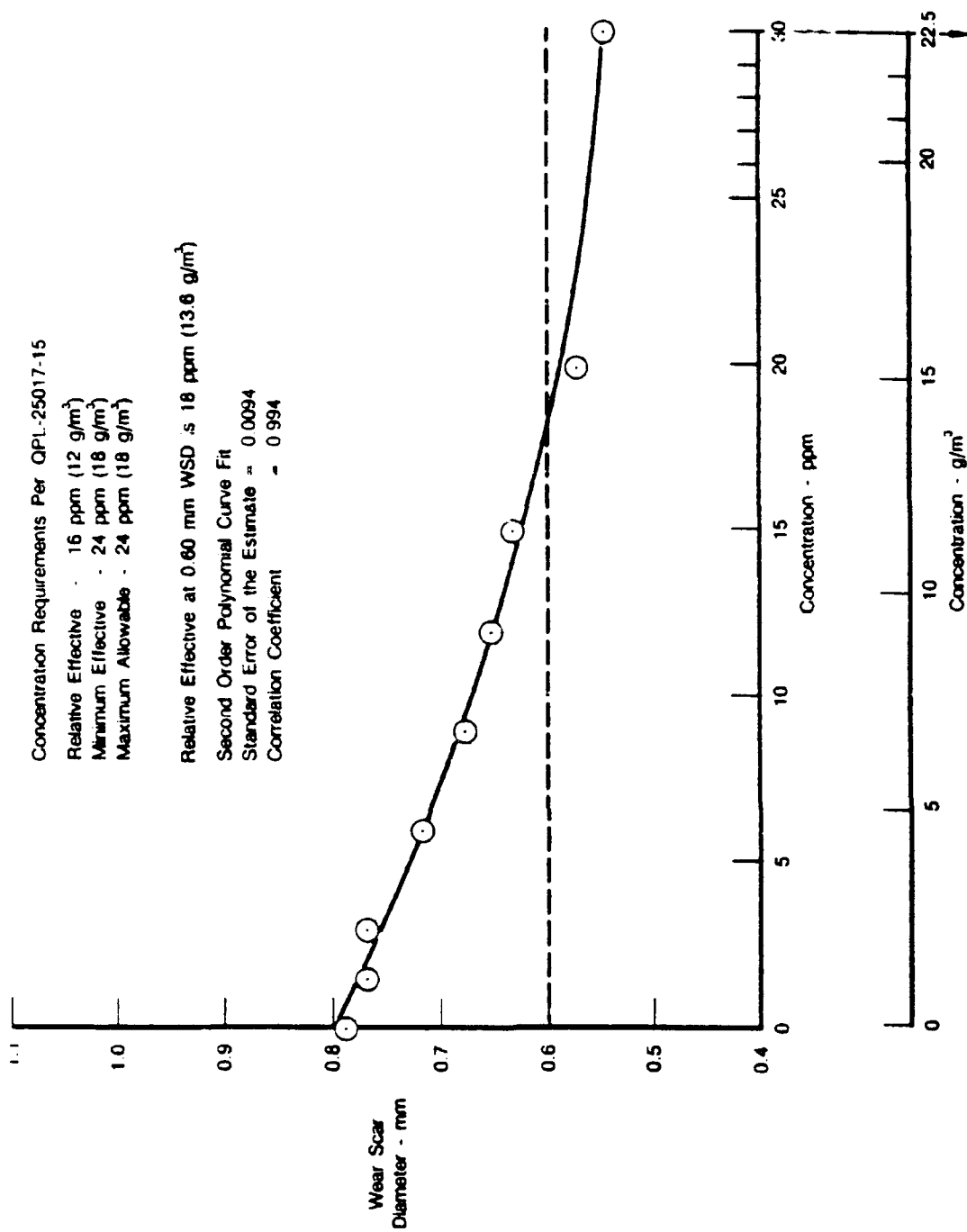


Figure D-16. Effect of NUCHEM PCI-105 in Isopar M

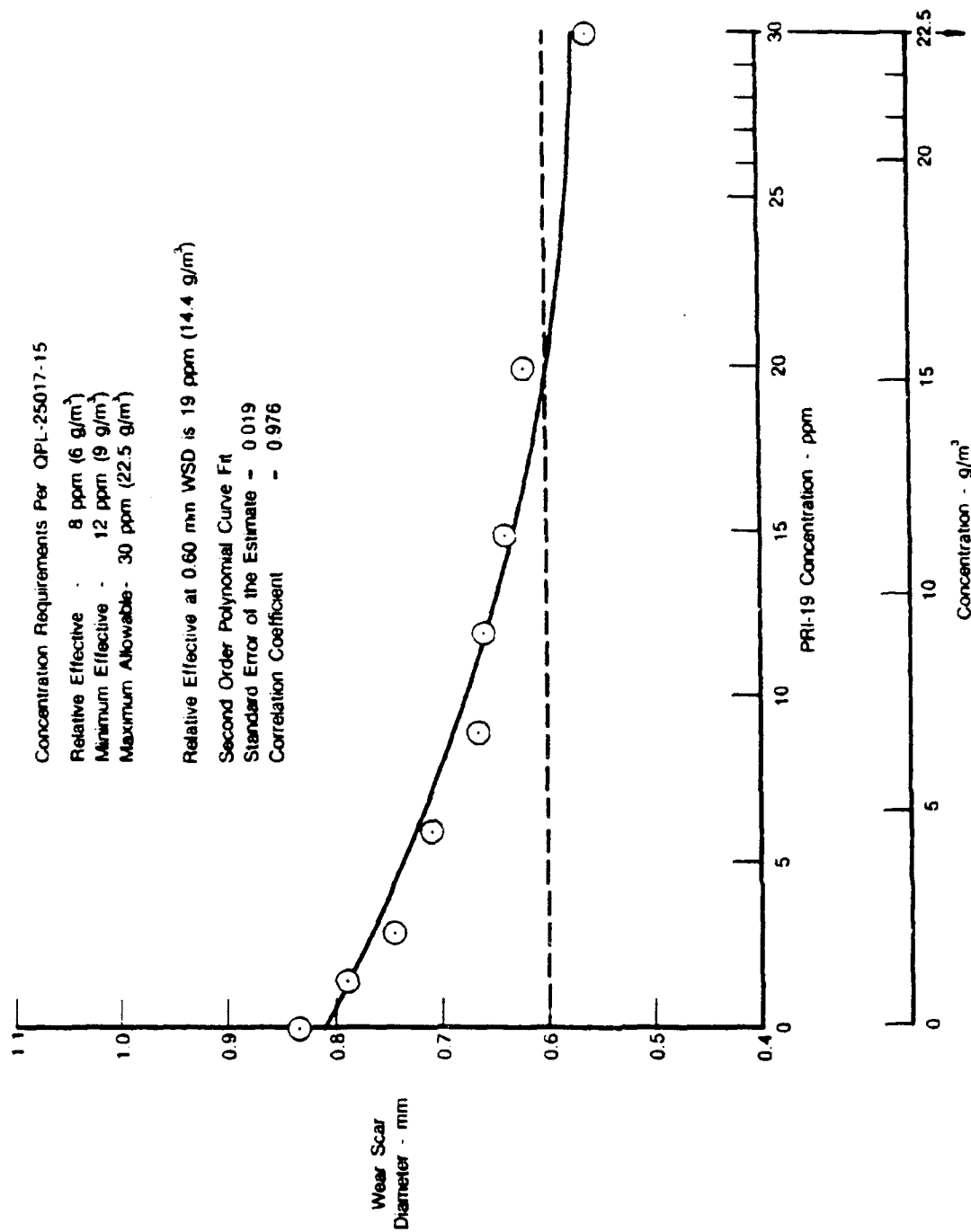


Figure D-17. Effect of Apollo PRI-19 in Clay Treated JP-4

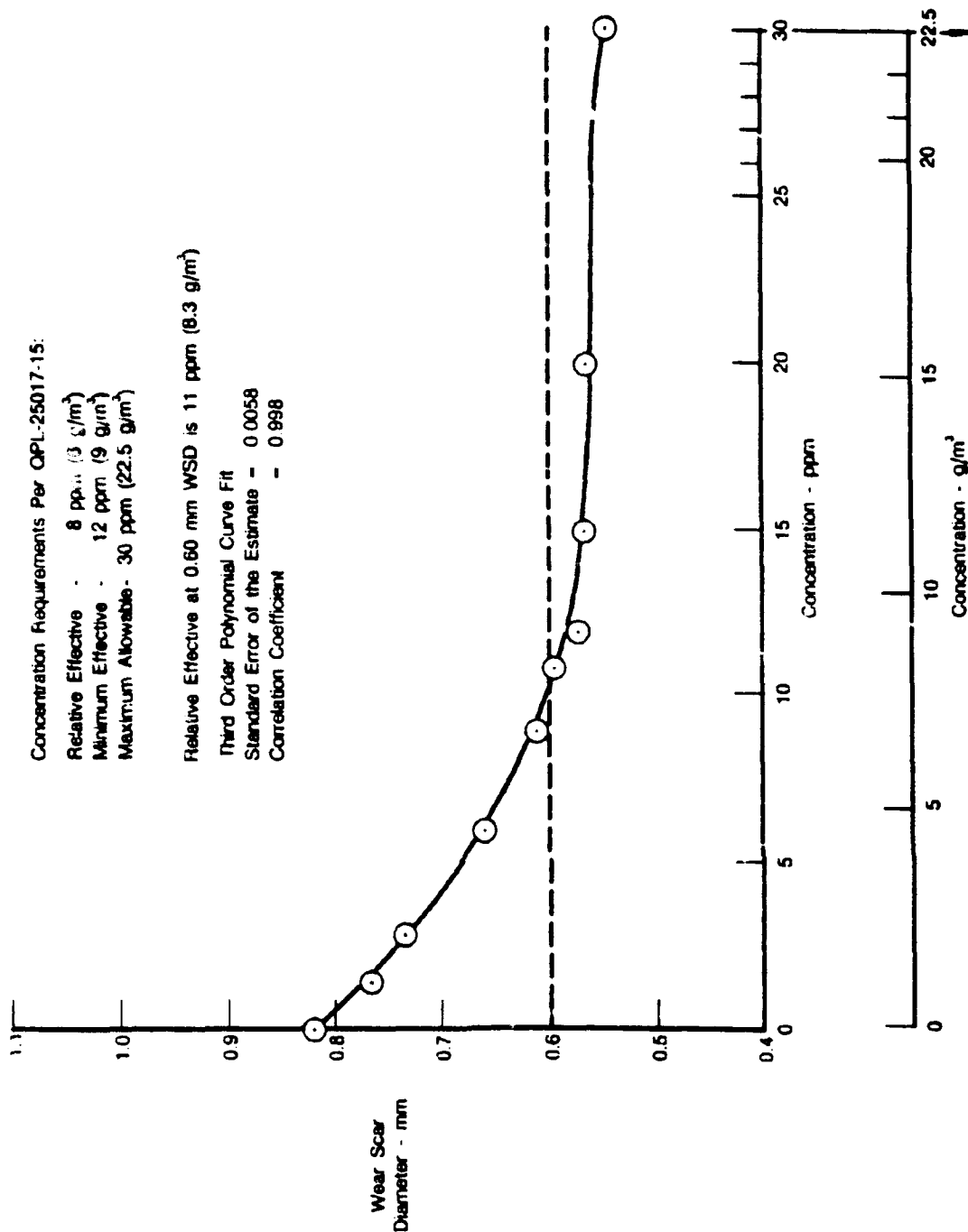


Figure D-18. Effect of HITEC E-580 in Clay Treated JP-4

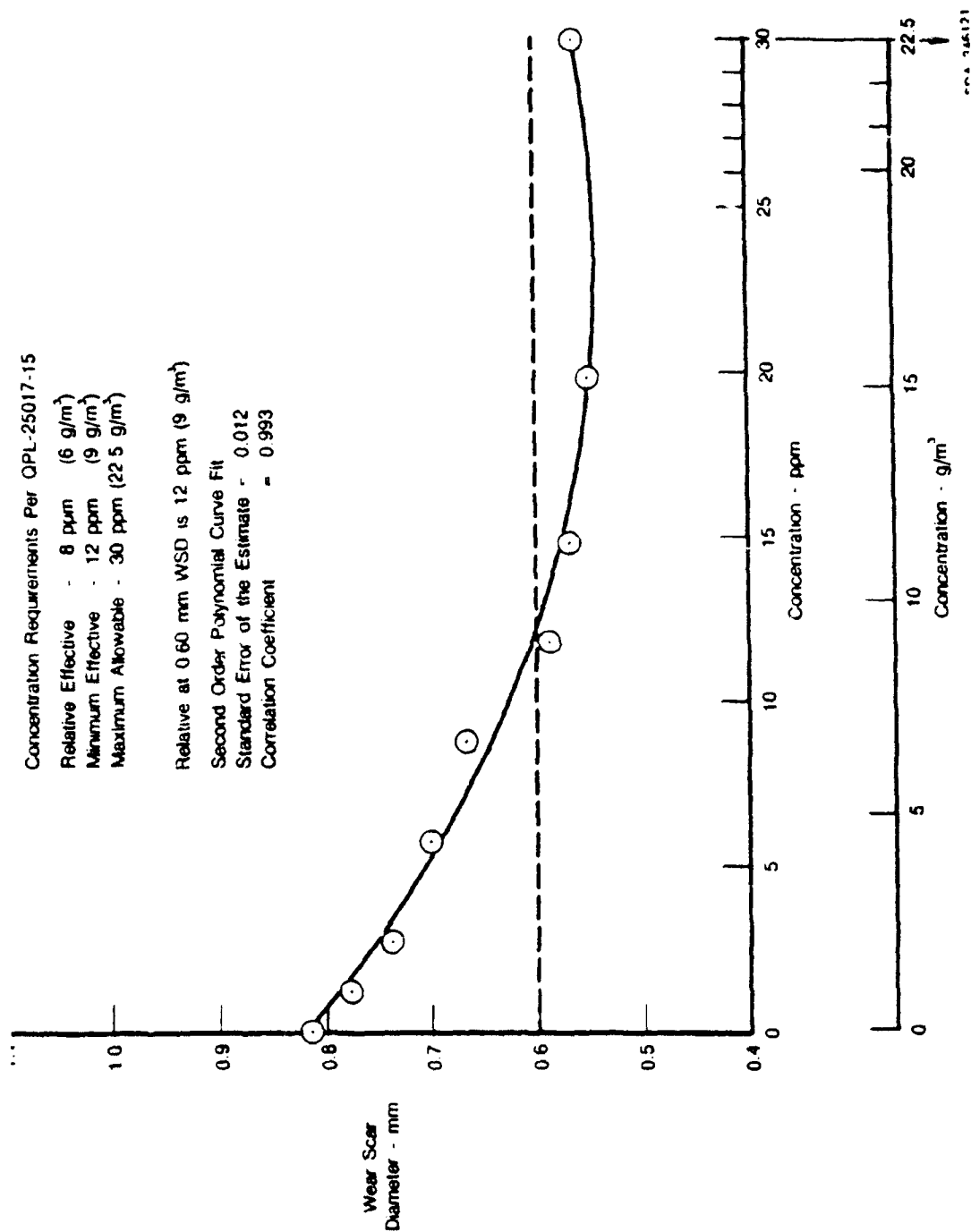


Figure D-19. Effect of DCI-4A in Clay Treated JP-4

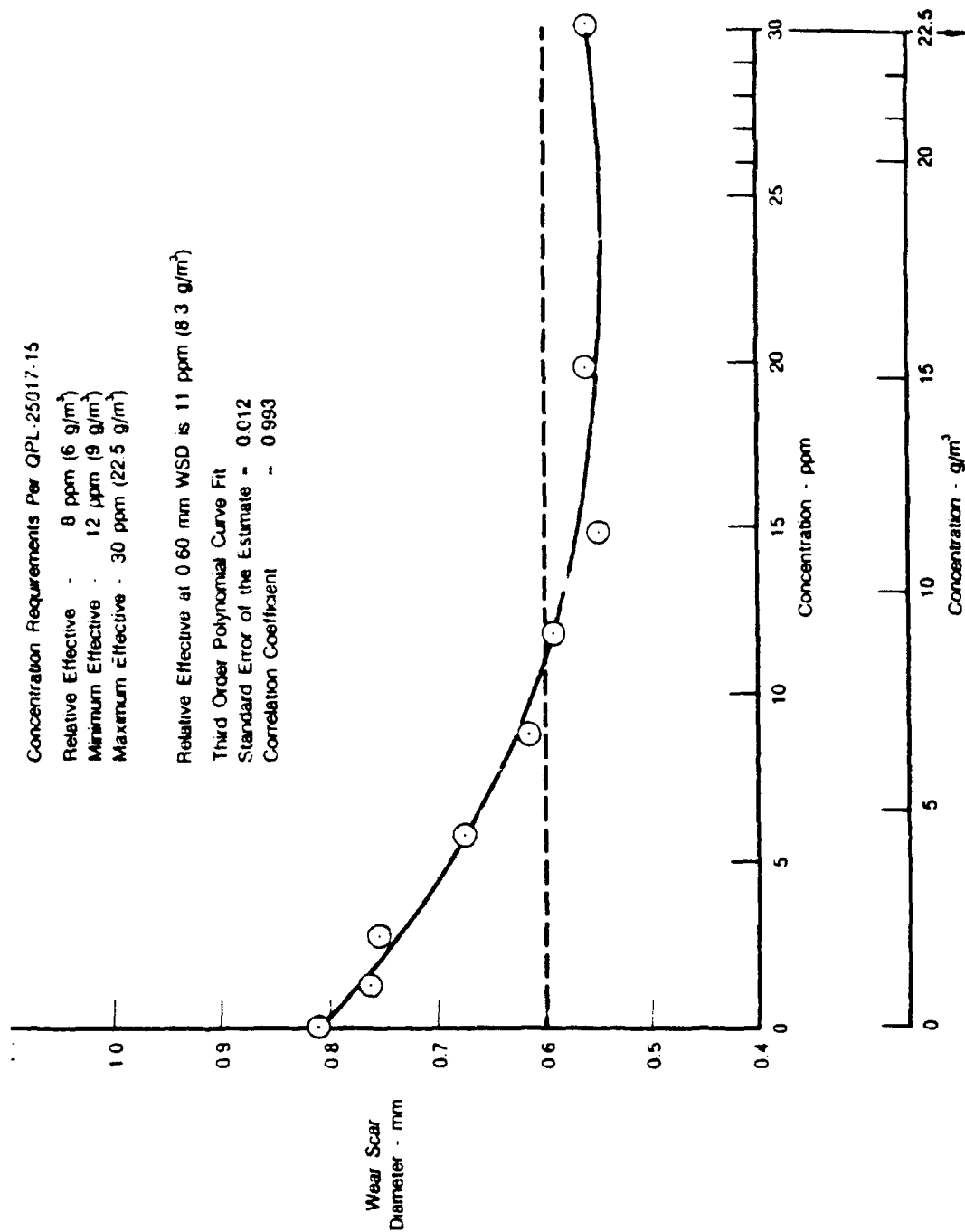


Figure D-20. Effect of DCI-6A in Clay Treated JP-4

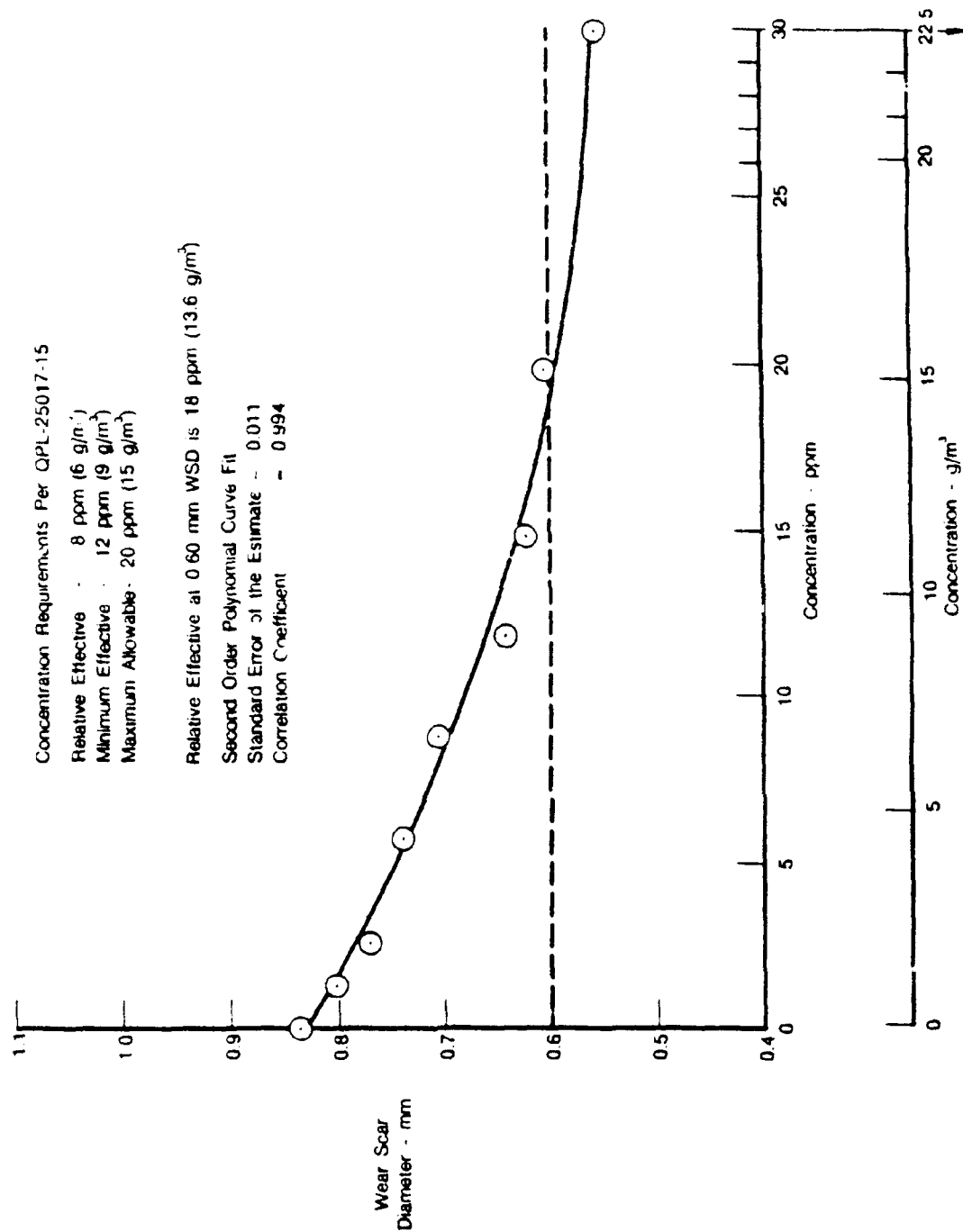
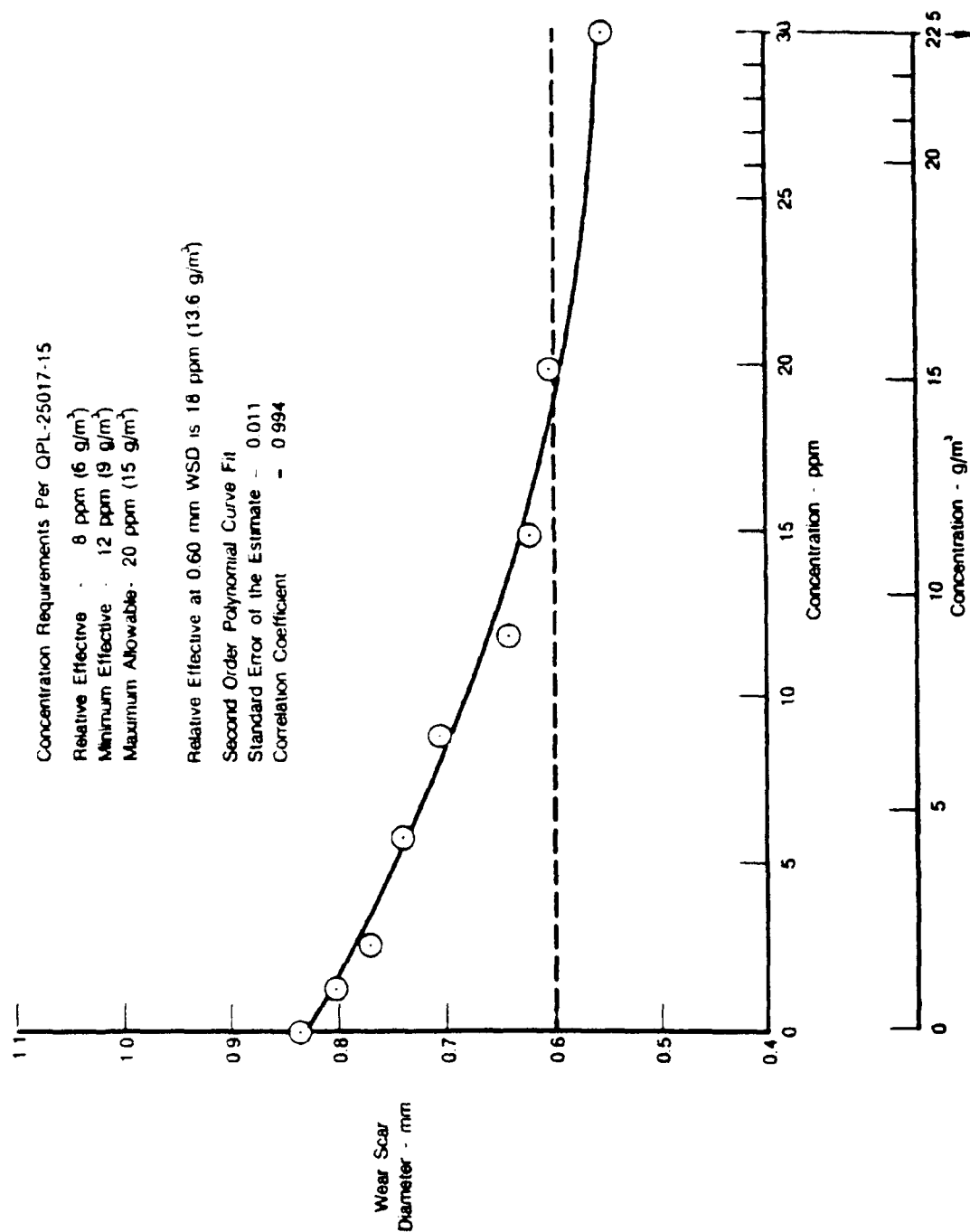


Figure D-21. Effect of LUBRIZOL 541 in Clay Treated JP-4



FDA 346123

Figure D-22. Effect of NALCO 5403 in Clay Treated JP-4

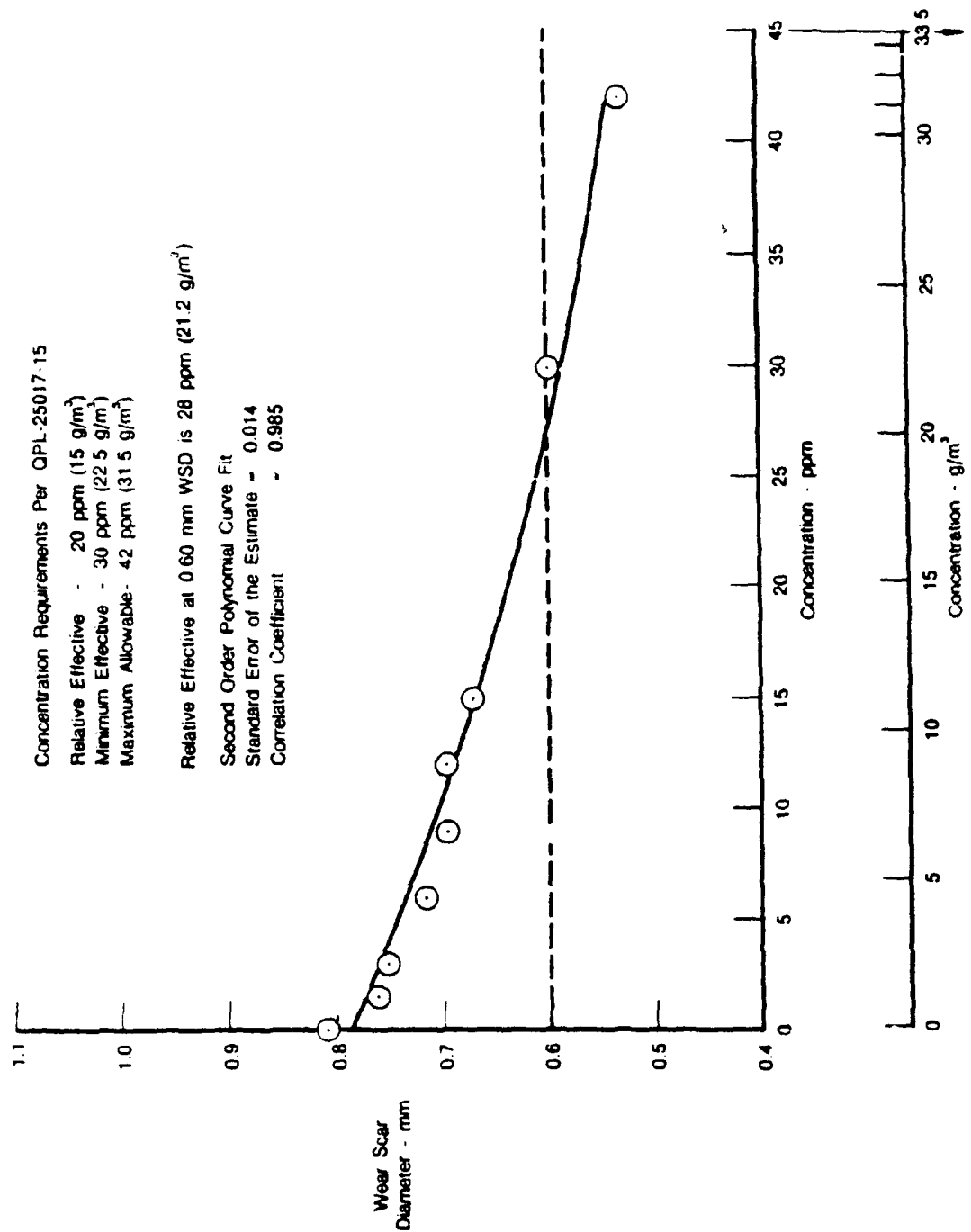


Figure D-23. Effect of TOLAD 245 in Clay Treated JP-4

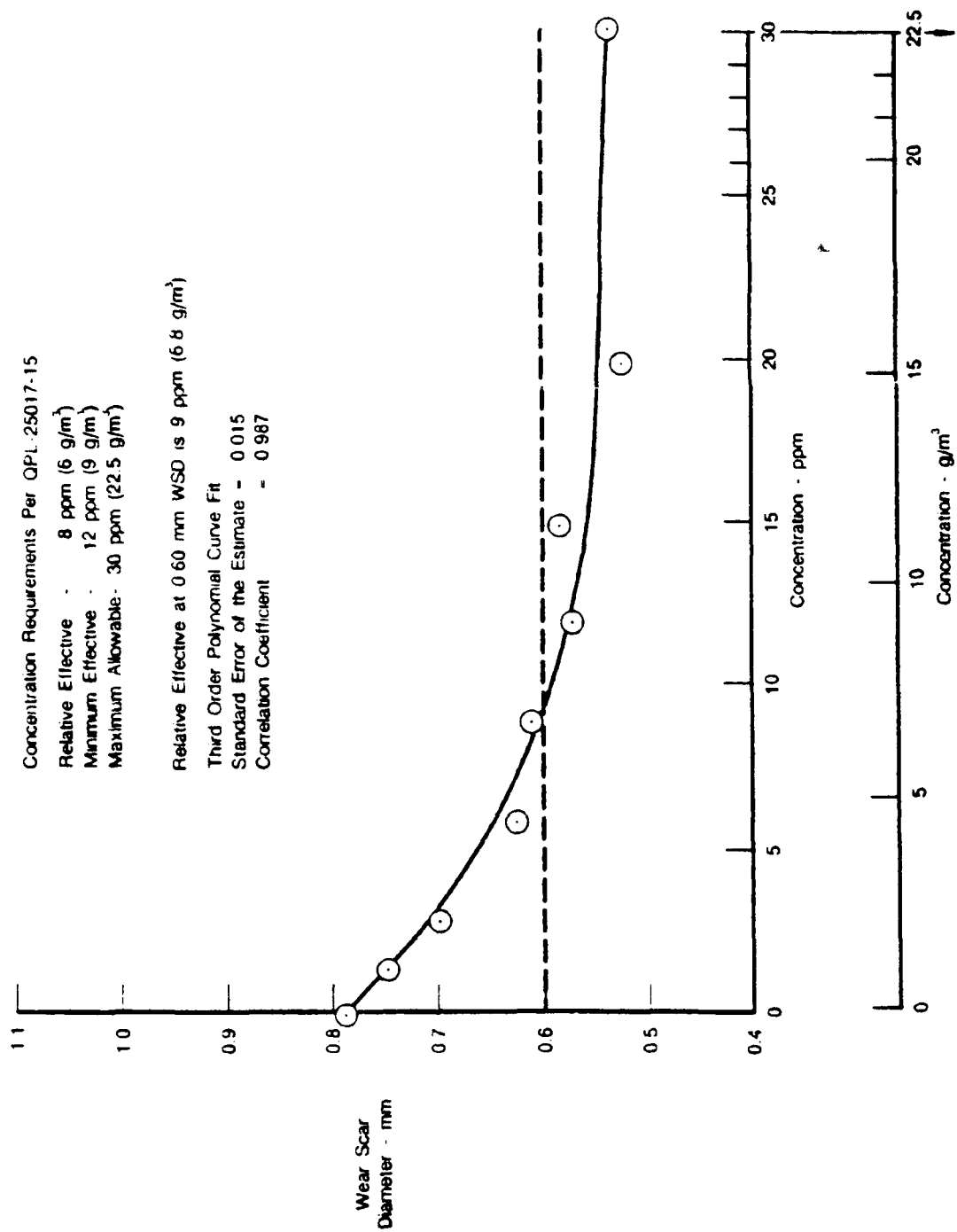


Figure D-24. Effect of UNICOR-J in Clay Treated JP-4

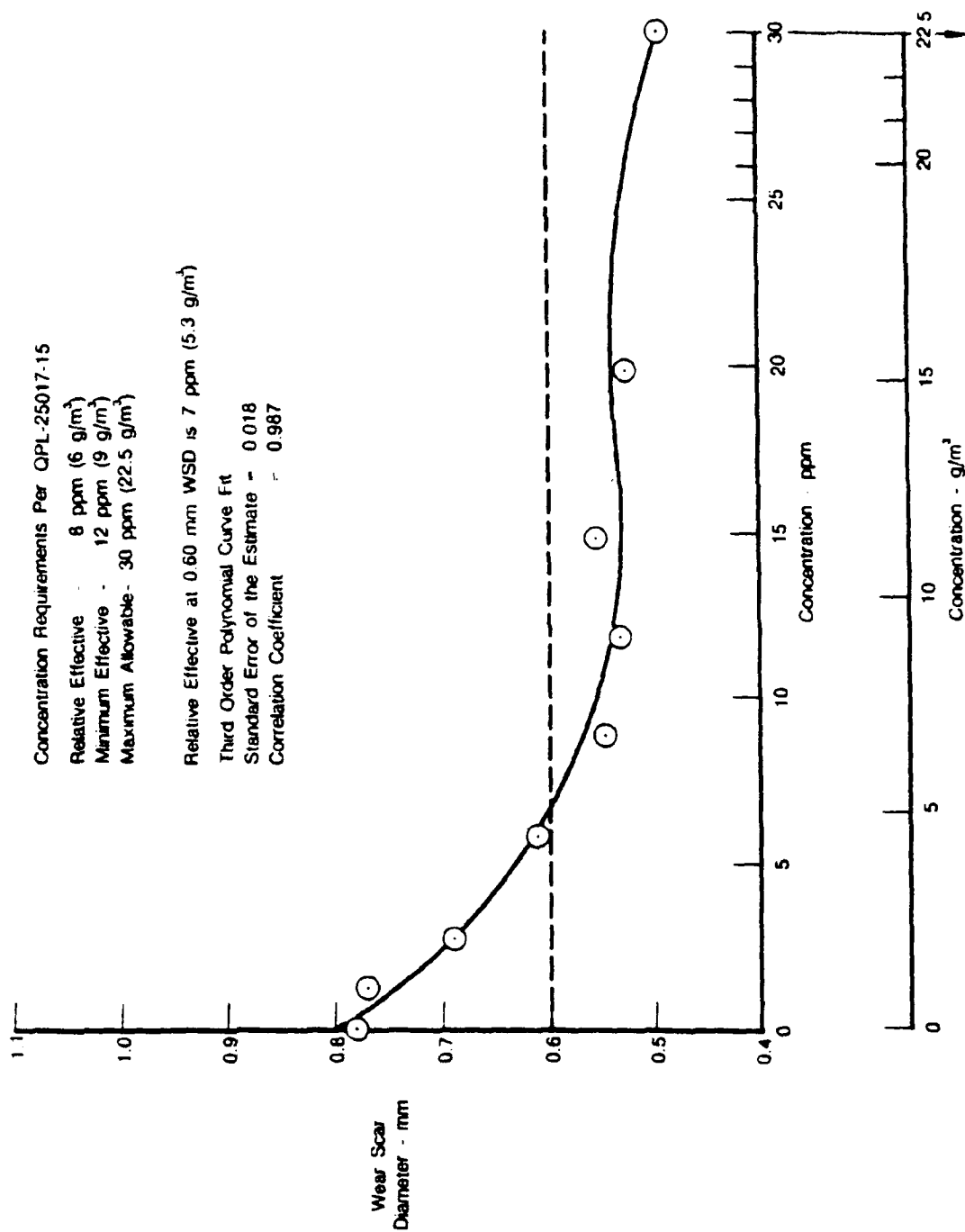


Figure D-25. Effect of IPC-4410 in Clay Treated JP-4

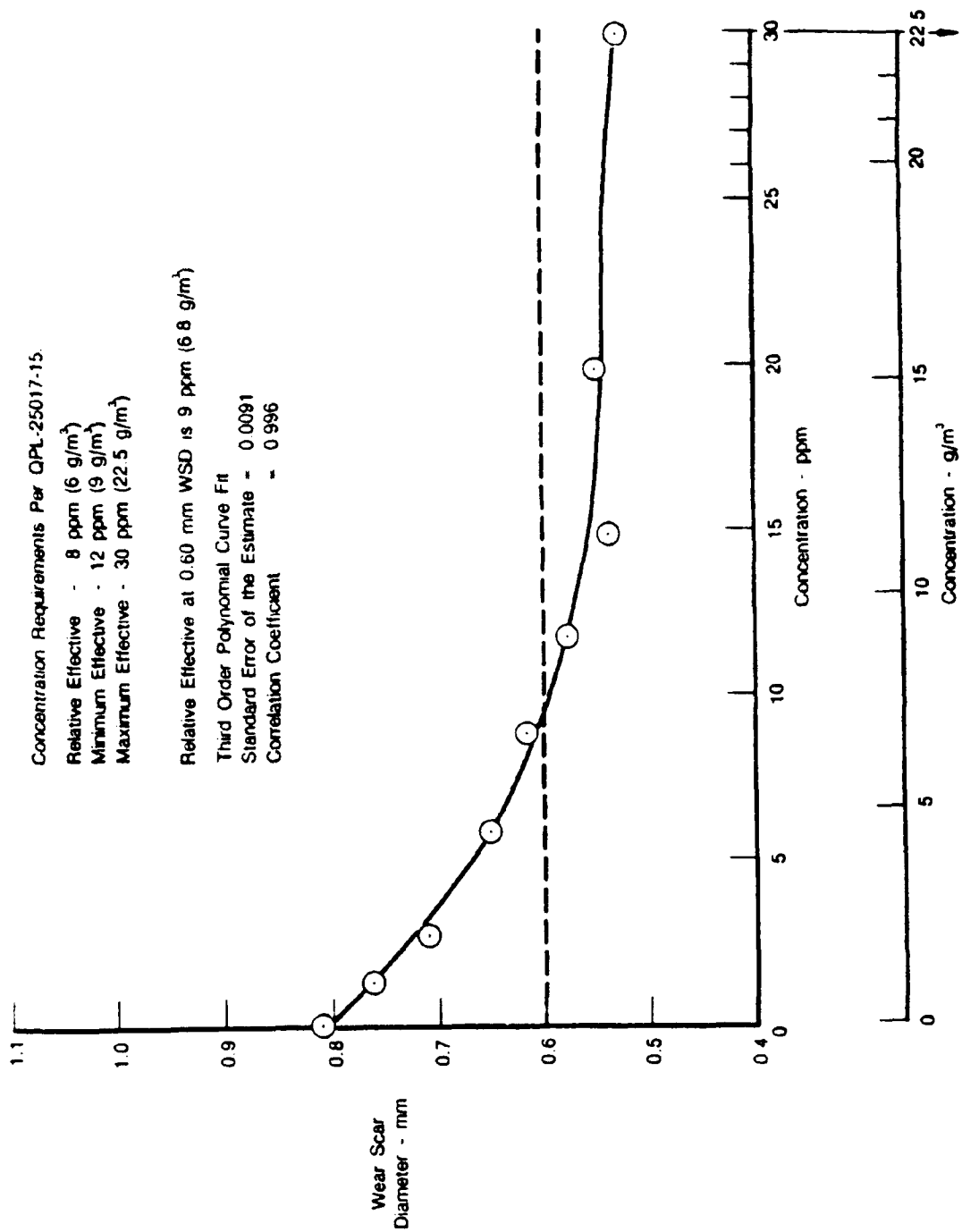


Figure D-26. Effect of MOBILAD F-800 in Clay Treated JP-4

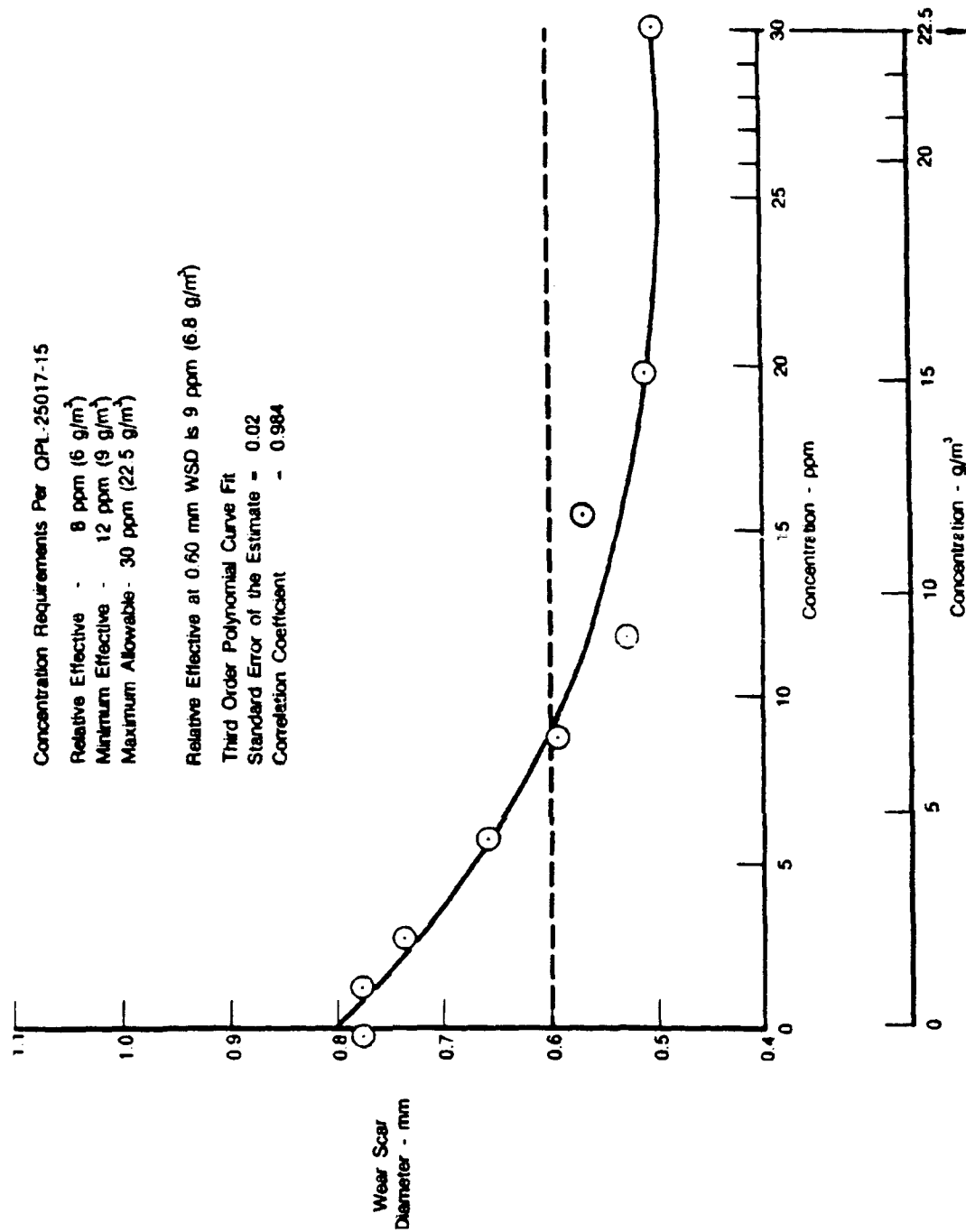


Figure D-27. Effect of NALCO-5405 in Clay Treated JP-4

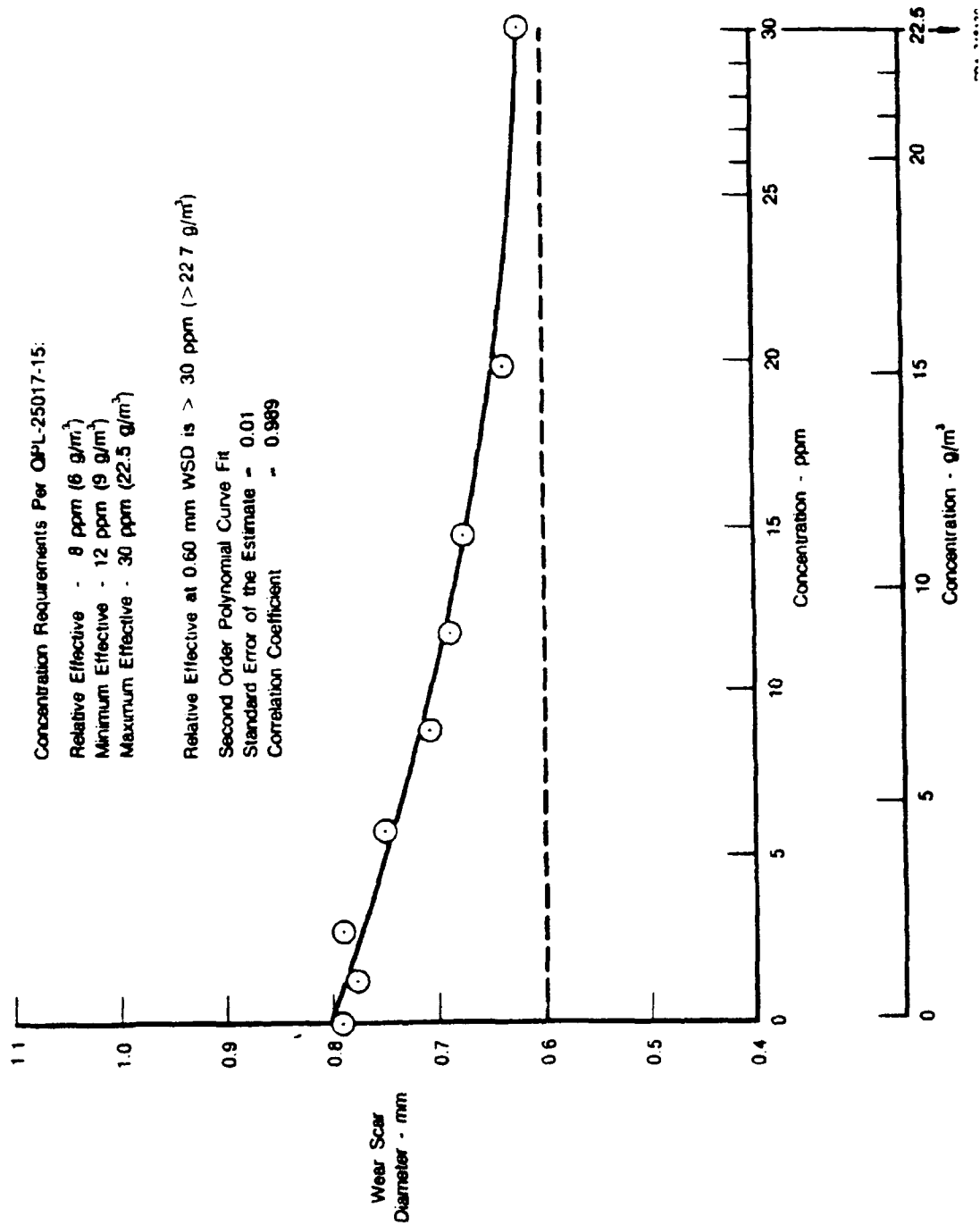


Figure D-28. Effect of TOLAD 249 in Clay Treated JP-4

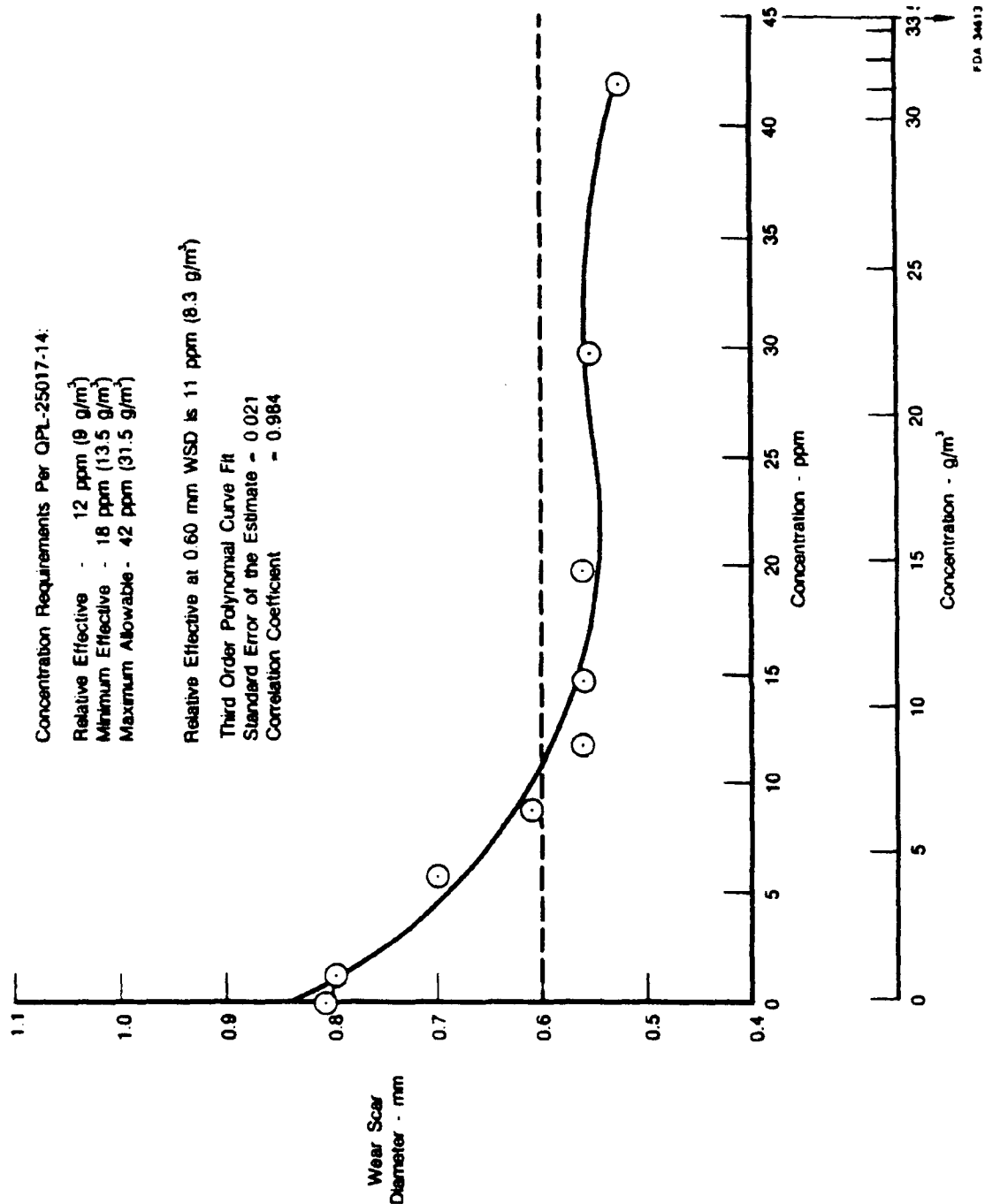


Figure D-29. Effect of P-3305 in Clay Treated JP-4

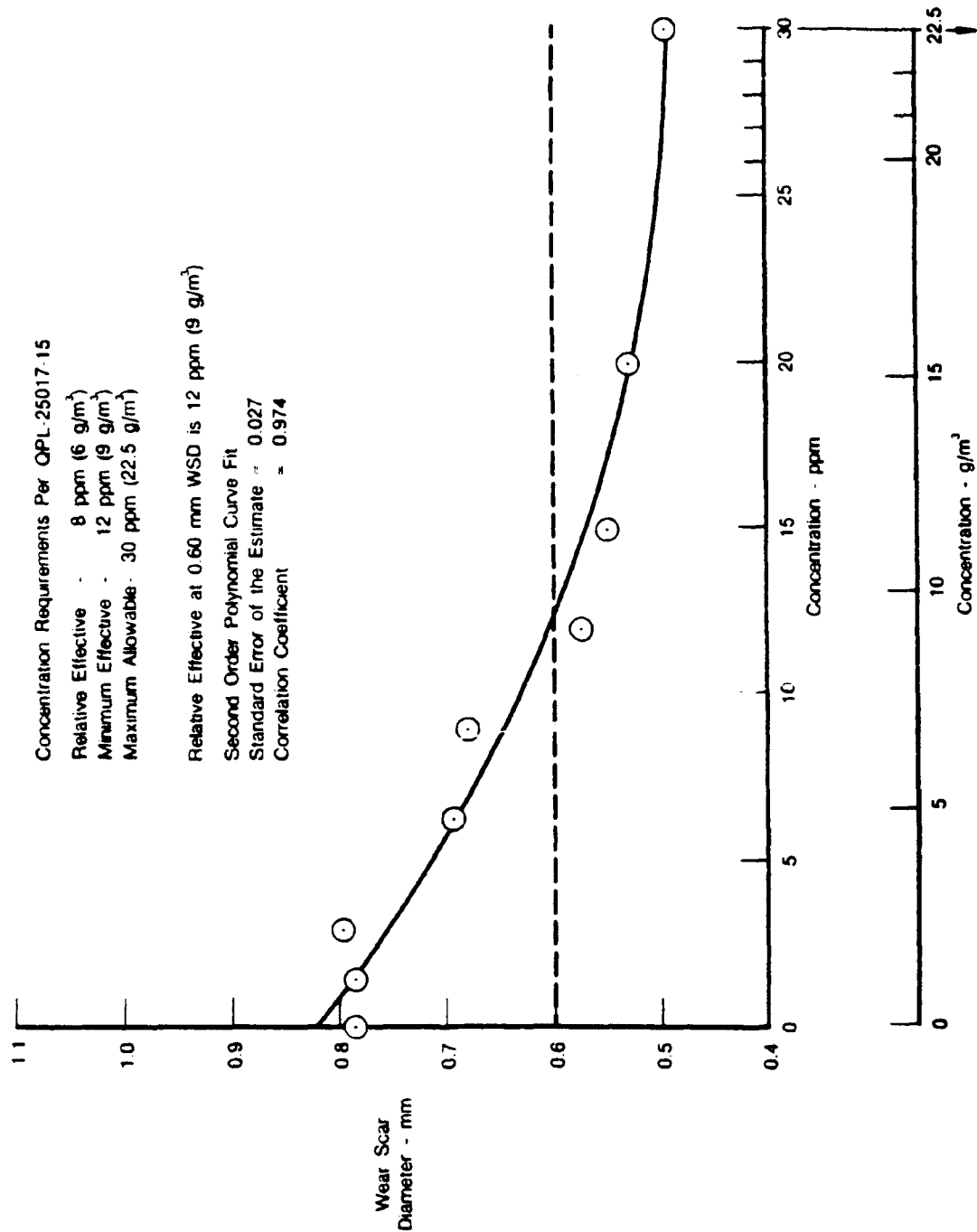


Figure D-30. Effect of IPC-4445 in Clay Treated JP-4

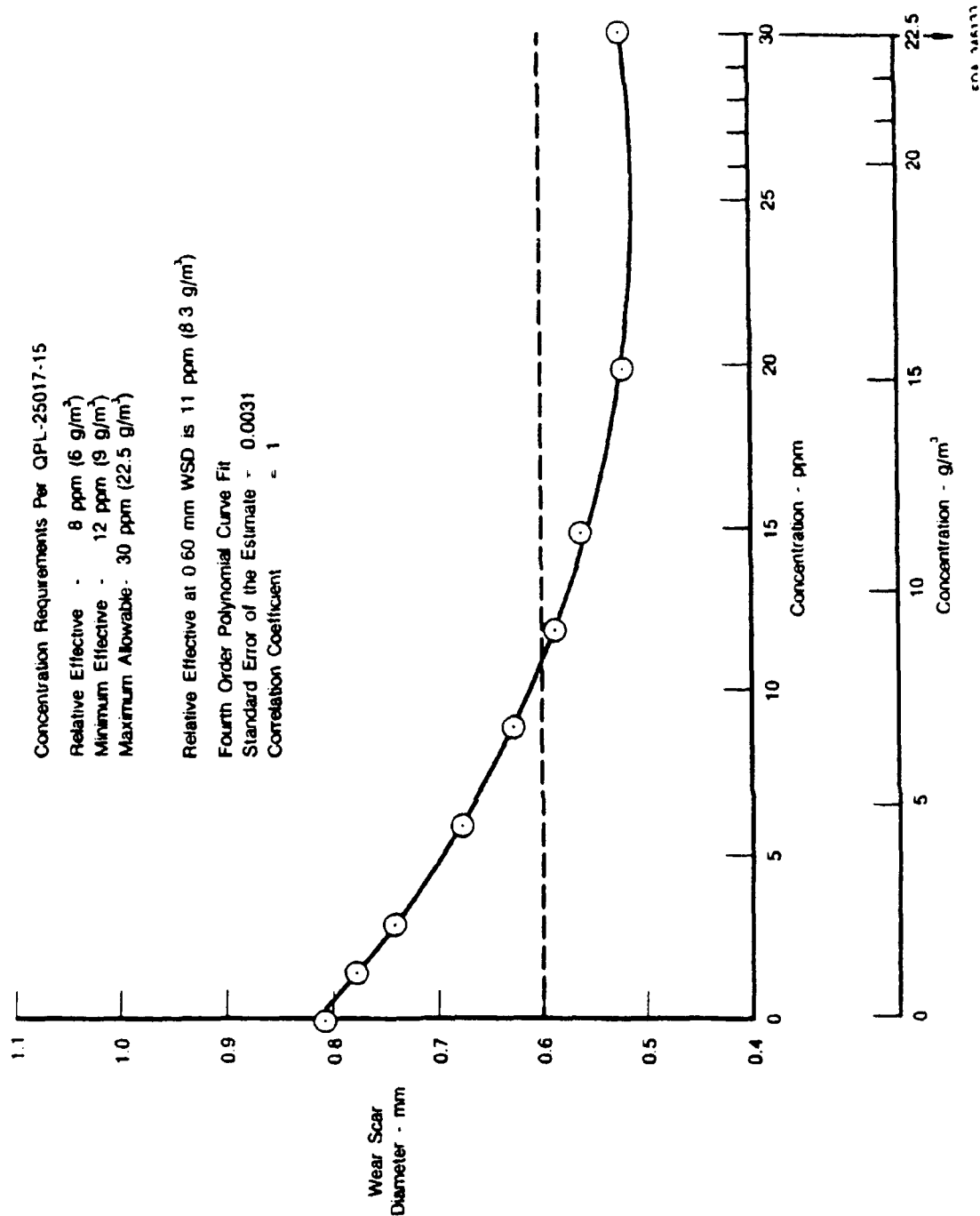


Figure D-31. Effect of WELCHEM 91120 in Clay Treated JP-4

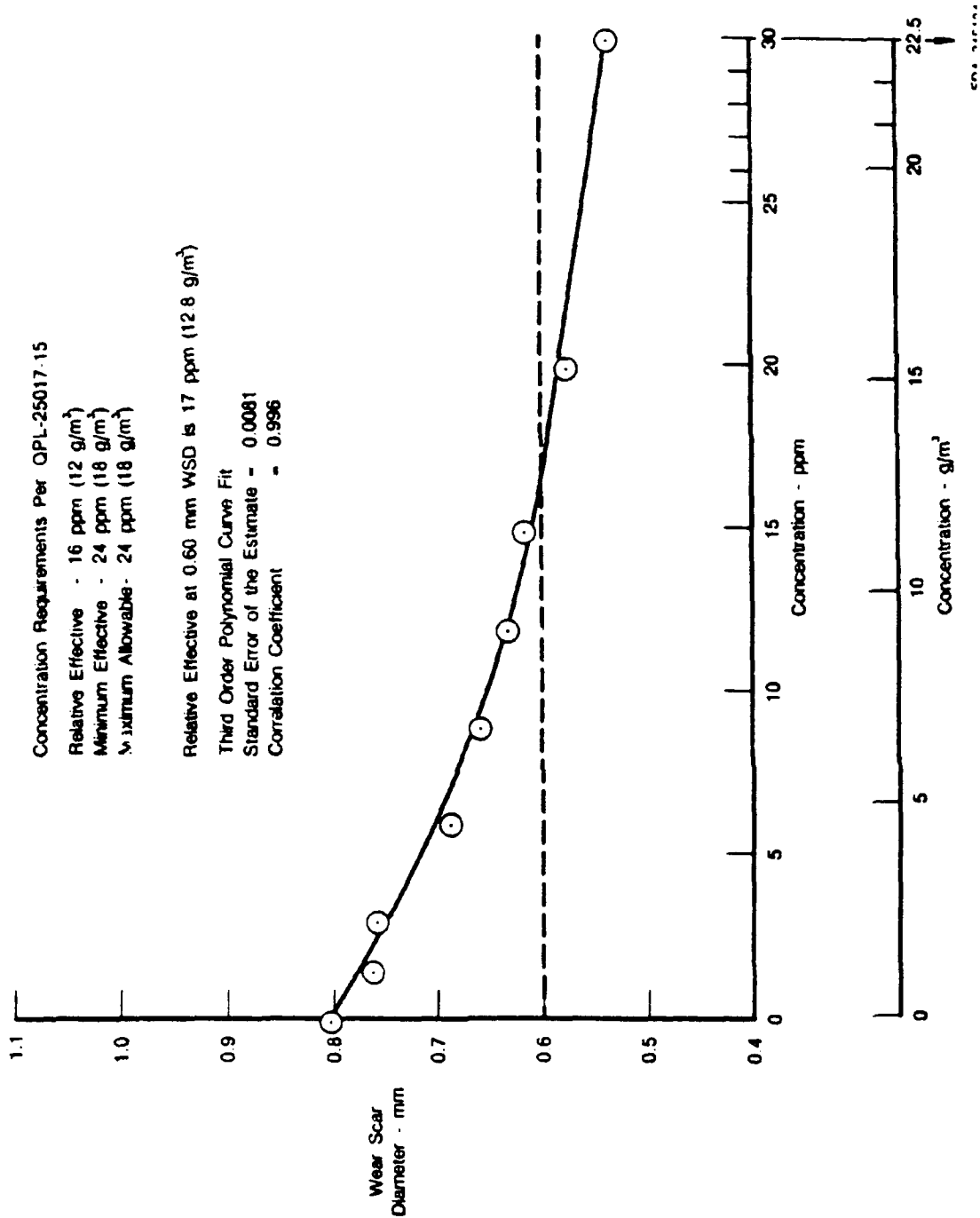


Figure D-32. Effect of NUCHEM PCI-105 in Clay Treated JP-4

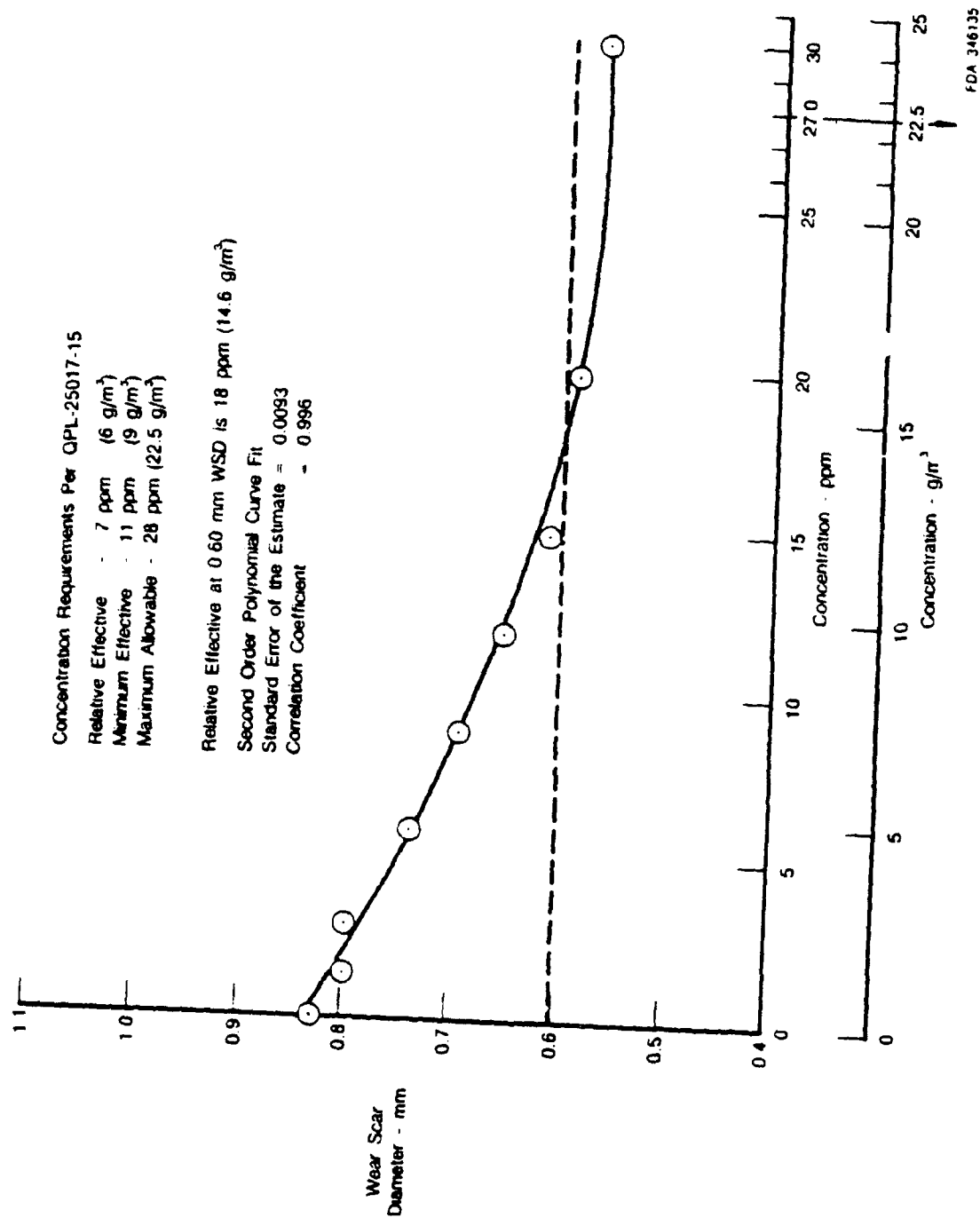


Figure D-33. Effect of Apollo PRI-19 in Clay Treated JP-8

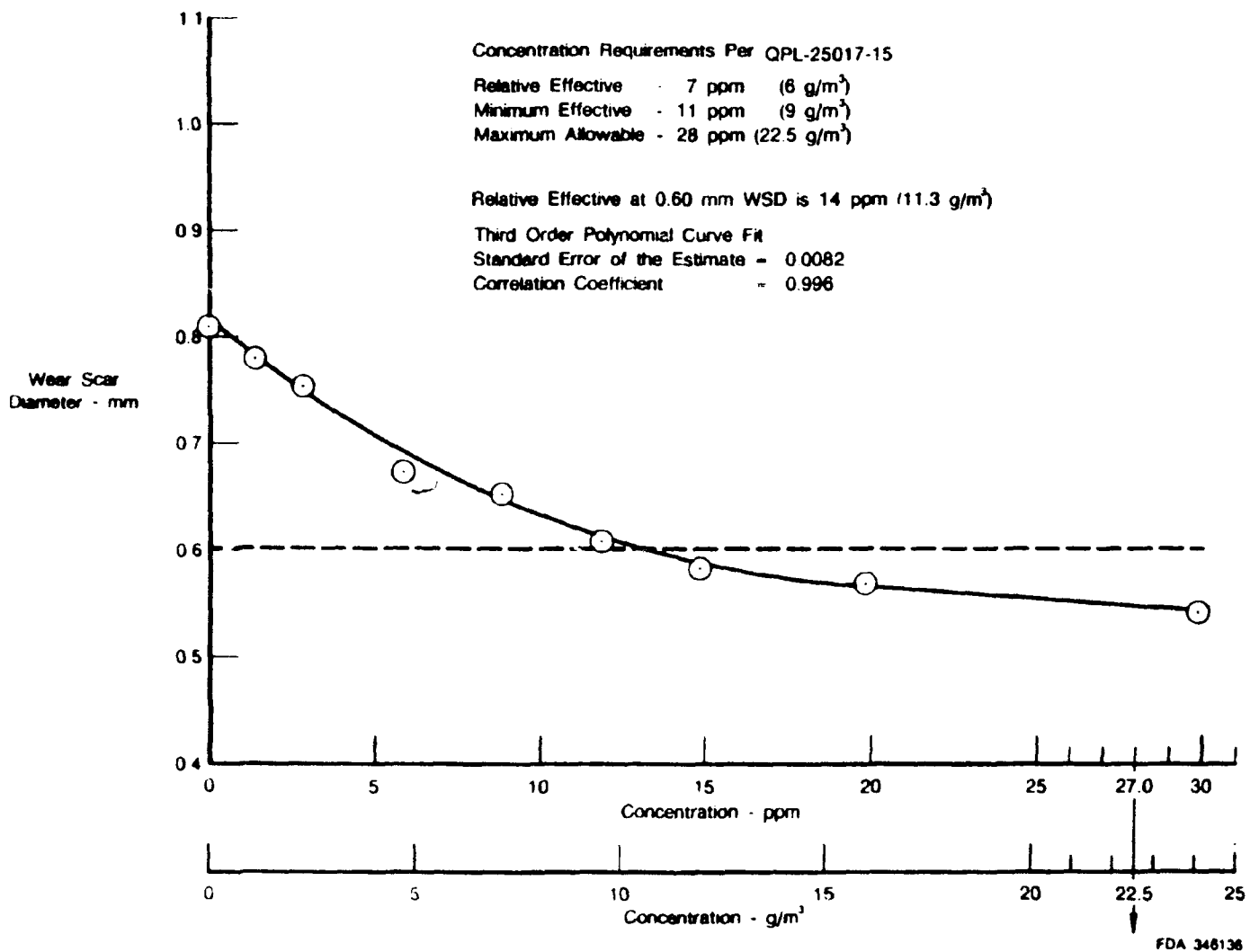


Figure D-34. Effect of HITEC E-580 in Clay Treated JP-8

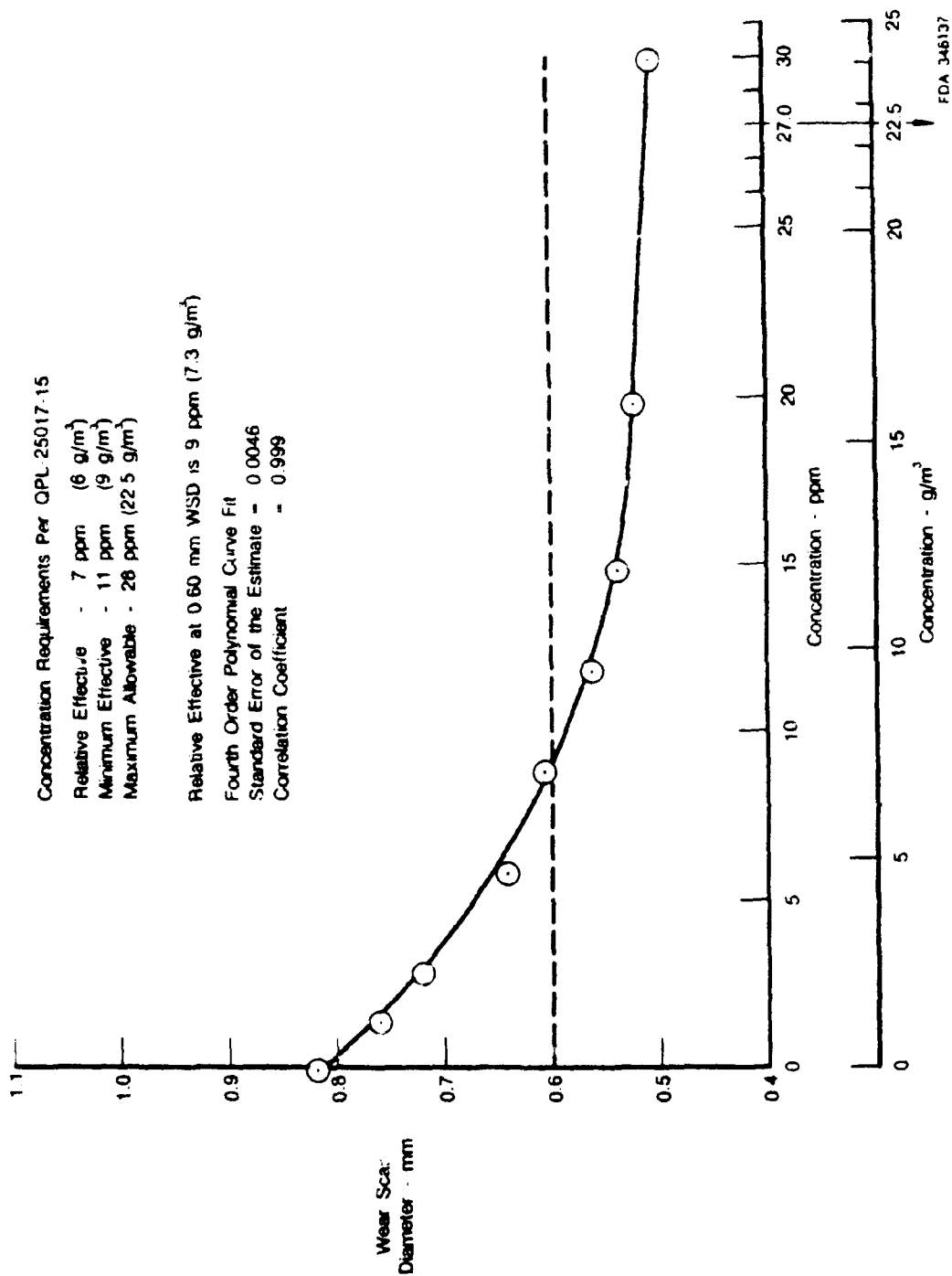


Figure D-35. Effect of DCI-4A in Clay Treated JP-8

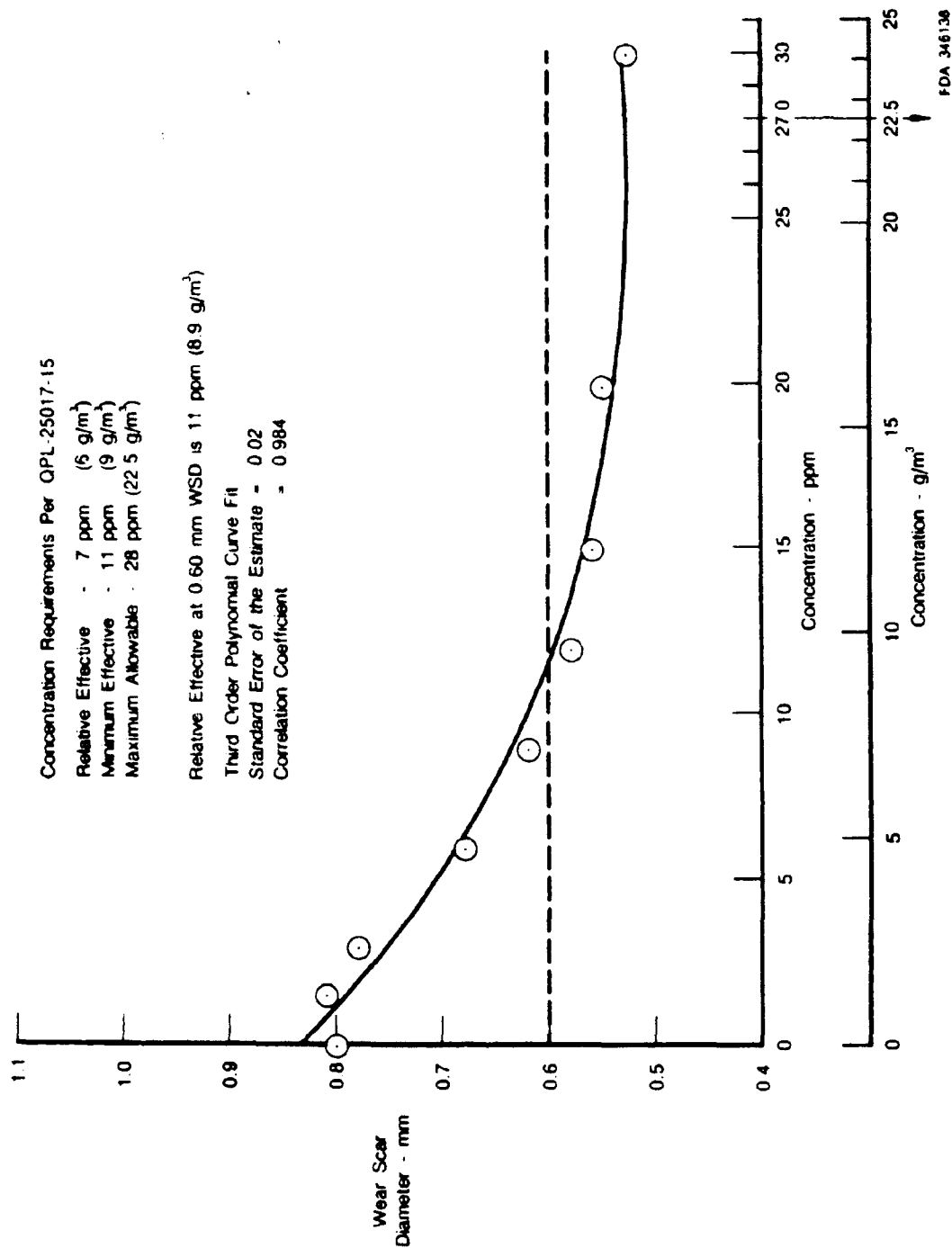


Figure D-36. Effect of DCI-6A in Clay Treated JP-8

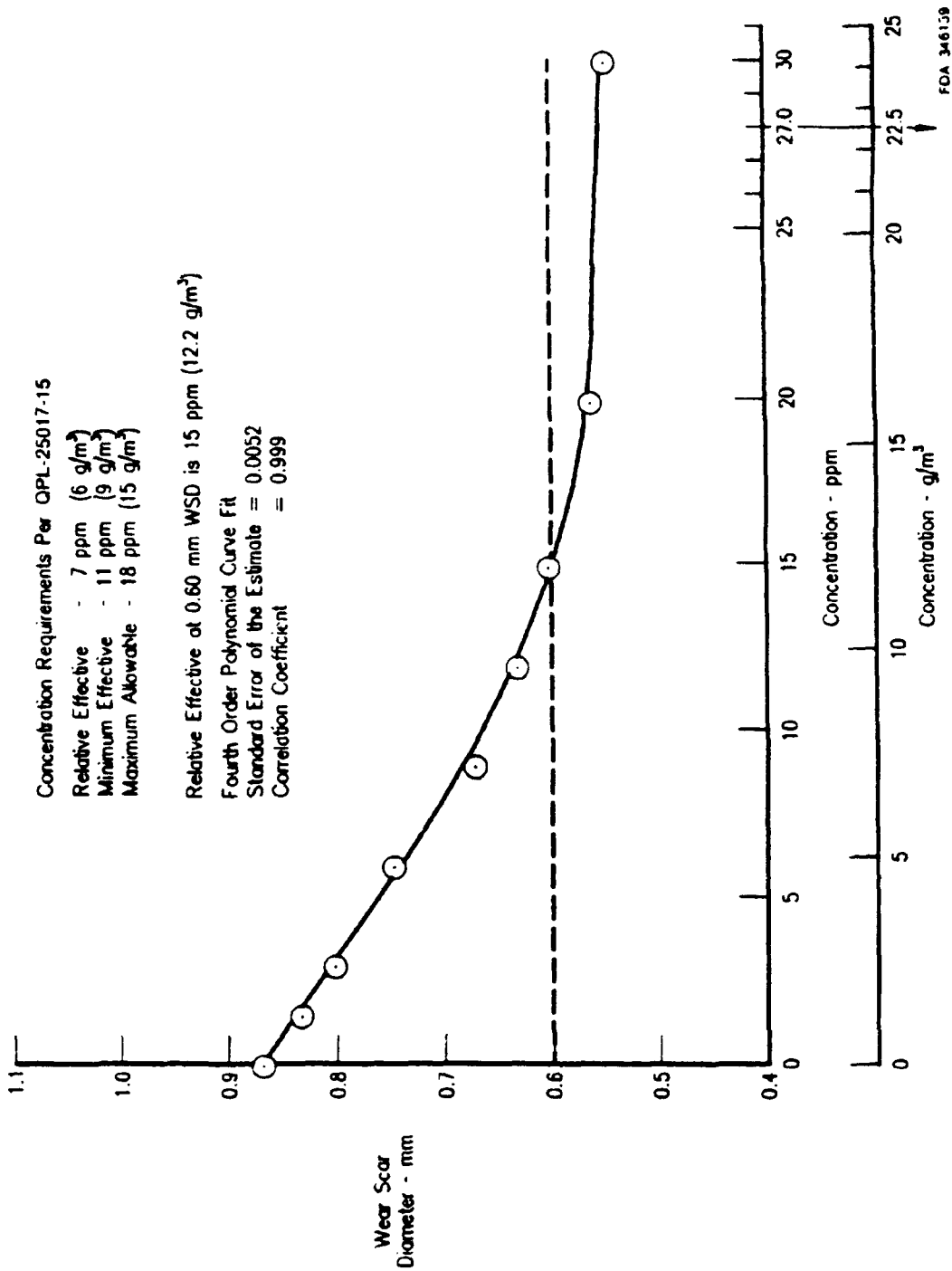


Figure D-37. Effect of LUBRIZOL in Clay Treated JP-8

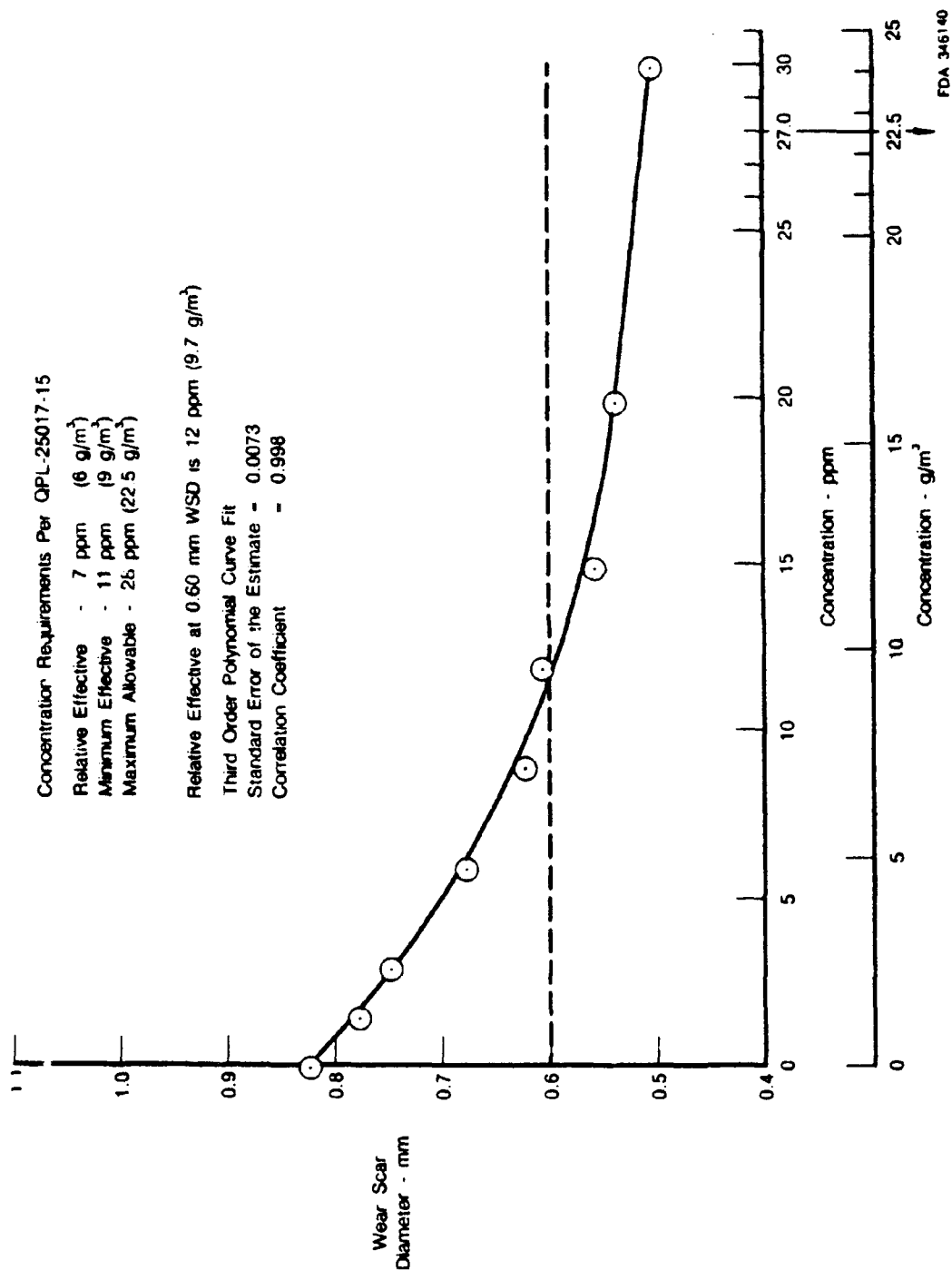


Figure D-38. Effect of NALCO 5403 in Clay Treated JP-8

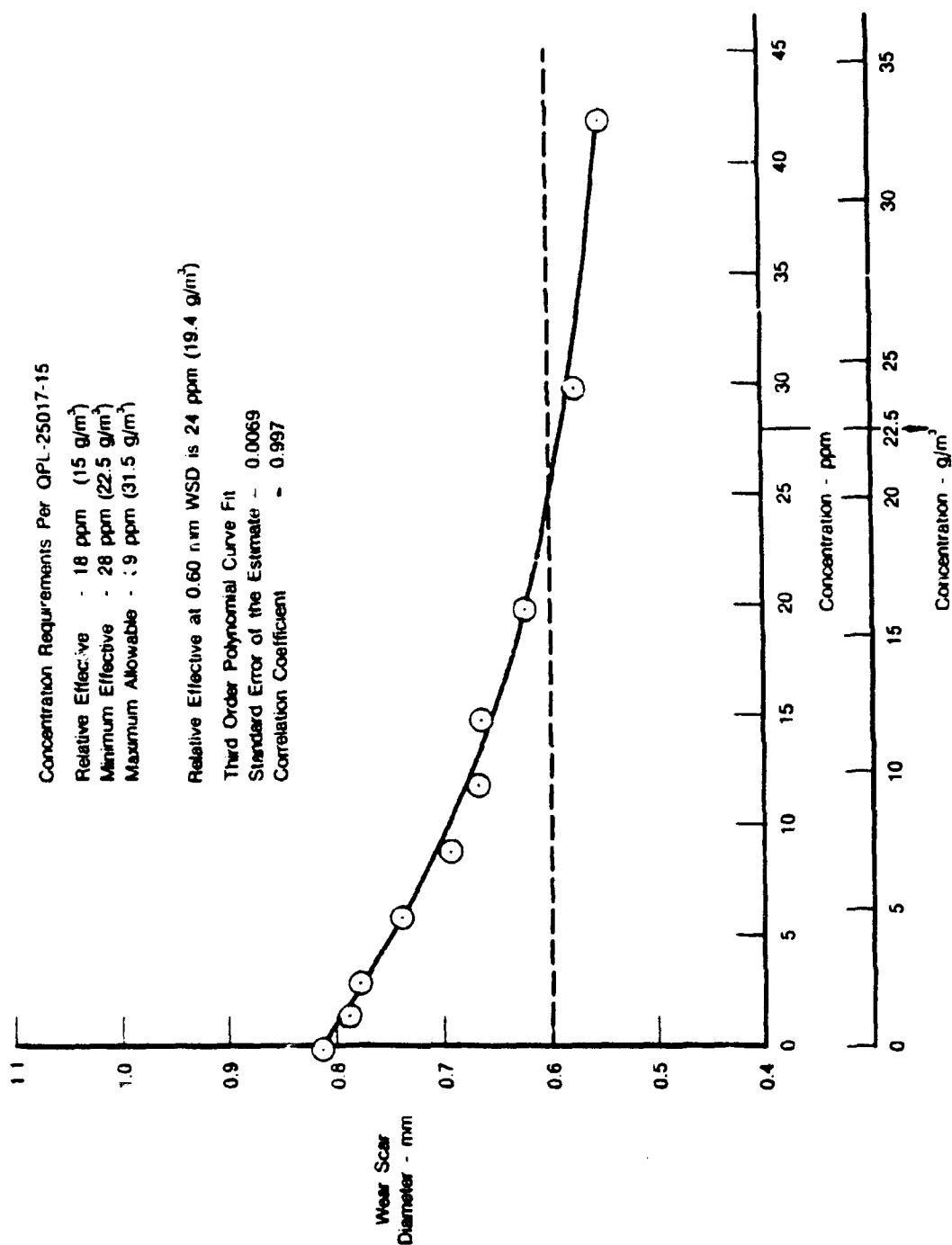


Figure D-39. Effect of TOLAD 245 in Clay Treated JP-8

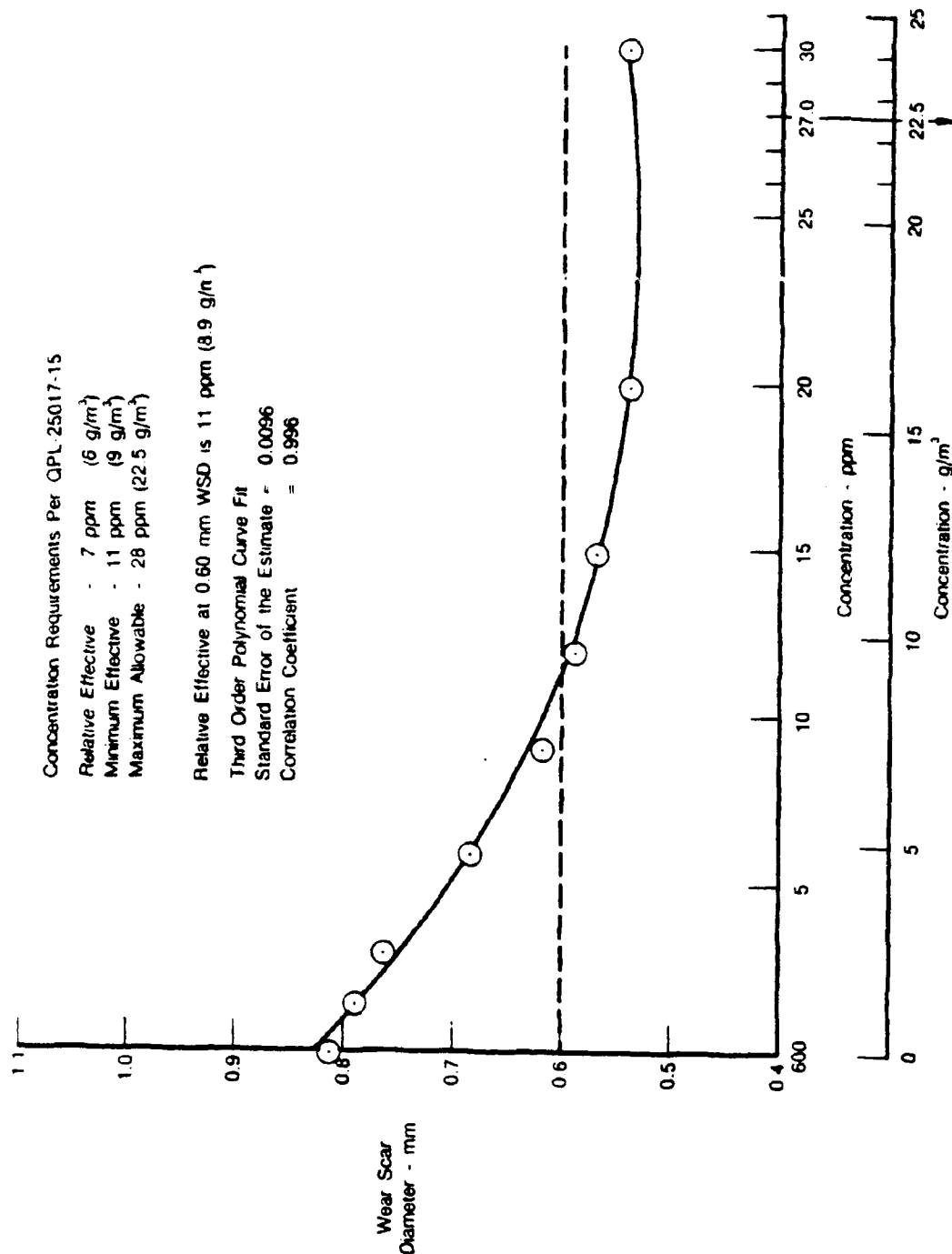


Figure D-40. Effect of UNICOR-J in Clay Treated JP-8

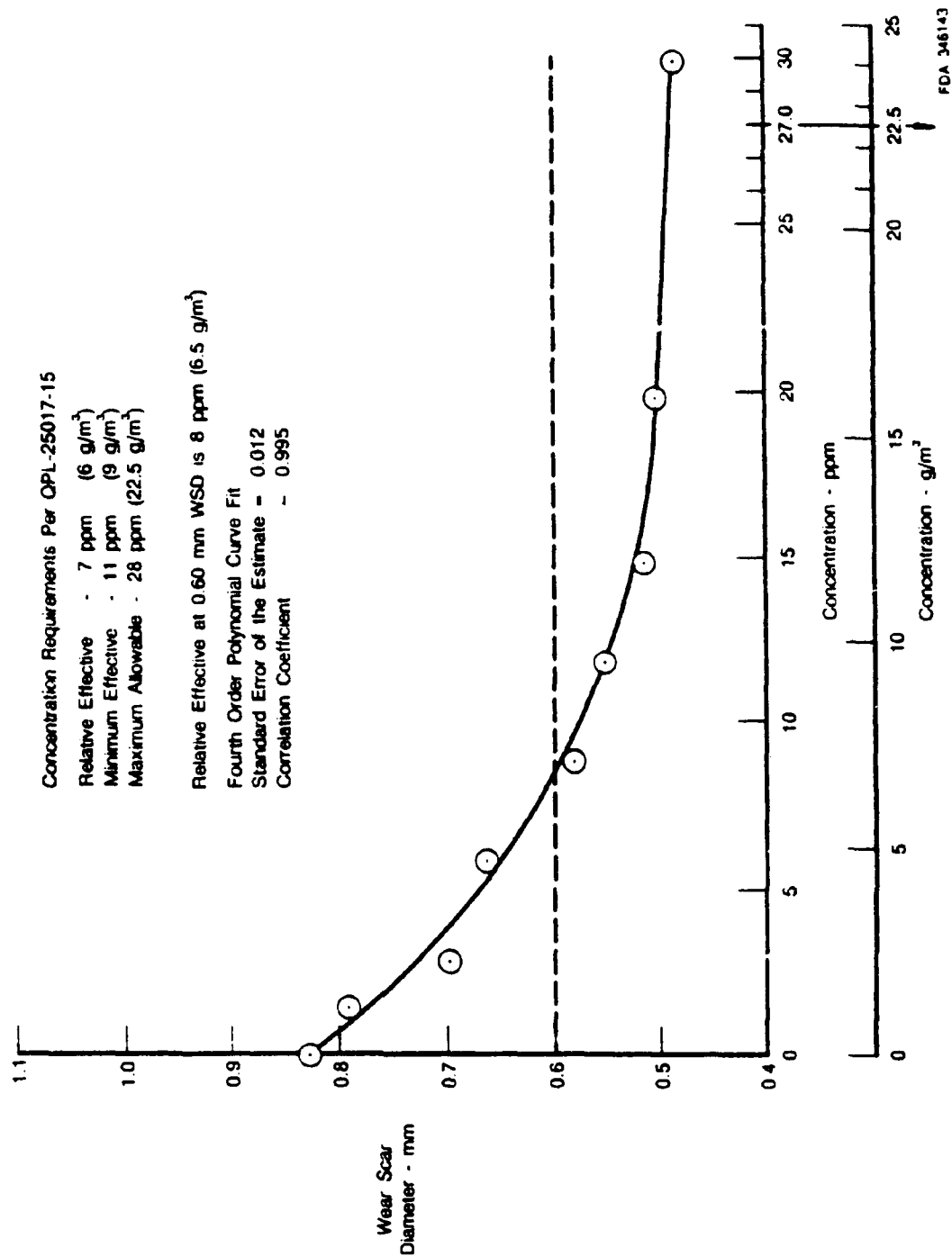


Figure D-41. Effect of IPC 4410 in Clay Treated JP-8

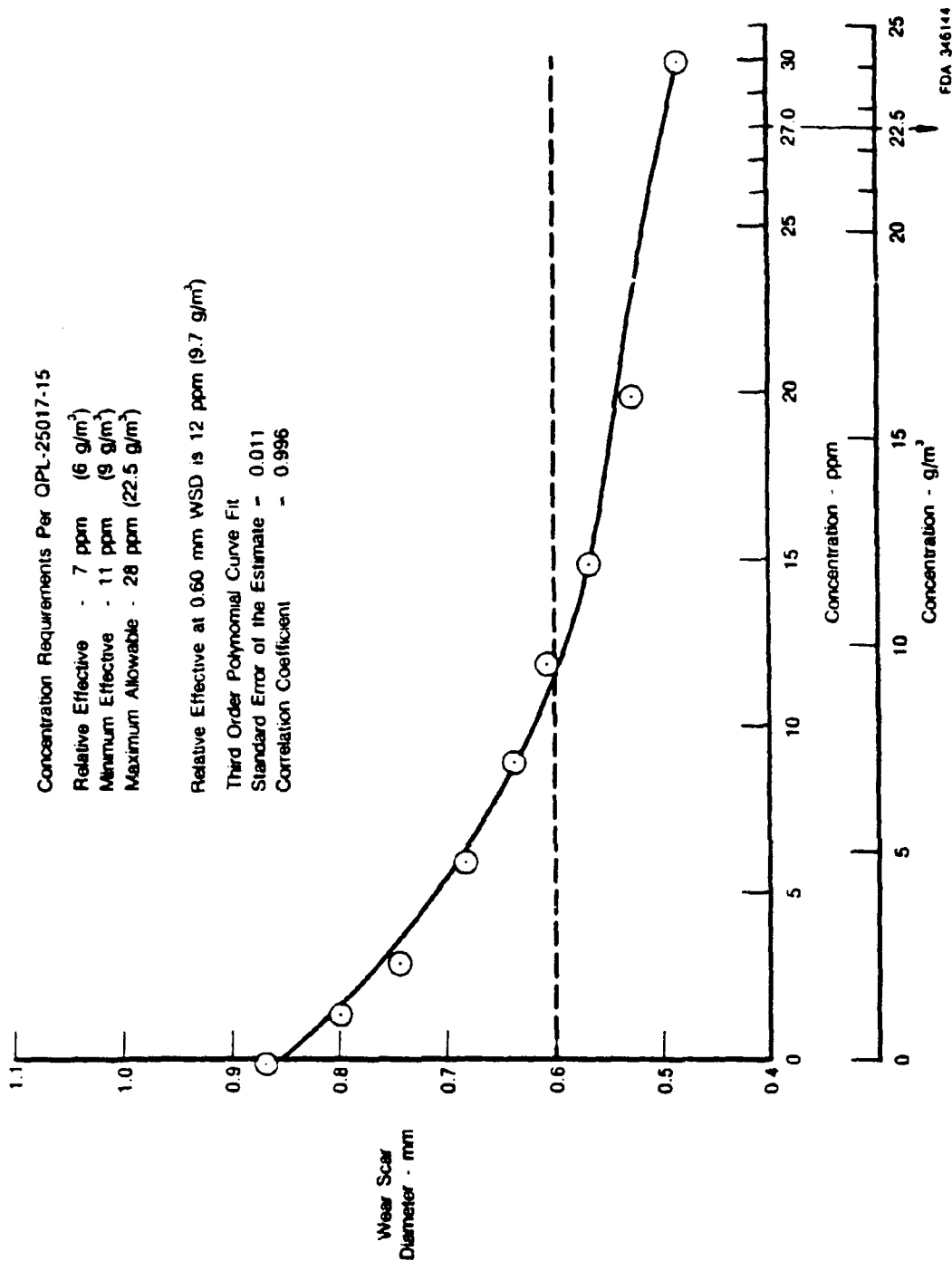


Figure D-42. Effect of MOBILAD F-800 in Clay Treated JP-8

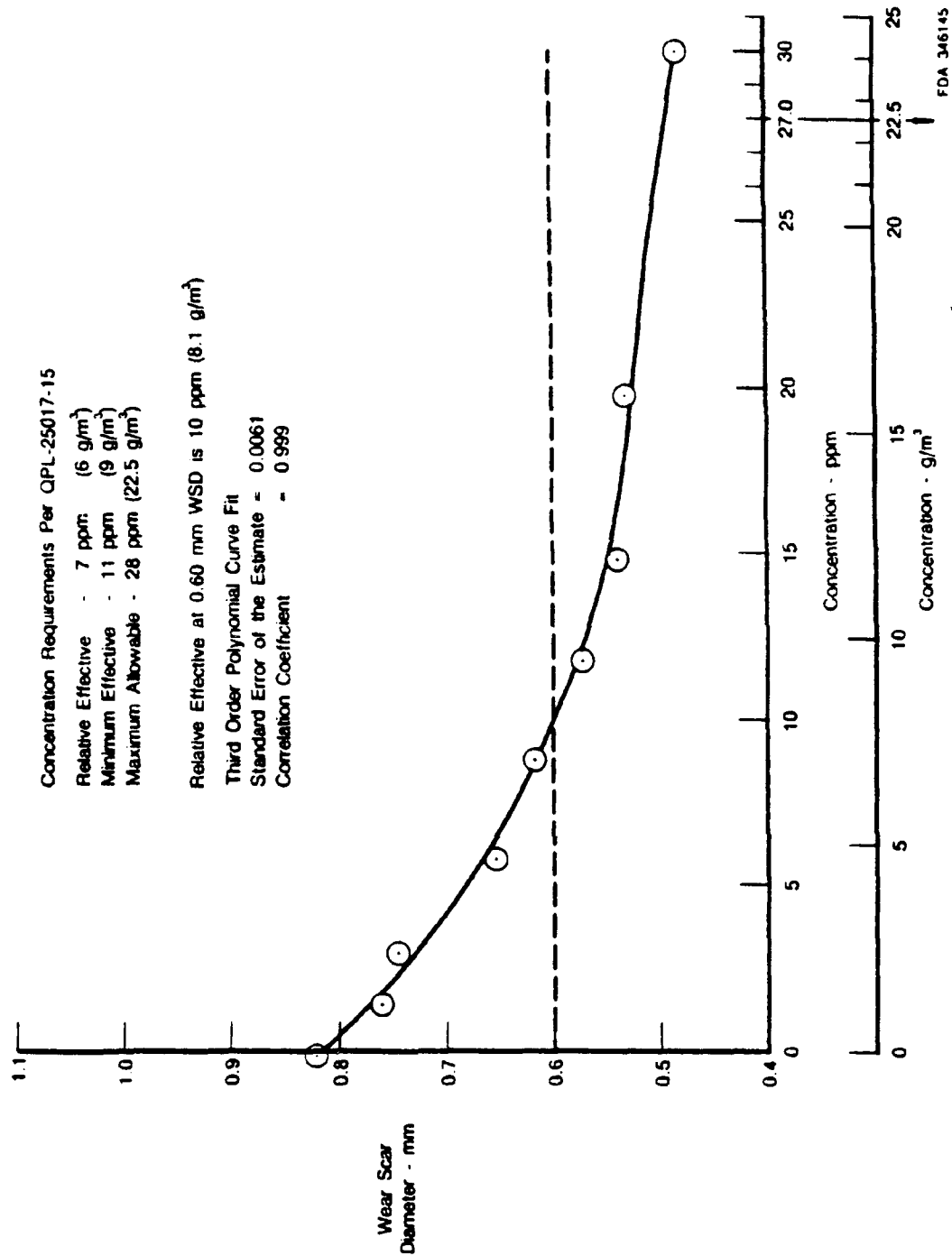


Figure D-43. Effect of NALCO 5405 in Clay Treated JP-8

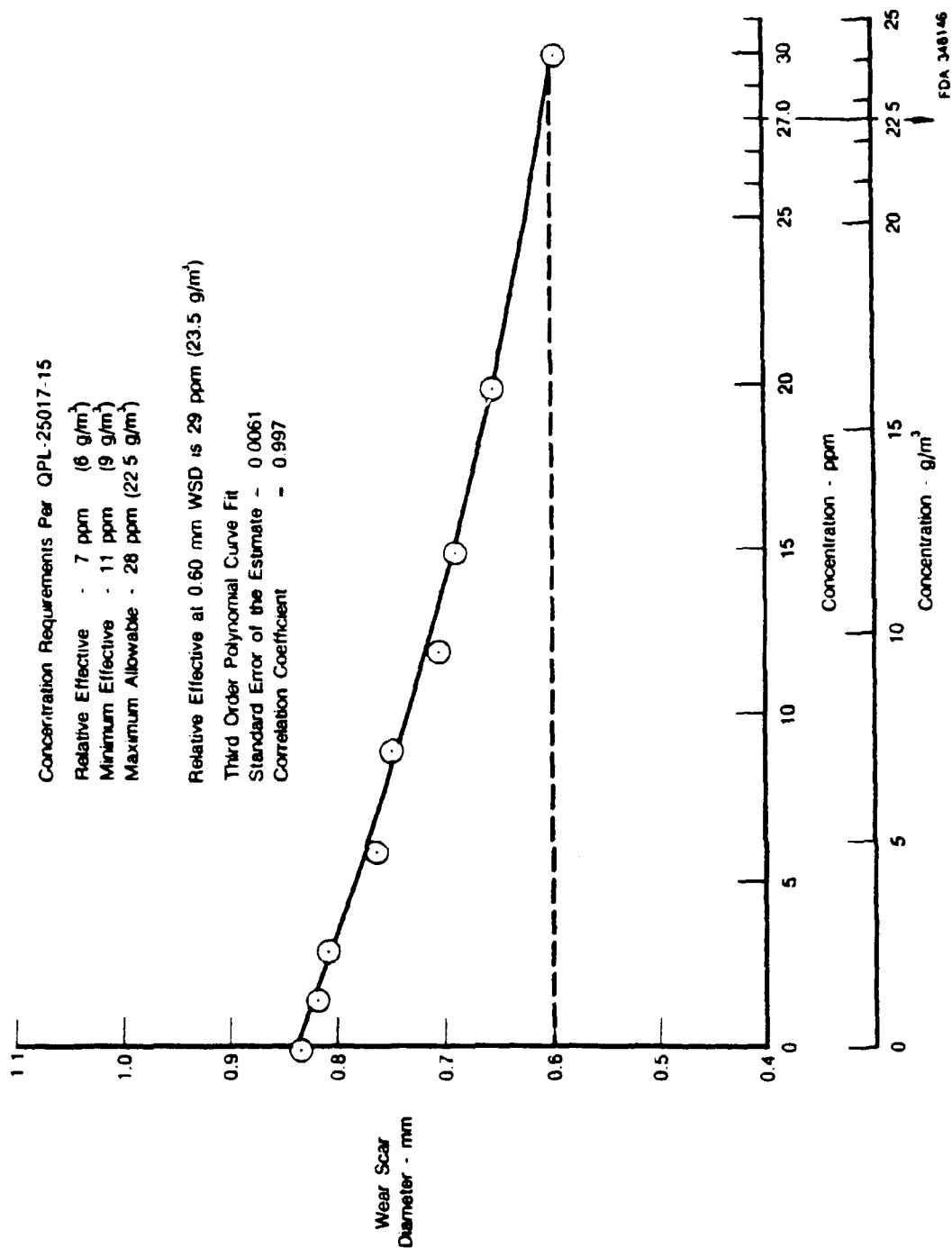
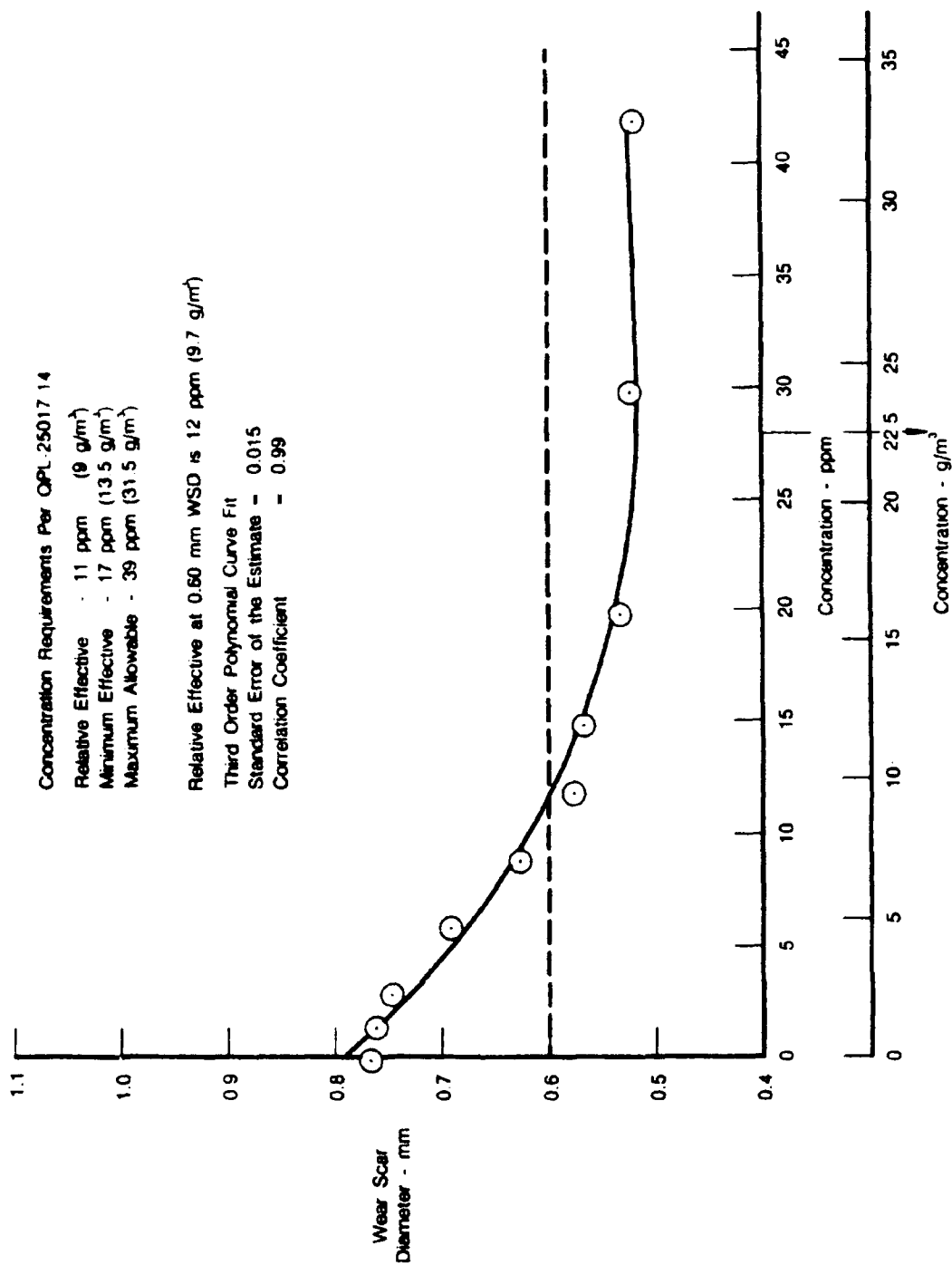


Figure D-44. Effect of TOLAD 249 in Clay Treated JP-8



FDA 346117

Figure D-45. Effect of P-3305 in Clay Treated JP-8

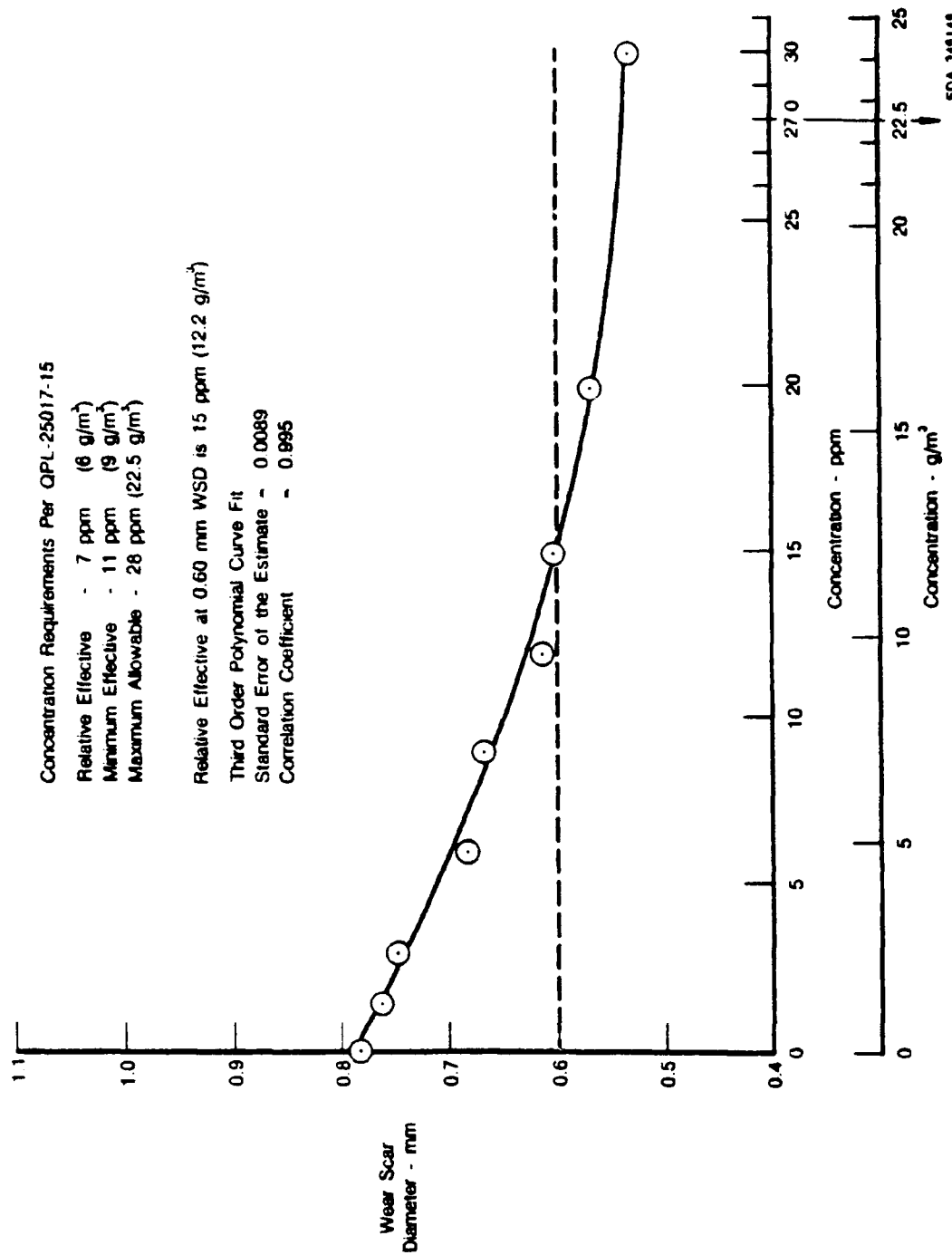


Figure D-46. Effect of IPR-4445 in Clay Treated JP-8

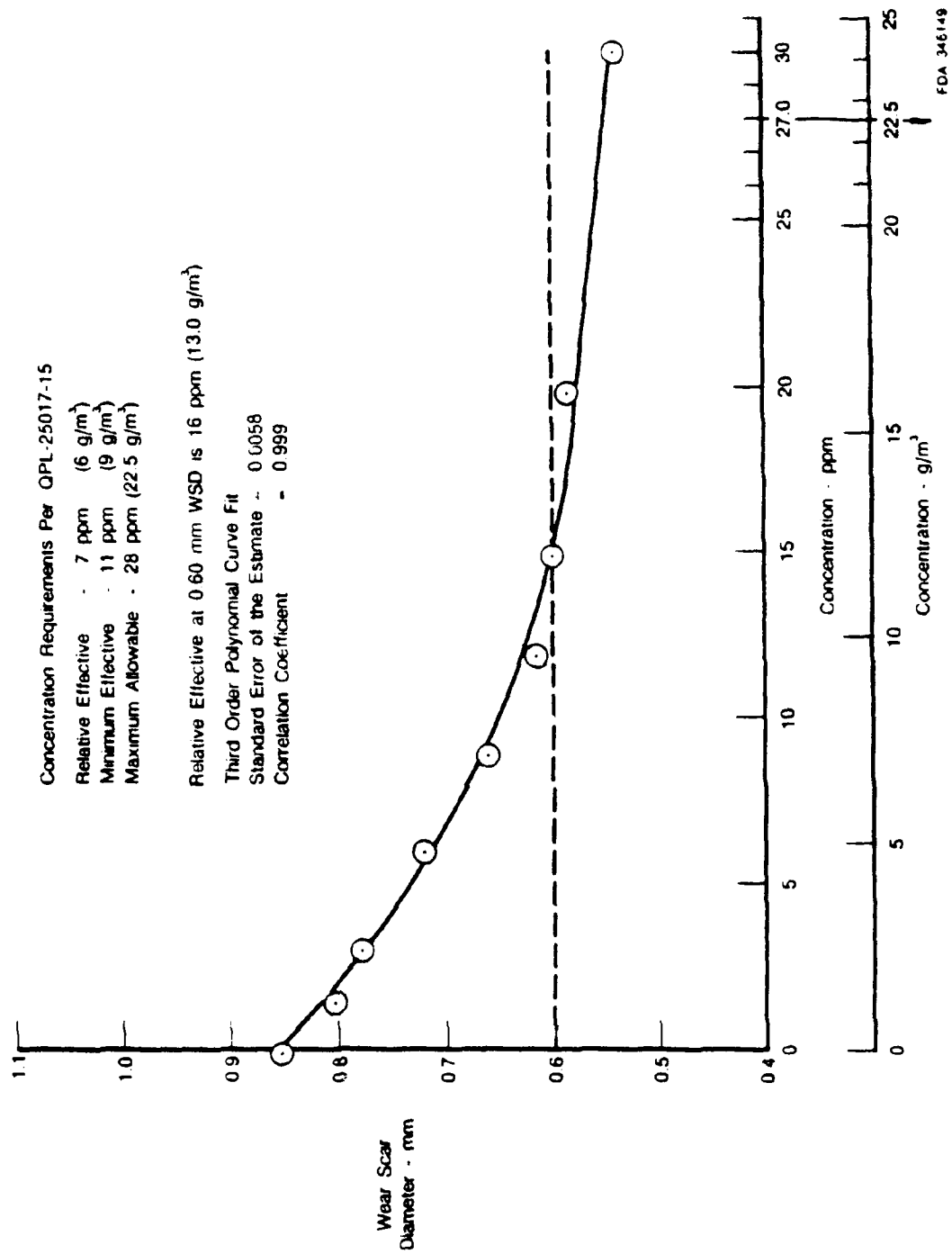


Figure D-47. Effect of WELCHEM 91120 in Clay Treated JP-8

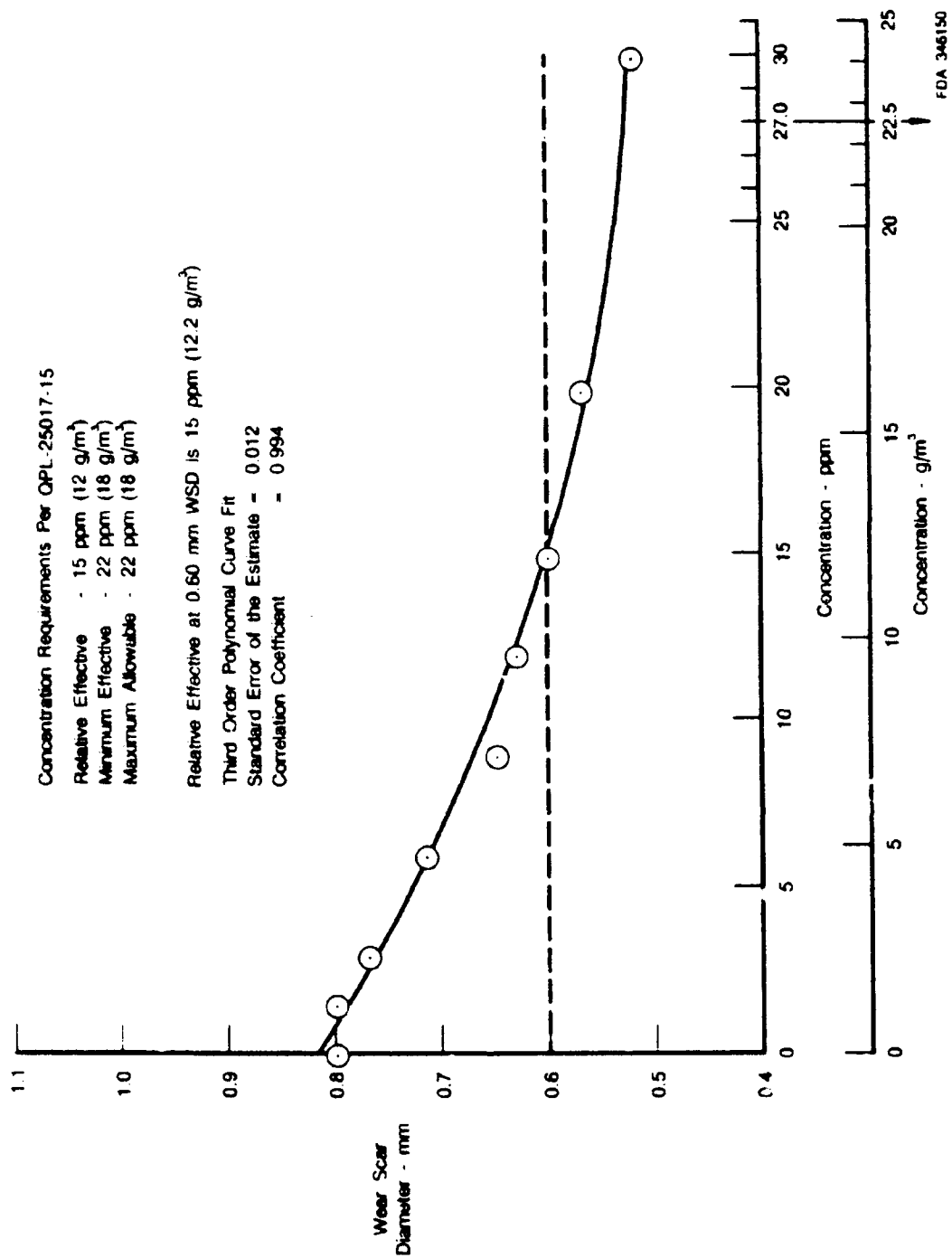


Figure D-48. Effect of NUCHEM in Clay Treated JP-8

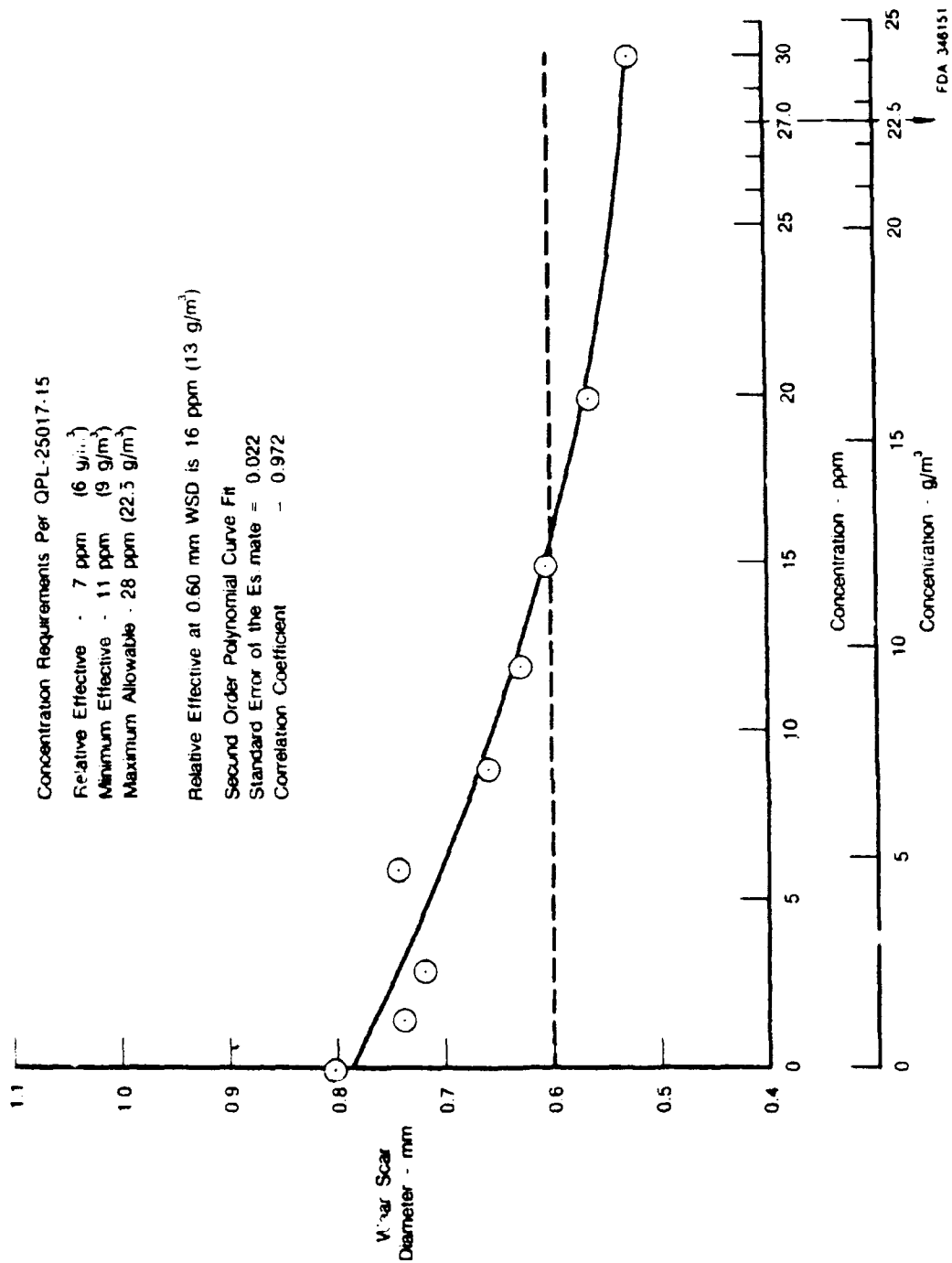


Figure D-49. Effect of Apollo PRI-19 in Clay Treated JP-8

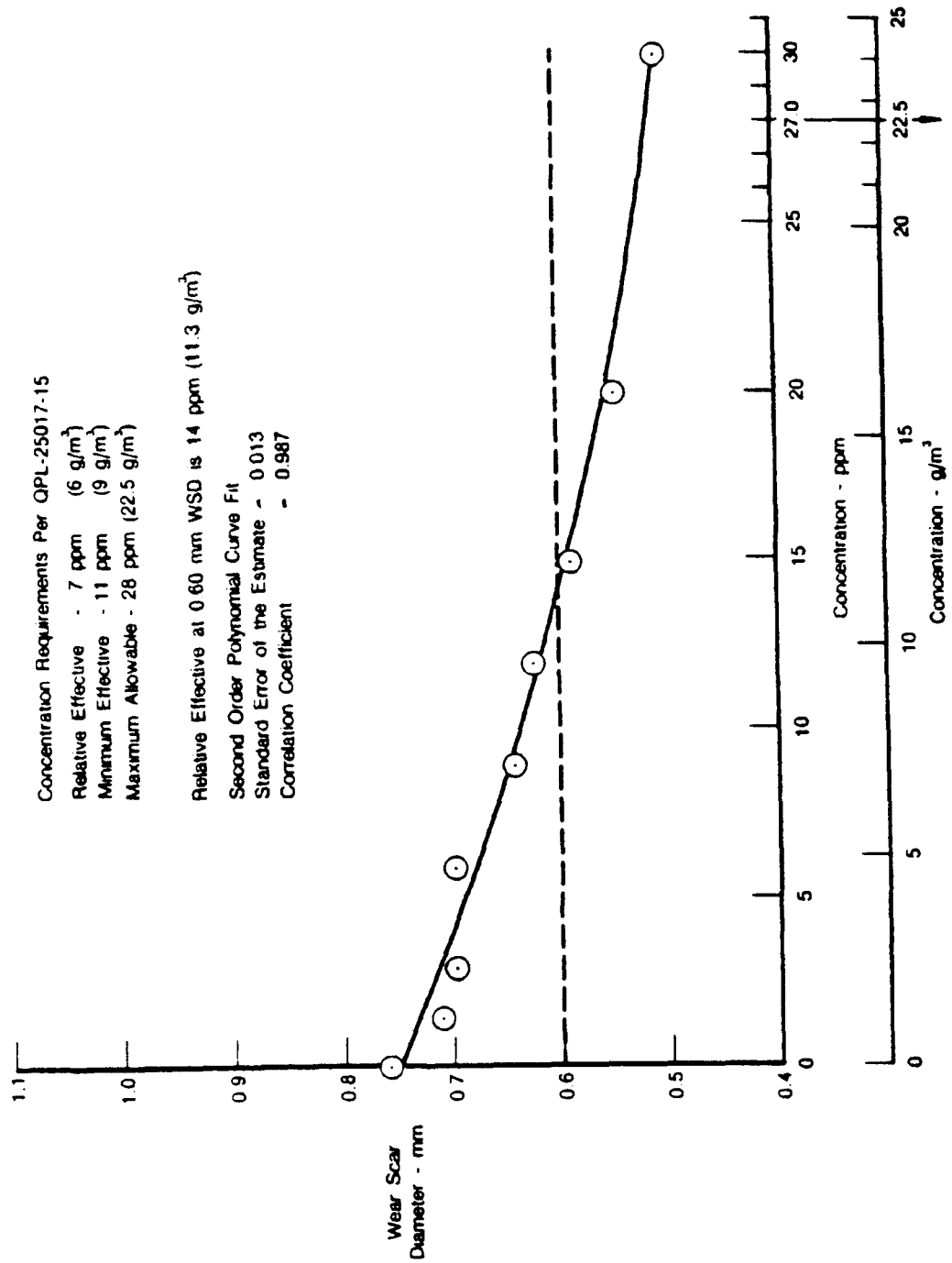


Figure D-50. Effect of HITEC E-580 in Clay Treated JP-5

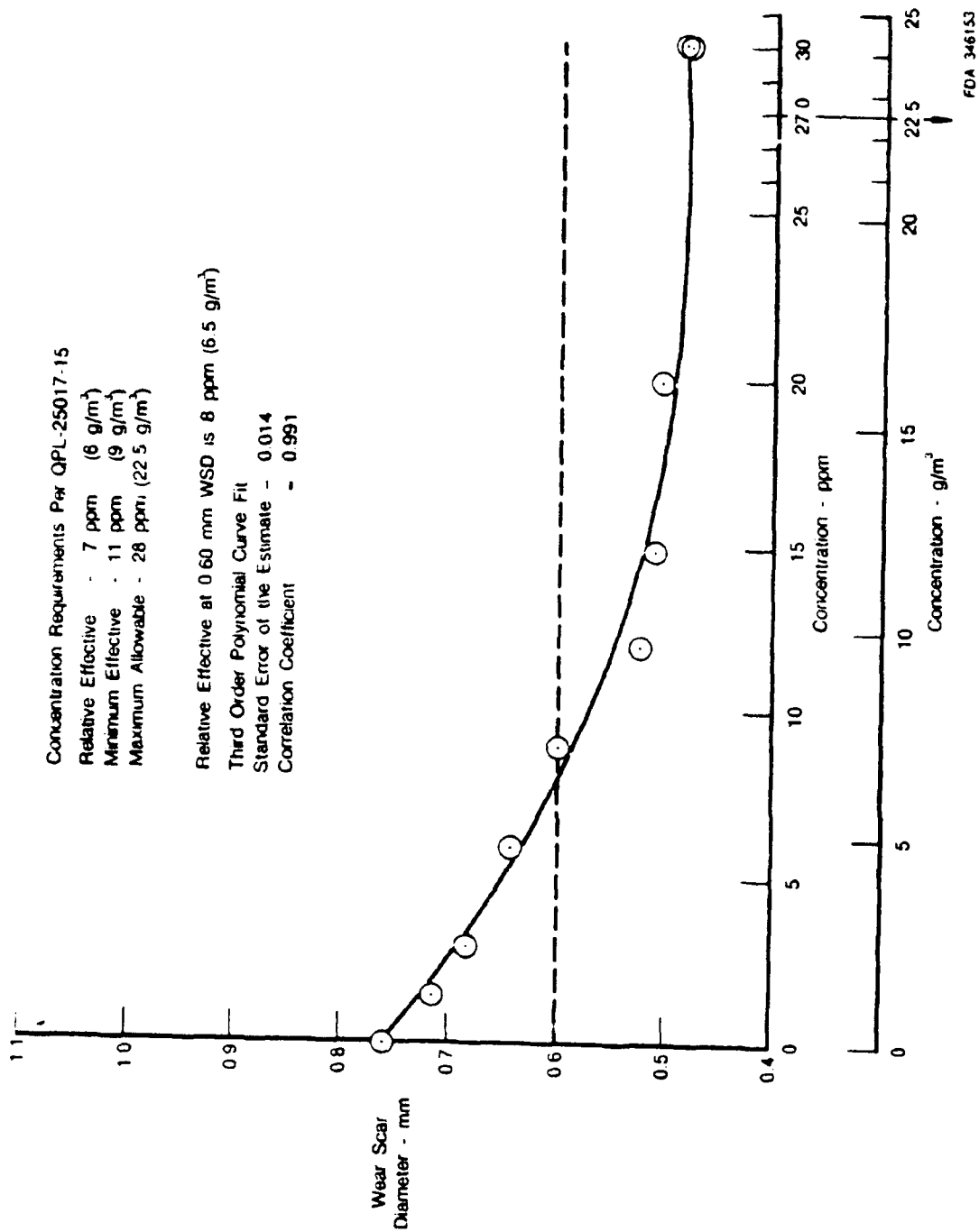


Figure D-51. Effect of DCI-4A in Clay Treated JP-5

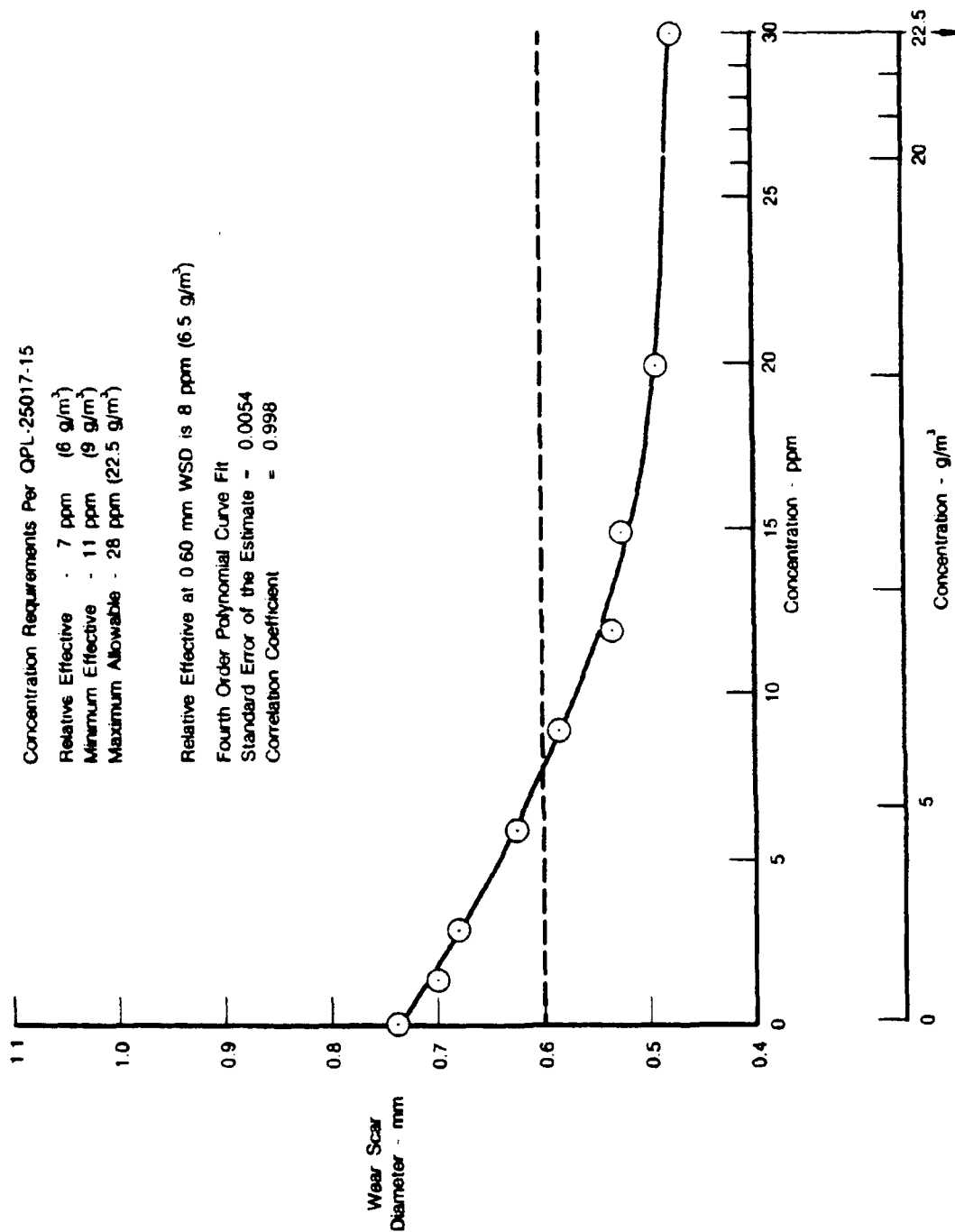


Figure D-52. Effect of DCI-6A in Clay Treated JP-5

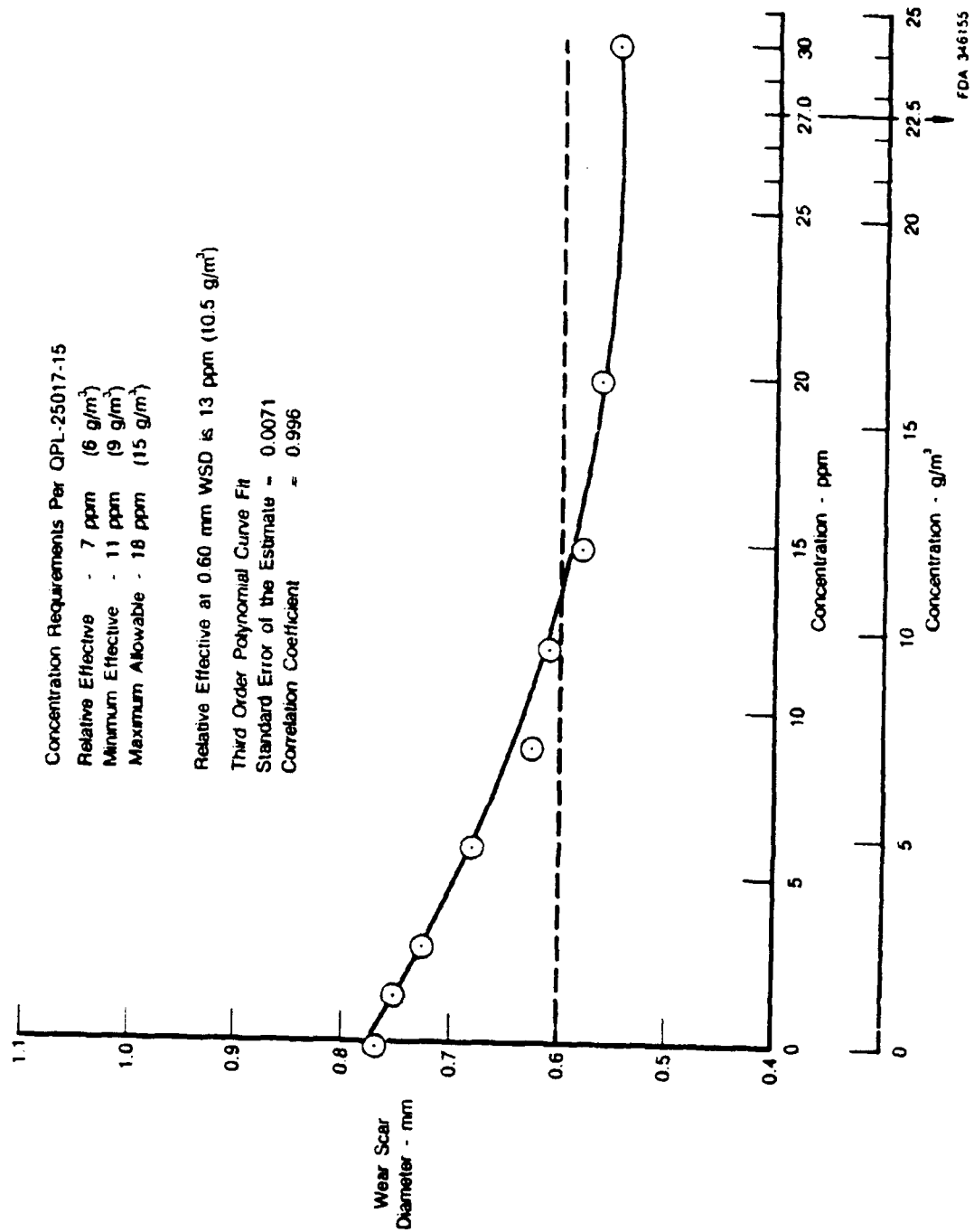


Figure D-53. Effect of LUBRIZOL 541 in Clay Treated JP-5

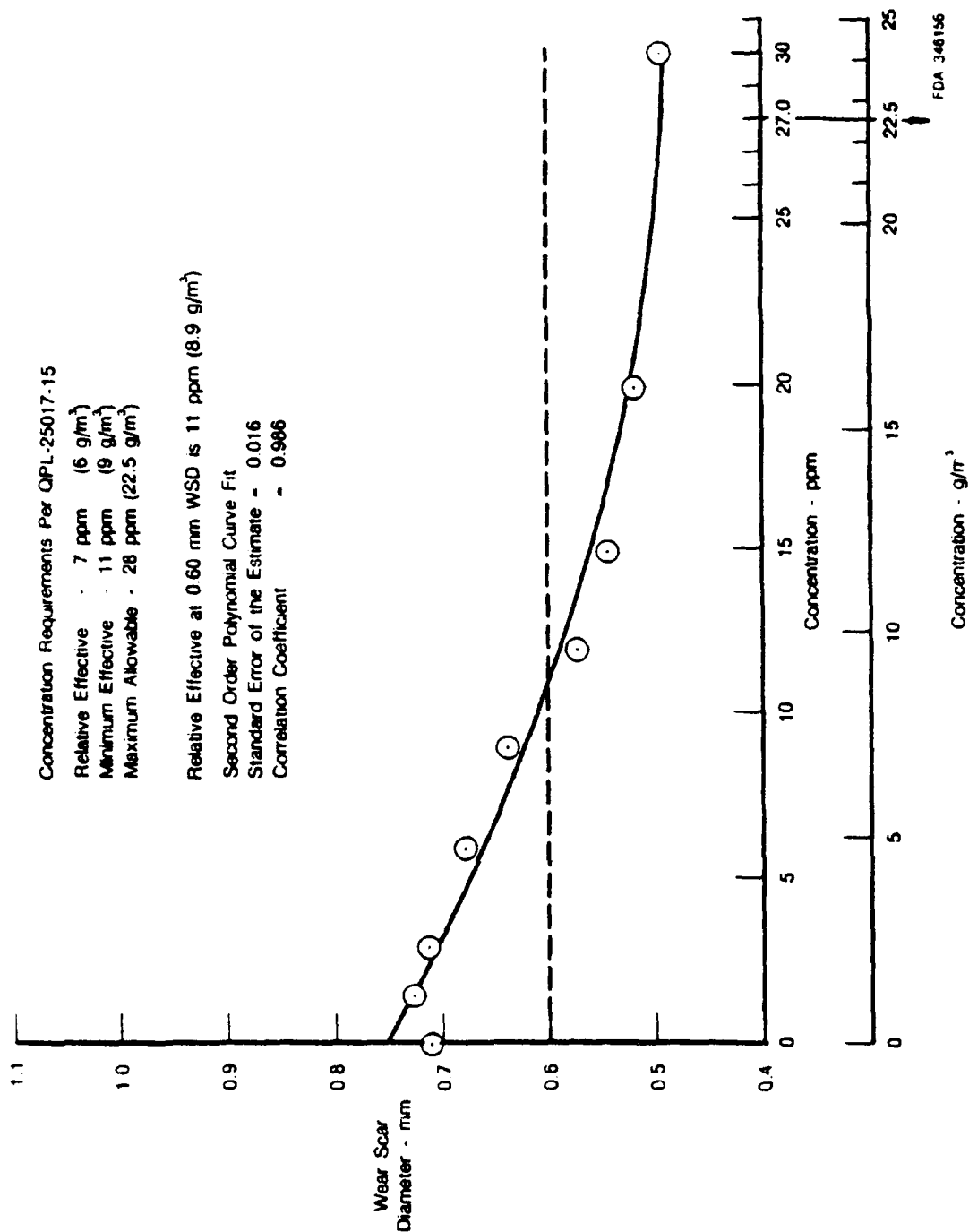


Figure D-54. Effect of NALCO 5403 in Clay Treated JP-5

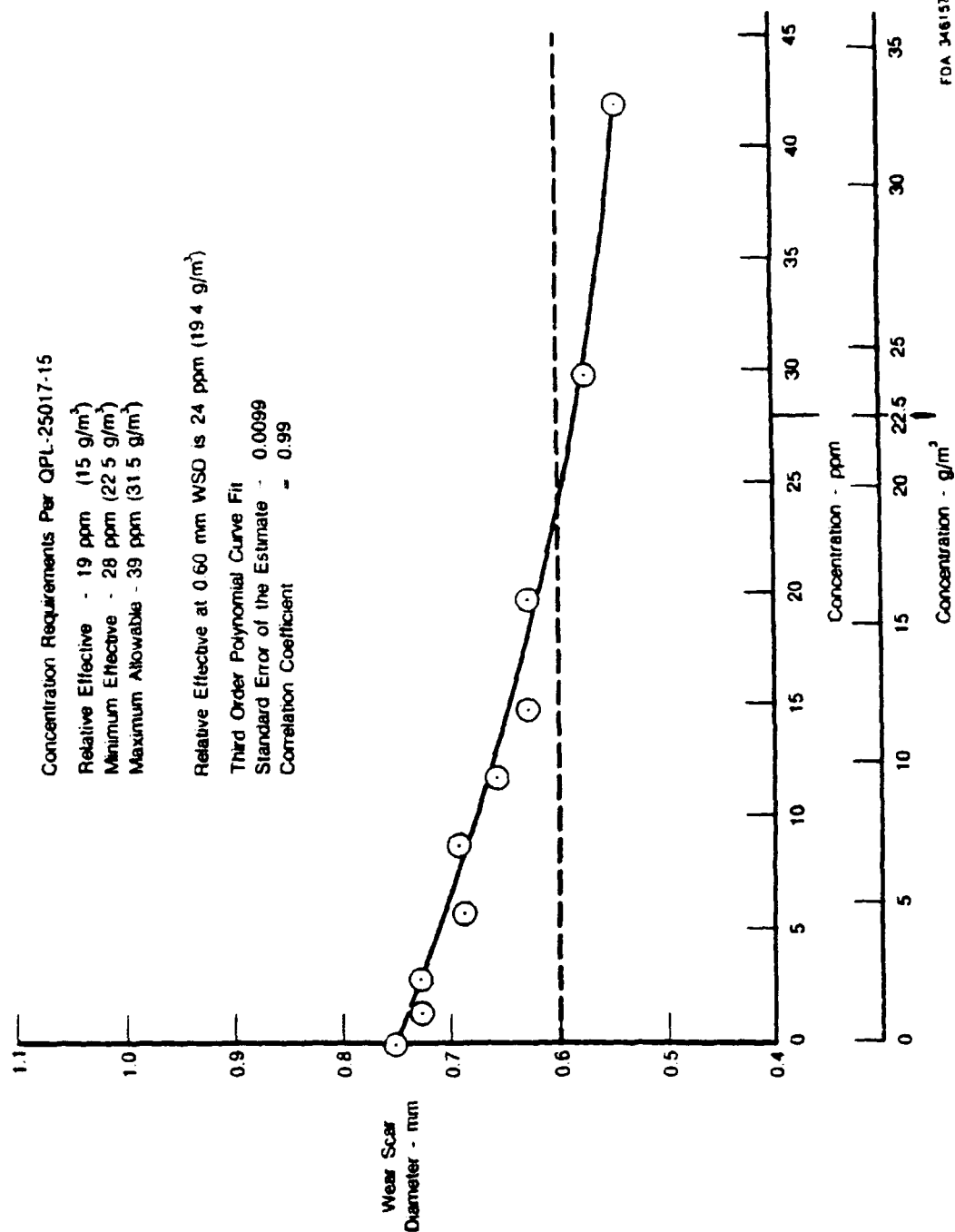


Figure D-55. Effect of TOLAD 245 in Clay Treated JP-5

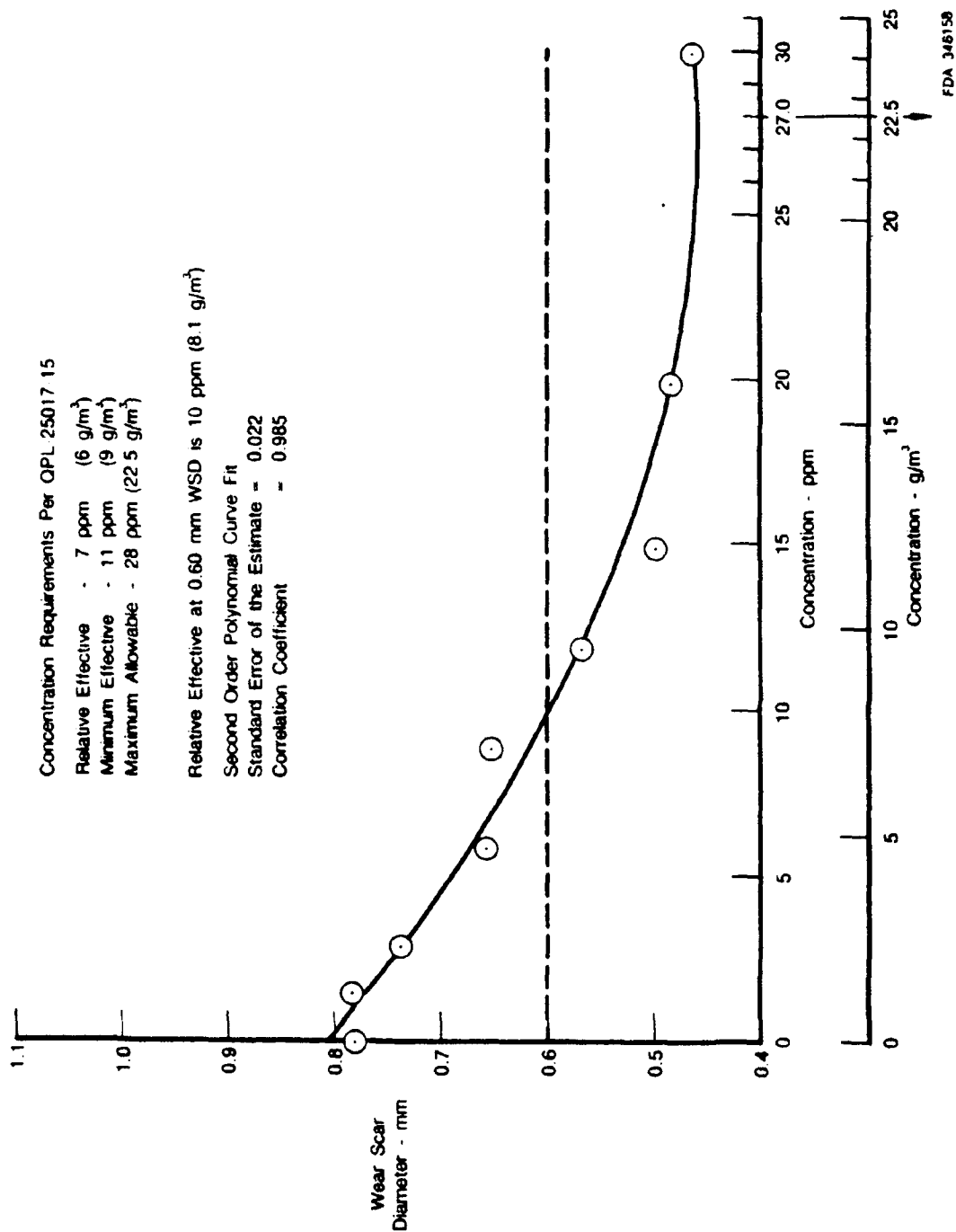


Figure D-56. Effect of UNICOR-J in Clay Treated JP-5

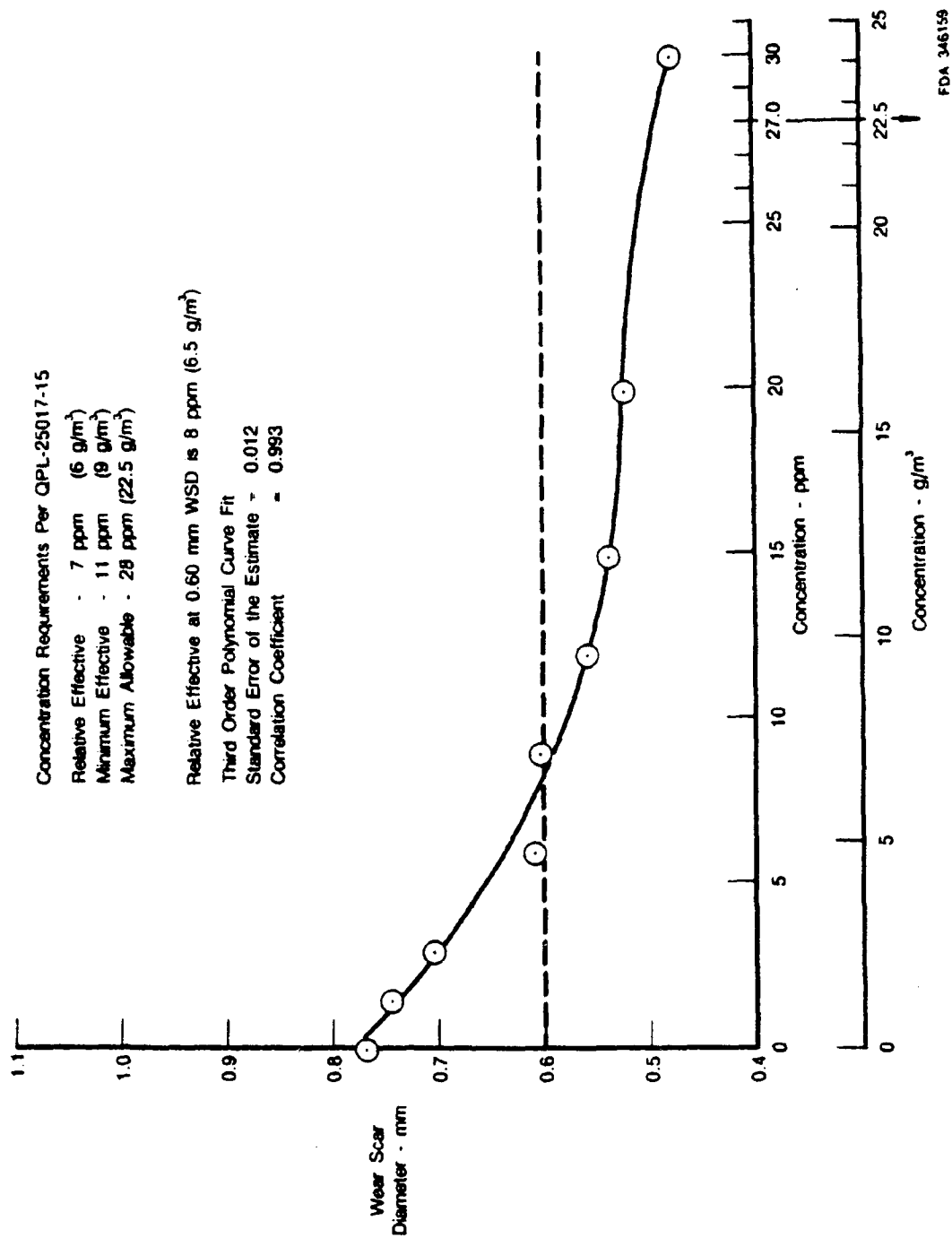


Figure D-57. Effect of IPC-4410 in Clay Treated JP-5

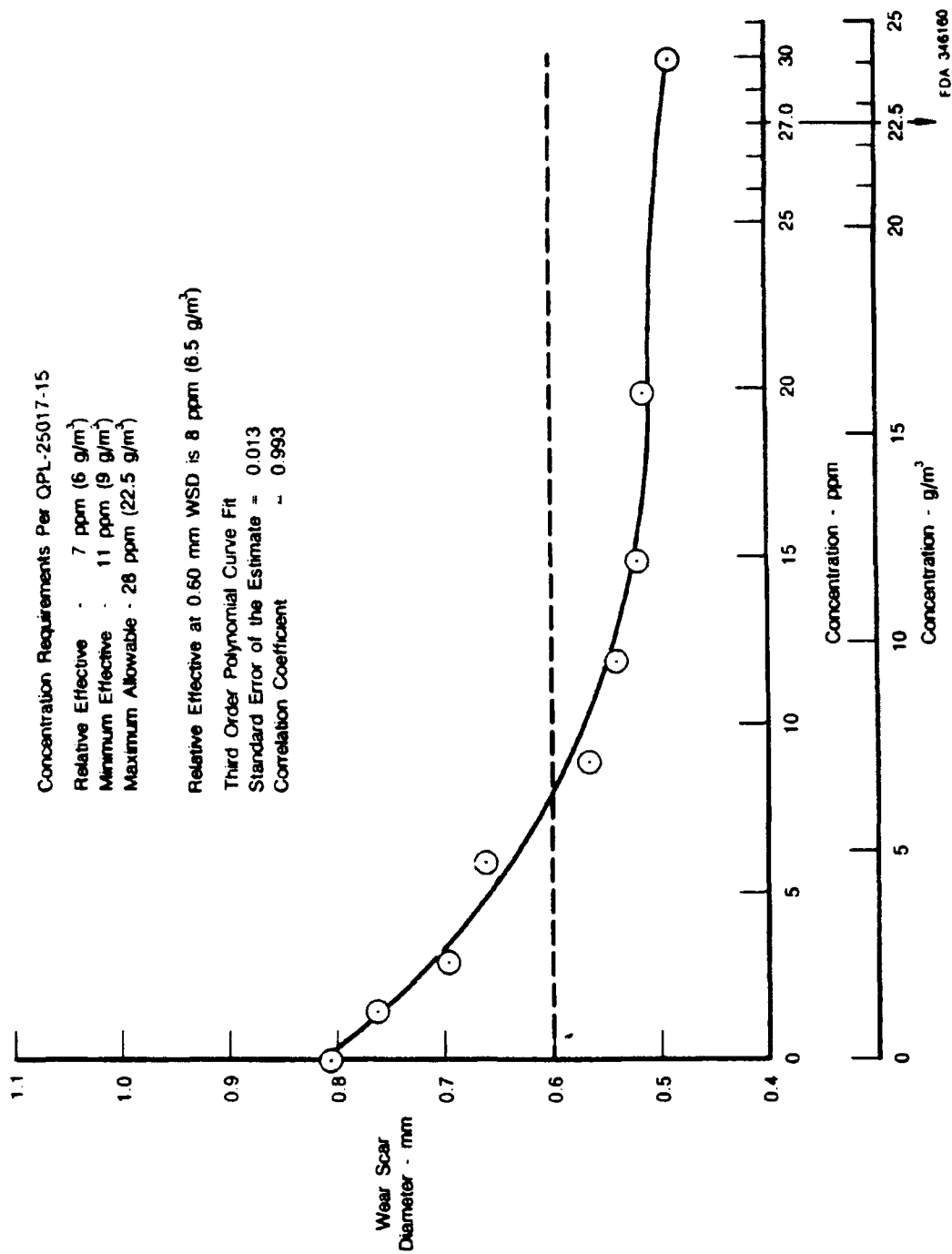


Figure D-58. Effect of MOBILAD F-800 in Clay Treated JP-5

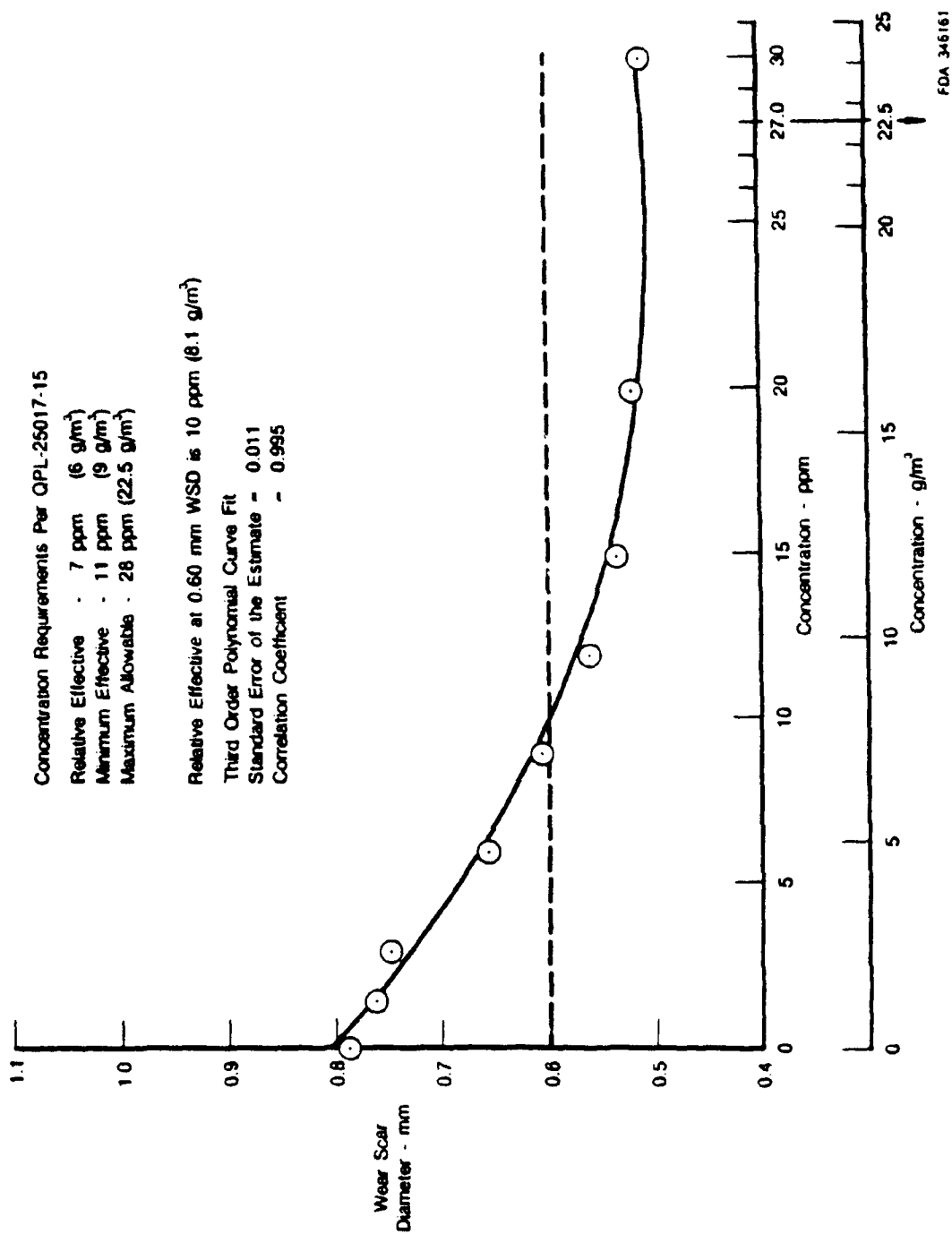


Figure D-59. Effect of NALCO 5405 in Clay Treated JP-5

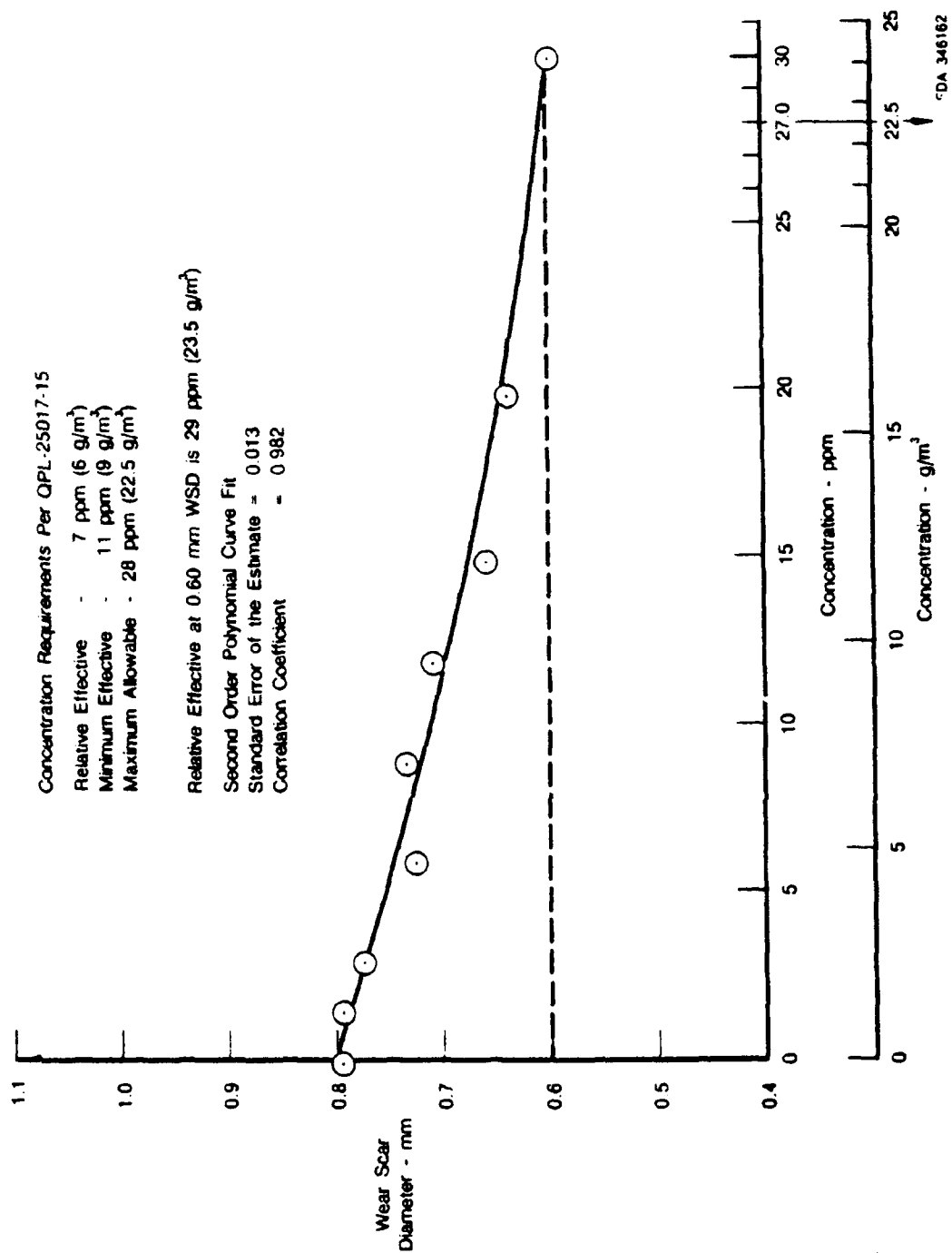


Figure D-60. Effect of TOLAD 249 in Clay Treated JP-5

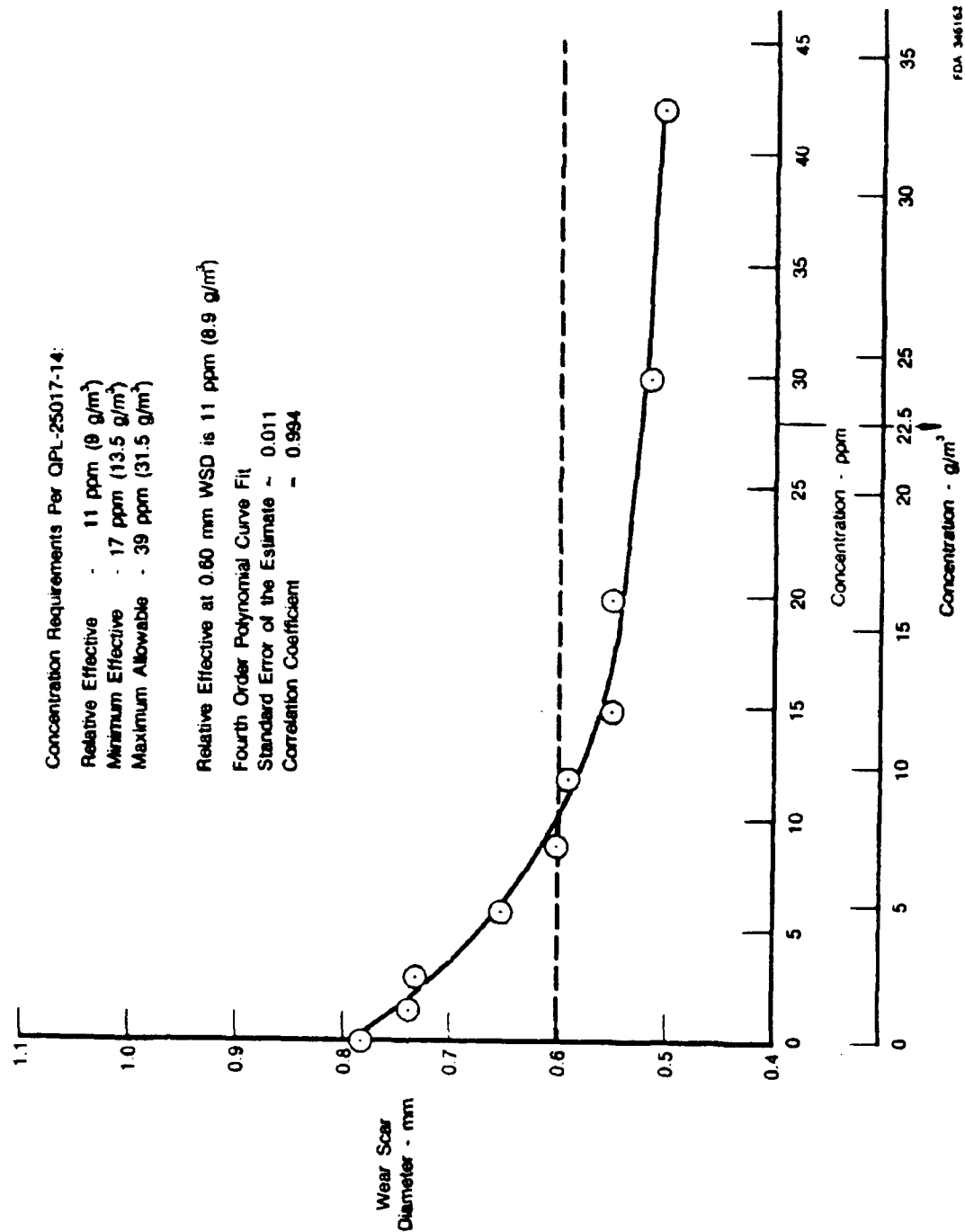


Figure D-61. Effect of P-3305 in Clay Treated JP-5

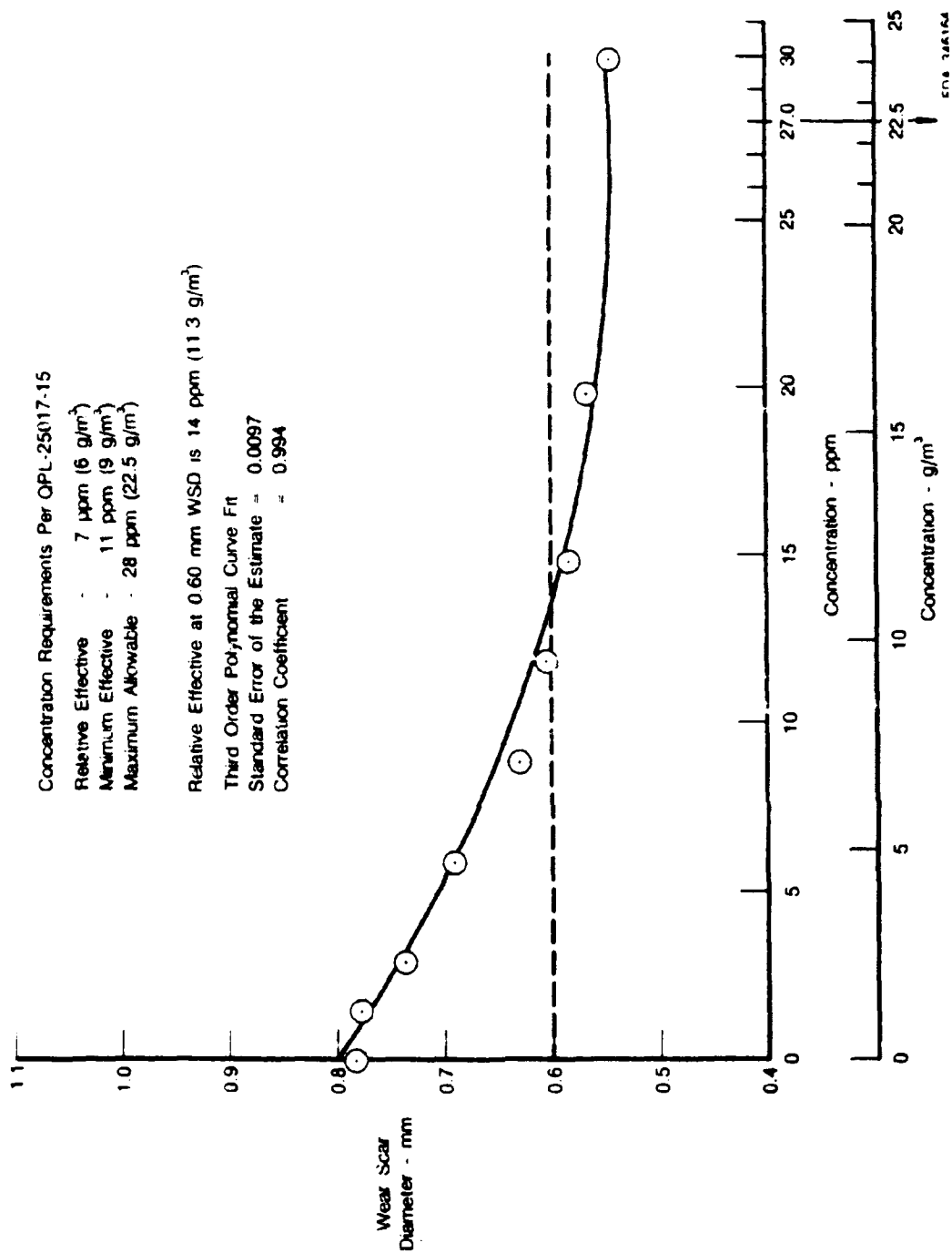


Figure D-62. Effect of IPC-4445 in Clay Treated JP-5

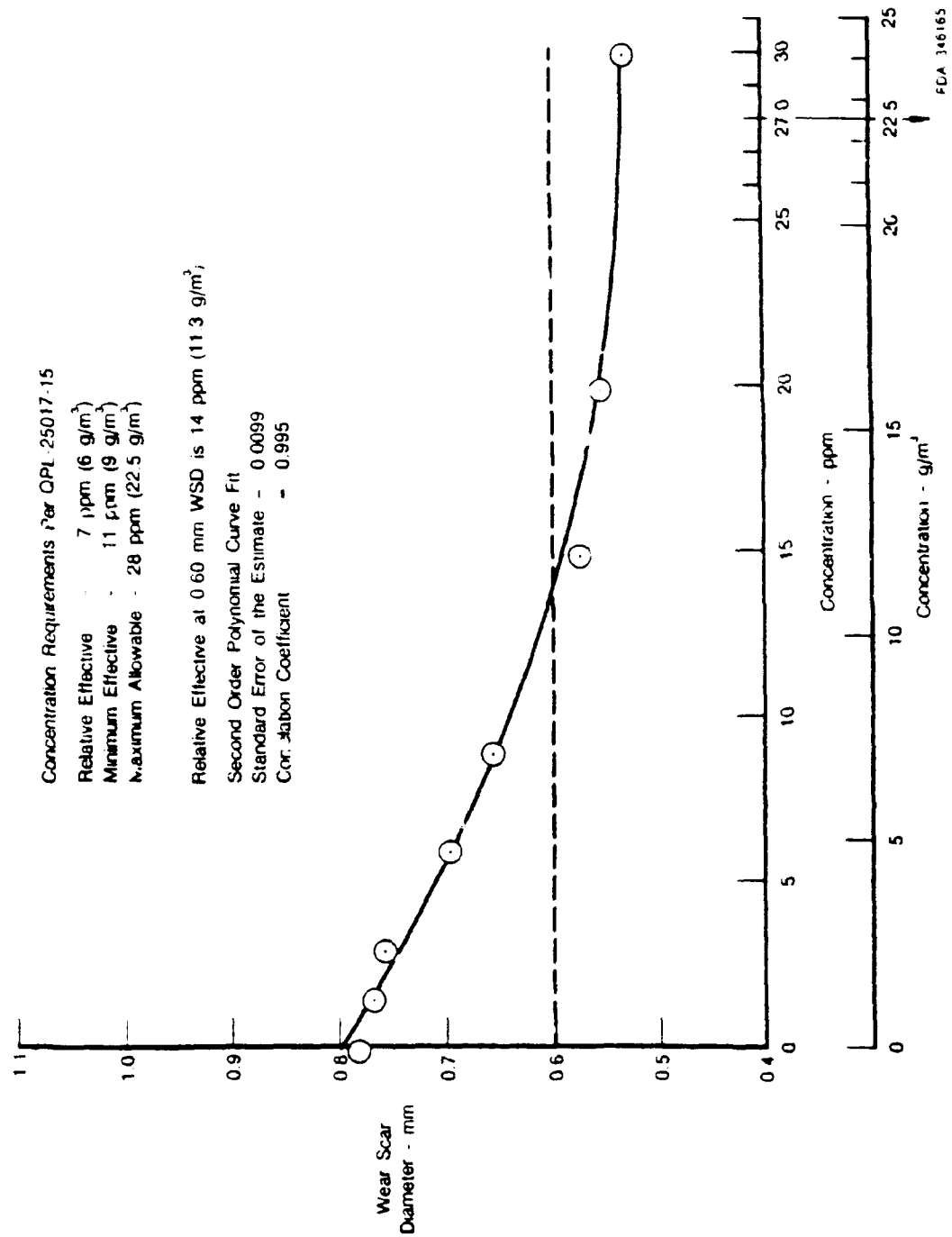


Figure D-63. Effect of WELCHEM 91120 in Clay Treated JP-5

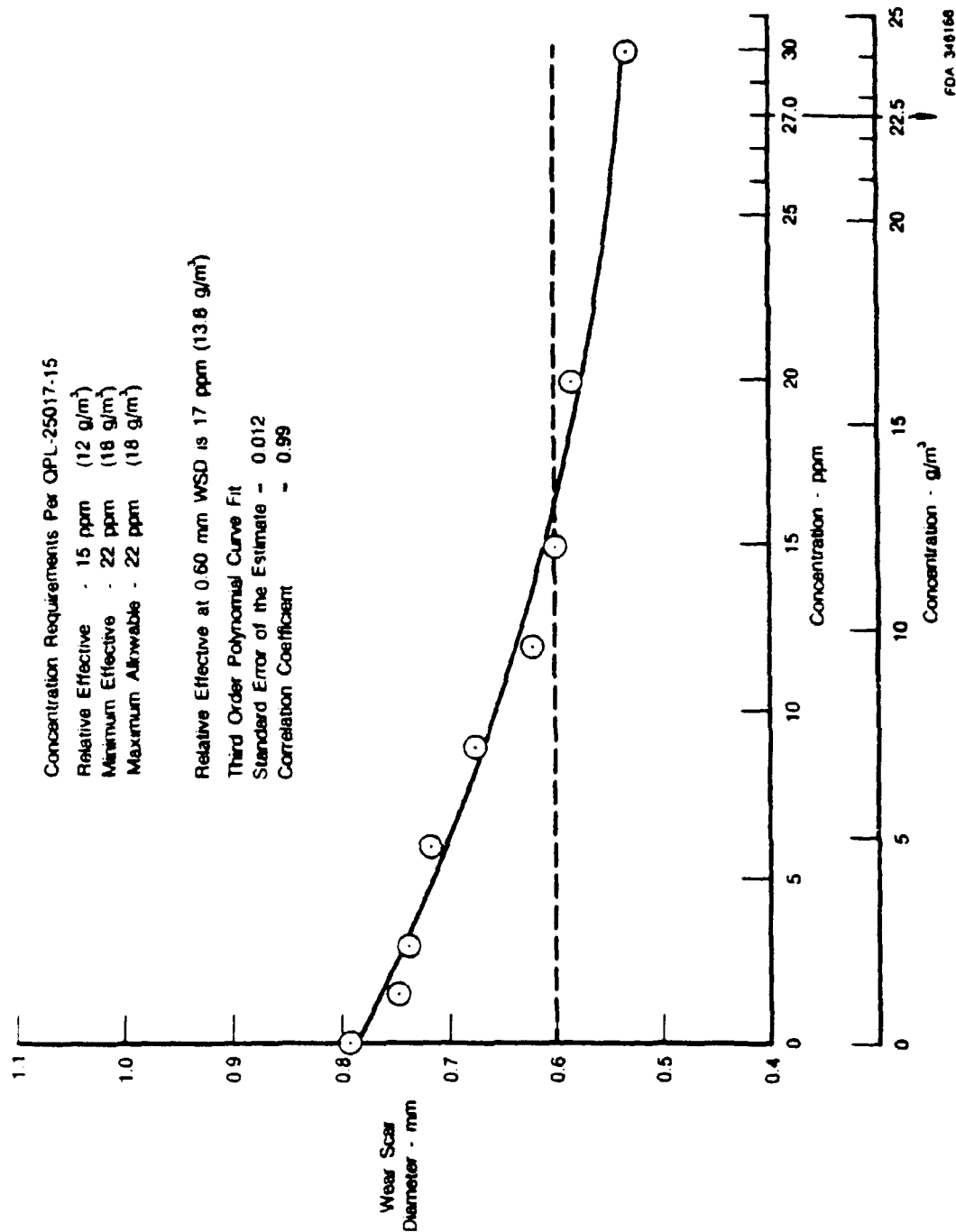


Figure D-64. Effect of NUCHEM PCI-105 in Clay Treated JP-5

APPENDIX E

INHIBITOR, CORROSION/LUBRICITY IMPROVER, FUEL SOLUBLE (METRIC)

This specification is approved for use by all Departments and Agencies of the Department of Defense.

1. SCOPE

1.1 Scope. This specification covers one type of fuel soluble corrosion inhibitor/lubricity improver additive for use in aviation turbine fuel, motor gasoline, diesel fuel, and related petroleum products.

2. APPLICABLE DOCUMENTS

2.1 Issues Of Documents. The following documents of the issue in effect on date of invitation for bids or request for proposal, form a part of this specification to the extent specified herein.

SPECIFICATIONS

Federal

TT-S-735	Standard Test Fluids; Hydrocarbon
W-F-0800	Fuel Oil, Diesel
W-G-1690	Gasoline, Automotive, Leaded or Unleaded

Military

MIL-G-3056	Gasoline, Automotive, Combat
MIL-T-5624	Turbine, Fuel, Aviation Grades JP- 4 and JP-5
MIL-C-7024	Calibrating Fluid, Aircraft Fuel System Components
MIL-L-7808	Lubricating Oil, Aircraft Turbine Engine, SYNTHETIC Base
MIL-F-25558	Fuel, Ramjet Engine, Grade IW-1
MIL-I-27686	Inhibitor, Icing, Fuel System
MIL-G-46015	Gasoline, Automotive, Combat, Referee Grade
MIL-F-46162	Fuel, Diesel, Referee Grade
MIL-T-83133	Turbine Fuel, Aviation, Kerosene Type, Grade JP-8

STANDARDS

Federal

FED-STD-791 Lubricants, Liquid Fuels, and Related Products; Methods of Testing

Military

MIL-STD-290 Packaging of Petroleum and Related Products

(Copies of specifications, standards, drawings, and publications required by contractors in connection with specific procurement functions should be obtained from the procuring activity or as directed by the contracting officer.)

2.2 Other publications. The following documents from a part of this specification to the extent specified herein. Unless otherwise indicated, the issue in effect on date of invitation for bids or request for proposal

shall apply.

American Society for Testing and Materials

ASTM A 108	Cold-Finished Carbon Steel Bars and Shafting
ASTM D 56	Test for Flash Point by Tag Closed Tester
ASTM D 97	Test for Pour Point of Petroleum Oils
ASTM D 270	Sampling Petroleum and Petroleum Products
ASTM D 445	Test for Kinematic Viscosity of Transparent and Opaque Liquids (and the Calculation of Dynamic Viscosity)
ASTM D 482	Test for Ash from Petroleum Products
ASTM D 664	Test for Neutralization Number by Potentiometric Titration
ASTM D 665	Test for Rust-Preventing Characteristics of Steam-Turbine Oil in the Presence of Water
ASTM D 1298	Test for Density, Specific Gravity, or API Gravity of Crude Petroleum and Liquid Petroleum Products, by Hydrometer Method
ASTM D 2274	Test for Stability of Distillate Fuel Oil (Accelerated Method)
ASTM D 2550	Test for Water Separation Characteristics of Aviation Turbine Fuels
ASTM D 2624	Test for Electrical Conductivity of Aviation Turbine Fuels Containing a Static Dissipator Additive
ASTM D 3114	Test for D-C Electrical Conductivity of Hydrocarbon Fuels

(Application for copies should be addressed to the American Society for Testing and Materials, 1916 Race Street, Philadelphia, PA 19013.)

Manufacturing Chemist's Association, Incorporated

Manual L-1 Warning Labels--A Guide for the Preparation of Warning Labels for Hazardous Chemicals

(Application for copies should be addressed to the Manufacturing Chemists' Association, Incorporated, 1835 Connecticut Avenue, N.W., Washington, DC 20009.)

3. REQUIREMENTS

3.1 Qualification. The inhibitors furnished under this specification are for use in aviation turbine fuels, motor gasoline, diesel fuel, and related petroleum products. The inhibitor shall be a product that has passed the applicable qualification tests listed below and has been listed on or approved for listing on the applicable qualified products list. Tentative approval for listing on the qualified products list shall be granted pending successful completion of the storage stability tests. Failure to pass the storage stability

requirement of 3.12 shall be cause for withdrawal of approval.

3.1.1 Qualification Requirements The qualification requirements for the inhibitors are listed for each type of fuel. All approved inhibitors shall meet the requirements of 3.2 through 3.12, 3.16, and 3.17 to be qualified for use in fuels conforming to MIL-T-5624, MIL-C-7024, MIL-F-25568, and MIL-T-83133. To qualify for use in motor gasolines (MIL-G-3056 and VV-G-1690) and diesel fuel (VV-F-800), the inhibitors shall also pass the applicable requirements of 3.13 through 3.15.

3.2 Materials. The composition of the finished inhibitor is not limited but is subject to review by the qualifying activity in order to assure service compatibility with previously qualified products.

3.2.1 Toxic products and formulations. The material shall have no adverse effect on the health of personnel when used for its intended purpose. Questions pertinent to this effect shall be referred by the procuring activity to the appropriate departmental medical service who will act as an advisor to the procuring activity.

3.3 Solubility. The maximum allowable concentration of inhibitor, as defined in 3.7, shall be readily and completely dissolved in all fuels for which it is qualified. There shall be no precipitation, cloudiness or other evidence of insolubility when tested as specified in 4.6.1.

3.4 Compatibility. The inhibitor shall be compatible with all inhibitors currently qualified under this specification and with the static dissipator additives listed in MIL-T-5624. There shall be no precipitation, cloudiness, other evidence of noncompatibility when tested as specified in 4.6.2.

3.5 Relative effective concentration. The relative effective concentration shall be determined in accordance with 4.6.3 and shall be expressed in grams of finished inhibitor per cubic meter of fuel. The relative effective concentration shall not be less than 6 grams of inhibitor per cubic meter of fuel (g/m^3) and shall be approved at concentrations divisible by 3 (e.g., 6, 9, 12, 15, . . . 33, and 36 g/m^3).

3.6 Minimum effective concentration. The minimum effective concentration shall be 1.5 times the relative effective concentration. This amount shall be not less than 9 grams of inhibitor per cubic meter of fuel.

3.7 Maximum allowable concentration. The maximum allowable concentration shall be the lowest of the following (all expressed in grams of inhibitor per cubic meter of fuel):

- a. Fifty-four grams of inhibitor per cubic meter of fuel
- b. Four times the relative effective concentration
- c. The highest concentration giving a Water Separator Index Modified value of 70 or higher when determined in accordance with 4.6.4
- d. The highest concentration giving less than a 40% change in electrical conductivity with fuel containing static dissipator additive (see 4.6.2.2).

The maximum allowable concentration shall be equal to or greater than the minimum effective concentration and shall be a value evenly divisible by 4.5 within the range of 9 to 54 g/m^3 .

3.3 Ash content. The ash content of the inhibitor shall not exceed 0.10 percent when determined in accordance with 4.6.5.

3.9 Pour point. The maximum allowable pour point of the finished inhibitor shall be -18°C when

determined as specified in 4.6.6.

3.10 Aircraft turbine engine operation. Grade JP-4 fuel (MIL-T-5624) containing twice the maximum allowable concentration (see 3.7) of the inhibitor shall be tested in accordance with 4.6.7 to determine its acceptability for turbine engine use. Engine operation shall not be adversely affected and the post-test condition of the engine shall indicate no excessive deposits, wear, corrosion, et cetera, which are attributed to the inhibitor.

3.11 Specification requirements. A blend of the inhibitor at its maximum allowable concentration in a representative fuel shall meet all of the requirements of each applicable specification when tested in accordance with 4.6.8. For example, to be qualified for use in a motor gasoline, a gasoline conforming to MIL-G-3056 shall continue to meet all applicable requirements of MIL-G-3056 after the maximum allowable concentration of the inhibitor is added.

3.12 Storage Stability. After storage for 12 months in accordance with 4.6.9, the inhibitor shall show no precipitation, layering, or other evidence of gross separation or degradation. Inhibitor representing the top half of the stored sample shall meet all requirements of this specification except 3.10.

3.13 Induction System deposit For use in motor gasolines conforming to V-G-1690 and MIL-G-3506, the inhibitor shall pass the induction system deposit test performed in accordance with 4.6.10.

3.14 Emulsification tendency. To obtain approval for use in motor gasolines conforming to VV-G-1690 and MIL-G-3056 and diesel fuel conforming to V-F-800, the inhibitor shall pass the emulsification tendency test performed in accordance with 4.6.11.

3.15 Accelerated stability. To obtain approval for use in diesel fuels conforming to W-F-800 the inhibitor shall pass the accelerated stability test performed in accordance with 4.6.12.

3.16 Identification qualification data. The following properties of the finished inhibitor shall be determined but not limited during qualification: density 15°C, viscosity at 37.8°C, flash point, neutralization number, pH, and type of metallic constituent, if present (see 4.6.13). The permissible production variation of individual properties will be established at the time of qualification by mutual agreement between the manufacturer and the qualifying activity. Individual batches of inhibitor subsequently subjected to qualification conformance inspections shall conform to the established range of properties. The ranges shall not adversely affect any of the inhibitor performance characteristics such as relative effective concentration and Water Separometer Index Modified.

3.17 Workmanship. The finished product in bulk or container shall be uniform in appearance and visually free from grit, undissolved water, insoluble components, or other adulteration. The material shall have no adverse effect on the health of personnel when used for its intended purpose. Evidence to this effect shall be subject to review by departmental medical authority (See 6.3).

4. QUALITY ASSURANCE PROVISIONS

4.1 Responsibility for inspection. Unless otherwise specified in the contract, the contractor is responsible for the performance of all inspection requirements as specified herein. Except as otherwise specified in the contract, the contractor may use his own or any other facilities suitable for the performance of the inspection requirements specified herein, unless disapproved by the Government. The Government reserves the right to perform any of the inspections set forth in the specification where such inspections are deemed necessary to assure that supplies and services conform to prescribed requirements.

4.2 Classification of inspections. The inspection and testing of the fuel soluble inhibitor shall be

classified as follows:

- a. Qualification inspection (see 4.3)
- b. Quality conformance inspection (see 4.4).

4.3 Qualification inspection. Qualification inspection and testing shall consist of tests specified under 4.6.

4.3.1 Test report. A certified test report shall be forwarded to the activity responsible for qualification before the qualification sample is supplied. The test report shall contain laboratory data showing the results required by 3.3, 3.4, 3.5, 3.7, 3.8, 3.9, 3.11, 3.12, and 3.16. The test report shall also contain laboratory data on any of the special tests conducted to qualify the inhibitor for use in motor gasoline and diesel fuel (e.g., 3.13, 3.14, and 3.15). In addition, complete formulation data shall be supplied to the qualifying activity. This data shall include chemical composition (I.U.P.A.C. nomenclature and structural diagrams of each ingredient), the percentages of each ingredient, the manufacturer and trade names of each ingredient, and where available, the purity of each ingredient. The contractor shall furnish toxicological data and formulations required to evaluate the safety of the material for the proposed use.

4.3.1.1 Qualification sampling. Unless otherwise specified by the activity responsible for qualification, an initial 1-liter sample of finished inhibitor shall be submitted for evaluation by all of the tests with the exception of the storage stability and aircraft turbine engine tests. If the product passes these tests, an additional sample of finished inhibitor will be requested for the storage stability and aircraft turbine engine tests. Samples shall be identified as required and forwarded to the laboratory responsible for testing as designated in the letter of authorization from the activity responsible for qualification (see 6.5).

4.3.1.2 Requalification. Requalification will be required in the event any change in composition or formulation, source of the inhibitor or its ingredients, or manufacturing sites is made.

4.3.1.3 Retention of qualification. The retention of qualification of products approved for listing on the qualified products list (QPL) shall be accomplished by a periodic verification to determine continued compliance of a supplier's product with the requirements of this specification. The verification intervals shall not exceed two years. Unless otherwise specified by the activity responsible for the qualified products list, verification of qualification may be made by certification.

4.4 Quality conformance inspection. Quality conformance inspection of a bulk lot of inhibitor shall consist of tests for conformance to requirements for solubility (3.3), ash (3.8), pour point (3.9), and property limits shown on the Qualified Products List. In addition, the product shall be required to pass a rusting test when blended in depolarized iso-octane at the relative effective concentration and tested in accordance with 4.6.3.1, and shall also be required to give a Water Separometer Index Modified of 70 or higher (average of three tests) when tested at the maximum allowable concentration in accordance with 4.6.4.

4.4.1 Inspection lot

4.4.1.1 Bulk lot. A bulk lot is defined as an indefinite quantity of a homogeneous mixture of material offered for acceptance in a single isolated container, manufactured as a single isolated batch, or manufactured by a single plant run (not exceeding 24 hours) through the same processing equipment with no change in ingredient material.

4.4.1.2 Packaged lot. A packaged lot is defined as an indefinite number of 55-gallon drums or smaller unit packages of identical size and type, offered for acceptance, and filled with a homogeneous mixture of material from a bulk lot.

4.4.2 Sampling. Each bulk or package lot of material shall be sampled for verification of product quality and compliance in accordance with ASTM D 270.

4.5 Inspection. Inspection shall be in accordance with Method 9601 of FED-STD-791.

4.6 Test methods

4.6.1 Other inhibitors. The maximum allowable concentration of inhibitor shall be mixed with each of the following fuels. The fuel shall contain no other inhibitors. Immediately after mixing and at the end of 24 hours, the samples shall be visually inspected for precipitation, cloudiness, or other evidence of insolubility.

- a. JP-4 fuel conforming to MIL-T-5624 containing the maximum allowable concentration of inhibitor conforming to MIL-I-27686
- b. A motor gasoline conforming to MIL-G-3056, MIL-G-46015, or VV-G-1690
- c. A diesel fuel conforming to VV-F-800 or MIL-F-46162.

4.6.2 Compatibility

4.6.2.1 Inhibitors. Grade JP-4 fuel (MIL-T-5624) containing the maximum allowable concentration of the inhibitor under test and no other inhibitors shall be mixed in equal proportions with samples of MIL-T-5624, grade JP-4 fuel containing the maximum allowable amount of each inhibitor previously qualified under this specification. The MIL-T-5624, grade JP-4 fuel used shall contain the maximum allowable amount of inhibitor conforming to MIL-I-27686. At the end of a 24-hour period, the samples shall be visually inspected for precipitation, cloudiness or other evidence of noncompatibility.

4.6.2.2 Static dissipator additive. Grade JP-4 fuel (MIL-T-5624), filtered through clay as described in appendix A.4 of ASTM D2550, shall be blended with each static dissipator additive approved in MIL-T-5624 to provide test fuels having a conductivity of 400 picosiemens per meter (pS/m) \pm 100 pS/m. After a 24-hour period, to insure that equilibrium fuel conductivity has been established the inhibitor under test shall be added and mixed. At the end of another 24-hour period, no more than \pm 40 percent change in the electrical conductivity of the fuel shall have occurred as a result of the test inhibitor. The fuel electrical conductivity shall be measured using either ASTM D 2624 or ASTM D 3114 test methods. The post-test visual inspection of the sample shall reveal no precipitation, cloudiness or other evidence of noncompatibility. (NOTE: Some loss in fuel conductivity with time may occur when bare glass bottles or bare metal cans are used with fuels containing static dissipator additives. The use of an epoxy-coated container is suggested. Also, fuel conductivity is temperature sensitive; no significant change in temperature should be allowed during the test.)

4.6.3 Relative effective concentration. The relative effective concentration of the inhibitor shall be determined by testing the inhibitor at various concentrations in depolarized iso-octane in accordance with 4.6.3.1. The inhibitor shall be tested at concentrations divisible by 3 (e.g., 6, 9, 12, 15, ... 33, and 36 grams inhibitor per cubic meter of fuel). No intermediate concentrations shall be tested. The relative effective concentration shall be defined as the lowest concentration giving a passing result in accordance with 4.6.3.1.6.

4.6.3.1 Rusting test method

4.6.3.1.1 Test apparatus. The test apparatus shall conform to the following requirements:

- a. Oil bath, conforming to ASTM D 665, with the additional requirement that it must be

capable of maintaining the test sample at a temperature of $38^{\circ}\text{C} \pm 0.5^{\circ}\text{C}$

- b. Beaker, beaker cover, stirrer, stirring apparatus, and chuck and motors for holding and rotating specimens while polishing shall conform to ASTM D 665
- c. Infrared heat lamp, 250 watts
- d. Hypodermic syringe, glass, 30-ml, with 6-inch stainless steel needles
- e. Disposable microliter pipets, consisting of calibrated capillary tubes containing 1, 2, 3, 4, 5, 10, 15, and 20 microliters
- f. Column, chromatographic, glass, 40 mm ID x 600 mm with poly (tetrafluoroethylene) stopcock. A separatory funnel, Squibb, 1-liter, with poly tetrafluoroethylene) stopcock may be substituted for the chromatographic column
- g. Specimen holder, poly (tetrafluoroethylene), dimensions as specified in ASTM D 665 for type 2 holder
- h. Specimen, dimensions as specified in ASTM D 665, made of grade 1018 steel in accordance with ASTM A 108. The specimen shall be fabricated from 0.625 inch diameter round stock by machining or grinding to the final diameter of 0.50 inch. The specimen may be reused from test to test but shall be discarded when the diameter is reduced to 0.375 inch.

4.6.3.1.2 Test materials. Test materials shall conform to the following requirements:

- a. Silica gel, 28-200 mesh, heated to 225°F for 2 hours and cooled in a desiccator before use.
- b. Test solvent, iso-octane conforming to TT-S-735, which has been freshly depolarized as follows: A glass chromatographic column or 1 liter separatory (Squibb) funnel is filled with silica gel to a height 20 cm above the stopcock, retaining the silica gel by means of a glass wool plug. (NOTE: Do not use stopcock grease). One gallon of iso-octane is passed through the silica-gel bed by gravity, discarding the first 50 ml and collecting the remainder in a chemically clean glass container. The depolarized iso-octane should be used within 1 week after treatment.
- c. Test water, type B medium hard, prepared as follows: Make up three stock solutions using ACS reagent-grade chemicals in distilled water. Each solution shall contain one of these chemicals 16.4 g/liter NaHCO_3 , 13.2 g/liter $\text{CaCl}_2 \cdot 2\text{H}_2\text{O}$, or 8.2 g/liter $\text{MgSO}_4 \cdot 7\text{H}_2\text{O}$. Pipet 10 ml of the NaHCO_3 stock solution into 800 ml of distilled water in a 1-liter volumetric flask, and shake vigorously. While swirling the contents of the flask, pipet 10 ml of the CaCl_2 stock solution and then 10 ml of the MgSO_4 stock solution into the flask, add distilled water to bring the volume to 1 liter, and mix thoroughly. The final blend shall be clear and free of precipitation.
- d. Isopropanol, ACS reagent grade.
- e. Glassware cleaning solution.
- f. Lintless paper tissue (NOTE: Cel-Fibe 1710 Wipes, available from CellFibe, Milltown, New Jersey, are satisfactory).

g. Abrasive cloth, 150-, 240-, and 400-grit metal working aluminum oxide abrasive cloth, closed coat on jeans backing. The abrasive cloth is available in rolls of 1-inch tape, the most convenient form for use in this test.

h. Disposable vinyl gloves.

4.6.3.1.3 Specimen preparation. The specimen, whether new or used from a previous test, shall be cleaned by solvent rinsing or brushing as needed to remove oily residues, loose rust, or foreign material. After this preliminary cleaning, the specimen shall be handled only with vinyl gloves. (NOTE: It is essential to avoid contamination of the specimen, particularly by perspiration residues, and care should be taken to avoid transfer of such contaminants to the specimen via the abrasive cloth or the lintless paper tissues.) The specimen shall then be ground successively with 150-, 240-, and 400-grit abrasive cloth while mounted in the chuck of the grinding and polishing apparatus and turned at 1700 to 1800 rpm, in accordance with the following procedures:

a. Grind with 150 grit cloth to remove all defects, irregularities, pits, and scratches as determined by visual inspection. Old 150-grit cloth may be used to remove rust or major irregularities, but the grinding shall be completed with new cloth. Stop the motor and scratch the static specimen longitudinally with one pass of new 150-grit cloth, using light pressure so that visible scratches appear.

b. Grind with 240-grit cloth, removing all marks from the 150-grit cloth, and finishing with new 240-grit cloth. Stop motor and scratch the static specimen longitudinally with one pass of new 240-grit cloth, using light pressure, so that visible scratches appear.

c. Polish with 400-grit cloth by wrapping a strip of cloth halfway around the specimen and applying a firm but gentle downward pull to the ends of the strip and moving the strip slowly along the specimen. Shift the position of the abrasive cloth frequently to expose fresh abrasive to the specimen. Continue this procedure, using new strips of abrasive cloth as required, until all marks from the previous 240-grit operation have been removed and the surface presents a uniform appearance, free of longitudinal or spiral scratches, with all polishing marks appearing to be circumferential. The final passes along the specimen shall be made with fresh abrasive cloth.

d. Remove the specimen from the chuck, wipe the lintless tissue, and store in a beaker of depolarized iso-octane in a desiccator containing silica gel or other noncorrosive desiccant until ready for use. The storage period in the iso-octane shall not exceed 7 days.

4.6.3.1.4 Preparation of test blend. The test blend shall be prepared in the test beaker, not more than 2 hours before the immersion of the specimen in the test blend. The test blend shall be prepared in accordance with the following procedure:

a. Clean the test beaker with a suitable cleaning solution (see note below). Clean the stainless steel stirrer and methyl methacrylate beaker cover by rinsing in any suitable aliphatic hydrocarbon solvent such as a light naphtha or iso-octane, washing thoroughly with hot distilled water, and oven drying (not over 65.6°C for cover). NOTE: If a glass stirrer or beaker cover is used, it should be cleaned in the same manner as the test beaker. Any suitable cleaning method that provides cleaning quality comparable to the use of chromic acid may be used. The use of a detergent cleaning solution is suggested. Use stainless steel forceps to handle the glassware. Wash with tap water and then with distilled water. Rinse with reagent grade isopropyl alcohol and dry in the air or oven. Detergent cleaning avoids the potential hazards and inconvenience associated with handling corrosive chromic acid solutions. The latter remains as the reference cleaning practice and as such may function as an alternative to the preferred use of detergent

solutions.

b. Prepare the blend of iso-octane and inhibitor in the test beaker with direct addition of the inhibitor. No intermediate blends, concentrates, or stock solutions are permitted. Prepare each test blend using between 300 and 400 ml of iso-octane in the test beaker. Use pipet or pipets to add integral numbers of microliters of the inhibitor to the beaker to increase measurement accuracy. Add the calculated volume of depolarized iso-octane to the test beaker. Fill the appropriate microliter pipet or pipets with inhibitor, wipe off excess, and force the inhibitor into the iso-octane. Allow the pipet to fill with iso-octane by capillary attraction and force this rinse into the test beaker. Repeat the rinse four times. Calculate the amount of iso-octane and inhibitor to be added to the test beaker using the instructions given in 4.6.3.1.4.c.

c. Calculate the volume of iso-octane required for each concentration desired using the following equation, where density is in g/ml at 15°C:

$$\text{ml of iso-octane} = \frac{(\text{density of inhibitor}) (\text{microliters of inhibitors}) (1000)}{(\text{desired inhibitor concentration, grams/cubic meter})}$$

For example, assume the inhibitor has a density of 0.95 and the desired concentration is 6 grams/cubic meter of fuel. Calculate the volume of iso-octane required when using 2 microliters of inhibitor

$$\text{ml iso-octane} = (0.95) (2) (1000)/(6) = 316.7$$

For inhibitor having a density less than 0.9 g/ml, the volume of iso-octane for many concentrations of interest will be less than 300 ml or more than 400 ml. Use the following procedure:

- (1) Calculate the volume of inhibitor required for 300 ml of iso-octane.
- (2) Increase the volume of inhibitor to the next integral microliter and add to 300 ml of iso-octane in the test beaker. Mix well.
- (3) Calculate the amount of inhibitor/iso-octane blend to be removed from the test beaker to leave the desired amount of inhibitor.
- (4) Remove the calculated amount of inhibitor/iso-octane blend and replace with an equivalent volume of depolarized iso-octane. Mix well. This approach is illustrated for the above example:

- (a) Using this equation, calculate the desired volume of inhibitor for 300 ml of iso-octane for an inhibitor with a density of 0.85 and for a desired concentration of 6 g/m³.

$$300 \text{ ml iso-octane} = (0.85) (X \text{ microliters inhibitor}) (1000)/(6),$$

$$X = 2.12 \text{ microliters of inhibitor}$$

- (b) Add the next integral volume of inhibitor (i.e., 3 microliters) to 300 ml iso-octane and mix well. This gives an inhibitor concentration of 3 microliters inhibitor/300 ml iso-octane or 1 microliter/100 ml.
- (c) The desired amount of inhibitor is 2.12 microliters. Thus, we need $(2.12)(100) = 212$ ml of inhibitor/iso-octane blend.

(d) Remove 88 ml of the inhibitor/iso-octane blend (i.e., $300 - 212 = 88$ ml). Replace with 88 ml of depolarized iso-octane. Mix well. This results in the correct volume of inhibitor (i.e., 2.12 microliters) in 300 ml of iso-octane.

d. Place the beaker in the oil bath which has been regulated previously to maintain a sample temperature of $38^{\circ}\text{C} + 0.5^{\circ}\text{C}$. The beaker is inserted in a hole of the bath cover and suspended at a level such that the oil level in the bath is not below the sample level in the beaker. Cover the beaker with the beaker cover and the stirrer in position. Adjust the stirrer so that the shaft is 6 mm (0.24 inch) off-center in the beaker, and the blade is within 2 mm (0.08 inch) of the bottom of the beaker. Then suspend a thermometer through the hole in the cover intended for that purpose, so that it is immersed to a depth of 57 mm (2.2 inches). Stir for at least 5 minutes. Turn off the stirrer. Using a clean pipet or syringe, withdraw enough test blend to leave exactly 300 ml in the beaker. Allow the test blend to come to $38^{\circ}\text{C} \pm 0.5^{\circ}\text{C}$. Replace the thermometer with a cork or plastic plug.

4.6.3.1.5 Test procedure. After preparing a test specimen as described in 4.6.3.1.3 and a test blend as described in 4.6.3.1.4, the test shall be performed in accordance with the following procedure:

a. Remove a test specimen from the iso-octane in the desiccator and wipe dry with a lintless paper tissue, handling with vinyl gloves throughout this step and the following operations. Repolish with 400-grit abrasive cloth by wrapping a strip of the cloth halfway around the specimen and applying a firm but gentle downward pull to the ends of the strip. Move the strip slowly along the specimen, twice in each direction, shifting the strip after the first back-and-forth pass so that fresh abrasive is exposed to the specimen. Inspect the specimen to insure that the surface presents a uniform appearance, free of longitudinal or spiral scratches, with all polishing marks appearing to be circumferential. Additional polishing is required if the specimen appearance is other than described. After polishing is completed, remove the specimen from the chuck, wipe lightly with lintless paper tissue, and screw the specimen into the specimen holder. Rinse the specimen with a stream of isopropanol from a wash bottle. Wipe dry immediately, wiping twice with fresh lintless paper tissues, using firm pressure and rotating the specimen while drawing through the tissue. NOTE: Under conditions of high ambient humidity, it is necessary to heat the specimen to prevent condensation of moisture and premature rusting. Under such conditions before the rinsing operation, place the specimen and holder 6 inches from a 250-watt infrared heat lamp and rotate for 1 minute. Keep the specimen under the lamp while proceeding with the rinsing and wiping operations.

b. Immediately after rinsing and wiping, insert the specimen and holder through the specimen hole in the beaker cover and suspend the specimen so that its lower end is 13 to 15 mm (0.51 to 0.59 inch) from the bottom of the beaker. Leave the specimen in the test blend for a 10-minute static soak, then turn on the stirrer and soak dynamically for 20 minutes. NOTE: When multiple tests are run simultaneously, it is permissible to extend the static soak period to not more than 40 minutes in the case of the "first-in" specimen, giving the "last-in" specimen a 10-minute soak.

c. Turn off the stirrer. Remove the cork or plug from the beaker cover, and add 30 ml of test water to the test beaker, adding it very carefully to the bottom of the beaker by means of a hypodermic syringe. Change to a clean needle for each test beaker. Replace the cork or plug in the beaker cover.

d. Start the stirrer immediately and run for 5 hours, holding the bath temperature at the same setting so that the test samples will be maintained at $38^{\circ}\text{C} \pm 0.5^{\circ}\text{C}$.

e. At the end of 5 hours, stop the stirrer, remove the specimen and holder, rinse immediately

with isopropanol, and allow to air-dry. Examine at once without magnification under normal indoor illumination, approximately 60-foot candles, scanning the surface very carefully, to detect any small pits. Record observations of visible rust, pits, stains, or deposits.

4.6.3.1.6 Interpretation of test results. A test shall be reported as failing if the center 48mm-(1.875-inch) section of the specimen shows six or more rust spots of any size, or if it shows any rust spot 1 mm in diameter or larger. (NOTE: The ends of the specimen, outside the center section, are ignored in rating the specimen.) Visible deposits or stains other than rust shall not constitute failure; deposits or stains may be examined microscopically to determine their classification. In order to assign a pass-fail rating to a given inhibitor at a given concentration, two tests shall be performed. The inhibitor shall be reported as passing at the given concentration if both tests give passing ratings, or failing at the given concentration if both tests give failure ratings. If the two tests give one passing rating and one failing rating, two additional tests shall be performed. If either or both of these additional tests give a failing rating, the inhibitor shall be reported as failing at the given concentration. If both of the additional tests give passing ratings, the inhibitor shall be reported as passing at the given concentration.

4.6.4 Water separator index modified. The inhibitor shall be blended into the reference fluid base, as described in ASTM D 2550, and tested in accordance with ASTM D 2550. For any given concentration of inhibitor, the average of three tests results shall be used to determine the conformance to the requirements of 3.7 or 4.4. In qualification testing to define the maximum allowable concentration, the inhibitor shall be tested at one or more concentrations selected from the following: 9, 13.5, 18, 22.5, 27, 31.5, 36, 40.5, 45, 49.5, or 54 grams inhibitor per cubic meter of fuel. No intermediate concentrations shall be tested. Only the ASTM CRC Water Separator apparatus shall be used for qualification testing.

4.6.5 Ash content determination. The ash content of the inhibitor shall be determined in accordance with ASTM D 482, using a platinum crucible.

4.6.6 Pour point determination. Pour point shall be determined in accordance with ASTM D 97.

4.6.7 Aircraft engine test. The engine shall be operated for 100 hours in accordance with the engine operating requirements of MIL-L-7808. Grade JP-4 fuel, conforming to MIL-T-5624 shall contain twice the maximum allowable concentration of the inhibitor. Upon completion of the test, components of the engine exposed to the fuel such as a fuel controls, fuel nozzles, combustion section, turbine blades, exhaust section, elastomers, fuel/oil heat exchangers, and fuel pumps shall be examined for evidence of excess wear, deposits, corrosion or other deleterious effects. This test shall be performed by the activity responsible for qualification (see 6.5).

4.6.8 Specification tests. The inhibitor shall be added at its maximum concentration to a base fuel that contains no inhibitor but is otherwise representative of each grade of fuel for which the additive is to be qualified. The blend of fuel and inhibitor shall be subjected to all of the tests of each applicable specification.

4.6.9 Storage stability test Two 1-quart amber glass bottles shall each be filled with 850 ml of the inhibitor and shall be tightly capped by means of a screw cap having a conical polyethylene liner. Each bottle shall be wrapped in a minimum amount of opaque packing material sufficient for protection against mechanical damage, but minimal in thermal insulation qualities. The wrapped bottles shall be enclosed in a tight wooden or metal box for further protection against breakage and sunlight. The crated samples shall be stored at ambient, outdoor conditions in a temperate climate. The box shall be kept off the ground and protected from direct sunlight and precipitation under a canopy, open roof shed, or similar ventilated shelter. The crated samples shall be stored undisturbed in an upright position for the specified period. One of the samples shall be stored for exactly 12 months and then removed for examination and testing, the other samples shall be stored for 12 months or less and may be removed for examination and testing at any time at the option of the qualifying activity. Whenever a sample is removed for

examination and testing, it shall be uncanted with minimum disturbance; the bottle shall not be shaken, inverted, or otherwise agitated. The contents of the bottle shall be inspected visually for precipitation, separation into layers, or other evidence of gross separation. The presence or absence and the nature of such separation shall be recorded. The top half of the liquid sample shall be carefully removed by suction or siphoning into another bottle, without disturbing the bottom half of the original sample. The top-half sample, after transfer to the second bottle, shall be shaken thoroughly and then used in laboratory testing, performed in accordance with 3.12. The bottom-half sample, in the original storage bottle, shall be retained for examination and possible additional testing to detect changes caused by storage.

4.6.10 Induction systems deposit test. The inhibitor, at its maximum concentration, shall be blended into a MIL-G-3056 motor gasoline. The test fuel shall then be tested for the formation of induction system deposits in accordance with Method 500 of FED-STD-791. The naphthawashed deposits shall not exceed 2 mg/100 ml of fuel. The MIL-G-3056 gasoline without the inhibitor shall also be tested in accordance with Method 500 of FED-STD-791 concurrently to define the level of deposition occurring as a result of the inhibitor.

4.6.11 Emulsification tendency test. The inhibitor, at maximum allowable concentration, shall be blended into a MIL-G-3056 motor gasoline and a MIL-F-46162 diesel fuel. Each test fuel shall then be examined for emulsification tendencies in accordance with Method 550 of FED-STD-791. Interface ratings in excess of three are evidence of unsatisfactory emulsification tendencies and shall not be allowed. The MIL-G-3056 motor gasoline and the MIL-F-46162 diesel fuel shall also be tested in accordance with Method 550 of FED-STD-791 to identify the quality of the fuels before the addition of the inhibitor.

4.6.12 Accelerated stability test. The test inhibitor, at its maximum allowable concentration, shall be blended into a diesel fuel (W-F-800) that contains no additives. Each test fuel shall be tested for the formation of total insolubles in accordance with ASTM D 2274. The total insolubles shall not exceed 1.5 mg/100 ml. The diesel fuel without the test inhibitor shall also be tested in accordance with ASTM D 2274 concurrently to define the level of insolubles occurring without the presence of the inhibitor. (NOTE: A suitable reference diesel fuel for this evaluation is described in Method 341.4 of FED-STD-791).

4.6.13 Identification tests. Identification tests shall be conducted in accordance with the following methods:

Density at 15°C	ASTM D 1298 or pycnometer
Viscosity at 37.8°C	ASTM D 445
Flash Point	ASTM D 56
Neutralization number	ASTM D 664, total acid number
pH	On 0.10 -- 0.11 g sample in 125 ml of ASTM D 664 Titration solvent. Read the constant pH as defined in note 9 of ASTM D 664.
Metallic constituent	Emission spectrograph not applicable for materials with ash contents of 0.05 percent or lower.

5. PACKAGING

5.1 Packaging, packing, and marking. The packaging, packing, and marking shall be in accordance with MIL-STD-290. In addition, package units shall be labeled to the extent applicable in accordance with Manual L-1.

6. NOTES

6.1 Intended use. The inhibitors covered by this specification are used, when specifically authorized, in jet engine fuels for the prevention of corrosion in fuel handling, transportation, and storage equipment and to improve the lubricating qualities of jet fuels. Certain of the inhibitors are also used in automotive gasoline, diesel fuel, and related petroleum products.

6.2 Ordering data. Procurement documents should specify the following:

- a. Title, number, and date of this specification
- b. Quantity required
- c. Selection of applicable levels of packaging and packing (5.1).

6.2.1 Amount of use of inhibitor. When Government procurement documents specify the use of inhibitors in fuels and related petroleum products, the concentration of inhibitor shall be specified in grams of inhibitor per cubic meter of fuel and shall not be less than the minimum effective concentration nor more than the maximum allowable concentration as listed on the Qualified Products List. Since the inhibitor is intended for use under many different environments, it is not possible to establish a single optimum concentration for all uses. Therefore, when a specific concentration is not required by the Government, the quantity of inhibitor used may vary to meet specific conditions.

6.3 Toxicity. Questions pertinent to toxicity should be referred by the procuring activity to the appropriate departmental medical service who will act as an advisor to the procuring activity. In case of Army procurement, the Surgeon General will act as advisor to the procuring activity.

6.4 Inhibitor for addition to fuels. When a fuel contractor or the Government purchases the inhibitor for addition to fuels to be used by the Government, the manufacturer of the inhibitor must certify to the purchaser that the product is an inhibitor that has been qualified under this specification. In addition, a test report showing compliance of the product with the requirements of 4.4 must be supplied to the purchaser. Additional data may be required by the purchasing activity to establish compliance with this specification.

6.5 Qualification. With respect to products requiring qualification, awards will be made only for products which are at the time set for opening of bids, qualified for inclusion in the applicable Qualified Products List whether or not such products have actually been so listed by that date. The attention of the contractors is called to these requirements, and manufacturers are urged to arrange to have the products that they propose to offer the Federal Government tested for qualification in order that they may be eligible to be awarded contracts or orders for the products covered by this specification. The activity responsible for the Qualified Products List is the Aero Propulsion Laboratory, Air Force Wright Aeronautical Laboratories (POSF), Wright-Patterson AFB, OH 45433, and information pertaining to qualification of products may be obtained from that activity.

6.6 Changes from previous issue. Asterisks are not used in the revision to identify changes with respect to the previous issue, due to the extensiveness of the changes.

Custodians:

Army- -ME

Navy- -AS

Air Force- - 11

Preparing activity:

Air Force- - 11

Project 6850-0597

Review activities:

Army- -MD,AV

Navy- -SH

Air Force- -68

User activity:

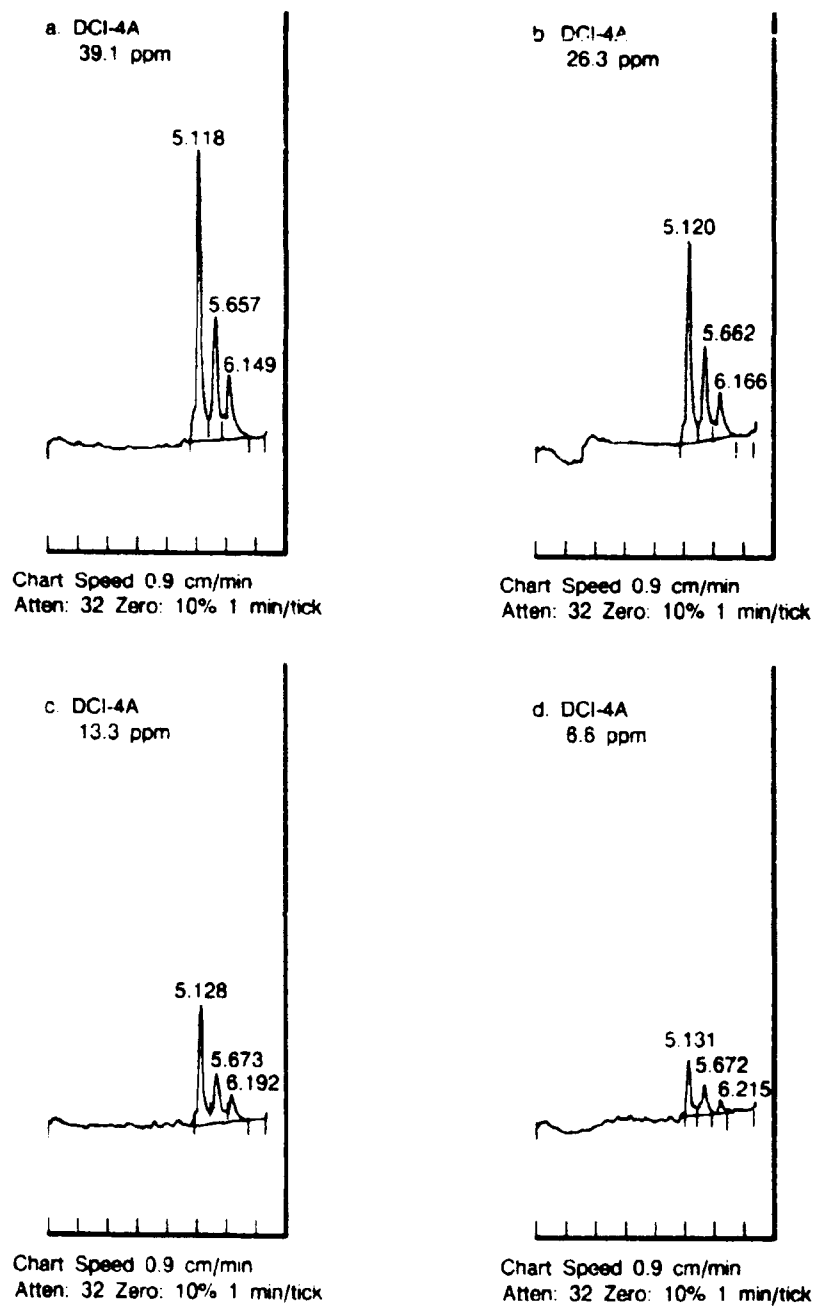
Army- -AT

APPENDIX F
RPHPLC CHROMATOGRAMS OF CORROSION INHIBITOR IN CT JP-4

LIST OF ILLUSTRATIONS

Figure

F-1	DCI-4A
F-2	DCI-6A
F-3	HITEC E-580
F-4	IPC 4410
F-5	IPC 4445
F-6	NALCO 5403
F-7	NALCO 5405
F-8	NUCHEM PCI 105
F-9	PRI-19
F-10	TOLAD 245
F-11	TOLAD 249
F-12	UNICOR J
F-13	LUBRIZOL 541
F-14	WELCHEM 91120
F-15	MOBILAD F800
F-16	CLAY TREATED JP-4 AND ADDITIVE FREE JP-4
F-17	TRIMER, DIMER, AND MONOMER LINOLEIC ACIDS



FDA 346

Figure F-1. DCI-4A

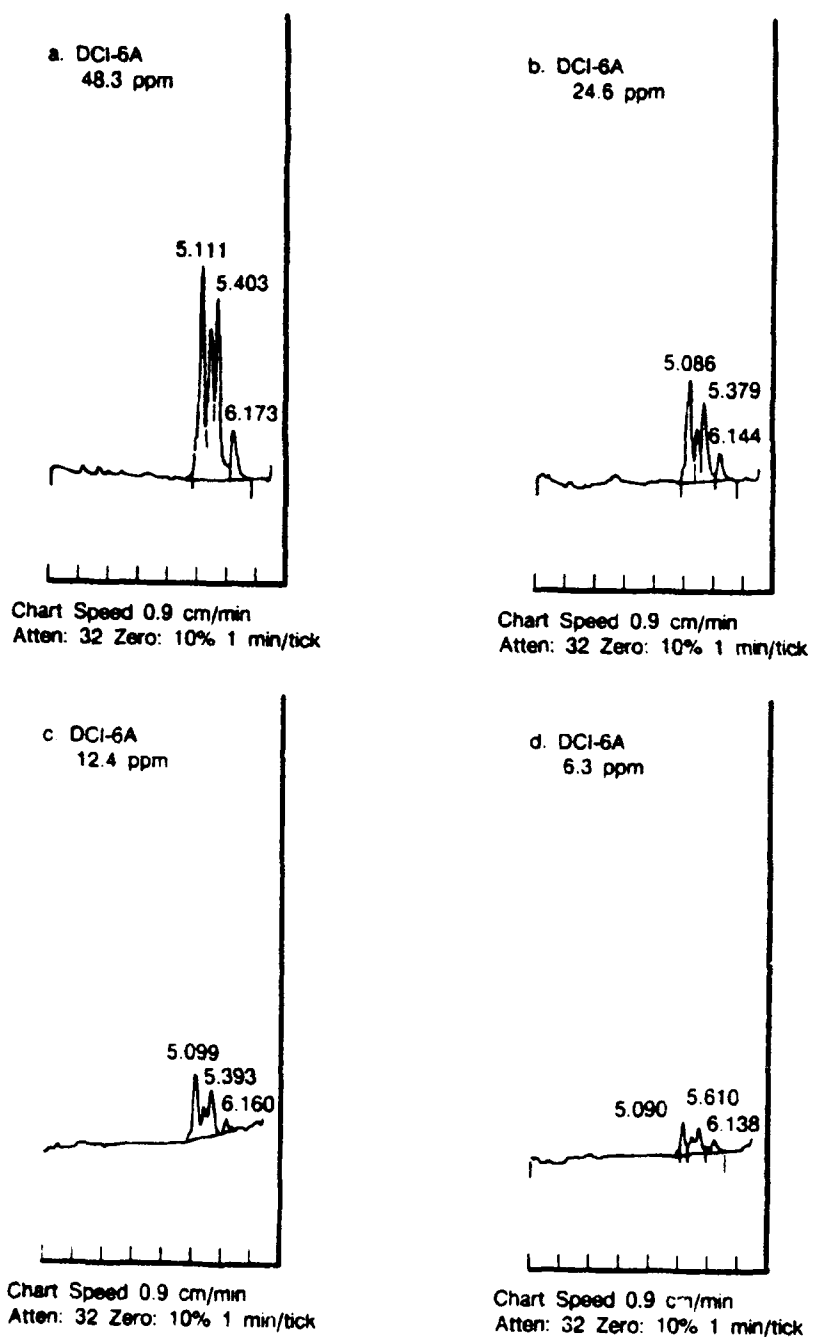


Figure F-2. DCI-6A

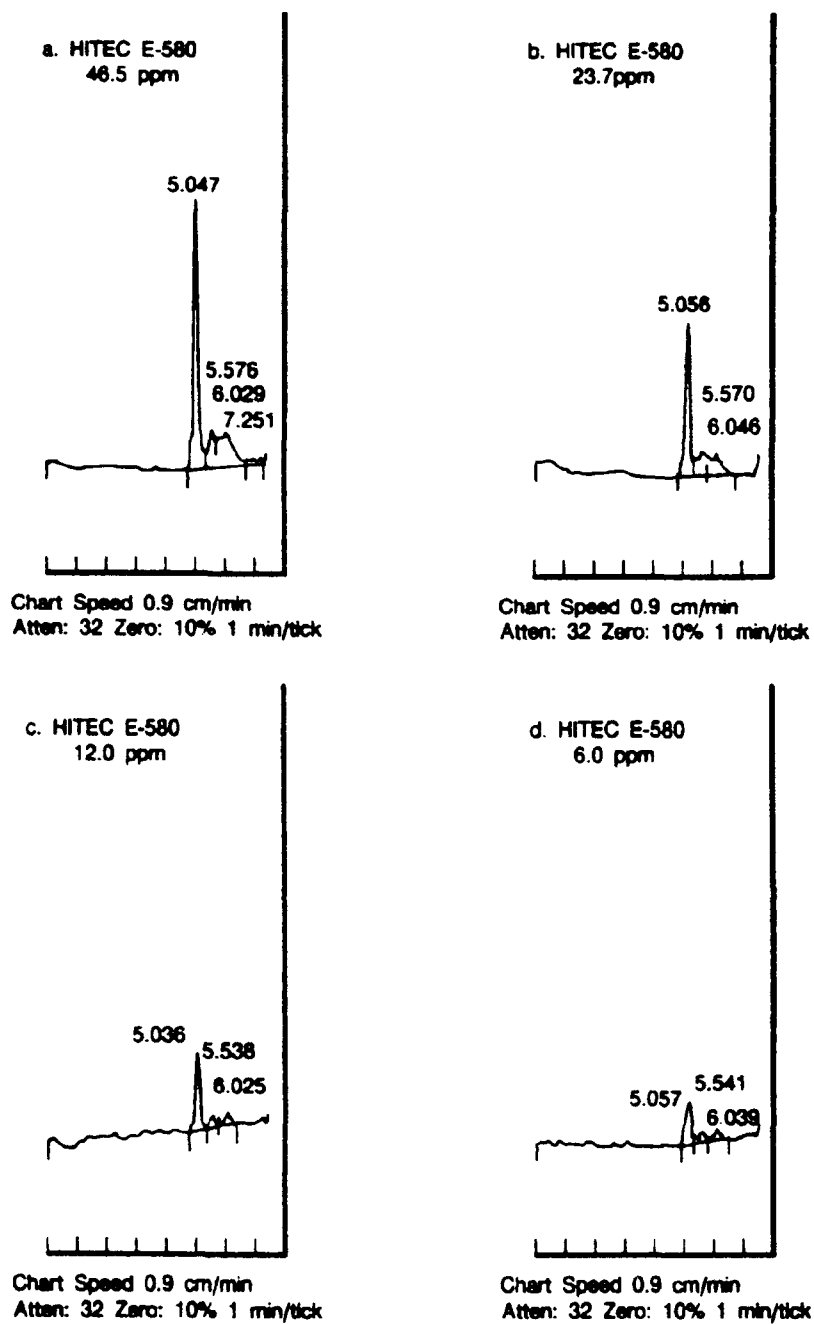
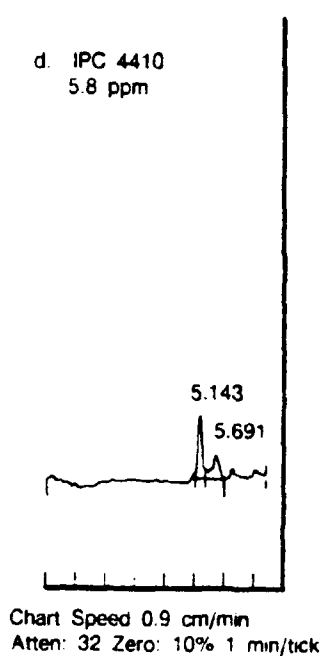
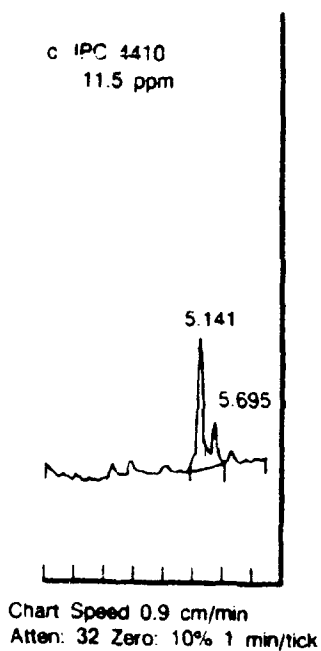
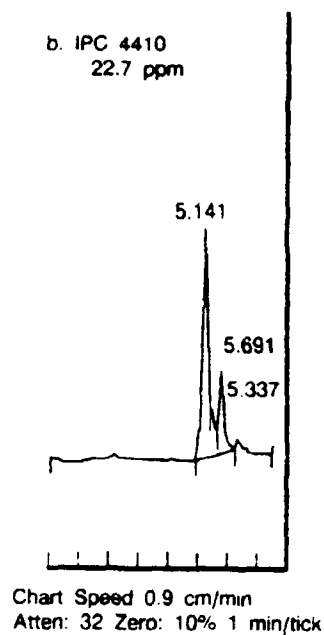
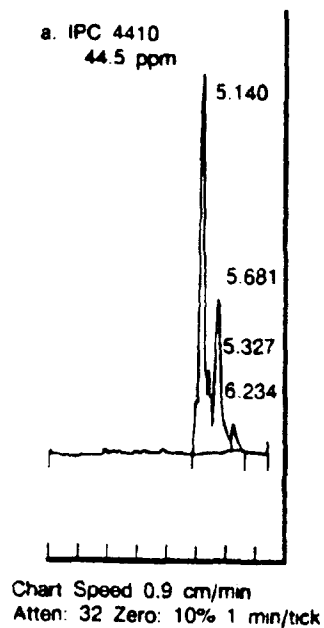


Figure F-3. Hitec E-580



FDA

Figure F-4. IPC 4410

a. IPC 4445
41.8 ppm

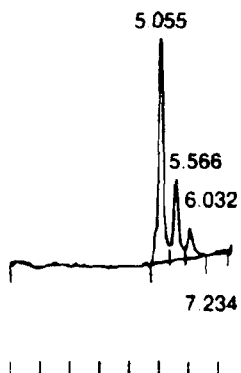


Chart Speed 0.9 cm/min
Atten: 32 Zero: 10% 1 min/tick

b. IPC 4445
21.3 ppm

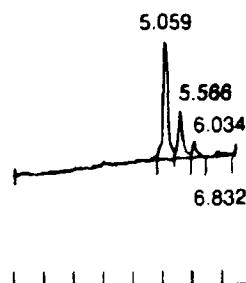


Chart Speed 0.9 cm/min
Atten: 32 Zero: 10% 1 min/tick

c. IPC 4445
10.8 ppm

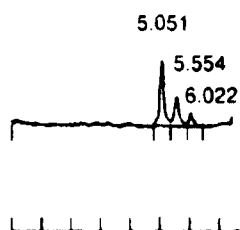


Chart Speed 0.9 cm/min
Atten: 32 Zero: 10% 1 min/tick

d. IPC 4445
5.4 ppm

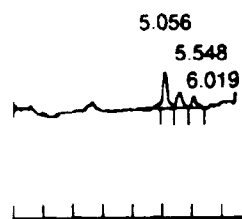


Chart Speed 0.9 cm/min
Atten: 32 Zero: 10% 1 min/tick

FDA 346172

Figure F-5. IPC 4445

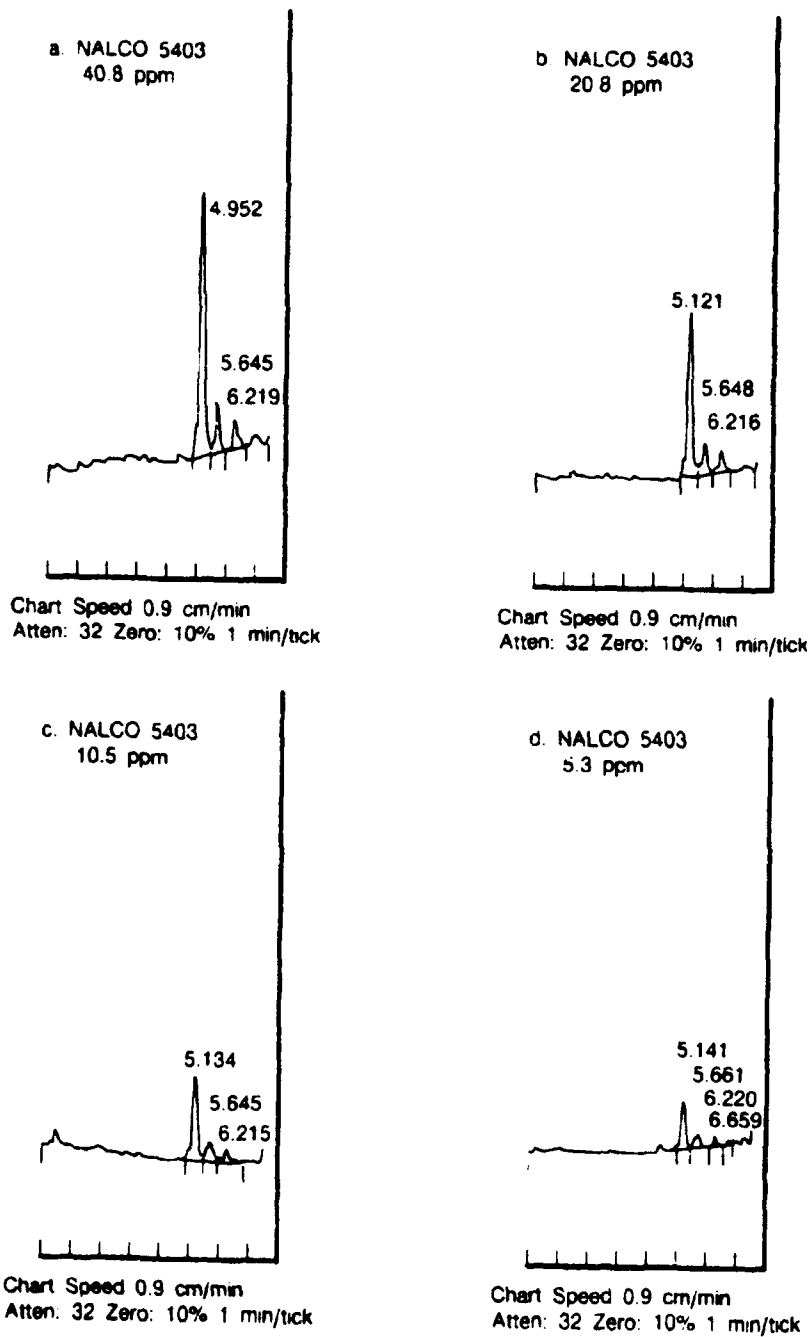


Figure F-6. Nalco 5403

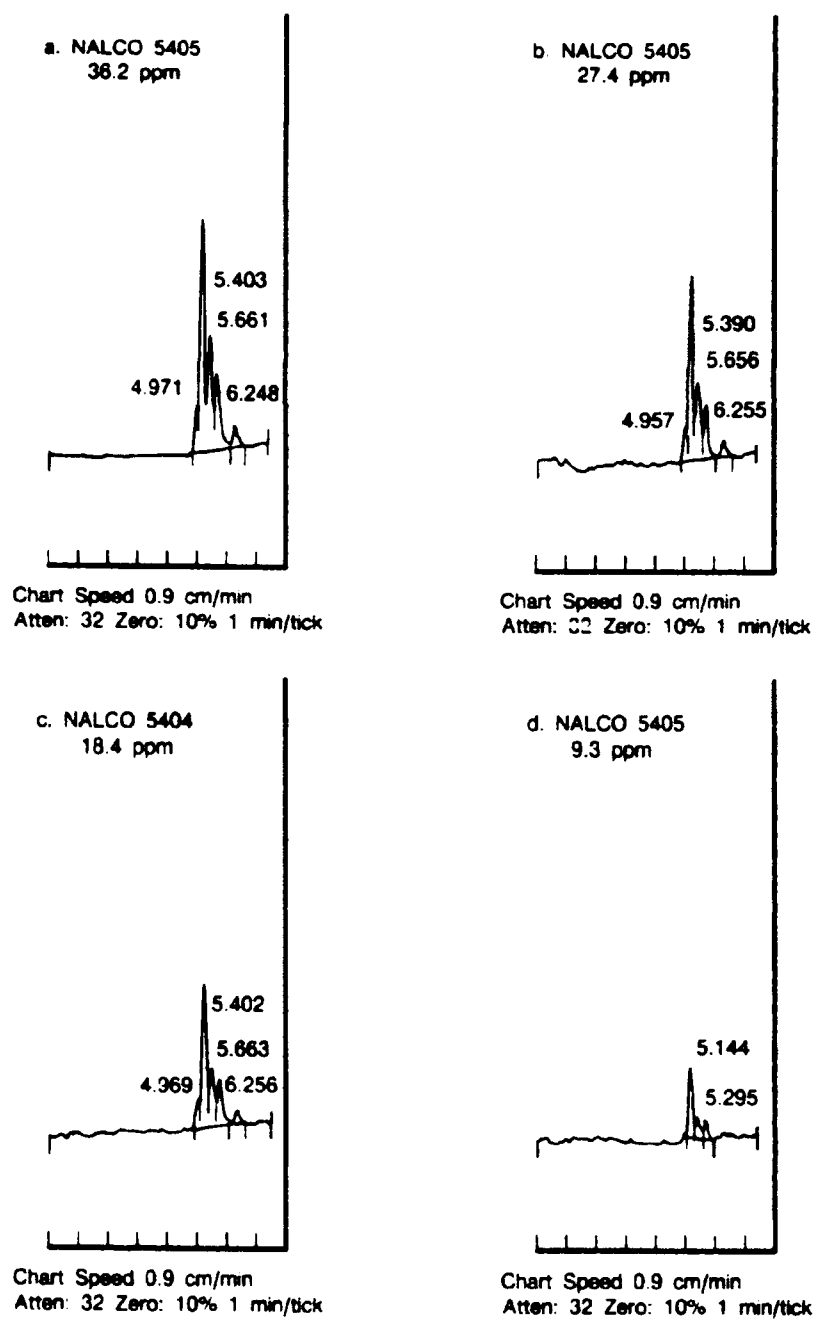
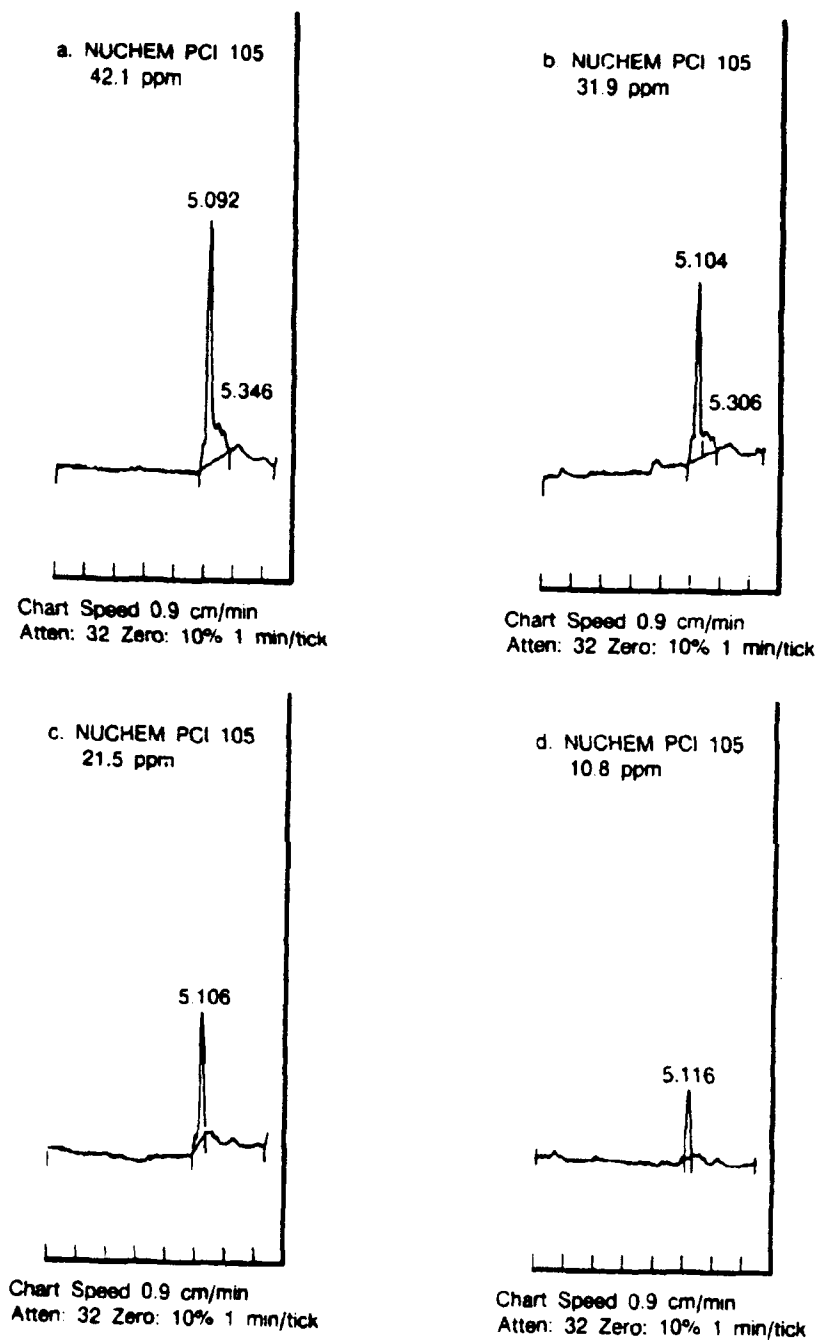
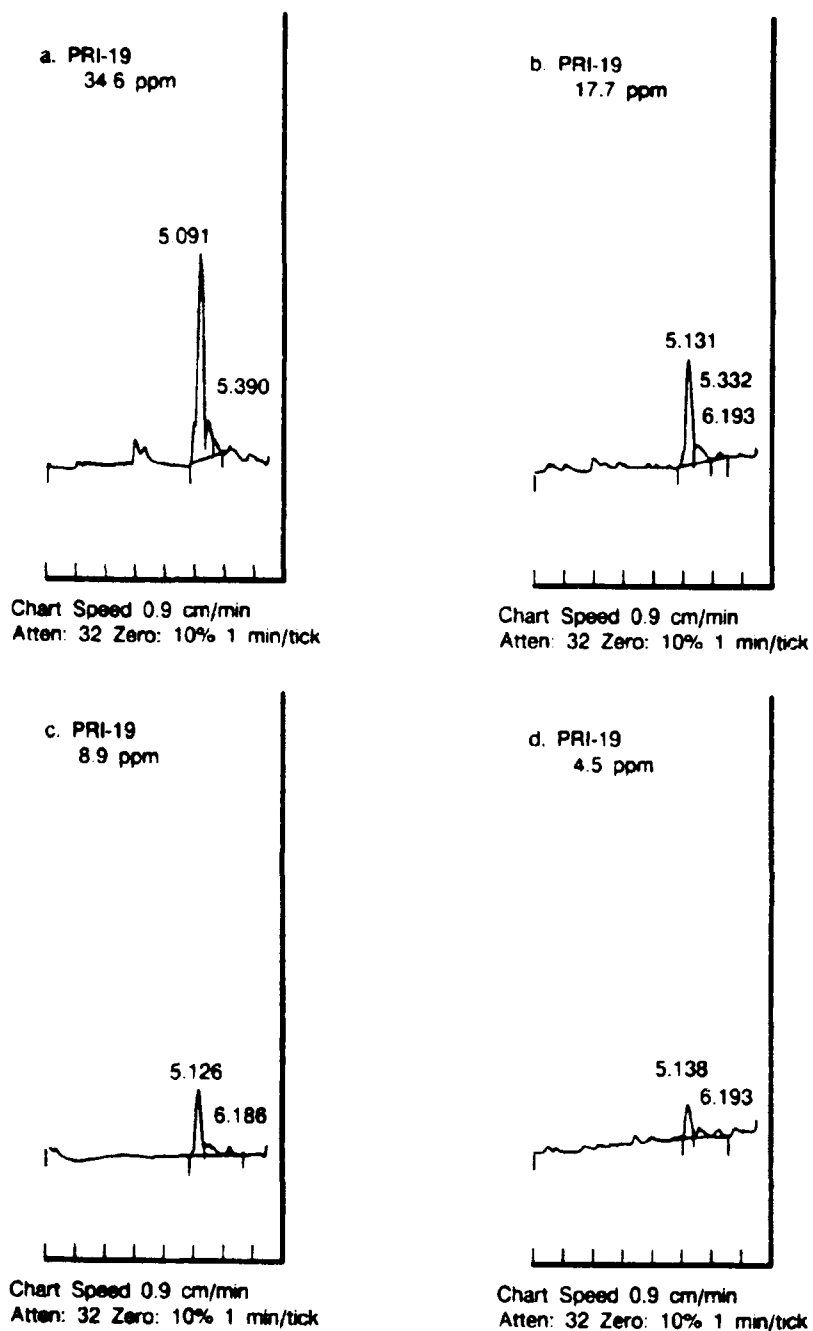


Figure F-7. Nalco 5405



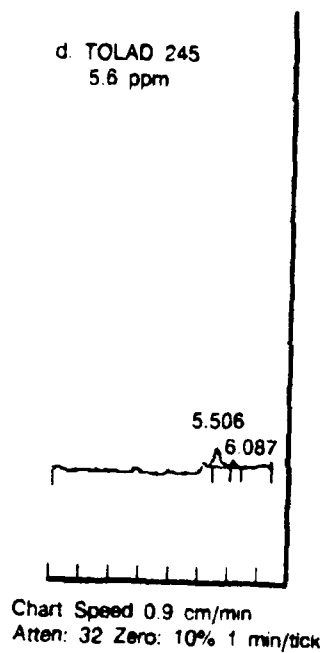
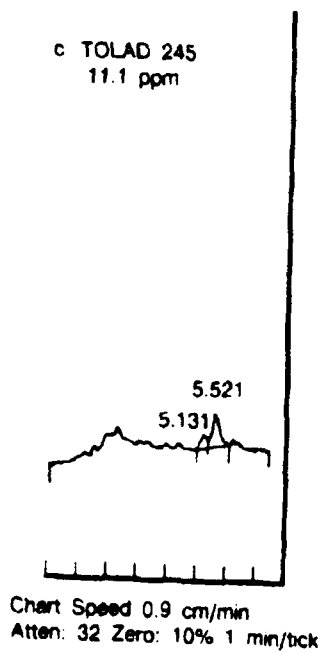
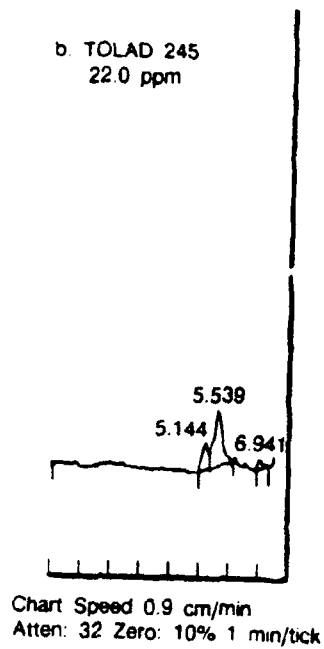
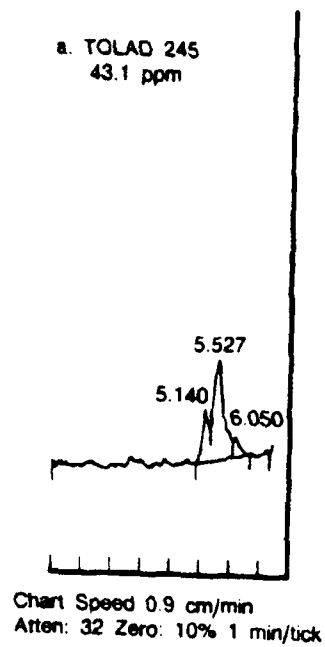
FDA 346175

Figure F-8. — NUCHEM PCI 105



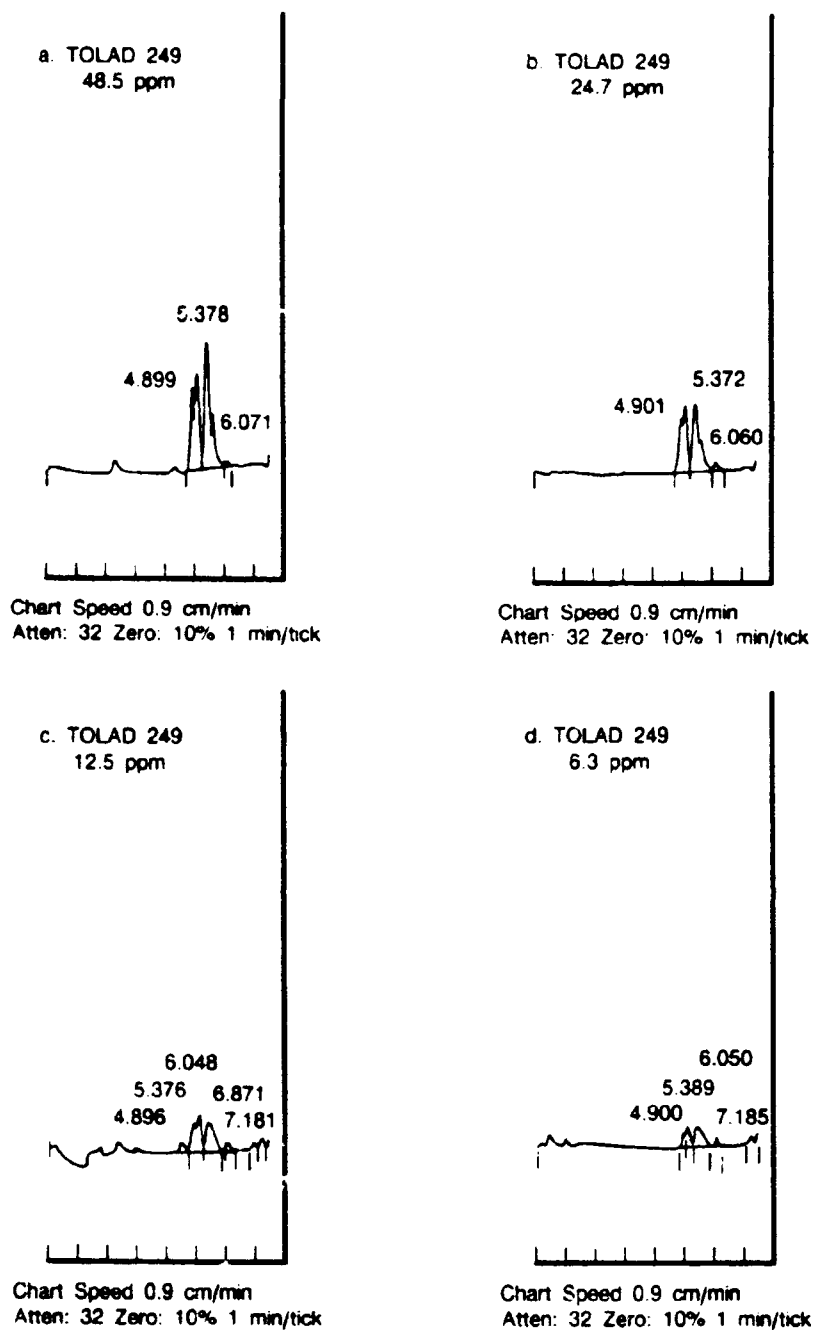
FDA 346176

Figure F-9. — PRI-19



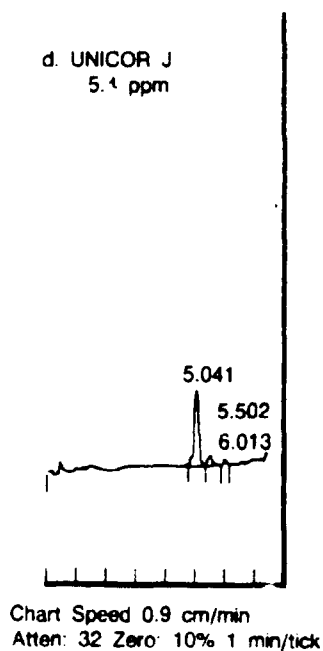
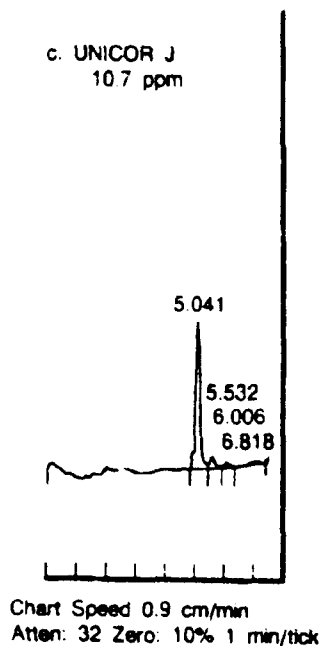
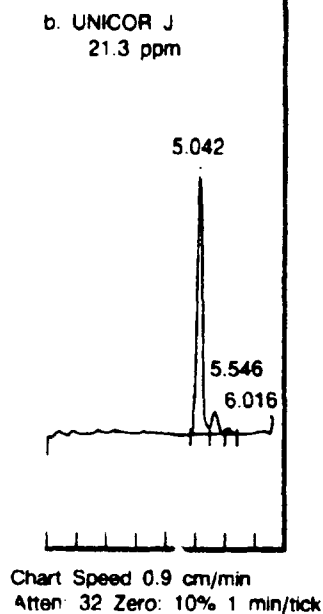
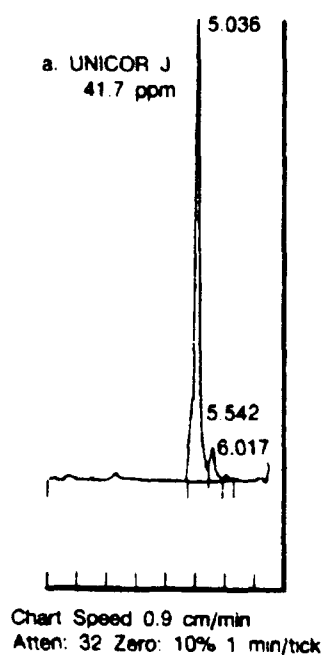
FDA 348177

Figure F-10. — TOLAD 245



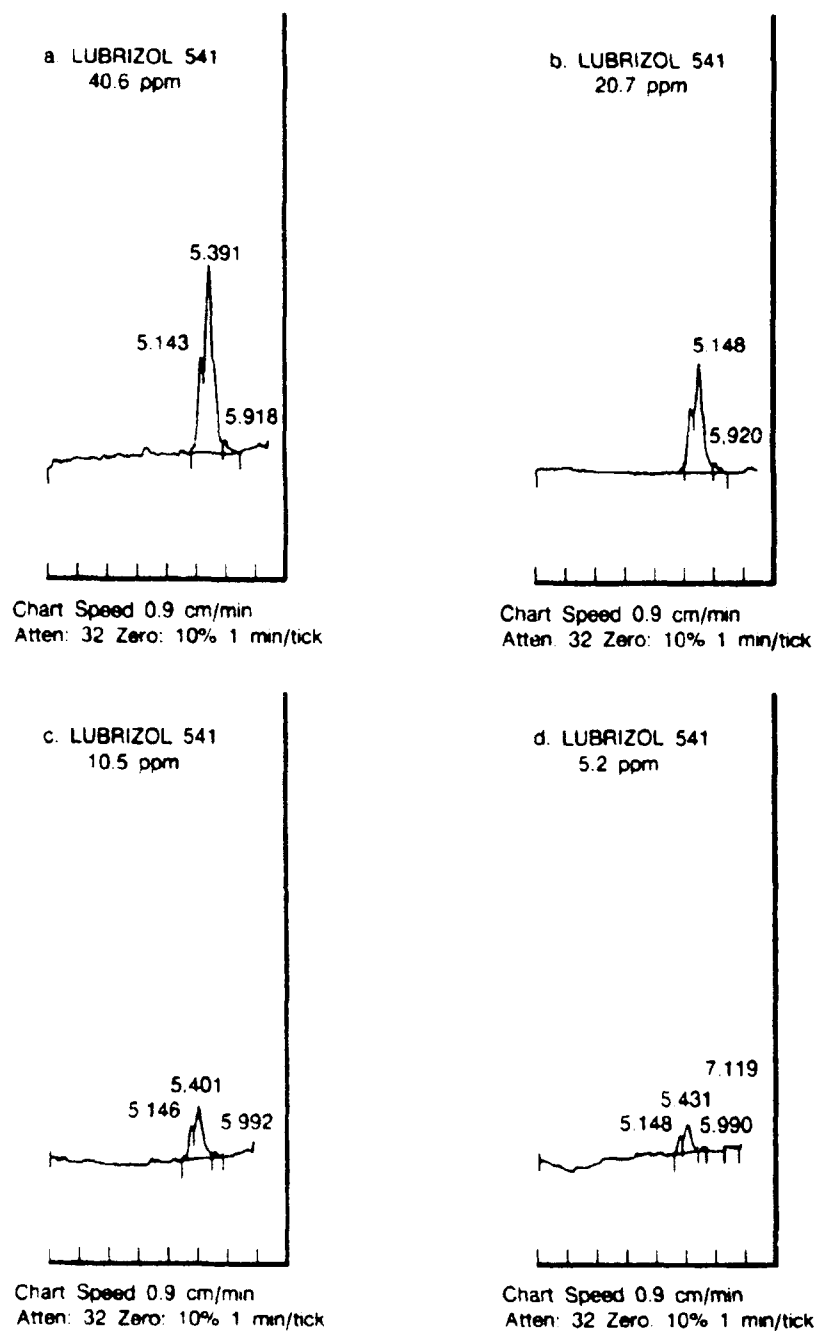
FI

Figure F-11. — TOLAD 249



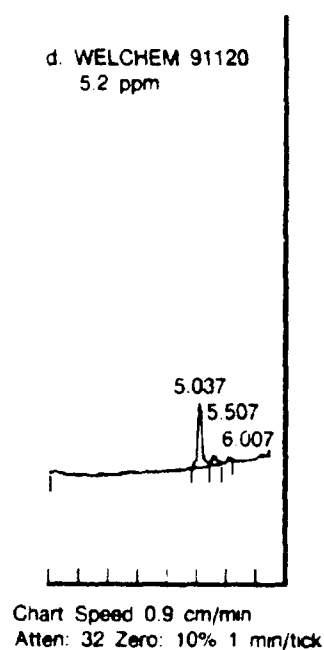
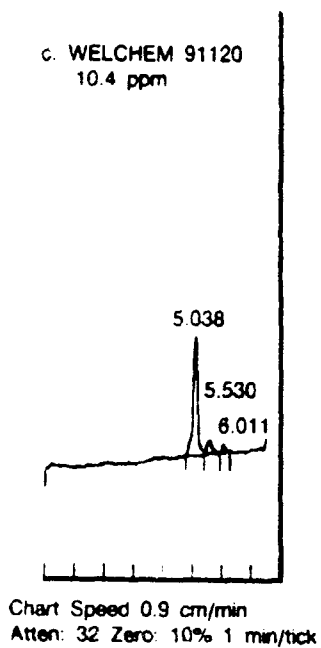
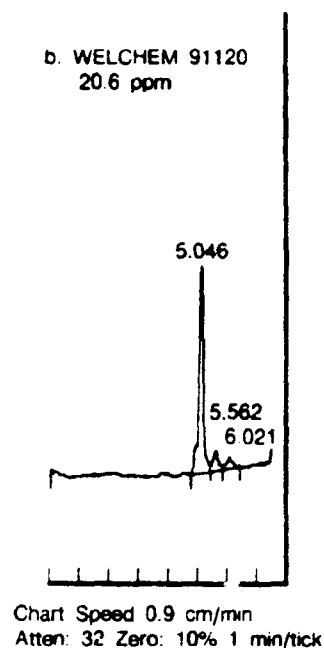
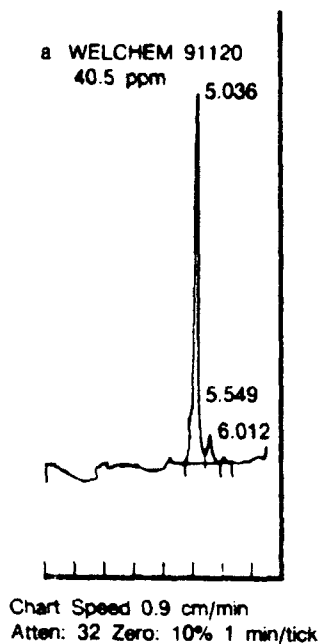
FDA 346183

Figure F-12. — UNICOR J



FDA 34

Figure F-13 — LUBRIZOL 541



FDA 341

Figure F-14. — WELCHEM 91120

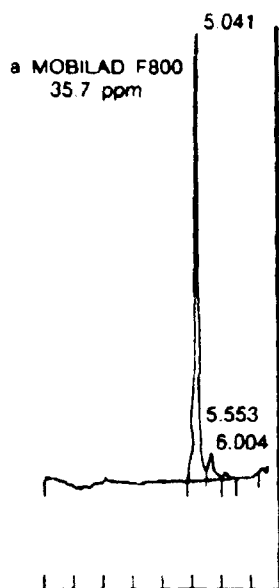


Chart Speed 0.9 cm/min
Atten: 32 Zero: 10% 1 min/tick

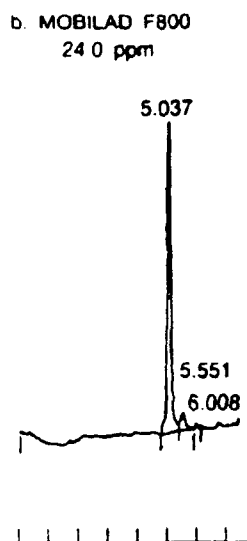


Chart Speed 0.9 cm/min
Atten: 32 Zero: 10% 1 min/tick

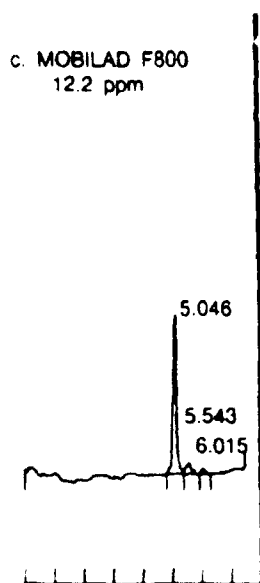


Chart Speed 0.9 cm/min
Atten: 32 Zero: 10% 1 min/tick

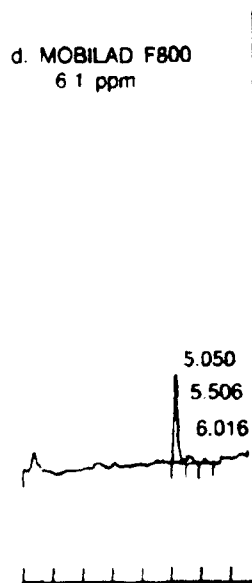
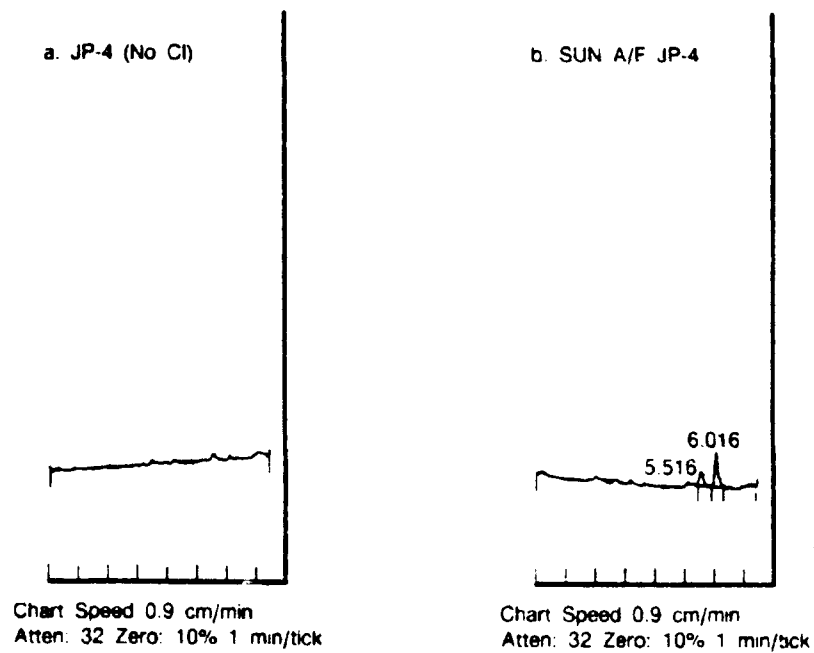


Chart Speed 0.9 cm/min
Atten: 32 Zero: 10% 1 min/tick

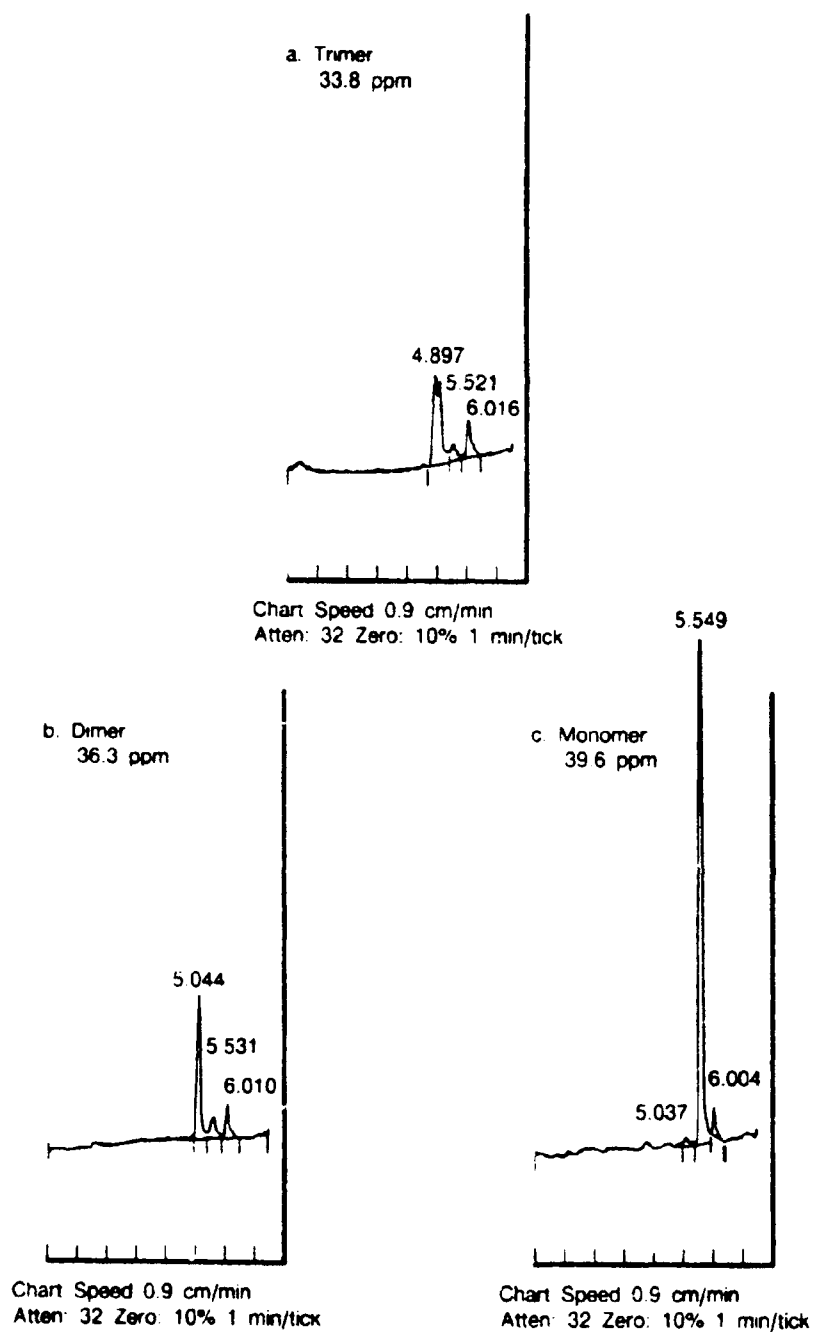
FDA 346186

Figure F-15. — MOBILAD F800



FDA 340829

Figure F-16. -- Clay Treated JP-4 and Additive Free JP-4



FDA 34083

Figure F-17. — Trimer, Dimer, and Monomer Linoleic Acids

DETERMINATION OF CORROSION INHIBITOR CONTENT IN AVIATION FUELS

Period of Performance

15 March 1986 through 13 March 1987

Reference

Task Order No. 6, Topical Report No. 7, March 1987, FR 19032-7, W.H. Edwards, T.B. Biddle, P.A. Warner

Abstract

An RPHPLC analytical method has been developed that quantitatively determines DLA in JP-4 type fuels. The method requires no sample pretreatment, allowing the direct additive analysis to be performed. Preliminary tests on 4 corrosion inhibitors with dissimilar active ingredients indicates that quantitative separation is accomplished. The high surface activity of DLA and CI products containing active ingredients of a similar nature require that standards be made daily and samples be analyzed within 8 hours after they are taken. Teflon type containers for preparation of standards and samples were found to contribute to the precision and accuracy of the test method. The reverse phase high performance liquid chromatography (RPHPLC) methodology developed during this investigation is based on the ability of the method to detect DLA which is the primary active ingredient present in many fuel soluble CI.

SECTION 1.0

INTRODUCTION

The recent use of severe processing conditions in industry to refine crude oil into finished transportation fuels has resulted in lubricity related fuel system wear problems. This has led to a dependence upon the use of fuel soluble corrosion inhibitors as lubricity improvers.

Currently, there are 14 approved corrosion inhibitors (CI) on the qualified products list of the MIL-I-25017 specification. CI additives work by adsorption to metal surfaces, providing corrosion inhibition and improved lubricity properties for fuels. This same mechanism, however, promotes additive depletion through adsorption on pipeline or vessel walls during fuel transport and storage. The ability to monitor the concentration of these additives is important to assure effective levels are present at the point of use in aircraft or test systems.

The acceptable method for evaluating the lubricity properties of fuels is the Ball on Cylinder Lubricity Evaluator (BOCLE) test. The fluid under test is placed in a controlled atmosphere test reservoir at 10% relative humidity. A non-rotating steel ball is held in a vertically mounted chuck and forced against an axially mounted steel cylinder at an applied load of 1000 grams. The test cylinder rotates at a fixed speed and receives a momentary exposure to the test fluid upon each revolution. The wear scar generated on the test ball is considered a measure of fluid lubricating properties. The method is a relative system of measurement for ranking fuel lubricity but can not determine actual levels of CI concentration.

In the past, several approaches for determining CI content in jet fuel have been investigated. These methods were based on detection of the dimer of linoleic acid (DLA) which was found to be the primary active ingredient in many of the qualified CI. One of the first methods for CI quantification in jet fuel

was developed by the DuPont Company (DuPont Petroleum Laboratory Analytical Method No. M14-78). This method uses open column ion exchange with infrared (IR) detection. The technique is labor intensive and the IR detection is subject to interference from the ion exchange resin.

More recent techniques use an alkali extraction to remove the fuel matrix and concentrate the additives for analysis. Infrared (IR) spectroscopy or gel permeation chromatography (GPC) with refractive index (RI) detection are methods that have been evaluated by industry (References 1,2,3,4). While these techniques have been moderately successful, they are time consuming and caution must be observed in their application. The technique of extraction and concentration requires considerable effort. Complete extraction, with no losses, is extremely difficult to achieve. This is especially true of surface active CI compounds. Infrared spectroscopy can deviate from Beer's Law in a random manner because of chemical and instrumental effects. The spectrum must be manually interpreted to achieve optimum quantitative data. The GPC-RI technique is used primarily in molecular weight distribution estimates for large molecular weight compounds such as polymers. It is not considered to be quantitative. Additionally, GPC column packings tend to swell and contract with variations in temperature and solvent. These variations can cause problems in the separation phase and also affect the refractive index detection of CI compounds. Furthermore, GPC repeatability and reproducibility have been shown to be poor.

Techniques are available using derivatization of fatty acid compounds to facilitate analysis by gas chromatography (GC) or high performance liquid chromatography (HPLC) (Reference 5). However, the polar impurities and high molecular weight aromatic hydrocarbons in jet fuel tend to interfere with an in-situ derivatization. For this technique to be successful, the additives would first have to be extracted.

Bergman, et al., described a simple and rapid colorimetric technique for non-esterified fatty acids (Reference 6). A modified version of this method was evaluated during this effort to determine the potential for quantifying DLA in a fuel matrix. The technique initially showed promise in that DLA in hexane standards appeared to yield linear calibration lines. Although the line slopes remained nearly the same, the relative absorbance values varied significantly between calibrations. This indicated a variation in analytical sensitivity. The problem worsened in jet fuel matrices. A white gelatinous material came out of solution after reaction. The absorbances of these solutions were significantly lower than the DLA/hexane standards and were non-linear. It was apparent that polymeric reactions were occurring involving two or more DLA molecules with divalent copper ions. As a result, these very large molecules were precipitating from solution and no quantitative information could be obtained.

Green, et al., recently reported an ion pairing HPLC technique for the isolation of carboxylic acids from petroleum (Reference 7). The technique requires no sample pretreatment, allowing the direct injection of the fuel sample into the chromatograph. Because of the obvious advantage of a direct injection method, a modification of the IPHPLC technique for the analysis of DLA was investigated. The modification consisted of a change in mobile phase to lower its ultraviolet (UV) cut off so that the DLA maxima at 202 nm could be used. To accomplish this, the hexane was replaced with pentane, the chloroform with isopropanol, and the methanol/tetramethylammonium hydroxide (TMA-OH) with acetonitrile/low UV TMA-OH. Percentage composition was adjusted to maintain solubility.

Using the modified mobile phase, an analysis of a standard consisting of DLA in pentane was conducted. Good sensitivity for DLA was apparent although the DLA peak shape was not optimum. However, when the fuel matrix DLA standards were run the DLA was not completely separated from the fuel matrix. Adjustments in the gradient program (i.e. varying the percentage of the solvents and the rates of these changes) did not resolve the DLA from the fuel matrix.

Assessment of the above candidate techniques provided the basis for the design of a reverse-phase HPLC (RPHPLC) approach to quantifying DLA in jet fuels. The rationale used for this approach was based upon the following: DLA has a molecular weight of about 560, which is very large compared to other fuel component molecules; DLA is very polar and soluble in aqueous base and several low UV absorbing organic solvents.

The RPHPLC method, developed and presented in the following section, uses the above properties to allow the rapid direct analysis of DLA in jet fuel. Data are presented for a DLA standard and container type stability study, standard calibration statistics, interferences study, and method applicability to four approved CI products.

SECTION 2.0

EXPERIMENTAL

2.1 MATERIALS

HPLC grade isopropanol and water were obtained from Burdick and Jackson (Muskegon, MI). Potassium phosphate, monobasic and sodium hydroxide were ACS Analytical Reagent grade obtained from Mallinckrodt, Inc. (Paris, KY). EMPOL 1010, a dilinoleic acid of 97% purity, was obtained from Emery Chemical Co. (Cincinnati, OH). Additive free JP-4 fuel samples were obtained from Sun Oil Co. (Philadelphia, PA), Ashland Oil Co. (Ashland, KY) and Hunt Oil Co. (Dallas, TX). Four samples of the 14 approved CI products listed on the QPL of MIL-I-25017 specification were obtained from the respective suppliers. Isopar M solvent was obtained from Exxon Co. (Houston, TX).

2.2 METHOD

A Varian Model 5560 Ternary Liquid Chromatograph was used to perform all HPLC analyses in this study. It was equipped with a Varian Model UV200 variable wavelength ultraviolet-visible detector set to 202 nm with a 0.5 second response time, a Rheodyne Model 7125 injector valve with 50 μ L sample loop and an electronic column heater. A cyanopropyl bonded phase column (Brownlee Labs), 5 micron particle size, 22 cm x 4.6 mm with 3 cm cyanopropyl guard column was used for the separations. Quantitation was accomplished with a Varian Model Vista 402 Chromatography Data System. All baseline treatment was peak valley to peak valley and peak height quantification was automatically determined by the Vista 402 software using the external standard calibration mode.

The mobile phase consisted of 60% isopropyl Alcohol (IPA) AND 40% Ph 7.0 buffer (0.0395 M $\text{KH}_2\text{PO}_4/\text{NaOH}$). The buffer solution was prepared by diluting 250 mL of 0.1 M KH_2PO_4 and 145 mL of 0.1 M NaOH to 1000 mL with HPLC grade water. The column heater was set to 28 C to eliminate the affect of temperature fluctuations on the chromatographic separation. It was found that a 1 C column temperature change altered peak retention times. A temperature of 28 C is sufficient to overcome this problem and yet not damage the column packing.

The standards and samples are syringe injected directly into the HPLC system via 50 μ L sample loop. A 500 μ L smooth bore glass and Teflon syringe is best for this purpose. The sample loop is first washed with a 500 μ L aliquot of sample from the syringe. The second 500 μ L aliquot is the analysis sample. This assures complete sample loop filling and that sample loss and cross contamination are minimized. Between samples the syringe plunger is removed and the syringe is thoroughly cleaned with isopropyl alcohol and acetone. It is then dried with clean nitrogen.

The additives elute first, ahead of the fuel matrix. After this it is necessary to remove the rest of the fuel sample from the column prior to the next analysis. To accomplish this a wash cycle begins at 4.0 minutes into the run using the ternary (3 solvent) capability of the chromatograph. Reservoirs A, B and C contain IPA, buffer solution and pure HPLC grade water, respectively. The sequence begins at sample

injection and the program is started. The initial conditions of 60% IPA, 40% buffer, and a flow rate of 0.8 mL/minute are held constant for the first four minutes. After 4.0 minutes a gradient to 100% water (reservoir C) is run over a one minute interval and then held at 100% water for two minutes. This assures removal of buffer so that no salt precipitation occurs which can damage both the chromatograph and analytical column. Flow rate is also adjusted to 1.3 mL/minute at this point.

At the end of the two minute water wash, now 7.0 minutes into the run, a gradient to 100% IPA (reservoir A) is made in 1.0 minute and held for two minutes. This assures complete removal of the fuel matrix from the column. Next, a one minute gradient is run back to 100% water (again required to prevent buffer salt precipitation) followed by an immediate one minute gradient to 60% IPA and 40% buffer. This completes 12.0 minutes into the analysis and is followed by a 4-minute flush with the original mobile phase at 1.3 mL/minute. At 16.0 minutes the flow rate is adjusted over a one minute interval back to 0.8 mL/min. Reequilibration to a stable baseline requires an additional 13.0 minutes for a total elapsed time of 30.0 minutes.

System pressure, in general, will vary depending upon the mobile phase, column length and packing type. However, for the conditions used in this work, an initial pressure of 215 atmospheres (3160 psi) is normal. Pressure will increase during the column wash cycle, reaching 300 atmospheres (4410 psi), but returns to about 215 atmospheres after adjustment of the flow rate to 0.8 mL/minute.

SECTION 3.0

RESULTS AND DISCUSSION

During the course of this study, Isopar M, a narrow cut isoparaffinic solvent, was found to fulfill the requirements for a pure, fuel-like solvent. Therefore, Isopar M was used for some experiments to serve as a standard matrix in evaluating HPLC parameters.

Figures 1 and 2 respectively, are composite calibration chromatograms of DLA in Isopar M, and DLA in additive free (neat) JP-4 from Hunt Oil Co. The DLA peak can be seen at a retention time of 2.6 minutes. The other peaks shown in chromatograms are believed to be polar compounds from the matrix since they appear in the neat fuel chromatograms as well.

Figures 3 and 4 are the results of linear regression analyses performed on the data from Figures 1 and 2, respectively. The standard error of the estimate (SEE) for DLA in Isopar M was 0.59 ppm. The SEE for DLA in neat JP-4 was 0.40 ppm. The correlation coefficient was 0.9993 for DLA in Isopar M and 0.998 for DLA in neat JP-4.

A time stability experiment using 100 mL glass containers and 100 mL Teflon containers was conducted to evaluate the effect of container type on the stability of DLA standards and CI analyses. Standards of 100 mL volumes were prepared at a concentration of 25.4 parts per million (ppm) DLA in Isopar M and monitored for DLA depletion as a function of time. Within 8 hours, the DLA standard in glass had depleted to 23.4 ppm, a 7.9% decrease, while the standard in Teflon had depleted to 24.7 ppm, a 2.8% decrease in concentration. After 3 days, the standards in both containers were shown to stabilize at a concentration of 20.0 ppm. No further changes in concentrations were noted at the conclusion of 8 days. The results of the investigation indicated that for a given DLA concentration and solution volume, (1) the container surface type dictates the rate of DLA depletion (i.e. glass > Teflon) and (2) the degree of depletion may be a function of container area in contact with the solution.

The additive free JP-4 fuels obtained from Ashland, Hunt and Sun Oil Companies were analyzed for

possible interferences to CI additive quantification. A standard calibration was made and each fuel analyzed. Only the Sun Oil Co. fuel sample produced a peak at the 2.6-minute retention time shown previously for DLA. This peak, however, was very small and did not present a significant interference problem. One additive free JP-5, obtained from the Naval Air Propulsion Center, was also analyzed. No interfering peaks were observed for that sample.

Applicability of the RPHPLC technique to several approved CI products was determined. The four CI products chosen for investigation were DCI-4A (DuPont), Nalco 5405 (Nalco Co.), Tolad 245 and Tolad 249 (Petrolite Co.). The DCI-4A, Nalco 5405 and Tolad 249 were reported to contain dimer acids, trimer acids and fatty acids as active ingredients. Tolad 245, however, was reported to contain acylated glycols and acylated alkanolamines as active ingredients.

Figure 5 shows RPHPLC chromatograms of DCI-4A, Nalco 5405, Tolad 245 and Tolad 249 in Isopar M solvent. The chromatograms show good separation of the additives from the solvent matrix and indicate separation will occur in a jet fuel matrix. In addition, the size, shape and resolution of the peaks shown in the chromatograms indicate quantification is possible, especially when the particular CI product used is known. If the additive used is not known, it may be possible to identify it from its unique chromatogram fingerprint. Work in this area still needs to be done. The diversity of active ingredients found in the four CI's evaluated indicates that for a fuel sample containing a mixture of these products quantification may not be possible. Such a situation could arise when a sample is taken from a bulk storage tank that receives fuels containing different CI products. This mixture could not be resolved with the present RPHPLC technique. The mixture of additives would prevent accurate calibration of standards. The technique could be used, however, to monitor the normalized total CI content. This would provide the basis for determining CI losses during fuel transport and storage.

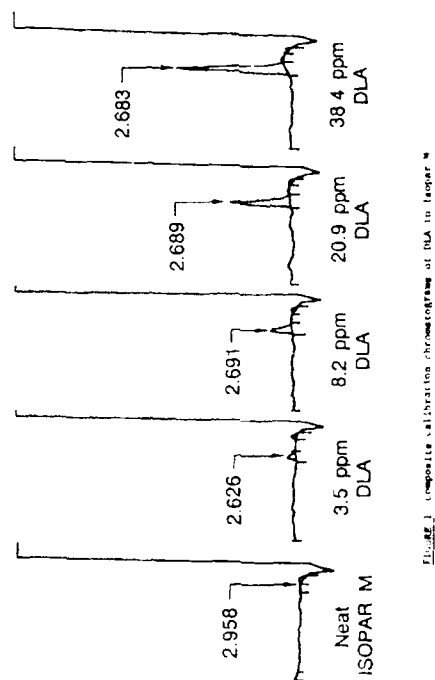


Figure 1. Composite Calibration Chromatograms of DLA in Isopar M

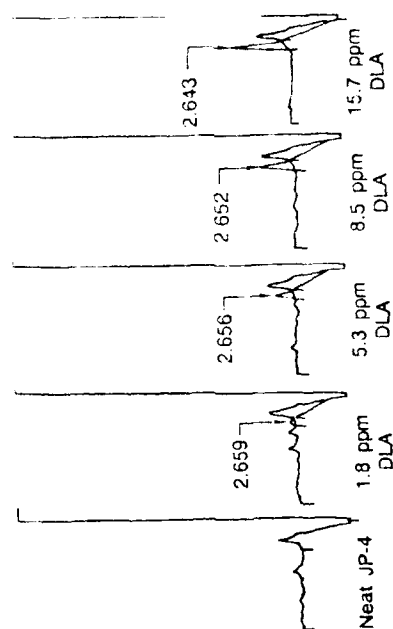


Figure 2. Composite Calibration Chromatograms of DLA in Additive Free JP-4

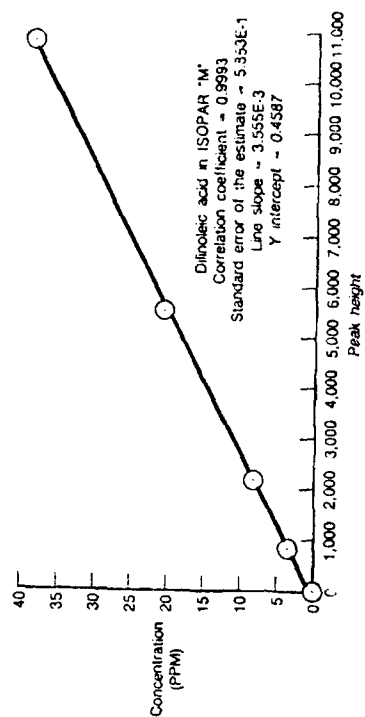


Figure 3. Linear Regression Analysis of Data From Figure 1

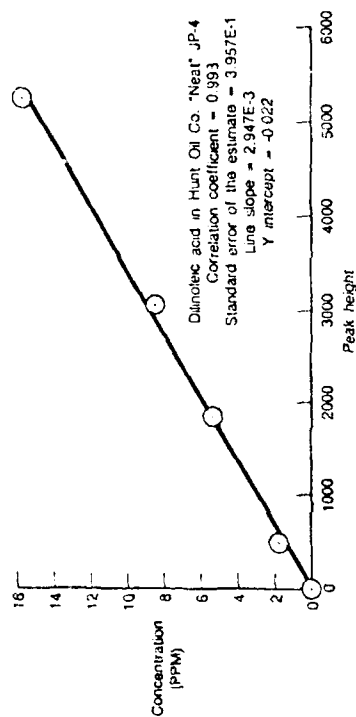


Figure 4. Linear Regression Analysis of Data From Figure 2

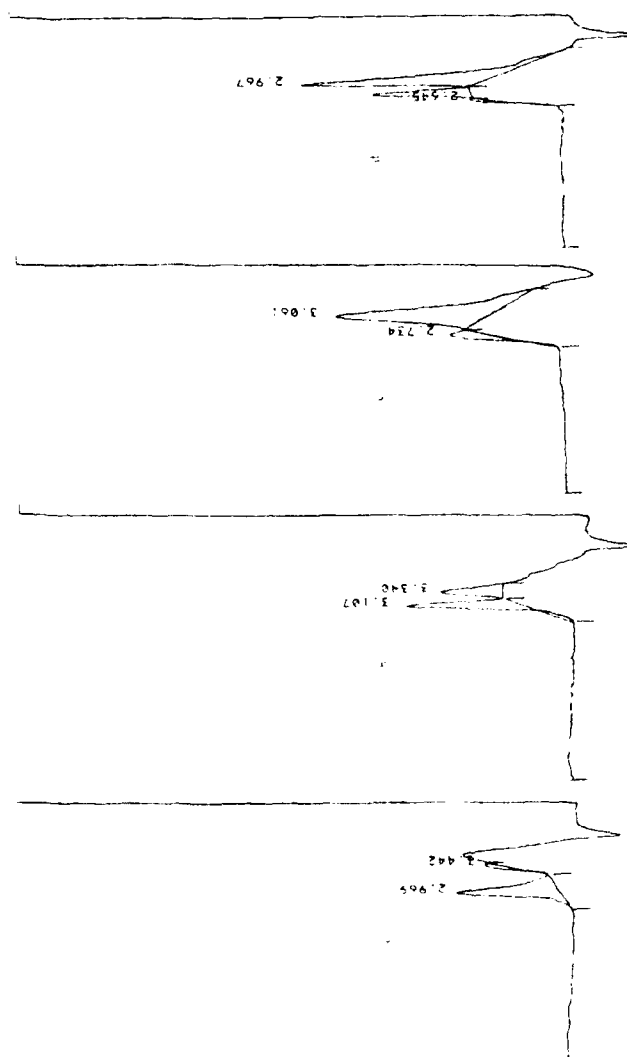


Figure 5. RPHPLC Chromatograms of (a) DCI-4A, (b) Nalco, (c) Tolad 245 and (d) Tolad 249

SECTION 4.0

CONCLUSIONS AND RECOMMENDATIONS

An RPHPLC analytical method has been developed that quantitatively determines DLA in JP-4 type fuels. The method requires no sample pretreatment, allowing the direct additive analysis to be performed. Preliminary tests on 4 corrosion inhibitors with dissimilar active ingredients indicates that quantitative separation is accomplished. The high surface activity of DLA and CI products containing active ingredients of a similar nature require that standards be made daily and samples be analyzed within 8 hours after they are taken. Teflon type containers for preparation of standards and samples were found to contribute to the precision and accuracy of the test method.

The RPHPLC methodology developed during this investigation is based on the ability of the method to detect DLA which is the primary active ingredient present in many fuel soluble CI. It is recommended that the applicability of the technique to all 14 approved CI in a variety of fuel types be determined. Additional development of the test method should be pursued to further refine instrumental parameters, identify CI containing active ingredients other than DLA and recommend modifications to the method which would permit a broader application for determining CI content in jet fuels.

REFERENCES

- 1) Morgan, T. G., Filtration and Separation, Sept./Oct., 1972, p585-589.
- 2) Hillman, D. E., Paul, J. I., and Cobbold, D. G., edited by D. R. Hodges, Recent Analytical Developments in the Petroleum Industry, 1974, John Wiley and Sons, chapter 3, p47-58.
- 3) "Determination of the Dilinoleic Acid Content of Aviation Turbine Fuels", NATO STANAG 3390, Edition No. 5, Annex C.
- 4) Wechter, M. A., "Quantitative Determination of Corrosion Inhibitor Levels in Jet Fuels by HPLC", NRL Contract No. N00014-85-M-0248.
- 5) Knapp, D. and Kruger, S., 1975, Anal. Letters, vol. 8, p603.
- 6) Bergman, S. R., Carlson, E., Dannen, E. and Sobel, B. E., Clinica Chimera Acta, 104, 1980, p53-63.
- 7) Green, J. B., et al., "Rapid Isolation of Carboxylic Acids from Petroleum Using High Performance Liquid Chromatography", Anal. Chem., 1985, 57, p2207-2211.

ASSESSMENT OF THE FIBER OPTIC MODIFIED JET FUEL THERMAL OXIDATION TESTER

Period of Performance

27 March 1987 through 15 July 1988

Reference

Task Order No. 14, Topical Report No. 11, FR 19032-11, July 1988, Tedd Biddle

Abstract

The Fiber Optic Modified-Jet Fuel Thermal Oxidation Tester was developed by Geo-Centers, Inc., Boston, Massachusetts, under Navy funding (Reference 1). Key features include a means for producing quantitative data with the JFTOT, real time data acquisition and display, and data at eight temperatures obtainable from one test. The objectives of this technical effort included the procurement, setup, and functional assessment of the FOM-JFTOT system hardware and software.

SECTION 1.0

INTRODUCTION AND BACKGROUND

Fuel thermal stability has been identified as a critical limiting factor in the development of propulsion systems for high speed aircraft. For advanced high speed aircraft flying at speeds greater than Mach 3, fuel is the only available heat sink. Fuel will undergo considerable thermal stress as the primary source for cooling cabin air, electronics, lubricants, hydraulic fluids, and some engine and airframe structural components. Fuel system coking has already been observed in some current engines, plugging spray rings, fuel nozzles, and heat exchangers. The result is reduced performance and reliability.

Although qualitative methods have been relied upon in the past to rate the tendency of a fuel to form fuel system deposits, it is widely agreed that a more quantitative system of measurement is needed. A less subjective, more quantitative method would have value in providing kinetic rate data, characterizing advanced fuel candidates, evaluating thermal stability improving additives, and improving the reliability of quality control testing. The concept of applying fiber optics to a standard Jet Fuel Thermal Oxidation Tester (JFTOT) may represent a significant step forward in providing quantitative, real time deposition rate data. If successfully developed, the Fiber Optic Modified JFTOT (FOM-JFTOT) could provide a means for getting the most out of the data currently available from a standard accepted test method while a comprehensive long range research program directs effort to techniques which more closely simulate actual engine conditions and thermal environments.

The FOM-JFTOT was developed by Geo-Centers, Inc., Boston, Massachusetts, under Navy funding (Reference 1). Key features include a means for producing quantitative data with the JFTOT, real time data acquisition and display, and data at eight temperatures obtainable from one test. The objectives of this technical effort included the procurement, setup, and functional assessment of the FOM-JFTOT system hardware and software. To facilitate and coordinate the preliminary validation, close communication was maintained with the Naval Air Propulsion Center (NAPC), Trenton, N.J. and AFWAL/POSF. Three NAPC supplied fuels were evaluated to provide a limited means for evaluating repeatability and reproducibility. Limitations of the FOM-JFTOT were identified as well as the potential for further development.

SECTION 2.0

EXPERIMENTAL

2.1 EQUIPMENT

2.1.1 Jet Fuel Thermal Oxidation Tester (JFTOT)

An InterAv Research Model JFTOT was used in this investigation. A fuel system schematic for the InterAv Research Model JFTOT is shown in Figure 1. All testing was conducted according to the method described in ASTM D3241. "Thermal Oxidation Stability of Aviation Turbine Fuels (JFTOT Procedure)". Aerated fuel, initially at ambient temperature, was passed at a rate of 0.05 mL/s over a heated aluminum tube and through a 17 micron filter. For breakpoint temperature determinations the stability of the fuel was determined by its propensity to lacquer the tube and block the filter during a 2.5-hour test. The color of the lacquer was assessed by visual comparison with an ASTM color chart. For visual tube ratings, the color of the lacquer produced was considered a failure if a rating of code 3 or greater was obtained. The pressure drop developed across the filter was considered a failure if it exceeded 25 mm Hg. Breakpoint temperatures were defined as the highest temperature at which the fuel passed the JFTOT test.

2.1.2 Configuration Of Fiber Optic Modified JFTOT

The fiber optic monitoring system was interfaced with the InterAv Research Model JFTOT. Configuration of the FOM-JFTOT is shown in Figure 2. The only hardware modification required was replacement of the standard heater tube test section with one on which fiber optic probes were mounted. The interior of the specially designed test section is circular, while the exterior is square. Threaded metal connectors for eight probes are welded to the exterior in a spiral arrangement along the length of the heater tube between stations 28 and 48 millimeters (mm). The ends of the probes are flush with the interior surface of the heater tube holder and are designed to be non-intrusive to the fuel flow. A cross section diagram of the heater tube holder is shown in Figure 3 (Reference 2). The probe positions correspond to the ASTM D3241 temperature profile for aluminum tubes and are shown in Table 1. Because the probes are located at positions of different temperature along the tube, the deposition rate at each of these temperatures can be determined from a single JFTOT run.

As shown in Figure 2, an electronics box (electro-optic module) contains both a source and a detector for each probe. Each probe consists of a fiber optic bundle containing seven fibers. The light from the source is transmitted through one fiber to the heater tube. The light reflected back from the heater tube and deposit surface is conducted back through the remaining six fibers to the photo detector. A Leading Edge computer receives and stores the data obtained during the run. An inverted plot of reflected light intensity (attenuation) versus time is continuously displayed on the monitor using a different color for each probe. Figure 4 is an example of the real time CRT display. Each minimum or maximum inflection point shown on the plot equates to a deposit thickness accumulation of 0.14 micron. A separate Hewlett Packard Vectra Series 9000 computer was used to perform all data analysis and plotting routines.

2.2 SOFTWARE

The Geo-Centers software consists of a data acquisition package and a data analysis package. The data acquisition software provides real time data collection and display and currently has allocated space for 600 data points per test. For example, 2 data points per minute would be taken for a test of 300-minute duration. The data analysis software package performs thickness calculations and plating routines for attenuation vs time, thickness vs time, and thickness vs tube position. The software permits printing tables of thickness vs time, probe number (therefore, position and temperature) vs total deposit, and

inflection point vs time.

2.3 THEORY

The application of fiber optics to a standard JFTOT for monitoring real time deposit formation is based on the principles of light interference or 'interferometry'. Changes in intensity of reflected light during film formation permits calculation of film thickness in microns. The thickness of the film is determined from the wavelength of the light and the number of cycles observed. The thickness measurement is corrected for the refractive index of the film and the angle at which the light passes through the film. The thickness of the film (d), in microns, is calculated using the following equation:

$$d = m\lambda / (2n \cos\phi)$$

where

m = number of reflected light cycles observed

(1 light cycle = 1 maximum plus 1 minimum inflection point)

λ = wavelength of light

n - refractive index of deposit = 1.6

ϕ = angle from the normal that light passes through the film = 6.9 degrees

($\cos 6.9 = 1$)

The light source used is a near infrared light emitting diode (LED) with a wavelength of 880 nanometers (nm). Geo-Centers measured the refractive indices of several jet and diesel fuel deposits and found that all those measured had refractive indices in a narrow band around 1.6. The wavelength of the light in the deposit is $880\text{nm} / 1.6 = 550\text{ nm}$, therefore, $1/4$ wavelength = $138\text{ nm} = 0.14\text{ microns}$, $1/2$ wavelength = 0.28 microns , $3/4$ wavelength = 0.42 microns , etc.

Figure 5 shows the theory upon which the FOM-JFTOT works: (1) Light from the source reflects off the front and back of the deposit and undergoes a phase change due to differences in the refractive indices of the deposit and the tube surface. (2) Wave 2 will emerge in or out of phase with Wave 1 depending on the distance Wave 2 travels through the film. (3) If Wave 2 emerges in phase with Wave 1, it will interfere constructively with Wave 1; if Wave 2 emerges out of phase with Wave 1, it will interfere destructively with Wave 1. (4) This interference effect results in changes in the intensity of the reflected light: constructive interference results in a maximum intensity of the reflected light, while destructive interference results in a minimum intensity of the reflected light. Figure 6 shows the effect of film thickness on reflected light.

2.4 TEST APPROACH

2.4.1 Test Fuels

Functional assessment of the FOM-JFTOT was conducted using three NAPC supplied fuels. The samples were identified as FF-3, a 470°F (243°C) breakpoint JP-5; NAPC 17, a 470°F (243°C) breakpoint diesel marine fuel; and FF-8, a 500°F (260°C) breakpoint JP-5. The FF-3 fuel had been used throughout much of NAPC's FOM-JFTOT development work. The fuels were reported to have been in outside storage for many months at the NAPC facility and subjected to severe temperature changes. Breakpoint temperatures were confirmed at P&W to determine if changes in thermal stability had occurred during the period of storage. P&W breakpoints agreed with those reported by NAPC.

2.4.2 FOM-JFTOT Test Conditions

With the exception of sample size, test duration, and tube rating technique, FOM-JFTOT tests were

performed according to the ASTM D3241 JFTOT procedure. Duplicate runs were performed on the three fuels at three different test temperatures to assess the effect of temperature and fuel quality on time to attain a 0.14 micron deposit thickness (first maximum inflection point). Test times were 300 and 960 minutes (5 hours and 16 hours, respectively). Test duration was dictated by the amount of time required to reach the first maximum inflection point.

2.4.3 Summary Of Test Matrix

		JFTOT <u>Break Point</u>
Fuels:	NAPC 17 (DFM)	470°F (243°C)
	FF-3 (JP-5)	470°F (243°C)
	FF-8 (JP-5)	500°F (260°C)
Test Temperature:	550, 500, 450°F (288, 260, 232°C)	
Test Duration (min):	300, 960	

SECTION 3.0

RESULTS AND DISCUSSION

3.1 ESTABLISHMENT OF HARDWARE MAINTENANCE PROCEDURE

Frequent, random, probe failures were experienced in a number of the early test runs. Probe failure resulted in a loss of data midway through a test. Of equal concern was loss of time required for test setup and execution. Additionally, there was a concern that replacement probe costs could prove to be prohibitive and detract from the feasibility of the FOM-JFTOT approach to thermal stability testing. Examination of the failed probes under a microscope revealed coke deposits on probe surfaces.

Removal of the coke was accomplished by applying a commercially available cleaner called "Micro Laboratory Cleaning Solution", manufactured by International Products Corporation, Trenton, N.J.. A 10% solution of the cleaner was applied with a cotton swab to the probe surface and allowed to soak for several minutes. Fresh cotton swabs were then used to remove the cleaning solution, apply a deionized water rinse, and dry the probe surface. Subsequent inspection of the probe surface under a microscope indicated whether repeating the procedure for further cleaning of the probe was necessary.

The careful, gentle, use of cotton swabs in the cleaning procedure was found to be important due to the fragility of the glass probe surfaces used for transmitting and receiving light. Implementation of the cleaning procedure restored the failed probes to good working order. Microscopic examination and cleaning of the probes at the conclusion of each FOM-JFTOT test was incorporated into the test method as a preventative maintenance procedure.

3.2 SOFTWARE LIMITATIONS AND IMPROVEMENTS

A number of improvements were made to the FOM-JFTOT system software to rectify significant limitations and errors identified during the collection and analysis of fiber optic data. Modifications to the acquisition program included storage of test data to disk as it is collected during the test run. Formerly, data was not stored on disk until the entire test had been completed. This resulted in a loss of

test data if momentary power interruptions were experienced. Further assessment of the software found that erroneous identification of inflection points (representing deposit accumulation) were resulting in incorrect calculations of deposit thickness. Modifications to the software, therefore, included establishment of appropriate limits for the computer identification of all valid inflection points. A subroutine was written to check for available disk space before initiating a test run and notify the operator if insufficient space as available. Prior to this modification, available disk space was incorrectly identified and resulted in a loss of data at the end of the test.

Figure 9 is a plot of deposit thickness vs time for probe 5. The data points represent actual data from a test performed at 550°F (288°C) on one of the test fuels. The Geo-Centers software drew a straight line between two points consisting of zero thickness at zero minutes and total deposit thickness at the end of the test. Because the validity of this line was suspected, a routine was incorporated into the data analysis software to permit plotting of a best fit line derived from all maximum and minimum inflection points. Figure 9 shows the least squares linear curve fit, the Geo-Centers line, and a polynomial curve fit. A comparison of these lines indicate that deposit accumulation as a function of time for each probe would be best represented using a first or second order polynomial curve fit. Additionally, routines were written for the generation of Arrhenius plots and the calculation of activation energies and FOM-JFTOT breakpoints.

3.3 EVALUATION OF NAVY FUELS

3.3.1 FOM-JFTOT Data

In the assessment of the FOM-JFTOT and evaluation of the Navy fuels, only data generated at heater tube positions represented by probes 1 through 5 (located at the hot spot and upstream of the hot spot) were considered. Data generated at probes 6, 7, and 8 (tube positions downstream of the hot spot) did not correlate well with data generated at probes 1 through 5. As shown in Figure 8, significantly greater deposits were generated downstream of the hot spot than at equivalent temperatures upstream of the hot spot. This may be attributed to prestressing the fuel during exposure to the temperature gradient in the region of the fuel inlet to the heater tube hot spot. Another possible cause for greater deposits downstream of the hot spot is the formation of decomposition products that are soluble in the fuel at the hot spot temperature but become insoluble at cooler temperatures downstream of the hot spot.

Data generated on the three NAPC supplied fuels, FF-3 (JP-5, NAPC 17 (DFM), and FF-8 (JP-5), are shown in Tables 2,3 and 4, respectively. The Tables represent FOM-JFTOT runs performed at test temperatures of 550°F (288°C), 500°F (260°C), and 450°F (232°C). Time to achieve the first maximum inflection point, i.e. the accumulation of a 0.14 micron deposit thickness, is shown in minutes for each of the 5 probe positions. Each probe position represents a different temperature according to the ASTM D3241 temperature profile for aluminum tubes.

Times to first maximum inflection point shown in these tables were identified by the computer software. In some cases, no data was obtained for a particular probe because the probe failed during the test. In other instances, depending on the thermal stability properties of a fuel, there was insufficient temperature at a particular probe location, or insufficient time at that temperature, to achieve a 0.14 micron deposit build up.

Tests performed on FF-3 at 550°F and 500°F were conducted over a 5-hour period. As shown in Table 2, at a test temperature of 500°F (260°C) probes 1 and 2 were at insufficient temperature to achieve a 0.14 micron deposit thickness in five hours. Runs performed on FF-3 at a test temperature of 450°F (232°C) were conducted over a 16-hour period. The longer test duration was necessary because of slower deposit formation at low temperatures. At 450°F (232°C), a 0.14 micron deposit thickness was only attainable at probe 5 (the hot spot temperature). A longer test would have resulted in 0.14 micron deposit thickness at the lower probe temperatures.

In Table 3, the test performed on FF-8 at 550°F (288°C) was conducted over a 5-hour period. Because FF-8 was a higher thermal stability fuel than FF-3, a 16-hour test was necessary at 500°F (460°C) to produce deposit thicknesses of 0.14 microns for probes 1 through 5 at the lower probe temperatures. A test performed at 450°F was not attempted because of the length of time that would be required to form sufficient deposits to measure.

3.3.2 Effect Of Fuel Quality And Temperature On Deposition Rate

A summary of the data for the three test fuels, along with test temperatures and test times is shown in Table 5. The summary is based on time to accumulate 0.14 micron deposit at probe 5 (the hot spot). The rate deposition to first maximum was compared to rate of deposition over the entire test period. Because of the limited amount of data, no trends were evident to evaluate the effects of metal surface passivation or initial deposit formation on subsequent deposition rates. Table 5 was used to assess the effect of fuel quality and temperature on deposition rate and total deposit formed over the 5-hour and 16-hour test periods. The FOM-JFTOT was able to quantitatively discriminate between fuels of varying quality as defined by known thermal stability JFTOT breakpoint values. Differentiation between fuels was evident at all test temperatures: the lower the JFTOT breakpoint, the less time required to achieve a first max (0.14 micron deposit thickness).

The effect of temperature was easily discernible: as temperature increased the rate of deposition increased, as did the total deposit formed over the total test period. It is interesting to note that the effect of temperature on the rates of deposition for FF-3 and FF-8 was considerably less than that for NAPC 17. Based on time to first max, an increase in temperature from 500°F (260°C) to 550°F (288°C) increased the rate of deposition for FF-8 and FF-3 by a factor of 3 to 4.5, while NAPC 17 increased by a factor of 11.

3.3.3 Repeatability And Reproducibility

A total of five tests were performed on FF-3 at 550°F (288°C) to make a preliminary assessment of the repeatability of the measurements. Repeatability was good as shown by the time required to reach the first maximum for probe 5 in Table 6. The deposit rates were essentially the same for all five tests. As shown in Table 7, excellent agreement was shown between the NAPC and the P&W laboratory analyses of FF-3 at 550°F (288°C). This table compares the average result from five test runs performed on FF-3 at P&W to that of a single run performed at NAPC.

3.3.4 Activation Energy And Fiber Optic Breakpoint Temperature

Using the P&W FOM-JFTOT software, Arrhenius plots were generated and activation energies calculated for the NAPC supplied fuels. Calculation of activation energy was based on the Arrhenius equation:

$$(1) \quad k = Ae^{(-E/RT)}$$

where

A = Preexponential factor

R = Universal gas constant (0.001987 kcal/mole Kelvin)

E = Activation energy

$$(2) \quad \ln k = -E/RT + \ln A \quad \text{(Equation of the line: } y = mx + b\text{)}$$

$$(3) \quad \text{slope (m)} = -E/R$$

$$(4) \quad E = \text{slope} / 1.8 \times R$$

where 1.8 converts the slope from Rankine to Kelvin. E is kcal/mole.

The software plots the FOM-JFTOT data in the form of the log of the reciprocal of time to achieve 0.14 micron deposit on the y axis versus the reciprocal of temperature in degrees Rankine on the x axis. For convenience, degrees F are shown on the x axis of the plots even though scaling and calculations were performed in degrees Rankine. This was done for ease of relating to the temperatures at which the tests were performed. The software performs a least squares linear curve fit of the data and determines the slope of the line. Activation energy (E) is then calculated using equation (4).

Fiber Optic Breakpoint temperature (FOBP) was calculated for each of the Navy fuels. The concept of FOBP temperature provided a unique method for rating the thermal stability properties of the test fuels. FOBP temperature is defined as the temperature required to achieve a first max (0.14 deposit thickness) in 150 minutes. FOBP is based on quantitative data derived from the Arrhenius equation instead of a visual rating system such as described in ASTM D3241 JFTOT procedure. A FOBP can be obtained in a single run whereas a standard JFTOT breakpoint requires four to six tests in order to define breakpoint to within 10°F. Figure 7 shows how the FOBP can be determined from an Arrhenius plot. FOBP temperature can be calculated using a derivation of the Arrhenius equation:

$$\text{FOBP Temperature (°F)} = (\text{absolute value of the slope} / 5.01 + b) - 460$$

where

5.01 = absolute value of $\ln 1/150$ minutes

b = y intercept

-460 = converts degrees Rankine to °F (°F = R - 460)

FOBP temperatures for the three test fuels are shown in Table 8 along with standard JFTOT breakpoints. FOBPs were found to be very repeatable and ranked the fuels in the same order as the JFTOT breakpoints. FOBP discriminated between the two 470°F (243°C) JFTOT breakpoint fuels. The higher breakpoint temperatures measured by the FOM-JFTOT are probably a result of the fact that 0.14 micron deposit corresponds to a thicker deposit than required to give a visual rating of greater than 3. NAPC has done work which shows that there is a correlation between FOBP and JFTOT breakpoint. More fuels need to be characterized to establish this correlation.

3.3.5 Arrhenius Plots

Among the criteria used to assess the FOM-JFTOT were linearity and repeatability of data from tests performed at different temperatures. This is important in accurately determining the rate of deposit formation as well as in calculating activation energies and FOBP temperatures, since they are all dependent on the slope of the best fit line through these data. Figure 10 is an Arrhenius plot of data obtained from tests conducted at 550°F (288°C) for 5-hours, 500°F (260°C) for 5 hours, and 450°F (232°C) for 16 hours on the FF-3 JP-5 fuel sample. Figure 11 is a similar plot for the FF-8 JP-5 sample showing plotted data from runs performed at 550°F (288°C) for 5 hours and 500°F (260°C) for 16 hours. Data at 450°F (232°C) was not obtainable over a 16-hour test duration due to the higher thermal stability properties of the FF-8 sample. An Arrhenius plot for data generated on the NAPC 17 sample at 550°F (288°C), 500°F (260°C), and 450°F (232°C) is shown in Figure 12.

In Figure 10, the best fit line, with a correlation coefficient of 0.9967, showed an excellent fit for data from three separate tests and from probes positioned at different temperatures along the heater tube. This

plot is comprised of five data points from the 550°F (288°C) test, three points from the 500°F (260°C) test, and one point from the 450°F (232°C) test. Only one of the five probes from the 450°F (232°C) test (the one located at the hot spot) had achieved a 0.14 micron deposit thickness at the end of the 5-hour test. The probes in this test located upstream of the hot spot were at insufficient temperatures to form deposits within the allotted test time. Similarly, only three probes produced 0.14 micron deposit thickness during the 5-hour test at 500°F (260°C). At 550°F (288°C), all five probes were at sufficient temperatures for form deposits within the allotted test period. Figure 10 shows the rate of deposit as linear from 450°F (232°C) to 550°F (288°C) for the JP-5 fuel. Figure 12, on the other hand, appears to indicate a rate change occurs between 550°F (260°C) and 550°F (288°C) for the NAPC 17 diesel fuel.

Figures 13 and 14, respectively, are Arrhenius plots of all data points produced from five replicate runs performed on FF-3 and two replicate runs on NAPC 17 at a test temperature of 550°F (288°C). The plots shows not only the repeatability of the FOM-JFTOT as a system for monitoring real time deposit accumulation but also the ability of the JFTOT to repeat the mechanism of deposit formation. Each of the FF-3 replicate runs were plotted separately in Figure 15 to determine variability in slope and the observed effect on activation energies and FOBP. The data from the replicate runs were extrapolated considerably beyond the narrow range at which they were measured. This was done on the assumption that Figure 10 was correct in depicting the rate of deposit as linear from 450°F (232°C) to 550°F (288°C). While variation in activation energy was noted, the FOBP for the five replicate runs were shown to agree within 7 degrees F.

The Arrhenius plot shown in Figure 16, used FOM-JFTOT data to compare the thermal stability properties of the three Navy fuels. The plot was generated from tests conducted at 550°F (288°C), 500°F (260°C), and 450°F (232°C). The FOM-JFTOT provided data consistent with the Arrhenius theory and the known thermal stability history of the fuel samples. the lower JFTOT breakpoint fuels, FF-3 and NAPC 17, showed significantly greater deposition rates than did the higher thermal stability FF-8 JP-5 fuel. As temperature increased, the time required to accumulate a 0.14 micron deposit thickness decreased. The FOBP temperatures ranked the three fuels in good agreement with that of the JFTOT breakpoint temperatures. The FOM-JFTOT data discriminated between the two different 470°F JFTOT breakpoint fuels; NAPC 17, a diesel marine fuel; and FF-3, and JP-5 fuel. FF-8, the most thermally stable of the three fuels, was shown to have the lowest activation energy, at 25 kilocalories per mole (kcal/mole). The lower thermal stability fuels, FF-3 and NAPC 17, exhibited activation energies of 30 and 33 kcal/mole, respectively.

3.3.6 Trace Interpretation

The following paragraphs discuss the effect of time and temperature on the traces used to monitor and quantify real time deposit formation. Discussion is directed at those traces selected as representative of the runs performed on FF-8 and FF-3. FF-8 demonstrated the higher thermal stability of the three Navy fuels with a JFTOT breakpoint temperature of 500°F (260°C), while FF-3 and NAPC 17 had equivalent JFTOT breakpoints of 470°F (243°C). Figures 17, 18, and 19 represent three separate tests performed on FF-3 at 550°F (288°C), 500°F (260°C), and 450°F (232°C), respectively. These figures show the effect of time and temperature on deposit formation as interpreted by the FOM-JFTOT traces. In Figure 17, the attenuation versus time trace shows well defined inflection point for all eight probes positioned along the heater tube. The temperature at each probe position is shown to the right of the plot. Each maximum and minimum inflection point represents 0.14 micron deposit thickness. These are additive such that counting the inflection points yield the total deposit accumulation over the total test time. The general upward slope of the lines indicates that the deposit is absorbing a small amount of light with time.

The time to first maximum inflection point (0.14 micron deposit) data used in generating the Arrhenius plots were a direct consequence of the data available from these traces. Probes yielding meaningful data were those which were at sufficient temperature to produce a well defined first maximum inflection point (0.14 micron deposit thickness) within the allotted test period. At a test temperature of 550°F (288°C),

all probes were at sufficient temperatures to cause between three to thirteen inflection points, depending on the specific location of the probe. As shown by the trace, the higher the probe temperature, the more numerous the inflection points and the greater the overall deposit thickness at the conclusion of the test. Since the three probes downstream of the hot spot were not used in the analysis of the Navy fuels, five data points were available for use in the Arrhenius plots.

As shown in Figure 18, the lower test temperature resulted in lower probes temperatures upstream of the hot spot. At these lower temperatures, the entire 5-hour test period was required to achieve a 0.14 micron deposit thickness (first maximum) at probe numbers 3, 4, and 5. Based on the thermal stability properties of FF-3, probe numbers 1, 2, and 3 were at insufficient temperatures to attain 0.14 micron deposit within the 5-hour test. Because the sensitivity limit of the FOM-JFTOT detection system is 0.14 microns, probes 1, 2, and 3 would have required additional test time to achieve a first maximum inflection point. A 16-hour test at 500°F would have produced two to three inflection points at these probes. Three data points, those yielded by probes 3, 4, and 5, were obtained from this trace for use in the Arrhenius plots.

The continued reduction in amplitude of the inflection points with decreasing temperature is shown in Figure 19. This test performed on FF-3 at 450°F (232°C) produced usable data only at the hot spot (probe 5). All probes upstream of the hot spot were at insufficient temperature to form a minimum 0.14 micron deposit thickness within a 16-hour test period.

Traces representative of those produced during tests performed on FF-8 at 550°F (280°C) for 5 hours and 500°F (260°C) for 16 hours are shown in Figures 20 and 21. Because of the higher thermal stability properties of FF-8, no data was obtainable at a test temperature of 450°F (232°C) at the end of a 16-hour run. FF-8 would have required a test time well beyond 16 hours to achieve a deposit thickness of 0.14 microns.

3.4 EVALUATION OF A P&W JP-5

During the course of this investigation, NAPC reported a significant limitation of the FOM-JFTOT. While the FOM-JFTOT had been used successfully at NAPC to characterize poor thermal stability fuels, critical problems were encountered when attempting to characterize fuels exhibiting good thermal stability.

At P&W, a typical JP-5 fuel with a JFTOT breakpoint temperature of 530°F (277°C) was selected for evaluation to confirm the NAPC findings. A FOM-JFTOT run was performed on the P&W JP-5 at 550°F (280°C) for 5 hours. The resulting trace, shown in Figure 22, indicated deposit formation only at probe number 8, downstream of the hot spot. Inspection of the heater tube revealed a nonuniform, narrow band of deposit of approximately 17 millimeters (mm) in width. Three deposit-free, shiny-aluminum, zones ran through the length of the deposit. The onset of deposit occurred 40 mm up from the inlet end of the heater tube. This was downstream of probes 1 through 5 and as such the trace correctly identified no deposit at those positions. Probe 6, 7, and 8 were located at stations which should have detected deposit formation. As shown in Figure 22, probe number 8 indicated the presence of deposit, while probes 6 and 7 did not. It is possible, however, that due to the nonuniformity of deposit around the circumference of the heater tube, probes 6 and 7 were located in regions where no deposit was formed.

A second test was performed on the P&W JP-5 to determine if an increase in test temperature would result in a wider deposit band to permit detection by probe number 5 located at the hot spot. This test was conducted at 575°F (302°C) for 5 hours. The attenuation vs time trace which resulted from this test is shown in Figure 23. The deposit band increased, moving in the direction of the fuel inlet, such that the lower band of the deposit was in the region where probe 5 is located. However, the same nonuniformity of deposit formation around the circumference of the heater tube was experienced as in the former test conducted at 550°F (288°C). The FOM-JFTOT trace resulted in an erratic plot of attenuation vs time. No meaningful data could be realized from any of the probes monitored.

Figure 24 is a photograph of the heater tubes from the tests performed on the P&W JP-5 fuel at 550°F (288°C) and 575°F (302°C). Also shown is a typical heater tube from tests performed on the three Navy fuels. It was suspected that the FO probes and special test section contributed to the nonuniform deposit by creating eddies within the laminar fuel flow through the test housing. Heat transfer would be effected resulting in an unequal distribution of temperature around the circumference of the heater tube. This effect would be more apparent on thermally stable fuels, laying down thin films, than it would on poorer thermal stability fuels which produce heavy deposit layers. A subsequent test on the same fuel, using a standard JFTOT test section with no probes, produced a similar nonuniform deposit.

SECTION 4.0

CONCLUSIONS AND RECOMMENDATIONS

4.1 STRENGTHS AND POTENTIAL

- The FOM-JFTOT represents a significant step forward in bridging the gap between qualitative go-no go type JFTOT tests and quantitative JFTOT data that can be used to characterize fuels and generate real time rate data. If successfully developed, the FOM-JFTOT could provide a means for getting the most out of the data available from a standard accepted test method. It would provide an inexpensive, short-term test that could be used to evaluate research quantities of fuel as well as qualify fuel system additives. After evaluation and selection of the most promising fuel/additive candidates, the more costly fuel system simulators, requiring hundreds or thousands of gallons of fuel, could be employed.
- The concept of FOBP provides a quantitative approach to ranking the thermal stability properties of jet fuels, eliminating much of the subjectivity associated with visual JFTOT breakpoint determinations. Because FOBP temperature can be obtained in a single run, the approach is significantly less labor intensive than JFTOT breakpoint determinations which required four to six runs. FOBP temperatures were shown to be very repeatable.
- In the evaluation of three Navy supplied fuels, the FOM-JFTOT was successfully used to assess the effect of temperature and fuel quality on time to accumulate a 0.14 micron deposit thickness. The FOM-JFTOT was able to discriminate quantitatively between the fuels which varied in quality as defined by known thermal stability JFTOT breakpoint values.
- Repeatability of the FOM-JFTOT data, within the P&W laboratory, and reproducibility between the NAPC and P&W laboratories was found to be excellent.
- Arrhenius plots generated from the FOM-JFTOT data were consistent with the known thermal stability properties of the test fuels. The lower JFTOT breakpoint fuels showed significantly greater deposition rates than did the higher thermal stability fuel. As temperature increased, the time required to accumulate a 0.14 micron deposit thickness decreased. Slopes, activation energies, and FOBP temperatures derived from the Arrhenius equation, ranked the three fuels in good agreement with that of the JFTOT breakpoint temperatures.

4.2 LIMITATIONS

- Sensitivity is limited to 0.14 micron deposit thickness. Due to the light source and detectors used, only deposits equating to a JFTOT visual code of 4 or greater can be characterized. This limitation severely restricts the usefulness of the FOM-JFTOT. The FOM-JFTOT is restricted to fuels and test

conditions which are conducive to deposit formation, i.e., poor thermal stability fuels and optimum test temperatures.

- A good thermal stability P&W JP-5 fuel tested at 550°F (288°C) and 575°F (302°C) produced a nonuniform deposit around the circumference of the heater tube. It is suspected that other thermally stable fuels may exhibit a similar anomaly.

4.3 DEVELOPMENT NEEDS

This investigation focused on assessing the merit of the FOM-JFTOT system of measurement with little effort directed at method development, other than resolving some immediate software problems and probe durability problems. Development efforts should be prioritized into modifying the FOM-JFTOT system to measure thinner tube deposits (0.07 microns) to permit characterization of more thermally stable fuels, and investigating the cause of nonuniform deposit bands.

REFERENCES

1. Kamin, R. A., "Fiber Optic Modified JFTOT Test Program," Presented at the Coordinating Research Council Oxidation Stability of Gas Turbine Fuels Group, Dayton, Ohio, April 23, 1987.
2. Darrah, S. D., "Development of New Optical Methods of Tube Deposit Rating in JFTOT Procedure," Presented at the Coordinating Research Council Aviation Committee Panel on Tube Deposit Rating Techniques, Dayton, Ohio, April 23, 1987.

JET FUEL THERMAL OXIDATION TESTER

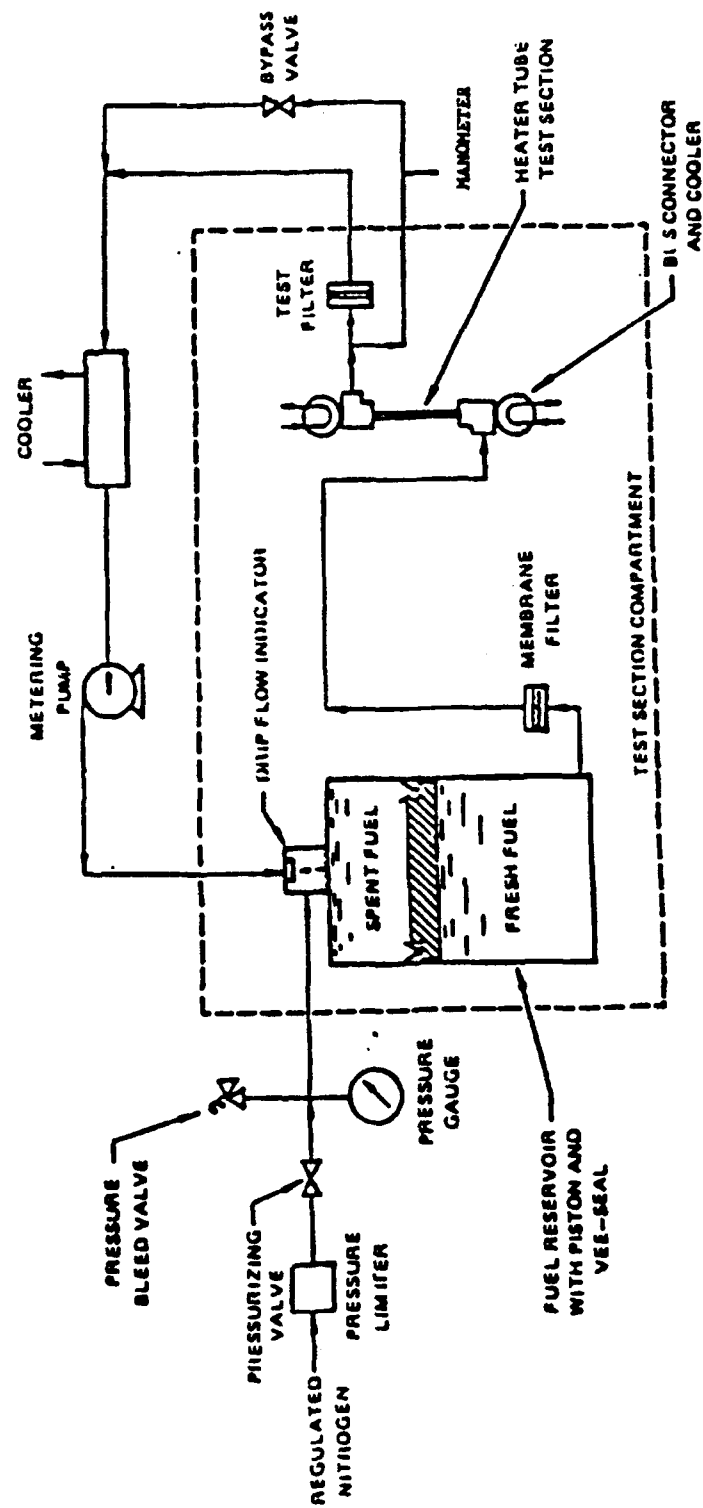
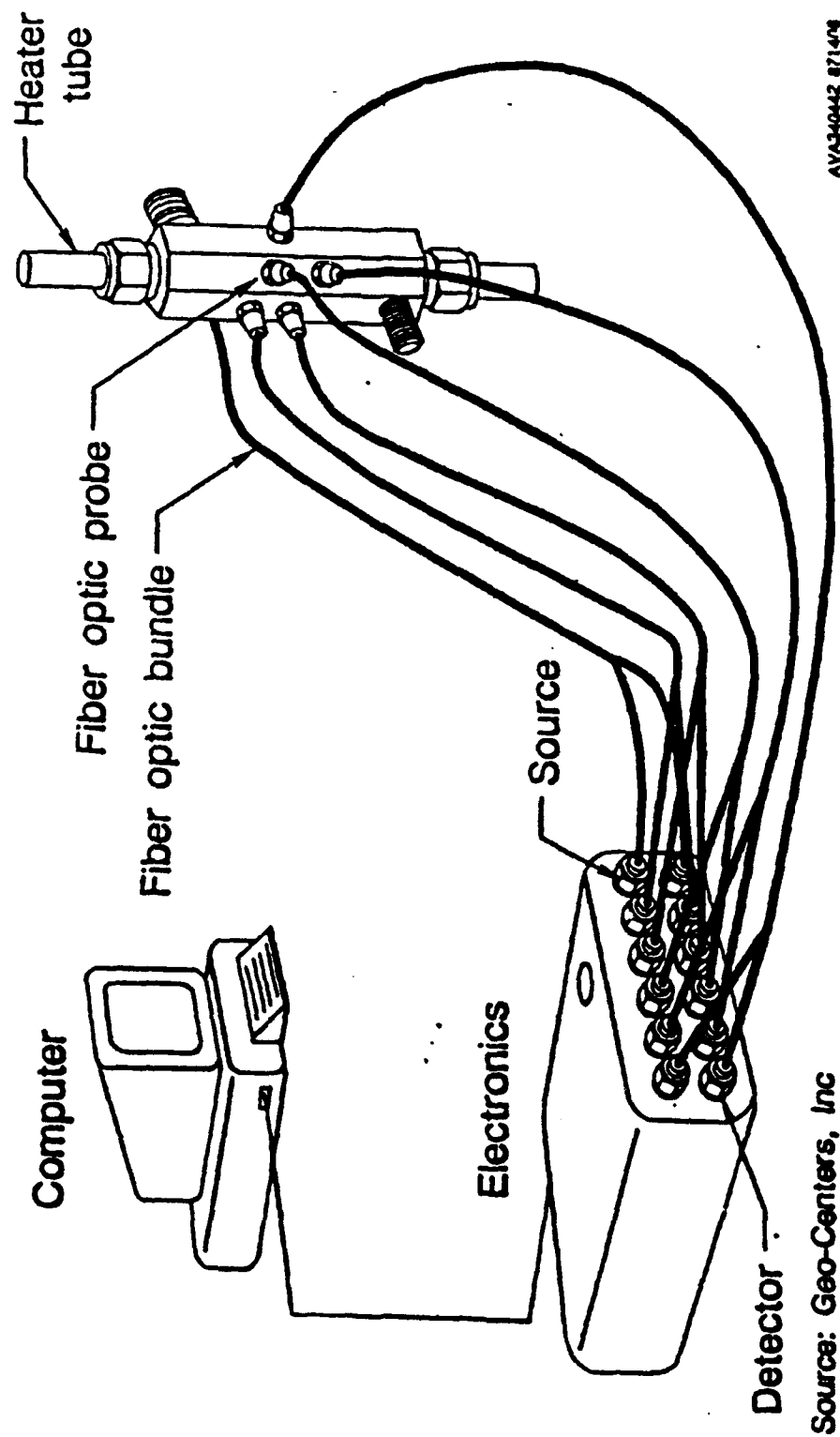


Figure 1. Jet Fuel Thermal Oxidation Tester

CONFIGURATION OF FIBER OPTIC JFTOT



AVA3-0442 871408

Figure 2. Configuration of Fiber Optic JFTOT

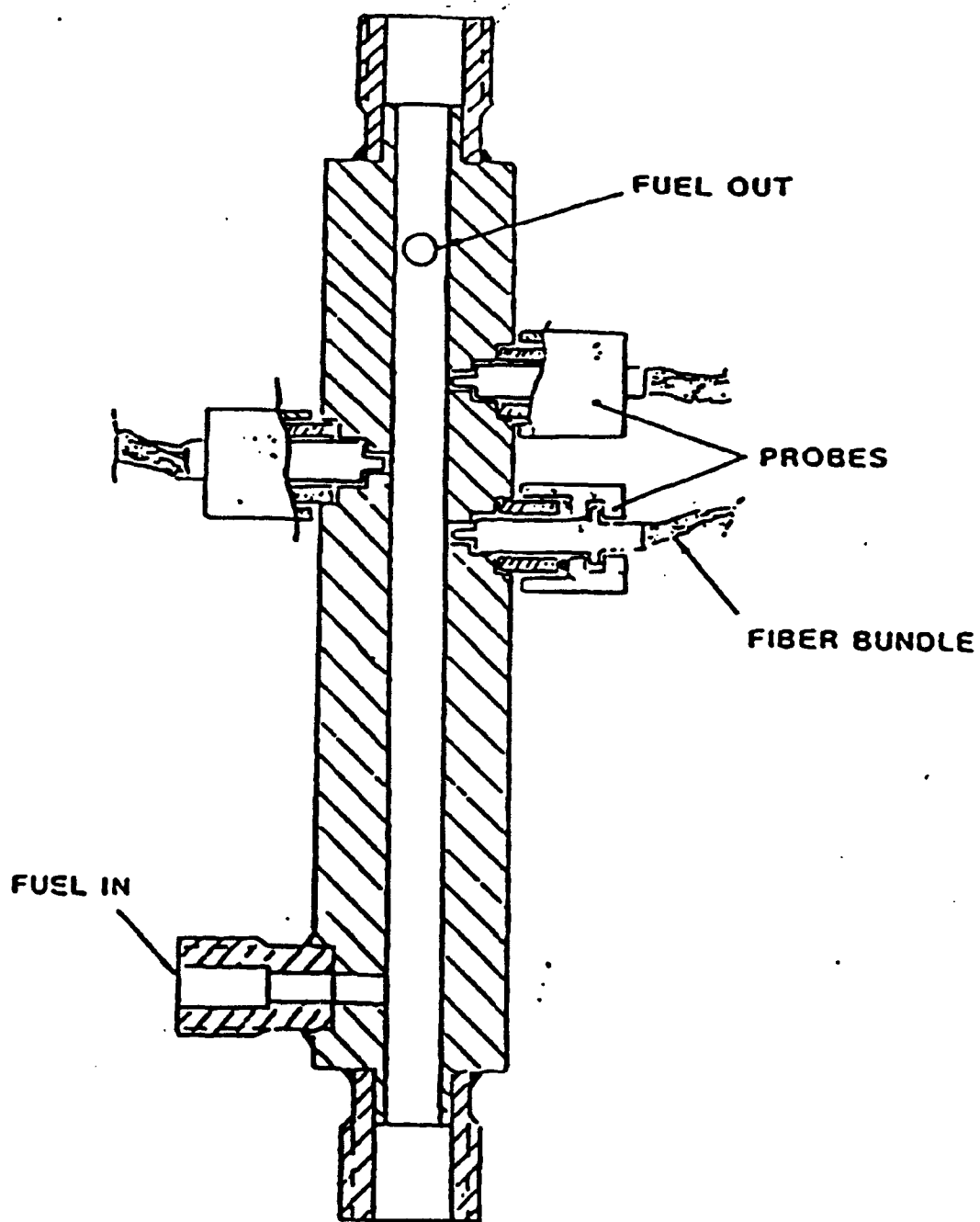


Figure 3. Cross Section of FOM-JFTOT Heater Tube

TABLE I
TEMPERATURE PROFILE OF ALUMINUM TUBES
CORRESPONDING TO FOM-JFTOT PROBES

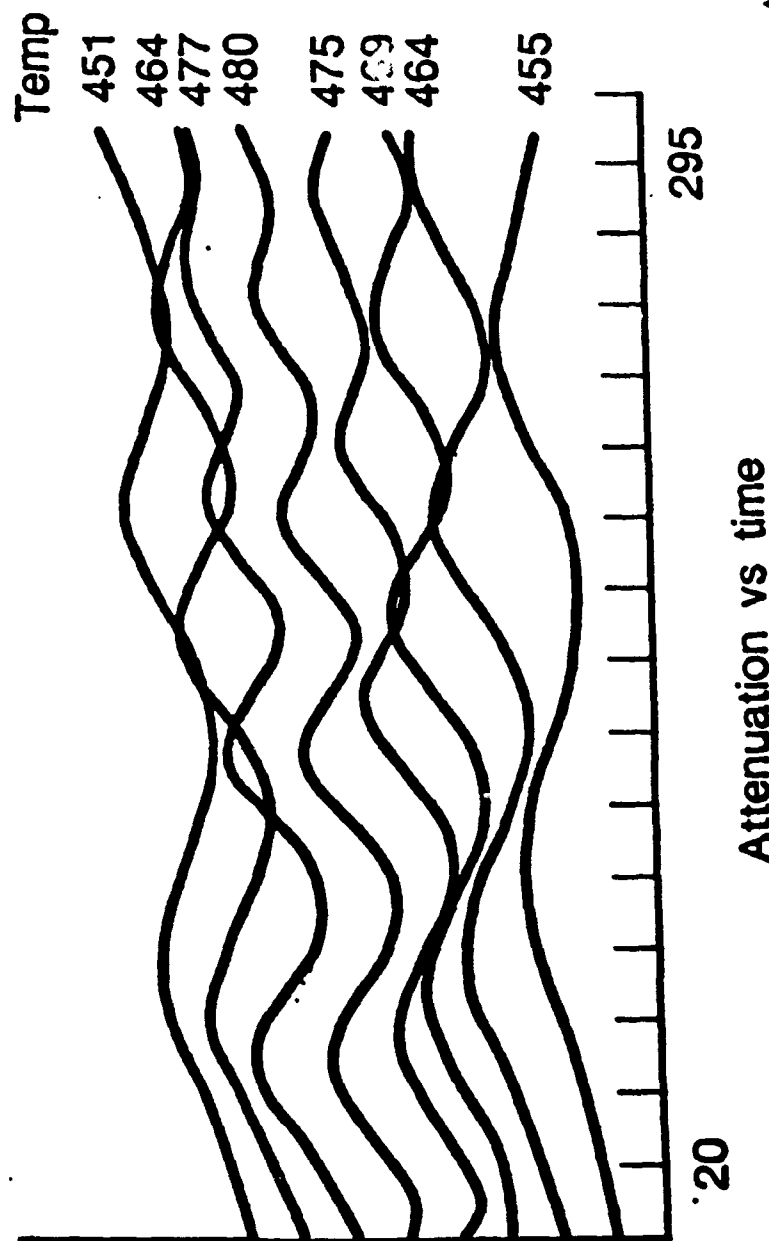
TEST TEMPERATURES, C(F)

PROBE NO.	PROBE POSITION(mm)	232(450)	260(500)	274(525)	288(550)	302(575)	316(600)
1	28	219(426)	246(475)	259(498)	272(522)	285(545)	298(568)
2	30	223(433)	250(482)	263(505)	277(531)	290(554)	303(577)
3	32	227(441)	254(489)	267(513)	281(538)	295(563)	308(588)
4	34	229(444)	257(495)	270(518)	284(543)	298(568)	312(594)
5	39	232(450)	260(500)	274(525)	288(550)	302(575)	316(600)
6	42	230(446)	258(496)	272(522)	286(547)	300(572)	314(597)
7	46	223(433)	250(482)	264(507)	277(531)	291(556)	305(581)
8	48	217(423)	244(471)	257(495)	270(518)	284(543)	297(567)

NOTE: TEMPERATURE PROFILES ARE FROM ASTM D3241, TABLE A4.1

REAL TIME CRT DISPLAY FOR FIBER OPTIC JFTOT

Displays attenuation (opposite of reflected light intensity)



AVA342414 87140

Figure 4. Real Time CRT Display For Fiber Optic JFTOT

FIBER OPTIC JFTOT THEORY

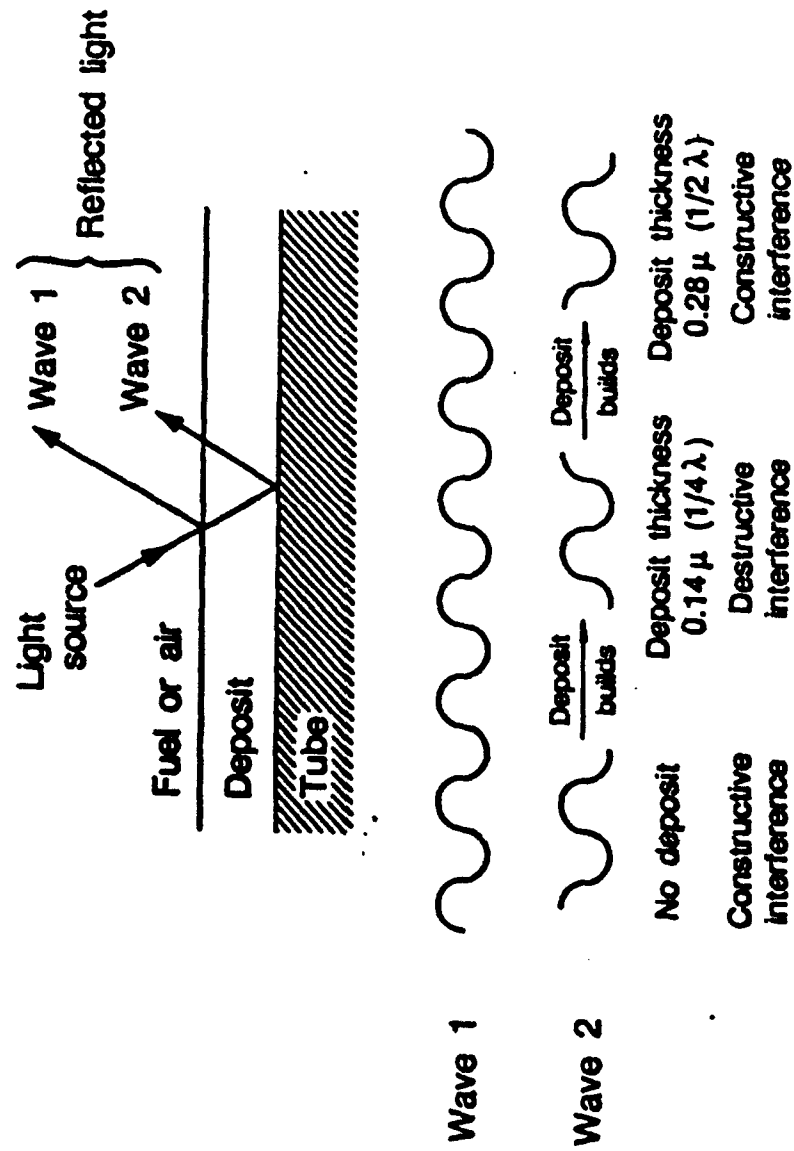


Figure 5. Fiber Optic JFTOT Theory

FIBER OPTIC JFTOT

Effect of film thickness on reflected light

Film thickness - μ	Relationship of 2 light waves	Interference of light waves	Effect on reflected light
0	In phase	Constructive	Maximum intensity
$0 < d < 0.14$	Out of phase	Destructive	Decreasing intensity
0.14	$\frac{1}{2} \lambda$ Out of phase	Completely destructive	Minimum intensity
$0.14 < d < 0.28$	Out of phase	Constructive	Increasing intensity
0.28	In phase	Constructive	Maximum intensity

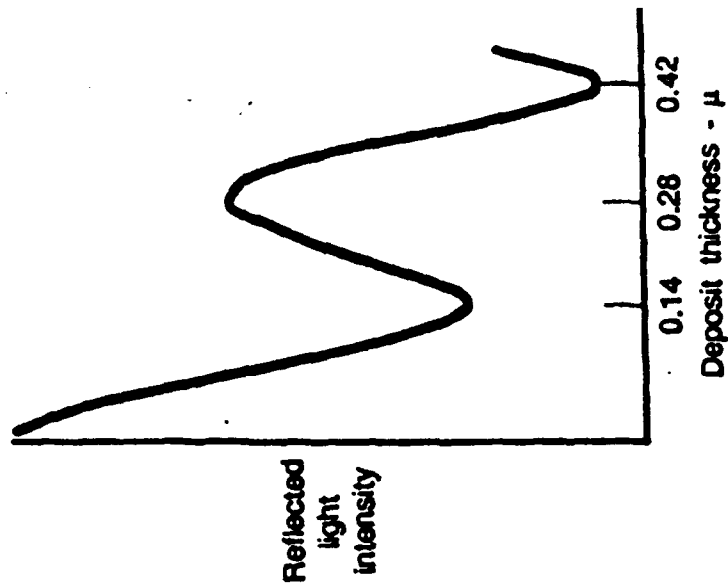


Figure 6. Effect of Film Thickness On Reflected Light

LINEARITY OF DEPOSIT RATE

Software interpretation

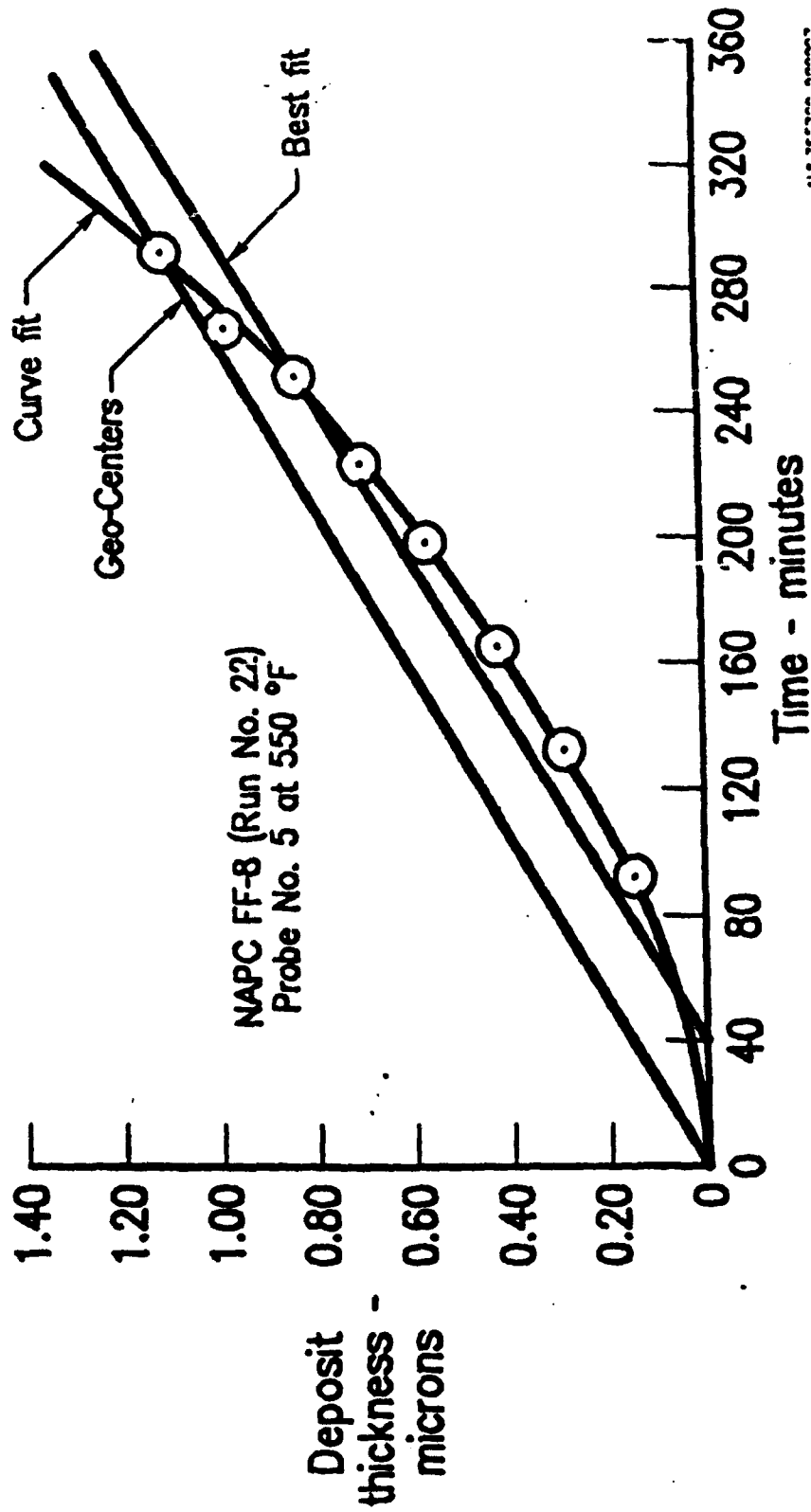


Figure 7. Linearity of Deposit Rate

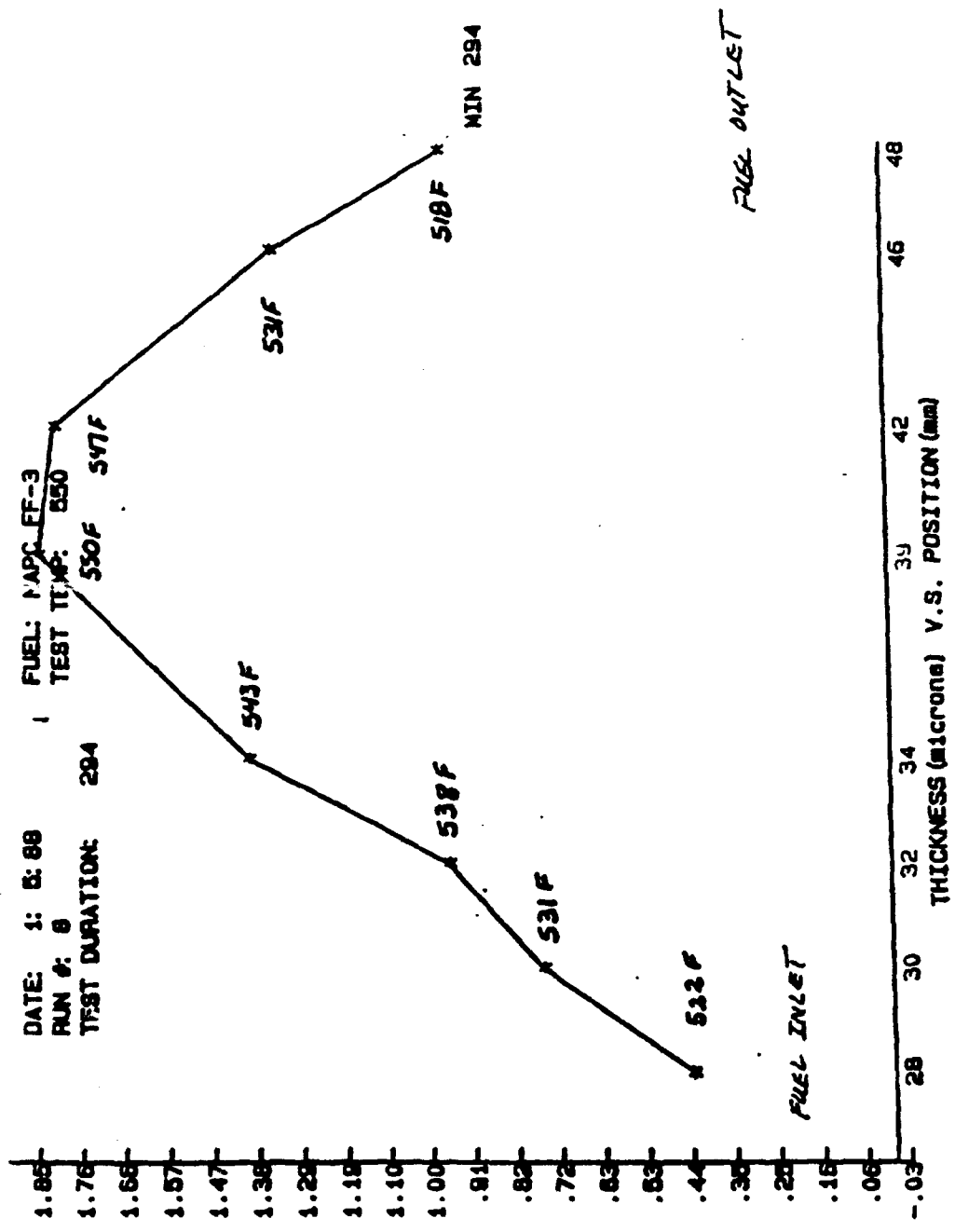


Figure 8. Thickness vs Tube Position for NAPC FF-3

TABLE 2
FF-3 JP-5 (470°F BP) TEST DATA - ALL RUNS

TIME TO ACHIEVE 1ST MAX (0.14μ DEPOSIT)

TEST TEMP (F)	PROBE NO.	POS. (mm)	TUBE TEMP (F)	MINUTES				
				RUN NO. 8	RUN NO. 9	RUN NO. 10	RUN NO. 11	RUN NO. 13
550	1	28	522	107.5	100.0	92.5	-	105.0
	2	30	531	71.0	63.0	64.0	74.5	70.5
	3	32	538	61.5	52.0	-	53.5	50.5
	4	34	543	44.0	37.0	46.5	45.5	47.5
	5	39	550	38.0	32.5	37.5	40.5	38.5
500	1	28	475	RUN NO. 15 -	RUN NO. 16 -			
	2	30	482	-	-			
	3	32	489	245.0	240.0			
	4	34	495	203.0	-			
	5	39	500	171.0	156.0			
450	1	28	426	RUN NO. 27 -	RUN NO. 28 -			
	2	30	433	-	-			
	3	32	441	-	-			
	4	34	444	-	-			
	5	39	450	763.3	713.3			

TABLE 3
NAPC 17 DFM (470°F BP) TEST DATA - ALL RUNS

TIME TO ACHIEVE ISI MAX (0.14μ DEPOSIT)

TEST TEMP (F)	PROBE NO.	POS. (mm)	TUBE TEMP (F)	MINUTES		
				RUN NO. 17	RUN NO. 18	
550	1	28	522	111.5	128.5	
	2	30	531	54.5	69.0	
	3	32	538	42.0	50.5	
	4	34	543	29.0	22.0	
	5	39	550	15.5	11.5	
				RUN NO. 19	RUN NO. 23	RUN NO. 24
500	1	28	475	-	-	-
	2	30	482	-	-	-
	3	32	489	-	-	-
	4	34	495	-	-	-
	5	39	500	-	142.0	149
				RUN NO. 25	RUN NO. 26	
450	1	28	428	-	-	
	2	30	433	-	-	
	3	32	441	-	-	
	4	34	444	-	-	
	5	39	450	645.0	555.0	

TABLE 4
FF-8 JP-5 (500°F BP) TEST DATA - ALL RUNS

TIME TO ACHIEVE 1ST MAX (0.14μ DEPOSIT)

TEST TEMP (F)	PROBE NO.	POS. (mm)	TUBE TEMP (F)	MINUTES	
				RUN NO. 20	RUN NO. 22
550	1	28	522	239.5	262.0
	2	30	531	183.5	200.5
	3	32	538	161.0	-
	4	34	543	121.0	120.5
	5	39	550	92.0	93.5
500				RUN NO. 29	RUN NO. 30
	1	28	475	676.7	600.3
	2	30	482	576.7	460.0
	3	32	489	453.3	445.0
	4	34	495	356.7	410.3
	5	39	500	310.3	276.7

TABLE 5
SUMMARY OF FIBER OPTIC JFTOT TEST RESULTS

FIBER OPTIC JFTOT - TEST RESULTS

SUMMARY

<u>Fuel Description</u>	<u>No. of runs</u>	<u>Test temp (F)</u>	<u>Break point temp (F)</u>	<u>Time to 1st max (min)</u>	<u>Rate of deposit 1st max (10⁻³ u/min)</u>	<u>Rate of deposit overall (10⁻³ u/min)</u>	<u>Total deposit test (u)</u>
Test duration: 300 minutes (5 hours)							
NAPC 17 (DFM)	2	550	470	13.5	11.0	5.4	1.62
FF-3 (JP-5)	5	550	470	37.5	3.8	6.1	1.84
FF-8 (JP-5)	2	550	500	92.8	1.5	3.6	1.08
NAPC 17 (DFM)	2	500	470	145.8	0.96	0.96	0.286
FF-3 (JP-5)	2	500	470	163.5	0.86	0.85	0.256
Test duration: 960 minutes (16 hours)							
FF-8 (JP-5)	2	500	500	297.5	0.48	0.92	0.890
NAPC 17 (DFM)	2	450	470	600.0	0.24	0.24	0.225
FF-3 (JP-5)	2	450	470	738.3	0.19	0.20	0.185

TABLE 6
REPEATABILITY OF FIBER OPTIC JFTOT TEST RESULTS

FIBER OPTIC JFTOT - TEST RESULTS
 Repeatability
 Test temperature: 550F
 Test duration: 300 minutes (5 hr)

<u>Fuel description</u>	<u>Run No.</u>	<u>Time to 1st max (min)</u>	<u>Rate of deposit 1st max (10⁻³ u/min)</u>	<u>Rate of deposit overall (10⁻³ u/min)</u>	<u>Total deposit test (u)</u>
FF-3	8	38.5	3.6	6.3	1.89
	9	32.5	4.3	6.1	1.84
	10	37.5	3.7	5.9	1.78
	11	40.5	3.5	5.8	1.75
	13	38.5	3.6	6.5	1.95

TABLE 7
REPRODUCIBILITY OF FIBER OPTIC JFTOT TEST RESULTS

FIBER OPTIC JFTOT - TEST RESULTS

Reproducibility

Fuel description: FE-3/JP-5 (470F BP)

Test temperature: 550F

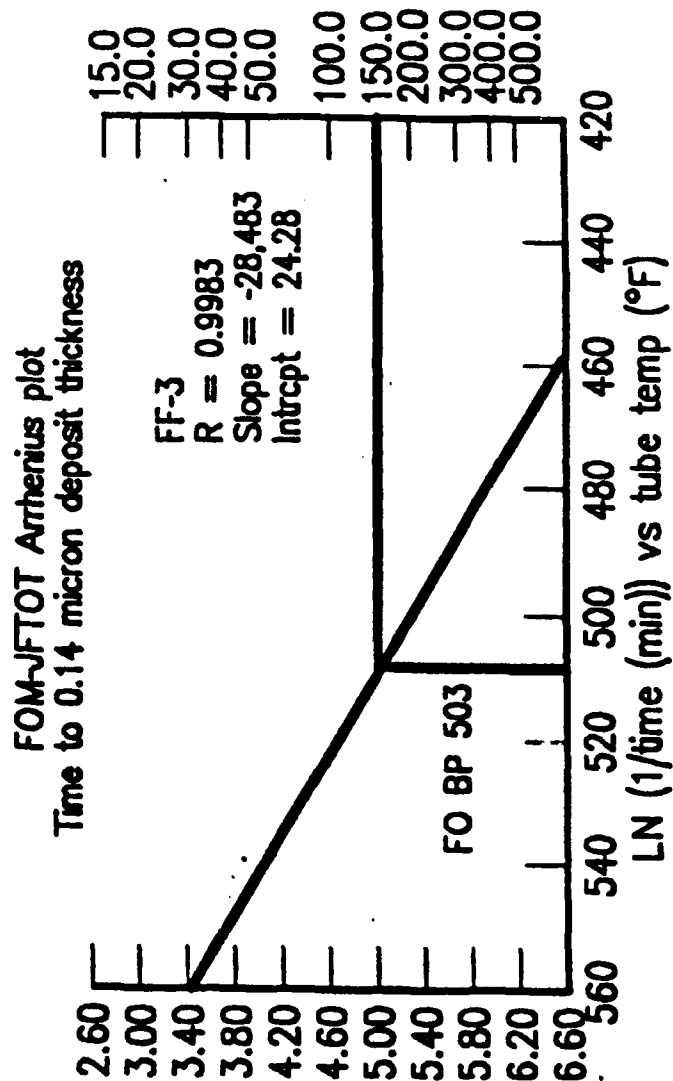
Test duration: 300 minutes

Laboratory	No. of runs	Time to 1st max (min)	Rate of deposit 1st max 10^{-3} μ /min	Rate of deposit overall 10^{-3} μ /min	Total deposit test (μ)
NAPC lab	1	39.0	3.6	5.3	1.58
P&W lab	5	37.5	3.8	6.1	1.84

FIBER OPTIC BREAK POINT TEMPERATURE

Definition

Temperature required to achieve first max (0.14 μ deposit thickness) in 150 minutes



ANL355771 880807

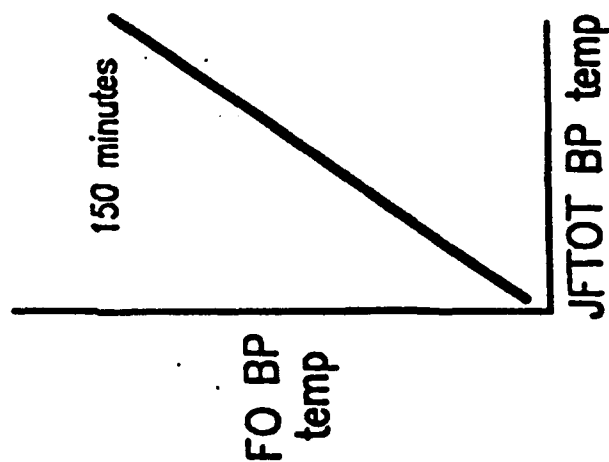
Figure 9. Fiber Optic Break Point Temperature

TABLE 8
NEED FOR CORRELATING FIBER OPTIC AND JFTOT BREAK POINT

FIBER OPTIC BREAK POINT TEMPERATURE

Need to correlate with standard JFTOT break point

Fuel description	JFTOT BP (°F)	FO-JFTOT BP (°F)
FF-3 (JP-5)	470	504
NAPC 17 (DFM)	470	495
FF-8 (JP-5)	500	536



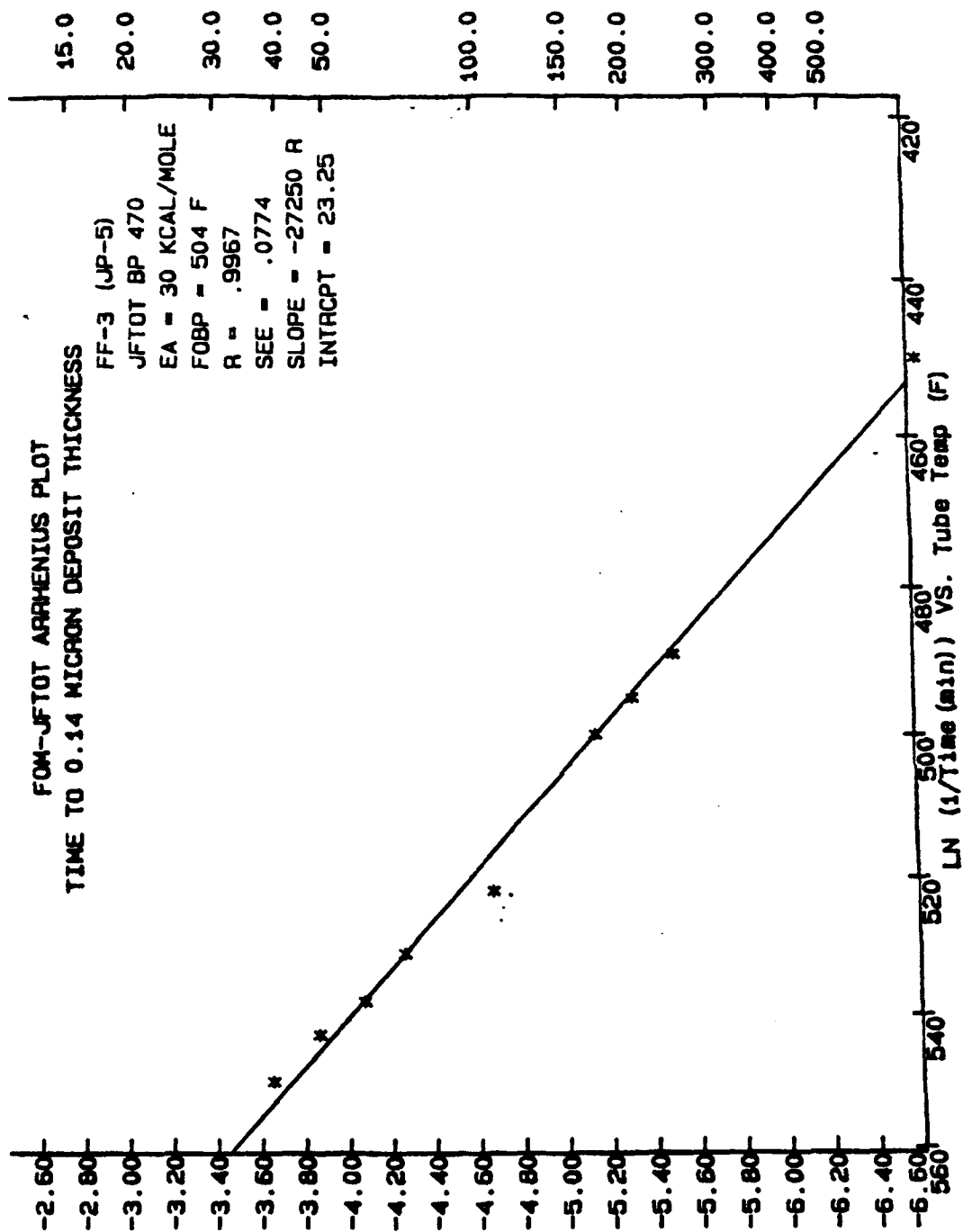


Figure 10. Arrhenius Plot for FF-3 JP-5

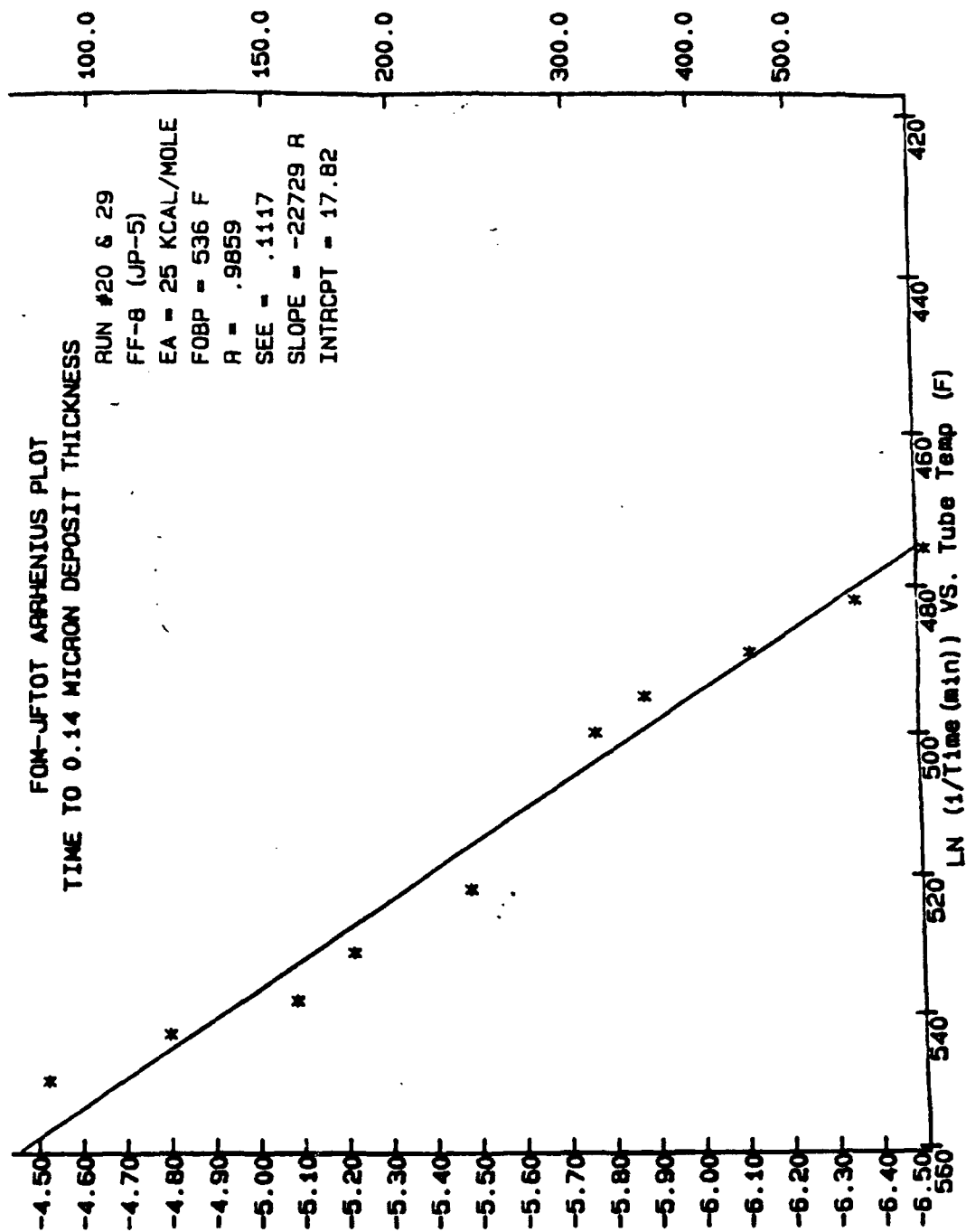


Figure 11. Arrhenius Plot for FF-8 JP-5

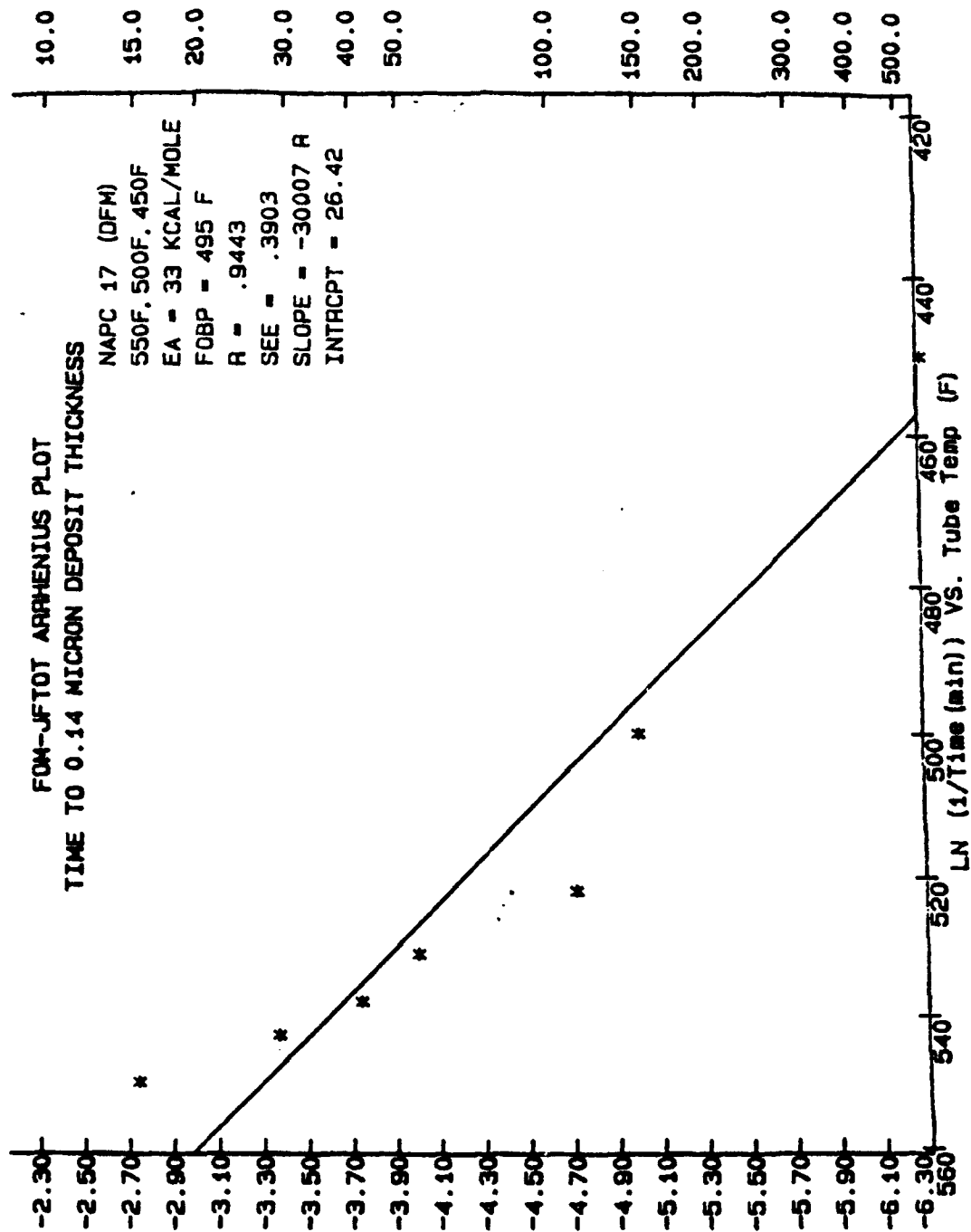


Figure 12. Arrhenius Plot for NAPC 17 (DFM)

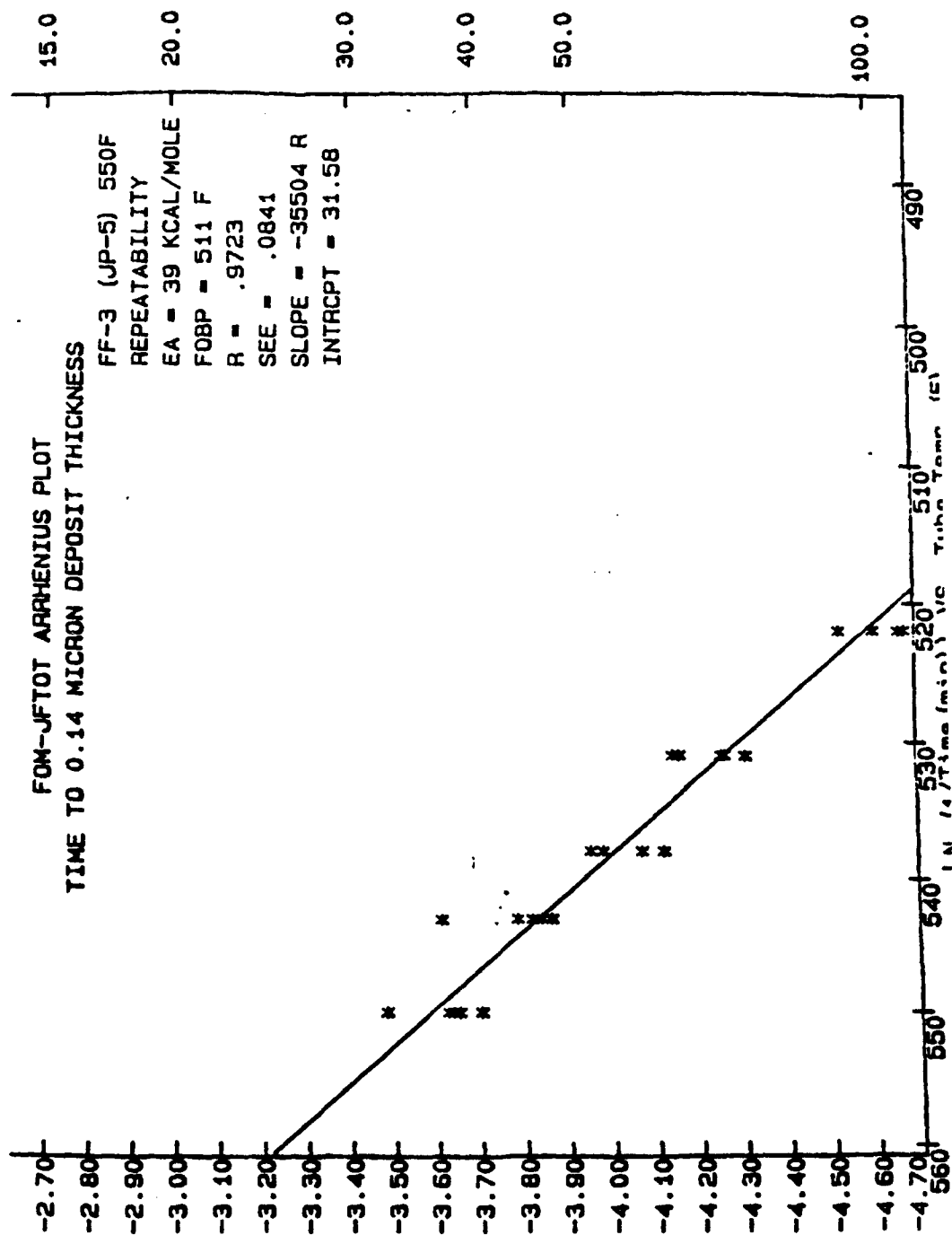


Figure 13. Arrhenius Plot for FF-3 JP-5 - Repeatability of Measurements

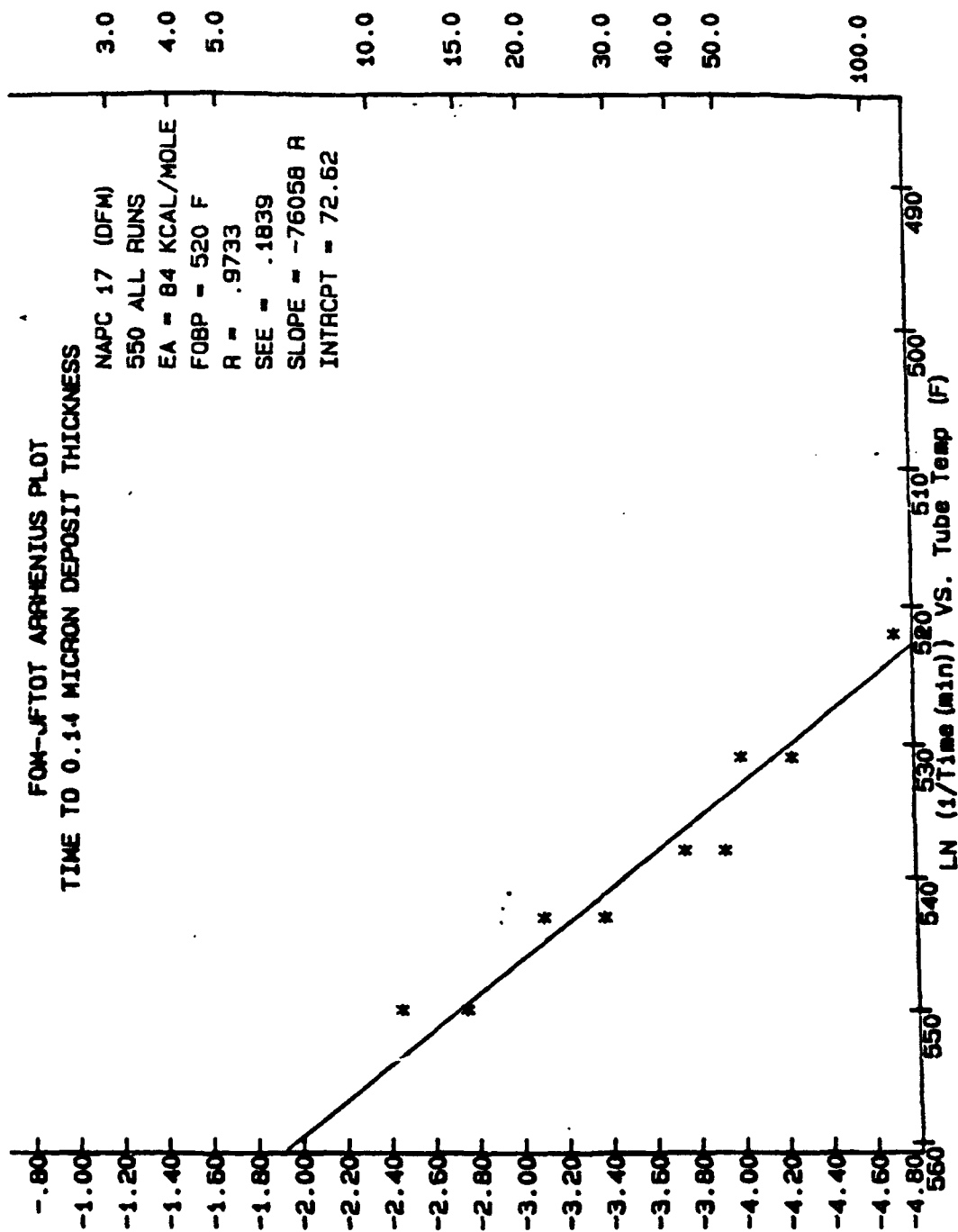


Figure 14. Arrhenius Plot for NAPC 17 (DFM) - All Runs

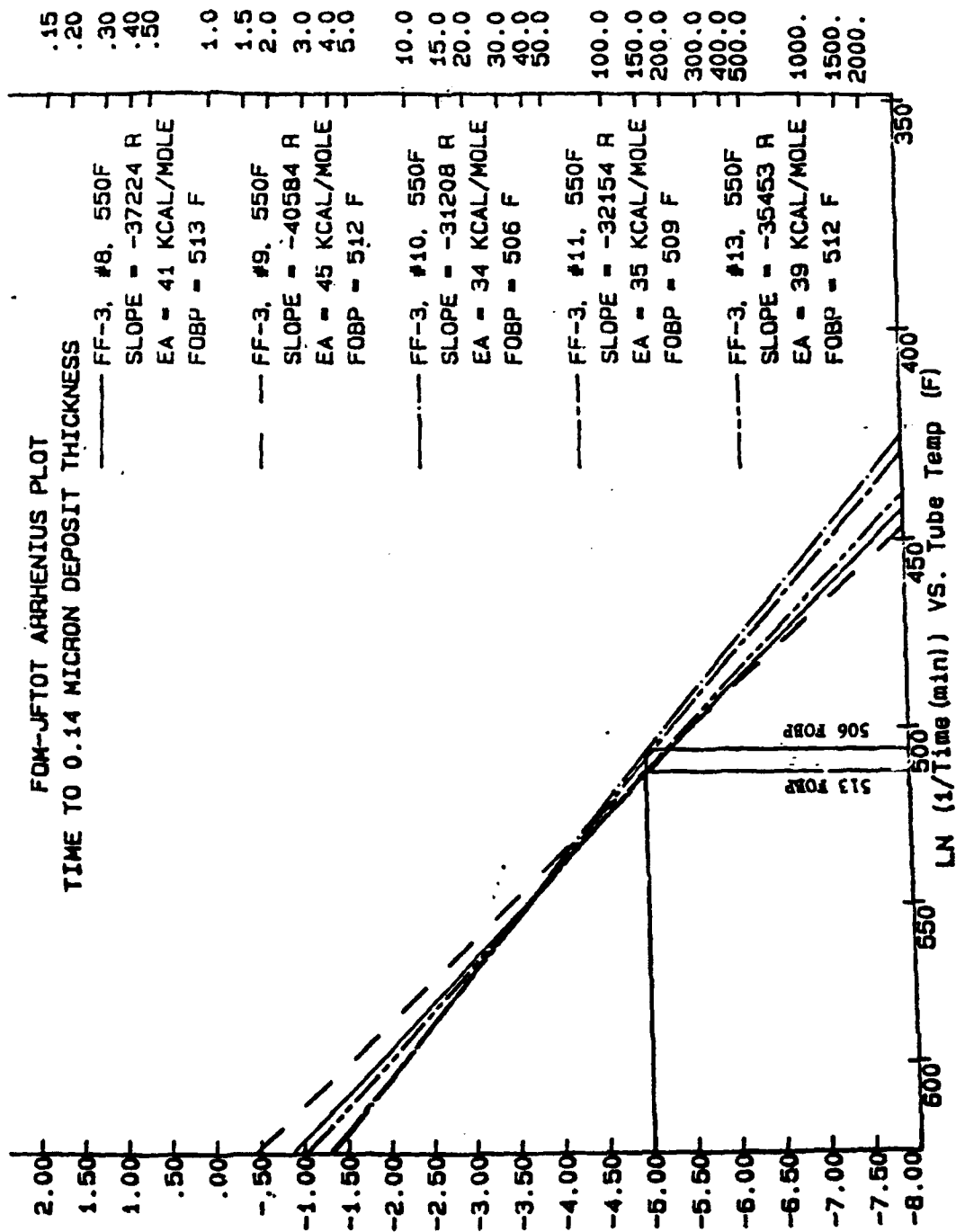


Figure 15. Repeatability of Fiber Optic Break Point Derived From Arrhenius Plot

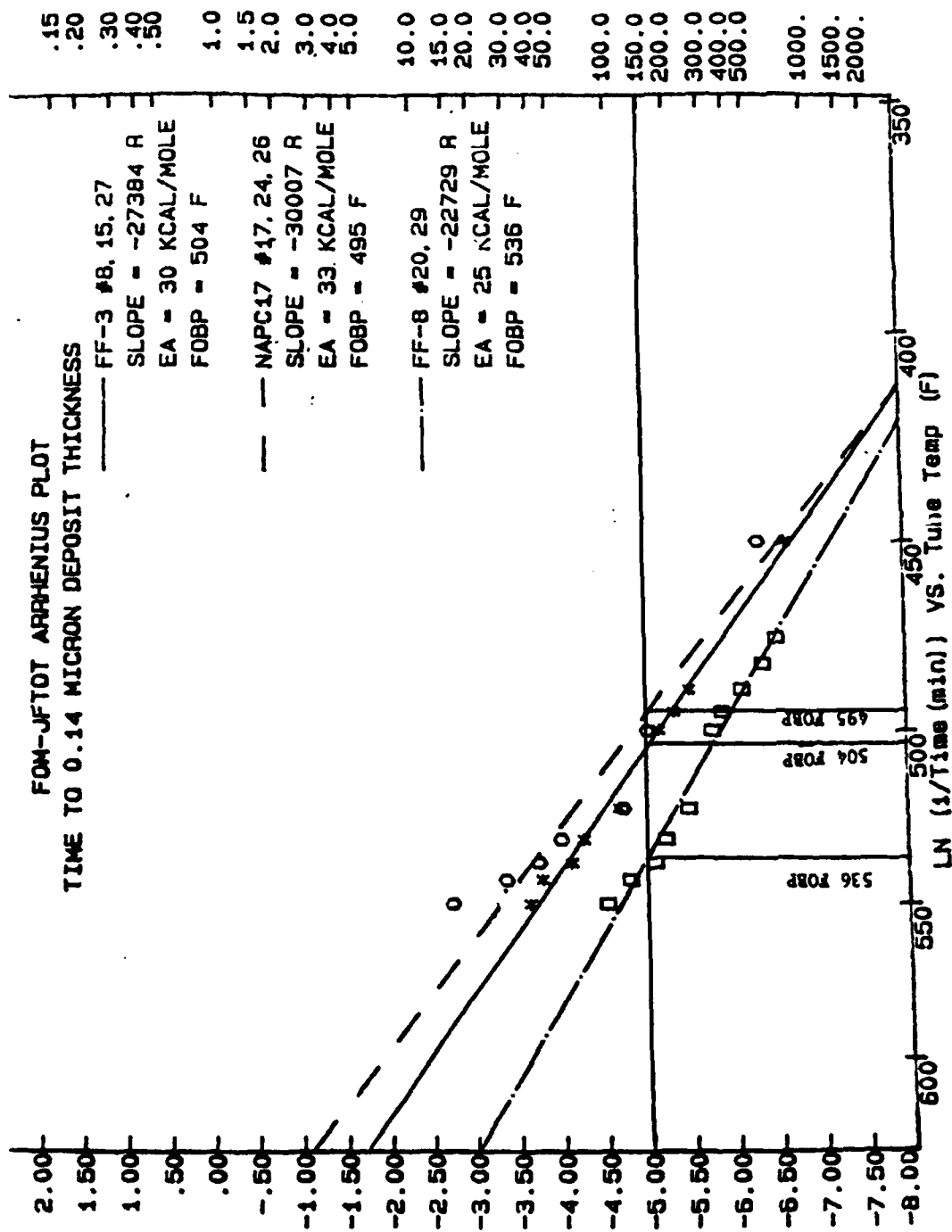


Figure 16. Fiber Optic Break Point Derived from Arrhenius Plot For Three Fuels

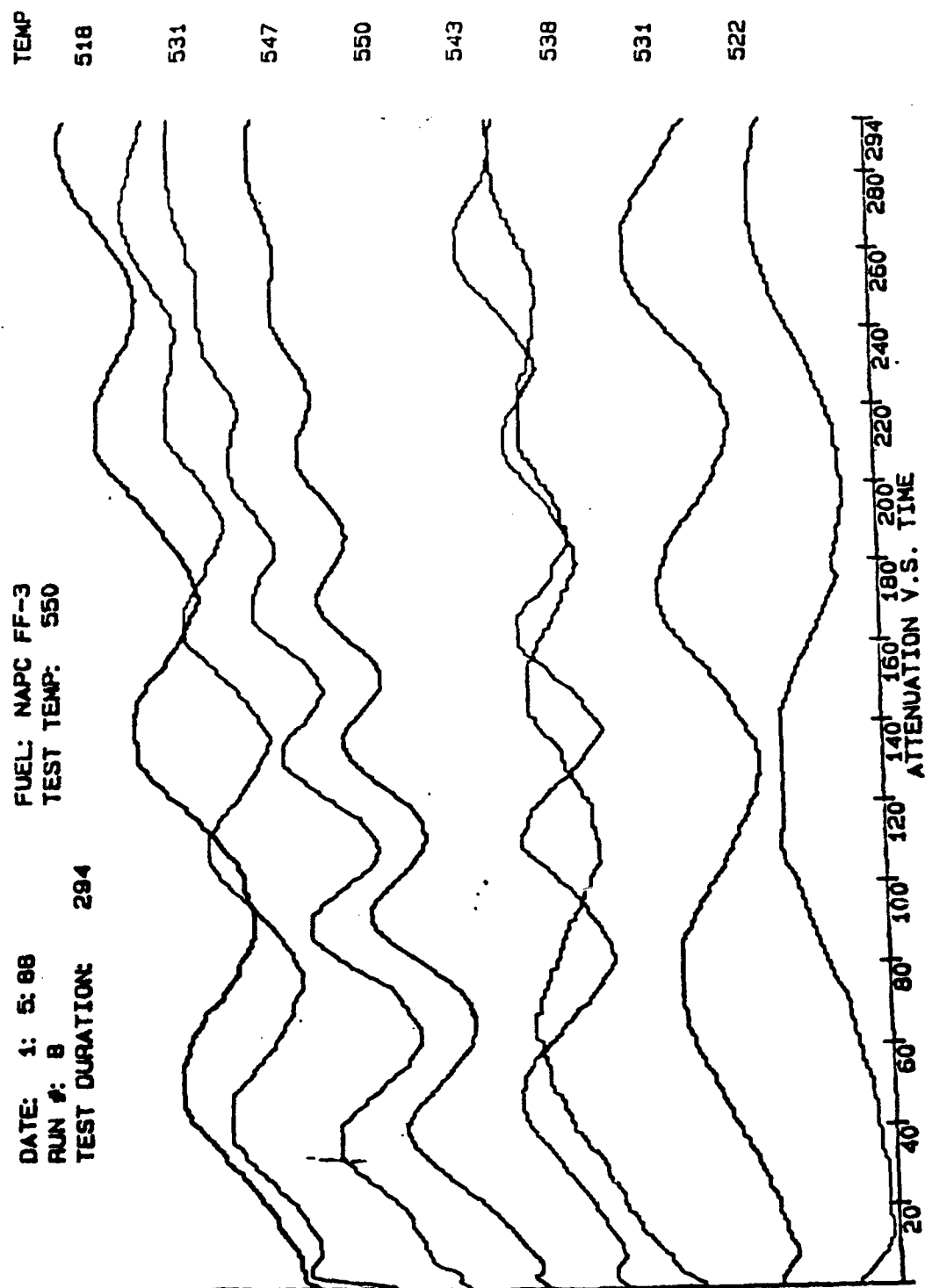


Figure 17. Real Time Display of Interferogram for NAPC FF-3 at 550°F Test Temperature

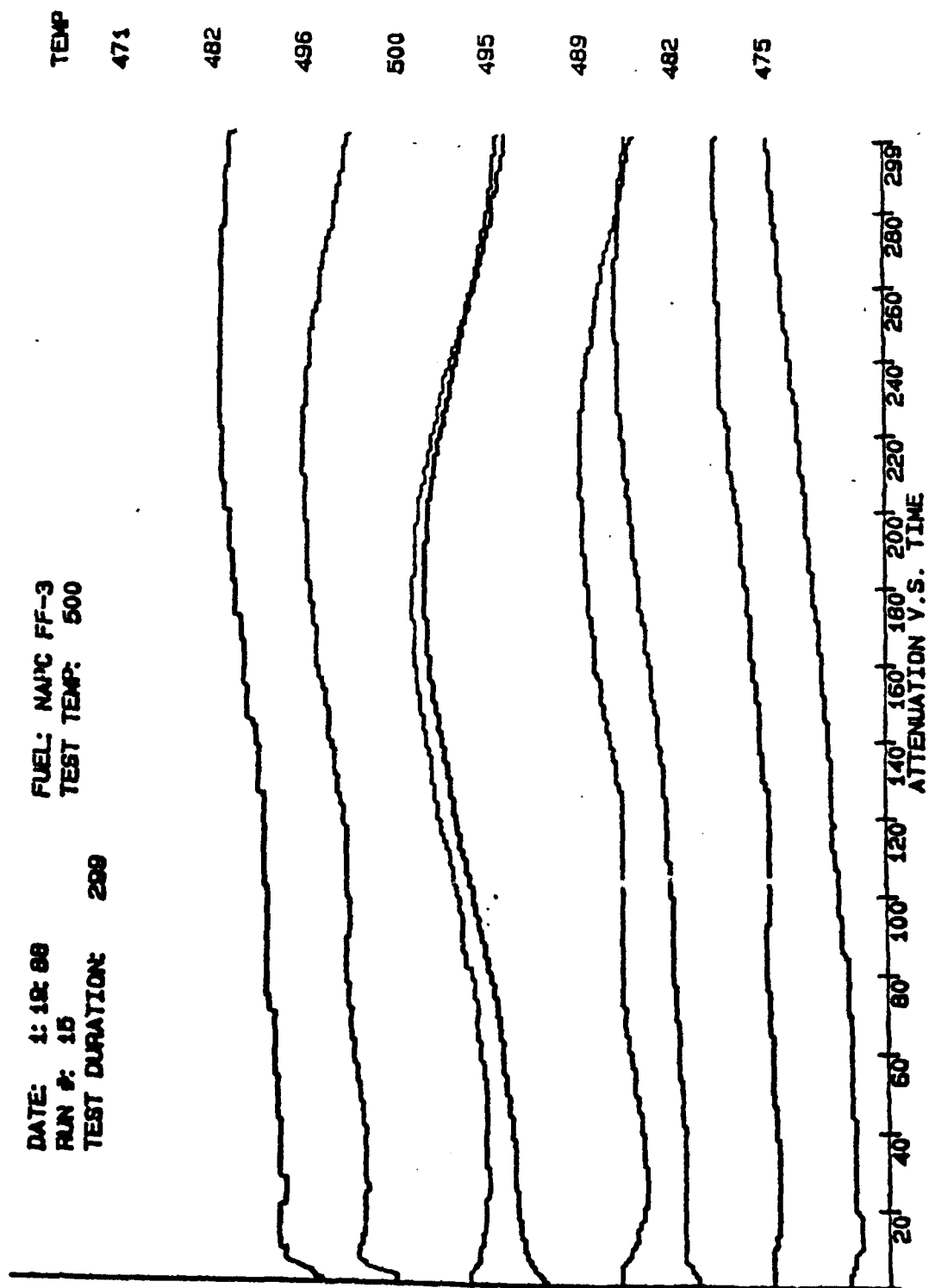


Figure 18. Real Time Display of Interferogram for NAPC FF-3 at 500°F Test Temperature

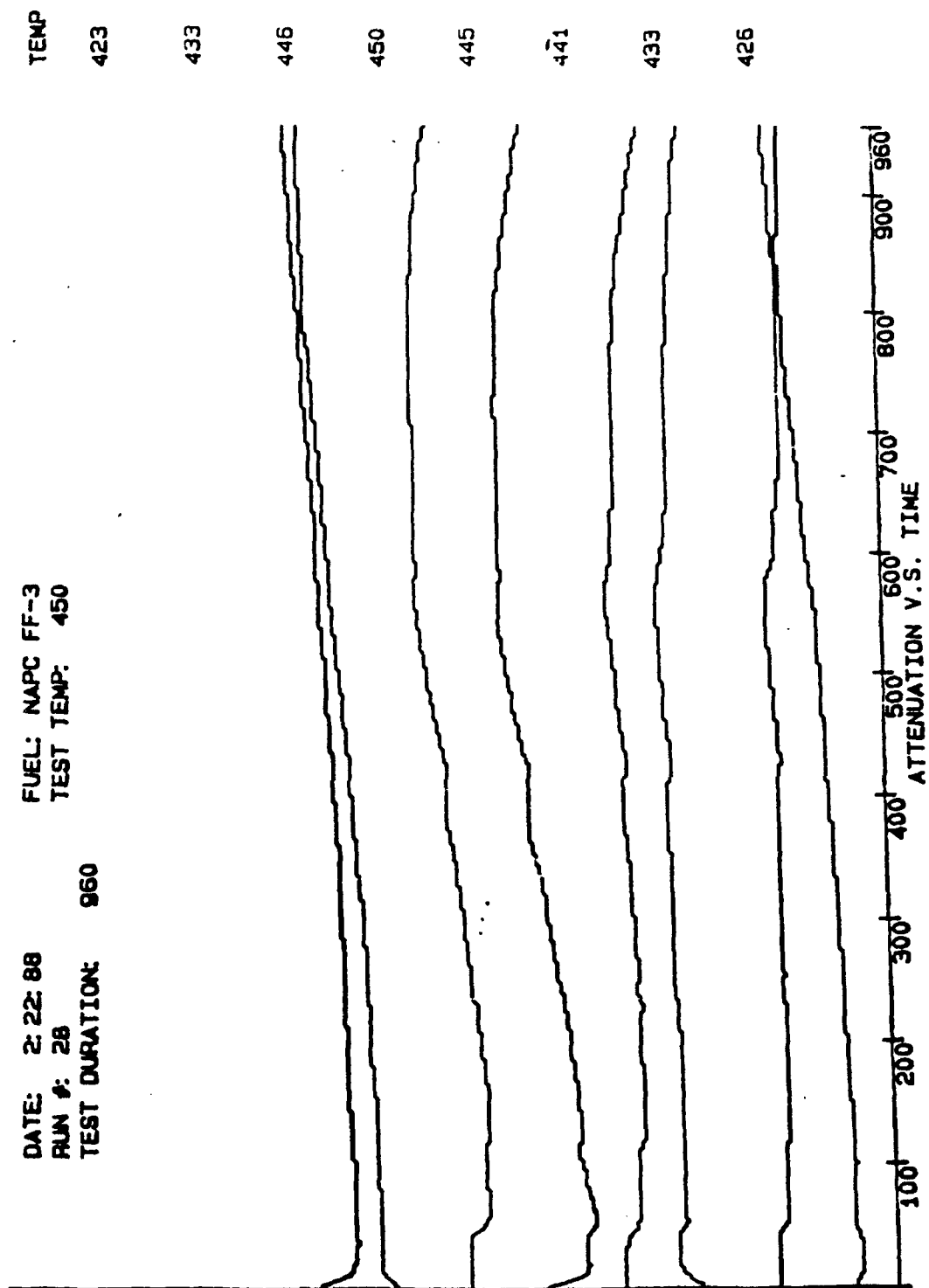


Figure 19. Real Time Display of Interferogram for NAPC FF-3 at 450°F Test Temperature

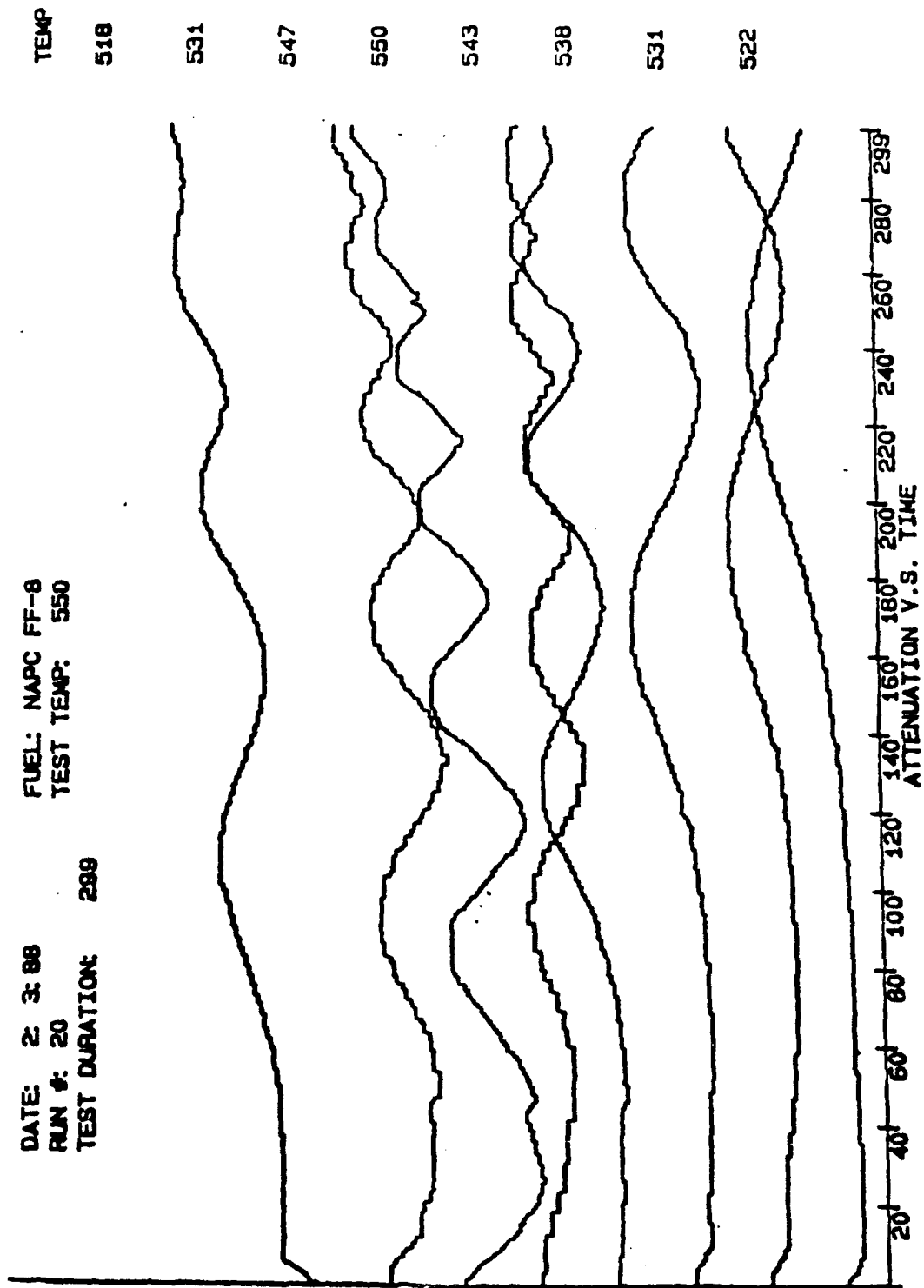


Figure 20. Real Time Display of Interferogram for NAPC FF-8 at 550°F Test Temperature

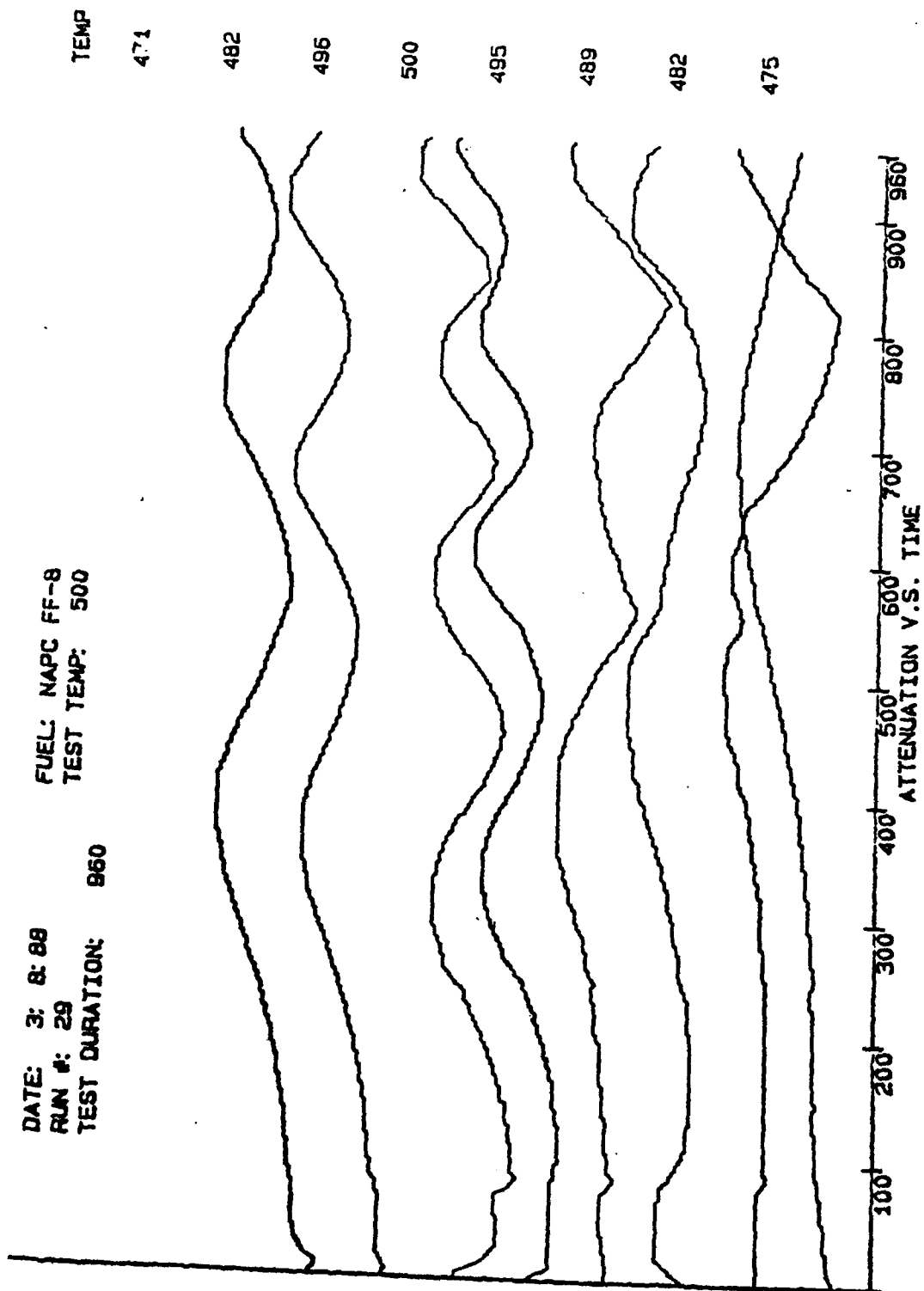


Figure 21. Real Time Display of interferogram for NAPC FF-8 at 500°F Test Temperature

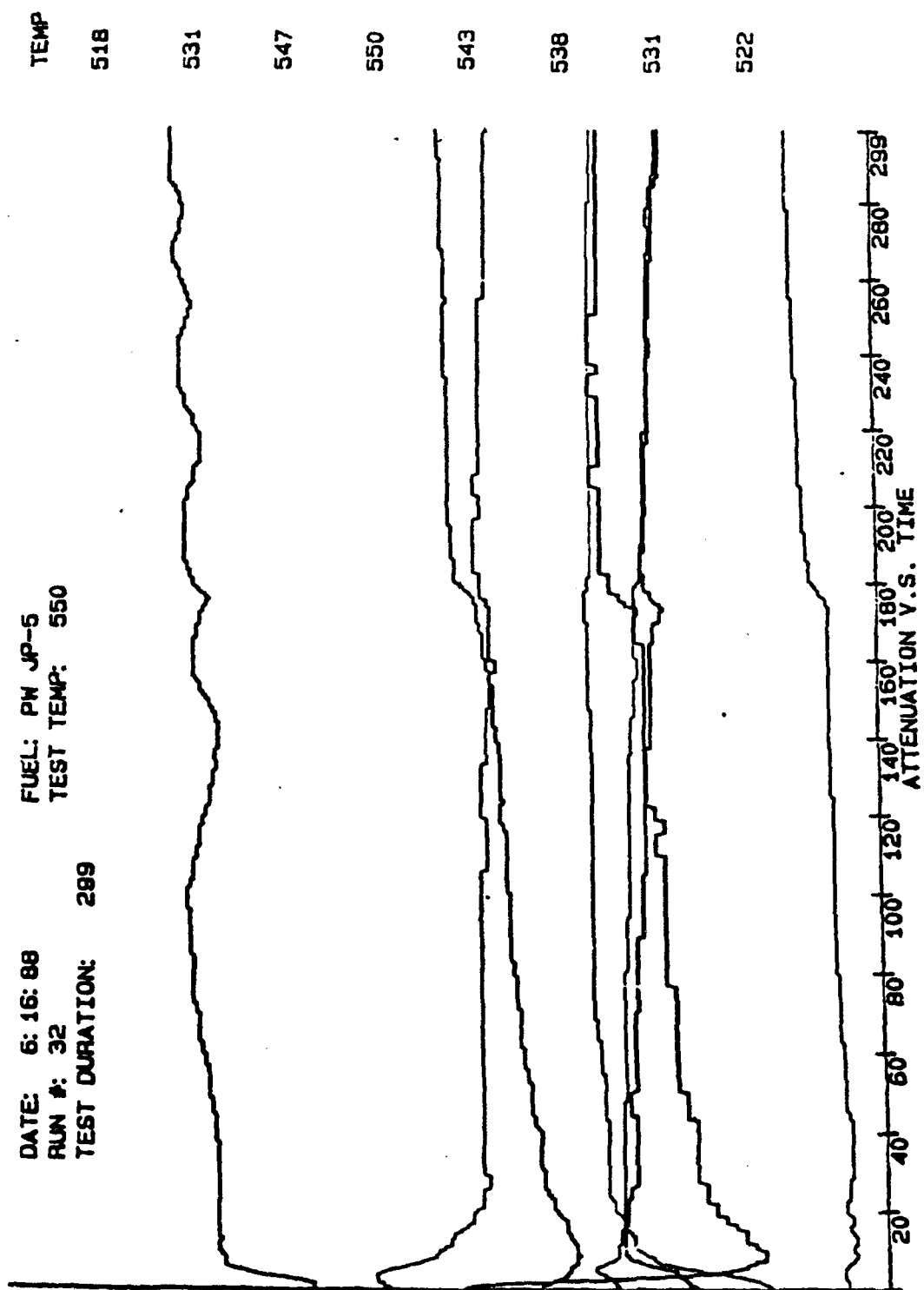


Figure 22. Real Time Display of Interferogram for P&W JP-5 at 550°F Test Temperature

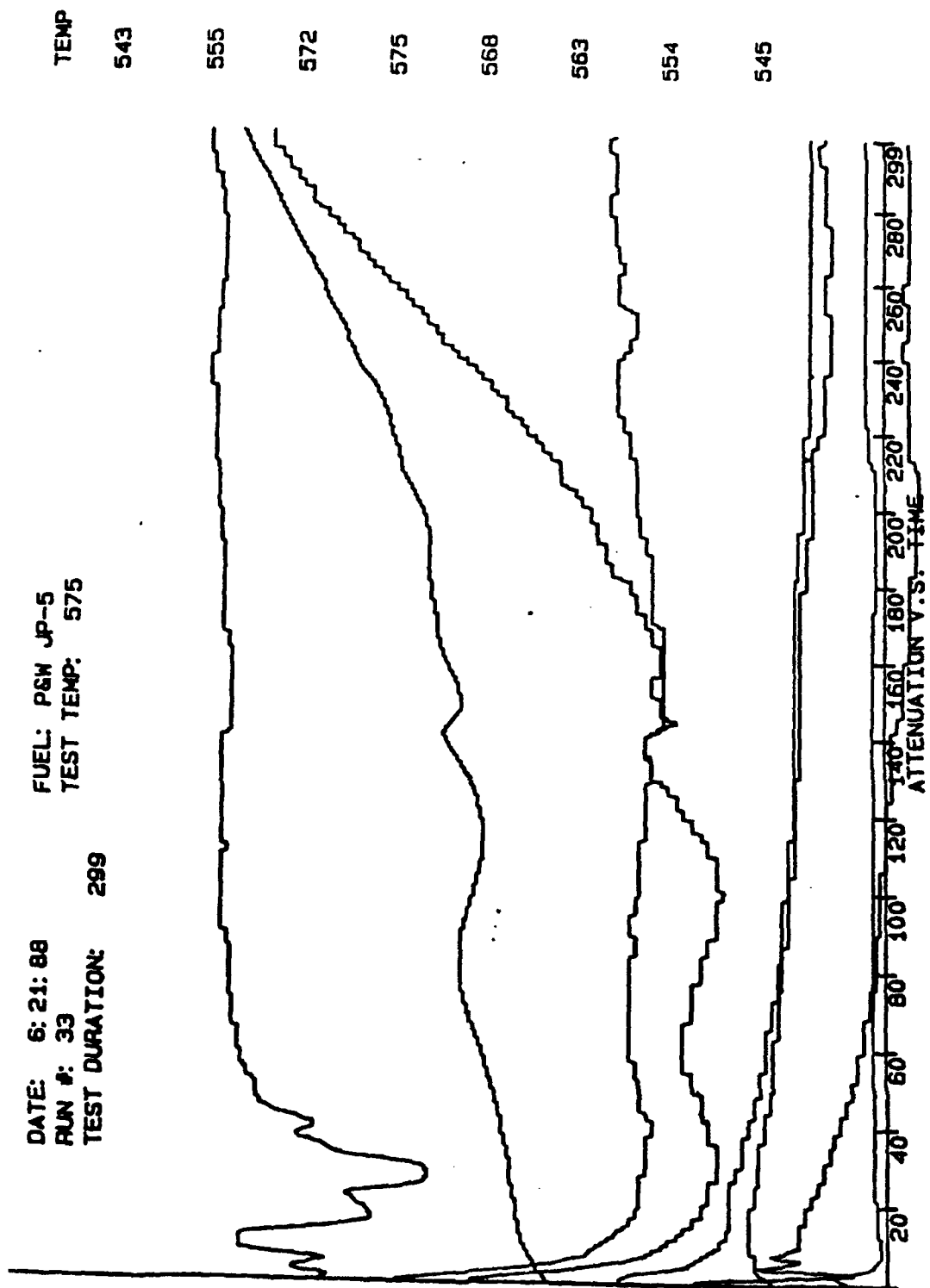


Figure 23. Real Time Display of Interferogram for P&W JP-5 at 575°F Test Temperature

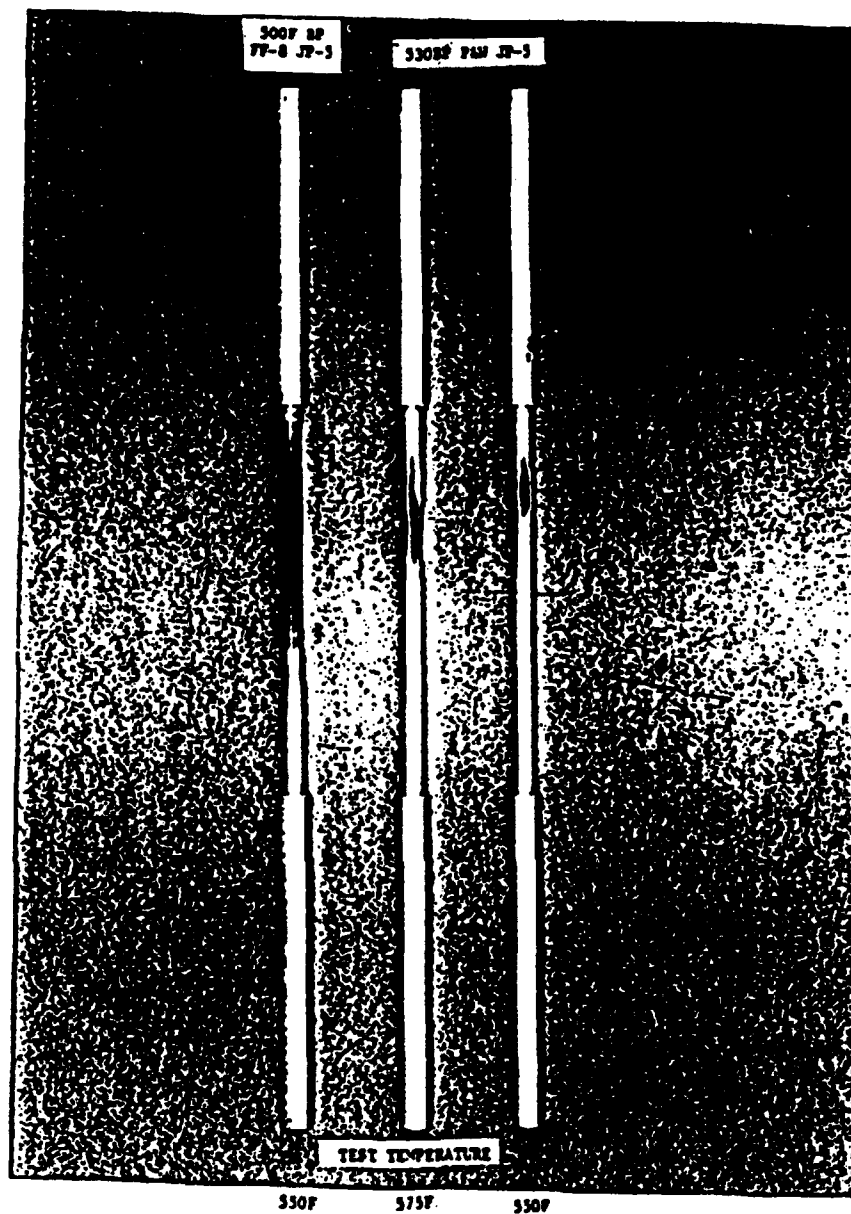


Figure 24. FOM-JFTOT Heater Tube Deposits

THERMAL OXIDATION CLOSED CELL EXPERIMENTS

Period of Performance

22 March 1989 through 22 March 1990

Reference

Task order No. 16, Topical Report 12, FR19032-12, William Edwards

Abstract

Closed test cells were designed and fabricated to assess the role of metallurgy in the fuel thermal oxidative deposition process. Any differences in deposition rates observed were investigated to determine whether a catalytic process was involved or whether differences were due to the affinity of deposits to adhere to a specific metal surface. In the static tests performed under this investigation, significantly lower levels of fuel degradation products were produced than reported in literature for dynamic flowing fuel test rigs. Repeatability was not as good as desired. Based on the amounts of filterable and tube wall carbon obtained, calculated activation energies, total carbon/total volume, and total wall carbon/total carbon ratios for each cell type, there appeared to be a difference between stainless steel and aluminum catalytic properties. These differences are most likely mechanistic in nature. However, the data does not allow the determination of which metallurgy is more catalytic. Any future effort using a static closed test cell approach will require further development in reactor design and a review of equipment and techniques available for providing rapid heat up to isothermal conditions.

SECTION 1.0

INTRODUCTION

A data base is needed for the development and calibration of a computational fluid dynamics and chemistry (CFDC) model for application to the thermal oxidative deposition of jet fuels. Generation of such a data base will require the performance of some simple thermal stability experiments conducted under precisely controlled conditions. One of the fundamental issues to be addressed is the role of different metallurgies on the deposition process.

Recent studies performed at Shell Research Ltd. using the Jet Fuel Thermal Oxidation Tester (JFTOT) indicated that metallurgy was significant at low levels of deposition. However, at higher levels of deposition, different metallurgies produced similar results presumably because lacquer was being deposited on a lacquered surface. While differences between metallurgies are clearly discernable under certain conditions, it is not evident that the metal surface actually serves to catalyze the formation of bulk fuel insolubles, or whether the increase in deposition is a function of existing insolubles having a greater affinity for a specific metallurgy.

SECTION 2.0

EXPERIMENTAL

Closed test cells were designed and fabricated to assess the role of metallurgy in the fuel thermal oxidative deposition process. These test cells were used to determine the effect of different metallurgies on deposition rates. Any differences in deposition rates observed were investigated to determine whether a catalytic process was involved or whether differences were due to the affinity of deposits to adhere to a specific metal surface. The role of test fuel chemical composition was not considered.

2.1 MATERIALS

The Thermal Oxidation Closed Cells (TOCC) were constructed of type 304 stainless steel (SS) and aluminum (Al). Chromatography grade tubing was used to minimize variations in tubing internal surface conditions. Two sizes, $\frac{3}{8}$ " and $\frac{3}{16}$ " O.D. of each tubing type were fabricated in 4" lengths. The smallest I.D. of these tubes was the Al $\frac{3}{16}$ " size which was 0.128 inches. I.D.'s smaller than this were considered too small for efficient oxygen flow and carbon combustion during carbon burn-off analysis. SS and Al Swagelok end-cap fittings were used, as appropriate, to terminate the ends of each TOCC.

Elemental analysis was performed on the tubing internal surfaces to verify that in fact type 304 SS and high aluminum tubing was obtained. No anomalies were reported.

The TOCC's were cleaned in a commercially available degreaser called Blue Gold (available from the Blue Gold Company, Highland, Ohio) with 1200 watts ultrasonic agitation for 10 minutes. The solution concentration was 10% by volume. Blue Gold is water based, halogen free and non-toxic. The Blue Gold/ultrasonic cleaning was followed by thorough rinsing with 12-megaohm ultra pure water. The parts were then acetone rinsed and GN_2 dried. This procedure produced low carbon analysis results and proved to be very repeatable.

The test fuel was Mil-T-83133 C, JP-8, containing no metal deactivator. The fuel was stored in an epoxy lined 5-gallon can in the laboratory to minimize compositional changes during the testing period.

2.2 INSTRUMENTATION

A heated aluminum block with four 2.5" by 12" vertical wells was used to provide uniform heating of the TOCC's. Temperature control precision was $\pm 1^\circ\text{F}$. Temperature distribution within the wells was less than $\pm 4^\circ\text{F}$, after equilibration. The top 3" of each well was insulated with glass wool to help maintain uniform temperatures within each well.

Carbon analyses were carried out using a LECO RC412 Multiphase Carbon/ Hydrogen/ Moisture Determinator Model 787-900-300. The carbonaceous deposits were "burned off" in a quartz tube furnace with a flowing oxygen atmosphere. The temperature was raised at 270°F (150°C) per minute to 1022°F (550°C) and held for 3 minutes. All organic carbon was converted to CO and CO_2 . The RC412 catalytically converts the CO to CO_2 and the total CO_2 is quantified by infrared detection. Results were calculated in milligrams/square foot. Calibration was done using LECO and NBS SRM carbon standards.

2.3 TECHNIQUES

The TOCC's were prepared just prior to thermal stressing as outlined above. Each TOCC was filled to 50% of its internal volume with test fuel and the end-caps sealed. Procedures recommended by Swagelok for setting the fittings were strictly followed for each TOCC. They were then labeled with an aluminum

tag to maintain identification, rinsed with isopropanol and acetone to remove finger prints and contamination, dried with GN_2 and placed in the heated aluminum block. At the end of the two hour thermal stress period, they were removed and allowed to cool to room temperature. Water quenching, to rapidly stop the thermal process, was evaluated, but was found to cause severe leaks in nearly every instance in both the SS and Al TOCC's.

Each TOCC was then opened, one at a time, and the fuel vacuum filtered through a 1.0 micron glass fiber filter (Gelman Type A/E). The filters and tubes were rinsed with three 10-milliliter (mL) portions of hexane. The vacuum was continued until all visible hexane was removed (10 to 15 seconds). The filters were then dried in a 212°F (100°C) convection oven for 15 minutes. After drying, the filters were put into 50 mm plastic petri dish type containers and placed in a desiccator until analyzed. Following a hexane wash, the TOCC tubes were oven dried and stored in ceramic dishes with covers in a desiccator until analyzed. All carbon analyses were performed within 24 hours with most completed within 8 hours of thermal stress period completion.

Glass fiber type filters were necessary for carbon analysis because other types, while having smaller pore sizes, contain carbon and either detonate and/or liberate fluorine during analysis. This can damage the quartz combustion tube of the analyzer. The Gelman type A/E filters are thicker than the other filters and, at reduced filtration rates, this increases its retentiveness somewhat beyond the 1.0 micron nominal value. It should be noted that techniques are available to allow the use of the other type filters. However, the increased probability of varying filter carbon content, and possible contamination due to the increased materials and handling that would be required, made these filters and techniques undesirable for this work.

The RC412 was calibrated with LECO part # 502-029, 1.07% \pm 0.03% by weight Synthetic Carbon standard. The accuracy of this calibration was checked using NBS SRM 112b Silicon Carbide with a certified free carbon content of 0.26% \pm 0.03% by weight.

The temperature ramp program from 212°F (100°C) to 1022°F (550°C) at the rate of 270°F (150°C) per minute was used for all analyses. This program was chosen after trial runs indicated that all fuel deposited carbon was removed under these conditions. Additionally, it was necessary to stay below the softening temperature of the Al tubing to prevent interstitial carbon from being included in the analysis result.

2.4 PROCEDURE DEVELOPMENT

Initial efforts involved establishing test temperatures and times. TOCC test sets consisting of three TOCC's containing fuel plus one blank TOCC were used for determining optimum conditions.

Leakage of both SS and Al TOCC's and rupture of the Al 3/8" TOCC was experienced over the temperature range of 300°F (149°C) to 700°F (371°C) within 30 minutes of heating when the TOCC's were filled with fuel. Expansion of the fuel and deformation of the Al tubing was determined to be the cause of these problems. The ANSI Code for pressure piping, ASME/ANSI B31.3, reports that the rated pressure capabilities for tubing must be reduced as use temperatures increase. When temperatures increase from 200°F (93.3°C) to 400°F (204.4°C), the aluminum alloy 6061-T6 reduction factor is 0.4 and for type 304 SS it is 0.93. This means that type 6061-T6 Al loses 60% of its strength over this temperature range. The type 304 SS would lose only 7%.

Further testing showed that by reducing the fuel volume to 50% of the TOCC internal volume, bursting of the Al 3/8" TOCC was eliminated and leakage was reduced for the other TOCC types. Fuel leaks were detected by observing a change in the appearance of the TOCC's. A color change from the original silvery color to that of an amber or brown was typical of fuel leakage and deposition on the outside of the TOCC.

A major cause of leakage was found to be ferrule galling during assembly of the TOCC's. Galling prevented the tube and ferrules from seating properly in the end-cap. A lubricant is applied by the manufacturer to the nut, ferrule, and end-cap threads to prevent galling. However, this lubricant was removed when the parts were cleaned to eliminate contamination prior to assembly for testing. Cleaning after seating of the ferrules improved sealing, but the end-caps still galled on the ferrules making removal without fuel loss very difficult. In addition, blank carbon values were higher and not repeatable.

Fuel leaks seemed to be eliminated, for the most part, by both reducing the test temperature range and using SS nuts, end-caps and aluminum ferrules instead of SS ferrules. The Al nuts and ferrules galled so badly that they could not be removed without significant loss of test fuel. The softer aluminum ferrules used with SS nuts and end-caps were found to provide a better seal with minimal galling than SS ferrules even on the Al tubes. In order to prevent the test fuel from contacting the SS end-caps used on the Al TOCC's, Al disks were made to fit over the end of the large and small Al tubes. When the end-cap fittings were tightened, these disks were pressed onto the tube ends, thus preventing the fuel from contacting the SS end-cap. TOCC rejection was based upon a TOCC color change from silver to amber/brown. This color change was taken to indicate leakage of a TOCC and the test set was discarded and a new run made.

A 500°F (260°C) SS $\frac{3}{8}$ " TOCC test was performed with sampling at 2, 4, 6 and 8 hour periods. A fifth set was allowed to run for 96 hours (4 days). Total carbon values for the 5 tests were not greater than the 2-hour test. Since these were run in triplicate and no sign of leakage was evident, it was felt that these results were valid. In a study conducted by United Technologies Research Center (UTRC) for NASA entitled "Experimental Study of the Thermal Stability of Hydrocarbon Fuels", P.J. Marteney, et. al. reported similar results using similar SS "static reactors". Fuel fouling tests were performed at temperatures of 300°F (149°C) to 800°F (427°C) with regular diesel fuel for periods of 30 minutes to 2.5 hours. These tests resulted in lower fuel deposition than was observed in a dynamic flowing fuel test apparatus under similar conditions. This was thought to be indicative of the importance of fluid transport in the deposition mechanism. It is probable that in the present study, the fixed fuel and air volumes are also limiting factors to the amount of deposition. The UTRC researchers also reported problems involving leakage and contamination during the course of their static reactor experiments.

TOCC experiments were conducted at 500°F (260°C) for 1, 2 and 4 hour periods to confirm the 2-hour optimum test period established in the first tests. The 1-hour test showed extremely low carbon values and there was poor agreement between the TOCC set individual tubes. Presumably, this represents the "induction period" for deposit formation under these test conditions. The 2 and 4-hour tests produced essentially the same amount of carbon. Therefore, 2 hours was chosen as the standard test time period for this study.

In the final tests performed, JP-8 fuel was aerated with a diffusion stone just prior to being volumetrically added to the TOCC's. The TOCC's were filled to 50% of their volumes with the test fuel. Thermal stressing was conducted every 50°F (27.8°C) from 300°F (149°C) to 500°F (260°C) for 2 hours. TOCC sets of each tubing type and size consisted of three cells with fuel, plus one empty cell to serve as the set blank.

2.5 DATA ANALYSIS

All raw filter and TOCC tube carbon data were corrected for blank carbon values and then normalized to yield uniform units of mg/mL/sq.ft./hr. This was designated Data Set 1 and was comprised of three groups: Total Filterable Carbon (TFC), Tube Wall Carbon (TWC) and Total Carbon (TC). TC is the sum of the TFC and the TWC.

Data Set 1 carbon values were averaged to provide a single "smoothed" point at each temperature for each TOCC type. This was designated Data Set 2. Data Sets 1 and 2 were then analyzed using least squares linear regression and Arrhenius equation analyses. The linear form of the Arrhenius equation was used:

$$\ln k = -E_a / RT + \ln A$$

where: k = Reaction product measured (i.e. carbon)

E_a = Energy of Activation, kcal/mole

R = Universal Gas Constant, 1.987 kcal/mole

T = Temperature in degrees Kelvin (K)

A = Preexponential factor (characteristic reaction constant)

TFC and TC activation energies and line fit statistical information were calculated and graphical representations made for each TOCC type.

SECTION 3.0

RESULTS AND DISCUSSION

Approximately six TOCC sets were run per temperature per TOCC type, except for the Al $3/16$ " type which had a severe leakage problem. Approximately 10 runs were made with it. Over 500 TOCC's were assembled and thermally stressed. Not all were analyzed for carbon because leakage was evident and they were discarded. Reuse was not possible. This reduced the number of usable TOCC sets to a great extent. There were instances where it was not clear whether leakage had actually occurred or not, especially at the 450°F and 500°F temperatures. Vaporization could have been such that the vapors simply moved away from the TOCC's, without forming the telltale deposits on the outside of the cells.

Data Sets 1 and 2 TFC, TWC and TC values in mg/mL/sq.ft./hr are summarized in Tables 1 and 2, respectively.

3.1 TOTAL CARBON

Figures 1 through 4 are plots of Data Set 1 Total Carbon (TC) values for SS $3/8$ ", Al $3/8$ ", SS $3/16$ " and Al $3/16$ " TOCC's, respectively. Activation energies in kcal/mole are given in the legends. These are quite low compared to the 8 to 12 kcal/mole generally reported in the literature for the below 500°F (260°C) temperature region. However, the literature values represent flowing fuel test conditions and are probably higher due to the greater fluid transport and lower fuel residence time inherent to that type of test apparatus.

Figure 5 is a TC composite plot of all four TOCC types using Data Set 2 values. This plot shows the relationship of Al and SS TOCC of different sizes in a less cluttered manner. The activation energies (E_a) are given in the legend.

In general, the data has quite a bit of scatter for all four TOCC types. The use of Al ferrules may have solved the galling related leakage, but because of aluminum's lower hardness, as compared to SS, small tube surface scratches and imperfections may not have been "coined out" as well. These would be sites for leakage and/or hidden fuel deposits. One other consideration is the fact that Swagelok fittings function by compression fit of the two part ferrule system to the tube. In the case of Al tubing, this force (especially at elevated temperatures) could deform the tubing and allow fuel to escape. This was considered in the design stage of the TOCC's. The thickest walled tubing available in chromatography grades was obtained in an effort to prevent this problem.

**TABLE 1.
DATA SET 1- NORMALIZED VALUES
FOR TOTAL FILTERABLE CARBON, TOTAL WALL CARBON, & TOTAL CARBON**

TOCC Type		300°F	350°F	400°F	450°F	500°F
SS 3/8"	TPC	0.41	0.63	1.06	1.06	0.52
		0.31	0.59	0.70	0.57	
		0.58		0.63		
	TWC	1.01	3.24	4.78	2.17	2.74
		0.89	1.92	1.34	2.44	
		1.64		3.07		
	TC	1.42	3.87	5.84	3.23	3.26
		1.20	2.51	2.04	3.01	
		2.22		3.70		
Al 3/8"	TPC	0.38	0.66	0.71	0.63	0.52
		0.32	0.62	0.58	0.47	
		0.66	0.58	0.62		
	TWC	0.86	1.10	2.26	1.48	1.49
		1.39	1.63	1.11	1.57	
		0.87	0.43	2.07		
	TC	1.24	1.76	2.97	2.11	2.01
		1.71	2.25	1.69	2.04	
		1.53	1.01	2.69		
SS 3/16"	TPC	1.43	3.18	3.77	7.73	2.47
		1.04	2.08	1.36	1.95	
		3.51	2.34			
	TWC	14.03	4.16	5.39	4.94	12.80
		8.25	15.33	13.19	13.90	
		2.86	7.70			
	TC	15.46	7.34	9.16	12.67	15.27
		9.29	17.41	14.55	15.85	
		6.37	10.04			
Al 3/16"	TPC	2.69	4.48	6.04	11.19	2.80
		1.45	3.13	4.14	3.13	2.80
		0.67	4.81	1.01		
	TWC	14.11	7.12	14.06	9.51	3.47
		16.25	27.47	7.36	7.37	3.47
		24.83	10.89	16.09		
	TC	37.02				
		16.80	11.60	20.10	20.70	6.27
		17.70	30.60	11.50	10.50	
		25.50	15.70	17.10		
		43.40				

TABLE 2. DATA SET 2-- NORMALIZED AND AVERAGED CARBON VALUES						
TOCC Type		300°F	350°F	400°F	450°F	500°F
SS 3/8"	TFC	0.43	0.62	0.79	0.82	0.53
	TWC	1.18	2.58	3.07	2.30	2.73
	TC	1.61	3.19	3.86	3.12	3.26
Al 3/8"	TFC	0.45	0.62	0.64	0.55	0.52
	TWC	1.04	1.05	1.83	1.53	1.50
	TC	1.49	1.67	2.45	2.08	2.01
SS 3/16"	TFC	2.01	2.53	2.60	4.87	2.47
	TWC	8.38	9.05	9.29	9.42	12.80
	TC	10.39	11.58	11.89	14.29	15.27
Al 3/16"	TFC	2.80	4.14	3.69	7.16	2.80
	TWC	23.05	15.11	12.53	8.45	3.47
	TC	25.85	19.25	16.22	15.61	6.27
Note: TFC = Total Filterable Carbon TWC = Total Wall Carbon TC = Total Carbon = TFC + TWC						

The Ea values of the averaged data in Data Set 2 are reduced as compared to the Data Set 1 values (unaveraged data). However, the statistical data for each TOCC is generally improved. Table 3 summarizes the standard deviation (SD), standard error of the estimate (SEE), goodness of the fit (R) and the Ea values calculated for Data Sets 1 (DS 1) and 2 (DS 2) TC data.

TABLE 3. DATA SETS 1 & 2 STATISTICAL ANALYSIS AND ACTIVATION ENERGIES (Ea) FOR TOTAL CARBON								
Stat.	SS 3/8"		Al 3/8"		SS 3/16"		Al 3/16"	
	DS 1	DS 2	DS 1	DS 2	DS 1	DS 2	DS 1	DS 2
SD	0.46	0.34	0.30	0.20	0.34	0.16	0.50	0.53
SEE	0.14	0.15	0.09	0.09	0.10	0.07	0.14	0.24
R	0.62	0.71	0.52	0.71	0.46	0.97	0.63	0.88
Ea	3.30	2.43	1.90	1.42	1.83	1.59	-3.71	-4.79

It would appear that as temperature increased, leakage of the small Al TOCC became worse and since more fuel would boil and vaporize, more was lost. If this were the case, then the very high carbon values

obtained at the lower temperatures could have resulted from a greater amount of the escaping fuel coking on the ferrules or other difficult place to observe. Outside the TOCC more oxygen would be available to encourage coking. Then, as test temperatures were increased for succeeding Al $3/16$ " TOCC sets, vaporization pressures would increase and thus leakage rates (and velocities) would also increase. The increased velocities would tend to carry the vaporized fuel away from the TOCC's and result in the lower carbon values obtained.

In spite of the problems experienced with the smaller I.D. Al TOCC's, the differences in TC between the large and small tube sizes are readily apparent as shown in Figures 6 and 7. Both SS and Al appear to be catalytic because more carbon was obtained in the small TOCC's as compared to the large TOCC's. Since the larger surface area to volume ratio diminishes the effect of mass transport, the presence of catalytic activity is inferred.

Catalysis is classically associated with a change in reaction rate. It can be either slower (negative catalyst) or faster (positive catalyst), but the reaction(s) final equilibrium and thus the amount of product obtained is not affected. Only the speed at which that equilibrium is reached is changed. Ea values are lowered as a result of positive catalysis.

Catalysts function by increasing the rate of one or more steps in a reaction mechanism by opening a reaction path having a lower activation energy. The reaction path is opened when a molecule or group of molecules gain enough energy to form activated complexes. The number of possible reactions and thus reaction steps that a catalyst may be able to activate, in a mixture like jet fuels, becomes theoretically enormous. It follows then that the final amount of deposit carbon formed for different catalysts will most likely be different. Put another way, in complex mixtures different catalysts, depending upon the particular catalyst's functional mechanism, can lead to different reactions and thus different product amounts. In addition, it is also known that competing reactions can alter even catalyzed primary reaction rates and equilibrium states. In fact, catalyst activity and efficiency can vary depending upon the reaction environment; even to the extent that the catalyst becomes neutralized or "poisoned".

It has been stated that both SS and Al appear to be catalytic, but because the smaller I.D. Al TOCC data was suspect, it was not possible to determine which metal was more catalytic. However, the fact that the calculated Ea values for the Al TOCC's are different from those found for the SS TOCC's indicates that there is probably a difference in the way SS vs Al catalyze reactions (i.e. different functional mechanisms). In order to evaluate this, further data analysis was conducted.

The TFC data was analyzed in a similar fashion as the TC data to evaluate whether any more information concerning the differences in catalytic functional mechanisms between SS and Al could be obtained. The rationale behind this approach was that the filterable carbon, being made up of large molecules and carbon particles, would not volatilize and be lost as readily as the liquid fuel. Thus the Al $3/16$ " TFC data might be of more use in this respect than the Al $3/16$ " TC data.

3.2 TOTAL FILTERABLE CARBON

Figure 8 is a composite plot of Data Set 2 TFC values for the four TOCC types. Ea values are given in the legend.

The TFC data indicate the same general relationships as the TC data, except that the Al $3/16$ " TOCC curve now has a negative slope. This was expected since the filterable carbon should not have been as affected by vaporization losses as was the TC values. Table 4 summarizes the statistical information and Ea data for Data Sets 1 and 2 TFC values.

TABLE 4. STATISTICAL ANALYSIS AND ACTIVATION ENERGIES FOR TOTAL FILTERABLE CARBON								
Stat.	SS 3/8"		Al 3/8"		SS 3/16"		Al 3/16"	
	DS 1	DS 2	DS 1	DS 2	DS 1	DS 2	DS 1	DS 2
SD	0.34	0.27	0.24	0.14	0.56	0.33	0.78	0.39
SEE	0.10	0.12	0.07	0.06	0.17	0.15	0.22	0.17
R	0.53	0.48	0.32	0.28	0.38	0.53	0.32	0.27
Ea	2.13	1.33	0.95	0.40	2.48	1.82	2.93	1.08

Again, as with the TC data, there is quite a bit of scatter in the data. However, even though the Al $3/16$ " TFC data is more believable, the contradiction between the large and small SS and Al TOCC's, with respect to carbon deposit amounts and Ea values, still exists.

3.3 TOTAL CARBON TO TOTAL FUEL VOLUME RATIO ANALYSIS (TC/TV).

The differences in deposit rates and amounts observed for both TC and TFC, can be further evaluated to determine whether these differences are the result of a catalytic effect on the bulk fuel insolubles or that of differences in their affinity for the metal surface. To do this, total carbon/total fuel volume (TC/TV) ratios were calculated and compared to the TC formed. Table 5 summarizes the Data Set 2 TC values and the calculated TC/TV ratios for the four TOCC types. Designations are: SS $3/16$ " (Rs1), SS $3/8$ " (Rs2), Al $3/16$ " (Ra1) and Al $3/8$ " (Ra2).

TABLE 5. TOTAL CARBON AND TOTAL CARBON TO TOTAL VOLUME RATIOS								
Run Temp.	SS 3/16"		SS 3/8"		Al 3/16"		Al 3/8"	
	Rs1	TC	Rs2	TC	Ra1	TC	Ra2	TC
300°F	17.0	10.4	0.7	1.6	65.0	25.9	0.6	1.5
350°F	19.0	11.6	1.3	3.2	48.0	19.3	0.6	1.7
400°F	20.0	11.9	1.6	3.9	41.0	16.2	0.9	2.5
450°F	24.0	14.3	1.3	3.1	39.0	15.6	0.8	2.1
500°F	26.0	15.3	1.4	3.3	16.0	6.3	0.8	2.0
Note: TC = Total Carbon Rs1 = TC/TV for SS 3/16" Ra1 = TC/TV for Al 3/16" TV = Total Fuel Volume Rs2 = TC/TV for SS 3/8" Ra2 = TC/TV for Al 3/8"								

It is evident that Rs1 > Rs2 and Ra1 > Ra2. In addition, both R1's have much higher TC values than the R2's. This implies that both SS and Al exhibit catalytic properties. However, because of the problems

experienced with the $\frac{3}{16}$ " O.D. Al TOCC's, it is not possible to determine with confidence which is more catalytic. Data for the larger O.D. TOCC's would indicate that SS was slightly more productive than Al, even though the SS Ea value is somewhat higher. This may, in fact, indicate something about the differences in the mechanism of catalysis between SS and Al. However, this is a speculative observation since it is based upon only the larger I.D. TOCC data.

3.4 TOTAL WALL CARBON TO TOTAL CARBON RATIO (TWC/TC)

The ratio of TWC/TC provides another tool for determining if the role of metallurgy is that of a catalytic effect on the bulk insolubles or that of increased affinity of the deposits for the wall surface. Low ratios with high total carbon values would indicate formation of catalytically induced insolubles within the fuel. High ratios with lower total carbon contents would indicate that deposit affinity for the wall surface was the dominating factor. Table 6 summarizes TC values and calculated TWC/TC ratios for Data Set 2.

In general, it appears that for all four TOCC types, the majority percentage of the TC was produced on the tube walls. This finding indicates that while catalysis seems to be a significant factor, the affinity of deposits to adhere to the SS and Al tube walls is essentially equal on a percentage of total carbon basis and for this JP-8 test fuel.

TABLE 6.								
TOTAL CARBON AND TOTAL WALL CARBON TO TOTAL CARBON RATIOS								
Run Temp.	SS 3/16" Rs1 TC		SS 3/8" Rs2 TC		Al 3/16" Ra1 TC		Al 3/8" Ra2 TC	
300°F	0.81	10.4	0.73	1.6	0.89	25.9	0.70	1.5
350°F	0.78	11.6	0.81	3.2	0.78	19.3	0.63	1.7
400°F	0.78	11.9	0.80	3.9	0.77	16.2	0.75	2.5
450°F	0.66	14.3	0.74	3.1	0.54	15.6	0.73	2.1
500°F	0.84	15.3	0.84	3.3	0.55	6.3	0.74	2.0
<div>Note: TC = Total CarbonTW = Total Wall Carbon</div> <div>Rs1 = TC/TW for SS 3/16"Rs2 = TC/TW for SS 3/8"</div> <div>Ra1 = TC/TW for Al 3/16"Ra2 = TC/TW for Al 3/8"</div>								

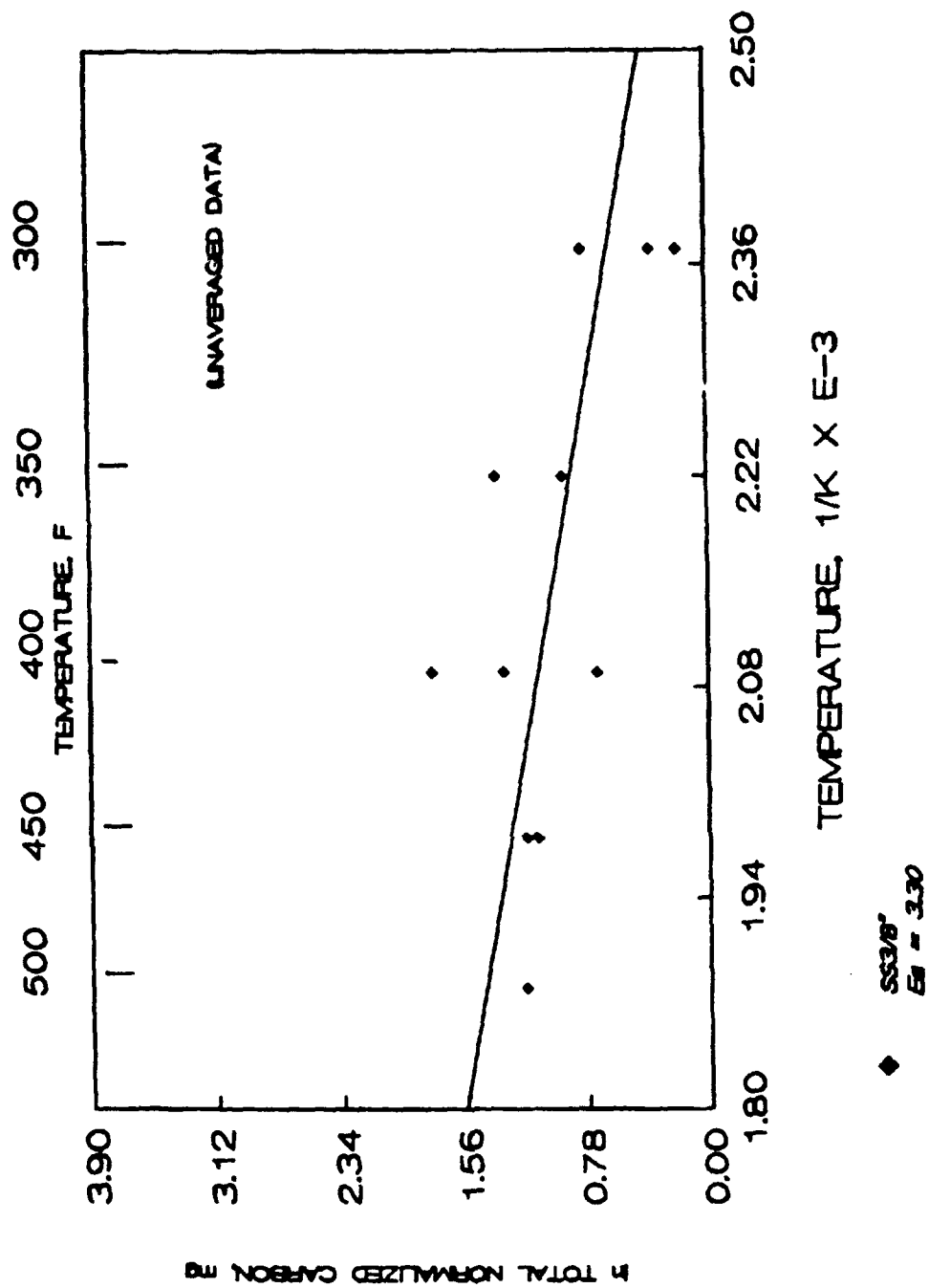


Figure 1. Arrhenius Plot of 3/8" Stainless Steel Total Carbon

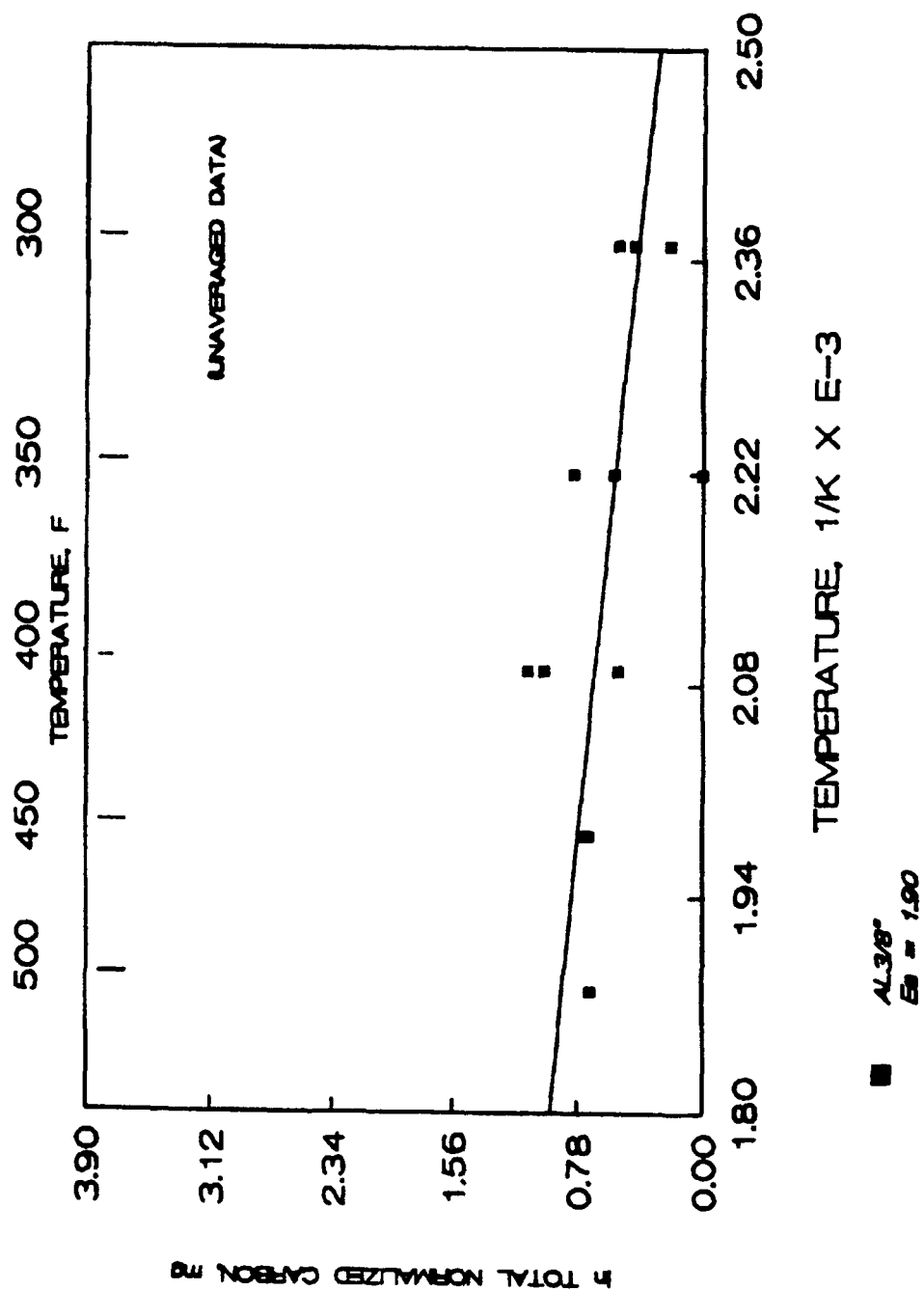


Figure 2. Arrhenius Plot of 3/8" Aluminum Total Carbon

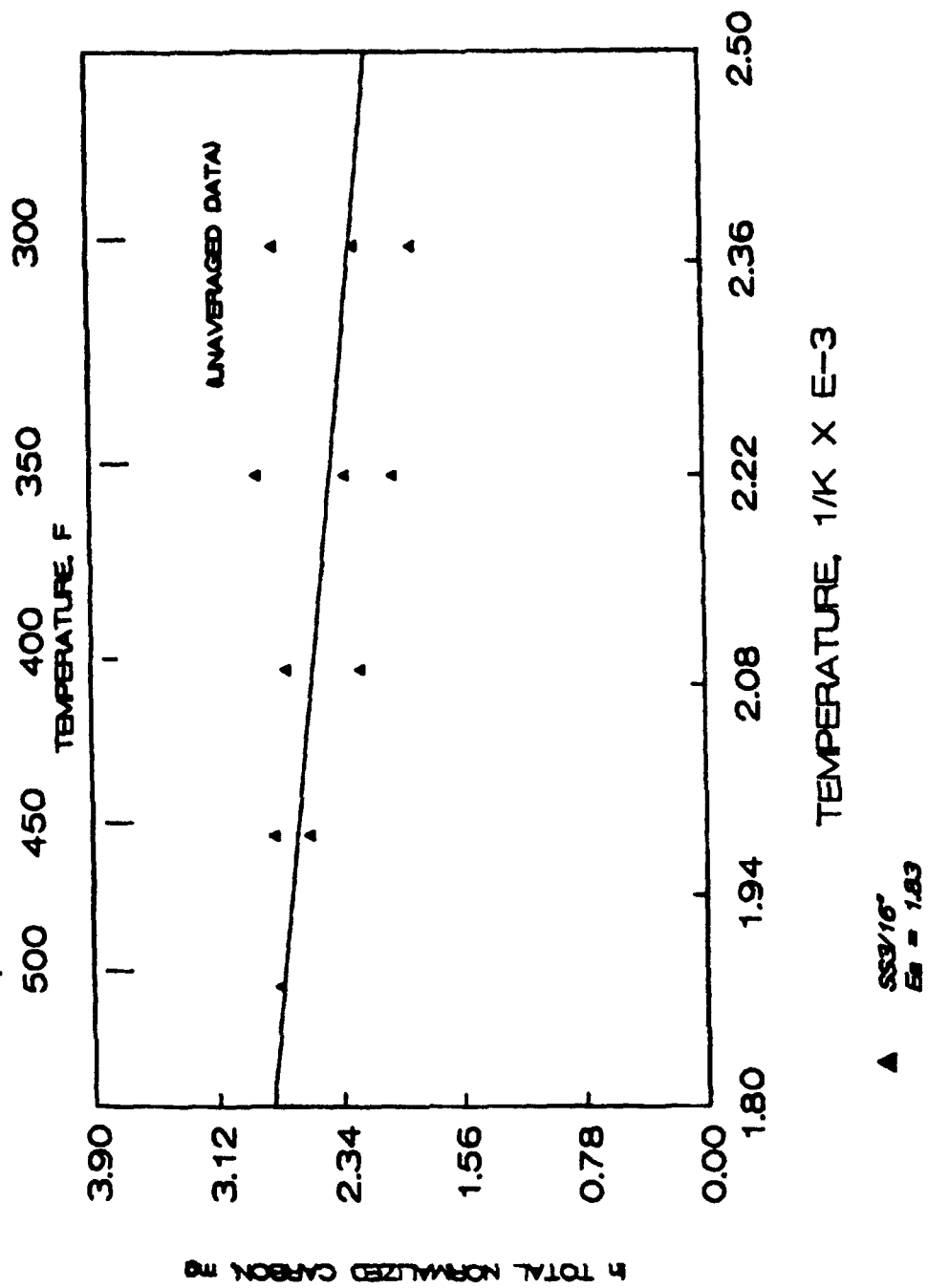


Figure 3. Arrhenius Plot of 316 Stainless Steel Total Carbon

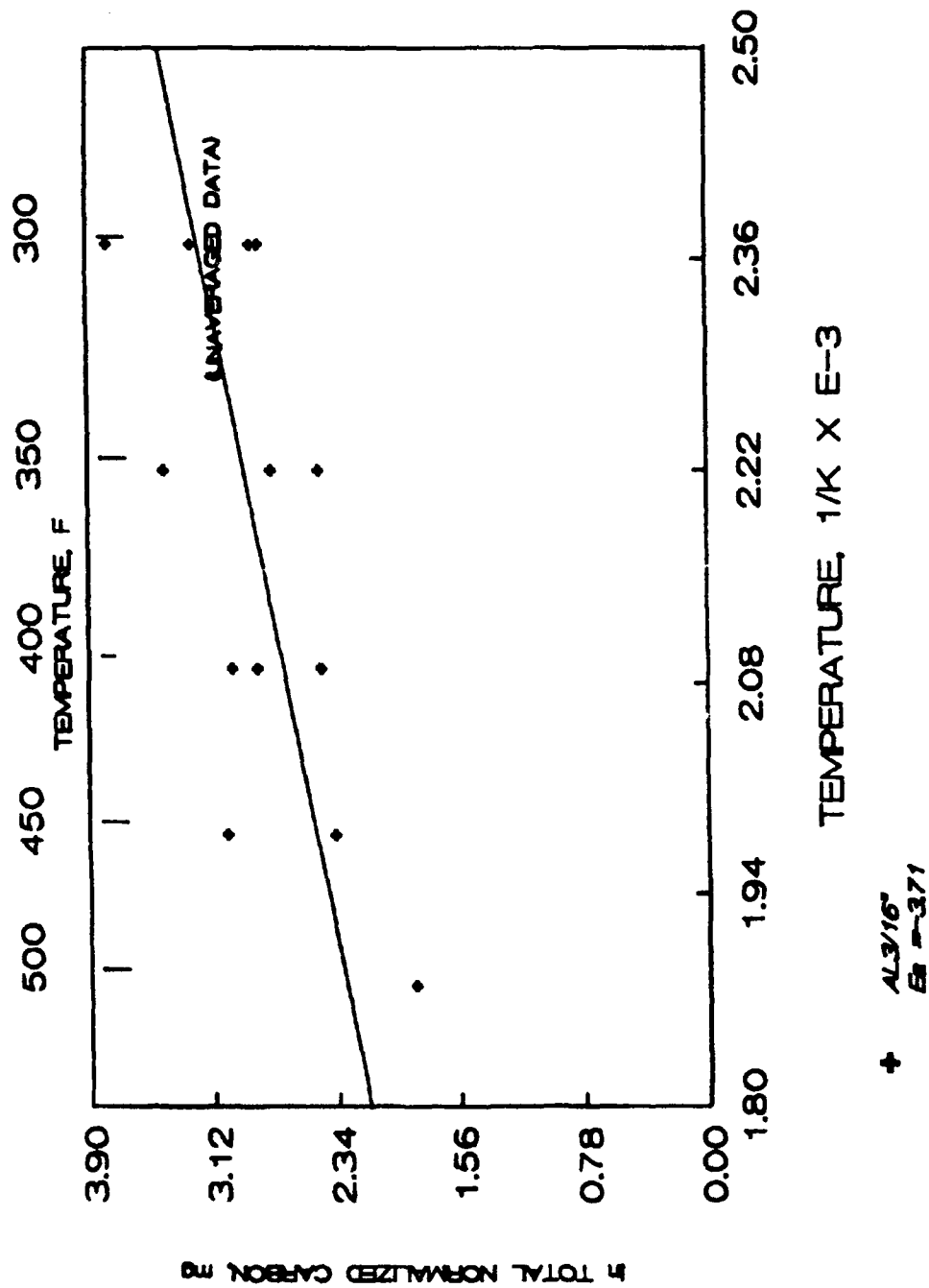


Figure 4. Arrhenius Plot of 3/16" Aluminum Total Carbon

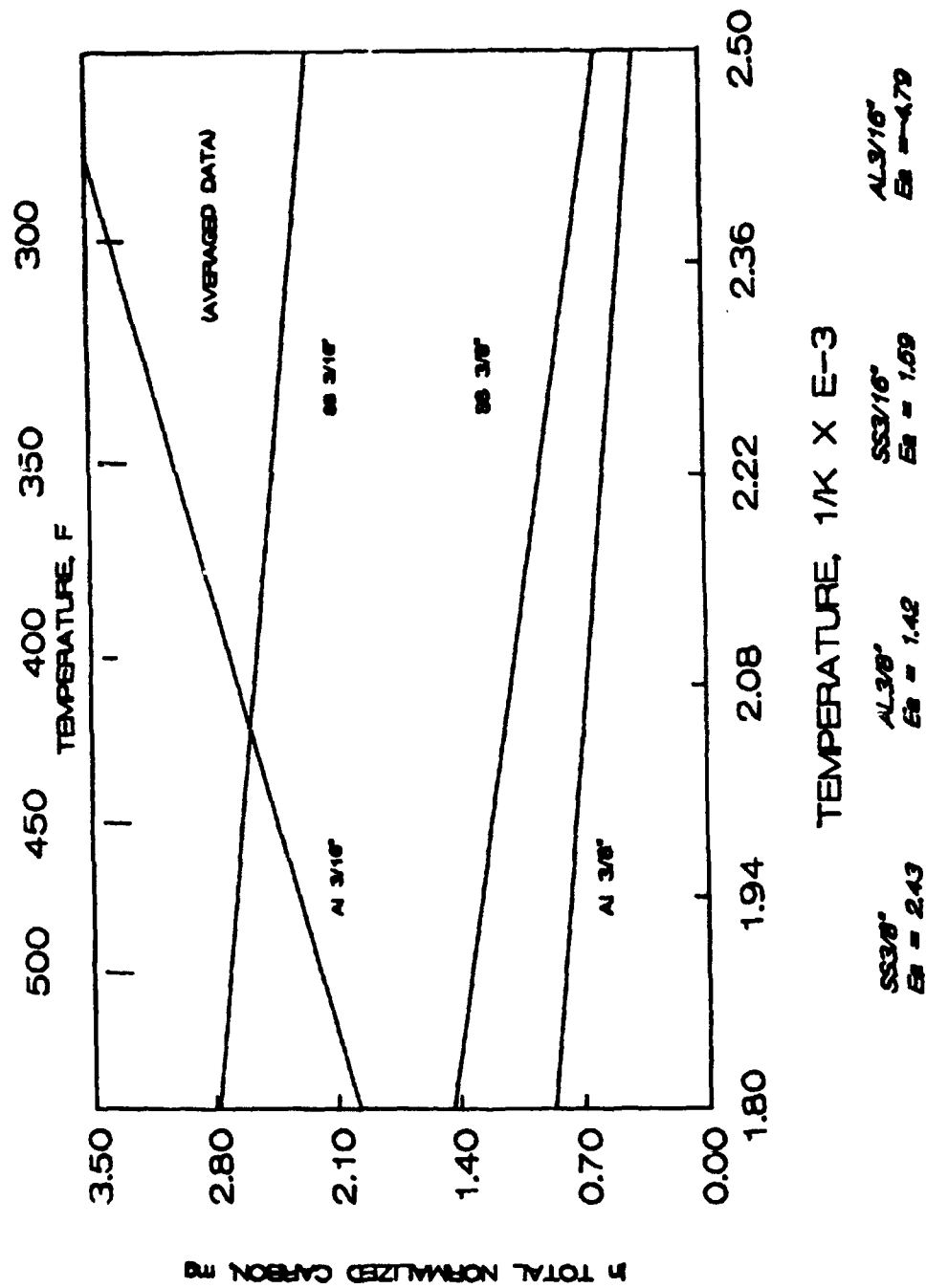


Figure 5. Arrhenius Plot of Composite TOCC

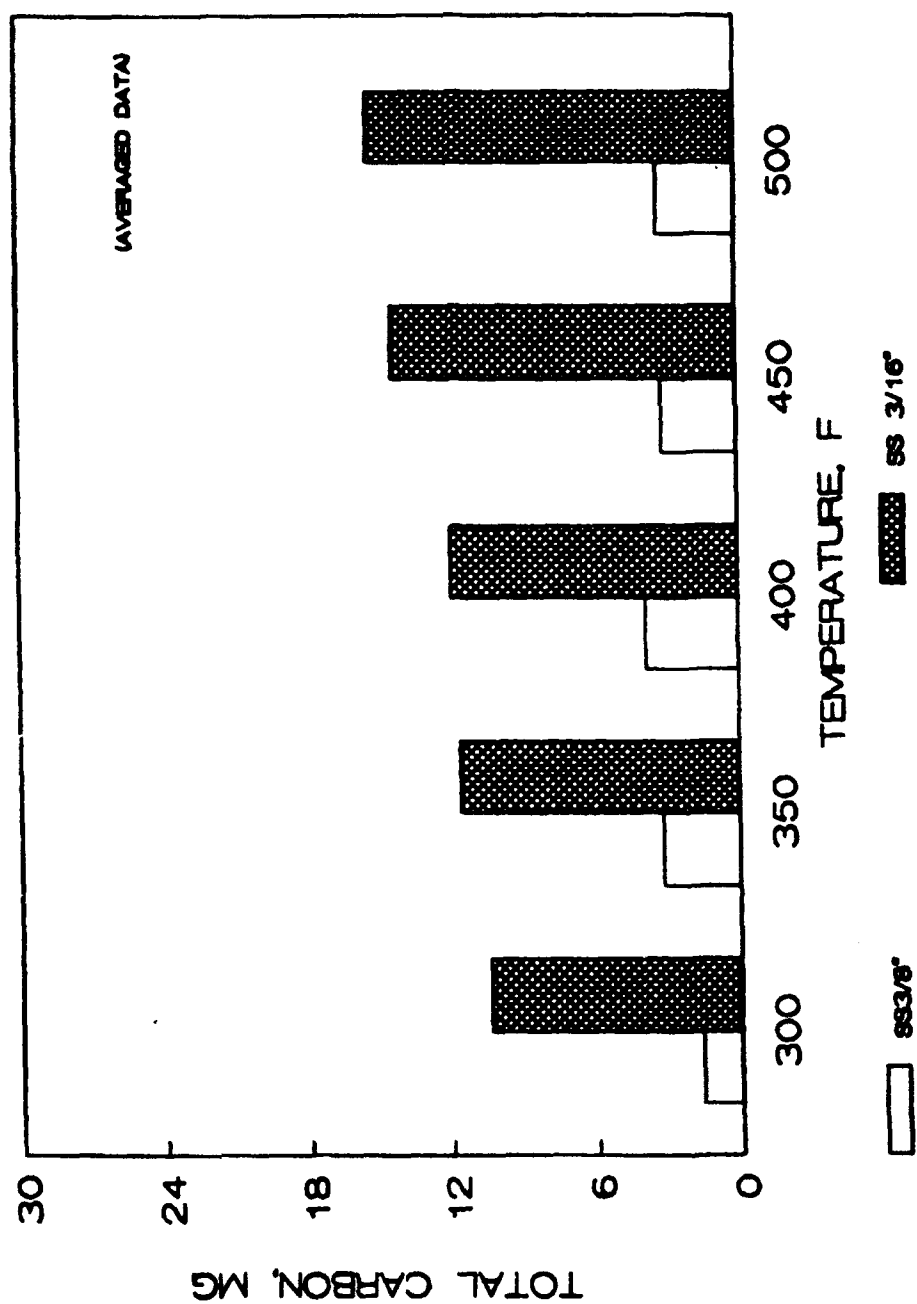


Figure 6. Normalized Total Carbon Comparison of 3/8" Stainless Steel vs 3/16" Stainless Steel

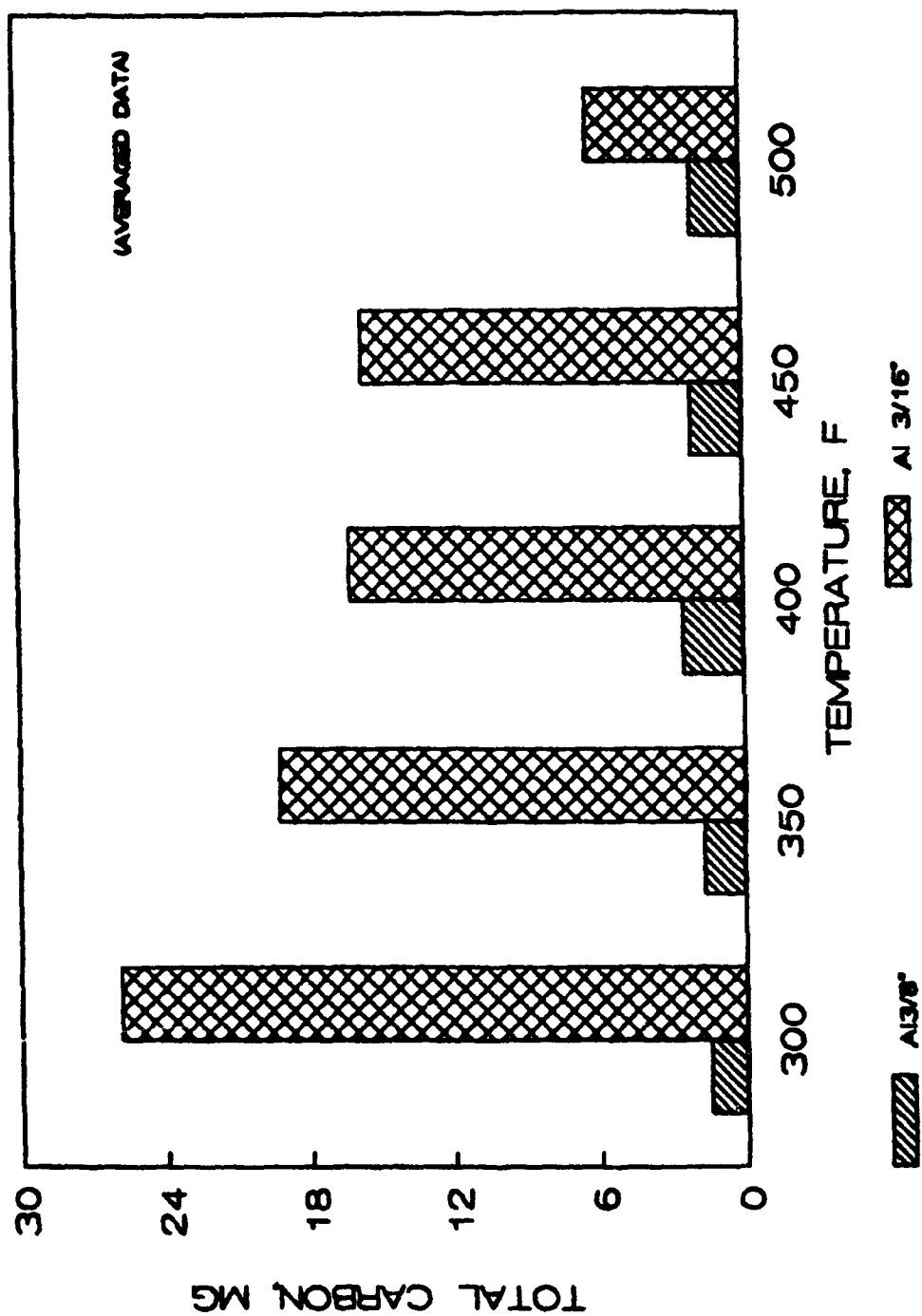


Figure 7. Normalized Total Carbon Comparison of 3/8" Aluminum vs 3/16" Aluminum

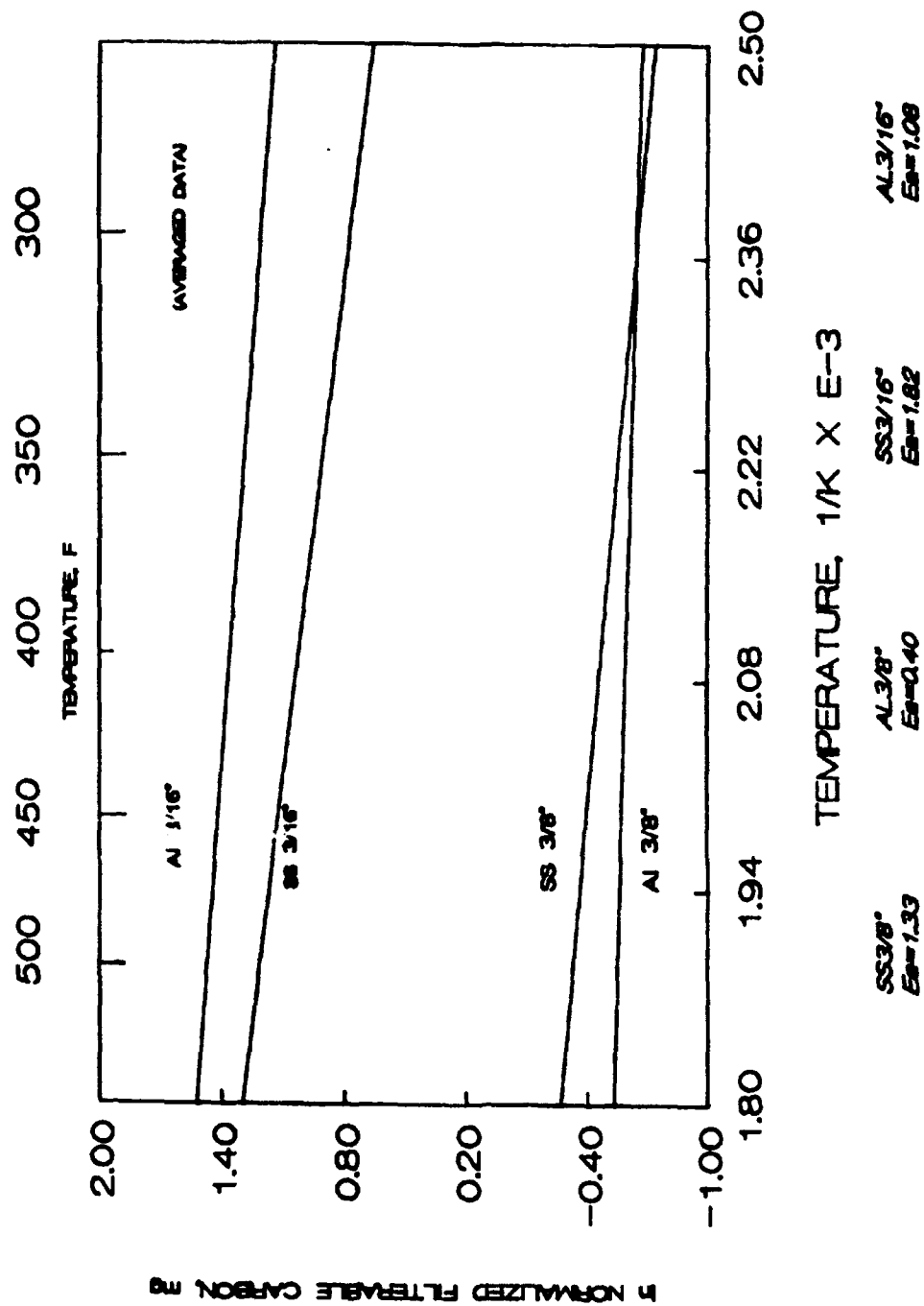


Figure 8. Arrhenius Plot of Filterable Carbon

SECTION 4.0

CONCLUSIONS AND RECOMMENDATIONS

In the static tests performed under this investigation, significantly lower levels of fuel degradation products were produced than that reported in literature for dynamic flowing fuel test rigs. This is attributed to the small sample volumes and limited air available to the TOCC's. However, the amounts were easily determined using the LECO RC412 Carbon Determinator.

Repeatability was not as good as desired. The smaller I.D. Al TOCC experienced the greatest leakage difficulties of the four TOCC types. It may be that the low carbon values contributed to the data scatter, but insidious leakage is also highly suspected.

The role of metallurgy, as indicated by the data in this investigation, appears to be catalytic. Both the small SS and Al TOCC's produced much more carbon than the larger I.D. TOCC's.

Based on the amounts of filterable and tube wall carbon obtained, the calculated activation energies and the TC/TV and TWC/TC ratio analyses for each TOCC type, there appears to be a difference between SS and Al catalytic properties. These differences are most likely mechanistic in nature. However, the data does not allow the determination of which metallurgy is more catalytic. Any future effort using a static closed test cell approach will require further development in reactor design and a review of equipment and techniques available for providing rapid heat up to isothermal conditions.

DESIGN REQUIREMENTS FOR A LABORATORY SCALE THERMAL OXIDATION STABILITY TEST

Period of Performance

22 March 1989 through 11 June 1990

Reference

Task Order No. 16, Topical Report No. 13, June 11, FR 19032-13, T.B. Biddle

Abstract

As the need for a valid thermal stability test becomes increasingly apparent with advanced engines in the design phase, so does the controversy over what a valid test should encompass. There is a need to develop a laboratory-scale device that generates information directly applicable to fuel behavior in a fuel system. Further, it should permit examination of chemical processes occurring in the fuel, yet incorporate the economics, ease of operation and versatility associated with bench-top devices. The objective of this study was to determine the design requirements for such a device. A survey of industry was conducted to assimilate information and transition it into requirements for a meaningful thermal stability test. Sources used in compiling information included industry and military personnel, overhaul and repair depots, research consortiums, and literature.

According to the guidelines of this study, design requirements were to focus on components identified as being most susceptible to fuel thermal stability problems. These components were found to be largely restricted to the hot section of the engine, i.e., fuel injector nozzles, nozzle supports, afterburner spray rings, fuel manifold assemblies, and fuel feeder tubes. Other components within the fuel system were reported as fuel sensitive during the course of the industry and military survey and literature search, but actual cases could not be identified or substantiated. Critical fuel system parameters reported for the hot section included small passage areas, Reynolds number, metal temperature, fuel temperature, and flow rate. The flight conditions most prone to result in thermal stability problems were found to be those involving low fuel flow and high environmental temperatures.

SECTION 1.0

INTRODUCTION

Thermal instability was first identified as a problem in aviation fuels in the 1950's. Since then an understanding of the deposition process has been sought through a variety of small scale test devices, fuel system simulators, and simply designed, closely controlled experiments. Thermal stability continues to be a concern not only because of random, intermittent, problems experienced by field engines, but largely due to the more stringent fuel demands of advanced systems currently under development.

Thermal stability has been recognized as a critical limiting factor in the design of advanced engines. Increased heat loads resulting from increases in lubricant and hydraulic fluid operating temperatures and extensive airframe electronics and hydraulics will rely on the cooling capabilities of the fuel. To accommodate these heat loads, engine hardware designers and fuel developers are faced with developing coke resistant hardware in combination with fuels with greater cooling capacities. It was assumed that development of advanced fuels would keep pace with advances in engine technology. It is now recognized that benefits of programs such as the Integrated High Performance Turbine Engine

Technology Initiative (IHPTET) may be partially offset due to the need for larger recirculating systems to maintain fuel temperatures below their thermal oxidative stability limits.

As the need for a valid thermal stability test becomes increasingly apparent with advanced engines in the design phase, so does the controversy over what a valid test should encompass. This is a complex problem because hardware designers have different fundamental needs than do fuel developers. From the commercial perspective, there is the desire for a simple, inexpensive, quality control test which will ensure that fuels tested as acceptable do not inadvertently result in field problems. Quantitative measurements, and as a result a more complex and elaborate test, are required by researchers involved in hardware design and advanced fuel development. Moreover, some researchers desire a test that duplicates or closely simulates actual engine conditions. Others propose that the device need not duplicate engine parameters. More importantly, it should provide data on a laboratory scale basis which can be used to predict how a fuel will behave in the fuel system. Most widely agreed upon is the desire for a convenient bench-top test using research size sample volumes.

The Jet Fuel Thermal Oxidation Tester (JFTOT) is the most widely accepted small scale laboratory device used to determine the thermal stability of jet fuels. It fulfills most of the requirements for a quality control test and has been used to study many facets of fuel decomposition. The JFTOT, however, is often criticized because of its subjective rating system and lack of direct correlation to fuel performance in an aircraft.

When it becomes necessary to predict fuel performance in an aircraft fuel system, simulators are used. These simulators provide bridges between small-scale devices and actual engine aircraft performance. In addition, simulators provide practical thermal stability information under simulated aircraft conditions. The hardware, environmental conditions, and fuel required by simulators, however, make it expensive and impractical for other than very limited testing.

There is, therefore, a need to develop a laboratory-scale device that generates information directly applicable to fuel behavior in a fuel system. Further, it should permit examination of chemical processes occurring in the fuel, yet incorporate the economics, ease of operation and versatility associated with bench-top devices. The objective of this study was to determine the design requirements for such a device.

SECTION 2.0

STUDY APPROACH

A working outline was generated which focussed on a number of fundamental concerns important in formulating design requirements for a valid thermal stability test. Each of the considerations shown below were explored in an effort to determine which fuel system components should be addressed and which operating parameters are critical and should be included as a design requirement for a thermal stability test. The feasibility of incorporating these design requirements in a test rig was considered. A conceptual configuration for a bench-top test device was formulated within the constraints of the scope of effort.

- Components Most Susceptible to Fuel Thermal Instability
- Fuel System Parameters Typical of Current and Near-Term Advanced Engines
- Critical Fuel System Parameters
- Type of Information Needed by Hardware Designers and Fuel Developers
- Capabilities and Limitations of Current Test Devices
- Collated Design Requirements For A Thermal Stability Test
- Conceptual Configuration of a Bench-Top Test Device

The rationale for this plan of study is discussed briefly in the paragraphs which follow.

2.1 COMPONENTS SUSCEPTIBLE TO THERMAL INSTABILITY

An important first step was to identify fuel system components most susceptible to thermal stability problems. In doing so, it was necessary to discriminate between fuel component problems that were directly related to fuel thermal stability and those which were not actually a consequence of the fuel, but rather the result of a system failure. Approached in this way, needless complications to a conceptual test configuration can be avoided by not addressing a component which in truth had no history of fuel related thermal stability problems. Documented cases that could be directly related to fuel were sought from industry, P&W engine project groups, and military overhaul and repair depots. After establishing in what manner the components identified were affected, an attempt was made to determine the build-up of deposit required to degrade performance.

2.2 FUEL SYSTEM PARAMETERS TYPICAL OF CURRENT AND NEAR-TERM ADVANCED ENGINES

Fuel system parameters were determined for a typical, generic, current engine and a near-term advanced engine. Fuel system parameters for each engine were surveyed at up to five flight conditions. Based on availability and the scope of this program, information such as fuel temperatures, metal temperatures, materials, flow rates, Reynolds numbers, and pressures were compiled to establish actual engine environmental conditions.

2.3 CRITICAL FUEL SYSTEM PARAMETERS

Knowing that it was unlikely that a test could be designed to address all environmental conditions for each component, those conditions considered the most critical in regard to thermal stability were identified.

2.4 TYPE OF INFORMATION NEEDED BY HARDWARE DESIGNERS AND FUEL DEVELOPERS

It is important that a conceptual test design provide information that is meaningful and useful to the user's specific application. The needs and concerns of a hardware designer will be different from that of a fuel developer. The type of information required by each had to be ascertained as well as the form in which the data should be generated. From a fuel system designer's standpoint, meaningful information might include rate of deposition as a function of fuel type; time at temperature; metal and surface finish; fuel flow rate, velocity, and Reynolds number; pressure; and effect of deposit on heat transfer. The form in which the data should be generated, e.g., deposit thickness, volume of deposit, heat transfer coefficients, etc. also was established.

From a fuel developer's perspective, changes in chemical composition as a function of thermal stressing (time and temperature), the influence of functional groups, heteroatomic species, refinery processes, and catalytic activity might be of interest. Determining what type of information was needed by a fuel developer was important in formulating a test design capable of defining relationships in terms of fuel chemistry.

2.5 CAPABILITIES AND LIMITATIONS OF CURRENT TEST DEVICES

A review of the capabilities and limitations of current test devices permitted comparison of what was already readily available to that of the needs of fuel system designers and fuel developers. This activity reviewed what existing rigs tell us, how they work, the fuel system parameters and components they simulate, how sample deposits are evaluated, and how the information is transitioned into hardware design and/or fuel development.

2.6 COLLATED DESIGN REQUIREMENTS FOR A THERMAL STABILITY TEST

Information compiled in the previous sections was collated and reduced to provide a workable approach for arriving at design requirements for a valid thermal stability test. In order to avoid what would turn out to be an elaborately instrumented fuel system simulator (the design of which was not the intent of this program), the input was carefully scrutinized in total then reduced based on conclusions from the following:

- ✓ Which of the most critical fuel system parameters can feasibly be duplicated or simulated in a bench-top configuration ?
- ✓ How would this be accomplished and what type of measurement is required ?
- ✓ What compromises must be made in actual fuel system parameters and direct engine correlation in order to accomplish the goals of an accelerated laboratory-scale thermal stability test using research quantities of fuel ?
- ✓ Can these compromises be made and still provide useful information to fuel system designers and fuel developers ?

2.7 CONCEPTUAL CONFIGURATION FOR A LABORATORY SCALE TEST DEVICE

Information compiled and collated in the previous sections, with emphasis on the most critical of the design requirements, was used to arrive at a conceptual configuration for a bench-top laboratory scale test device.

SECTION 3.0

SOURCES USED FOR COMPILING DESIGN REQUIREMENTS

A number of different avenues were pursued to explore the design considerations discussed in the previous section. The intent was to assimilate information and transition it into requirements for a meaningful thermal stability test. Sources used in compiling information included industry and military personnel, overhaul and repair depots, research consortiums, and literature.

3.1 ASTM/CRC ACTIVITIES

At the onset of this technical effort, ASTM subcommittee J submitted a request to the Coordinating Research Council (CRC) for a research effort to further define the requirements for jet fuel thermal stability. In addition, the request asked for a critical review of test methods for determining whether quality requirements were being met. CRC responded by forming the CRC Ad Hoc Panel on Jet Fuel Thermal Stability Test Methods. This action coincided neatly with the needs of the WRDC activity as it provided a forum for industry input. ASTM's list of concerns and objectives were carefully reviewed by P&W along with a 'strawman' proposal prepared by the Panel Chairman (Jerry Ohm of Boeing). Although fundamental differences exist between the ASTM/CRC quality control objectives and the Air Force's need for an analytical research tool, it was felt that active participation in the panel would permit much common ground information to be funnelled into the Air Force effort.

The CRC Ad Hoc Panel concluded that compiling fuel system parameters was an important first step in accomplishing their specific goals. Consequently, Kurt Strauss, as an independent consultant, was commissioned by the CRC to compile fuel system parameters from engine manufacturers and airframers. The efforts of the CRC and the interests of the Air Force were discussed so as to eliminate as much redundant activity as possible. It was agreed that close contact would be maintained and information shared where ever possible. It was further agreed that it was in the best interest of all parties involved that efforts be coordinated so as to mutually benefit the research and quality assurance communities. The information compiled by Mr. Strauss from the engine and airframe manufacturers was to be presented to the CRC panel in coded form so as not to disclose specific engine models or manufacturers.

At the December 1989 meeting of ASTM, the focus of the Air Force sponsored investigation was presented to members and attenders of the J-08 High Temperature Stability Panel. As a follow-up, a survey and working outline for compiling information was mailed to members of industry experienced and knowledgeable in fuel thermal stability.

3.2 UNITED KINGDOM THERMAL STABILITY STEERING GROUP

The Ministry of Defense (MOD) Thermal Stability Steering Group in the United Kingdom was consulted in regard to reported activities paralleling the CRC research program. Richard Clark (Shell Research), chairman of the UK Thermal Stability Steering Group, disclosed that while a similar study to that of CRC's had been proposed by the Steering Group, only Shell was willing to commit manpower to accomplish the effort. Consequently, Shell is pursuing its own thermal stability program on a proprietary basis. Shell Research's main thrust is in continued development of a laboratory-scale test rig which incorporates turbulent fuel flow into its design. Minutes from the UK Steering Group meeting were reviewed for insight into the UK perspective.

Bryan Rayner of Rolls Royce, who is a frequent liaison between MOD and the U.S., advised that Rolls Royce was currently working on a test configuration which will act as a bridge between bench-top thermal stability rigs and fuel system simulators. This is needed to qualify bench-top rigs based on

correlations to engine tests. Mr. Rayner was not at liberty to disclose further details of the Rolls Royce effort.

3.3 P&W PROJECT GROUPS

Project Groups within P&W, including 'Combustion Design', 'Mechanical Components and System Design', and Engine Controls' were commissioned with the task of compiling fuel system parameters for a typical current and near-term advanced engine.

3.4 OVERHAUL AND REPAIR DEPOTS

Air Logistics Centers (overhaul and repair facilities) at Tinker Air Force Base, Oklahoma City, OK and Kelly Air Force Base, San Antonio, TX were contacted to identify fuel system components that exhibited coking problems in the field. Components were reviewed on the basis of evidence of deposits at regular scheduled tear-down intervals, and problems which resulted in unscheduled maintenance. In addition, P&W Customer Support International Offices in Saudi Arabia, Pakistan, Venezuela, Korea, Israel, and Japan were contacted concerning thermal stability related component failures.

3.5 INDUSTRY AND MILITARY SURVEY

The working outline discussed in Section 2.0, describing important considerations in the design of a thermal stability test, was expanded upon and presented to industry and the military in the form of a survey. The survey consisted of an outline structured to capitalize on industry's experience relating to sensitivity of engine components to fuel thermal instability. A follow-up letter to the survey requested the components identified be based on first-hand knowledge rather than hear-say, i.e., documented malfunctions and failures due to deposit formation directly related to the fuel. In addition, the survey sought to determine critical fuel system parameters and design features which should be incorporated into a laboratory scale test rig.

Those receiving the outline included, but were not limited to, members of the CRC Ad Hoc Panel on Fuel Thermal Stability Test Methods, WRDC, the Naval Air Propulsion Center (NAPC), the Naval Research Laboratory (NRL), United Technologies Research Center (UTRC), and P&W combustion and component design groups. A copy of the survey and distribution is contained in Appendix A. Personal telephone contacts and a follow-up letter urged participation by industry in this effort. Twenty-eight survey responses were received out of the forty-two individuals and organizations solicited for input.

3.6 LITERATURE SEARCH

In addition to the industry and military survey, a literature search was performed to further investigate the design considerations discussed in Section 2.

SECTION 4.0

STUDY RESULTS

Input received from industry and the military, and information compiled from foreign Air Force bases, U.S. overhaul and repair depots and P&W Project Groups are summarized in the paragraphs which follow.

4.1 FUEL SYSTEM COMPONENTS AFFECTED BY THERMAL STABILITY

The Air Logistics Centers (overhaul and repair depots) contacted reported that tear-down inspections are performed at regular scheduled intervals. Deposits are regularly observed on the following fuel wetted components: fuel feeder tubes, fuel manifold assemblies, main burner nozzles, nozzle support assemblies, augmentor nozzle actuators, and augmentor spray ring and spray bar assemblies. Thermal stability related field problems resulting in unscheduled maintenance are rarely encountered.

One overhaul and repair depot reported that, in general, minor coking is tolerated and corrective action is not taken until such time as the component fails a bench-type flow test. The second overhaul depot advised that parts are cleaned immediately upon evidence of coking or deposits, flow checked, recycled through cleaning if required, and then flow checked a second time. The parts are condemned if they do not pass the second flow check. Coke removal is typically accomplished by flowing hot (~200°F) alkali permanganate through the component, followed by a mild acid rinse, a water rinse, then air dried. Manual scrubbing is often required using a variety of solvents, wire brushes and reamers. The parts most difficult to clean are the fuel manifold assemblies and fuel nozzle supports.

P&W Program Managers and Customer Support Groups responsible for maintaining product integrity and resolving engine hardware and fuel related problems for the air forces of Saudi Arabia, Pakistan, Venezuela, Korea, and Japan report no instances of thermal stability related problems. One customer reported experiencing thermal stability problems with the No. 1 through 5 augmentor spray ring; the No. 3 spray ring being the most susceptible to coking. It is suspected that this customer's more demanding flight missions contribute to spray ring coking.

P&W Project and Support Groups (Mechanical Components, Combustion Design, and Engine Controls) associated thermal stability problems with fuel nozzles, fuel feeder tubes at the nozzle support assembly, augmentor spray rings and spray bars. Fouling of the fuel/oil heat exchanger is an extreme rarity; possibly, in part, because it is located upstream of the hottest fuel temperatures. Historically, only one instance of fuel/oil heat exchanger fouling has been documented at P&W. It's been P&W's experience in general, that fuel controls, pumps, and filters are not affected because the design of the system limits the temperature they can reach. Occasional system failures, e.g., seal leaks or line leaks, allow enough hot engine air to leak past a fuel system component to result in local over heating and excessive coke formation. This is an anomaly and not a typical system problem. While P&W has not experienced fuel control or filter problems in normal operation, other sources within industry reported occurrences.

In response to the survey (which requested first-hand knowledge), industry reports the following components to be affected by thermal stability: fuel/oil heat exchangers, fuel injector nozzles, nozzle support assemblies, fuel controls, fuel filters, fuel feeder tubes, fuel manifold assemblies, augmentor spray rings and spray bars, and augmentor nozzle actuators. Literature cited many of the same components. In addition, one airframer cited the compressor inlet temperature (CIT) sensor, and the variable bleed valve (VBV) gear motor. It is generally believed that the problem of fuel decomposition normally occurs downstream of the engine pump and becomes progressively worse as the fuel progresses toward the point of injection.

The manner in which fuel components are affected and tolerance levels, where available, are summarized in the paragraphs which follow.

◆ *Fuel Controls*

In the fuel control, which is generally downstream of the fuel/oil heat exchanger, heated fuel passes through many close clearance valves and actuators in the servo system. Flow is quite low, sometimes resulting in long residence time at high temperature. Fuel derived deposits, lacquer, or gum can form on sliding surfaces causing sticking and result in malfunction of the fuel metering system. Throttle stagger and unstable idle can be a consequence. In the fuel control, problems can result from deposits less than 0.001 inch thick.

◆ *Fuel Filters*

Fuel-derived deposits can plug filters and reduce fuel flow. Instances of filter clogging with a gelatinous substance have been reported to be the consequence of thermally unstable fuel.

◆ *CIT Sensor*

Temperatures shift due to screen clogging.

◆ *VBV Gear Motor*

Seizure due to sticky film.

◆ *Fuel/Oil Heat Exchangers*

Although rarely encountered, coking can cause heat transfer effectiveness to degrade which can result in higher oil temperatures. Pressure drop across the heat exchanger also increases with coking. Tolerance levels for fuel/oil heat exchangers are not well known. Any amount of deposit build-up degrades heat exchanger performance. Heat exchangers are normally over-sized so that the thermal performance is acceptable even with some deposits and/or scaling. The increased pressure drop tends to improve heat transfer which partially offsets the decrease in effectiveness due to the deposits.

◆ *Fuel Injector Nozzles*

Deposits affect fuel spray pattern and flow rate. Fuel nozzles for modern engines typically consist of a variable area metering valve, stem, and fuel injection tip. Sufficient deposit build-up in any of these areas can degrade nozzle performance. The distribution valves are usually sliding spool devices. The spool is lapped to the bore with a diametral clearance on the order of 0.0002 inch. Thus, virtually any build-up of hard deposit would inhibit spool movement and cause significant deviation from design flow schedules. Softer deposits may be scraped away during normal movement of the spool.

The stem, which carries fuel from the valve to the nozzle tip, typically has passages on the order of 0.188 inch diameter. Therefore, significantly larger deposits can be tolerated without significant restriction. Of greater concern, however, is the flaking of these stem deposits and subsequent plugging of the nozzle tip. Minimum passage dimensions in the tips are held to 0.020 inch or larger in most fighter and transport engines, but the allowable stem deposit thicknesses cannot be defined due to the random nature of flaking. In the tip, the 0.020 inch or larger minimum passage dimension applies to pressure atomizing components such as the primary nozzle in a hybrid airblast or high shear injector. The secondary passages in these tips are relatively large, and a deposit build-up on the order of 0.005 to 0.010 inch would cause a 10 % reduction in flow which is ample cause for replacement of the nozzle.

◆ *Fuel Manifold Assemblies*

Fuel manifolds under normal operating conditions seem to develop fuel fouling only after long periods of service. This is probably due to their position in a moderate temperature regime directly upstream of the fuel nozzles. Varnish builds up over time to cause reduced fuel flow.

◆ *Fuel Feeder Tubes*

Fuel feeder tube fouling appears to only occur where these tubes enter elevated temperature environments. Fuel feeder tube points of connection to augmentor spray rings have been found to be frequent sites of fuel fouling. Evidence suggests that during periods between augmentation, when fuel handling hardware temperatures peak, the residual static fuel in this hardware thermally degrades and forms coke deposits.

◆ *Augmentor Spray Rings / Spray Bars*

The design and position of this hardware within the augmentor environment seem to affect coking rates. Spray ring designs which use fuel pressure actuated spray valves ('pintles') tend to foul more than spray rings using an open orifice design. The spray ring's position in the thermal environment (i.e. core or duct air streams) seem to be a factor as well. Pintle type spray rings exposed to duct air stream tend to foul most often. Apparently, residual fuel trapped in these rings form small amounts of deposit. With each augmentor cycle, more deposits build-up until the spray ring becomes substantially fouled.

◆ *Augmentor Nozzle Actuators*

Actuator fouling may be related to the formation of varnishes and gums rather than crystalline type carbon deposits. Fine orifices coupled with long fuel residence times contribute to the problem.

In summary, the components cited by industry, military, overhaul centers, foreign air bases, P&W Project groups, and literature as the most frequently plagued by thermal stability problems are fuel feeder tubes at the nozzle support assembly, fuel nozzles, and augmentor spray rings and spray bars. These components show performance degradation directly related to fuel thermal instability. Components such as fuel controls, actuators (with fuel used as the hydraulic fluid), and fuel/oil heat exchangers have had problems due to fuel degradation, but the problems seem to be rare, transient, and illusive in nature.

4.2 FUEL SYSTEM PARAMETERS TYPICAL OF CURRENT AND NEAR-TERM ADVANCED ENGINES

Fuel system temperatures were determined for a typical current and near-term advanced engine by the P&W Component Design Technology Group. Thermal management models for IHPTET Phase II and III engines were unavailable at this writing. Table 1 shows fuel temperatures representative of current technology engines at five different flight conditions. Table 2 shows fuel temperatures representative of a near-term advanced engine at four different flight conditions. Fuel residence times for a near-term advanced engine are shown in Table 3.

Additional fuel system parameters were compiled or derived for the following specific components:

◆ *Developmental Engine Heat Exchanger*

The following heat exchanger data were generated for a development engine cruise condition: Including recirculation, 53 lb/minute of fuel enters the heat exchanger at 257°F and exits at 298°F. Oil in and out temperatures are 320°F and 296°F, respectively. Tube temperature is close to 300°F. The heat exchanger contains 319 aluminum U-shaped fuel tubes with an average diameter of 0.072 inches. Pressure is approximately 1500 psi. Flow velocity is 2.38 ft/second which yields a fuel residence time in the tubes of less than 1 second.

◆ *Hot Section For Near-Term Advanced Engine*

Typical hot section parameters are shown in Table 4 for a near future engine. The minimum and maximum values shown were generated from conditions over the entire flight envelope. These values were derived from an analysis of nozzle flow passages in both the primary and secondary circuits of a typical fuel nozzle. The primary fuel circuit usually sees relatively small fuel flow rates (0.42-1.3 Lb./min. per nozzle), and, hence low velocities and Reynolds numbers. The secondary circuit, however, can flow up to 22 Lb./min. per nozzle, providing much higher nozzle velocities, heat transfer rates and Reynolds numbers.

The primary fuel circuit is always used and provides good droplet atomization at low fuel flows. At higher fuel flows, the secondary circuit kicks in (usually around 100-115 psi difference) and eventually supplies virtually all of the fuel flow at higher nozzle delta P's. Note that the items asterisked are those considered the most critical with regard to thermal stability by the P&W Combustion Design Group. Specific values at the critical flight points (high Mach number, high altitude) are shown in Table 5.

◆ *Main Burner Nozzle Materials For Near-Term Advanced Engine*

Main burner nozzle materials for a near-term future engine are shown in Table 4.

◆ *Fuel Pump And Fuel Control Materials For Typical Current Engine*

Castings are typically made of C-355 and CO-356 aluminum. Internal parts are AMS 5616, 5735, 5688, 5630, AISI 410, CPM 10-V and other similar material.

◆ *After Burner Spray Ring/Spray Bar Materials For Current And Near-Term Advanced Engines*

After burner spray rings/spray bars in typical current engines are made of Waspaloy. Near-term advanced engine spray rings will be made of Inco 625 (high nickel alloy).

4.3 CRITICAL FUEL SYSTEM PARAMETERS

The fuel system parameters widely agreed upon as being among the most critical were time, temperature and pressure. Of these, fuel system pressures are considered the easiest to simulate. Pressure is very important since high fuel temperatures resulting from increasing heat loads in air vehicles may result in two-phase and/or supercritical conditions. These high fuel temperatures will make it difficult, if not impossible, to trade time for temperature in test devices. Thus, it may become necessary to operate the test device at actual temperatures which will result in very long test times unless a very sensitive means of measuring decomposition is developed.

Flow rate, velocity, and Reynolds number were also considered very important. Deposit erosion, variations in average fuel temperature, and extent of deposition can be affected by these parameters and can be very significant in trying to use results from a test device to predict fuel performance in fuel

system components with widely varying conditions. The thing that makes it difficult to simulate these parameters is that all are important and to simulate all three you would have to vary the cross-sectional area of the test device in addition to varying the flow rate.

Materials exposed to the fuel can be very important due to the catalytic effect. Simulating or duplicating the material type can be very difficult or relatively easy depending on the design of the test device. For example, it is difficult to change materials in a test device that is heated by passing current directly through a test section due to wide differences in resistivity of the materials. Conversely, it is easy to change materials in static test devices that are heated externally.

TABLE 1
TYPICAL CURRENT ENGINE THERMAL MANAGEMENT SYSTEM
MAXIMUM FUEL TEMPERATURES, °F

<i>Flight Point</i>	<i>Ground Idle</i>	<i>Loiter</i>	<i>Subsonic Cruise</i>	<i>Supersonic Dash</i>	<i>Idle Descent</i>
Engine Fuel Pump Exit	250	200	260	160	255
Fuel/Oil Cooler Exit and Into Gas Generator	290	245	320	220	*350

* Highest temperature during transient condition. Derived from a series of steady state conditions. Transient model not available.

TABLE 2
NEAR-TERM ADVANCED ENGINE THERMAL MANAGEMENT SYSTEM
FUEL TEMPERATURES, °F

<i>Flight Point</i>	<i>Ground Idle</i>	<i>Loiter</i>	<i>Subsonic Cruise</i>	<i>Supersonic Dash</i>
Main Fuel Pump Exit	305	295	260	210
Fuel/Oil Cooler Exit and Into Gas Generator	320	325	300	270

Maximum fuel temperature of 325°F is maintained by recirculation system

TABLE 3
NEAR-TERM ADVANCED ENGINE THERMAL MANAGEMENT SYSTEM
COMPONENT RESIDENCE TIMES, SECONDS

<i>Flight Point</i>	<i>Ground Idle</i>	<i>Loiter</i>	<i>Subsonic Cruise</i>	<i>Supersonic Dash</i>
Main Fuel Pump	1.4	0.9	0.6	0.5
Fuel/Oil Cooler	1.4	0.9	0.6	0.5

TABLE 4
HOT SECTION FOR NEAR-TERM ADVANCED ENGINE OVER ENTIRE ENVELOPE

	<i>Minimum</i>	<i>Maximum</i>
Fuel Passage Diameter (inch)	0.02	0.188
Flow Velocities (ft/sec)	0.1 (stem)	150(stem)
Reynolds Number	45 (stem)	886,000(stem)
Fuel Residence Time (sec)	0.02	1.80
Fuel Temperature (°F)	200	325
Metal Temperature (Wetted Surfaces) (°F)	200	400
Pressures (psia)	30	1200

Fuel Passage Materials: 347 SS, Hastelloy X, Stellite 31, 440C SS
 Fuel Filter Materials: 304 SS, 321 SS, 347 SS
 Fuel Filter Pore Size: 380 micron total flow; 117 micron primary flow
 Fuel Filter Area: 0.9 - 1.0 sq. in.

TABLE 5
HOT SECTION FOR NEAR-TERM ADVANCED ENGINE AT CRITICAL FLIGHT POINTS

	<i>Primary Circuit</i>	<i>Secondary Circuit</i>
* Minimum Fuel Passage Diameter	0.02	0.05
Flow Velocity (at min. dia., ft/sec)	90	20
* Reynolds Number (from above values)	25,000	14,000
Fuel Residence Time in Nozzle (sec)	1.5	1.6
Fuel Temperature Entering Nozzle (°F)	300	300
* Metal Temperature (°F)	350	400
Pressure difference (psi)	135	135
* Nozzle Flow Rate (Lb./min.)	0.75	1.07

* Represents worst case coking conditions. Although not the highest fuel temperatures, under these conditions experience the hottest wall temperatures (walls are insulated).

4.4 FLIGHT CONDITIONS AFFECTING COMPONENTS SENSITIVE TO FUEL THERMAL STABILITY

Fuel thermal stability problems generally arise during flight conditions involving high fuel temperatures and high nozzle environmental (metal) temperatures. For engines without recirculating flow, these conditions typically occur at high altitude flight points at augmented and non-augmented conditions. Fuel temperatures at the nozzle inlets are high at the upper left hand corner of the flight envelope at low Mach numbers where engine burn flow is low. They are also high at the upper right-hand corner of the envelope at high Mach numbers where inlet air to the engine is aerodynamically the hottest.

For engines requiring recirculating fuel systems, high fuel temperatures typically occur during steady state cruise between 0.5 and 0.8 Mach number from low altitude (sea level) to high altitude (>50,000 feet). High nozzle environmental temperatures generally occur at high Mach numbers. Augmented/military power points above cruise power are of short duration. They will have higher total fuel flows and thus reduced fuel temperatures entering the nozzle.

The relationship between altitude and Mach number to fuel temperature and metal temperature can be described as follows: Fuel temperature goes up as fuel flow goes down. Increasing altitude decreases fuel flow for a given throttle setting, thereby raising fuel temperature. Increasing Mach number at a constant altitude requires a higher throttle setting which increases fuel flow and decreases temperature. Increasing Mach number also raises ram air temperature and causes nozzle environmental temperature to rise.

Altitude reduces engine fuel flow rate as the mass of air pumped by the engine decreases with air density. As fuel flow decreases, the fuel heat sink capacity decreases and heat rejected from fuel system components, lube system, and avionics to a smaller heat sink results in a higher temperature rise of the fuel. In general, the smaller the heat sink becomes, the higher the temperature of the sink becomes. For recirculating flight engines, recirculation flow is used to increase the heat sink capacity which carries away heat in order to avoid high fuel temperatures. Recirculation systems result in higher tank temperatures and system weights.

For non-recirculating flow engines, the following summarizes the effect of altitude and Mach number on fuel flow and fuel temperatures.

- Condition: High Altitude/High Mach Number

Result: Moderate fuel flow ----> Moderate fuel residence time ----> High fuel temperatures ----> High nozzle temperatures ----> Potential for thermal stability problems

- Condition: High Altitude/Low Mach Number

Result: Low fuel flow ---> Increased fuel residence time ---> High fuel temperatures ---> Low nozzle temperatures ---> Potential for thermal stability problems

- Condition: Low Altitude/Low Mach Number

Result: High fuel flow rates ---> Decreased fuel residence time ---> Low fuel temperatures ---> Low nozzle temperatures ---> Little potential for thermal stability problems

- Condition: Augmented Power Points

Result: High fuel flows ---> Decreased fuel residence time ---> Low fuel temperatures ---> High nozzle temperatures ---> Some potential for thermal stability problems

For recirculating flow engines, the following summarizes the effect of altitude and Mach number on fuel flow and fuel temperatures.

- Condition: High Altitude/High Mach Number

Result: Moderate fuel flow ----> Moderate fuel residence time ----> Relatively high fuel temperatures ----> High nozzle temperatures ----> Potential for thermal stability problems

- Condition: High Altitude/Low Mach Number

Result: Low fuel flow ---> Increased fuel residence time ---> High fuel temperatures ---> Low nozzle temperatures ---> Potential for thermal stability problems

- Condition: Very Low Altitude (<5000 feet)/Very Low Mach Number(<0.3)

Result: High fuel flow rates ---> Decreased fuel residence time ---> Low fuel temperatures ---> Low nozzle temperatures ---> Little potential for thermal stability problems

- Condition: Low Altitude/High Mach Number

Result: High fuel flow rates ---> Decreased fuel residence time ---> Low fuel temperatures ---> High nozzle temperatures ---> Little potential for thermal stability problems

- Condition: Augmented Power Points

Result: High fuel flows ---> Decreased fuel residence time ---> Low fuel temperatures ---> High nozzle temperatures ---> Some potential for thermal stability problems

The highest fuel temperatures are normally experienced on an idle descent. Although the time is short at each altitude, the cumulative time could be 10 to 30 minutes or longer. During idle descent, Mach number is low, altitude is high, fuel flow is low, residence time is high, and fuel temperature is high. Component temperature reflects fuel temperature and would be high, although ambient temperature would be low.

Loiter also results in prolonged high fuel temperature. Loiter is similar to the above except fuel flow is higher and the condition is sustained for longer periods of time. Loiter usually occurs at the lowest throttle setting and fuel flow rate that will allow the aircraft to sustain the desired altitude.

For engines without recirculation flow, the aircraft can fly indefinitely without adverse effects below a maximum altitude boundary. The boundary is fixed by maximum fuel temperatures of 325°F and maximum engine oil supply temperatures of 330°F. At altitudes above the boundary, flight is time limited. Experience has shown that there is no adverse effect during the time-limited flights. This altitude limit could be raised if the cause of fuel deposits and breakdown was better understood.

In addition to the above discussion, an interesting condition has been observed which accelerates coke buildup. This condition was noticed during the course of a P&W program which required ongoing visual inspection of coked regions of augmentor spray rings. The visual observations were related to specific engine conditions experienced during test and in the field. The observations indicated that only minimal lacquering takes place during fuel flow. The lacquering is the consequence of long time exposure to temperature and is, in itself, of little significance. In a typical military flight scenario, fuel is heated as it travels through the fuel system on its way to the combustor and/or augmentor to be burned. Generally, the fuel flow rate is high enough to limit serious fuel decomposition. However, during flight when the augmentor is shut off, spray ring temperatures rise considerably, going from about 350°F (177°C) to 1000°F (538°C) and higher in some areas. The fuel left in these rings boils as a result of the soak-back temperatures and, with no where to go, degrades rapidly to form insoluble 'sticky' products. The same scenario occurs in the combustor fuel nozzles at engine shut down. Since the augmentor is cycled on and off more frequently than the engine is, it is understandable that the augmentor fuel plumbing would have a higher coking rate than the combustor fuel nozzles.

Manifold drain valves which open when the engine or augmentor is turned off and rapidly drains the fuel out of the hot manifolds and nozzles has been an historical solution to this problem. However, environmental considerations and the need to eliminate augmentor cancellation "signature" has eliminated or degraded the benefits of the manifold drain valves.

Another troublesome condition occurs in engines using duplex fuel nozzles and separate feed manifolds. The fuel "split" is normally controlled by an externally mounted flow divider valve. As the flow rate approaches the transition point where the second manifold begins to flow, the flow divider schedules a very low or essentially a leakage flow into the secondary feed line and nozzle. The flow is very low, almost zero, and boils off almost as fast as it leaks which forms the same heavy deposits as noted in the spray rings and feed tubes of the augmentor.

Similar deposits occur in fuel operated valves which control hot engine air flow where fuel is on one end of a shaft and hot air is on the other. Heat transfer down the shaft can form heavy coke deposits on the fuel-wetted end of the shaft. If the seal leaks, a similar buildup occurs on the air side.

4.5 TYPE OF INFORMATION NEEDED BY FUEL SYSTEM DESIGNERS AND FUEL DEVELOPERS

Input from fuel users, fuel system designers, and fuel developers ranged from the general to the specific. Within the hardware design and the fuel developer constituencies, respectively, there was general agreement in the type of information that is needed. Conflicting views, however, were apparent in the constraints under which the information would be truly meaningful. One point of view argued that in order for the data to be meaningful, the fuel system environment should be duplicate in a test rig. The other point of view emphasized that the test need not duplicated engine conditions, but need only to provide data on a laboratory scale which can be used to predict how a fuel will behave in the fuel system.

The following paragraphs describe both in general and specific terms, the type of information perceived as important to the fuel system designer and fuel developer as related through industry and military input. These are contributors thoughts and should not be construed as final conclusions of the study.

Fuel Users

From a fuel user's point of view, a thermal stability test rig should indicate which fuels are acceptable, and more importantly which are not.

Hardware Designers

A fuel system designer needs to be able, given the conditions within the entire fuel system, to predict the performance degradation of each component as a function of time for various flight profiles. This cannot be accomplished considering only the conditions within individual components since preconditioning of the fuel upstream of the component can have a significant impact on the extent to which the performance of the component is affected.

From a hardware designer's point of view, a test rig should indicate the maximum fuel and surface temperatures which can be tolerated to provide trouble free operation given conditions of surface material and finish, Reynolds number, velocity, residence time, pressure, and heat transfer. In brief, the test rig results should be relatable to what actually occurs in an engine.

A test rig is desired which will permit evaluation of thermal stability characteristics of fuels over a wide range of temperature, hydrodynamic and surface material conditions with a minimum of testing. For example, it should be able to establish thermal stability break points in a single run and should determine whether a given fuel might present a problem at a lower temperature while seeming to be acceptable at higher temperatures. The test rig should also have a reasonably precise, reproducible, and quantitative means of evaluating its results.

The designer wants fuel information in terms of engineering properties that can be used in calculations. This could include maximum allowable temperatures for some specific time interval. Rate of deposition versus temperature for different component materials would provide useful information. It is necessary to define the range of available fuels to provide the designer some landmarks. There is a desire for a test which profiles fuel characteristics that can be related to engine conditions such that maximum allowable conditions can be formulated. The conditions at which the onset of deposition occurs need to be determined. If a component must operate in a regime where degradation occurs, the rate of deposition and effect of deposits on system performance must be determined.

Other input suggested that relevant design features of a test apparatus should include:

- Both dynamic and static fuel delivery systems.
- A fuel flow regime similar to that in the aircraft fuel system, i.e., turbulent rather than laminar flow to model passages through fuel management controls and heat exchanger elements.
- Operating temperature raised over that in the aircraft system, in order to accelerate the deposit forming process and make it practical for test purposes.

The P&W Combustor Design Group suggested that from a fuel nozzle designer's standpoint, thermal stability testing should address three areas of concern in nozzle design. These include:

- 1.) Coking of the small, high velocity fuel passages in the nozzle tip which can produce an unacceptable reduction in flow rate.

- 2.) Coking of the relatively large, low velocity passages in the fuel nozzle stem which can produce an unacceptable reduction in flow rate through either restriction of the passage or through coke flaking which can plug the smaller passages in the tip.
- 3.) Gumming or coking of the distribution valves which can produce unacceptable flow hysteresis.

Thus, a thermal stability test should include the following elements:

- A "standard" pressure atomizing fuel nozzle or orifice configuration with passages on the order of 0.020 inch. The nozzle should be encased in insulation to ensure similar liquid and passage temperatures. Flow versus pressure drop characteristics would be monitored as a function of fuel temperature and hours of operation.
- A heated tube test similar to the current JFTOT test but with quantitative measurement of deposition on the tube as a function of fuel temperature, wall temperature and hours of operation. A filter screen with 0.020 inch passages should be installed downstream of the heated tube and its pressure drop monitored to address flaking. The heated tube should be vibrated to simulate engine vibration.
- A "standard" sliding spool-in-sleeve valve periodically cycled over a range of fuel flows. Growth in hysteresis should be monitored as a function of fuel temperature and hours of operation.

The following is a cumulative list of the type of information that fuel system designers say is needed from a thermal stability test. Different component groups or disciplines within industry perceived different specific needs based on specific component areas. The following applies to one or more of the components identified as affected by thermal oxidative stability.

Onset And Rate Of Deposition As A Function Of:

- Fuel Type
- Fuel Temperature
- Metal Type and Surface Finish
- Fuel Flow Rate (Turbulent and Laminar)
- Fuel Velocity
- Pressure
- Thermal Prestressing
- Cyclic Operation
- Heat Soaking

Additional Needed Information Includes:

- Thermal Conductivity of Deposits (i.e. the effect of deposits on heat transfer)

Form In Which Data Should Be Generated:

- Deposit Thickness
- Deposit Mass
- Heat Transfer Coefficients
- JFTOT Break Points

Fuel Developers

The needs of the fuel developer are similar in many respects to that of the fuel system designer, that is, there is a need to know the environmental conditions influencing the onset and rate of deposition (e.g. fuel type, temperature, etc.). In addition, a fuel developer's efforts are focused on studying the chemistry involved in the deposition process. The type of information needed is that which will permit a better understanding of the following:

- Autoxidation process
- Intermediate species
- Nature of deposits
- Identity and concentration of reactive species
- Role of compounds containing hetero atoms
- How and where deposits are formed (bulk fuel or boundary layer)
- How bulk fuel deposits are transported to surface and what makes them adhere to surface
- How incipient deposits grow
- Role of component surface materials and finishes
- How fuel chemistry can be modified to resist deposition
- How fuel chemistry can be modified to reduce deposition
- What fuel additives are effective and how they work
- Role of dissolved oxygen and trace impurities in the fuel
- Which fuel constituents contribute to stability and which ones degrade thermal stability
- Effects of different refining processes
- Chemical onset of instability and formation of insolubles in a fuel
- Activation Energies
- Pre exponential factors
- Basis for a predictive model

The complexity of the chemical processes involved in the above are well beyond the scope of a single test apparatus, method, or approach. However, a well instrumented, multifaceted, test device could be used in conjunction with a series of well defined, closely controlled experiments to provide greater insight into the questions posed. Computational fluid dynamic models coupled with fuel degradation chemistry could significantly aid in this endeavor. Modeling can help design experiments and interpret the results. A primary design requirement for a laboratory scale test device is the ability to generate meaningful, quantitative data that can be used in the development, qualification, and evaluation of computational models.

There was wide spread agreement that the fuel researcher needs to relate quality to chemical composition parameters. The test result should allow him to quantitatively rank fuels by their deposit forming tendencies. He is helped in his understanding of the deposition process by having knowledge of the point of incipient deposit formation as well as the magnitude of deposit. The point of incipient deposit formation is preferably defined by the temperature at which insolubles begin to appear in the test device operated under specified conditions. Suggestions for measuring incipient deposits included light reflectance methods. Suggestions for determining the magnitude of deposit included measurement of thickness, weight, or carbon content. In addition, it was suggested that the thickness of the deposit layer could well be inferred from indirect measurements such as conductivity, dielectric breakdown, or interferometry. Further, a fuel developer needs a laboratory-scale test device that can provide real time data acquisition in terms of deposit rates and chemical compositional changes.

4.6 CAPABILITIES AND LIMITATIONS OF CURRENT TEST DEVICES

◆ JET FUEL THERMAL OXIDATION TESTER (JFTOT)

The JFTOT test is an accepted ASTM test method (ASTM D3241). It is the most widely used laboratory scale test device for ranking the thermal stability properties of jet fuels.

How It Works

In the JFTOT apparatus, the fuel under test moves from a reservoir at 3 milliliters per minute, passes through a 0.45-micron filter, and enters a test housing where it flows over a resistively heated polished aluminum tube. Upon exiting the test housing, the fuel flows through a 17-micron filter where insoluble degradation products are captured, and then returns to the top of the reservoir. The spent fuel is separated from the fresh fuel by a rubber-sealed piston which descends in the reservoir as the fresh material is withdrawn. The JFTOT fuel system is pressurized with nitrogen at 500 pounds per square inch (psig) during operation. Standard test conditions are 2.5 hours at 500°F (260°C) for MIL-T-5624, MIL-T-83133 (JP-4 / JP-5 and JP-8, respectively), and Jet A type fuels. Standard test conditions for MIL T 38219 (JP-7) are 5.0 hours at 671°F (355°C).

Thermal stability of the fuel is determined by its propensity to lacquer the heated tube or block the 17-micron filter. The color of the lacquer is assessed via simple visual comparison to a standard ASTM color chart. Military specifications require that under standard test conditions, the color of the lacquer produced not be darker than a visual code rating of less than 3. In addition, pressure drop across the 17-micron filter must be less than 25 millimeters (mm) of mercury. Although not part of the ASTM procedure, the thermal stability "break point" of a fuel is defined within industry and the military as the highest temperature at which the fuel can be tested and still yield a passing test result. The repeatability of this break point temperature measurement is approximately 10°F (5°C).

Limitations

Laminar Flow

There is general concern that the JFTOT's laminar flow does not accurately reflect flow dynamics in aircraft fuel systems. Calculated Reynolds numbers for the JFTOT and the TOFT (Thermal Oxidative Fouling Tester) are approximately 16 and 54, respectively. Reynolds numbers more representative of an aircraft fuel system are in the range of 5,000 to 25,000 (in some cases higher).

As a point of interest, the effect of flow rate and fuel temperature on Reynolds number (Re) were calculated for the HLPS configuration and are shown below. All calculations are based on a test section inlet diameter of 2.5 mm and JP-8 viscosities at 25, 260, and 300°C (77, 500, and 572°F).

- Re at 3 mL/minute and 25°C = 16
- Re at 3 ml/minute and 260°C = 118
- Re at 10 ml/minute and 25°C = 54
- Re at 10 ml/minute and 260°C = 379
- Flow rate required for JFTOT to achieve Re 4,000 at 25°C
= 706 ml/minute (i.e. 106 Liters / 2.5 hour test)
- Flow rate required for JFTOT to achieve Re 4,000 at 300°C
= 87 ml/minute (i.e. 13.1 Liters / 2.5 hour test)
- Flow rate required for JFTOT to achieve Re 7,000 at 25°C
= 1237 ml/minute (i.e. 185.6 Liters / 2.5 hour test)
- Flow rate required for JFTOT to achieve Re 7,000 at 300°C
= 152 ml/minute (i.e. 22.9 Liters / 2.5 hour test)

Mass-Transfer Effects

According to Shell Thornton Research Center, flow rate and activation energy experiments indicate that mass transfer effects as well as chemical reactions may dominate the JFTOT deposition process. Shell attributes the formation of a stagnant boundary layer to the JFTOT's laminar flow. Fuel flow within a turbulent regime would ensure a test which responds more to fuel chemistry and is less dependent on physical transport (i.e. the rate in which reactants diffuse from the bulk fuel into the stagnant boundary layer).

Sensitivity To Surface Passivating Agents

It has been suggested that the JFTOT is overly responsive to the beneficial effects of surface passivating agents. If proven to be a valid concern, longer test durations on a stainless steel tube could resolve this shortcoming. In a research environment, this would be an acceptable approach. For specification testing, longer test periods would not be desirable.

Fuel Preheating

Lack of fuel preheating is considered by some researchers to be a shortcoming of the standard JFTOT test procedure. This is because it fails to simulate aircraft fuel systems in which bulk fuel temperatures in excess of 100°C (212°F) are found. When the JFTOT replaced the CRC Fuel Coker as the standard thermal stability test, the requirement for fuel preheating was dropped. It was dropped because fuels had a tendency to fail on pressure differential rather than tube deposits and this was considered inconsistent with the rating system. The JFTOT apparatus, however, has the capability for main reservoir heating as well as using a Mini Heated Reservoir.

Fuel Prefiltration

The significance and requirement for the 0.45 micron prefilter has been questioned. The presence of the filter can affect JFTOT results, particularly in cases of fuel contamination. Filtration at the 1-micron

level at refueling installations is common place. It has been suggested that some prefiltration on the JFTOT is required, but that a membrane of higher porosity might be more suitable

Residence Time

In the standard JFTOT test, the fuel takes 13 seconds to traverse the heater test section from inlet to outlet. In an aircraft fuel system, it takes typically less than 1 second to pass through the hottest parts of the heat exchanger. In some engines employing primary and secondary burners, lower flow rates and hence longer soak periods can be encountered in the burner system itself. The HLPS does provide for adjustable flow rates from 1 to 10 mL per minute in which to affect residence times.

Tube Material

JFTOT tube composition is critical in determining the extent of fuel degradation and/or the formation of tube deposits. Visual ratings using ASTM color standards is reliant upon the use of aluminum tubes. Use of aluminum tubes limits high temperature fuel investigations because they begin to deform at temperatures above 700°F (371°C). Some researchers conclude that the aluminum tube exerts a rate-determining effect on deposition. It has been reported that at high temperatures, migration of magnesium in the alloy to the tube surface forms a magnesium oxide layer which passifies deposit formation. Other researchers have been unable to substantiate this conclusion. NRL reports that carbon burn-off analysis has shown that use of stainless steel tubes leads to increased levels of deposit. Fuels are ranked in the same order of stability as with the aluminum tubes. Several researchers have concluded that it is more appropriate to use stainless steel tubes for fuel studies.

Deposit Assessment

The JFTOT test has been useful over the years as a quality control test. Its usefulness as a research tool, however, is limited. This is in part due to the subjective nature of the visual rating system which excludes quantitative measurements. In its current configuration, its inability to provide rate data limits studies directed at investigating the deposition process and environmental effects. Early efforts to quantitate tube deposits focused on the Tube Deposit Rater (TDR). Based on this light reflectance method, a maximum TDR value of 12 is required for JP-7 per MIL-T-38219 military specification. In April 1990, the CRC solicited Alcor to refine the TDR by way of implementing current material and design technology. Other attempts to quantitate JFTOT tube deposits have included carbon burn-off, gravimetric analysis, dielectric breakdown, and interferometry.

Dielectric breakdown and interferometry represent two of the most unique approaches. Dielectric breakdown was the focus of the thermal stability Deposit Measuring Device (DMD) developed by Southwest Research Institute (SWRI). It capitalizes on the electrical insulation properties of the varnish-like JFTOT tube deposits. In this method, an electrode is attached to one end of the JFTOT tube and a second electrode placed on the deposit at the desired measurement location. Voltage is then applied and increased until dielectric breakdown occurs providing a measurement of deposit thickness.

Among the most promising approaches for quantifying JFTOT tube deposits was the Fiber Optic Modified-Jet Fuel Thermal Oxidation Tester (FOM-JFTOT) developed by the Naval Propulsion Laboratory and Geo-Centers. In this method, a fiber optic monitoring system is interfaced with a JFTOT. The only hardware modification required is replacement of the standard heater tube test section with one on which fiber optic probes were mounted. The interior of the specially designed test section is circular, while the exterior is square. Threaded metal connectors for eight probes are welded to the exterior in a spiral arrangement along the length of the heater tube between stations 28 and 48 millimeters (mm). The ends of the probes are flush with the interior surface of the heater tube holder and are designed to be non-intrusive to the fuel flow. The probe positions correspond to the ASTM D3241 temperature profile for aluminum tubes. Because the probes are located at positions of different temperature along the tube, the deposition rate at each of these temperatures can be determined from a single JFTOT run.

The FOM-JFTOT system includes an electric-optic module which contains both a source and a detector for each probe. Each probe consists of a fiber optic bundle containing seven fibers. The light from the source is transmitted through one fiber to the heater tube. The light is reflected back from the heater tube and deposit surface through the remaining six fibers to a photo detector. A personal computer receives and stores the data obtained during the run. An inverted plot of reflected light intensity (attenuation) versus time is continuously displayed on the monitor using a different color for each probe. Each minimum and maximum inflection point shown on the plot equates to a deposit thickness accumulation of 0.14 micron.

There are limitations associated with each of the methods described above. TDR readings are somewhat repeatable but are not proportional to the amount of deposit formed. The carbon combustion method is extremely sensitive to contamination. Tube preparation includes preburn-off and repolishing. In addition to the tedium, the procedure needs refining to improve repeatability. The Geo-Centers Interferometry method is limited to a minimum thickness of 0.14 microns which equates to a code 4 JFTOT visual rating, and assumes a typical refractive index for all fuel deposits of 0.16. Probes are extremely fragile and expensive to replace. The SWRI dielectric method is limited to tube deposits which typically contain more than 60 micrograms of carbon.

Capabilities

The JFTOT uses research quantities of fuel. Time, temperature, pressure, and flow rate are controlled. Oxygen levels from sample to sample are controlled by sparging with air prior to testing. Break point determinations permit a degree of quantification, permitting direct comparisons of the temperature capabilities of fuels.

Role of JFTOT Data in Fuel System Component Design

The Combustion Design Group at P&W reported that the JFTOT has had only a minor role in fuel nozzle design and is viewed as a method of assuring full minimum quality. It is used as a correlating parameter in assessing suitability of a nozzle design for operating on alternative fuels.

Additional Comments From Industry and Military Survey

There is concern that the JFTOT sometimes fails to screen out problem fuels. The most recent examples of this occurred in China and Brazil. In Brazil, General Electric (GE) engines experienced fouling of the main fuel control. In China, GE CFM 56 engines experienced plugging of a main fuel control filter screen, while P&W JT8D engines experienced severe fuel pump and nozzle fouling. In the Brazil occurrence, the JFTOT was unable to simulate fouling of GE engines in Boeing aircraft when using initial batches of Brazilian chemically sweetened fuel. In China, the presence of carbon disulfide in the fuel was suspected of contributing to fouling of the JT8D nozzles. However, JFTOT experiments failed to confirm that carbon disulfide degraded thermal stability.

Since actual fuel samples from the affected aircraft were unobtainable, it is difficult to conclude with confidence that the JFTOT failed to screen out the bad fuels in either occurrence. In the China incident, a hardware problem is possible since BOCLE measurements performed on representative samples indicated hydrotreating. Hydrotreated fuel would be expected to have excellent thermal stability properties. Never-the-less, because these are rare occurrences, the majority of users interested exclusively in quality control are still quite satisfied with the JFTOT in its current configuration.

Some fuel researchers, however, have misgivings about the JFTOT test and do not believe it tells us anything about thermal stability, other than screening out the very bad from the very good. These researchers believe that the Hot Liquid Process Simulator (HLPS), if run in a non-JFTOT mode, may offer some clues, especially when coupled with a good way of rating tubes. These researchers believe

that the United Technology Research Center (UTRC), Shell Thornton, and GE single tube heat exchanger work is a step in the right direction. Although there are some concerns about the configuration of some of the test equipment, these rigs may have the potential for controlling more experimental variables than a JFTOT. A single tube heat exchanger coupled with advanced diagnostics is seen as a promising approach.

For quantifying deposits, the Nanometric Interferometry method and carbon burn-off are viewed as the most worthy of pursuing at the present time. Some researchers suggested that methods such as carbon burn-off, weight measurement, direct accumulation measurements by acoustics or laser diagnostics, and post test interferometry should be evaluated. Analysis of the deposit on the surface of the test specimen using techniques such as scanning electron microscopy, Auger spectroscopy and other novel methods should also be explored.

Other researchers believe that when properly applied, the JFTOT provides unambiguous information on fuel oxidative thermal stability. The break point temperature identifies the temperature at which a fuel will begin to show evidence of insoluble thermal stability degradation under very specific test conditions. This was felt to be a valid indication of a fuel's relative sensitivity to thermal oxidative reactions. In fact, tests have shown that the JFTOT ranks fuels in the same order as the old (1960-70) Air Force Fuel System Simulator and with burner feed arm/nozzle fouling tests. In addition, work performed by UTRC for the Naval Air Propulsion Center (NAPC) showed break point correlation with TF-30 nozzle coking.

Further input suggested that the JFTOT test is controversial because of attempts to quantify deposits, especially at temperatures above and below the break point temperature. The weight, volume or area of deposit does not provide the same information as break point temperature and attempts to correlate these results may be ambiguous.

Some researchers felt that given certain modifications, the JFTOT could remain a quality control test and at the same time become significantly more useful in research applications. Suggested modifications included double length JFTOT tubes so that the temperature scale is not so greatly compressed, and a means for quantifying mass or thickness as a function of temperature. Quantifying weight of deposit by carbon burn-off, deposit thickness by interferometry, and deposit composition by Auger spectroscopy could provide useful research information. This information could be correlated with fuel compositional parameters if approached correctly.

The laminar flow regime of the JFTOT has been criticized because it is not representative of the turbulent flow experienced in actual engines. It has not been shown, however, that turbulent flow is a critical engine parameter (as an after thought, this is true for many other fuel system parameters - that's why we need a test). In addition, it has been postulated that a mass transport effect dominates JFTOT deposition due to a stagnant boundary layer induced by laminar flow in the test section. Reactions occur in this stagnate boundary layer and are governed by the rate of diffusion of reactants from the bulk fuel.

If mass transport is proven to have a dominating effect on JFTOT deposition due to laminar flow, and if it can be proven that turbulent flow is not a critical parameter in actual engines, then any approach that sufficiently mixes the fuel to preclude a stagnant boundary layer would resolve the problem. It is possible that eliminating the stagnant boundary layer can be accomplished in a much easier fashion than attempting to incorporate turbulent flow with high Reynolds number in the JFTOT. Baffles, rifling, or a turbulent (low Reynolds number) inducing "dimpled" test section design (similar to the design of some heat exchanger tubes), along with increased flow rate, could provide a manageable and straight forward solution.

◆ UTRC RESISTANCE-HEATED TUBE RIGS

How It Works

Small diameter, stainless steel tubes of 3 to 8 ft. length are resistively heated to produce initial wall temperatures up to 900°F (482°C). Tests can be performed for periods up to 750 hours. At the conclusion of the test, the tubes are sectioned and the carbon mass determined by carbon burn-off.

Limitations

Although the temperature span over a typical tube section is small and the mass well defined, the analysis is labor intensive and growth can be determined only at the conclusion of the test. A multiple-tube apparatus with three parallel legs has been used to expedite the acquisition of data, but the experiments remain time and labor intensive. In addition, as in the JFTOT, the effects of tube wall and fuel temperature can not be independently determined, since the heated wall is the thermal source. It is possible, however, to adjust the wall/fuel temperature difference by varying the tube length.

Capabilities

Capabilities include good temperature control, multiple temperatures per test, realistic flow parameters, and the ability to determine fuel heat transfer properties.

◆ UTRC MATERIALS TEST REACTOR

How It Works

The description which follows is a rig proposed by UTRC and is based on refinement of a prototype system. Its intended use is for evaluating the effects of different materials and surface finishes on deposition rate. The UTRC Materials Test Reactor (MTR) incorporates 24.5 mm diameter sample discs within a 3.5 foot long rectangular flow channel. Sample ports are directly opposite each other at the inlet and exit. This provides for exact match of fuel conditions or allows optical access to the samples across the channel. Specimens are individually heated by small cartridge heaters embedded in copper holders. The temperature of each specimen is measured by a thermocouple at the back side and regulated by a proportional controller. Fuel is preheated in a separate upstream heater (typically less than 350°F). With the exception of a small leakage of heat from the front surface of the heated samples and the copper holder fuel temperature is well controlled. Deposition on the planar samples is measured by carbon burn-off. Plans are underway to incorporate optical diagnostics using fiber optic probes.

Limitations

Disadvantages include large fuel quantity, large assembly.

Capabilities

If successful, this approach will permit several temperature / material test combinations to be performed in a single run. In addition, independent control of fuel and wall temperature is possible.

◆ SHELL THORNTON SINGLE-TUBE HEAT-TRANSFER RIG (STHTR)

The STHTR was developed to realistically simulate an aircraft fuel system and specifically examines the degradation of fuels in a simulated fuel/oil cooler. The fuel undergoes heating in three stages: 1.)

simulated fuel tank heating, with a one hour residence time; 2.) preheater, to reproduce hydraulics and avionics coolers; and 3.) test heat-exchanger, to simulate the oil-cooler. The conditions employed are designed to maintain realistic, turbulent fuel flow. Fuel flow rate is 13.6 kg/h with a Reynolds number of 5,000. Fuel degradation during the 24-hour test manifests itself as a brown lacquer on the inside of the test heat-exchanger. As the fuel passes through the rig its stability is assessed by the rate of loss of heat transfer efficiency between the test heat exchanger wall and the fuel.

Limitations

Requires large volumes of fuel. Its large scale more closely approaches a fuel system simulator than a laboratory scale test.

4.7 THERMAL STABILITY CRITERIA CURRENTLY USED IN FUEL SYSTEM COMPONENT DESIGN

The thermal stability criteria most used in fuel nozzle design is field experience. Coking data generated in heated tube rigs has been used on a limited basis and has been useful in determining the effect of wall temperature on hours of operation. Coking rates are also monitored during actual engine development testing. Fuel temperature is verified and the component disassembled and the coking rate determined based on the projected mission cycle and run times. This data is used to establish maximum fuel and wall temperature based on required life of the latest component and the corresponding coking rate.

System design is selected to maintain fuel nozzle wall temperature to a value which, for the required 4-6000 hour engine life, would not result in a coke buildup in the flow passages thicker than a specified amount. The limit is based on a maximum/minimum deposition rate for JP-4, which is rumored to be worse than JP-5 or JP-8. Field experience involving out-of-spec flow rate, flow hysteresis, spray characteristics, etc. is factored into design and method of operation. Service revisions are made as needed once a design is in production.

SECTION 5.0

SUMMARY AND CONCLUSIONS

According to the guidelines of this study, design requirements were to focus on components identified as being most susceptible to fuel thermal stability problems. In current engines, these components are largely restricted to the hot section of the engine, i.e., fuel injector nozzles, nozzle supports, afterburner spray rings, fuel manifold assemblies, and fuel feeder tubes. Other components within the fuel system were reported as fuel sensitive during the course of an industry and military survey and literature search, but actual cases could not be identified or substantiated. Efforts were made to do so by contacting air bases around the world, overhaul and repair depots, P&W component design groups and members of the CRC Thermal Stability Test Methods Panel. The Brazilian and China occurrences of fuel pump coking may be an exception. However, fuel history, documentation, and other pertinent information is sketchy and makes it difficult to conclusively link the problem to fuel thermal instability. Hot section components, on the other hand, are regularly reported and well documented.

Critical fuel system parameters reported for the hot section include small passage areas, Reynolds number, metal temperature, fuel temperature, and flow rate. The flight conditions most prone to result in thermal stability problems are those involving low fuel flow and high environmental temperatures. Alternately, a theory has been proposed that only minimal lacquering occurs at the conditions described above, and that coking is much more likely to occur during periods of no flow when the augmentor is shut off. During these times, soak-back temperatures rise rapidly to high levels and residual fuel boils off forming liquid and vapor phase deposits. Cyclic conditions compound the problem. A similar theory is advanced for fuel injector nozzle fouling.

Ideally, the type of test a fuel system designer requires is a test which directly measures changes in component performance as a function of critical fuel system parameters. In addition, a fuel system developer requires a test which addresses activation energies and pre-exponential factors, formation and concentration of precursors, trace contaminants, types and concentration of heteroatomic species, and quantification of deposits. Data acquisition is most desirable in real time. The above information is relevant in understanding the deposition process and, in turn, the development of high temperature fuels and additives. The ultimate goal is the development of a numerical model that can predict the extent to which fuel decomposition affects system performance.

None of the current bench-top test devices (or those which approach fuel system simulators) satisfy all of the perceived needs, or provide the specific type of direct information sought by fuel system designers and developers. This is largely due to the logistics of incorporating features which simulate actual engine conditions, e.g., high pressures, high flow rates, turbulent flow with high Reynolds numbers, and sophisticated state-of-the-art instrumentation for monitoring chemical activity. In addition, there is an unwillingness to trade time for temperature. The suspected dominance of mass transport effects, the indirect and subjective nature of rating deposits and determining deposition rates, and little direct correlation to engine testing further limits the desirability of existing rigs. On the other hand, there is an understandable, but contradictory, reluctance to deal with prohibitive sample sizes, and forego the convenience, flexibility and ease of operation offered by accelerated test approaches.

The need for a convenient, inexpensive, quality control test to ensure adequate fuel quality will continue to dominate much of the concern of fuel users. In this respect, the JFTOT appears to perform adequately when used as intended. For limited research purposes, many of the short comings associated with the JFTOT could be resolved upon inclusion of a fuel mixing test section design to reduce mass transport effects, an objective rating system, the use of steel tubes, and longer test periods when evaluating additives.

In formulating the design requirements for a thermal stability test, a dilemma is encountered. Although this study identified the engine hot section to be most sensitive to thermal stability problems, much of today's concerns are directed at future engine designs. Current and near-term advanced thermal management systems were reviewed in this study but fuel system parameters projected for the advanced engines of IHPTET Phase II and III are not yet available. Components not affected by today's standards may well be subject to the rigors of the heat loads and environmental conditions of tomorrow's systems. For fuel developers, there is a critical need to develop fuels of greater heat sink capacity for these advanced systems.

The dilemma posed is whether a test design should address only today's most sensitive components, fuel chemistry, and operating parameters, or include the flexibility to also address potential problem areas of tomorrow's advanced systems. The question is rhetorical. The requirements for a thermal stability test must include all potentially critical parameters for a number of components. It is, after all, the test itself that will be used to determine which fuel system parameters affect thermal stability. Due to the complexity of the task, it is felt that such a test can only be accomplished in a step-like modular fashion. Using an "open-end" design approach, a manageable number of features should be incorporated, proven in concept, then used as a foundation to build upon. In retrospect, this study did not simplify test design, but brought realization to the complexity of the problem.

5.1 DESIGN REQUIREMENTS

Preliminary design requirements should include the following:

- ***Requirement: Flexibility***

The basis for a beginning design should include system flexibility such that extensive redesign and qualification of the central assembly is not required each time an additional feature is incorporated. This will require considerable planning and careful study of future add-on features that will be required to predict a fuel's performance in an engine. The approach should be that of a modular design. The system should not be locked into a strict configuration which addresses a specific application. Versatility should be considered foremost in system design such that it can be built upon. To preserve the concept of a bench-top test, design of each modular assembly should be capable of being evaluated on its own merits after having established the soundness of the central assembly.

- ***Requirement: Direct Measurement of Changes In Component Performance***

Through the use of specially designed plug-in modules, the system should be capable of directly measuring changes in component performance. Ultimately, such measurements should include heat transfer coefficients, fuel flow versus pressure drop, small orifice and screen plugging, and resistance to sliding motion.

- ***Requirement: Temperature Control***

The test design must be capable of precisely controlling fuel temperatures up to 425 °F (218°C) in accordance with the near-term goals of JP-8 + 100°F nozzle design temperatures. Provision for metal temperatures up to 1000°F (538°C) are required to represent the soak back temperatures experienced at the nozzle. Resistive and isothermal heating modes should be provided. Power requirements should consider resistivity of the different metals which potentially could be used as test specimens (e.g. aluminum, stainless steel, and Waspaloy).

- ***Requirement: Fuel Delivery System***

The fuel delivery system should include a pump capable of delivering high fuel flows for assessing the effect of flow rate and for achieving Reynolds numbers in the 4,000 to 6,500 range. Interchangeable fuel pumps may be required to precisely deliver and maintain flows from 3 mL/minute to 1.4 L/minute. A fuel flow of 1.4 L/minute is required to achieve a Reynolds number of 6,500 based on 1/8" tubing and JP-8 viscosity at 25°C. At these conditions, one 55-gallon drum of fuel would be consumed in a 2.5 hour test. Fuel supply design should permit easy conversion to a 1-liter sample reservoir, or one or more 55-gallon drums in tandem.

- ***Requirement: Pressure Capability***

Pressures up to 1500 psi to simulate those found in aircraft fuel systems.

- ***Requirement: Test Section Fuel Flow Dynamics***

Interchangeable test sections or reactors should provide for static or dynamic operation. Dynamic testing should include laminar (Re 16 to $<4,000$) and turbulent flow regimes. Test sections should be designed for self-induced turbulent flow (fuel mixing) as well as turbulent flow defined by Reynolds numbers in the 4,000 to 6,500 range. Depending on the flow regime selected, residence times should be variable from 1 second to 13 seconds.

- ***Requirement: Optical Assess***

The user-selected test sections and static reactors must provide optical assess for data acquisition. This is required for real time measurement of deposit growth and fuel composition changes, as well as for mapping temperature profiles and flow dynamics.

- ***Requirement: Test Specimen Configuration***

Standard test specimens should be flat to optimize optical measurements. However, a flexible open-end system should permit a variety of specimen configurations for use with specially designed plug-in test modules when assessing specific components.

- ***Requirement: Quantification of Deposits***

A precise, objective measurement system is required for quantifying the on-set of deposition. Measurement of deposit thickness should be possible down to 300 angstroms for detecting incipient deposits.

- ***Requirement: Fuel Compositional Changes During Thermal Stressing***

A means for monitoring gross changes in fuel composition during thermal stressing is required. Ultimately, high resolution tracking is required for identifying precursors and intermediate reaction species which lead to deposit formation.

- ***Requirement: Measurement of Dissolved Oxygen***

A simple, straight forward approach for monitoring oxygen consumption during thermal stressing is required. Oxygen levels of 1-50 ppm should be considered for low level detection.

- **Requirement: Real Time Data Acquisition**

Real time data acquisition is required to establish deposition rates, activation energies, and pre-exponential factors.

5.2 TRADE-OFFS

Fuel flows representative of an actual engine fuel system are prohibitive and cannot feasibly be achieved in a bench-top test rig. To do so would require a fuel flow between 69 and 243 lbs/minute depending on the fuel system component simulated. Reynolds numbers approaching the lower limits of actual fuel system operation can be duplicated. However, Reynolds numbers more typical for most components are unapproachable in a laboratory scale rig ($Re > 7,000$ to 25,000 and beyond) due to the required fuel flow rates.

Trading time for temperature traditionally has been used as a means for accelerating testing. A provision for automated long-term testing at realistic temperatures is possible. However, incorporating this feature would result in hundreds of hours of operating time and would require extremely low flow rates because of the prohibitive volume of fuel required. In addition, the validity of the result could be questionable due to the atypical fuel flow. Realistic flow rates, high Reynolds numbers, and time for temperature are likely trade-offs for a laboratory-scale test device. The significance of these trade-offs should be determined in a limited investigation directed at assessing worst case extremes.

5.3 FEASIBILITY OF CONSTRUCTING THE CONCEPTUAL TEST DEVICE

It is unlikely that all of the design requirements identified in this study can be incorporated into a bench-top test device in a single leap. Due to the nature of the problem and the complexity of the device, it must be an evolutionary process. The features required to satisfy so many needs would introduce such a multitude of variables that the logistics of evaluating proof of concept and qualifying the apparatus would be overwhelming. A "starter" system, however, is well within the realm of current technology.

It is feasible to build a modular starter system, operating in a static or dynamic test mode, having as its foundation the ability to quantify deposits and monitor gross changes in chemical composition. This can be accomplished in both a post test and real time mode. The most promising approach is through the use of fiber optics. These features within themselves would represent a significant step forward. Closely controlled temperatures, times, and pressures and automation for extended long term testing is not viewed as a significant problem. Considerably higher flow rates and temperatures than provided by the JFTOT are feasible in a laboratory-scale rig. In addition, two alternative user-selected heated tube test section configurations can be included into the basic design. One such test section could resemble the JFTOT tube in which fuel flows over the test piece, while the alternative test section would resemble a heat exchanger design in which fuel flows through the tube.

Having developed and evaluated the basic configuration, incorporation of turbulent flow of Reynolds numbers in the 4000 range would be a feasible next step. It is felt that this can be accomplished without a great deal of difficulty. A straight forward approach for monitoring oxygen concentration does represent a significant problem and will require an exhaustive survey of instrument manufacturers and procedure development time.

Upon accomplishing these near-term objectives, and subsequent to their evaluation and validation, means for directly assessing component performance can be approached. This might best be accomplished by emulating the approach used by the Air Force in the Reduced Scale Fuel Simulator. Auxiliary devices such as the "small orifice device" and the "nozzle screen device" currently used by the Reduced Scale Fuel System Simulator could be specially designed as a plug-in module to the basic configuration of the conceptual test rig. The feasibility of this approach will be dependent upon required fuel flows

applicable to the component being simulated. An intensive, well thought out design and development effort will be required in design of the plug-in modules.

Measurements such as heat transfer coefficients can be incorporated into a test device by way of thermocouples to assess the effect of deposit on heat exchanger performance. This add on module could take on a heated tube configuration where fuel flows through aluminum 0.072 diameter tubes. Design of an add-on modular configuration with passages on the order of 0.020 inch should be included and allow flow versus pressure drop characteristics to be monitored to assess effect on nozzle performance. To simulate lacquering of sliding surfaces in a fuel control, a module could be designed that features a heat loaded dynamic piston/sleeve arrangement exposed to fuel. A similar module could be designed to simulate fuel nozzle sliding spool devices.

It is proposed that a second generation system address the complexities and sophisticated instrumentation required to track precursors involved in the deposition process and the manner in which deposits adhere to metal surfaces. The feasibility of accomplishing these long-term goals are governed by available technology as well as its applicability to a small-scale laboratory device.

Two of the most challenging features of the near-term conceptual design are being addressed by P&W under two government funded research programs. A Navy funded program entitled "Development of a Fiber Optic Interferometer for Determining Jet Fuel Deposition Rates" has as its primary objective development of an optical diagnostics system capable of measuring incipient deposit formation in real time. Under the auspices of an Air Force sponsored program entitled "Development of an Advanced JP-8 Fuel", P&W IR&D funded efforts are being directed at development of a procedure for monitoring on-line fuel compositional changes during thermal stressing. This program has a targeted start date of August 1990.

APPENDIX A

A copy of the survey distributed to industry and military for use in compiling design requirements for a thermal stability test is contained in Appendix A. A list of the individuals and companies receiving the survey is included.

DESIGN REQUIREMENTS FOR A THERMAL STABILITY TEST

I. Fuel System Parameters for Current and Advanced Generic Engine

1. Which fuel system components are affected by fuel thermal stability ?
e.g.
 - o fuel/oil heat exchangers
 - o fuel injector nozzles
 - o fuel controls
 - o fuel pumps
 - o fuel filters
 - o other
2. How are they affected ?
e.g.
 - o fuel/oil heat exchangers
 - o fuel injector nozzles
 - o fuel controls
 - o fuel pumps
 - o fuel filters
 - o other
3. For each component, what are the tolerance levels before the component is affected, i.e., how much deposit build up is required to degrade performance ?
4. What flight condition (s) in a typical, generic, current and advanced engine is most prone to effect the above ?
e.g.
 - o cruise
 - o descent
5. What are the fuel system parameters for the flight condition(s) identified above in a typical, generic, current and advanced engine ?
e.g.

	<u>Current</u>	<u>Advanced</u>
o Heat Exchangers		
- Tube temperature		
- Fuel temperature		
- Tube diameter and length		
- Flow velocity		
- Reynolds number		
- Tube Material		
- Fuel residence time		
- Pressure		
o Fuel Pumps (Low and High Stage)		
- Pump materials		
- Pressure		
- Fuel residence time		
- Fuel temperature		

o Fuel Filter

- Filter media and surface area
- Filter pore size
- Fuel temperature
- Fuel residence time
- Pressure

o Fuel Control Unit

- Fuel passage diameters (Main & Servo)
- Fuel passage lengths
- Fuel velocity
- Reynolds number
- Fuel residence time
- Fuel temperature
- Fuel passage materials
- Internal filter material, pore size, and area
- Pressure

o Hot Nozzle Section

- Fuel passage diameters or areas
- Fuel passage materials
- Filter material, pore size, and area
- Flow velocity
- Reynolds No.
- Fuel residence time
- Fuel temperature
- Metal temperature
- Pressure

o Interconnecting Plumbing

- Material
- Fuel temperature
- Residence time

o Fuel tank

- Typical fuel temperature history (sub & supersonic)
- Fuel residence time
- Tank materials
- Tank surface temperature (supersonic)
- Pressure (supersonic)
- Fuel oxygen content

6. Which are the most critical fuel system parameters for each component in regard to fuel thermal stability ?

7. From a fuel system designer's standpoint, what type of information is needed - i.e., what is it you want to know ?

e.g. rate of deposition as a function of fuel type, temperature, time, metal, surface finish,

velocity, Reynolds number, pressure, effect on heat transfer, etc.

8. In what form (s) should this data be generated ?
e.g. deposit thickness, volume of deposit, heat transfer coefficients, etc.
9. From a fuels researcher's standpoint, what type of information is needed to aid in understanding the deposition process and in the development of advanced fuels ?

II. Capabilities and Limitations of Current Test Devices

1. What do existing rigs tell us and how do they work ?
e.g.
 - o JFTOT/HLPS
 - o UTRC rigs
 - o Shell Single Tube Heat Transfer Rig (STHTR)
 - o Fuel System Simulators
2. How are deposits evaluated and data interpreted in existing rigs ?
e.g.
 - o Visual Comparison to ASTM Color Chart
 - o Alcor Tube Deposit Rater (TDR) - Light Reflectance
 - o Erdco Townsley Optical Densitometer
 - o SWRI Dielectric Strength of Deposit (Dielectric Breakdown)
 - o Geo-Centers Interferometry Method
 - o Nanometric Interferometry/Algorithm Method
 - o Carbon burn-off

III. Design Requirements For A Thermal Stability Test

1. Which of the most critical fuel system parameters can feasibly be duplicated or simulated for a valid thermal stability test?
2. How would this be accomplished and what type of measurement is required ?
3. What compromises must be made in actual fuel system parameters and direct engine correlation in order to accomplish the goals of an accelerated laboratory-scale thermal stability test using research quantities of fuel ?
4. Can these compromises be made and still provide useful information to fuel system designers and fuel developers ?
5. What criteria should be used for assessing the data ?

IV. Conceptual Design Features To Be Incorporated Into a Bench-Top Test Rig

1. Determined from conclusions formulated under III.

V. Feasibility of Constructing the Conceptual Test Apparatus Based On Design Requirements

1. Logistics and cost determined from a preliminary design configuration directed at satisfying the requirements identified in the study.

SURVEY DISTRIBUTION

CONTACT

Gunter Datchefski
 Perry Kirklin
 Ted Lyon
 Charles Martel
 Jack Muzatko
 Bud Nesvig
 Tom Peacock
 Bryan Rayner
 Dr. William Taylor
 George Wilson
 Dr. Peter E. Wolveridge
 Richard Clarke
 Dennis Harding
 Robert Morris
 Dr. Robert Hazlett
 Steve Anderson
 Robert Morris
 Royce Bradley
 Dr. Ron Butler
 Bill Harrison
 Rick Kamin
 Buck Nowack
 Cy Henry
 Al Zengel
 Kurt Strauss
 Gerry Ohm
 Dave Naegeli
 Pierre Marteney
 Dr. Lou Spadaccinni
 Robert Lohmann
 Pat Deskin
 Jim Shadowen
 Charlie Graves
 Sam Arline
 Vince Lee
 Paul McClure
 Jim Mohn
 Nat Kosowski
 Ed Kichura
 Bennett Crowswell
 Ray Bruchez
 William Edwards

COMPANY

Esso Research Centre
 Mobil Research and Development Corp.
 General Electric Company
 Universal Energy Systems
 Chevron Research Company
 ERDCO Engineering Corp.
 Douglas Aircraft Co.
 Rolls Royce
 Exxon R&D Company
 Alcor, Inc.
 Shell Research Limited
 Shell Research Limited
 Naval Research Laboratory
 Naval Research Laboratory
 Consultant
 Wright Research & Development Center
 Wright Research & Development Center
 Wright Research & Development Center
 Wright Research & Development Center
 Wright Research & Development Center
 Naval Air Propulsion Center
 Naval Air Propulsion Center
 E.I. duPont de Nemours & Co.
 Coordinating Research Council
 Consultant
 Boeing Commercial Airplanes
 Southwest Research Institute
 United Technologies Research Center
 United Technologies Research Center
 P&W - Commercial Engine Business
 P&W - Systems Analysis
 P&W - Combustor Design
 P&W - Combustor Design
 P&W - Engine Controls
 P&W - Mechanical Components and Systems
 P&W - Mechanical Components and Systems
 P&W - Mechanical Components and Systems
 P&W - Mechanical Components and Systems
 P&W - Mechanical Components and Systems
 P&W - Preliminary Design & Advanced Engines
 P&W - F100 Engine Projects
 P&W - Fuels & Lubricants Laboratory

HIGH TEMPERATURE FUEL REQUIREMENTS AND PAYOFFS STUDY

Period of Performance

May 1989 through May 1990

Reference

Task Order No. 17, Topical Report No.16, FR19032-16, 25 August 1990, B.M.Croswell

Abstract

This program was directed at defining the fuel temperature capability requirements for future tactical fighter applications and to quantify the payoff which would be realized by achievement of this capability. The study was sponsored by the Air Force Wright Research and Development Center (WRDC), Aero Propulsion Laboratory, Wright-Patterson Air Force Base, Ohio in association with the Naval Air Propulsion Center (NAPC), Trenton, New Jersey.

SECTION 1.0

INTRODUCTION

1.1 OVERVIEW

The Integrated High-Performance Turbine Engine Technology Initiative (IHPTET) is a joint Department of Defense/NASA/industry effort to develop and demonstrate revolutionary and innovative technologies that will double propulsion system capability. The technologies which result from this initiative will allow future gas turbine engines to operate at much higher temperatures, pressures and rotational speeds. As a result the next generation of propulsion systems will exhibit vastly improved levels of engine thrust-to-weight and fuel burned. These increased propulsion system capabilities will translate into significantly improved aircraft system performance including missions with long range, high speed cruise capabilities.

Improvements in both the propulsion and aircraft systems will place a much greater requirement on the fuel, which will act as the primary heat sink for both the airframe and engine. Under the program described herein, P&W conducted analytical studies to establish the maximum temperature capability requirements for advanced JP fuels for each IHPTET Technology Phase. In addition, the study quantified the payoffs of high temperature fuel capability and showed that development of these fuels is critical to the IHPTET initiative.

1.2 BACKGROUND

The overall objective of the IHPTET initiative is the identification and development of the advanced propulsion system concepts and technologies required to maintain the superiority of our military aircraft. Toward this end, P&W has established the goals shown on Figure 1.2-1. Each phase represents a significant advance in the state-of-the-art in gas turbine propulsion. Achievement of these goals will require that technologies be developed throughout the engine. Failure to address any one area will significantly jeopardize the overall achievement of the IHPTET goals. This is especially true in the area of high temperature fluids and fluid system materials development. The high speed and temperature goals of the IHPTET initiative will require bearings, lubricants, gears and seals with high temperature capability. Increased heat generation in both the airframe and engine hydraulic system will demand the

development of nonflammable, high temperature hydraulic fluids or the use of high temperature fuels. Finally, the greater heat generation associated with high speed missions and advanced propulsion systems and aircraft demand the additional heat sink capacity associated with high temperature, thermally stable fuels. To address these requirements, P&W has established the high temperature fluid development goals for each IHPTET Phase shown on Table 1.2-1.

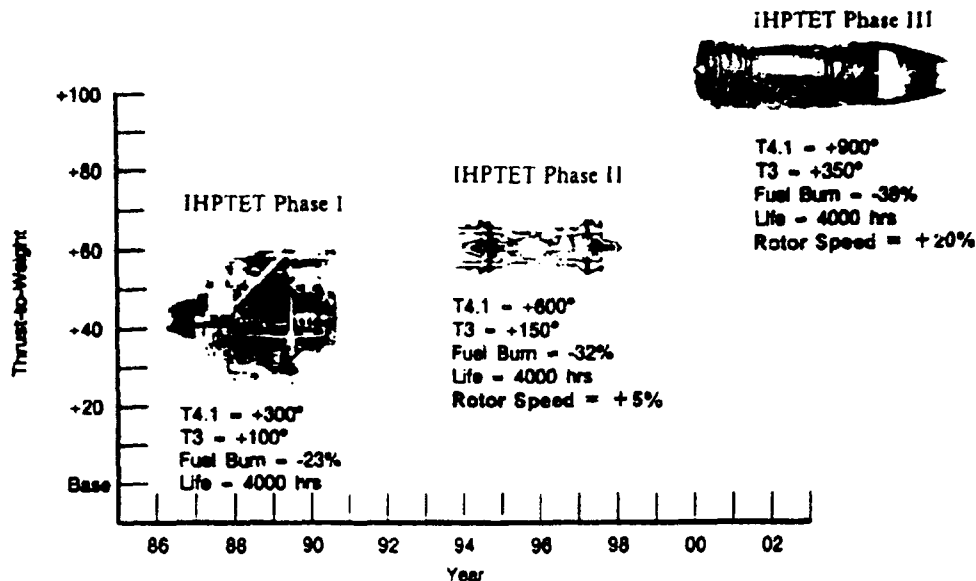


Figure 1.2-1 P&W IHPTET Turbofan/Turbojet Goals

TABLE 1.2-1
P&W HIGH TEMPERATURE FLUID DEVELOPMENT GOALS

	Base	IHPTET Phase I	IHPTET Phase II	IHPTET Phase III
Liquid Lubricants (°F)	400	400	625	700
Fuels (°F), JP-4/JP-8	325	425	550	700
JP-7	550			

Before beginning efforts to develop advanced, high temperature fluids, the requirement for this capability and the resulting payoff must be established. An example of this type of effort was the Lubricant and Mechanical Component Requirements Assessment for the High Performance Turbine Engine Initiative study. This AFWAL/POSL contract (F33657-84-C-2137) was performed by P&W during the October 1986 to August 1987 time period. The study helped to establish the liquid lubricant goals shown in Table 1.2-1. Achievement of these goals will allow the design of a lubrication system that will reduce the weight of mechanical component systems by 25% for an IHPTET Phase II propulsion systems and by 31% for IHPTET Phase III systems. By showing these significant payoffs, studies like this one have resulted in the development of liquid lubricants becoming part of the IHPTET initiative.

The High Temperature Fuels Requirements and Payoff Study represents a similar effort for fuels. For missions with very severe operating environments such as those associated with very high speed flight, defining the requirement for high temperature fuels is fairly straightforward. Figure 1.2-2 shows that heat sink capacity is a barrier for flight speeds above Mach 5. Without advanced fuels like endothermic or cryogenic fuels, these systems cannot achieve their missions.

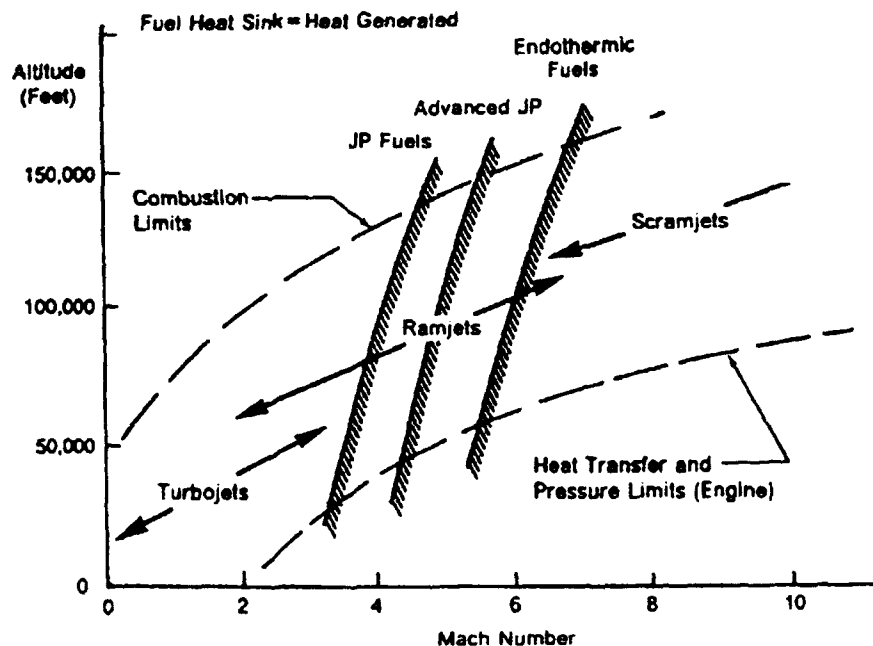


Figure 1.2-2. Cooling Capacity of Fuels Defines Thermal Barrier at High Speed

For more conventional JP fueled propulsion systems in more traditional missions, justification for the development of high temperature capability is more difficult. The use of existing JP fuels, while requiring some design compromises, would not likely restrict the engine flight envelope. This has been demonstrated on several weapon systems which are currently in or are nearing service. An example is the Advanced Tactical Fighter (ATF) aircraft which uses a fuel recirculation system to provide sufficient heat sink for the airframe and engine. This approach could continue to be used for future weapon systems but with an increasing penalty as the heat generation of both the airframe and engines become greater. For this reason, establishment of the requirement for high temperature fuel will be dependant on what will be an acceptable recirculation system size and weight for future aircraft.

1.3 APPROACH

Two primary objectives were established for this study. The first was to define development goals for advanced JP fuels by determining the maximum fuel temperature capability requirements for the future generation of tactical fighter missions. The second was to show how the development of high fuel temperature capability would contribute to the achievement of the IHPTET goals.

Figure 1.3-1 shows the basic approach used to accomplish the study goals. The first step was to define the advanced aircraft missions to be investigated, which determined the engine operating environment and power levels. Following selection of a propulsion system concept, engine performance was modeled to

establish engine internal gaspath temperatures, pressures and flows, as well as the levels of engine fuel flow. This information was used to conceptually design the engine flowpath and to determine the rotor speeds. This is also where configuration issues such as rotor support arrangement were determined. All of this information along with assumed airframe heat loads were used in the development and exercise of engine thermal management models. These models established recirculation flow requirements and temperatures throughout the fuel system. With the fuel heat sink requirements determined, relative sizing of the fuel system components was accomplished to establish payoffs in terms of reduced weight that will be realized with high temperature fuel development.

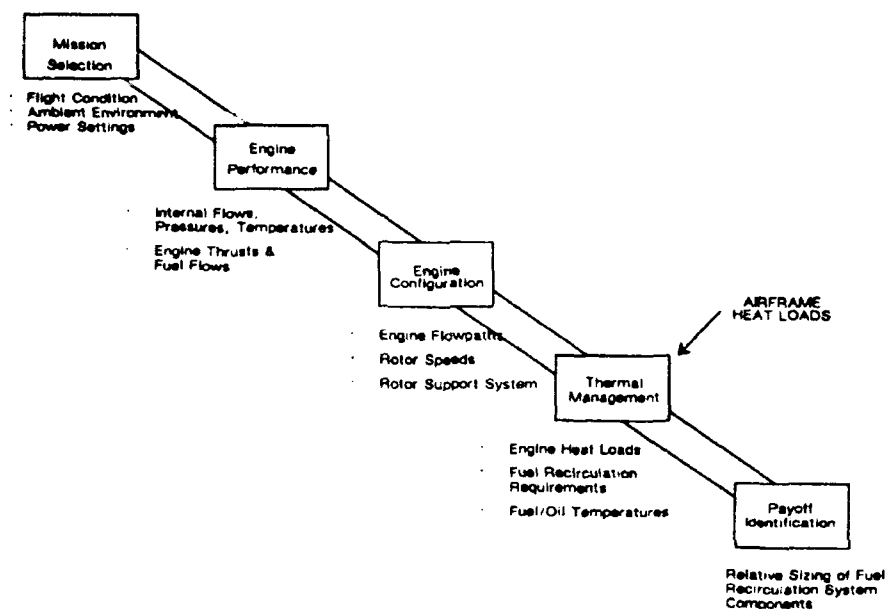


Figure 1.3-1. High Temperature Fuel Requirements and Payoffs Study Approach

This approach sought to maximize use of available resources. For example, the aircraft missions and engine performance simulations that were used had been generated in previous studies and were provided at no cost to the contract. In addition, the thermal management models were adapted from the Lubricant and Mechanical Component Requirements Assessment contract mentioned earlier.

Accomplishment of the goals of this study were complicated by several factors. The first is the fact that, as was discussed in the previous section, fuel recirculation can be used to provide the required heat sink when the fuel temperature capability is not sufficient. For this reason, future fuel temperature requirements for each IHPTET Phase cannot be defined in terms of a single answer but instead are dependant on what is an acceptable fuel recirculation system size and weight.

Defining a payoff to IHPTET for the development of high temperature fuel is directly related to reducing the weight of the of recirculation system. This is where a second complicating factor was encountered. Sizing of the fuel recirculation system is the responsibility of the airframer and is bookkept as part of the airframe weight. This created a two-fold problem, the first being that Pratt & Whitney has little experience and no data base for the sizing of most fuel recirculation components. Secondly, while the development of high temperature fuel capability will result in major weight savings in the recirculation system, most of the savings would be in the airframe and little would be realized by the engine. It is, therefore, difficult to show a high payoff to the IHPTET initiative because IHPTET is

focused exclusively on propulsion system improvements. In addition, there is little definitive information relative to the future levels of airframe heat load. This is important since the airframe heat loads greatly influence the heat sink requirements of the fuel.

With these considerations in mind, a two phase approach to accomplish the study goals was agreed upon by P&W, the Air Force and the Navy:

1. Fix airframe heat loads near the levels projected for the prototype of the next generation of tactical fighter aircraft. Determine the maximum fuel temperature capability required to realize the significant aircraft weight savings resulting from elimination of the fuel recirculation system.
2. Perform a parametric varying maximum fuel temperature capability and airframe heat load to establish how these factors influence fuel recirculation rates. For these various rates, use relative sizing of the recirculation system fuel/air heat exchanger to show how development of high temperature fuels influences recirculation system component weight.

This approach was used within the following study ground rules:

- Only JP fuels and fuel capabilities were considered in the study. Endothermic fuels were not addressed.
- Missions investigated were limited to the more conventional advanced military tactical missions. Special missions with very high speed requirements (greater than Mach 3.0) were not considered.
- Although P&W's technology plan calls for the development and demonstration of magnetic bearings in IHPTET Phase III, for the purposes of this study, high temperature liquid lubricants and conventional high speed bearings were assumed.

SECTION 2.0

FACTORS INFLUENCING FUEL TEMPERATURE REQUIREMENTS

2.1 ADVANCED APPLICATIONS / MISSIONS

The significant propulsion system improvements realized from the IHPTET initiative will result in lighter weight, smaller diameter engines and lower takeoff gross weight (TOGW) aircraft. Reduced drag associated with these smaller aircraft will allow sustained flight at much higher speeds and require future aircraft and propulsion systems to operate in much harsher thermal environments. To determine the impact of these missions on required fuel temperature capability, this study evaluated the advanced missions shown in Table 2.1-1.

Table 2.1-1. Advanced Missions Selected for High Temperature Fuel Requirements & Payoff Study

MISSION	IHPTET TECHNOLOGY PHASE		
	I	II	III
• Advanced Tactical Fighter (ATF)	x		
• Advanced Navy Fighter (ANF)		x	
• Mach 2.5 Air Superiority Fighter (ASF)		x	x
• Mach 1.5 Lightweight Fighter (LWF)		x	x

The ATF mission is classified and a description of this mission cannot be provided in this document. The ANF mission used is based on the Navy Advanced Tactical Fighter. This mission is also classified and no details of that mission are included in this report. Descriptions of the other two missions investigated in this study are provided below:

MACH 2.5 AIR SUPERIORITY FIGHTER (ASF)

The ASF mission profile is shown on Figure 2.1-1. This mission has an overall range of 700 nautical miles, with a 300 mile supersonic (Mach 2.5) dash leg and a two turn Mach 0.9 combat segment. Other performance requirements for this mission include a 35 second acceleration time from Mach 0.8 to Mach 1.6 at 30,000 feet, a 6.5 g (force of gravity) sustained turn at Mach 0.9/30,000 feet, and a 1500 feet balanced field takeoff and landing.

MACH 1.5 LIGHTWEIGHT FIGHTER (LWF)

Figure 2.1-2 presents the LWF mission profile. This mission has an overall range of 200 nautical miles, with a Mach 1.5 cruise out, a combat segment with three max power turns and a subsonic cruise back. Additional requirements include carrying an 1800 lb payload, a specific excess power (Ps) of 500 ft/sec and a 5.0 g sustained turn at Mach 0.9 / 30,00 feet.

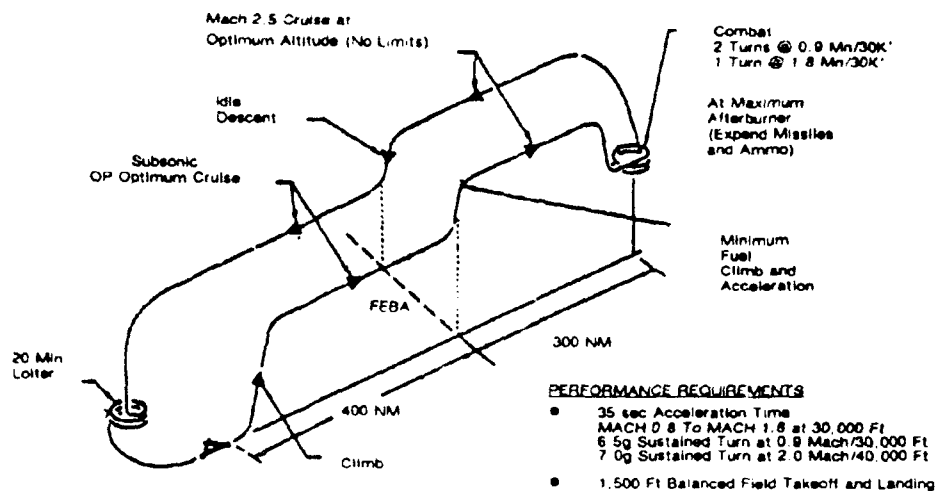


Figure 2.1-1 Air Superiority (Mach 2.5) Mission Profile

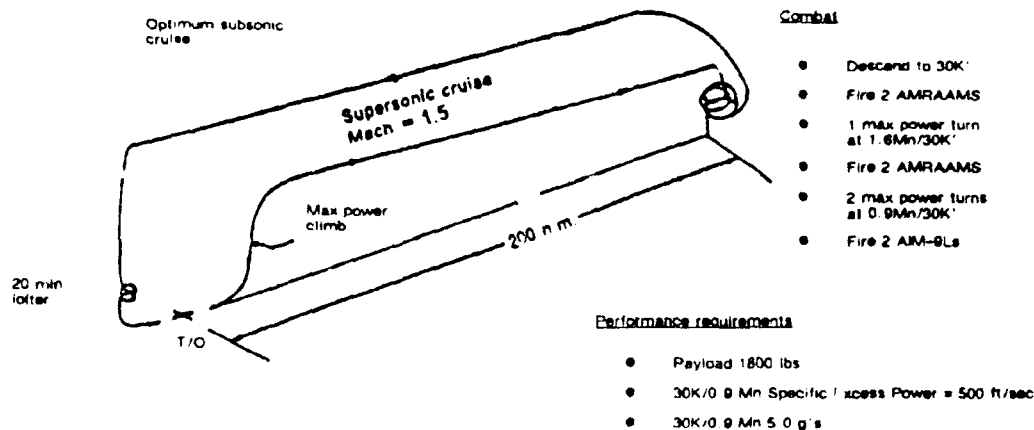


Figure 2.1-2 Lightweight Fighter (Mach 1.5) Mission Profile

2.2 AIR FRAME HEAT LOADS

The levels of heat loads generated by future aircraft are unclear at this time but an extrapolation of operational systems indicates that the fuel will be required to absorb much greater thermal loads. Figure 2.2-1 shows the historical trend of airframe heat load for typical two-engine Air Force fighters as well as projections for the ATF. The increasing levels of heat generated can be attributed to a number of factors. These include more stringent missions which results in higher airframe skin temperatures, the increased hydraulic system requirements associated with large control surfaces, and the requirement to provide cooling for environmental control systems and advanced airframe avionics.

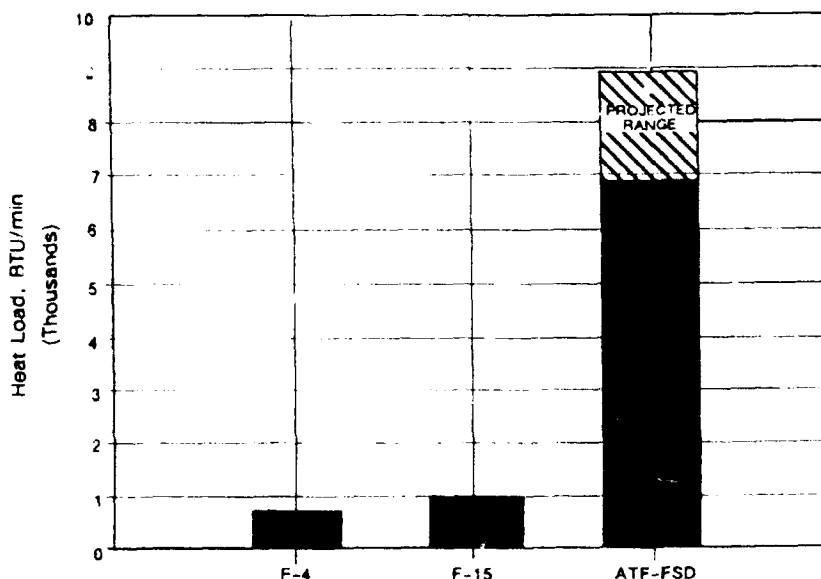


Figure 2.2-1 Increasing Heat Sink Demand On Fuel From Airframe Heat Loads (Per Engine)

2.3 PROPULSION SYSTEM HEAT LOADS

The propulsion system cycles used in this study reflect the IHPTET trend of increased capability through higher operating speeds, pressures and temperatures. These cycles have also been optimized to meet the individual requirements of each mission. For example, the ASF and LWF missions require propulsion systems with high specific thrust (thrust-per-pound of airflow). Accordingly, these engines have high fan pressure ratios (6.0-8.0) and low bypass ratios (0.1-0.3). The engine operating pressure ratios for the ASF engines are lower than those for the LWF. This reflects the requirement to avoid compressor discharge temperature limits at the higher cruise Mach numbers of that mission. The propulsion systems for both of these missions will have turbine temperatures which are 600 - 700°F higher than current engines. In addition, the engine rotational speeds for the Phase II propulsion systems are approximately 5% higher than current engines while the Phase III speeds are 12% - 20% greater.

The mission for the ANF application includes an extended loiter requirement. A major goal of advanced Navy systems will be to extend the time-on-station capability at this loiter condition. This requirement places a premium on propulsion systems with reduced fuel consumption. As a result, this engine has a higher operating pressure ratio and more moderate bypass ratio than the cycles selected for the ASF and LWF. While the rotational speeds for the engine will be similar to the ASF and LWF, turbine temperatures for this application are 300°F lower.

The higher rotor speeds, internal gas path pressures and temperatures of the propulsion system cycles just described are the primary factors effecting engine heat generation. Increased speeds will translate to higher tangential velocity and friction between moving components like gears, seals and bearings. Lubrication system heat generation will also be higher due to increased lubricant shear and churning. The result will be higher lubricant temperatures and a requirement for greater fuel heat sink capacity.

SECTION 3.0

THERMAL MANAGEMENT MODELS

3.1 OVERVIEW

The propulsion system heat loads, as well as the fuel, lube oil and hydraulic fluid temperatures are determined and maintained within design limits by the Integrated Thermal Management System. Figure 3.1-1 presents a diagram of the model used in this study. The model uses system requirements and operating limits determined by aircraft operations, engine/airframe equipment and the physical and chemical properties of the system fluids. Aircraft operations take into account the flight envelope and aircraft mission. Engine equipment includes the bearings, seals, gearbox mechanical requirements, fuel/oil/hydraulic pumps and engine controls. Airframe equipment affecting system requirements include avionics, the cockpit environmental control system and the flight control surface hydraulic system.

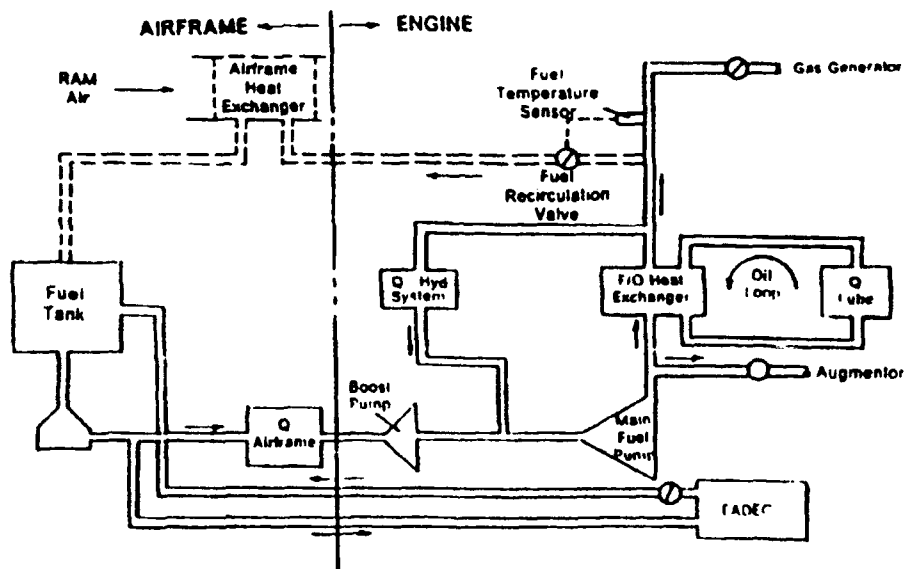


Figure 3.1-1 Fuel System Model Used in The High Temperature Fuel Requirements and Payoffs Study

Engine fuel is the principal heat rejection medium. In addition to the heat generated by the fuel system components, heat is transferred to and from the fuel by a complex system incorporating fuel/oil, fuel/hydraulic fluid and fuel/air heat exchangers. In the systems studied, heat rejected to the fuel is either burned or recirculated back to the airframe fuel tank after passing through a airframe mounted fuel/air heat exchanger.

The key assumptions made in the generation of this model include:

- Temperature of the fuel in the tank is 110°F. This assumption includes any heat which is picked-up by the fuel in the process of cooling the engine Full Authority Digital Electronic Control (FADEC). The study assumes that future systems with higher Mach number cruise requirements will have increased insulation to maintain this fuel temperature in the tank.
- Increased temperature capable oil and hydraulic fluids will be available for use with the higher temperature capable fuel. This is an obvious requirement since the fuel must act as the heat sink for the lubrication and hydraulic systems. To achieve positive heat flow out of these systems will require the oil and hydraulic fluid to always be at a higher temperature than the fuel.

- Related to the previous assumption is the requirement for increased temperature capable fuel system components. The components in this study, e.g. fuel lines, fuel pumps, heat exchanger components and fuel nozzles, have all been assumed to have adequate temperature capability.
- Fuel will be used as the engine hydraulic fluid which eliminates the need for an engine fuel/hydraulic fluid heat exchanger.
- For the IHPTET Phase I system studied, airframe heat loads in the range of 3000-3700 BTU/minute were assumed depending on the flight condition. For the IHPTET Phase II and III system, an airframe heat load of 4000 BTU/minute was assumed at all flight conditions.

An existing model for a current airframe/engine thermal management system (Figure 3.1-2) served as the baseline for the model used in these studies. Several revisions were made to this baseline during the development of the model. They include:

- The location for removal of fuel to route through the hydraulic system was revised. The baseline removes the portion of the fuel used as the engine hydraulic fluid before sending the remaining fuel through the fuel/oil heat exchanger. By moving the point-of-removal of the fuel for the hydraulic system to after this heat exchanger, more fuel is available to serve as a heat sink for the engine lubrication system. This also raises the temperature of the fuel routed through the hydraulic system. At many flight conditions, this higher fuel temperature will be greater than the ambient adiabatic wall temperature. This results in the engine actuators acting as a heat exchanger with a positive outflow of heat from the fuel and a decrease in fuel temperature across the engine hydraulic system.
- A new subroutine was added to better predict engine lubrication system heat generation. This new subroutine considers the heat flux into each bearing compartment as well as the heat generation of each bearing compartment. The model also provides a means of adjusting the amount of compartment insulation to control this heat flux. Buffer air condition and compartment oil flow rates are also considered in the model.
- Modifications were made to the main and boost fuel pump heat generation rate to provide a better estimate of the heat-up of the fuel across these components.

A more detailed description of two of the key thermal management model systems; the engine lubrication and the fuel recirculation systems is provided in the next two sections.

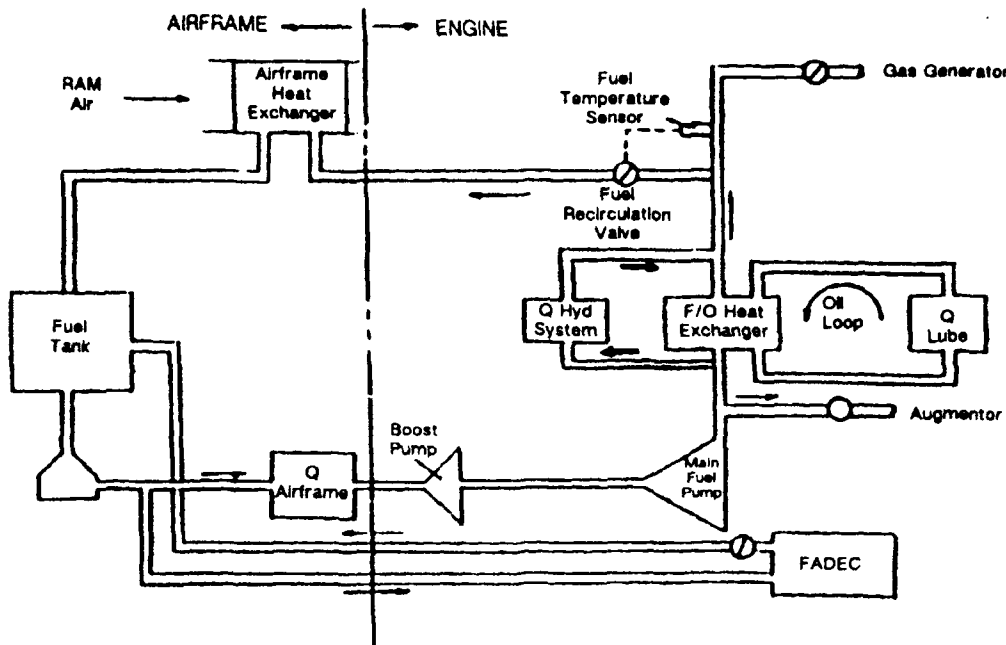


Figure 3.1-2 Fuel System Model Baseline - Current Airframe/Engine Fuel System Model

3.2 ENGINE LUBRICATION SYSTEM

The rotor support/lubrication system models used to establish the engine heat generation were similar in concept for all the missions/propulsion systems considered in the study. In each system, the low speed (inner) shaft is supported by three mainshaft bearings. Roller bearings are located at the No. 1 and No. 5 positions and an angular contact ball bearing is located at the No. 2 position. The high speed (outer) shaft is supported by a ball bearing in the No. 3 position and a roller bearing in the No. 4 position. The No. 4 bearing is a counter rotating roller bearing and is positioned between the low and high shafts. The bearing inner is located on the high shaft for better bearing clearance and operating control. The outer ring is supported by the low shaft by means of a wrap-around hub.

The IHPTET Phase I engine has three bearing compartments. The No. 1 roller bearing is housed in its own compartment forward of the fan. The No. 2 and 3 ball bearings, as well as the towershaft and bevel gear drive system are contained in a common mid-engine compartment located between the high compressor and fan. A common rear compartment houses the No. 4 and 5 roller bearings. Both of these bearings are located aft of their respective turbines. The No. 5 bearing supports not only the low shaft radial load but also the high shaft through the No. 4 bearing.

The rotor support arrangement of the IHPTET Phase II and III engines differ from the Phase I engine in that the five mainshaft bearings are located in two rather than three bearing compartments. In this configuration, the fan rotor is overhung with the No. 1 bearing in a common compartment with the No. 2 and 3 bearings and the gearbox tower shaft and bevel gear drive system. This results in a reduction in engine weight through the elimination of a bearing compartment and the use of a non-structural inlet case.

The liquid lubrication system used in this study is a state-of-the-art hot tank type system shown schematically on Figure 3.2-1. Starting at the oil tank, the lubricant enters the main oil pump where sufficient energy is added to the fluid to overcome the resistances to flow offered by the downstream

circuits and to enable the lubricant to traverse the closed cycle at a pre-established flow rate. Initially when the lubricant is cold and its viscosity high, the lubricant bypasses the heat exchanger and oil filter downstream of the main oil pump and flows through a bypass valve around these components.

When the engine is in sustained operation and the lubricant is hot, the oil filter and heat exchanger bypass valves close. The hot lubricant then passes some of its acquired thermal energy to the fuel supply in a fuel/oil heat exchanger. The lubricant is then delivered to the various bearing compartments where it cools and lubricates the bearings, shaft seals, gears, dampers and compartment walls. While in the compartment, the oil also picks up additional heat from windage and churning losses as well as from high temperature buffer air which leaks into the compartment. The oil is then scavenged from the compartments by pumps which return the oil to the system tank where it passes through a deaerator. Compartment seal leakage air containing some entrained lubricant is routed to the gearbox, and is passed through a deoiler before being discharged overboard.

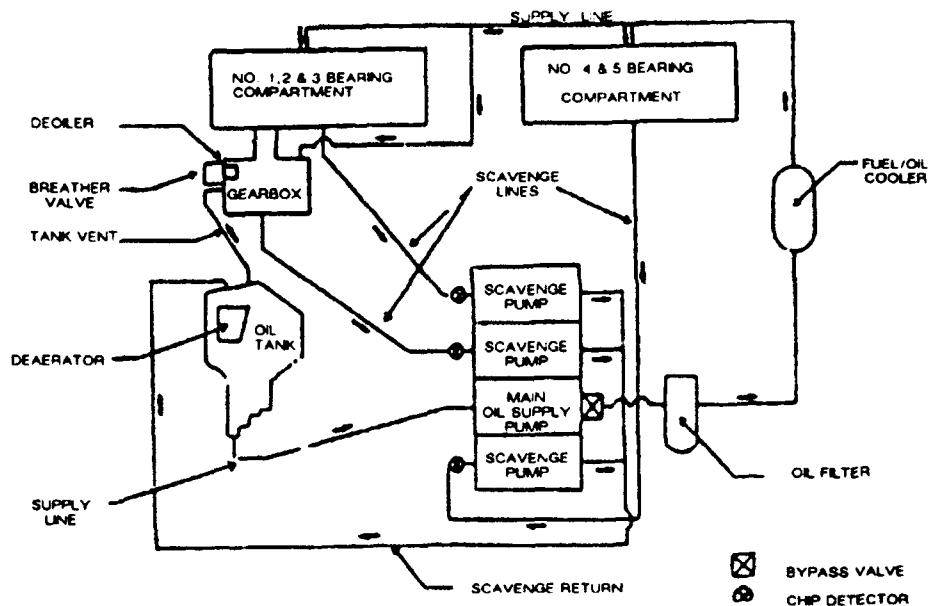


Figure 3.2-1 Typical Hot Tank Lubrication System

3.3 FUEL RECIRCULATION SYSTEM

Where used, the fuel recirculation system assumed in this study is very similar to systems used on the latest generation of tactical fighter aircraft. A sensor indicates fuel temperature limits are being reached and a fuel recirculation valve opens. Fuel in greater amounts than is required for operation of the engine is routed through the fuel system to provide a sufficient heat sink for the airframe and engine. The hot fuel not used for engine combustion is routed through the recirculation valve to a fuel/air heat exchanger before being reintroduced into the tank. While this cooling does not reduce the returned fuel to the same temperature as the fuel in the tank, the system does minimize the heat-up of the tank. Air for the heat exchanger is brought in through an inlet on the aircraft. For static conditions such as ground idle where recirculation is required, a flow inducing device is used to bring airflow into the system.

As was mentioned earlier in this report, the majority of the fuel recirculation system design responsibility falls to the airframer. The fuel recirculation valve is the only major component of this system which is

the responsibility of the engine company. Based on an industry survey, baseline fuel recirculation system weights were estimated for purposes of calculating payoffs for advanced fuels development. These estimated weights are shown in Table 3.3-1

Table 3.3-1. Estimated Fuel Recirculation System Component Weights

Fuel/Air Heat Exchanger (One per engine)	30 lbs.
Fuel Recirculation Valve (One per engine)	10 lbs.
Ram Circuit (Inlet, Flow Inducer)	100 lbs.
Plumbing, Lines, etc.	20 lbs.
<hr/>	
Total (Single engine aircraft)	160 lbs.
Total (Twin engine aircraft)	200 lbs.

SECTION 4.0

STUDY RESULTS

4.1 FUEL REQUIREMENTS WITH FIXED AIRFRAME HEAT LOADS AND NO RECIRCULATION SYSTEM

The development of high temperature fuel capability would realize it's greatest payoff if sufficient heat sink capacity could be generated without a fuel recirculation system. As discussed in the previous section, for the next generation of tactical fighters the elimination of this system would save approximately 200 lbs. of weight in the airframe and engine. As heat sink requirements increase in the future, these systems will likely weigh even more. With this in mind, the first approach taken in this study was to identify the fuel temperature capability required to eliminate the recirculation system.

In this first phase of the study, the following five flight conditions were considered when determining maximum fuel temperature requirements:

- 1.) Ground Idle
- 2.) Subsonic Cruise
- 3.) Idle Descent
- 4.) Loiter

Ground idle and loiter were selected because these are conditions where the engine operates at very low levels of fuel flow and require high levels of recirculation flow or high fuel temperature capability to achieve the necessary heat sink. The high flight speeds associated with supersonic cruise, while providing a higher level of fuel flow to act as the heat sink, also result in more stringent operating temperatures for the fuel system. Somewhere in between these two extremes are the subsonic cruise flight points that combine moderate levels of fuel flow and operating temperatures.

The final flight condition considered was idle descent. This occurs when the pilot, in order to reduce flight speed and altitude, cuts engine power to an idle setting. When this happens after a supersonic flight point, the worst case combination of low fuel flow and high operating temperatures is encountered. These are transient conditions since the thermal environment becomes less severe as flight speed decreases. The thermal management models used in this study are steady state models and do not handle conditions such as these in a transient manner. The idle descent points were still felt to be critical to defining fuel temperature requirements and for this study were investigated using the steady state models. Estimated maximum fuel temperatures determined at these flight conditions may be somewhat higher than if transient models were available and used.

Maximum fuel temperature requirements were established for a system without fuel recirculation and airframe heat loads in the range of 3000-4000 Btu/hr. These heat loads were selected because they are in the range anticipated for the prototype of the next generation of tactical fighter aircraft. All of the flight conditions described previously were investigated for the following three missions:

- 1.) IHPTET Phase I Advanced Tactical Fighter
- 2.) IHPTET Phase II Air Superiority Fighter
- 3.) IHPTET Phase III lightweight Fighter

Preliminary results from this portion of the study were presented to the Air Force and Navy in July and August of 1989. Subsequent to that presentation, further investigation of the thermal management models indicated that the three computational iterations used to generate these results were not sufficient to insure temperature convergence. As a result, hydraulic and gas generator fuel temperature requirements were found to be underestimated at flight points with low fuel flows. Flight points with higher fuel flows very nearly reached convergence with three iterations and were only slightly effected. To insure accuracy, all results presented in this report have been generated using ten convergence iterations. Comparisons of these results with those previously presented indicate very little change in the projected requirements for high temperature fuels.

The results of the first phase of this study indicated idle descent was the flight condition where the maximum fuel temperatures were encountered. Ground idle was also considered to be a critical condition since this is the sizing point for the recirculation system. Due to funding and time considerations, only these two flight points were considered for the final three missions studied:

- 4.) IHPTET Phase II Advanced Navy Fighter
- 5.) IHPTET Phase II Lightweight Fighter
- 6.) IHPTET Phase III Air Superiority Fighter

When examining the results of this portion of the study, note that total heat load on the fuel at each flight condition does not necessarily increase with each IHPTET Phase. Table 4.1-1 shows the sources and levels of heat that the fuel must absorb at the supercruise flight condition. As propulsion system technology improves with each IHPTET Phase, the resulting increase in engine rotational speeds and flowpath temperatures will result in higher heat loads from the bearing lube system. Since heat load from the fuel pump is directly related to fuel flow, the improvements in engine technology that result in lower fuel consumption will actually reduce heat load from this source. Fuel consumption is also greatly effected by the flight condition and power setting. As a result, the low fuel flows required for the high altitude supercruise condition of the Phase II ASF greatly reduces heat load from the main fuel pump. Finally, we can attribute the reduced hydraulic system heat loads for the IHPTET Phase II and III systems to a combination of fuel temperature and flight conditions that result in heat actually being lost in the hydraulic system. This is especially true for the IHPTET Phase III LWF which supercruises at a relatively low Mach number and has very high fuel temperatures in the hydraulic loop. As a result, all but 156 Btu/min of the heat generated by this hydraulic system is lost to the atmosphere. The remaining 156 Btu/min must be absorbed by the fuel.

Table 4.1-1 Summary of Fuel Heat Loads (Btu/min) for the Supercruise Flight Condition

	IHPTET Phase/Mission		
	I/ATE	II/ASE	III/LWF
Hydraulic System	1253	1061	156
Main Fuel Pump	4466	1959	3055
Airframe	3650	4000	4000
Bearing Lube System	4319	5130	8534
Misc	1053	954	672
Total	14741	13104	16417

4.1.1 IHPTET Phase I Advanced Tactical Fighter Mission

For an IHPTET Phase I propulsion system in an ATF mission, Figure 4.1-1 shows that without recirculation, current fuels (JP-4, JP-8) with 325°F capability would have insufficient heat sink at all flight conditions except supersonic cruise. Fuel temperature capability was then allowed to vary until sufficient heat sink capacity was provided. Figure 4.1-2 indicates a fuel temperature capability of approximately 655°F would be necessary to provide the heat sink needed for the idle descent flight condition. This capability would result in an excess heat sink capacity for all other flight conditions; although the margin is relatively small at the subsonic cruise conditions. Fuel with this capability would, however, require a bearing lubrication fluid capability of approximately 660°F.

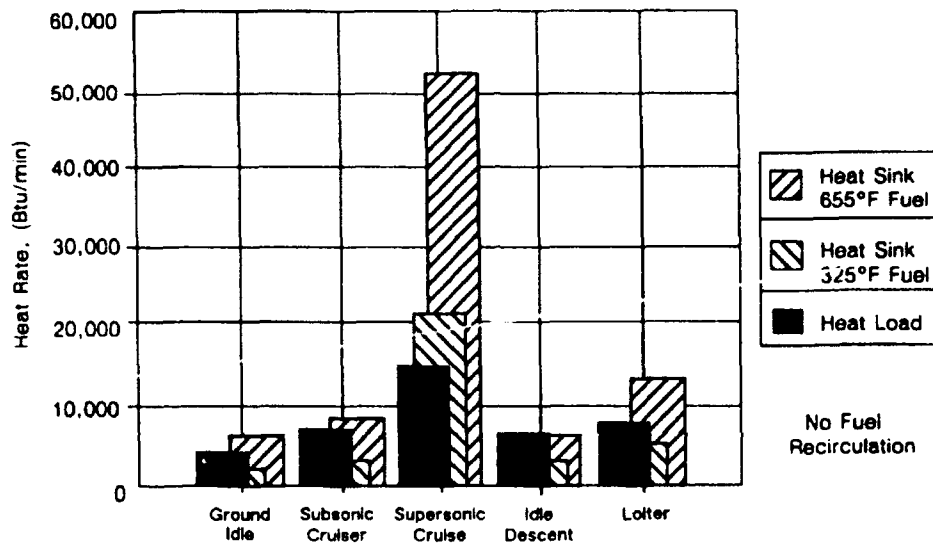


Figure 4.1-1. HPTET Phase I ATF Mission - Heat Load vs. Heat Sink

Figure 4.1-2 shows that maximum fuel temperatures are encountered at the gas generator inlet for all flight conditions except supersonic cruise. For this high speed flight point, the increased actuator adiabatic wall temperature results in a heat gain for the fuel and a maximum fuel temperature in the hydraulic system loop. Conversely, the low speed, subsonic flight points have an adiabatic wall temperature lower than the fuel temperature, resulting in a fuel temperature drop across the hydraulic system. Simply put, at the low speed flight conditions, the hydraulic system actuators act as a fuel/air heat exchanger.

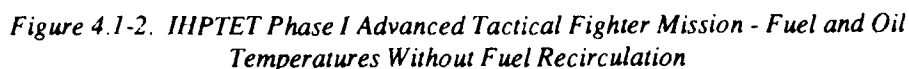
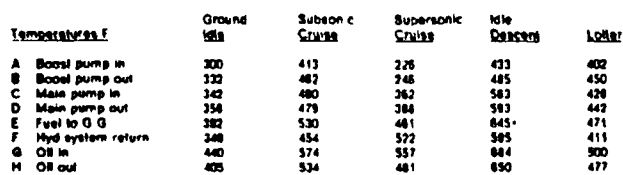


Figure 4.1-3 shows that at an IHPDET Phase II engine technology level, current fuels would be unable to provide the required heat sink at all ASF mission flight conditions investigated. For this mission, the requirement for a Mach 2.5 descent at idle power sets the need for a 645°F capable fuel if the required heat sink is to be provided without recirculation. Figure 4.1-4 shows that this is by far the most difficult condition in this mission and requires fuel temperature capability over 100F higher than the other flight points. This is reflected by the excess heat sink capacity which results when a 645°F fuel is used at the other flight conditions.

481



• **Measurement**

482

4.1.3 IHPTET Phase III Air Superiority Fighter (ASF) Mission

For a LWF mission using IHPTET Phase III technology level engines, Figure 4.1-5 indicates inadequate heat sink capacity at all flight points in the mission except supersonic cruise. Figure 4.1-6 shows that idle descent is again the flight condition which sets the maximum fuel temperature requirement. In this case, an 840F capable fuel would be necessary to provide the heat sink capacity without recirculation.

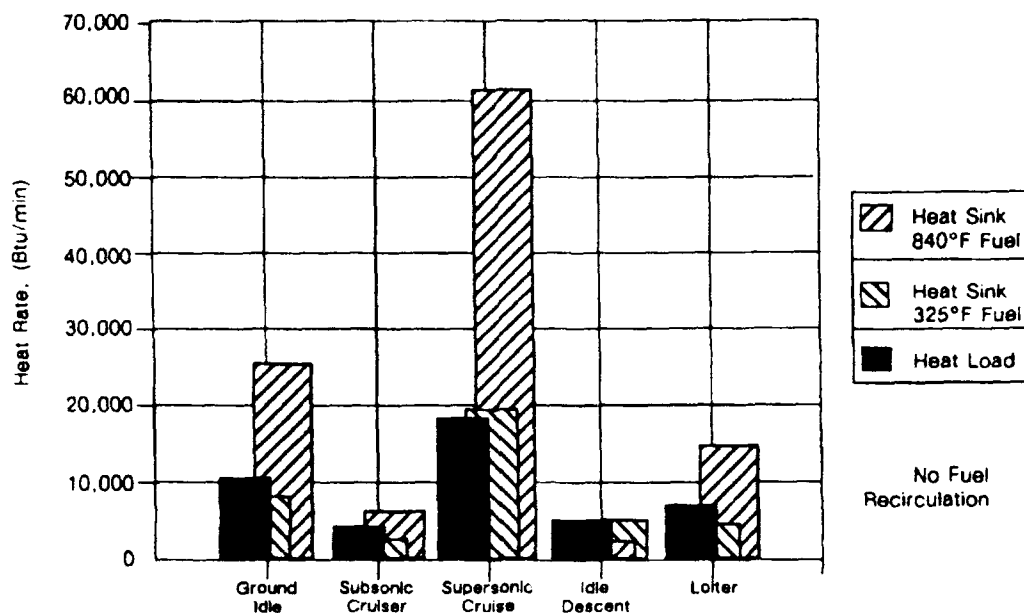


Figure 4.1-5. IHPTET Phase III LWF Mission - Heat Load vs. Heat Sink

A significant difference between the LWF and the ASF application is that maximum fuel temperature is encountered not at the gas generator inlet, but instead at the exit of the fuel boost pump. This occurs because of the lower engine cycle overall pressure ratio selected for the LWF. Engines operating at altitude idle flight conditions often must run at higher idle power settings than is necessary for the mission. This is required so the engine can provide sufficient engine bleed air pressure to meet airframe power requirements. The ASF engines have lower engine pressure ratios than the LWF engines. As a result, the ASF engines must run to higher idle power setting to meet this bleed pressure requirement. Because of this, the ASF propulsion systems have approximately twice the fuel flow to absorb the same 4000 Btu/min airframe heat load as do the LWF engines. As a result, the fuel entering the LWF engines, following heat pickup from the airframe, is at a significantly higher temperature than the ASF mission. In fact, the boost pump fuel temperatures for the idle descent and subsonic cruise flight conditions are such that the remainder of the fuel system has a net heat loss. This is again the result of heat being lost from the fuel in the hydraulic system loop.

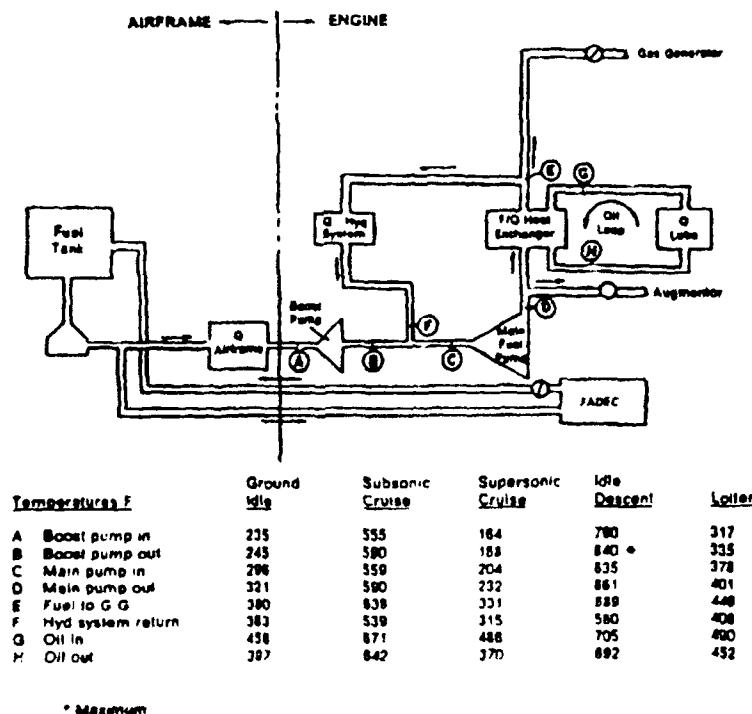


Figure 4.1-6 IIP/TET Phase III Lightweight Fighter Mission - Fuel and Oil Temperature Without Fuel Recirculation

4.1.4 Other Missions Investigated

For the final three missions studied, only the idle descent and ground idle flight conditions were investigated. Figure 4.1-7 summarizes the fuel temperatures at idle descent for all the missions investigated. Out of all of the missions investigated, the Advanced Navy Fighter exhibited the highest maximum fuel temperature (870°F). Like the LWF mission, this can be traced to the optimum propulsion system cycle that has a high operating pressure ratio (OPR) for good fuel consumption characteristics. This cycle allows the engine to run to very low idle fuel flows and as a result, creates very high fuel temperatures when absorbing the airframe heat load. Again, like the LWF mission, the remainder of the fuel system has a net heat loss. Here again, the actuators are acting as a fuel/air heat exchanger with the fuel showing a significant reduction in temperature across the hydraulic system loop.

Comparison of predicted temperatures for the Phase II and III ASF and LWF yielded expected results. The higher speeds and lower fuel flows of the Phase III propulsion systems result in increased fuel temperatures. The differences are not large since the same mission profile and airframe heat loads were considered in both phases.

The results for ground idle are shown on Figure 4.1-8. While this flight condition has significantly lower fuel temperatures than idle descent, it is critical for sizing the recirculation system. These results provide a baseline for the next phase of the study which focuses on fuel recirculation requirements in a parametric manner.

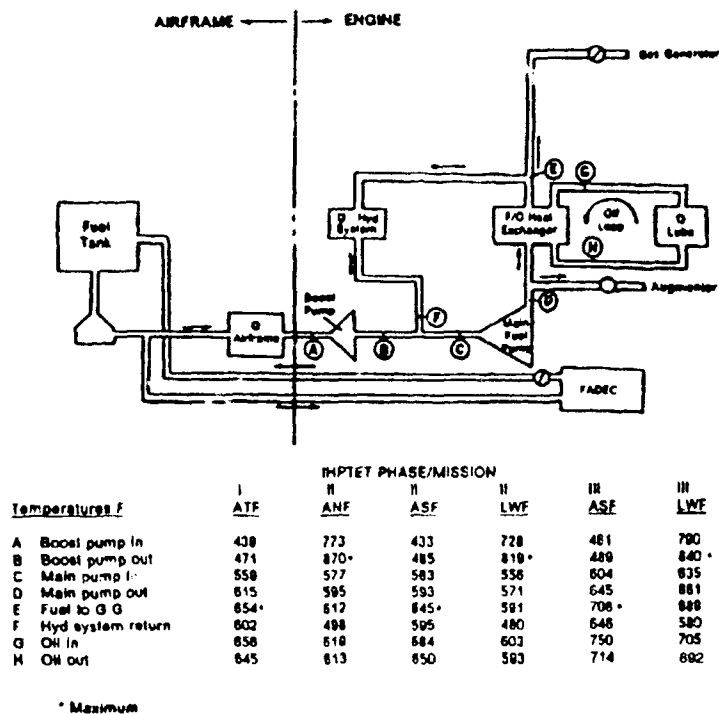


Figure 4.1-7. Maximum Fuel Temperature for Idle Descent Flight Condition Without Fuel Recirculation

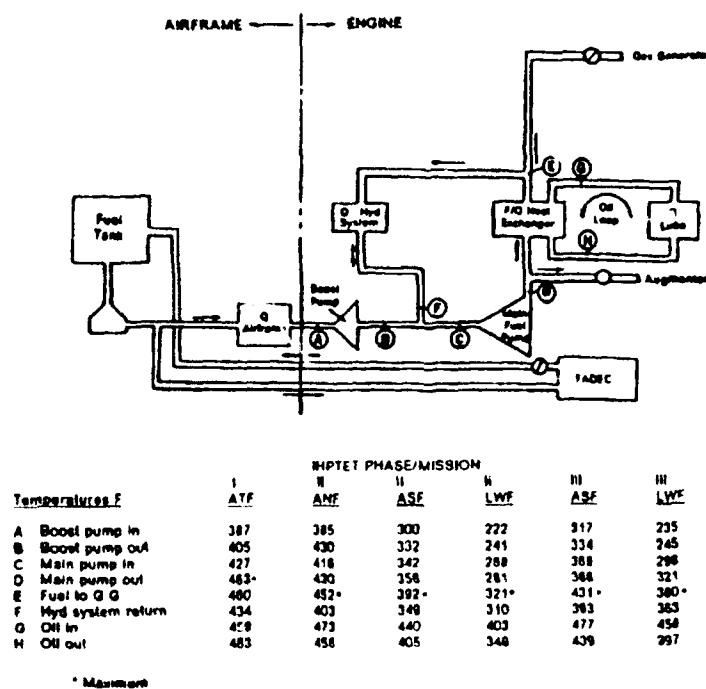


Figure 4.1-8. Maximum Fuel Temperature for Ground Idle Flight Condition Without Fuel Recirculation

4.1.5 Summary

Table 4.1-1 summarizes the maximum fuel temperatures with no fuel recirculation for each mission. This table also compares these results to the IHPTET goals for high temperature fluids presented earlier in Table 1.2-1. Realization of the technologies to reach these fuel temperature capabilities probably will still not allow future tactical fighters to eliminate the recirculation system. This is because a number of factors are likely to drive heat loads up even further and because several other factors will limit the usable fuel temperature capability:

- There is no definitive projection of what will be the future levels of airframe heat load. The trends do indicate that future heat loads will exceed the 3000-4000 Btu/min used in the first phase of this study. This means that without recirculation, even higher fuel temperatures than were projected in this study could result.
- For a twin-engine aircraft, some kind of failure analysis for a one-engine out situation needs to be considered. This situation would require the fuel system of the remaining operational engine to handle the entire airframe heat load. Recirculation provides a way to handle this type of situation
- No matter how much fuel capability is increased, fuel temperature will still have to be kept at a lower level than oil and hydraulic fluids to insure outflow of heat from these systems. For this reason, any fuel temperature capability above the development goals for these other fluids will not be useable in a conventional tactical fighter fuel system.
- A great amount of technology development in the area of fuel system components would need to occur to run these elevated levels of fuel temperatures. A prime example is the fuel pumps. Current pumps can handle max fuel temperatures in the range of 200 to 240°F. The first phase of this study indicated fuel pump temperatures of up to 840°F for some of the missions investigated. This would require a significant increase in pump material temperature capability and pump designs to avoid cavitation at these elevated fuel temperatures.

Table 4.1-2. Maximum Fuel Temperatures Relative To IHPTET Fluid Development Goals

	IHPTET PHASE/MISSION					
	IHPTET PHASE I	IHPTET PHASE II			IHPTET PHASE III	
		ANF	ASF	LWF	ASF	LWF
Max Fuel Temperature (Study Results with No Recirculation)	654	870	645	819	708	840
Fuel Development Goals						
Fuels	425		550			700
Liquid Lubricants	400		625			700

4.2 PARAMETRICS OF MAXIMUM FUEL TEMPERATURE AND AIRFRAME HEAT LOAD TO ESTABLISH RECIRCULATION SYSTEM REQUIREMENTS

Based on results from the first phase of the study, a decision was made that rather than elimination of the fuel recirculation system, a more reasonable goal was to show how high fuel temperature capability can minimize the weight penalty associated with fuel recirculation. Since future levels of airframe heat load are unclear, a parametric study for each of the missions of interest was performed. The parametric looked at fuel recirculation requirements for different levels of fuel temperature capability and airframe heat load.

To show the potential weight payoff for reducing recirculation flow, the results of the parametric for the IHPTET Phase II Air Superiority Mission (ASF) were used to do a relative sizing of a fuel recirculation system component. In this case, the recirculation fuel/air heat exchanger was selected. Since ground idle is the critical flight condition for sizing of the fuel recirculation system, the parametrics were performed at that condition. The point must be made again that the fuel/air heat exchanger is the design responsibility of the airframer and the estimates made here by P&W should be used to show relative component weight improvements.

4.2.1. Recirculation Requirements

The results of parametric studies to determine fuel recirculation requirements as a function of maximum fuel temperature and airframe heat load for each mission are presented on Figures 4.2-1 thru 4.2-6. This study was directed at the ground idle flight condition. Discussions with airframers indicated this was the critical flight point in sizing the recirculation system. A summary of the results of this parametric study is presented on Table 4.2-1 using the P&W fuel temperature goals and a best guess of airframe heat loads for future tactical fighters.

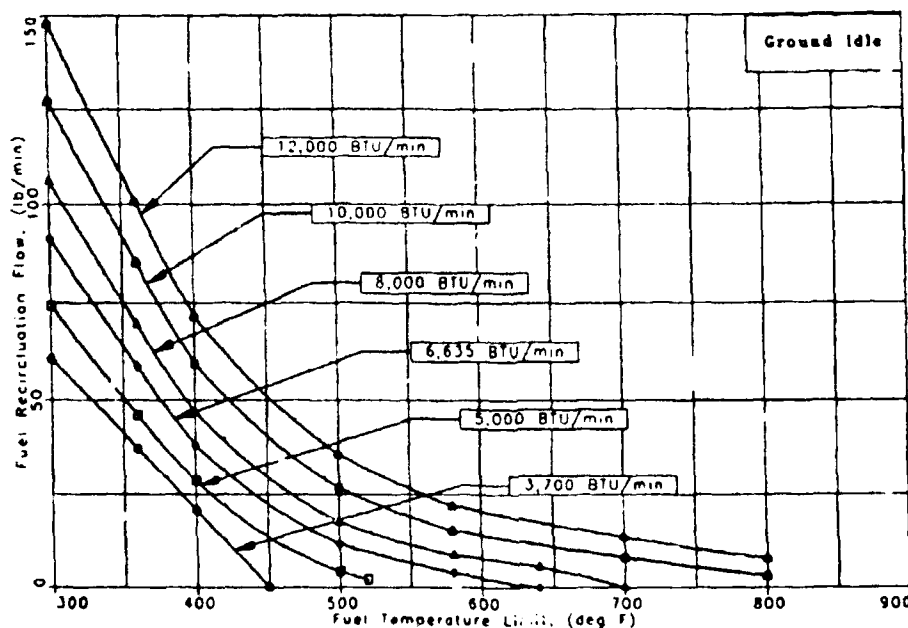


Figure 4.2-1 IHPTET Phase I Fuel Recirculation Requirements For Advanced Tactical Fighter Mission

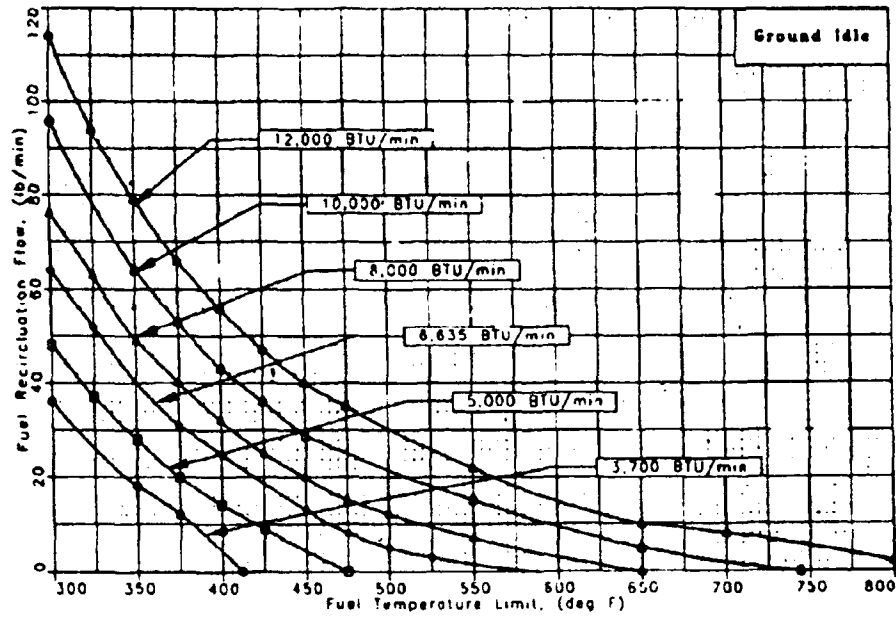


Figure 4.2-2 IHPTET Phase II Fuel Recirculation Requirements For Advanced Navy Fighter Mission

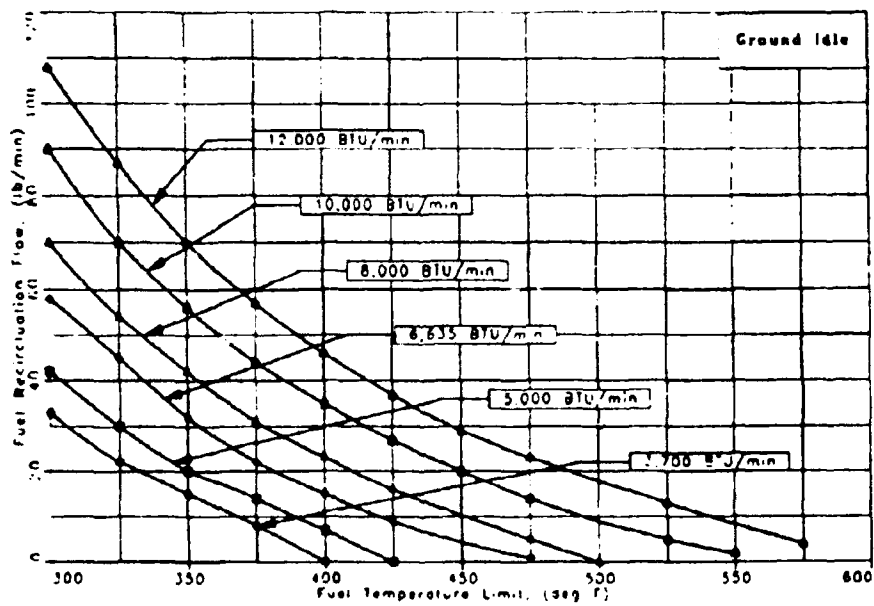


Figure 4.2-3 Fuel Recirculation Requirements For IHPTET Phase II Air Superiority Fighter Mission

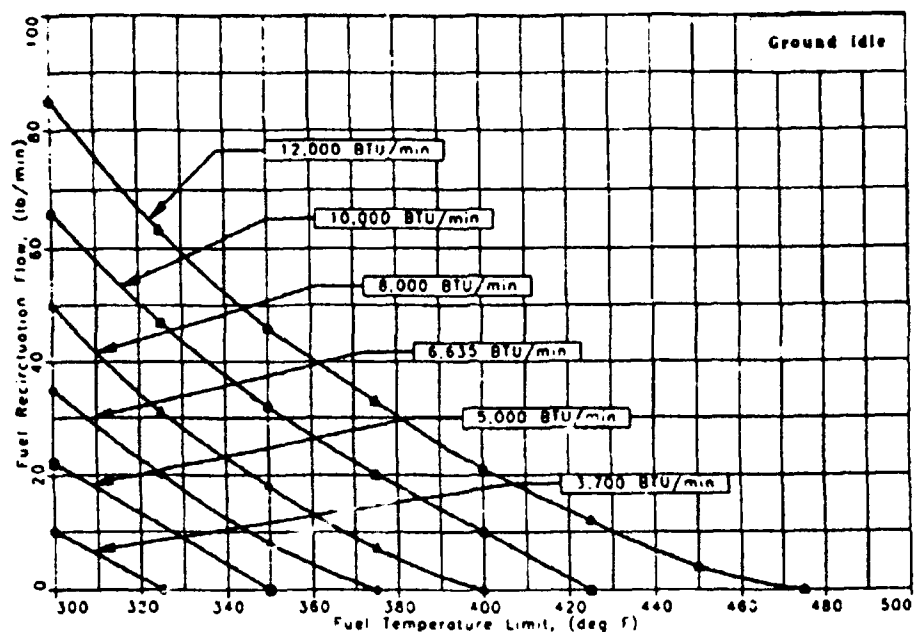


Figure 4.2-4 Fuel Recirculation Requirements For IHPTET Phase II Lightweight Fighter Mission

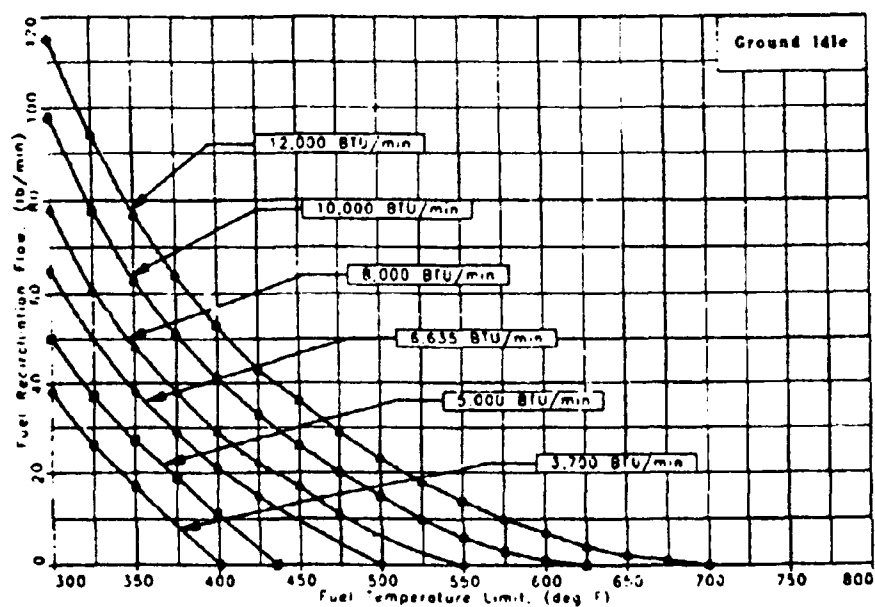


Figure 4.2-5 IHPTET Phase III Fuel Recirculation Requirements for Air Superiority Fighter Mission

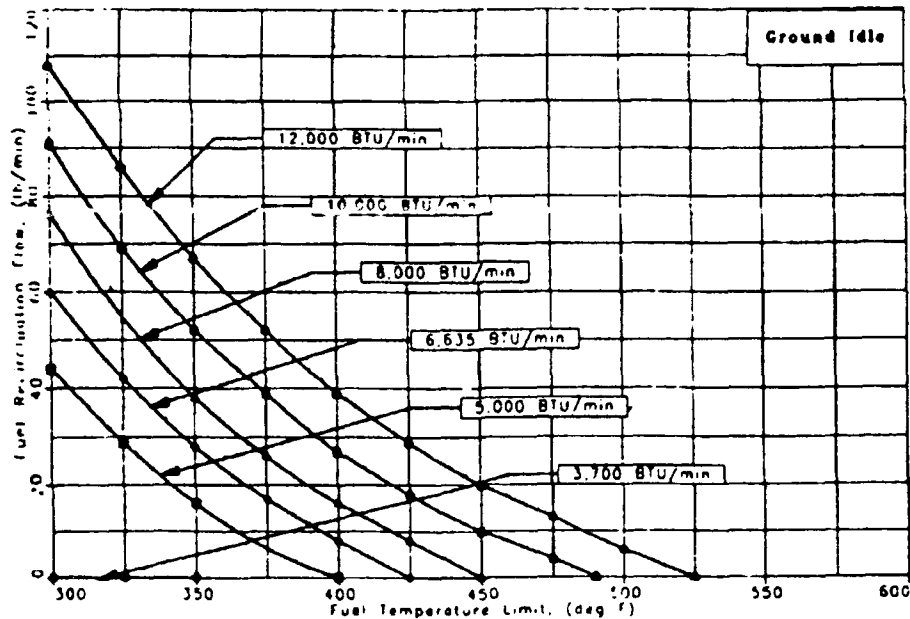


Figure 4.2-6. IHPTET Phase III Fuel Recirculation Requirements for Lightweight Fighter Mission

IHPTET Phase		Max Fuel Temp (°F)	Airframe Heat Load (BTU/min)	Fuel Recirculation (lb/min)
I	Advanced Tactical Fighter	325	5,000	62
		425	5,000	20
II	Air Superiority Fighter	325	8,000	55
		550	8,000	0
II	Advanced Navy Fighter	325	8,000	55
		550	8,000	7
II	Lightweight Fighter	325	8,000	31
		550	8,000	0
III	Air Superiority Fighter	325	10,000	78
		700	10,000	0
III	Lightweight Fighter	325	10,000	69
		700	10,000	0

These results indicate that achievement of P&W's fuel development goals will allow the system to operate with significantly reduced or with no fuel recirculation at ground idle. Earlier results indicated that fuel recirculation would be required at the idle descent flight condition even with high temperature fuel capability. This would seem to contradict the idea that ground idle is the critical sizing

point for the recirculation system. Again, the explanation for this may be that the idle descent requirements identified earlier are estimates of transient conditions using a steady state model. As a result, the estimated idle descent fuel heat sink requirements may be too high. Despite this, the trend established here of significantly reduced recirculation flow should apply at both flight conditions.

4.2.2 Preliminary Sizing of Recirculation System Components

The results of the IHPTET Phase II ASF fuel recirculation parametric were used to estimate the relative effect of recirculation flow on the weight of the fuel/air heat exchanger. The results, shown on Figure 4.2-7, were generated at the ground idle flight condition. Discussions with airframers indicated this to be the critical sizing point for these components. Although fuel recirculation rate is higher at the idle descent points, the air heat sink is at a lower temperature. As a result, the required level of airflow for the recirculation system is less than for the idle descent condition.

The recirculation system configuration used in this study is consistent with the configuration described in Section 3.3. The baseline ram air heat exchanger was sized for a max fuel temperature of 300F and a 3700 Btu/min airframe heat load. Using Figure 4.2-3, a fuel recirculation rate of 33 lb/min is indicated for these conditions. As was shown on Table 3.3-1, the baseline recirculation system ram air heat exchanger weight was assumed to be 30 lbs. This weight is representative of a state-of-the-art compact core heat exchanger. Performance curves indicate that the baseline heat exchanger would have a 1600 Btu/min heat return rate to the tank at the ground idle flight point.

When investigating the other fuel temperature limits and recirculation requirements, the heat return rate was held at 1600 Btu/min. Recirculation heat loads greater than this level represent the amount of heat that must be transferred from the fuel to the air in the heat exchanger. If the recirculation heat load was greater than zero but less than 1600 Btu/min, the heat exchanger can be removed but the recirculation line would be retained. Once the heat load and recirculation rate from Figure 4.2-3 was established, generalized design charts were used to establish the heat transfer coefficient and the required effective area of the heat exchanger. Weights were then predicted based on the assumption that weight is directly proportional to the required heat transfer areas of the heat exchanger.

The results on Figure 4.2-7 show that increasing the fuel temperature limit increases the amount of airframe heat load that can be rejected without increasing heat exchanger weight. The results also suggest that there is a point of diminishing return where increasing the heat exchanger weight does not proportionally increase exchanger heat transfer. This can be attributed to the assumption that the airflow rate is constant for all the parametric points studied. Increasing the airflow would require a redesign of the recirculation system inlet, inducing fan and ducting. Instead this study fixed the size (and weight) of these components and parametrically looked at the weight impact on the fuel/air heat exchanger with a fixed airflow. The results show that a 25 degree increase in fuel temperature capability decreases the heat exchanger weight by approximately 60%.

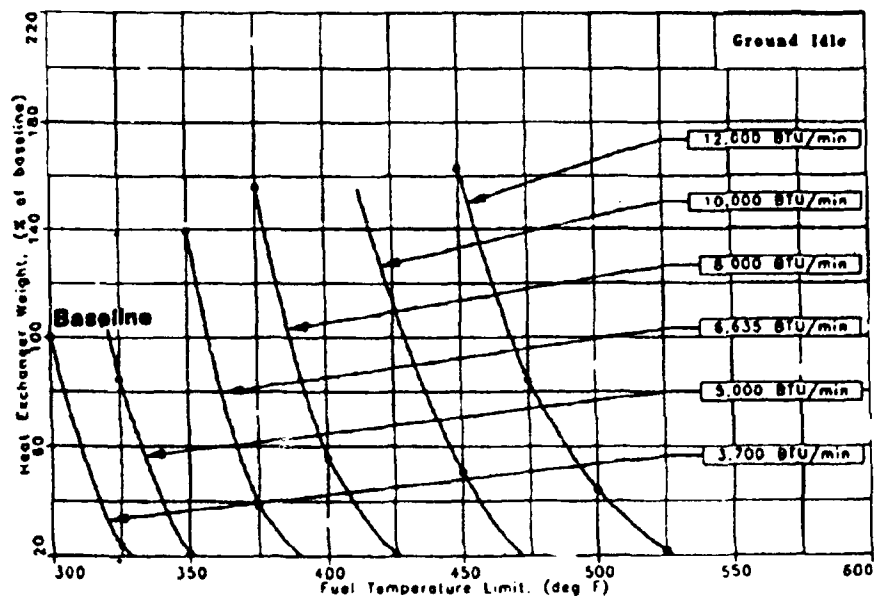


Figure 4.2-7 IHPTET Phase II Air Superiority Fighter Heat Exchanger Weight Payoff -
Based on Reduced Recirculation Requirements

Another approach that could be used to take advantage of higher fuel temperature capability would be to fix the heat exchanger size and use the increased capability to reduce (to a limit) the amount of heat returned to the tank below the assumed level of 1600 Btu/min. This would be accomplished by taking advantage of the higher exchanger effectiveness that would result with a higher fuel temperature. In reality, a system designer would trade both system weight and heat return rate to achieve the maximum benefit from increased fuel temperature capability.

4.2.3 Summary

Study results which showed that at the higher end of the curves, the heat exchanger size (as exhibited in terms of weight) has little effect on the required fuel temperature can attributed to the fact that this parametric was generated at a consistent heat exchanger airflow. In an aircraft design, the ejector and heat exchanger would be optimized to provide the required airflow and heat transfer with the minimum weight. This type of study detail would require the support of an airframer to capture the true impact of fuel temperature on recirculation weight. Still, this parametric provides an indication of the kind of payoff in terms of recirculation system weight reduction that is possible with improved fuel temperature capability.

SECTION 5.0

CONCLUSIONS

Based on this investigation, the following conclusions can be made:

1. Many airframer related issues such as future tactical fighter airframe heat loads and fuel tank insulation that effects the temperature of fuel in the tank have not been determined, making the definitive establishment of fuel temperature requirements difficult.
2. Payoff studies, the projection of future fuel system capabilities and the temperature development goals for other fluids indicate that the following are reasonable advanced JP fuel development goals:

Max Fuel Temp., °F

IHPTET Phase I	425
IHPTET Phase II	550
IHPTET Phase III	700

3. Achievement of these goals will not likely eliminate the requirement for a fuel recirculation system of future tactical fighters
4. Achievement of these goals will permit a significant reduction in the size and weight of the fuel recirculation system. While this does not result in a major reduction in the engine weight, the payoff in terms of reduced airframe recirculation system weight is significant.

SECTION 6.0

RECOMMENDATIONS

Increasing heat loads on the fuel and the desire to minimize the penalty associated with the recirculation system demands that higher fuel temperature capability be developed. While the engine itself will realize little weight savings, the benefit to the total airframe and propulsion system should be significant. The fact that fuel is a critical component to gas turbine operation makes the IHPTET initiative a logical vehicle for the development of advanced fuels.

This study has served as a starting point for establishing the requirements and payoffs for advanced fuels. The study also pointed out that fuel temperature requirements are driven by a wide variety of factors ranging from the mission, the airframe and the engine hydraulic and lubrication systems. With this in mind, a follow-on study should be considered that would look at the fuel, hydraulic and lubrication systems as a total package. Critical elements of this study would include:

- Use of an airframer as a subcontractor to establish projections of airframe heat loads and to get accurate estimates of fuel recirculation system weights.
- Definition of fuel system component capabilities that are projected and will be required in the future. Components like fuel lines, and pumps have temperature limits that should be considered when setting fuel development goals.
- Definition of the requirement that high temperature fuels make on the engine itself (i.e. high temperature fuel nozzles, etc.) and the impact of fuels at elevated temperatures on engine operation.
- An assessment of the impact of transient conditions like the idle descent flight points on fuel temperature requirements. If these situations are felt to be significantly different than the steady state conditions, the development of transient thermal management models may be considered.

Until these fuel development requirements are firmly defined, efforts should continue toward achievement of what would seem to be a definite requirement for high temperature capable fuels.